

## Evolution and variability of East Asian monsoon and the potential relationship with Himalaya-Tibet uplift

TADA, Ryuji<sup>1\*</sup>

<sup>1</sup>Graduate School of Science, the University of Tokyo

Monsoon is climatic phenomenon driven by heat capacity contrast between the continent and ocean, so every continent has its own monsoon system. Asian Monsoon is by far the largest monsoon system on the globe. Although it is regional phenomenon, it exerts significant influence on the global climate. The extremely large size of Asian Monsoon system is considered as having been caused by the presence of Himalaya and Tibetan Plateau (HTP). The large size and high altitude of HTP resulted in higher temperature at ca. 5000 m altitude compared to the surrounding area during summer that resulted in ascending air and development of low pressure cell over the plateau. Topographic effect could be also important to enhance summer monsoon. Large size of Asian continent enhanced cooling over continent during winter, resulted in development of high pressure cell known as Siberian High. HTP plays a role of topographic barrier that keeps Siberian High stronger and stable. Consequently, presence of HTP could have been playing a crucial role to strengthen Asian Monsoon. If correct, uplift of HTP could have resulted in intensification of Asian Monsoon.

Climatic simulations can be used to test the hypothesis that uplift of HTP has intensified Asian Monsoon if uplift history of HTP is known well. However, timings, modes, and magnitudes of HTP uplift have been poorly understood until recently. Situation is rapidly improved recently due to accumulation of thermo-chronological data from the various parts of HTP. Namely, collision of Indian Subcontinent against Eurasian Continent approximately at 40 Ma caused the 1st phase of Tibetan uplift that raised southern Tibet close to the present height by 35 Ma. From 25 Ma to 15 Ma, Main Central Thrust (MCT) and South Detachment System (STDS) in frontal Himalaya were activated and lower crust was extruded and eroded extensively. Approximately at 15 Ma, these fault system ceased their movements and east-west extension started in Tibet. From 15 Ma to 10Ma is the 2nd phase when Tibetan Plateau grew southeastward and possibly also northward. The 3rd phase of uplift started from approximately 5 Ma when northwestern Tibet, TienShan and Altai Mountains uplifted. Using this uplifting history of HTP as a boundary condition, it is possible to estimate what kind of paleoclimatic changes are expected in response to these 3 uplift phases based on climate simulation results.

In this presentation, I will review a recent progress in researches on tectonics-climate linkage as HTP uplift and Asian Monsoon evolution as an example.

Keywords: Monsoon, Himalaya-Tibet, Tectonics-Climate Linkage, East Asia, Japan Sea, Westerly Jet

## Pre-Miocene Birth of the Yangtze River

ZHENG, Hongbo<sup>1\*</sup> ; CLIFT, Peter<sup>1</sup> ; WANG, Ping<sup>1</sup> ; TADA, Ryuji<sup>1</sup> ; JIA, Juntao<sup>1</sup> ; HE, Mengying<sup>1</sup> ; JOURDAN, Fred<sup>1</sup>

<sup>1</sup>Nanjing Normal University

The development of fluvial systems in East Asia is closely linked to the evolving topography following India-Eurasia collision. Despite this, the age of the Yangtze River system has been strongly debated, with estimates ranging from 40-45 Ma, to a more recent initiation around 2 Ma. Here, we present new <sup>40</sup>Ar/<sup>39</sup>Ar ages from basalts interbedded with fluvial sediments from the lower reaches of the Yangtze together with detrital zircon U/Pb ages from sand grains within these sediments. We show that a river containing sediments indistinguishable from the modern river was established before ~23 Ma. We argue that the connection through the Three Gorges must post-date 36.5 Ma because of evaporite and lacustrine sedimentation in the Jiangnan Basin before that time. We propose that the present Yangtze River system formed in response to regional extension throughout eastern China, synchronous with the start of strike-slip tectonism and surface uplift in eastern Tibet and fed by strengthened rains caused by the newly intensified summer monsoon. Birth of the eastward flowing Yangtze River around the Oligocene/Miocene boundary changed largely the 'source to sink' regime in the East Asia-West Pacific region

Keywords: Yangtze River, birth, Tibetan Plateau, drainage capture, Asian monsoon

## The missing volcanic record captured by dispersed ash in sediment of the Japan Sea/East Sea and NW Pacific Ocean

MURRAY, Richard<sup>1\*</sup> ; SCUDDER, Rachel P.<sup>1</sup> ; DUNLEA, Ann G.<sup>1</sup> ; IKEHARA, Ken<sup>2</sup> ; IRINO, Tomohisa<sup>3</sup> ; TADA, Ryuji<sup>4</sup> ; ALVAREZ-ZARIKIAN, Carlos A.<sup>5</sup> ; KUTTEROLF, Steffen<sup>6</sup> ; SCHINDLBECK, Julie<sup>6</sup> ; SCIENTIFIC PARTY, Expedition 346<sup>5</sup>

<sup>1</sup>Boston University, <sup>2</sup>Geological Survey of Japan, <sup>3</sup>Hokkaido University, <sup>4</sup>University of Tokyo, <sup>5</sup>IODP-TAMU, <sup>6</sup>GEOMAR, Kiel

Volcanic ash in marine sediment provides a wealth of information not only about volcanism and arc evolution, but also potentially regarding climate change, geochemical mass balances, hydration of marine sediment during alteration, the geodynamics of subduction zones, and other key components of the earth-ocean-atmosphere system. Ash occurs both as discrete *layers* as well as isolated grains and shards *dispersed* throughout the bulk sediment, and with highly variable grain sizes.

The study of this dispersed component has lagged behind the sedimentologic and chemical assessment of the ash layer record. For example, while decades of smear-slide studies of bulk sediment in volcanic-rich regimes have presented visual estimations of the abundance of volcanic glass, shards, and other components, the quantitative importance of the dispersed ash or cryptotephra remains largely unconstrained on local, regional, and global scales. Also, compared to the often visually stunning ash layer records, which in certain settings can leave single layers with thicknesses of 10s of cm, the dispersed ash component and cryptotephra are unable to be visually differentiated from detrital clay.

We summarize here preliminary results regarding the distribution, composition, and accumulation of dispersed ash in sediment from the Japan Sea/East Sea (gathered during IODP Expedition 346, Asian Monsoon, and ODP Legs 127/128), and compare it to the record provided by discrete ash layers. We will interpret our work in the context of our ongoing studies of dispersed ash throughout the northwest Pacific, Nankai, and Izu-Bonin regions, which is based on sediment from DSDP/ODP/IODP Sites 52, 444, 579/581, and 1149, as well as from Sites C0011 and C0012.

Multivariate statistical treatments are an integral part of our approach, as the bulk determination of the major, trace, and REEs provides the chemical context for our determination of provenance, and the statistical models allow distinctive resolution of the different aluminosilicate components based on their individual geochemical signature(s). A corollary benefit of our approach is an improved determination of the eolian component, as we are able to discern how contributions of dispersed ash have been inadvertently attributed to the eolian aluminosilicate inventory. Q-mode Factor Analysis can help determine the number, and composition of, potential end member contributions. Applying these results in conjunction with Total Inversion, a linear regression technique, allows determination of the compositional variation of these end members.

Consistent with the qualitative smear-slide estimates, in these ash rich regions we find that the dispersed component can account for up to 40% of the total sediment. We are able to document abundances to a relatively high degree of precision (+/- 3-5%) on a sample-by-sample basis, and are further able to distinguish between different chemistries of the dispersed component, and document sources that change through time and space. In addition to providing an overview of “ the missing volcanic record ” , we will discuss some ongoing challenges, including how to best examine the relationship between the composition of the discrete ash layers compared to the discrete component, and what information can be gained from examining similarities and differences between their respective sources.

Keywords: volcanic ash, sediment chemistry, Japan Sea, East Sea, volcanism

## Tephrochronology and evolution of volcanic activities in Japanese islands during late Cenozoic

IKEHARA, Ken<sup>1\*</sup>

<sup>1</sup>Geological Survey of Japan, AIST

The Japanese islands are located along an active plate margin, and are home to many active volcanoes along an island arc. Large, explosive volcanic eruptions have yielded numerous volcanic ash layers (tephras) over geological time. Because tephra are deposited in both onland and seafloor areas, they represent a unique and important link between the geological records of the two settings. There are several source volcanoes to provide tephra to the Japan Sea floor. These are, for example, Kikai, Aira and Aso volcanoes in Kyushu, Sanbe and Daisen volcanoes in Chugoku, Asama volcano in north Kanto, Towada volcano in Tohoku, Toya volcano in Hokkaido, Ulleung volcano on Ulleung Island in the western Japan Sea, and Baegdusan volcano on Korean Peninsula. Most of the previous marine tephra studies in the Japan Sea have been concentrated for the late Quaternary in age. Because of shallow CCD and shallow gateways of the Japan Sea, oxygen isotope stratigraphy is not a perfect tool for age determination, especially in the deep-sea basins. Under the condition, wide-spread tephra works as a key bed connecting among marine cores, and give us a good time-marker. Quaternary Japan Sea sediments are characterized by alternating light- and dark-colored layers. The late Quaternary dark layers were deposited basin-wide in relation to enhanced summer monsoon during the interstadials of the Dansgaard-Oeschger cycles. Recent study on marine tephra among several marine cores in the central Japan Sea suggested the synchronicity of the dark layer deposition. This is clear evidence on significance of marine tephra study for inter-core correlation. Furthermore, tephra may connect the events in marine environments and those in terrestrial and lacustrine environments. Thus, tephra in the Japan Sea sediments are important for the paleoceanographic and paleoclimatic study in and around the Japan Sea. Information on longer time-scale occurrence of tephra layers and their source volcanoes will give us spatio-temporal variation of volcanic activities and their relations to the regional tectonic movements around the Japan Sea, because the continuous and muddy Japan Sea has been a good recorder of tephra layers after its opening.

Keywords: tephra, Japan Sea, stratigraphy

## Identification of Asian dust in hemipelagic sediments of East Asian marginal seas

IRINO, Tomohisa<sup>1\*</sup>

<sup>1</sup>Hokkaido University

Detrital fraction contained in marine sediments can be generally used as climate proxies because variations in provenance and mineralogy could be affected by the precipitation distribution and weathering intensity. Element composition of marine sediment is essentially controlled by the mineral composition that is also affected by sorting effect during their transport process. The inland deserts such as Taklimakan and Gobi are large detrital sources for the East Asian marginal seas, and the detrital fraction in the sediments collected from the abyssal part of the Japan Sea / East Sea has been regarded as the mixture of eolian dust and the detritus derived from the Japan Arc. This feature can be used to reconstruct the variability of provenance and transport pathway of detrital fraction in the sediments. Relative contribution of dust from Taklimakan / Gobi could be strongly affected by dust availability in source area and wind system transporting the dust. Major changes in such detrital provenance are more easily reconstructed from the proximal soil record at loess plateau, where many provenance studies have been conducted. Loess can be classified into two types based on their element composition. One is typical loess distributed close to desert area. The other is peripheral soil (weathered loess) distributed surrounding typical loess and desert area. Weathered loess is distributed in the northeastern and southern China in modern times. Spatial distribution of these two types of soils have been also changed from time to time. In order to detect the change in provenances and interpret the terrestrial environment using detrital proxies in the marginal sea sediments, it is necessary to know the variability or range of the element and mineral composition of a particular provenance during the targeted time periods as well as the sorting biases during the transportation.

Keywords: hemipelagic sediment, aeolian dust, provenance, mineral composition, element composition, isotope composition

## Carbon and Sulfur Cycling in Shallowly Buried Sediment of the Japan Sea/East Sea

DICKENS, Gerald<sup>1\*</sup>; KINSLEY, Christopher W.<sup>2</sup>; DUNLEA, Ann G.<sup>3</sup>; ANDERSON, William A.<sup>4</sup>; DA COSTA GURGEL, Marcio H.<sup>5</sup>; LEE, Kyung eun<sup>6</sup>; MURRAY, Richard W.<sup>3</sup>; TADA, Ryuji<sup>7</sup>; ALVAREZ ZAREKIAN, Carlos<sup>8</sup>; EXPEDITION 346, Scientific party<sup>8</sup>

<sup>1</sup>Rice University, <sup>2</sup>Massachusetts Institute of Technology, <sup>3</sup>Boston University, <sup>4</sup>Florida International University, <sup>5</sup>Universidade de Sao Paulo, <sup>6</sup>Korea Maritime University, <sup>7</sup>University of Tokyo, <sup>8</sup>Texas A&M University

Continental slopes cover about 10% of Earth's surface and represent the primary repository for sediment and organic carbon accumulation on long-time scales. For decades, the geochemical community has introduced and discussed various models for how ocean carbon and sulfur chemistry changes over time. Remarkably, in most of these models, the seafloor on continental slopes is either absent or passive. In the latter case, the prevailing view is as follows. During burial, organic carbon passes through a gauntlet of microbially mediated reaction in shallow sediment, especially including organoclastic sulfate reduction and methanogenesis. Although these reactions generate dissolved species (HCO<sub>3</sub><sup>-</sup>, HS<sup>-</sup>, CH<sub>4</sub>), burial fluxes exceed those of upward advection or diffusion. The end process, therefore, is accumulation of remnant solid organic carbon, authigenic carbonate, and authigenic Fe-sulfides. As suggested in several recent papers, this view may be incorrect. Instead, on the slope, a good fraction of solid organic carbon bypasses organoclastic sulfate reduction to produce dissolved inorganic carbon, dissolved organic carbon, and methane at depth. Large portions of these species return toward the seafloor because upward dissolved fluxes exceed burial. However, upward migrating methane reacts with dissolved SO<sub>4</sub><sup>2-</sup> to produce HCO<sub>3</sub><sup>-</sup> and HS<sup>-</sup> via AOM in shallow sediment. The end process is still accumulation of remnant solid organic carbon, authigenic carbonate, and authigenic Fe-sulfides, but the fluxes are linked through the formation, storage and consumption of methane.

It is entirely possible that variations in methane cycling within slope sediments drive significant long-term and short-term changes in ocean carbon and sulfur concentrations. To entertain this idea, however, the broad Earth Science community needs quantified fluxes of solid and dissolved components from appropriate settings. One current problem is that very few locations on continental slopes that have detailed pore water profiles extending 200 m below the seafloor with companion sedimentary records.

IODP Expedition 346 drilled multiple holes at seven sites across the Japan Sea/East Sea. The primary objective behind this cruise was late Neogene and Quaternary paleoceanography: more specifically, to reconstruct changes in surface and deep ocean water properties, riverine outflow, and dust input over the last 5-10 million years, which might be linked to the evolution and temporal differences in the Asian monsoon system. One interesting outcome of this goal was that the sites span a wide range of slope environments with considerable variation in organic carbon accumulation. Another was exquisite sediment recovery, with spliced cores between holes giving complete records from the seafloor to several hundred meters.

Expedition 346 provided a golden opportunity to chase the dynamic geochemical cycling of carbon and sulfur on continental margins. Using a combination of rhizon sampling and whole round squeezing, about 680 pore water samples were collected at the seven sites and analyzed for a broad array of dissolved species. The shipboard pore water geochemistry profiles generated on Expedition 346 are truly remarkable in terms of species examined, their detail across zones of chemical reaction, and the ability to directly couple them to the sedimentary record. Here, on behalf of the Expedition 346 scientists, we discuss the generation of the pore water profiles and their significance to carbon and sulfur cycling on continental slopes. For example, at Site U1427, there is no question as to the dominant process and where species are being produced and consumed in shallow sediment. Upward migrating CH<sub>4</sub> is reacting with SO<sub>4</sub><sup>2-</sup> via AOM to produce HCO<sub>3</sub><sup>-</sup> and HS<sup>-</sup>, the first product leaking to the seafloor, the latter product being consumed into sulfide minerals.

Keywords: Methane, AOM, carbon cycle, sulfur cycle

## N.incompta Mg/Ca-paleothermometry in the Japan Sea and its application to Holocene climate reconstruction

HORIKAWA, Keiji<sup>1\*</sup> ; KODAIRA, Tomohiro<sup>1</sup> ; IKEHARA, Ken<sup>2</sup> ; MURAYAMA, Masafumi<sup>3</sup> ; ZHANG, Jing<sup>1</sup>

<sup>1</sup>University of Toyama, <sup>2</sup>AIST, <sup>3</sup>The Center for Advance Marine Core Research, Kochi University

We present new core-top calibration for *Neogloboquadorina incompta* Mg/Ca-paleothermometry in the Japan Sea using 15 core-top surface sediments taken from the southern Japan Sea. Using this new Mg/Ca-paleothermometry, we generate the first high-resolution Mg/Ca-derived SST record for the past 7000 years from the sediment core (YK10-7-PC09) taken from 738 m water depth off Niigata. The age model for core YK10-7-PC09 was based on 8 AMS <sup>14</sup>C data of mixed planktic foraminifera, and the conventional <sup>14</sup>C ages were converted to the calendar ages using Marin13 and delta R of 0±100 yr. Trace metal/Ca ratio of *N.incompta* was measured by a SF-ICP-MS (Thermo Fisher Element II) and the precision (1sigma) of Mg/Ca ratios of the international CaCO<sub>3</sub> standard (BAM-RS3) was 0.786±0.008 (n=100).

We have performed paired analyses of δ<sup>18</sup>O<sub>c</sub> and Mg/Ca ratios of *N. incompta* at 15 sites. First, to calculate the mean temperatures of waters in which the foraminiferal shells were formed (i.e., calcification temperature), we have used modern local salinity and temperature data (<http://www.jodc.go.jp/>) in the following paleotemperature equation; T (°C) = 21.4-4.19×(δ<sup>18</sup>O<sub>c</sub>-δ<sup>18</sup>O<sub>sw</sub>) + 0.05×(δ<sup>18</sup>O<sub>c</sub>-δ<sup>18</sup>O<sub>sw</sub>)<sup>2</sup> (Oba, 1980). The δ<sup>18</sup>O<sub>sw</sub> was calculated from the following salinity-δ<sup>18</sup>O<sub>sw</sub> equation in the Japan Sea (δ<sup>18</sup>O<sub>sw</sub> (‰ VSMOW) = 0.27×Salinity-8.98; this study). The comparison of the predicted δ<sup>18</sup>O<sub>c</sub> values with the measured δ<sup>18</sup>O<sub>c</sub> shows that *N. incompta* shells were formed at 0-125 m water depths from June to December in the Japan Sea. Given that previous studies show that *N.incompta* dwells in the shallow waters (<100 m) in November to December (Kuroyanagi and Kawahata., 2004; Sagawa et al., 2013), we calculated the calcification temperatures at each site assuming shells were formed in November to December. The cross plot of the calcification temperatures and the Mg/Ca ratios for our core-top samples gives the following equation; Mg/Ca (mmol/mol) = 0.361×exp (0.043×Temp).

Using this new Mg/Ca-paleothermometry, the 7000-years *N.incompta* Mg/Ca records (0.6 to 0.9 mmol/mol, n=127) from core YK10-7-PC09 were converted to the temperature record. Compared to the present winter SST of ca.15 °C, the 7000-year SSTs varied from 13.5 °C to 20.8 °C. We identified four periods (ca.6000 yr BP, 4000-3500 yr BP, 3000-2300 yr BP, and 800 yr BP) that were warmer than the present and distinct colder periods at ca.4500 yr BP and ca.1500 yr BP than the present. This SST variability for the past 7000 years was almost consistent with the record of relative abundance of *F.doliolus*, which is the dominant species in the Tsushima Current (Koizumi et al., 2006). This finding indicates that the Tsushima Current influx might have changed with time and altered the heat transport into the Japan Sea, and probably induced significant changes in terrestrial precipitation and vegetation over the northern part of Japan facing the Japan Sea.

Keywords: Japan Sea, Holocene climate change, Mg/Ca-paleothermometry, Tsushima Current, *Neogloboquadorina incompta*

## Shallow water environmental change in the Sea of Japan during the last 30 kyr deduced from foraminiferal isotopes

SAGAWA, Takuya<sup>1\*</sup> ; UCHIDA, Masao<sup>2</sup> ; MURAYAMA, Masafumi<sup>3</sup> ; TADA, Ryuji<sup>4</sup>

<sup>1</sup>Department of Earth and Planetary Sciences, Faculty of Sciences, Kyushu University, <sup>2</sup>National Institute for Environmental Studies, <sup>3</sup>Center for Advanced Marine Core Research,, Kochi University, <sup>4</sup>Department of Earth and Planetary Science, Graduate School of Science, The Univeristy of Tokyo

The Sea of Japan is a marginal sea that connects with North Pacific and adjacent marginal seas by four shallow straits. Because water depth of the deepest straits today is ~130 m (Tsushima Strait and Tsugaru Strait), environments of Sea of Japan have been strongly affected by sea level fluctuations related to the glacial-interglacial cycles. Previous studies report that foraminiferal oxygen isotope variation from Sea of Japan is distinct from that commonly seen in seas of the world. Since Sea of Japan is nearly isolated from adjacent seas during the glacial maxima, salinity of surface water significantly decreases, and therefore foraminiferal isotopes show the lowest values due to the unique fresh water balance. The peak value of oxygen isotope is ~0.5 per mil at the last glacial maximum, which is ~2.5 per mil lighter than at 30 ka. We review literature data and present new results of two sediment cores from northeastern and southern part of Sea of Japan. The new data from southern core has ~70-yr resolution and shows abrupt shift that may correspond to abrupt climate change reported from the Greenland ice core and Asian monsoon proxy data of Chinese Cave and Loess. The new results suggest that the surface environment of Sea of Japan is sensitive to eustatic sea level change as well as abrupt climate changes.

Keywords: Sea of Japan, oxygen isotope, planktonic foraminifer



## Micropaleontological evidence of oceanic circulation changes in the Japan Sea during Pliocene to Pleistocene transition

ITAKI, Takuya<sup>1\*</sup>

<sup>1</sup>Geological Survey of Japan, AIST

Oceanic circulation in the Japan Sea is characterized by flowing of the Tsushima Warm Current and deep-water formation during the interglacial periods, while deep circulation was stagnant due to weakened deep convection with development of the low salinity surface water during the glacial periods. Such cycles of oxic and anoxic deep-water conditions recorded in sediments as alternations of light and dark hemi-pelagic mud layers occurred since ca. 2.5 Ma near Pliocene to Pleistocene transition. The results of micropaleontological studies from previous ocean drilling sites and many onshore sequences have provided various insights into oceanic changes related to global climatic and regional tectonic events during Pliocene to Pleistocene.

Fossil records of shallow dwelling plankton and shelf related benthos are composed of the assemblage associated with upper water environments. Warm-water ostracods and molluscs are rarely recognized from onshore sequences in Japan along the Japan Sea side during the Pliocene climatic optimum (3.2 to 2.7 Ma), and they were most likely associated with subtropical water mass entered from the southern strait. However, planktonic foraminiferal and radiolarian assemblages in hemipelagic sediments suggest that the warm-temperate water was originated from the northern strait during this period. Such conflict interpretation could be explained by a characteristic surface circulation, which was composed of two different water sources from the northern and southern straits. The warm water mass from the southern strait was restricted flowing along the Japanese coastal area, while another water mass from the northern strait was present offshore areas of the sea. Abundance of cold-water calcareous nannofossil species increased significantly at 2.75 Ma corresponding to the global cooling. In this period, ostracode assemblage also indicates cooling in the intermediate water. According to planktonic foraminifers and radiolarians, significant inflow of the subtropical water from the southern strait started at 1.7 Ma, which might be related to the deepened Tsushima Strait and the Okinawa Trough (ca. 2 Ma).

Deep-water environments in the Japan Sea are little known compared with that of shallow environments. Benthic foraminifers in deep-sea sediments changed their faunal composition from agglutinated fauna to calcareous fauna through 3 to 2 Ma. Similarly, deep-water radiolarians show faunal replacement from the Pacific-type deep dwellers to the Japan Sea-type deep dwellers at ca. 2.6 Ma. Such faunal changes recognized from benthic foraminifers and radiolarians imply that the unique deep-water circulation in the Japan Sea was formed with geographical isolation from the Pacific deep water. In actual, this timing is almost coincident with beginning of oxic and anoxic cycles in the Japan Sea. It is likely resulted from either the global cooling or local tectonic motion during the Pliocene to Pleistocene transition.

Keywords: Microfossils, Paleoceanography, Grobal cooling event, Tectonic event, Tsushima Warm Current, Deep water

## Evolution of the Kuroshio Current and its impact on East Asian marginal seas

LEE, Kyung eun<sup>1\*</sup>

<sup>1</sup>Korea Maritime and Ocean University

Quaternary is characterized by the onset of the Quaternary ice ages as well as the progressive cooling of the high latitude. Many proxy records from high latitude evidence this. On the other hand, records from low latitudes indicate that the sea surface temperature of the tropical warm pool regions remained relatively stable during the last 4 Ma. Hence these suggest a dramatic increase in the zonal (west?east) and meridional (north?south) gradients in sea surface temperature, which was accompanied by a progressive cooling of the water upwelled along the eastern margins of the Pacific. It is most likely believed that the evolution of the west-east and north-south temperature gradients in the North Pacific is closely related to the evolution of the western boundary current and North Pacific subtropical gyre during the Plio-Pleistocene. It, in turn, caused changes in weather and climate patterns of East Asian margins. In this presentation, previously published data and hypothesis will be reviewed to clarify future researches related to these.

Keywords: Kuroshio, North Pacific Subtropical Gyre, sea surface temperature

## Variations in intermediate water and ocean circulation during the last 26 ka based on a new benthic Mg/Ca calibration

KUBOTA, Yoshimi<sup>1\*</sup> ; KIMOTO, Katsunori<sup>2</sup> ; ITAKI, Takuya<sup>3</sup> ; YOKOYAMA, Yusuke<sup>4</sup> ; MATSUZAKI, Hiroyuki<sup>5</sup>

<sup>1</sup>National Museum of Nature and Science, <sup>2</sup>Japan Agency for Marine-Earth Science and Technology, <sup>3</sup>Geological Survey of Japan, AIST, <sup>4</sup>Atmosphere and Ocean Research Institute, University of Tokyo, <sup>5</sup>School of engineering, University of Tokyo

In order to understand variations in ocean circulation at intermediate depth in the North Pacific in subtropical area, bottom water temperatures (BWT), carbon isotope of benthic foraminifera, and oxygen isotope of seawater were reconstructed since 26 ka off east main Okinawa Island, northwestern Pacific. A new regional Mg/Ca calibration for benthic foraminifera *Cibicides wuellerstorfi* was established in order to convert benthic Mg/Ca value to temperature, based on twenty-nine surface sediment samples, including core top samples, retrieved around main Okinawa Island. On the other hand, in order to reconstruct changes in water properties since 26 ka, core GH08-2004 that was retrieved from water depth of 1166 m off east main Okinawa Island was used in this study. As a result, during the LGM from 24 ka to 18 ka, BWT showed relatively constant as approximately 2 °C, which was ~1.5-2 °C lower than today. One of the prominent features of our BWT records was a millennial scale variation in BWT during the last deglaciation. During the last deglaciation, BWT was higher in Heinrich Stadial 1 (H1) (~17 ka) and Younger Dryas (YD) (~12 ka), while lower in Bølling/Allerød (BA) interval (~14 ka). During the interval from 17 to 15 ka, BWT tended to decrease in association with a decrease in carbon isotope of *C. wuellerstorfi*, likely interpreted as increased upwelling of the older water mass that was stored in the abyssal Pacific during the glacial time. The timing of the signal of the upwelling coincided with deglacial atmospheric CO<sub>2</sub> rise initiated at ~17 ka, suggesting the increased upwelling in the subtropical northwestern Pacific from 17 to 15 ka contributes the carbon release to the atmosphere from the Pacific.

## Long-term evolution of the North Pacific subtropical gyre: Implication from the late Quaternary record

UJIIE, Yurika<sup>1\*</sup>

<sup>1</sup>Faculty of Science, Shinshu University

The North Pacific subtropical gyre drives a transportation of huge amount of heat from low to high latitude area to maintain warm climate in the northwestern Pacific area. This gyre system largely controls the zonal temperature gradient and west-east asymmetric climate, currently observed in the Pacific Ocean. The stepwise enhancement of these temperature gradients has partly been observed in the equatorial and east Pacific area since the late Pliocene. However, a lack of long-term observation in the west Pacific Ocean impedes a better understanding of the development of the Pacific climate.

The Kuroshio Current, flowing from the Okinawa Trough to eastward off the Japan, act as a heat-transfer along the North Pacific subtropical gyre margin. The variation in this surface current would reflect to the changes of the West Pacific climate. Especially, the Okinawa region is an ideal place for paleoclimatographic reconstruction, as (1) the Kuroshio Current shows an oscillation with surrounding water masses and (2) the sediments are buried in high rate. Through the short-term paleoceanographic records in the Okinawa region, the planktonic foraminiferal assemblage showed the decrease of the Kuroshio indicator and increase of the coastal- and cold-water masses indicators under the modern Kuroshio path (the East Chia Sea) during MIS 2. Interestingly, the long-term record, which was the first to cover the past 200 kyrs in this region, represented different oceanic condition during MIS 6. The indicator of the upper intermediate water in the subtropical gyre increased over whole of the Okinawa region at this time. Moreover, the Mg/Ca paleo-temperatures in the surface and upper intermediate layers showed that warming in the upper intermediate layer was continuing from MIS 6 to MIS 5e, while warming in this layer was rapidly stopped at MIS 2. Both records of the paleo-temperature and planktonic foraminiferal assemblage congruently suggest the development of the intermediate water in the North Pacific subtropical gyre during MIS 6, instead of the dominance of cold water mass observed during MIS 2. The intermediate water has likely been undergone an independent process from the changes of the surface water masses at least by MIS 5. Even the 200 kyrs record successfully inferred two different glacial mechanisms of MIS 2 and 6, associating with the changes of surface water masses and deeper waters. Future study with longer record will lead a comprehensive understanding how the modern water column structure has been developed in the Pacific Ocean.

Keywords: North Pacific subtropical gyre, Kuroshio, water column structure, Pleistocene

## Changes of water structures in the Sea of Japan during the Late Pliocene

YAMADA, Katsura<sup>1\*</sup> ; IRIZUKI, Toshiaki<sup>2</sup>

<sup>1</sup>Shinshu University, <sup>2</sup>Shimane University

An analysis of fossil ostracode assemblages in the Kuwae Formation, central Japan, clarify the paleoenvironmental changes related to glacial and interglacial cycles during MIS G19 and G10 (Irizuki et al., 2007). Added to this, temperate intermediate waters which were warmer than those of today, were existed in interglacial periods during 3.5 to 2.8 Ma. Radiolarian faunas inferred that enhancement of ventilation due to global cooling started at approximately 2.5 Ma (Kamikuri and Motoyama, 2007). However, temperatures of the temperate intermediate waters and the timing are uncertain. So, our aims are to clarify quantitative temperatures of shallow and intermediate waters during the late Pliocene based on Mg/Ca, and to discuss change of water structures in the Sea of Japan.

Siltstones collected from the Kuwae Formation along the Tainai River were soaked in H<sub>2</sub>O<sub>2</sub> for 24 hours before they were washed. Ostracode shells of genus *Krithe* (intermediate water species) and *Cytheropteron miurense* and *Cytheropteron sawanense* (shallow water species) were taken from the residues, and their Mg/Ca were measured by ICP-AES at Kochi University. Two intervals were identified in the study section based on quantitative temperature of intermediate and shallow waters and their vertical changes. Intermediate water temperatures ranged between 0 and 10 °C and fluctuated in short-time intervals during MIS G19-G16, although they were stable and showed a small amplitude between 3 and 7 °C during MIS G15-G13. Moreover, difference in temperature between shallow and intermediate waters was large in MIS G19 and G16, but was small in MIS G15-G13. These temperature difference and shifts suggest that strong stratification of shallow and intermediate waters during MIS G19-G16 changed to a condition in which temperature gradients were small due to enhance of ventilation in the Sea of Japan. MIS G15 and G13 were characterized by a large oxygen isotope values compared with those in other inter-glacial periods of the study intervals. The relative cooling in inter-glacial periods might be caused a beginning of ventilation in the Sea of Japan.

Keywords: Sea of Japan, Late Pliocene, ostracode, Mg/Ca, water structure

## Sedimentary Rhythms in the Middle Miocene Onnagawa Formation in Northern Japan

KUROKAWA, Shunsuke<sup>1\*</sup> ; TADA, Ryuji<sup>1</sup> ; TAKAHASHI, Satoshi<sup>1</sup> ; MIZUTANI, Akane<sup>1</sup> ; KUBOKI, Yui<sup>1</sup>

<sup>1</sup>Department of Earth and Planetary Science, Graduate School of Science, The University of Tokyo

The Middle to Late Miocene bedded siliceous rocks, are widely distributed in the Pacific rim. Typical examples are the Monterey Formation, distributed along the coast of California, and the Onnagawa Formation in northern Japan. The Onnagawa Formation is mainly composed by alterations of porcellanite and siliceous mudstone, called "hard-soft alternation", and finer alternations of light and dark porcellanites, in which parallel lamination is relatively well preserved. These alternations show centimeter- to meter-scale rhythms, where meter-scale rhythm is interpreted as reflecting variations in the water mass structure within the Japan Sea induced by sea-level oscillations paced by Milankovitch cycles (Tada, 1991). On the other hand, centimeter-scale rhythm reflects millennial-scale changes whose origin and cyclicity are still poorly understood.

In this study, we aim to reveal origin and cyclicity of light-dark alternation in the Onnagawa Formation, their relationship with variation of water mass structure in the Japan Sea, and implication to global climatic change.

We will create the perfectly continuous column of the Onnagawa Formation and construct detailed age model based on microfossil biostratigraphy and cyclo-stratigraphy. Then we will calculate the silica and detritus fluxes, respectively, from chemical composition of the siliceous rocks. We will discuss temporal variation of the water mass structure in the Japan Sea and its relation with global climatic changes.

In this presentation, we will introduce the results of our field study in Yashima area in northern Japan.

Keywords: Miocene, Onnagawa formation, Sedimentary rhythm

## Reconstruction of detrital flux to Lake Suigetsu during the past 20kyrs based on Color and XRF data

SUZUKI, Yoshiaki<sup>1\*</sup>; TADA, Ryuji<sup>1</sup>; NAKAGAWA, Takeshi<sup>2</sup>; NAGASHIMA, Kana<sup>3</sup>; HARAGUCHI, Tsuyoshi<sup>4</sup>; GOTANDA, Katsuya<sup>5</sup>; IRINO, Tomohisa<sup>6</sup>; SUGISAKI, Saiko<sup>1</sup>; SG12/06, Project members<sup>7</sup>

<sup>1</sup>Univ. Tokyo, <sup>2</sup>Univ. Newcastle, <sup>3</sup>JAMSTEC, <sup>4</sup>Osaka City University, <sup>5</sup>Chiba University of Commerce, <sup>6</sup>Hokkaido University, <sup>7</sup>SG12/06 Project

Lake Suigetsu is known for its highly precise age-depth model based on numerous <sup>14</sup>C dating combined with varve counting and wiggle matching with Chinese stalagmite record. For this reason, the sediments are capable of providing extremely precise and high resolution records of past climatic changes. Several paleo-climate reconstruction studies have been conducted based on pollen and diatom analyses of the Lake Suigetsu sediments. However, studies focusing on its detrital material were rare because its detrital component is expected to be a mixture of eolian dust, detrital material derived from surrounding slope of the lake, and suspended material derived from Hasu River that flew into Lake Mikata and came into Lake Suigetsu through a narrow and shallow channel, and it is difficult to separately evaluate materials from these different sources. However, our recent study revealed that it is possible to evaluate the contribution of the detrital material derived from Hasu River through Lake Mikata (See our presentation #01575 in Paleoclimatology and paleoceanography session).

In this study, we tried to reconstruct temporal changes in the flux of detrital material derived from Hasu River during the past 20kyrs based on Color data and XRF data of the major element composition of the sediments analyzed by XRF. We estimated the end-members to explain variations in major element chemical composition using Q-mode factor analysis and oblique rotation of reference vectors. We extracted 4 end members and found that characteristics of factor 2 resemble those of Hasu River suspension. Because number of major element composition data are limited, we estimate contribution of factor 2 to the sediment based on color data. We estimated contents of factor 2 using Multi-regression analysis between color data and factor 2 loading (composition). Factor 2 flux was calculated from factor 2 contents, dry bulk density, and linear sedimentation rates, and the result shows long-term and short-term trends. The short-term trend is characterized by sudden increases and subsequent gradual decreases of factor 2 flux where the sudden increases coincides with sedimentation of "event layers" that could represent earthquake. The long-term trend, which seems to reflect intensity of river discharge from Hasu-River, seems to reflect rainfall intensity, shows mirroring image against stalagmite record in China suggesting that precipitation decreased in Suigetsu area when precipitation increased in South China.

Keywords: Lake Suigetsu, Deglaciation, Holocene, Factor analysis, Multi-regression analysis

## The East Asian winter monsoon variability during the past 150,000 years

YAMAMOTO, Masanobu<sup>1\*</sup> ; SAI, Hiroataka<sup>1</sup> ; CHEN, Min-te<sup>2</sup> ; ZHAO, Meixun<sup>3</sup>

<sup>1</sup>Faculty of Environmental Earth Science, Hokkaido University, <sup>2</sup>National Taiwan Ocean University, <sup>3</sup>Ocean University of China

The response of the East Asian winter monsoon variability to orbital forcing is still unclear, and hypotheses are controversial. We present a 150,000 yr record of sea surface temperature difference (delta SST) between the South China Sea and other Western Pacific Warm Pool regions as a proxy for the intensity of the Asian winter monsoon, because the winter cooling of the South China Sea is caused by the cooling of surface water at the northern margin and the southward advection of cooled water due to winter monsoon winds. The delta SST showed dominant precession cycles during the past 150,000 yr. The delta SST varies at precessional band and supports the hypothesis that monsoon is regulated by insolation changes at low-latitudes (Kutzbach, 1981), but contradicts previous suggestions based on marine and loess records that eccentricity controls variability on glacial-interglacial timescales. Maximum winter monsoon intensity corresponds to the May perihelion at precessional band, which is not fully consistent with the Kutzbach model of maximum winter monsoon at the June perihelion. Variation in the East Asian winter monsoon was anti-phased with the Indian summer monsoon, suggesting a linkage of dynamics between these two monsoon systems on orbital timescale.

Keywords: The East Asian winter monsoon, The South China Sea, The Western Pacific Warm Pool, Precession, Sea surface temperature



## Geochemical and molecular biological characterization of nitrogen dynamics in (had)opelagic sediments

NISHIZAWA, Manabu<sup>1\*</sup> ; HIRAI, Miho<sup>1</sup> ; NOMAKI, Hidetaka<sup>1</sup> ; YANAGAWA, Katsunori<sup>1</sup> ; MAKABE, Akiko<sup>2</sup> ; KOBAYASHI, Keisuke<sup>2</sup> ; NUNOURA, Takuro<sup>1</sup>

<sup>1</sup>JAMSTEC, <sup>2</sup>TUAT

Great progress has been made in understanding the nitrogen cycle in oceanic waters by the recent identification of ammonia-oxidizing archaea and anaerobic ammonia oxidizer (anammox), and by the following comprehensive approaches to clarify the abundance and activity of each component in the nitrogen cycle. However, nitrogen dynamics in marine sedimentary habitats is still uncertain. To further characterize nitrogen dynamics in the deep-sea sediments, we have quantified i) gene abundance of putative nitrifiers, denitrifiers and anammox, and ii) potential rate of denitrification in the hadopelagic sediment cores taken from the Ogasawara Trench (water depth of 9760m). We have also determined nitrogen and oxygen stable isotopic compositions of nitrate in the interstitial water in the hadopelagic sediments. Abundance of potential proteobacterial denitrifiers correlated with that of nitrifiers through the depth, and anammox also likely co-occurred with nitrifiers. Further, nitrate isotope compositions suggest the enrichment of  $^{18}\text{O}$  by nitrification process and co-occurrence of nitrification and denitrification in nitrate reduction zone. The data suggest that aerobic and anaerobic processes of the nitrogen cycle coupled in the nitrate reduction zone in the hadopelagic sediments.

## Niche separation of nitrifiers and anammox in deep-sea sediments.

NUNOURA, Takuro<sup>1\*</sup> ; HIRAI, Miho<sup>1</sup> ; NISHIZAWA, Manabu<sup>1</sup> ; -, Juliarni<sup>1</sup> ; NOMAKI, Hidetaka<sup>1</sup> ; SUGA, Hisami<sup>1</sup> ; TASUMI, Eiji<sup>1</sup> ; MIYAZAKI, Junichi<sup>1</sup> ; MAKABE, Akiko<sup>2</sup> ; KOBAYASHI, Keisuke<sup>2</sup> ; TAKAI, Ken<sup>1</sup>

<sup>1</sup>JAMSTEC, <sup>2</sup>TUAT

We revealed the distribution patterns of nitrifiers and anammox along with geochemical gradients in a hadopelagic sediment core from the Ogasawara Trench (Nunoura et al. 2013). The results presented novel insights into the inorganic nitrogen cycle in deep-sea sediments as shown below. 1) Thaumarchaeotes and *Nitrospina* predominates in the ammonia and nitrite-oxidizing communities, respectively. 2) The pore-water nitrate recorded isotopic signatures of nitrification. 3) Abundance of anammox was likely regulated by not only by redox potential but also by nitrite supply from ammonia oxidation. 4) Maximum abundance of denitrifier occurred at sediment surface.

The purpose of this study is to know the roles of benthic microbial inorganic nitrogen cycle in diverse deep-sea environments. In this study, we compared pore water chemistry, and abundance and composition of nitrifier and anammox populations in 6 distinct regions, and will discuss about the roles of dynamic nitrogen cycle in deep-sea benthic environments.

Keywords: nitrification, anammox

## Ecology of viruses in deep-sea hydrothermal vents

YOSHIDA, Yukari<sup>1\*</sup>

<sup>1</sup>JAMSTEC

Since the discovery of ubiquitous and highly abundant viruses in aquatic ecosystems, many studies have been conducted to discern the role of viruses within aquatic microbial communities. As a result, viruses are now recognized to be significant components of all aquatic ecosystems. It has been suggested that they affect global nutrient and biogeochemical cycles in the world's oceans, and play a role in regulating abundance and composition of microbial communities. Viruses can also mediate lateral gene transfers and drive the diversification of microbial communities and the co-evolution between viruses and hosts.

Deep-sea hydrothermal vents are sites having great microbial biomass, high productivity, and physiologically and genetically high diversity, contrasting sharply with the surrounding sparsely populated deep-sea environments. The primary production in the deep-sea vent ecosystem is sustained by chemolithoautotrophic microorganisms that utilize reduced chemical compounds from the earth interior as energy sources. To date, the biogeochemical processes, ecophysiological functions, and evolutionary significance of deep-sea vent microbial communities have been extensively studied, but the ecological and evolutionary impacts of viruses on the deep-sea vent microbial communities remain to be fully elucidated.

Here, I provide an overview of current hot research topics related to viruses in aquatic ecosystems, and then introduce our studies on the viral functions and ecology in deep-sea hydrothermal vents in addition to several previous studies on virus-host interactions.

Keywords: virus, hydrothermal vent, chemolithoautotrophs

## Iron redox cycling and subsurface offshore transport in the eastern tropical South Pacific oxygen minimum zone

KONDO, Yoshiko<sup>1\*</sup> ; MOFFETT, James W.<sup>2</sup>

<sup>1</sup>National Institute of Polar Research, <sup>2</sup>University of Southern California

Iron (Fe) is well known as an essential element involved in a number of biochemical processes in the ocean such as nitrogen metabolism. The distribution of dissolved Fe in seawater depends on the nature and magnitude of the sources and sinks, and the transport mechanisms. The thermodynamically favored oxidation state of Fe, Fe(III), is strongly hydrolyzed and its removal is mainly constrained by the formation of strong complexes with natural organic ligands such as humic substances and siderophores. These organic ligands control not only the solubility of dissolved Fe in seawater, but also the bioavailability of Fe(III) for phytoplankton. Fe(III) in seawater can be reduced to Fe(II), which is more soluble and kinetically labile, although is rapidly oxidized in the oxygenated seawater. Recent studies have suggested that dissolved Fe(II) substantially exists in surface seawater (e.g., Hansard et al., 2009), suboxic layers in oxygen minimum zones (OMZs) (e.g., Kondo and Moffett, 2013), hypoxic shelf waters and sediments (Lohan and Bruland, 2007), hydrothermal vents and shallow submarine eruption (Santana-Casiano et al., 2013). Since Fe(II) is more bioavailable than Fe(III), the existence of Fe(II) could provide a big advantage for the organisms in these environments even though it is ephemeral. These results suggest the importance to investigate chemical and redox speciations of Fe to elucidate carbon and nitrogen cycles in the ocean.

The distribution of dissolved Fe, Fe(II) and Fe(III)-binding organic ligands were investigated in the upper 1000 meters of the eastern tropical South Pacific from January to March 2010, during El Nino event. Dissolved Fe concentrations were exceedingly low in surface waters, showed minima near chlorophyll maximum, and increased below that depth. While high rates of nitrogen fixation have been inferred for this region from models, our data suggest that surface Fe is much too low to support diazotrophs. Dissolved Fe and organic Fe(III) ligands concentrations at mid-depth were elevated in the nearshore stations, where virtually all dissolved Fe(III) was bound to these ligands. Maxima in the concentration of Fe(II) were seen in the oxygen-deficient and high-nitrite layers of the OMZ. Fully 8 to 68% of dissolved Fe existed as Fe(II) in the samples collected at these depths. Dissolved Fe concentration was higher in the OMZ where Fe(II) and nitrite were present. We propose that this region, the most reducing part of the OMZ, plays an important role in subsurface, offshore Fe transport.

Keywords: iron, Fe(II), oxygen minimum zone, eastern tropical South Pacific, organic ligand

## Biogeochemical cycles on the deep-sea floor revealed by isotope labeling experiments

NOMAKI, Hidetaka<sup>1\*</sup>

<sup>1</sup>JAMSTEC

Deep-sea benthic food webs are mainly sustained by sinking aggregates of phytodetritus derived from the water column. Although the majority of organic matter is consumed before reaching the deep-sea floor, phytodetritus still transports a significant amount of fresh material from the surface ocean to the seafloor. A portion of the phytodetritus is converted to benthic biomass, and the remaining refractory organic matter not utilized by the benthic community is preserved in the sedimentary record. The activity of the benthic community is thus expected to be an important factor in controlling the quality of organic matter, and biogeochemical cycles on the deep-sea floor. We carried out some different types of *in situ* isotope labeling experiments to reveal these benthic processes. Results quantitatively demonstrated the fate of phytoplankton, bacteria, dissolved organic carbon, and dissolved inorganic carbon on the deep-sea floor.

Keywords: Sediment-water interface, Benthos, isotope tracer, Biogeochemical cycle

## Nitrogen isotopic record of chlorophylls as a tool for understanding of nitrogen dynamics in the oceanic photic zone

OGAWA, Nanako O.<sup>1\*</sup> ; YOSHIKAWA, Chisato<sup>1</sup> ; SUGA, Hisami<sup>1</sup> ; OHKOUCHI, Naohiko<sup>1</sup>

<sup>1</sup>JAMSTEC

Nitrogen isotope record of chlorophylls has a large potential as a tool for reconstructing the nitrogen cycle and its dynamics in the photic zone. In this study, we determined the nitrogen isotopic compositions of chlorophyll *a* ( $\delta^{15}\text{N}_{chl}$ ) and pheophytin *a* ( $\delta^{15}\text{N}_{Phe}$ ) as well as nitrate ( $\delta^{15}\text{N}_{NO_3}$ ) collected from two sites (S1 and K2) in the northwest Pacific as a case study. Both chlorophyll *a* and pheophytin *a* were extracted from the particulate organic matter (POM) and purified by the fraction collector of high-performance liquid chromatography. The nitrogen isotopic composition of the isolated chlorophylls was determined by our ultra-sensitive elemental analyzer / isotope ratio mass spectrometry. The estimated isotopic fractionation associated with the chlorophyll synthesis is -7.9 ‰ to -13.1 ‰, confirming the previous studies. However, the  $\delta^{15}\text{N}$  of POM is not consistent with those of chlorophylls, suggesting that the POM from both sites is a mixture of phytoplankton and other materials like detritus of zooplankton. The  $\delta^{15}\text{N}_{chl}$  value provides pure  $\delta^{15}\text{N}$  signature of phytoplankton, which is crucial for better understanding of nitrogen dynamics in the surface ocean. Chlorophylls are also buried and preserved in the sediments for long, and thus useful for the reconstruction of nitrogen cycle in the surface ocean in the geological past. In this presentation, we will summarize the evidence and discuss advantages and pitfalls of this tool for the future use in the oceanography and paleoceanography.

Keywords: nitrogen isotope, oceanic photic zone, nitrogen dynamics, photosynthetic pigments, nitrate

## Heterotrophic bacterial production and extracellular enzymatic activity in sinking particulate matter

YAMADA, Namiha<sup>1\*</sup> ; FUKUDA, Hideki<sup>2</sup> ; OGAWA, Hiroshi<sup>2</sup> ; SAITO, Hiroaki<sup>3</sup> ; SUZUMURA, Masahiro<sup>1</sup>

<sup>1</sup>AIST, <sup>2</sup>AORI, The University of Tokyo, <sup>3</sup>Fisheries Research Agency

Heterotrophic activities on sinking particulate matter (SPM) have important role for flux of SPM. To demonstrate regional differences in heterotrophic activities on SPM, we measured heterotrophic bacterial production (HBP) in seawater and SPM as well as potential extracellular enzyme activity (EEA) in SPM on a transect along 155E in the western North Pacific Ocean in the subarctic (44N), the Kuroshio Extension area (35N), and the subtropical gyre (20N).

Samples were collected from the western North Pacific Ocean during cruise KH08-2 (Leg 2) on R/V Hakuho-maru from 23 August to 16 September 2008.

Hydrographic data were provided by a shipboard CTD profiler equipped with a carousel multi-sampling system. We obtained water-column depth profiles of dissolved nutrients including nitrate, phosphate, and silicate, Chl a, bacterial cell abundance (BA), and HBP.

We deployed standard cylindrical multi-traps, with eight acrylic trap tubes mounted at each depth. The traps were set vertically on the array line at three targeted depths of 50 m, 200 m, and 500 m at 44N, and 100 m, 200 m, and 500 m at 35 and 20N. The upper deployment depths were chosen to be just under or near the bottom of the euphotic zone. The euphotic zone was defined as the depth at which photosynthetically active radiation was 1% of the value just below the surface.

Before deployment, all trap tubes except tube for HBP and EEA in SPM on each array were filled with seawater that had been collected from 4 m below the surface at each station using the ship's pump, pre-filtered through a 0.2- $\mu$ m capsule cartridge filter to minimize biological contamination, and mixed with sodium chloride to a final concentration of 4% (w/v) to create a density gradient. Trap tube at each depth was used for collecting samples for measuring HBP and EEM in SPM, and was filled with seawater filtered as described above that was collected just before deployment from the depth corresponding to the target layer of trap deployment with a 12-L Niskin bottle. The arrays were attached to a buoy and allowed to drift freely for 24 h at 44N, and 48 h at 35 and 20N.

Upon recovery, the traps were stored upright in the dark and left to settle for 1 h. After the contents had settled, the upper portion of the trap volume above the collection cup was gently drained by siphoning. During the siphoning, only about trap tube for HBP and EEA, an aliquot of the supernatant was subsampled approximately 30 cm from the top of the tube. After siphoning was complete, the upper cylinder of the trap tube was separated from the collection cup. The particle-rich water in each collection cup was pre-screened through a 500- $\mu$ m-mesh sieve to remove swimmers and then mixed to disrupt large amorphous particles. The pre-screened filtrates were used for measurements of total mass flux of SPM, particulate organic carbon (POC) and nitrogen (PON) content, and HBP and EEA (leucine aminopeptidase (LAPase),  $\alpha$ -glucosidase (BGase), lipase, and alkaline phosphatase (APase)).

Depth-integrated HBP in seawater from the surface to 500 m was comparable between the locations, whereas HBP in SPM at 44N was substantially lower than at the other sites. We found the highest POC export flux and export efficiency to bathypelagic depths, and the lowest water temperatures, at 44N. We found significant correlations between LAPase activity, BGase activity, POC flux and particulate organic nitrogen flux. LAPase activity was two orders of magnitude higher than BGase activity, with a BGase:LAPase activity ratio of 0.027. There were no significant correlations between HBP and EEA in SPM except for lipase, and lipase activity was significantly correlated with temperature. We propose that hydrographic conditions are an important factor controlling heterotrophic bacterial activity and export efficiency of organic carbon to the deep ocean, as are the sources and abundance of SPM produced in the euphotic zone via primary production.

**Keywords:** Sinking particulate matter, Sediment trap, Heterotrophic bacterial activity, Extracellular enzyme activity, western North Pacific

## Enigmas concerning sterols and their surrogates in eukaryotic cell membranes

TAKISHITA, Kiyotaka<sup>1\*</sup>; YABUKI, Akinori<sup>1</sup>; CHIKARAISHI, Yoshito<sup>1</sup>; TAKAKI, Yoshihiro<sup>1</sup>; YOSHIDA, Takao<sup>1</sup>; OHKOUCHI, Naohiko<sup>1</sup>

<sup>1</sup>Japan Agency for Marine-Earth Science and Technology

A large fraction of eukaryotes and bacteria respectively possess sterols and hopanoids, which function as potent stabilizers of cell membranes. Sterols are also associated with fluidity and permeability of eukaryotic cell membranes, and are key to fundamental eukaryotic-specific cellular processes such as phagocytosis. Several steps of *de novo* sterol biosynthesis require molecular oxygen. For example, the epoxidation of squalene is the first oxygen-dependent step in the sterol pathway; the epoxidized squalene is then cyclized to either lanosterol or cycloartenol by the enzyme oxidosqualene cyclase. In contrast, prokaryotic hopanoid biosynthesis does not require molecular oxygen as a substrate, and the squalene is directly cyclized by the enzyme squalene-hopene cyclase.

Until now, it was unclear how bacterivorous unicellular eukaryotes that are abundant in anoxic or low oxygen environments could carry out phagocytosis. These eukaryotes cannot obtain sterols from food bacteria as the latter generally lack them and sterols cannot be synthesized *de novo* in the absence of molecular oxygen. We have previously provided evidence that the molecule tetrahymanol is synthesized by some anaerobic/microaerophilic eukaryotes and possibly functions as an analogue of sterols in these organisms. Nevertheless, neither sterol, nor tetrahymanol, nor their related molecule has been found in the other anaerobic/microaerophilic eukaryotes, and so it is still enigmatic how these organisms maintain their fluid and permeable membrane system specific to eukaryotes.

One more area of confusion is regarding sterols in bivalves with chemosynthetic bacteria inhabiting areas of deep-sea hydrothermal vents and methane seeps, such as *Calyptogena* spp. and *Bathymodiolus* spp. In general, bivalves cannot synthesize sterols *de novo* and it is necessary for them to obtain these molecules from small eukaryotic prey. On the other hand, *Calyptogena* spp. and *Bathymodiolus* spp. mainly or exclusively acquire nutrients produced by their bacterial symbionts, rather than from eukaryotes rich in sterols. Nevertheless, these "chemosynthetic bivalves" contain sterols. More curiously, *Calyptogena* spp. have intermediate metabolites of phytosterols (24-methylenecycloartanol, cycloeucalenol, and obtusifoliol), while *Bathymodiolus* spp. have high amounts of cholesterol typical of animals. Little attention has been given to how chemosynthetic bivalves produce or acquire these kinds of sterols.

In my talk, I will discuss potentially controversial topics regarding sterols and their surrogates in eukaryotic cell membranes, which do not appear in biochemical and geochemical textbooks.

Keywords: eukaryotes, sterols, tetrahymanol, cell membrane



## Structural differences of humic acid isolated from estuarine sediments at several fields around Ariake Sea

IWAMOTO, Yuya<sup>1</sup> ; YAMAUCHI, Noriaki<sup>2\*</sup> ; NARAOKA, Hiroshi<sup>2</sup>

<sup>1</sup>Dept. of Earth and Planetary Sci., Grad. School of Sci., Kyushu Univ., <sup>2</sup>Dept. of Earth and Planetary Sci., Fac. of Sci., Kyushu Univ.

Material transfer and circulation of coastal areas, and the form and state of the organic matter in the estuary tidal flat area, is attracting attention at various angles from the biological importance of the river estuaries. Analysis and evaluation of the sediment material and coastal water has been carried out around the river basin. So far, we have analyzed the chemical structure of humic substance in the Chikugo River basin near or vary by region. The Ariake Sea, from the fact that environmental issues such as hypoxic water and red tide has occurred, environmental analysis have been made from various points of view in recent years. However, research of organic matter deposition simultaneous in a wide range of areas of the Ariake Sea coast is a few instances.

In this study, humic acid fraction were extracted from the surface sediment of the tidal flat areas, including rivers and estuaries tidal flats, tidal flats as well as less affected by other rivers a broad area of the northern half of the Ariake Sea. Then, the extracted humic acids were analyzed such as stable isotopic analysis and elemental composition, and regional differences were compared. And the use of humic acid as environmental indicator was evaluated from the point of some differences to the several conventional analyses of the environmental indicators at the coastal area.

Sediment samples were collected at a total of seven locations of tidal flat (estuaries at Hayatsue-gawa, Rokkaku-gawa, Hama-gawa, Kikuchi-gawa, Shira-kawa, and tidal flat at Arao and Tara) and two places of the downstream of Chikugo River from May 2011 to August 2013. Humic acid fraction were prepared according to the IHSS soil humic acid extraction method. Multiple analysis, such as the elemental analysis, stable isotope ratios, ultraviolet-visible absorption analysis (application of (A<sub>2</sub>/A<sub>4</sub>) ratio of 270nm/407nm that has been proposed by Fookan and Liebezeit (2000)) were applied to the humic acid of coastal areas.

Correlation derived from the source materials was observed between stable isotope ratio, and the atomic ratio calculated from elemental analysis, ultraviolet-visible absorption ratio and the regional differences of humic acid. Contribution of terrigenous organic matter is poor at Hama-gawa estuary Tara and Arao tidal flat. Further, trend in nitrogen isotope ratio is different from the other regions and the 2 points (Hama-gawa mouth and Tara tidal flat). Conditions such as denitrification and nitrogen sources is somewhat different in the Ariake Sea northwest side was suggested.

Keywords: Ariake Sea, estuarine, stable isotope ratio, UV, humic substance

## Origin of fluorescent dissolved organic matter in forested headwater stream during base-flow period

OBARA, Akihiro<sup>1\*</sup>; OHTE, Nobuhito<sup>1</sup>; EGUSA, Tomohiro<sup>1</sup>; TOKUCHI, Naoko<sup>2</sup>; KOBAYASHI, Keisuke<sup>3</sup>; YAMASHITA, Youhei<sup>4</sup>; SUZUKI, Masakazu<sup>1</sup>

<sup>1</sup>Graduate School of Agricultural and Life Sciences, The University of Tokyo, <sup>2</sup>Field Science Education and Research Center, Kyoto University, <sup>3</sup>Graduate School of Agriculture, Tokyo University of Agriculture and Technology, <sup>4</sup>Graduate School of Environmental Science, Hokkaido University

In this study, we focus on fluorescent dissolved organic matter (FDOM) such as humic substances (HSs) and aromatic amino acids, which constitutes the main portion of streamwater DOM. Our objective is to estimate the origin of streamwater FDOM during baseflow period, by comparing its composition with soil infiltration water, saturated groundwater and bedrock spring water.

Our study site is Inokawa watershed (watershed area 503 ha) in The University of Tokyo Chiba Forest. We collected stream water samples and bedrock spring water at 142 points in the watershed in 2009, 2010 and 2012, and also soil waters and groundwater in Fukuroyamasawa Experimental Watershed (2ha) which is one of most headwater hollows. Rainwater was collected at the weather station in the watershed. The water samples were filtered with 0.45mm membrane filters and analyzed for DOC concentration by wet-oxidation method, and Excitation-Emission Matrix (EEM) using 3D-spectrofluorometry. EEMs were compiled and further analyzed by Parallel Factor Analysis based on Murphy et al., (2013), and decomposed into five components with distinctive fluorescence spectra. Chemical characteristics of components were identified by comparing their spectral shapes with previous studies as follows: C1 as humic acid type HS-like, C2 as fulvic acid type HS-like, C3 as microbial-derived HS-like, C4 as tryptophane-like and C5 as tyrosine-like.

Groundwaters and bedrock spring waters were classified into three groups based on the ratio of three HS-like components, as C1-dominant group, C2-dominant group and C3-dominant group. Although groundwater in Fukuroyamasawa watershed belonged to C1-dominant group, and showed seasonal change in DOC concentration, the composition of HS-like components of groundwaters and bedrock spring waters in three groups were temporally relatively stable. This suggests that these groups can be used as end-members in identification of the origin of streamwater FDOM.

Ratios of three HS-like components in streamwaters fell in between groundwater groups and soil waters in about half of the samples. In other samples, however, ratios could not be explained by mixing of such hillslope end-members. FDOM of those streamwaters had higher abundance of C1 and C2, and also relatively higher DOC concentrations, suggesting that it was originated not only from soil and/or groundwater in the hillslope, but also from organic materials in the stream such as deposited litters, woody debris and/or other organic-containing sediments. As to aromatic amino acid-like components, streamwater FDOM tended to have lower C5/C4 ratio relative to hillslope waters, and often had C5 undetectable, suggesting that C5 was more labile than C4 in stream environment.

This study showed that HS in streamwater is produced not only in hillslope but also in stream itself, and in-stream produced HS can show different fluorescence spectral characteristics from hillslope-produced HS.

**Keywords:** fluorescent dissolved organic matter (FDOM), forested watershed, streamwater chemistry, excitation-emission matrix (EEM), parallel factor analysis (PARAFAC)

## Pseudopolarographic estimation of copper complexing ligands in freshwater of Lake Biwa, Japan

MARUO, Masahiro<sup>1\*</sup> ; OBATA, Hajime<sup>2</sup>

<sup>1</sup>School of Environmental Science, The University of Shiga Prefecture, <sup>2</sup>Atmosphere and Ocean Research Institute, The University of Tokyo

Pseudopolarography (Croot P. L. et al., *Mar. Chem.*, 67, 219-232 (1999), Wiramanaden C. I. E., et al., *Mar Chem.*, 110, 28-41 (2008)) is useful method to detect metal (copper) complexation that is very stable compared with that detected by other methods: AdCSV: adsorptive cathodic stripping voltammetry, ion selective electrode etc. in water. It was applied in seawater analysis especially for coastal area where large amount of organic material with high complexing capacity was detected. Also in freshwater lake, there is high potential of existence of very stable copper complexes in water, as it sometimes includes high concentration of sulfur containing compounds and concentration of competing metals such as calcium and magnesium are very low compared with those in seawater. Existence of very stable ligands was investigated using freshwater sampled in Lake Biwa, Japan.

As reference ligands, EDTA, DPTA and CDTA were used at pH 8.8 using borate buffer solution. Copper was deposited on HDME (hanging mercury drop electrode) by varying potential from -0.2 to -1.5 V, and deposition time was 420 s. After deposition, deposited copper was stripped by scanning from the deposition potential to 0 V. Peak height was plotted against deposition potential, and half wave potential was determined. By comparing the half wave potential with that of reference ligands, stability of copper complexing ligands in the sample was estimated.

Half wave potentials measured by references were -0.4 V for EDTA, -0.58V for CDTA, and -0.65 V for DTPA, respectively. By measuring water sampled at north basin of Lake Biwa, half wave potentials at -0.5 V and -1.1 V was obtained for surface water. Only single half wave potential at -0.5 V was obtained for waters at 2m and 10m depth. Existence of strong ligands that has stability close to EDTA was detected all samples tested. These ligands were also detected by AdCSV using salicylaldoxime as competing ligands. But ligand detected at half wave potential at -1.1 V is not detected or undetectable. It might suggest significance of very stable complexes in water of Lake Biwa.

Keywords: freshwater, Lake Biwa, copper, ligand, electroanalysis

## Isotopic composition of chlorophylls as a new indicator of energy flow in stream ecosystems

ISHIKAWA, Naoto F.<sup>1\*</sup> ; SUGA, Hisami<sup>1</sup> ; OGAWA, Nanako O.<sup>1</sup> ; OHKOUCHI, Naohiko<sup>1</sup>

<sup>1</sup>JAMSTEC

In most freshwater (e.g., stream) ecosystems, periphytic algae attached to a substrate (periphyton) play an important role as benthic primary producer. However, the energy flow, which is transferred from periphyton to animal consumers through trophic pathways, has not yet been adequately assessed because few studies have traced algal signatures from periphyton matrix to food webs. Here we present a new application of the isotopic composition of chlorophylls in periphyton to the tracer of *in situ* primary production. Chlorophylls can be used as a biomarker of photosynthetic autotrophs, including periphytic algae. We purified chlorophylls from periphyton matrix using a high performance liquid chromatograph (HPLC), and measured carbon and nitrogen stable isotope ratios of chlorophylls, pheophytins, the bulk of periphyton, and algal grazing specialists (e.g., *Epeorus latifolium*: mayfly larva) using an elemental analyzer coupled with an isotope ratio mass spectrometer (EA/IRMS). We will compare the results with traditional isotope maps, and discuss the potential of the isotopic composition of chlorophylls in aquatic food web studies.

Keywords: periphyton, photosynthetic pigments, biomarker, HPLC, stable isotopes

## Biodiversity indicators of trophic structure measured by stable isotope ratios

TAYASU, Ichiro<sup>1\*</sup> ; KATO, Yoshikazu<sup>1</sup> ; ISHIKAWA, Naoto F.<sup>2</sup> ; YOSHIMIZU, Chikage<sup>1</sup> ; HARAGUCHI, Takashi, F.<sup>1</sup> ; OKUDA, Noboru<sup>1</sup> ; TOKUCHI, Naoko<sup>3</sup> ; KOHMATSU, Yukihiro<sup>3</sup> ; TOGASHI, Hiroyuki<sup>4</sup> ; YOSHIMURA, Mayumi<sup>5</sup> ; OHTE, Nobuhito<sup>6</sup> ; KONDOH, Michio<sup>7</sup>

<sup>1</sup>Center for Ecological Research, Kyoto University, <sup>2</sup>Japan Agency for Marine-Earth Science and Technology, <sup>3</sup>Field Science Education and Research Center, Kyoto University, <sup>4</sup>Tohoku National Fisheries Research Institute, Fisheries Research Agency, <sup>5</sup>Kansai Research Center, Forestry and Forest Products Research Institute, <sup>6</sup>Graduate School of Agricultural and Life Sciences, The University of Tokyo, <sup>7</sup>Faculty of Science and Technology, Ryukoku University

The term "biodiversity" is considered as multi-level diversity, ranging from genetic, species, to ecosystem level. However, it is difficult to measure arbitrary level of biodiversity, therefore, biodiversity assessment at species level is often applied to an ecosystem. Biodiversity assessment at species cannot directly be related to ecosystem function, thus, a grouping method, such as functional feeding group (FFG), is often used in stream ecology.

Our project, funded by the Environment Research and Technology Development Fund (4D-1102), aimed at developing a method to evaluate functions of biodiversity in watershed ecology, especially streams. Stable isotope tools have been used to study watershed ecology, which covers researches on nutrient cycling and food web structure among forest, river, lake and coastal ecosystems. Recently, nitrogen isotope ratios of individual amino acids have been measured to estimate trophic positions of animals. However, this technique has not been applied to complex food web analysis, such as freshwater systems, which are based on both autochthonous and allochthonous productions. We have proved that this method is applicable to various freshwater food webs, including the system to which the bulk-isotope method could not be applied. Application of the method to archived biological specimen allows us to study long-term trophic changes in the ecosystem. Natural abundance of radiocarbon is another signature that separates carbon sources in freshwater ecosystems.

We suggest that a trophic structure estimated by various isotope signatures, together with estimated biomass of each taxonomic group, is an alternative index of describing biodiversity in watershed ecosystems.

Keywords: Stable isotope ratios, Food web, Trophic position

## Vertical distribution of the triple oxygen isotopic compositions of DO in oligotrophic/mesotrophic environments

TSUNOGAI, Urumu<sup>1\*</sup> ; MINAMI, Sho<sup>1</sup> ; SAKUMA, Hiroki<sup>1</sup> ; KOMATSU, Daisuke<sup>1</sup> ; NAKAGAWA, Fumiko<sup>2</sup>

<sup>1</sup>Graduate School of Environmental Studies, Nagoya University, <sup>2</sup>Faculty of Science, Hokkaido University

In order to quantify the gross production rate of dissolved oxygen molecules (DO) in hydrosphere beneath thermocline, vertical distributions of the triple oxygen isotopic compositions of DO in oligotrophic/mesotrophic lakes were determined, together with their temporal variations.

Keywords: oligotrophic lake, mesotrophic lake, dissolved oxygen, triple oxygen isotopes, vertical profile, seasonal variation

## Biogeochemistry on glaciers and icesheets ? Microbial process of glacier darkening and material cycles

TAKEUCHI, Nozomu<sup>1\*</sup>

<sup>1</sup>Chiba University

Glaciers and icesheets have been reported to shrink worldwide, probably caused by recent global warming. They are inhabited by diverse organisms, which adapted to the cold environment. Snow and ice algae grow photosynthetically on their surface and sustain heterotrophic microbes. Organic matter including their bodies and products can reduce surface albedo and accelerate melting of glaciers. Thus, shrinkage of glaciers and icesheets is not only due to climate change, but also possibly due to change of glacier ecosystems. Therefore, it is important to assess quantitatively biogeochemical process of carbon and nitrogen cycles on glaciers. In this talk, I would like to review our present knowledge on glacial ecosystems including Asian and polar glaciers and discuss possible reasons of recent darkening of the Greenland icesheet.

Keywords: glacier, Greenland, albedo, algae, microbe, carbon cycle

## How does anthropogenic nitrogen input affect the nutrient dynamics and food web structures?

OHTE, Nobuhito<sup>1\*</sup>; TOGASHI, Hiroyuki<sup>3</sup>; TOKUCHI, Naoko<sup>2</sup>; YOSHIMURA, Mayumi<sup>6</sup>; KATO, Yoshikazu<sup>7</sup>; ISHIKAWA, Naoto F.<sup>5</sup>; KONDO, Michio<sup>4</sup>; TAYASU, Ichiro<sup>7</sup>

<sup>1</sup>Graduate School of Agricultural and Life Sciences, University of Tokyo, <sup>2</sup>Tohoku National Fisheries Research Institute, Fisheries Research, <sup>3</sup>Field Science Education and Research Center, Kyoto University, <sup>4</sup>Kansai Research Center, Forestry and Forest Products Research, <sup>5</sup>Center for Ecological Research, Kyoto University, <sup>6</sup>Japan Agency for Marine-Earth Science and Technology, <sup>7</sup>Faculty of Science and Technology, Ryukoku University

In last five decades, impacts of anthropogenic nutrient inputs on river ecosystems have continuously been a major concern for the governments and residents of the catchments in Japan. Major sources of anthropogenic nitrogen (N) include leachate from forest ecosystem, surplus fertilizers and sewage. Impacts of anthropogenic N inputs on nutrient dynamics and food web structures were investigated using stable N isotope techniques in the Arida river catchment, Japan. Riverine survey utilizing 5 regular sampling points showed that  $\delta^{15}\text{N}$  of nitrate ( $\text{NO}_3^-$ ) increased from forested upstream ( $\sim 2\text{‰}$ ) to the downstream ( $\sim 7\text{‰}$ ) due to the sewage loads and fertilizer effluents from agricultural area. Correspondingly the  $\delta^{15}\text{N}$  of benthic algae and aquatic insects increased toward the downstream. This indicates that primary producers of each reach strongly relied on the local N sources and it was utilized effectively in their food web. Simulation using a GIS based mixing model considering the spatial distributions of human population density and fertilizer effluents revealed that strongest impacts of N inputs was originated from organic fertilizers applied to orchards in the middle to lower parts of catchment. Differences in  $\delta^{15}\text{N}$  between primary producers and predators were  $\sim 6\text{-}7\text{‰}$  similarly at all sampling points. Food web structural analysis using food network unfolding technique based on observed  $\delta^{15}\text{N}$  suggested that the structure of nutrient pyramid did not differ significantly along the riverine positions, while the members of species in each trophic level changed and the impact of anthropogenic N input was visible along the river.

Keywords: river ecosystem, nitrogen input, stable isotope, food web



## Aerobic methane production in oxygenated water column of a lake ecosystem

IWATA, Tomoya<sup>1\*</sup> ; KOBAYASHI, Ai<sup>1</sup> ; NAITO, Azusa<sup>1</sup> ; KOJIMA, Hisaya<sup>2</sup>

<sup>1</sup>University of Yamanashi, <sup>2</sup>Hokkaido University

Methane is a potent GHG with about twenty times the global warming potential of carbon dioxide. Globally, half of CH<sub>4</sub> emissions are linked to industry and the extraction of fossil fuels, while the remainder of emissions is related to natural sources such as wetlands, freshwaters, oceans, forests, and termites. Among such various natural sources, lake ecosystems are now recognized as the important source of atmospheric CH<sub>4</sub>, evading the 8-48 Tg CH<sub>4</sub> yr<sup>-1</sup> (6-16% of total natural CH<sub>4</sub> emissions and greater than oceanic emission)(Bastviken et al. 2004). Therefore, identifying the pathways and mechanisms of CH<sub>4</sub> production in lake ecosystems is prerequisite to predict the GHG concentrations in the atmosphere and the resultant global warming in the future of the earth.

In lake ecosystems, the majority of methane production has long been believed to occur in anoxic sediments via methanogenesis. However, we have recently found the novel pathway of methane production in aerobic environments with well-oxygenated water in oligotrophic lakes. In particular, in lakes with phosphorus-deficient conditions, dissolved CH<sub>4</sub> concentrations often exhibit a large subsurface maximum during the stratified period. Moreover, seasonal occurrence of the CH<sub>4</sub> maximum was closely related to the abundance of planktonic microbes (such as *Synechococcus*) in the oxygenated water, suggesting active methane production by microbes even in the presence of O<sub>2</sub>. Furthermore, the microcosm experiments confirmed the aerobic methane production when methylphosphonic acid (MPn) was added to the P-deficient lake water, suggesting the expression of *phn* genes encoding a carbon-phosphorus (C-P) lyase pathways for P utilization and producing methane from MPn. These findings are contradict to the conventional theory of methane production (methanogenesis in the absence of oxygen) but correspond to the recent findings on the aerobic CH<sub>4</sub> production in the North Pacific gyre (Karl et al. 2008); this study showed that marine microorganisms use MPn as a source of phosphorus when inorganic phosphate is scarce and generate CH<sub>4</sub> as a byproduct of MPn metabolism.

In this session, we will present such novel methane production pathway observed in an oligotrophic lake, central Japan. Spatial and temporal dynamics of dissolved methane and planktonic microbes, as well as the laboratory microcosm experiments show the causal relationships between aerobic microorganisms, their phosphonate metabolism, and aerobic methane production in lake ecosystems.

Keywords: Aerobic methane production, cyanobacteria, *Synechococcus*, methylphosphonic acid, P-deficient lake

## Effect of fertilizer use and N deposition on global terrestrial nitrogen cycling in 1960-2010

NISHINA, Kazuya<sup>1\*</sup> ; ITO, Akihiko<sup>1</sup> ; HANASAKI, Naota<sup>1</sup> ; MASAKI, Yoshimitsu<sup>1</sup>

<sup>1</sup>National Institute for Environmental Studies

Human activities have considerably disturbed terrestrial nitrogen cycling especially after the industrial revolution. Because Haber-Bosch techniques and fossil fuel combustions have been large sources of reactive nitrogen to the terrestrial ecosystems. The recent N loading derived from these sources on terrestrial ecosystems was estimated 2 times higher than biogenic N fixation in terrestrial ecosystems (Gruber et al., 2009). In this study, we evaluated N fertilizer and N deposition on global terrestrial N cycling using ecosystem model 'VISIT' and global datasets. For the cropland, we made spatial temporal explicit N fertilizer input data (as NH<sub>4</sub><sup>+</sup> and NO<sub>3</sub><sup>-</sup> respectively) made by FAO statistics, historical land-use dataset and global crop calendar in SAGE dataset. For N deposition, we used global grid data from Galloway et al. (2004) with simple interpolation in time-series. From the simulation results, we evaluated historical N cycling changes by land-use changes and N depositions in N cycling (e.g., N leaching, N<sub>2</sub>O, NO) at global scale.

Keywords: N fertilizer, N deposition, N<sub>2</sub>O, Land use change, N leaching

## The diversity-stability relationship in soil microbial community investigated by a diversity-manipulation experiment

USHIO, Masayuki<sup>1\*</sup>

<sup>1</sup>Center for Ecological Research, Kyoto University

How biodiversity influences the stability of ecosystem processes is the central question in environmental science, but empirical investigations on the biodiversity-stability relationship in soil microbial community is still limited. To investigate the diversity-stability relationship in soil microbial community, microbial community composition was manipulated using taxon-specific biocides, and changes of community functions (i.e., soil decomposition activities) against changes in external environmental factors (i.e., plant materials to be decomposed) imposed to the soil microbial communities were investigated in a microcosm experiment.

Distilled water, bactericide (oxytetracycline) and fungicide (cycloheximide) were added to forest soils to create communities that are intact (i.e. fungi and bacteria are coexisting), fungi dominated and bacteria dominated, respectively. For decomposition substrates, fresh leaves of eastern hemlock and sugar maple were collected from the same location as the soil collection. The leaves, whose chemical qualities differ from each other, were dried, powdered, then mixed to fixed proportions to produce the substrate quality variations. The substrates were then added to each microbial community, and soil decomposition activity (soil respiration rate and activities of acid phosphatase, *N*-acetyl-glucosamidase,  $\beta$ -*D*-glucosidase and cellbiohydase) was measured after the substrate addition.

Soil respiration rates of the bacterial and fungal communities showed highly significant change along the substrate quality variation, but those of the coexisting community changed less significantly. Dependence of the enzyme activity on the substrate quality in the coexisting community was the weakest in general. These results indicated that the decomposition activity of the coexisting community was generally more stable than those of the less-diverse communities. In addition, microbial community compositions, which were estimated by soil lipid profile, changed more flexibly along the substrate quality variation for the coexisting community. These results can be interpreted as that, for the coexisting community, substrate quality influenced the microbial composition, and in turn, the shift in the microbial composition buffered the influences of the changes of substrate quality. The results could indicate that belowground microbial diversity as well as aboveground plant biodiversity is essential for the stability of terrestrial ecosystem processes, which are driven by the interaction of production and decomposition.

Great cautions should be taken because the specificity of the taxon-specific biocides used in this study was not perfect. For example, there must be many bacteria species that could not be inactivated by the addition of the bactericide. In order to understand the diversity-stability, or diversity-function, relationship in microbial community, more sophisticated methodology to manipulate microbial community composition is required. Limitations of current methodologies as well as possible techniques for the better manipulation of microbial community composition will be discussed in this presentation.

Keywords: biocides, enzyme activity, diversity, soil microbial community, soil respiration rate, stability

## Determination of phosphorus species and bioavailability in allophanic and non-allophanic Andisols

TAKAMOTO, Akira<sup>1\*</sup> ; HASHIMOTO, Yohey<sup>1</sup> ; WAGAI, Rota<sup>2</sup>

<sup>1</sup>Tokyo University of Agriculture and Technology, <sup>2</sup>National Institute for Agro-Environmental Sciences

Andisols have high phosphorus (P) retention capacity due to abundant active aluminums (Al) and irons (Fe). Such characteristics result in a significant inhibition of plant growth in Andisols, if not properly managed. Andisols are categorized into two groups on the basis of the difference in the clay mineral compositions. One group is called as allophanic Andisols, including allophane and imogolite in the clay fraction. The other is called as non-allophanic Andisols, including Al- and Fe- humus complexes and 2:1 phyllosilicates. These soil colloids are considered a major cause of high P retention capacity of allophanic and non-allophanic Andisols. Soil P forms have been investigated using chemical extraction methods. Chemically extracted P fractions of H<sub>2</sub>O-P and NaHCO<sub>3</sub>-P are considered readily soluble P, while NaOH-P is modelately labile P associated with Al and Fe, and HCl-P is apatite-like P. However, there are no studies determining chemical species and hosting phases of P in allophanic and non-allophanic Andisols at the molecular levels. This study was conducted to characterize the species and sorption hosts of P in allophanic and non-allophanic Andisols using Hedley's sequential P extraction method, solution <sup>31</sup>P-NMR and X-ray absorption near-edge structure (XANES) spectroscopy. For revealing the behavior of P in soils precisely, it is required to separate the different soil colloids along with their density and then identify P speciation and hosting mineral phases. This study used a density separation method that can classify soil colloids including humus and Al/Fe (oxy)hydroxides by their density.

The total concentration of P in the allophanic and non-allophanic Andisols was 6.2 g P kg<sup>-1</sup>. The sequential fractionation of bulk soil showed that the largest P pool of both allophanic and non-allophanic Andisols was NaOH-P. The density fractions of 2.0-2.25, 2.25-2.5, and >2.5 g cm<sup>-3</sup> accounted for 88% of allophanic Andisols, and among five fractions, the 2.0-2.25 g cm<sup>-3</sup> fraction was largest (44%). On the other hand, the density fractions of 1.8-2.0, 2.0-2.25, 2.25-2.5, and >2.5 g cm<sup>-3</sup> accounted for 88% of non-allophanic Andisols. The sequential fractionation of allophanic Andisols showed that the NaOH fraction had a large proportion of inorganic P (Pi, 76-92%) and organic P (Po, 72-99%). The sequential fractionation of non-allophanic Andisols also showed NaOH-Pi (46-83%) and Po (54-97%) were consisted largely of phosphorus pool, with exceptions in >2.25 g cm<sup>-3</sup> fractions. The results combined with the density separations and sequential extraction indicated that i) P in allophanic and non-allophanic soils is primarily associated with Fe and Al minerals, ii) Pi and Po in the 2.0-2.25 g cm<sup>-3</sup> fraction accounted largely for the total P of allophanic Andisols (Pi: 61%, Po: 68%), iii) Pi and Po in 1.8-2.0 g cm<sup>-3</sup> fraction accounted largely for allophanic Andisols (Pi: 48%, Po: 64%). According to the solution <sup>31</sup>P-NMR results, orthophosphate monoester accounted largely for Po in allophanic and non-allophanic Andisols. Further investigations on XANES and NMR spectroscopy will be presented for more detailed P speciation in the soils.

Keywords: phosphorus, ecosystem, Andisols

## Development of a carbonized wood passive sampler for atmospheric mercury

OKUMA, Akihiro<sup>1\*</sup> ; SATAKE, Kenichi<sup>1</sup>

<sup>1</sup>Geo-environmental Sci, Rissho Univ

### [Intro]

UNEP and WHO require reduce the amount used and mercury emission because it is a toxic metal. As a result, reduce and discharge in the world but Southeast Asia and China increase coal production and used by gold mining, And so increase emission to atmosphere. Emitted mercury to atmosphere is Hg<sup>0</sup> (elemental mercury) with over 95%. It can be transported and deposited to remote place from the sources because calculated atmospheric residence time of Hg<sup>0</sup> was estimated about 1 to 2 year. Furthermore deposited Hg can be converted to organic mercury and accumulated in the food chain, posing a potential threat to human's health. As a result, it is important to monitoring atmospheric mercury pollution. The present, atmospheric mercury sampler is active sampler with gold amalgam collection glass tube, but it is difficult to sampling cover wide area for high costs and need electrical power. So we made simple passive sampler for mercury monitoring with carbonized wood and experimented.

### [Method]

Sticked a wood (*c.japonica*) to acrylic laboratory dish with double-stick tape after it had been cut to 2.5cm×4.5cm×1.5cm and carbonized at 300 °C 2h in a electric muffle furnace. We conducted Uryu Exoerimental Forest of Hokkaido University, Sapporo campus of Hokkaido University, Kumagaya campus of Rissho University, Kuniiriyama in Gunma , Kanazawa University, Tottori University, Hiroshima University and Chiang Mai University (Thailand). Moreover, we compared the active sampler at Center for Environmental Science in Saitama.

### [Result]

Mercury concentration in propose passive sampler increased as day passed at All conducted sites. Mercury concentration in part of carbonized woods were 0.39 (for 33 days), 0.44 (for 66 days), 0.63 (for 95days), 0.86 (for 127 days), 0.91 ng Hg cm<sup>-2</sup> (for 158 days), and correlation coefficient was 0.95 at Center for Environmental Science in Saitama.

Atmospheric mercury concentration range were 2.0 to 2.6 ng Hg m<sup>-3</sup> during experiment. Absorption mercury speed into carbonized wood was uniform in steady atmospheric mercury. Propose passive sampler and active sampler were correlated, slope was  $y=14.7x$ , correlation coefficient was 0.95. Propose passive sampler was agreement with the data obtained by an active sampler by these results.

Keywords: mercury, carbonized wood, passivesamplerq, monitoring of air pollution

## Mechanisms and regulating factors of dissolved organic matter production in beech forest soils in northern Kyoto

FUJII, Kazumichi<sup>1\*</sup> ; NAKADA, Yuji<sup>2</sup> ; YOSHIDA, Makoto<sup>2</sup> ; HAYAKAWA, Chie<sup>3</sup> ; SUGIHARA, Soh<sup>3</sup> ; FUNAKAWA, Shinya<sup>3</sup>

<sup>1</sup>Forestry and Forest products Research Institute, <sup>2</sup>Tokyo University of Agriculture and Technology, <sup>3</sup>Kyoto University

In forest ecosystems, most of the organic matter supplied to the organic layer mineralizes to CO<sub>2</sub>, but a proportion (~30%) is leached as dissolved organic matter (DOM), as soil water percolates. DOM plays important roles in carbon and nutrient cycling in forest soils, however, the controlling factors and mechanisms of DOM production remain to be clarified. Since DOM contains high concentrations of aromatic compounds derived mainly from lignin, the roles of microorganisms in lignin solubilization and DOM production were investigated under field condition.

The concentrations and fluxes of dissolved organic carbon (DOC) in soil solution were quantified under beech forest in northern Kyoto. The activities of lignin-degrading enzymes, lignin peroxidase (LiP) and manganese peroxidase (MnP), and fungal community composition were analyzed.

The DOC fluxes increased in the organic layer (344 kg C ha<sup>-1</sup> yr<sup>-1</sup>), followed by a decrease with depth in the mineral soil layers (20 kg C ha<sup>-1</sup> yr<sup>-1</sup>). The seasonal fluctuation of DOC concentrations showed that DOC production increased in summer with increasing temperature, highlighting the importance of microbial activity to DOM production. The activities of both lignin-degrading enzymes, MnP and LiP, were detected in the organic layers, and several potential producers of enzymes, namely basidiomycete fungi, were also identified. These findings could support the central roles of fungi in lignin solubilization and DOC production in organic layers under beech forest in northern Kyoto, where the large fluxes of DOM leaching was observed.

## Soil nitrite transformation along a forest slope and controlling factors

KUROIWA, Megumi<sup>1\*</sup> ; ISOBE, Kazuo<sup>1</sup> ; KATO, Hiroyu<sup>1</sup> ; MURABAYASHI, Sho<sup>1</sup> ; KANEKO, Yuka<sup>1</sup> ; ODA, Tomoki<sup>1</sup> ; OHTE, Nobuhito<sup>1</sup> ; OTSUKA, Shigeto<sup>1</sup> ; SENOO, Keishi<sup>1</sup>

<sup>1</sup>Graduate School of Agricultural and Life Sciences, The University of Tokyo

We conducted a tracer study to clarify the spatial heterogeneity of nitrite ( $\text{NO}_2^-$ ) dynamics in forest soils. Because of its reactive nature,  $\text{NO}_2^-$  does not usually accumulate in forest soils. This low concentration and experimental difficulties of accurate quantification have hampered quantitative detailed analyses of gross  $\text{NO}_2^-$  production and consumption in terrestrial environments. However,  $\text{NO}_2^-$  is an intermediate in many N transformation processes including nitrification and denitrification. Furthermore  $\text{NO}_2^-$  can also be reduced to gaseous N and react with organic matter not only biologically but also chemically. Thus  $\text{NO}_2^-$  dynamics may control whole N retention/emission characteristics in forest soils.

We added  $^{15}\text{NO}_2^-$  to mineral top soils derived from a slope of a Japanese cedar forest. Primary properties of soils such as concentration of inorganic N, pH and water content differed geographically; N concentration, pH and water content are lower in the upper soils.  $\text{NO}_2^-$  production and consumption rates gradually increased from upper slope to lower slope. Quite short mean residence time of  $\text{NO}_2^-$  implies that  $\text{NO}_2^-$  consumed very rapidly anywhere in slope. The dominant pathway of  $\text{NO}_2^-$  consumption change geographically. It is suggested that the conversion to DON and gaseous N is more important in upper soils. On the other hand, conversion to  $\text{NO}_3^-$  (nitrification) is dominant in lower soils.

At this presentation, we focus on geographical difference of  $\text{NO}_2^-$  dynamics and their regulation by environmental factors.

Keywords: Forest soil, Nitrite,  $^{15}\text{N}$  tracer, Dissolved organic nitrogen, Nitrification

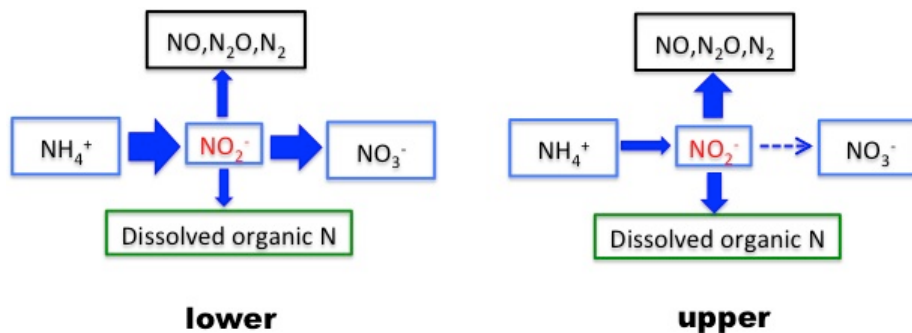


Fig.1 Schematic picture of nitrite dynamics along a forest slope.  
 Difference between upper and lower soils.

## The availability of atmospheric nitrate in a forested ecosystem

OSAKA, Ken'ichi<sup>1\*</sup> ; KOMAKI, Naoto<sup>1</sup> ; KAWAMURA, Yuya<sup>1</sup> ; MURATA, Tetsuya<sup>1</sup> ; KUGO, Tatsuro<sup>1</sup> ; NAKAMURA, Takashi<sup>2</sup> ; NISHIDA, Kei<sup>2</sup> ; NAGAFUCHI, Osamu<sup>1</sup>

<sup>1</sup>University of Siga prefecture, school of environmental science, <sup>2</sup>University of Yamanashi, ICRE

Nitrogen is an important element for forest ecosystems; shortage of nitrogen limits plant growth [Vitousek and Howarth, 1991], however, nitrogen discharged from forested ecosystems link to various environmental problems, such as eutrophication of aquatic ecosystems and deterioration of drinking water quality. Recently, atmospheric nitrogen deposition into terrestrial ecosystems is increasing [Galloway et al., 2008]. However, influence of the increase of atmospheric nitrogen deposition on forested ecosystem is not clear because the interaction between nitrogen input/output and inner nitrogen cycle is not sufficiently understood. In this study, to clarify the interaction between nitrogen input/output and inner nitrogen cycle, we investigate the atmospheric nitrate discharge rate from forested watershed and discuss the availability of atmospheric nitrate deposited into forested watersheds.

Keywords: forested watershed, stable isotope, nitrate, atmospheric deposition



## Estimation of leaf biomass and nitrogen uptake in a hinoki cypress forest

INAGAKI, Yoshiyuki<sup>1\*</sup> ; SAKAI, Atsushi<sup>1</sup> ; MIYAMOTO, Kazuki<sup>1</sup>

<sup>1</sup>Forestry and Forest Products Research Institute

Nitrogen uptake by aboveground vegetation in forest ecosystems is determined from nitrogen loss by litterfall plus nitrogen allocated to aboveground biomass increment. Nitrogen in litterfall is accurately estimated by littertrap while that in stem increment is by measurement of tree growth. In contrast, estimation of leaf biomass increment is difficult. Although there is close correlation between leaf biomass and cross-sectional area at lowest live branch in the crown, it is difficult to measure diameter at the lowest live branch. Recently, the simple method to estimate leaf biomass is developed by using tree height, height at lowest live branch and diameter at breast height. The applicability of this method depends on tree species and information about hinoki cypress is not known. In this study, we determined the equation for estimating leaf biomass by this method to hinoki cypress trees in Kochi prefecture, southern Japan. In addition the obtained equation is applied for a hinoki cypress forest where tree biomass and litterfall is measured for 20 years.

In two areas at different altitude in Kochi prefecture, 14 hinoki trees were felled and leaf biomass was measured. The relationship between leaf biomass ( $W_{\text{leaf}}$ ), and tree height ( $H$ ), height at lowest live branch ( $H_b$ ), and cross-sectional area at breast height ( $A_{1.3}$ ) was determined by following equation.

$$W_{\text{leaf}} = 1.02[0.0364AB^{1.10}] \quad (r^2 = 0.926, p < 0.0001)$$

$$AB = A_{1.3} [(H - H_b) / (H - 1.3)].$$

This equation is applied for a hinoki cypress forest in Kochi prefecture. Leaf biomass is determined at seven periods between 21 to 41 years old. Leaf production is calculated as leaf-litterfall plus increase of leaf biomass. Nitrogen uptake was calculated as sum of nitrogen in litterfall, increase of nitrogen in leaf and stem biomass. Nitrogen use efficiency of aboveground biomass was calculated as sum of leaf and stem production divided by nitrogen uptake. There was no significant correlation between forest age and leaf biomass, leaf production, stem production, nitrogen uptake and nitrogen use efficiency. However, nitrogen uptake was positively correlated with leaf biomass and leaf production. Nitrogen uptake was not correlated with stem production. These results suggest that nitrogen use of hinoki cypress does not show clear trend in relation to stand age but hinoki cypress utilize nitrogen efficiently to sustain stem production when nitrogen uptake is lower.

Keywords: hinoki cypress, leaf biomass, Stem, nitrogen, forest age

## A metabolic model of stable isotope dynamics

ISHII, Reiichiro<sup>1\*</sup> ; NOGUCHI, Maki<sup>1</sup> ; WADA, Eitaro<sup>1</sup>

<sup>1</sup>JAMSTEC

Carbon and nitrogen stable isotope analysis have been a powerful tool used for identifying food-web structures. Our recent study suggested that the ratios of trophic fractionation of carbon and nitrogen isotopes ( $\Delta\delta^{15}\text{N}/\Delta\delta^{13}\text{C}$ ) throughout food chain are similar in various ecosystems (Wada et al. 2013), although the general mechanisms determining isotopic incorporation rates and discrimination factors are poorly understood.

Here, we developed a mechanistic model of the isotopic fractionation in metabolic processes that are common to animals composing most grazing food chains. Particularly, we calculate fluxes of carbon and nitrogen stable isotopes within an organism by following fluxes of molecules involved in some of physiological reactions: the synthesis of amino acids and their carbon skeletons, the rates of which are governed by energy-producing systems such as glycolysis, the TCA cycle, and oxidative phosphorylation, that is, the ratio of the rate of amino-acid syntheses to that of energy-yielding processes. The active metabolic pathways above are assumed to be changed by the conditions of supply (diet quantity and quality) and demand (growth rate).

The model result suggests that the instant isotopic composition of animals are sensitive to the change of their diet composition and growth rate, but on the other hand, the isotopic composition converges as the integrating period becomes long. With further temporal scaling-up, in turn, the isotopic compositions of animal body reflect the spatio-temporal variability due to their life history, migration and foraging patterns. This gives mechanistic insight to what information we can acquire from the observation.

## Tracing environmental history of macroalgae by the use of radiocarbon and stable isotope ratio analyses

SATO, Naomi<sup>1\*</sup> ; FUKUDA, Hideki<sup>1</sup> ; MIYAIRI, Yosuke<sup>1</sup> ; YOKOYAMA, Yusuke<sup>1</sup> ; NAGATA, Toshi<sup>1</sup>

<sup>1</sup>Atmosphere and Ocean Research Institute, the University of Tokyo

In the bays located along the Sanriku coastal area (northeast Japan), where the Kuroshio and Oyashio mix in a complex manner, environmental conditions (e.g. water temperature, irradiation and nutrients) may largely change depending on which current predominantly enters into the bays. Changes in environmental conditions, in turn, may exert a large influence on growth of and interactions between organisms residing there. However, knowledge is limited regarding relationships between shifts in hydrographic conditions and physiological responses of organisms to environmental variability. The purpose of this presentation is to report our attempt to trace environmental history of individual macroalgae (wakame, *Undaria pinnatifida*), a widespread benthic primary producer and an important aquaculture product in the Sanriku area, by a combined use of radiocarbon and stable isotope ratio analyses. The key concept was to use distinct <sup>14</sup>C abundance between the two water currents, i.e., <sup>14</sup>C abundance of dissolved inorganic carbon in the Oyashio water is lower than that in Kuroshio water due to upwelling of old deep water. We assumed that <sup>14</sup>C abundance profile of pinnate blades of macroalgae (blades near the top are older than those near the bottom) reflects a temporal change in dissolved inorganic carbon <sup>14</sup>C (hence, shift in water current) via photosynthetic fixation. We also analyzed carbon and nitrogen stable isotope ratios ( $\delta^{13}\text{C}$  and  $\delta^{15}\text{N}$ ) of the blades to gain insights into changes in physiological state of the macroalgae during their growth.

We collected sporophytes of *U. pinnatifida* cultured between October 2012 and March 2013 at two stations (one located near the bay center and the other located near the river mouth) in Otsuchi Bay. One individual (length, ca. 190 cm) was collected at each station. For each individual, a tip of each pinnate blade was cut, treated with HCl, reduced to graphite, and served for determination of radiocarbon composition ( $\Delta^{14}\text{C}$ ) profile using an accelerator mass spectrometer.  $\delta^{13}\text{C}$  and  $\delta^{15}\text{N}$  of the corresponding samples were also measured using a stable isotope ratio mass spectrometer.

$\Delta^{14}\text{C}$  of pinnate blades of the saprophyte collected near the bay center varied between 0 and 40 permil.  $\Delta^{14}\text{C}$  values were high for the blades located at the upper and lower parts of the macroalgae, whereas they were low for the blades situated at the middle part. These results indicate that the sporophyte experienced the intrusion of the Oyashio water during the period of the development of the middle blade. Similar to the pattern in  $\Delta^{14}\text{C}$ ,  $\delta^{13}\text{C}$  and  $\delta^{15}\text{N}$  values were also lowest at the middle part, although the position of the minimum was skewed toward bottom relative to the position of the  $\Delta^{14}\text{C}$  minimum. There was a significant positive correlation between  $\delta^{13}\text{C}$  and  $\delta^{15}\text{N}$ , suggesting that the variation in stable isotope ratios reflected macroalgal physiological responses and associated shifts in isotope fractionation. Collectively, these results were interpreted as an indication that the physiological state of the saprophyte was altered with a time lag after the intrusion of the Oyashio water into the bay. In contrast,  $\Delta^{14}\text{C}$  profile of pinnate blade was complex for a saprophyte collected near the river mouth. For this individual, there was no clear pattern in distribution of  $\delta^{13}\text{C}$  and  $\delta^{15}\text{N}$  among blades. Complex variations in isotopic compositions for this individual might be ascribed to the influence of inflow river water.

Keywords: macroalgae, Sanriku coast, water current, radiocarbon, stable isotope

## Accumulation of humic-like fluorescent dissolved organic matter in the Japan Sea interior

TANAKA, Kazuki<sup>1</sup> ; KUMA, Kenshi<sup>2</sup> ; HAMASAKI, Koji<sup>3</sup> ; YAMASHITA, Youhei<sup>4\*</sup>

<sup>1</sup>Graduate School of Environmental Science, Hokkaido University, <sup>2</sup>Faculty of Fisheries Science, Hokkaido University, <sup>3</sup>Atmosphere and Ocean Research Institute, The University of Tokyo, <sup>4</sup>Faculty of Environmental Earth Science, Hokkaido University

Marine dissolved organic matter (DOM) is the largest reduced carbon reservoir in ocean. Most marine DOM is produced by marine biota and is resistant to rapid microbial degradation. Thus, it is crucial to know the dynamics of recalcitrant DOM for determining whether the marine DOM reservoir is stable or not. Even though there have been several hypotheses regarding with the recalcitrant mechanism of marine DOM, the microbial production of recalcitrant DOM (defined as microbial carbon pump) has been considered as the main process. Humic-like fluorescent DOM (FDOM<sub>H</sub>) has found to produce during microbial incubation. Even though FDOM<sub>H</sub> has known to easily degrade by sunlight, linear relationships between fluorescence intensity of FDOM<sub>H</sub> and indicators of microbial remineralization, e.g., apparent oxygen utilization (AOU), have been observed throughout the ocean. These experimental and observational results imply that FDOM<sub>H</sub> is a product of microbial carbon pump. Another important source of FDOM<sub>H</sub>, especially in coastal environments and marginal seas, is riverine supply. Even though the major fractions of FDOM<sub>H</sub> have been considered to be photo-degraded in coastal environments, substantial contribution of terrestrial FDOM<sub>H</sub> into ocean interior has been suggested. Thus, in addition to accumulation of in situ produced FDOM<sub>H</sub>, recalcitrant terrestrial FDOM<sub>H</sub> might occur in deep ocean, especially in marginal seas. However, it is not clear whether recalcitrant autochthonous and/or terrestrial FDOM<sub>H</sub> is accumulated in deep ocean of marginal seas or not.

We determined vertical profiles of FDOM<sub>H</sub> at 5 stations in the Japan Sea and 5 stations in the western North Pacific using excitation emission matrix fluorescence with parallel factor analysis (EEM-PARAFAC). Seawater samples from surface to bottom waters of the Japan Sea and the western North Pacific were collected during T/S Oshoro-maru (C184) and R/V Taisei-Marui (KT-11-17) cruises, respectively. Two FDOM<sub>H</sub> were obtained after EEM-PARAFAC and assigned as traditional terrestrial and marine (microbial) FDOM<sub>H</sub>, respectively. In the Japan Sea, levels of both FDOM<sub>H</sub> were lowest in surface waters, gradually increased with depth below surface waters, and were highest in waters distributed depths greater than 2000 m that were corresponding to the lower part of Japan Sea Proper Water (JSPW), i.e., lower part of the Japan Sea Deep Water (JSDW) and the Japan Sea Bottom Water (JSBW). Levels of both FDOM<sub>H</sub> were linearly correlated with AOU in the JSPW, suggesting that both FDOM<sub>H</sub> were produced in situ in the JSPW. Interestingly, levels of both FDOM<sub>H</sub> in the JSPW were similar or slightly higher compared with those in deep waters of the western North Pacific, even though AOU in the JSPW were significantly lower than those in deep waters of the western North Pacific. Such distributional characteristics of FDOM<sub>H</sub> in the JSPW imply that FDOM<sub>H</sub> is accumulated in the interior of the Japan Sea. We will discuss possible origin and accumulation mechanism of FDOM<sub>H</sub> in the Japan Sea interior.

Keywords: Japan Sea, Dissolved Organic Matter, Humic-like fluorescence

## Sources of hydroxyl radical photochemically produced in headwater streams from nitrogen-saturated forest

CHIWA, Masaaki<sup>1\*</sup>; HIGASHI, Naoko<sup>1</sup>; OTSUKI, Kyoichi<sup>1</sup>; KODAMA, Hiroki<sup>2</sup>; MIYAJIMA, Tohru<sup>2</sup>; TAKEDA, Kazuhiko<sup>3</sup>; SAKUGAWA, Hiroshi<sup>3</sup>

<sup>1</sup>Kyushu University Forest, <sup>2</sup>Graduate School of Science and Engineering, Saga University, <sup>3</sup>Graduate School of Biosphere Science, Hiroshima University

Hydroxyl radical ( $\cdot\text{OH}$ ) is the most oxidative reactant among the active oxygen species and oxidation reactions with  $\cdot\text{OH}$  are involved in important biogeochemical processes. In this study  $\cdot\text{OH}$  photoformation rate ( $R_{\text{OH}}$ ) was determined in headwater stream samples from nitrogen (N)-saturated forests, 1) to quantify the sources of  $\cdot\text{OH}$  in headwater streams and 2) to evaluate the nitrate ( $\text{NO}_3^-$ )-induced enhancement of  $\cdot\text{OH}$  formation in stream water caused by N saturation in forested watersheds. Stream water fulvic acid extracted from the forested watersheds was used to quantify the contribution of dissolved organic matter (DOM) to  $R_{\text{OH}}$ . The results showed that almost all (97%; 81-109%)  $R_{\text{OH}}$  sources in our headwater stream samples were quantitatively elucidated; the photolysis of  $\text{NO}_3^-$  (55%; 34-75%), nitrite [N(III)] (2%; 0.5-5.2%), and DOM-derived  $\cdot\text{OH}$  formation, from which photo-Fenton reactions (18%; 12-26%) and the direct photolysis of fluorescent dissolved organic matter (FDOM) (22%; 10-40%), was successfully separated. FDOM, which accounted for 53% (24-96%) of DOM in total organic carbon bases, was responsible for  $\cdot\text{OH}$  formation in our headwater streams. High  $\text{NO}_3^-$  leaching caused by N saturation in forested watersheds increased  $R_{\text{OH}}$  in the headwaters, indicating that N-saturated forest could significantly change photoinduced and biogeochemical processes via enhanced  $\cdot\text{OH}$  formation in downstream water.

Keywords: hydroxyl radical, dissolved organic matter, nitrate, photo-Fenton reaction, stream, photoinduced processes

## Effects of clear-cutting on the loss of ion and DOC from cool-temperate forested watershed in northern Japan

FUKUZAWA, Karibu<sup>1\*</sup> ; SHIBATA, Hideaki<sup>1</sup> ; TAKAGI, Kentaro<sup>1</sup> ; NOMURA, Mutsumi<sup>1</sup>

<sup>1</sup>FSC, Hokkaido University

Nitrate and dissolved organic carbon (DOC) concentrations in stream water before and after clear-cutting of trees and subsequent strip-cutting of understory vegetation, dwarf bamboo (*Sasa* spp.) were investigated to understand the effect of these disturbances on biogeochemical processes in forested watershed in Teshio Experimental Forest in northern Japan. Trees of 8 ha watershed except riparian zone were clear-cut in January-March of 2003. *Sasa* was strip-cut in October of 2003 and larch seedlings were planted on the cut line immediately after the *Sasa* cutting. Stream water was sampled every two or three weeks from 2002 to 2013. Tree-cutting did not cause a significant increase of nitrate concentration in stream water during the growing season after the cutting. Subsequent *Sasa*-cutting caused significant increase of stream nitrate concentration to ca. 15 micro mol L<sup>-1</sup>. At the cut site, it has been reported that *Sasa* compensated the decrease in tree fine root biomass. Thus, we suggest that nitrogen uptake by *Sasa* was very important in mitigating nitrogen leaching after tree-cutting, and the decline of this nitrogen uptake after *Sasa*-cutting lead to marked nitrate leaching to the stream. However, after that stream nitrate concentration fluctuated in the range of <0.1 to >20 micro mol L<sup>-1</sup> depending on date and year, and was especially high in 2007 throughout the year. It did not get back to pre-cutting level. Cation (K<sup>+</sup>, Na<sup>+</sup>, Ca<sup>2+</sup>, Mg<sup>2+</sup>) concentration and pH fluctuated much depending on the flow rate and changes by both cutting were not observed. On the other hand, ammonium was detected in 2007 and synchronized with increase in nitrate concentration. DOC concentration in stream water was not changed after both cuttings of tree and *Sasa* and had clear seasonal pattern that peaked in late summer. Stream DOC concentration increased in growing period with low runoff from late May to August and then decreased after runoff increased in fall, indicating that dilution by the runoff reduce stream DOC concentration after late summer. However, DOC concentration remained low during winter when runoff was stably low, suggesting that high temperature also promote DOC production in soil during the early summer. DOC loss from ecosystem was not influenced by the cutting of trees and *Sasa* in this watershed owing to the adsorption to the soil at the cut area. These results indicate the response to cutting is different between NO<sub>3</sub><sup>-</sup> and DOC due to the different source area of these solutes in the watershed with cool climate and the gentle basin topography.

Keywords: nitrate, DOC, cation, *Sasa*, stream discharge

## Microbial contributions to biochemical commonalities of decaying organic matter

HOBARA, Satoru<sup>1\*</sup> ; AE, Noriharu<sup>1</sup> ; HASEGAWA, Yuki<sup>1</sup> ; OGAWA, Hiroshi<sup>2</sup> ; SATOU, Takayuki<sup>3</sup> ; IMAI, Akio<sup>3</sup> ; BENER, Ronald<sup>4</sup>

<sup>1</sup>Rakuno Gakuen University, <sup>2</sup>The University of Tokyo, <sup>3</sup>National Institute for Environmental Studies, <sup>4</sup>The University of South Carolina

Natural organic matters including dead organisms are decayed (decomposed) under various environmental conditions, but some parts of them, residues, remain for long time. Organic matter residues are major components of organic matter in soil and marine ecosystems, and play important functions and roles. The residues are originated from various organisms, organs, and cellular components, and in various stages of organic matter decay. Recently, it has been suggested that organic matter produced by microorganisms increase its percentage in residues during decay process. However, researches are limited especially on the quality of the produced organic matter and its producing processes. In this research, we investigate biochemical differences between original organic matters and organic residues and biochemical changes of organic matter during decaying process to clarify microbial contributions to the organic matter residues. Biochemical molecular compositions of original organic matters was more variable than those of organic residues in soil and water: for example, glycine:lysine (Gly/Lys) ratio and glucosamine:galactosamine (GlcN/GalN) ratio of original organic matters varies widely with origins, while those of decayed residues indicates considerably narrower ranges for both ratios. An incubation test, litterbag experiment, in a terrestrial ecosystem showed a clear trend that Gly/Lys ratio increased and GlcN/GalN ratio decreased during decay for all three species litter. These changes were also observed for litterbag experiments conducted in water, suggesting that it might be uniformly-observed biochemical directivity for decaying organic matter. In addition, amino acids and amino sugars are biomolecules, which increase during decaying processes, suggesting that this directivity results from microbial products. Another biochemical directivity was observed for molecular weight distribution of decaying organic matters, suggesting that organic residues derived from microbial products contribute to biochemical directivities and commonalities of decaying organic matter in various environmental conditions.

Keywords: Organic matter decay, Soil, Ocean, Amino acids, Amino sugars, Molecular weight distribution

## Spatial modelling of water, nitrogen and sediment for systematic conservation of multiple ecosystem services

FAN, Min<sup>1\*</sup> ; SHIBATA, Hideaki<sup>2</sup>

<sup>1</sup>Graduate School of Environmental Science, Hokkaido University, <sup>2</sup>Field Science Center for Northern Biosphere, Hokkaido University

Spatial modelling and analysis of multiple ecosystem service (ES) under land use and climate changes provides useful support for decision making in sustainable planning, management and policies of large landscapes. This study aimed to integrate the GIS modelling approach of spatial explicit ESs (water yield, and retention of nitrogen (N) and sediment) into system conservation model under various land use and climate changes in Teshio river watershed located in northern Hokkaido, Japan. In this study, we applied hydrology and material flow model (Soil and Water Assessment Tools, SWAT model), land use change model (CLUED) and system conservation model (Marxan). The multiple scenario includes three different land use maps in past (1976), current (2006) and future (2036), and three climate change scenarios (short-term (2010-2039), mid-term (2040-2069), and long-term (2070-2099)).

Our results indicated that various land use and climate change scenarios showed different impact on ES and system conservation in the watershed. The forest land use change significantly affected on magnitudes and spatial patterns in water yield, sediment and N retention. It was suggested that south western and northern part of the studied watershed should be conserved to match the given conservation targets of multiple ESs (0.3 and 0.5 of maximum ES values). The protection area to satisfy each ES conservation target increased with increase of differences between each ES and maximum ES values under land use and climate changes. Our results indicated that the land distribution and area of optimal ES protection for multiple ESs were totally different from those for single ES. The conservation area for multiple ESs was more compact than those for single ES. The proposed approach in this study provided useful information to assess the responses of ESs and system conservation under the land use and climate changes. The system conservation area of ES protection for multiple ESs provided an effective trade-off tool between environmental protection and agriculture expansion.

Keywords: Ecosystem services, SWAT, Marxan, Land use and climate change



## Spatial variability of mineralization and nitrification in soil nitrogen along the hillslope in Japanese cedar forest

KATO, Hiroyu<sup>1\*</sup> ; OHTE, Nobuhito<sup>1</sup> ; ISOBE, Kazuo<sup>1</sup> ; ODA, Tomoki<sup>1</sup> ; MURABAYASHI, Sho<sup>2</sup> ; URAKAWA, Rieko<sup>1</sup> ; SENOO, Keishi<sup>1</sup>

<sup>1</sup>University of Tokyo, graduate school of agricultural and life sciences, <sup>2</sup>University of Tokyo, faculty of agriculture

**Introduction** Precise understandings of mechanism of nitrogen (N) cycle is one of the most important subjects for ecosystem conservation in forests and rivers. Especially, the responses of N mineralization and nitrification to environmental changes are especially important due to their role in entire N cycling. Previous studies suggest that nitrification and mineralization have spatial variation in forest, which are controlled by the geophysical condition such as topography and water condition. The aim of this study is to clarify the mechanisms behind the spatial variety of nitrification and mineralization rate in soil along the hillslope.

**Methods** The field observations and soil samplings were conducted at Fukuroyamasawa Experimental Watershed (Catchment Area 0.8ha) which belongs to the University of Tokyo, Chiba forest. Dominant vegetation on the slope consisted of *Cryptomeria japonica* plantation. Along the hillslope (entire length: 110m), soil samples were collected at organic layer (O-layer) and mineral layer (0-10cm) at 10m intervals. After measuring water content and pH, the  $\text{NO}_3^-$  and  $\text{NH}_4^+$  concentration of soil extract (by 2M KCl solution) were measured. The net mineralization and nitrification rate were measured by laboratory incubations (28 days). Then, the gross mineralization and nitrification rate were determined using the  $^{15}\text{N}$  pool-dilution method.

**Results** Soil moisture content was higher at the down slope part. Similarly, the pH value was higher at down slope part. The pool size of  $\text{NO}_3^-$  was significantly low at the up slope part, and gradually increased along the slope toward the lower portion. On the other hand, the pool size of  $\text{NH}_4^+$  did not have visible pattern along the slope. Moreover, there was not significant spatial variations in net and gross mineralization rate over the hillslope while net and gross nitrification had significant spatial pattern with higher rate at the down slope part.

**Discussion** Difference in the spatial patterns of mineralization and nitrification suggested that nitrification is more sensitive to the geophysical conditions such as the soil moisture content. We are attempting to explain the mechanisms of these spatial patterns from the spatial distributions of related microbial communities in the next step of this study

## Nitrogen mineralization rates in forest soils in the Japanese archipelago measured by field incubation

URAKAWA, Rieko<sup>1\*</sup> ; OHTE, Nobuhito<sup>1</sup> ; SHIBATA, Hideaki<sup>2</sup> ; ODA, Tomoki<sup>1</sup> ; WATANABE, Tsunehiro<sup>2</sup> ; FUKUZAWA, Karibu<sup>2</sup> ; INAGAKI, Yoshiyuki<sup>3</sup> ; TATENO, Ryunosuke<sup>4</sup> ; OYANAGI, Nobuhiro<sup>5</sup> ; HATTORI, Daichi<sup>6</sup> ; NAKATA, Makoto<sup>6</sup> ; HISHI, Takuo<sup>7</sup> ; FUKUSHIMA, Keitaro<sup>4</sup> ; NAKANISHI, Asami<sup>4</sup> ; TODA, Hiroto<sup>8</sup>

<sup>1</sup>Graduate School of Agricultural and Life Sciences, University of Tokyo, <sup>2</sup>Field Science Center for Northern Biosphere, Hokkaido University, <sup>3</sup>Forestry and Forest Products Research Institute, <sup>4</sup>Field Science Education and Research Center, Kyoto University, <sup>5</sup>Environmental Science Research Niigata, <sup>6</sup>Graduate School of Science and Technology, Niigata University, <sup>7</sup>Graduate School of Agriculture, Kyushu University, <sup>8</sup>Graduate School of Agriculture, Tokyo University of Agriculture and Technology

### 1. Introduction

To predict the effect of climate change on nitrogen dynamics in the forest ecosystem, it is necessary to investigate nitrogen mineralization and nitrification at various locations allowing for modeling of nitrogen dynamics in soils. In this study, we selected 20 sites from the Japanese archipelago and conducted field incubation for measuring net nitrogen mineralization and nitrification. We also considered whether parameters obtained from laboratory incubation were applicable in the field by comparing the ratios between field and laboratory incubations (Urakawa et al., 2013).

### 2. Method

We conducted buried bag method to investigate field net nitrogen mineralization and nitrification rate. In autumn 2012, we established an experimental plot (20 \*20 m) at each site, and at each plot, five soil sampling locations were established. At each sampling location, mineral soil samples were collected from 0-10, 10-30, 30-50 cm depths. Soil samples were sieved (4 mm mesh) to remove roots and gravel, and composited soils from five plots into one sample at each depth. After collecting soils for the initial extraction, buried bags were made and buried in the plots again. We collected them in spring, summer, and autumn 2013, and measured net nitrogen mineralization and nitrification for three seasons (autumn 2012 - spring 2013, spring - summer, summer - autumn). Soil samples were extracted with 2M-KCl solution (1:10) and concentrations of ammonium nitrogen and nitrate nitrogen were measured by colorimetric method. Net nitrogen mineralization and nitrification amount of each season were summed to evaluate the annual amount.

Simultaneously with the field incubation, inorganic nitrogen leaching was investigated by resin column method. Resin columns containing ion exchange resin was installed at depths of 0 and 50 cm. Inorganic nitrogen absorbed by ion exchange resin was extracted with 1M-KCl and concentration of inorganic nitrogen was analyzed by colorimetric method.

### 3. Results and Discussion

Annual net nitrification in 0-50 cm layer ranged widely from 40 to 140 kgN ha<sup>-1</sup> y<sup>-1</sup>. Nitrification amount in 10-50 cm layer was comparable to that in surface soil layer (0-10 cm) due to large bulk density and thickness, while nitrification in 0-10 cm layer accounted for about a half of that of all soil layers.

There was a significant positive correlation between nitrification measured by field and laboratory incubation. This suggests that estimation of field nitrification using parameters obtained from laboratory incubation is possible.

### 4. Reference

Urakawa et al. (2013) Characteristics of nitrogen mineralization rates and controlling factors in forest soils in Japanese archipelago, 2013 AGU Fall Meeting, San Francisco, 9-13 December 2013

Keywords: forest soil, nitrogen mineralization, nitrification, field incubation, nitrogen leaching, ion exchange resin

## Analysis of transportation and consumption processes of atmospheric nitrate in forested watershed by using oxygen isotop

KUGO, Tatsuro<sup>1\*</sup> ; OSAKA, Ken'ichi<sup>1</sup> ; NAKAMURA, Takashi<sup>2</sup> ; II, Yumi<sup>1</sup> ; IWAI, Misako<sup>1</sup> ; NISHIDA, Kei<sup>2</sup> ; NAGAFUCHI, Osamu<sup>1</sup>

<sup>1</sup>University of Shiga Prefecture, <sup>2</sup>ICRE University of Yamanashi

Some studies reported that atmospheric nitrogen deposition into terrestrial ecosystem has recently increased due to increase of anthropogenic emission of nitrogen compound into atmosphere. However, dynamics of atmospheric nitrogen deposition in forested watersheds is not clearly understood. Moreover, that leads our poor understanding of influence of increasing atmospheric nitrogen deposition on nitrogen cycle in forested ecosystem and nitrogen discharge from forested ecosystem. The purpose of this study is to clarify the mechanisms of transportation and consumption of atmospheric nitrate deposition in forested ecosystems. We collected rainfall, throughfall, surface water, soilwater (10cm, 30cm), groundwater, spring water and streamwater at a forested watershed planted with Japanese cypress in central Japan at biweekly. Samples were analyzed for total nitrogen, dissolved nitrogen, nitrate, ammonium, nitrite, and oxygen isotope of nitrate. Isotope analysis was conducted at ICRE in University of Yamanashi. We also collected soil at several month intervals, and measured nitrate, ammonium in soil and net mineralization rate, and net nitrification rate. We are planning to present transportation rate of nitrogen compounds and atmospheric nitrate through the forested watersheds and discuss the interaction between nitrogen cycle and atmospheric nitrate deposition in forested ecosystem.

Keywords: oxygen isotope of nitrate, transportation and consumption processes of nitrogen, forested watershed

## The effect of soil freeze-thaw on nitrogen transformation though the root litter changes

HOSOKAWA, Nanae<sup>1\*</sup> ; WATANABE, Tsunehiro<sup>2</sup> ; FUKUZAWA, Karibu<sup>2</sup> ; TATENO, Ryunosuke<sup>3</sup> ; SHIBATA, Hideaki<sup>2</sup>

<sup>1</sup>Graduate School of Environmental Science, Hokkaido University, <sup>2</sup>Field Science Center for Northern Biosphere, Hokkaido University, <sup>3</sup>Field Science Education and Research Center, Kyoto University

Soil freeze-thaw cycles are considered to alter soil nitrogen (N) cycle through physical disturbances of soil, changes in root litter quality, inhibition of microbial N immobilization and others. However, these mechanisms have not been well elucidated yet. Plant litter is important substrate for N mineralization by soil microbes. It has been reported that root litter mass is quantitatively comparable to those of leaf litter in various forest ecosystems. Previous studies suggested that physical disruption of root litter by freeze-thaw cycle in winter affect soil N dynamics through the change in substrate availability. In this study we aimed to clarify that effect of root litter on the rates of soil N mineralization and nitrification under various conditions of soil freeze-thaw.

This study was conducted at Shibeche experimental forest, Kyoto University located in Eastern Hokkaido, Japan. The study site is dominated by Natural oak (*Quercus crispula*) with dense dwarf bamboo (*Sasa niponica*) as understory vegetation. Soil is Humic Andosol. In July 2013, we collected 0-10cm mineral soil and fine root (<2mm) of oak in the 2500 cm<sup>2</sup> square plot. The collected soil was sieved to 2mm to remove coarse gravel and coarse organic matter. Fine roots for incubations were separated manually from the organic matter. The fine roots were added to 25g soil as 0, 5 and 15 mg g soil<sup>-1</sup>, respectively. The soil were exposed to three different freeze-thaw treatments: +5 °C ~-5 °C, -5 °C ~0 °C, -5 °C constant and +5 °C constant for 7days in low temperature incubator. After these freeze-thaw treatments, the soil were incubated at +5 °C for 2 days. For the samples exposed at +5 °C ~-5 °C and -5 °C constant were also incubated at +5 °C for 7 days and at +10 °C for 2 and 7 days. Each treatment had four replications. Soils were extracted using potassium chloride (KCl) before and after incubations, and were measured for ammonium (NH<sub>4</sub>) and nitrate (NO<sub>3</sub>) concentrations in the extracts. Net production rates of NH<sub>4</sub> and NO<sub>3</sub> were calculated as differences of NH<sub>4</sub> and NO<sub>3</sub> contents in soil between before and after the incubations. After the freeze-thaw treatment, roots were extracted using distilled water, and were measured for dissolved organic nitrogen (DON) in the extracts.

Root litter addition significantly increased the net NH<sub>4</sub> production incubated at 5 °C for 2 days after all freeze-thaw treatments (15 mg added >0mg added) with maximum at -5 °C ~0 °C treatment followed by -5 °C constant treatment. However, these effect were not observed in higher incubation temperature (10 °C) and longer incubation period (7days), rather dominated by N immobilization in those treatments. Similarly, the root litter additions significantly increased the net NO<sub>3</sub> production rate (nitrification rate) incubated at 5 °C for 2 days after all freeze-thaw treatments (15 mg added >0mg added) with maximum at +5 °C ~-5 °C treatment. However, these effect were not observed in higher incubation temperature (10 °C) and longer incubation period (7days) as same as the effects to the NH<sub>4</sub> production. The DON supply by water extraction from root litter tended to be large at -5 °C ~0 °C treatment.

These results indicated that increases of soil freeze-thaw cycles with root litter addition increased the net NH<sub>4</sub> production and nitrification. It was suggested that DON supply from root litter by soil freeze-thaw cycle related to these impacts. These effect seems to be remarkable in shorter period (2 days) and lower temperature (5 °C incubation). Furthermore, net NH<sub>4</sub> production, the sum of net NH<sub>4</sub>+NO<sub>3</sub> productions and DON supply from root rate were higher at -5 °C ~0 °C treatment than those at +5 °C ~-5 °C treatments, implying that magnitude (temperature ranges) of freeze-thaw cycle was not simple explain variables to impact of freeze-thaw on the microbial NH<sub>4</sub> production and nitrification activities.

## Estimation of trace gas fluxes in the forest of Mount Fuji using the multi layer model

NIJIMA, Kohei<sup>1\*</sup>; HIDA, Yuki<sup>1</sup>; WADA, Ryuichi<sup>1</sup>; MOCHIZUKI, Tomoki<sup>2</sup>; TANI, Akira<sup>2</sup>; NAKAI, Yuichiro<sup>3</sup>; TAKANASHI, Satoru<sup>3</sup>; NAKANO, Takashi<sup>4</sup>; TAKAHASHI, Yoshiyuki<sup>5</sup>; MIYAZAKI, Yuzo<sup>6</sup>; UEYAMA, Masahito<sup>7</sup>

<sup>1</sup>Teikyo University of Science, <sup>2</sup>University of Shizuoka, <sup>3</sup>FFPRI, <sup>4</sup>Yamanashi Institute of Environmental Science, <sup>5</sup>National Institute for Environmental Studies, <sup>6</sup>Hokkaido University, <sup>7</sup>Osaka Prefecture University

We measured vertical profiles of nitrogen oxide, NO, nitrogen dioxides, NO<sub>2</sub>, ozone, O<sub>3</sub>, and VOC in the atmosphere in Fujiyoshida and Hokuroku forest observation sites at the foot of Mt. Fuji in summer 2012. The concentration of ozone increased gradually with the height, but the concentrations of NO and NO<sub>2</sub> did not changed obviously. VOCs showed characteristic vertical profiles. We calculated O<sub>3</sub> fluxes at parts of in and under the canopy, and around the surface layer as  $-2.6 \pm 3.2 \text{ nmol m}^{-2} \text{ s}^{-1}$ ,  $0.2 \pm 2.9 \text{ nmol m}^{-2} \text{ s}^{-1}$ ,  $-8.7 \pm 5.2 \text{ nmol m}^{-2} \text{ s}^{-1}$ , respectively.

Keywords: forest, atmosphere, nitrogen oxides, ozone, VOC, vertical profile

## Localization of delta-34S value distribution in tree ring of Japanese cedar and evaluation on the S deposition history

ISHIDA, Takuya<sup>1\*</sup> ; TAKENAKA, Chisato<sup>1</sup> ; TAYASU, Ichiro<sup>2</sup>

<sup>1</sup>Nagoya univ., <sup>2</sup>Kyoto univ.

Anthropogenic sulfur emissions have been changed with human activities and affected sulfur dynamics in terrestrial ecosystems. Therefore, the information on sulfur deposition change should be important for understanding of the effects of anthropogenic sulfur on its dynamics. The stable sulfur isotope ratios ( $\delta^{34}\text{S}$ ) in tree rings are a useful archive for the history of sulfur deposition (Kawamura et al. 2006), since the  $\delta^{34}\text{S}$  of various origins have specific values and there is few isotopic fractionation through absorption of sulfur by plant. However, only few studies have been conducted about the  $\delta^{34}\text{S}$  in tree ring, and factors affecting the  $\delta^{34}\text{S}$  in tree ring have not been understood.

The aim of this study is to clarify the localization of  $\delta^{34}\text{S}$  distribution in tree ring. We also perform the evaluation of sulfur deposition history at locations received heavy anthropogenic sulfur deposition using tree ring.

The investigation was carried out at two study sites, Yokkaichi (YOK) and Inabu (INA) in central Japan. Both study sites have different histories of sulfur deposition. YOK had been affected by quite high anthropogenic sulfur deposition during 1960s. INA is located about 60 km NE of main urban area (Nagoya City). Three disk samples were obtained from Japanese cedar (*Cryptomeria japonica*) stump in 2013 at YOK and in 2012 at INA. The stumps at YOK were 63-year-old cut down in 2012 and those at INA were 170-year-old cut down in 2007. In addition, at INA, three 40-year-old living stems were cut down in 2013 at INA and the disk samples were obtained. After washing and dried, the tree ring samples were divided into 5 year increments from bark toward the pith, and ground using power mill. The ground samples were digested with  $\text{HNO}_3$  and  $\text{H}_2\text{O}_2$  on a hot plate and after filtration  $\text{BaCl}_2$  was added to obtain the  $\text{BaSO}_4$ . The  $\delta^{34}\text{S}$  values (VCDT) were measured using EA-IRMS.

To evaluation the localization of  $\delta^{34}\text{S}$  in sapwood, heartwood and pith, the data from the stump and the living wood samples at INA were compared. These samples showed the different localization of  $\delta^{34}\text{S}$  against the age. There were no difference of  $\delta^{34}\text{S}$  between the sapwood (living wood) and the heartwood (stump) at the same age. However, the  $\delta^{34}\text{S}$  values of the pith (living wood) were higher than those of heartwood (stump). This result indicated that the specific composition of sulfur compound might be consisted in pith and the  $\delta^{34}\text{S}$  of the pith should be unsuitable for evaluation of sulfur deposition history.

The  $\delta^{34}\text{S}$  values in ring at YOK declined from the late 1950s to early 1970s and then increased again. This trend was almost homologized in ring at INA and air  $\text{SO}_2$  concentration at near the YOK. In contrast, the minimum value of at YOK (-7.3 ‰) was lower than that at INA (-1.6 ‰). These results should be reflected by the deposition history of anthropogenic sulfur with low  $\delta^{34}\text{S}$  value at each site.

Keywords: Tree ring, Sulfur isotope, Morphology, Sulfur deposition

## Distribution of radiocesium in a small forest at Namie town in Fukushima Prefecture

OGATA, Hiroko<sup>1\*</sup>; KUROSHIMA, Hiroto<sup>1</sup>; OKOCHI, Hiroshi<sup>1</sup>; TOKONAMI, Shinji<sup>2</sup>; SORIMACHI, Atsuyuki<sup>3</sup>; HOSODA, Masahiro<sup>4</sup>; IGARASHI, Yasuhito<sup>5</sup>; KATAOKA, Jun<sup>1</sup>; OHSUKA, Shinji<sup>6</sup>

<sup>1</sup>Waseda University, <sup>2</sup>Hirosaki University, <sup>3</sup>Fukushima Medical University, <sup>4</sup>Hirosaki University Graduate School, <sup>5</sup>Meteorological Research Institute, <sup>6</sup>Hamamatsu Photonics K.K.

Fresh leaf/needle, litter, surface soil, stream water and bottom sand were monthly collected in a deciduous broadleaf forest and an evergreen needleleaf forest in Fukushima Prefecture during non-snowfall period. The concentration of radiocesium (<sup>134</sup>Cs and <sup>137</sup>Cs) was measured by commercially available NaI(Tl) scintillation detector.

The air dose rate at a broadleaf forest (5.64  $\mu$ Sv/h) was higher than that at a needleleaf forest (4.11  $\mu$ Sv/h) in November 2012. The average concentration of radiocesium in each sample was also higher at broadleaf forests than at needleleaf forests. The order of the concentration of radiocesium was litter > surface soil > fresh leaf/needle > bottom sand at both sites, indicating that radiocesium was accumulated in litter. Radiocesium was not detected in precipitation, throughfall, and stream water.

Surface soil samples at each sampling point were taken using a scraper plate in April and December 2013. Samples were taken with 0.5 cm increments for the depth of 0-5 cm and 1.0 cm increments for the depth of 5-10 cm. The maximum concentration was found at the surface at the broadleaf forest in April and December 2013. The maximum concentration was also found at the surface at the needleleaf forest in April 2013 but at 1-1.5 cm in December 2013, indicating that the radiocesium in surface soil penetrated deeply at the needleleaf forest. These differences were likely caused by the soil type and the composition of tree species at the sampling points.

A photostimulable phosphor (PSP) image plate was used to record a two-dimensional image of radioactivity distribution on the leaf/needle and root of the broadleaf tree samples. We used the CR<sup>x</sup>25P (General Electric Company). The image of the needleleaf sample of Japanese cedar showed some high intensity spots on the needles, indicating the presence of radioactive dusts attached onto the plant's surface. On the other hand, the image of the broadleaf showed uniform distribution, suggesting that contamination with radiocesium occurred internally.

In the presentation, we will also report about the runoff processes of the radiocesium with the stream bottom sand.

## Monitoring of atmospheric mercury pollution using a leaf camphor tree ( *Cinnamomum camphora* (L.) Sieb. )

CHIKAMASA, Takaya<sup>1\*</sup> ; KAMIYAMA, Naoko<sup>1</sup> ; SATAKE, Kenichi<sup>1</sup>

<sup>1</sup>Faculty of Geo-environmental Science, Rissho University

Source of mercury is divided into two anthropogenic sources such as incineration and sludge of fossil fuel and natural sources, such as by volcanic activity. Mercury discharged from these sources is present in the gaseous atmosphere mainly. On the other hand, trees are accumulated by adsorption or absorption in the leaves and bark of contaminants in the atmosphere. I am thought to absorb atmospheric pollution from the pores in the case of accumulation by the leaves. I was aimed at performing mercury pollution monitoring of air by measuring the mercury content in the leaves in this study. The absorption in the two years up fallen leaves from the deployment of new buds and evergreen broad-leaved tree, using the camphor tree( *Cinnamomum camphora* (L.) Sieb. ) accumulation is expected to indicators of mercury pollution in the atmosphere. I was monitoring for the full year, including the winter an increase in use of fossil fuels is expected by this. It was possible sampling points you ' ve covered as being human influenced due to its proximity to urban areas, in Rissho University campus is located in Kumagaya, Saitama Prefecture. In addition, a point of performing region comparison was a sampling Kirryu City in Gunma, Ogose town in Saitama, Ueno Park in Tokyo, Sarue Park in Tokyo and Katsuura City in Chiba.

### 1. Changes in mercury concentration due to dry and weight change due to drying temperature of leaf

After drying for five hours, respectively 70 °C leaves, at 130 °C, it was found that 60 minute in 70 °C , it is 10 minute at 130 °C to constant weight. Mercury concentration at each temperature was 33.4ngg<sup>-1</sup> at 70 °C, 33.0ngg<sup>-1</sup> at 130 °C.

### 2. Mercury concentration in the leaves within the site-specific mercury concentration in leaves

I was measuring the mercury concentration of each site by dividing the top, middle, at the bottom toward the petiole from the tip of the leaf camphor tree. As a result, mercury concentration was 62.0ngg<sup>-1</sup> at the top, 67.0ngg<sup>-1</sup> at middle, 66.5ngg<sup>-1</sup> at the bottom. In addition, I compared the mercury concentration in leaves in removing the mercury deposited in the leaf and total mercury concentration in the leaves. It is a leaf inside was revealed that much of the mercury contained in the leaves.

### 3. Changes in mercury concentration in the leaves by the time series variation

I investigated the time series changes in mercury concentration accumulated in the leaves by the use of leaves of different leaf age.

Keywords: mercury, camphor tree, environment



MIS21-P16

Room:Poster

Time:April 28 18:15-19:30

## Restoration of Soil Physical Properties by No-tilled Management in Tropical Sugarcane.

MORI, Yasushi<sup>1\*</sup> ; ARAI, Miwa<sup>2</sup> ; KANEKO, Nobuhiro<sup>2</sup> ; SWIBAWA, Gede<sup>3</sup> ; NISWATI, Ainin<sup>3</sup>

<sup>1</sup>Okayama Univesity, <sup>2</sup>Yokohama National University, <sup>3</sup>Univresity of Lampung

...

Keywords: Non-till, Sugarcane, Infiltration

## A study of soil organic matter stabilization using physical fractionation, isotopic, and spectroscopic approaches

WAGAI, Rota<sup>1\*</sup> ; ASANO, Maki<sup>1</sup> ; HAYAKAWA, Chie<sup>1</sup> ; INOUE, Yudzuru<sup>2</sup> ; KAJIURA, Masako<sup>1</sup> ; HIRADATE, Shyuntaro<sup>1</sup> ; YAMAGUCHI, Noriko<sup>1</sup> ; INAGAKI, Yoshiyuki<sup>7</sup> ; UCHIDA, Masao<sup>3</sup> ; TAKEICHI, Yasuo<sup>4</sup> ; SUGA, Hiroki<sup>5</sup> ; JINNOU, Muneaki<sup>4</sup> ; ONO, Kanta<sup>4</sup> ; TAKAHASHI, Yoshio<sup>5</sup>

<sup>1</sup>National Institute for Agro-Environmental Sciences (NIAES), <sup>2</sup>Kyushu University, <sup>3</sup>National Institute of Environmental Studies (NIES), <sup>4</sup>High Energy Accelerator Research Organization (KEK), <sup>5</sup>Hiroshima University, <sup>6</sup>TOYAMA Co. Ltd., <sup>7</sup>Forestry and Forest Products Research Institute

Volcanic-ash soil (Andisol) is unique among the world soil types due to the strong physical stability of organo-mineral aggregate structure at micro and submicron scales (Asano and Wagai, 2013, Geoderma) and its high capacity to store organic matter (OM) even in upland surface horizons under warm, moist climate regime where microbial heterotrophic activity is high. Several hypotheses have been proposed to account for these features of Andisol including (i) strong interaction of OM with dissolved metals (Al, Fe) and/or short-range-order (SRO) minerals that are quite abundant in this soil type, and (ii) preservation of recalcitrant compounds such as char.

Here we present some highlights from the 3-year project (GR091, NEXT Program, JSPS) examining the mechanisms of soil OM stabilization with a focus on organo-mineral interactions at various spatial and temporal scales using multiple analytical methods and experimental approaches. After careful consideration of the degree of soil aggregate disruption levels, we physically fractionated Andisol surface horizon sample based on particle size and density. Chemical composition of each physical fraction was assessed by elemental analysis, selective dissolution of inorganic phases, and solid-state <sup>13</sup>C-NMR. The origin and degree of microbial alteration of OM was estimated from C and N stable isotope ratios while the turnover time of C was assessed by radiocarbon measurements. Physical features of soil mineral and organo-mineral aggregate surfaces were characterized by specific surface area (N<sub>2</sub>-BET), XPS, and microscopic methods. We also conducted tracer experiments to further assess the residence time of the OM in each density fractions. Based on these results, we will discuss the progression of organo-mineral associations from fresh plant detritus to the aggregates of varying structure and stability for the studied Andisol.

## Formation evaluation and production interval determination at the 1st offshore methane hydrate production test site

FUJII, Tetsuya<sup>1\*</sup> ; TAKAYAMA, Tokujiro<sup>1</sup> ; SUZUKI, Kiyofumi<sup>1</sup> ; YAMAMOTO, Koji<sup>1</sup>

<sup>1</sup>Japan Oil, Gas and Metals National Corporation

In order to evaluate productivity of gas from marine methane hydrate (MH) by the depressurization method, on March 2013, the first offshore production test from MH concentrated zone (MHCZ) was conducted by the Research Consortium for Methane Hydrate Resource Development in Japan (MH21) at the AT1 site located in the north-western slope of Daini-Atsumi Knoll in the eastern Nankai Trough, Japan.

Before the production test, during the pre-drilling campaign conducted in 2012, extensive geophysical logging and pressure coring using Hybrid Pressure Coring System were conducted at monitoring well (AT1-MC) and coring well (AT1-C), in order to obtain fundamental information about reservoir properties of MH bearing formation for reservoir characterization, and also to decide on the production interval.

The MHCZ confirmed by the geophysical logging at AT1-MC has a thin-turbidite assemblage (from several tens of centimeters to a few meters) with 60 m of gross thickness; it is composed of lobe/sheet type sequences in the upper part, and relatively thick channel sand sequences in the lower part. The MHCZ at AT1-MC is thicker than those found in wells drilled in 2004 ( $\beta$ 1, 45 m), which were located about 150 m northeast of MT1-MC. This fact indicates that the predictions provided by a seismic interpretation and an inversion analysis were reasonable. Moreover, we confirmed that the silt-dominant formation just above the MHCZ was more than 20 m thick ; this was expected to be a seal formation. The well-to-well correlation between two monitoring wells (AT1-MC and MT1) in a 40 m distance shows fairly good lateral continuity of these sand layers (upper part of MHCZ), indicating an ideal reservoir for the production test.

In the upper part of the MHCZ, hydrate pore saturation (Sh) estimated from resistivity log showed distinct difference in value between sand and mud layers, compared to Sh from Nuclear Magnetic Resonance (NMR) log. Resistivity log has higher vertical resolution than NMR log, so it is favorable for these kinds of thin bed evaluation. In this part, 50 to 80% of Sh was observed in sandy layer. On the other hand, lower part of the MHCZ, Sh estimated from both resistivity and NMR log showed higher background value and relatively smoother curve than upper part. In this part, 50 to 80% of Sh was observed in sandy layer as well.

On the basis of the above observations, a production interval was planned. When we consider an effective depressurization, the existence of sealing layers is critical both above and below the interval. We expect that thin silty layers within the lower part of MHCZ will serve as a sealing layer that will prevent water coning from water-bearing layers. Therefore, we stopped drilling the production well at about 20 m above BSR, and decided to produce from approximately 40 m from the top of the MHCZ.

Our future (ongoing) work is to integrate reservoir characterizations based on well logs and pressure core data for the history matching of production test results.

This study is a part of the program of the Research Consortium for Methane Hydrate Resources in Japan (MH21 Research Consortium).

Keywords: methane hydrate, offshore production test, formation evaluation, production interval, eastern Nankai Trough, Daini-Atsumi Knoll

## P-wave velocity features of Methane Hydrate-Bearing turbidity sediments sampled by Pressure Core Tool

SUZUKI, Kiyofumi<sup>1\*</sup> ; SANTAMARINA, Carlos J.<sup>2</sup> ; WAITE, William<sup>3</sup> ; WINTERS, William J.<sup>3</sup> ; ITO, Takuma<sup>4</sup> ; NAKATSUKA, Yoshihiro<sup>1</sup> ; KONNO, Yoshihiro<sup>4</sup> ; YONEDA, Jun<sup>4</sup> ; KIDA, Masato<sup>4</sup> ; JIN, Yusuke<sup>4</sup> ; EGAWA, Kosuke<sup>4</sup> ; FUJII, Tetsuya<sup>1</sup> ; NAGAO, Jiro<sup>4</sup> ; YAMAMOTO, Koji<sup>1</sup>

<sup>1</sup>JOGMEC/TRC, <sup>2</sup>Georgia Institute of Technology, United State, <sup>3</sup>USGS, <sup>4</sup>AIST/MHRC

Turbidity sediments around the production test site at Daini-Atsumi knoll were deposited under channels and lobes of a submarine fan environment. It implies that sediments contain property difference caused by depositional environment, fundamentally. In addition, MH crystals among sediment grains overprint their original physical properties. Thus, difficulties in MH reservoir arise in clarifying the properties of MH-bearing sediments and normal sediments from logging data. To analyze their physical properties, core samples of MH-bearing sediments were taken at the first offshore production test site using a wireline tool called the hybrid pressure coring system (Hybrid PCS), which prevents dissociation of MH in the sampled cores.

Nondestructive, high-pressure analyses were conducted in both the 2012 summer drilling campaign and the 2013 winter collaboration study. To handle Hybrid PCS cores during the pressure coring campaign in the summer of 2012, a pressure core analysis and transfer system (PCATS) was installed on the research vessel Chikyu (Yamamoto et al., 2012). The measurements can be taken at the in situ water pressure at depth without causing any core destruction or MH dissociation. In January 2013, GT, USGS, AIST, and JOGMEC researchers conducted a collaborative study. In this study, the pressure core characterization tools (PCCTs) developed by GT also measured P-wave velocity of MH-bearing sediments.

In the PCATS analysis, the results showed a difference of more than 1,200 m/s in P-wave velocities between the MH-bearing sandy and muddy layers. This difference in P-wave velocities was confirmed by PCCTs measurements. Also, P-wave velocity of a turbidite interval tend to decrease upward as same as grading of a turbidite. The result implies that MH concentration is related with pore size of sediments.

### Acknowledgement

Authors would like to express thanks to Geotek at 2012 pressure core operation/analysis. Authors are grateful to USGS and Georgia Tech members who struggled with PCCTs operation/experiments in AIST Hokkaido. This research is conducted as a part of MH21 research and the authors would like to express their sincere appreciation to MH21 and the Ministry of Economy, Trade and Industry for disclosure permission for this research.

Keywords: Gas hydrate, P-wave velocity, Turbidite, Pore-filling type, Grain size distribution

## Reservoir Characterization and geological modeling for methane hydrate-bearing sediments around the 1st Offshore Product

TAMAKI, Machiko<sup>1\*</sup> ; SUZUKI, Kiyofumi<sup>2</sup> ; FUJII, Tetsuya<sup>2</sup> ; SATO, Akihiko<sup>1</sup>

<sup>1</sup>Japan Oil Engineering Co., Ltd., <sup>2</sup>Japan Oil, Gas and Metals National Corporation

The eastern Nankai trough is considered as an attractive potential resource of methane hydrates (MHs) and the first offshore production test was performed around the Atsumi-oki in 2013. The objective of this study is to conduct MHs reservoir characterization of methane hydrate (MH)-bearing turbidite sediments around the test site.

The depositional environment of MH-bearing sediments around the production test site is a deep submarine-fan turbidite system (e.g., Takano et al., 2009). To evaluate MH dissociation and gas production performance, we require precise geological models that describe facies variations of turbidite sediments and their corresponding petrophysical properties. In this study, we performed MHs reservoir characterization integrated from well log, core and 3D seismic data, and the 3D geological models were constructed based on geostatistical approach.

In accordance with the geological modeling workflow, (1) layering and gridding along the geological horizon and facies variations (framework modeling) and (2) defining internal properties (property modeling) were performed for the reservoir. Property modeling includes calculation of the distribution of facies and petrophysical properties such as hydrate saturation, porosity, and permeability, which are required as input to the reservoir flow simulation for predicting gas production performance.

This study is a part of the program of the Research Consortium for Methane Hydrate Resource in Japan (MH21 Research Consortium).

## Source of iodine and methane in gas hydrate layers in the Kumano Basin, Nankai Trough

YAMAMOTO, Itsuki<sup>1</sup> ; TOMARU, Hitoshi<sup>1\*</sup> ; MATSUZAKI, Hiroyuki<sup>2</sup>

<sup>1</sup>Department of Earth Sciences, Chiba University, <sup>2</sup>MALT, University of Tokyo

Because iodine has a strong biophilic behavior in marine system, pore waters in methane hydrate layers are often enriched in iodine as well as methane. The presence of long-lived radioisotope of iodine in nature therefore provides the potential age of source formations for methane. We have determined iodine isotopic ratios of pore waters collected frequently from sandy methane hydrate zone between 200 and 400 m below the seafloor in the Kumano Basin, Nankai Trough to examine the loci of source formations and processes to deliver and accumulate methane in the present methane hydrate stability.

Concentrations of iodine dissolved in pore waters peak at the top of sandy gas hydrate layers at 200 mbsf, where the iodine isotopic ratios also show the lowest/oldest values. Methane and iodine could have been derived from the landward old sediments through the sandy aquifers to the present methane hydrate zone. Transport of methane from old organic-rich sediments to the hydrate stability preferentially accumulates methane hydrates in thick sandy layers in the Kumano Basin.

Keywords: Methane hydrate, Iodine isotope, Pore water

## Trials of the methane hydrate observations in the local governments

AOYAMA, Chiharu<sup>1\*</sup>

<sup>1</sup>Japans Independent Institute

Nine prefectures of 1 local government prefecture of the Sea of Japan side established "Association of Ocean Energy Exploitation of Resources Promotion Sea of Japan" (the following, Association of Sea of Japan) in September, 2012. They support methane hydrate exploitation of resources of the government and aim at the local activation and job creation. Niigata and Hyogo that were members of the association of Sea of Japan carried out a prefecture original methane hydrate investigation. They appeal to the government for development promotion of the government by showing the result. On the other hand, Wakayama located on the Pacific side wants to appeal to the government for the reexamination of the development sea area by showing that outer layer type methane hydrate exists to the sea area that is nearer the landside than the sea area that the government develops. The Independent Institute carried out collaborative investigation each with Niigata, Hyogo and Wakayama in 2013. I show the results of research.

In the joint investigation with Niigata, plural plumes were observed in Mogami trough east slope (from depth of the water 200m 600m) .

In the joint investigation with Hyogo, I carried out observation of a methane plume and the structure and the seafloor topography under the sea bottom in Oki east sea area. Furthermore, I performed a piston core ring and gathered five samples and confirmed plural traces of the methane hydrate.

In the joint investigation with Wakayama, plural plumes were observed in Shionomisaki canyon (from depth of the water 1,700m 2,200m). There is hardly the report of the plume on the Pacific side so far. Therefore I want to continue observing it in future.

Keywords: methane hydrate, methane plume, quantitative echo shouder, piston core

## Quantify methane seeping flux from Ashizuri knoll, Nankai Trough

HARA, Shuichi<sup>1\*</sup>; TSUNOGAI, Urumu<sup>1</sup>; KOMATSU, Daisuke<sup>1</sup>; ASHI, Juichiro<sup>2</sup>; NAKAMURA, Ko-ichi<sup>3</sup>; SUNAMURA, Michinari<sup>4</sup>; NAKAGAWA, Fumiko<sup>5</sup>; TOKI, Tomohiro<sup>6</sup>

<sup>1</sup>Graduate School of Environmental Studies, Nagoya Univ., <sup>2</sup>ORI, Tokyo Univ., <sup>3</sup>National Institute of Advanced Industrial Science and Technology, <sup>4</sup>Division of Earth and Planetary Sciences, Grad. School Sci., Tokyo Univ., <sup>5</sup>Division of Earth and Planetary Sciences, Grad. School Sci. Hokkaido Univ., <sup>6</sup>Department of chemistry, Biology and Marine Science, Ryukyu Univ.,

The Ashizuri Knoll is located on the southern margin of Tosa Basin (ca. 1000 m depth) in the western Pacific Ocean. The top of the knoll is 534 m depth. The BSR have been detected around the knoll. Besides, seepage methane bubbles were found at top of the knoll. Extensive geochemical surveys on the water column around Ashizuri Knoll were done in September, 2013. The primary purpose of the study was to quantify the seeping flux of methane from the knoll by measuring the spatial distribution of methane around the knoll. Besides, we also tried to clarify the origin of methane by determining both  $\delta^{13}\text{C}$  and  $\delta\text{D}$  values.

Enrichment of thermogenic methane up to 145 nmol/L was detected just above the top of knoll. Besides, the methane enriched plume spread northeastward of the knoll at the water depth of 450- 660 m. The calculated methane flux was almost the same with that of off Joetsu hydrate area.



## Characteristics of natural gas hydrates retrieved off the southeastern and southwestern Sakhalin Island

HACHIKUBO, Akihiro<sup>1\*</sup> ; SAKAGAMI, Hirotohi<sup>1</sup> ; MINAMI, Hirotsugu<sup>1</sup> ; YAMASHITA, Satoshi<sup>1</sup> ; TAKAHASHI, Nobuo<sup>1</sup> ; SHOJI, Hitoshi<sup>1</sup> ; VERESHCHAGINA, Olga<sup>2</sup> ; JIN, Young K.<sup>3</sup> ; OBZHIROV, Anatoly<sup>2</sup>

<sup>1</sup>Kitami Institute of Technology, <sup>2</sup>Pacific Oceanological Institute, FEB RAS, <sup>3</sup>Korea Polar Research Institute

Gas hydrate samples were retrieved at the southeastern and southwestern Sakhalin Island in the cruises of LV59 and LV62 (R/V Akademik M. A. Lavrentyev). Sakhalin Slope Gas Hydrate (SSGH) project started in 2007, and we retrieved sediment cores including gas hydrates off northeastern Sakhalin Island in 2009-2011. In the recent cruises (2012-2013), we sampled sediment cores at the Terpeniya Ridge and the Tatarsky Trough (SE and SW Sakhalin Island, respectively). We found a lot of gas plumes ascend from the sea bottom and the dissolved methane in sediment pore water was rich. Gas hydrate crystals were recovered from both areas and stored into liquid nitrogen tank. Their dissociation heat and hydration number were measured by a calorimeter and Raman spectrometer, respectively. Dissociation heat of gas hydrates was almost the same as that of pure methane hydrate. Raman spectra showed that the hydrate crystals of both Terpeniya Ridge and Tatar Trough belonged to the structure I, and the hydration number was estimated about 6.0. Molecules of hydrogen sulfide were detected in both large and small cages of the structure I. Therefore, the hydrate crystal is similar to that obtained from NE Sakhalin Island in our previous cruises.

We obtained hydrate-bound gas and dissolved gas in pore water on board and measured their molecular and stable isotope compositions. Empirical classification of the methane stable isotopes;  $\delta^{13}\text{C}$  and  $\delta\text{D}$  indicated that the gases obtained at the Terpeniya Ridge are microbial origin via carbonate reduction, whereas some cores at the Tatarsky Trough showed typical thermogenic origin. We retrieved three sediment cores with gas hydrate at the Tatarsky Trough, and their  $\delta^{13}\text{C}$  of hydrate-bound methane were -47.5 ‰, -44.2 ‰, and -68.8 ‰, respectively. Therefore, gas hydrates encaged both microbial and thermogenic gases yield at the Tatarsky Trough. Ethane-rich (up to 1% of the total guest gas) hydrates were found at the Terpeniya Ridge and the Tatarsky Trough, and encaged ethane was also detected in their Raman spectra. Ethane  $\delta^{13}\text{C}$  of the all gas samples suggested their thermogenic origin.

Keywords: gas hydrate, stable isotope, Sea of Okhotsk, Raman spectroscopic analysis, Calorimetry

## First attempt to drill down hydrate mound and gas chimney by BGS Rockdrill 2

MATSUMOTO, Ryo<sup>1\*</sup> ; WILSON, Michael<sup>2</sup>

<sup>1</sup>Meiji University-Gas Hydrate Laboratory, <sup>2</sup>British Geological Survey

A series of shallow piston coring (PC) has identified dense accumulation of massive gas hydrates in the upper part of hydrate mounds and gas chimneys in Japan Sea since 2004, however, because of limited penetration of PC, distribution and resource potential of gas hydrate below ~10 mbsf have not been clearly answered as yet. On the other hand, 3D seismic profiles have revealed significant pull-up structure, a characteristic velocity pseudo-structure, in gas chimneys, suggesting an accumulation of significant amount, probably 20 to 30 vol.%, of gas hydrates in gas chimneys. In the summer 2013, Meiji University and British Geological Survey deployed BGS benthic drilling machine, Rockdrill 2, on hydrate mounds in Joetsu basin, Japan Sea, and successfully drilled through inhomogeneous, gas hydrate- and carbonate-bearing hard sediments and occasional soft and gassy sediments down to 32 mbsf. Core recovery was unfortunately low throughout the coring due to extensive dissociation of gas hydrate and gas expansion during and after coring. However, we could recover massive gas hydrate samples, 5 to 12 cm long, from a number of horizons down to 32 mbsf. Several 2 to 7 m thick zones of gas hydrate accumulation have been inferred from integrated profiles of drill logs, video-monitor observation, and discontinuous sediment core record. Shallow drilling of Rockdrill 2 is likely to have proved a dense distribution of gas hydrates in deeper part of hydrate mounds and gas chimneys.

Keywords: gas hydrate, Japan Sea, hydrate mound, gas chimney, Rockdrill 2

## Formation of shallow gas hydrates and geochemistry of gas and pore water from UT13 cruise in the Japan Sea

OWARI, Satoko<sup>1\*</sup> ; SUZUKI, Yoshiharu<sup>1</sup> ; TOMARU, Hitoshi<sup>1</sup> ; UCHIDA, Takashi<sup>2</sup> ; KOBAYASHI, Takeshi<sup>3</sup> ; TANI, Atsushi<sup>5</sup> ; NUMANAMI, Hideki<sup>4</sup> ; MATSUMOTO, Ryo<sup>6</sup>

<sup>1</sup>Graduate school of Science , Chiba university, <sup>2</sup>Akita Univesity Faculty of Engineering and Resource Science, <sup>3</sup>Tokyo University of Marine Science and Technology, <sup>4</sup>Department of Home Economics, Faculty of Home Economics, Tokyo Kasei-Gakuin University, <sup>5</sup>Dept. Earth and Space Science, Graduate School of Science, Osaka University, <sup>6</sup>Gas Hydrate Laboratory

Active gas venting and distribution of massive gas hydrates are largely observed on the summits of the Umitaka Spur and Joetsu Knoll in the eastern margin of the Japan Sea, where the fault system associated with strong anticline structure constrains the accumulation of gas and following gas hydrate formation. The UT13 cruise has conducted to collect shallow sediments from the Oki Trough, north eastern of Noto Peninsula, and offshore Akita-Yamagata areas, where gas chimney structure and strong backscatter indicate migration of gas-charged fluid and potential formation of gas hydrates near the seafloor. Geochemistry of pore water, dissolved gas, and hydrate-dissociated gas reflect the geochemical environments associated with the delivery of gas and fluid and formation/dissociation of gas hydrates in the shallow sediments.

Flake-like and nodular gas hydrates were observed at 1-6 mbsf in the Oki Trough and offshore Akita-Yamagata, respectively. Concentrations of methane dissolved in pore water are high, comparable to those in the Umitaka Spur and Joetsu Knoll area, and the SMI depths are accordingly shallow at ~2.7 mbsf in the entire research area, indicating high potential of gas hydrate accumulation in the shallow sediments. Concentrations of chloride are sporadically low in all areas due to gas hydrate dissociation during core recovery, accumulations of small gas hydrates with saturations up to 20% were observed, reflecting ubiquitous formation of gas hydrates in the research area. Concentrations of calcium and magnesium show fine increase and decrease in response to sulfate changes at deeper than SMI, reflecting the change of the methane flux mainly, the formation/dissociation of gas hydrates may have changed seafloor topography and geochemical properties of pore water and gas in the shallow sediments.

Contrary to the Umitaka Spur and Joetsu Knoll area where thermogenic gas dominates in the shallow gas hydrates, chemical and isotopic compositions of gas indicate that the majority of gas is of biogenic origin with minor contribution from thermogenic ethane and hydrogen sulfide, the latter may result in expanding gas hydrate stability and forming gas hydrates near the seafloor.

This research is supported by the MEXT Grand-in-Aid for Scientific Research (KAKENHI) to R. Matsumoto (Meiji University).

Keywords: Shallow gas hydrates, pore water, dissolved gas, SMI

## Distribution of methanogenic and methanotrophic archaea in subseafloor sediment collected during UT12

IMAJO, Takumi<sup>1\*</sup> ; KOBAYASHI, Takeshi<sup>1</sup> ; IMADA, Chiaki<sup>1</sup> ; TERAHARA, Takeshi<sup>1</sup> ; MATSUMOTO, Ryo<sup>2</sup>

<sup>1</sup>The graduate school of marine science and technology, TUMSAT, <sup>2</sup>Meiji University

Methane hydrate is now one of the most popular energy sources in the world, and various amounts are presumed to be buried around Japan's continental margins. Methane contained in methane hydrate in the deep sea sediment is produced by microbial or thermogenic system. In the microbial system, methanogenic and methanotrophic archaea play an important role in this environment. However, the studies on characteristics and abilities of these microorganisms are still underway in the Sea of Okhotsk. Therefore, this study focuses on isolation of the methanogenic archaea and analysis of community construction and diversity of these microorganisms.

Sediment samples were collected from the subseafloor by the piston coring, during UT12 (Umitaka-maru Gas Hydrate Research Cruise 2012). Samples were collected from each core sample at appropriate intervals. The samples were stored at 4 °C for the microbiological cultivation experiment use, and at -80 °C for the microbiological diversity analysis use, respectively.

For the isolation, cultivation was carried out by enrichment culture using H<sub>2</sub>/CO<sub>2</sub> medium. The cultivation temperatures were 15 °C and 30 °C, respectively. We successfully isolated several methanogenic archaea from the samples of the surface of the subseafloor. The result of the 16S rRNA gene sequence analysis showed that some of the strains were identified as closely related strains of *Methanogenium marinum*. In a previous literature, *M. marinum* was isolated from the cold marine sediment from the Scan Bay, Alaska. We also conducted the experiment to measure the methane productivity of our isolates by the range of the cultivation temperature.

For the analysis of community structure and diversity of methanogens, DNA was extracted from each sediment sample, using the ISOIL kit following the manufacturer's protocol. The 16S rRNA gene of methanogenic archaea and the mcrA gene of methanogenic and methanotrophic archaea were amplified by PCR. The PCR product was purified by FastGene Gel/PCR Extraction Kit following the manufacturer's protocol. The purified products were analyzed by T-RFLP method and clone library method. The results of the T-RFLP analysis showed that the various fragments were observed. Clone library sequencing analysis of mcrA genes indicated that some of them were identified as related sequences to *Methanogenium*. Also, results from T-RFLP method were used for MDS (Multi-Dimensional Scaling) analysis.

This experiment was supported by grants-in-aid for scientific research <KAKENHI>(Ryo Matsumoto, Meiji University).

Keywords: shallow gas hydrate, methanogenic archaea, methanotrophic archaea

## Environmental variability of the Japan Sea clarified by

OGIHARA, Shigenori<sup>1\*</sup>

<sup>1</sup>Earth and Planetary Science, The University of Tokyo

Environmental variability of the Japan Sea was presumed using MD179 Cruise 3312 sediment core by inorganic and organic geochemical analysis. Analysis of this study went focusing on mainly thin-laminated dark layer (TL-1 to 3). TOC was about 0.8% in TL-2 and 3, on the other hand, the TL-1 layer showed nearly 2%. In the central part of TL-2 to the upper part, all the samples of a C/S ratio are 1 or less. This has suggested strong reduction environment at the upper part of TL-2 layer.

The Pristane/Phytane ratio (Pr/Ph ratio) traditionally used as an oxidation-reduction index is shown that most analysis data are <3.0 and it was the reductive environment. Pentamethylcosane (PMI) which is the membrane lipid origin of the anaerobic methanotrophic archaea (ANME), C18-isoprenoid ketone characteristically detected to a cold-seep carbonate and hop-22 (29) ene (diploptene) also the origin were not clear, characteristically found out at a methane seeping point, those depth distribution was plotted and considered. Distribution of the AMNE marker in the inside of TL layers is heterogeneous, and the possibility of the sudden methane eruptions during the TL-2 deposition was suggested.

This study was supported by MH21, Research Consortium for Methane Hydrate Resources in Japan.

Keywords: Japan Sea, biomarker, TL layer, sulfur isotope composition, anoxic environment, C/S ratio

## Overview of well logging operations at the 1st offshore methane hydrate production test in the eastern Nankai Trough

TAKAYAMA, Tokujiro<sup>1\*</sup>

<sup>1</sup>Japan Oil, Gas and Metals National Corporation

Overview of well logging operations at the 1st offshore methane hydrate production test in the eastern Nankai Trough

T.Takayama\*, T.Fujii, K.Suzuki, K.Yamamoto (JOGMEC)

### Objective

The objective of well logging operations at the 1st offshore methane hydrate production test is to evaluate the formation lithology and reservoir properties. We will construct an integrate reservoir model based on the well logging data for assessing an accurate prediction of production performances for the methane hydrate (MH) production test.

### Well logging results

Our focused area around the offshore production test site comprised unconsolidated turbidite formations with a thickness of thin turbidite sand and mud layers according to the previous well logging data. These formations typically show significant washed out after the drilling and its effect of the quality of data is serious issues for the formation evaluation by well logging data.

The well logging results in the monitoring wells indicate that the significant washed out was found particularly in the intervals of thin bed turbidite formations above the reservoir interval and below the BSR(Bottom Simulating Reflectors). However, other intervals exhibit stable caliper logging data, which indicating there are no significant washed out effect even in the WL(Wireline Logging) data. This is probably due to the tight formation of the mud-rich and MH-rich intervals.

### Conclusions and Future works

- a) Operation of both LWD(Logging While Drilling) and WL was successfully completed without any significant trouble.
- b) Borehole condition was bad due to the borehole washed out above the reservoir interval and below the BSR. This was mainly due to the unconsolidated turbidite formation with the thin thickness of sand and mud layers. In spite of the washed out effect, reservoir and seal intervals showed good quality of well logging results which correspond to significant tight formations of mud-rich and MH-rich sediments.
- c) In LWD operation, we used pulse neutron generator without radioactive sources. This operation was quite rare in the world and we could successfully obtain fairly good well logging data in the seal and reservoir intervals.
- d) In the drilling of the MH reservoirs in the offshore exploration, the borehole washed out is inevitable because it exists in the shallow marine unconsolidated sediments. Hence, several challenging and technical issues are significantly important for our future study.

### Acknowledgment

This work was supported by Methane Hydrate 21 Research Consortium. We would like to thank the Ministry of Economy, Trade and Industry for providing permission to publish this paper.

Keywords: methane hydrate, offshore methane hydrate production test, Nankai Trough, Well logging

## Depicting Thermal History of the Forearc Basin Pleistocene Turbiditic Sedimentary Sequences around Daini Atsumi Knoll

AUNG, Than tin<sup>1\*</sup> ; FUJII, Tetsuya<sup>1</sup> ; UKITA, Toshiyasu<sup>1</sup> ; KOMATSU, Yuhei<sup>1</sup> ; SUZUKI, Kiyofumi<sup>1</sup>

<sup>1</sup>Methane Hydrate R&D Division, Technology & Research Center, JOGMEC

Thermal history of sedimentary basin is a key to understand hydrocarbon maturation and generation of the source rock within the basin. In terms of gas hydrate accumulation, high pressure and low temperature boundaries, the gas hydrate stability zone, is mandatory to simulate in order to understand accumulation mechanisms of gas hydrate in the studied basin. We have determined heat flow history of Pleistocene sedimentary sequences in the forearc basin round the Daini Atsumi knoll, along the eastern Nankai Trough, Japan, by simulating gas hydrate stability zone. World first offshore production test of gas hydrate was successfully done in the vicinity area of Daini Atsumi knoll during March 2013.

Simulation in 3D gas hydrate petroleum systems of the forearc basin filling with Pleistocene turbiditic sedimentary sequences around the Daini Atsumi knoll was firstly performed by applying assumed heat flow of 45 mW/m<sup>2</sup>. Temperature at seabed is applied as 3.5 C throughout the model area and depositional period. Simulated sedimentary sequences consist of Pleistocene Ogasa Group of sand and shale alternative turbiditic sedimentary layers. Older upper Kakegawa Group is also included between the model basement and Ogasa group. Lithologies are interpreted from grain size analysis of cores data. Lateral facies distribution are based on seismic facies analysis. Global sea level changes are considered in applying paleo-water depths of the geologic horizons.

Simulated hydrostatic pressure matches hydrostatic pressure calculated from XPT data at well A1-L. Simulated temperature was calibrated by DTS (distributed temperature sensor) Temperature of gas hydrate reservoir zone at well AT1-MC. Calibration result reveals that heat flow has to low down to 32 mW/m<sup>2</sup> in order to fit pressure and temperature at well. Result of simulated temperature using calibrated heat flow matches with a resolution of ~1C of the well data. This heat flow value is lower than the reported value (~50 mW/m<sup>2</sup>, Harris et al., 2014) around the vicinity of the studied area. Validation of this heat flow value requires 1) to reanalyze model layer thickness and total thickness of model, and 2) to reanalyze thermal conductivity of applied lithology.

In addition to above works, model is planned to update with paleo-water depth based on paleo-bathymetry from structural restoration, and reported depth from foraminiferal measurement of core samples at A1-L well. Because mass and lateral distribution of gas hydrate accumulation are considerably affected by tectonic uplift at Daini Atsumi Knoll.

This study is a part of the program of the Research Consortium for Methane Hydrate Resources in Japan (MH21 Research Consortium).

Keywords: Gas Hydrate Petroleum Systems, Daini Atsumi Knoll, Heat Flow, Pleistocene Ogasa Group, 3D, Simulation

## Methane Hydrate trapping system of the turbidite channel complex in Daini-Atsumi Knoll, eastern Nankai Trough, Japan

KOMATSU, Yuhei<sup>1\*</sup> ; FUJII, Tetsuya<sup>1</sup> ; SUZUKI, Kiyofumi<sup>1</sup>

<sup>1</sup>Japan Oil, Gas and Metals National Corporation

The 1<sup>st</sup> offshore gas hydrate production test was conducted at gas hydrate concentrated zone (reservoir) of the Eastern Nankai Trough, which is considered stratigraphic accumulation. However, the accumulation mechanism for this concentrated zone is not yet well understood.

In this study, in order to examine gas hydrate trapping system in the accumulation mechanism, we identify the depositional process and controlling factors based on facies analysis and sequence stratigraphy using the core and geophysical log data.

Seven depositional sequences are identified based on grain size, bed thickness, sedimentary structure, and stacking pattern in this study. The sequence boundaries are also identified by terminations of seismic reflection. These sequences are attributed to a fourth to fifth-order eustatic sea-level changes, because the stacking pattern cycle is in phase with global oxygen isotope curves, the cycle is also identified in the onshore formation during the same period. The reservoir was interpreted as Falling-Stage Systems Tract (FSST) and Lowstand Systems Tract (LST).

In the reservoir, it was observed the channel complex set characterized by relatively strong reflections and paleocurrent flowing from northeast to southwest on 3-D seismic data. The channel complex set changes into muddy facies in the south direction. The channel complex set is characterized by hemipelagic setting or slope (F1), abandonment mud drape (F2), nonamalgamated channel element (F3), and semiamalgamated channel element (F4). The channel elements (F3, 4) are the fundamental unit and record a single phase of downcutting and filling. The muddy deposits (several 10 m; F1) above reservoir are interpreted as condensed section because they are consistent with a peak of foraminifer abundance. The condensed section divide different sediments of gas hydrate saturation.

These features suggest that condensed section deposits become top seal and channel deposits interpreted as FSST and LST become reservoir in gas hydrate trapping formation. The trapping system has the ability to seal lateral gas leakage because the channel reservoir is located around structural wing, the direction of sand pinch-out to structural highs becomes oblique to the direction of sediment supply. Consequentially, gas hydrate trapping system is constrained by sedimentary facies, systems tracts, and geographic and tectonic setting. Concepts and data generated in this study can be used for gas hydrate petroleum system analysis such as basin simulation.

Keywords: gas hydrate system, sequence stratigraphy, sea level change, submarine channel, sedimentary facies



## Relationship of permeability and particle breakage of experimental fault -Evaluation for the methane-hydrate reservoir-

KIMURA, Sho<sup>1\*</sup> ; KANEKO, Hiroaki<sup>1</sup> ; ITO, Takuma<sup>1</sup> ; MINAGAWA, Hideki<sup>1</sup>

<sup>1</sup>Reservoir Modeling Team, Methane Hydrate Research Center, AIST

Methane hydrate is expected to be an energy resource in the future. As results of coring and logging, the existence of a large amount of methane-hydrate is estimated in the east Nankai Trough, offshore central Japan, where many folds and faults have been observed. Permeability in methane hydrate-bearing sediment is important factors for estimating the efficiency of methane gas production. In this study, we use a ring-shear apparatus to examine the relationship between the permeability and grain size reduction of silica sand sample after large displacement shearing under tested effective normal stresses ranging from 0.5 MPa to 8.0 MPa. The grain size distribution in the shear zone of sand specimen after ring-shearing at each normal stress level is analyzed by laser particle analyzer. The permeability and grain size reduce with the increasing the effective normal stress due to particle breakage. The relationship between permeability and grain size distribution after ring-shearing is expressed well by a curve in each sand, silt and clay size content. In the first group, the sand size content is up to about 80 %, permeability drastically decreases by two orders of magnitude. In the second group, the sand size content is less than about 80 %, the permeability is almost constant. In the silt and clay size, the both contents are up to about 10 %, the permeability abruptly decreases, while, the permeability gradually decreases over about 10 %. The results are indicated that the grain size reduction and the effective normal stress during shearing are one of the controlling factors of the permeability in fault of sand. This study is financially supported by METI and Research Consortium for Methane Hydrate Resources in Japan (the MH21 Research Consortium).

Keywords: Fault, Particle breakage, Permeability, Grain size distribution, Ring-shear test

## Methane seepage and possibility of hydrate-bearing layers around Kuroshima Knoll, SW Ryukyu

MATSUMOTO, Takeshi<sup>1\*</sup> ; AOKI, Tae<sup>2</sup>

<sup>1</sup>University of the Ryukyus, <sup>2</sup>Weathernews Inc.

A reconnaissance survey expedition of Kuroshima Knoll, located south of Ishigaki Island, southwest Ryukyu Islands, was carried out for the first time in 1996. During the expedition dead Calyptogena shells were identified on the summit plane of the knoll. Several advanced reconnaissance survey expeditions afterwards for the geological study in this area by 2001 revealed an active eruption of methane, which suggested a methane hydrate layer beneath the knoll. In this study, we carried out a mapping of the bottom sediment on the top flat plane of Kuroshima Knoll from the video images obtained by JAMSTEC submersibles and ROVs since 2002 in order to create a complete geological route map. The result shows that the whole area of the summit plane of the knoll with the water depth of around 640m was covered by dead Calyptogena community and calcareous rocks. Live Bathymodiolus community was located densely around 24deg. 07min. 48sec.N, 124deg. 11min. 33sec.E. Bubble eruption was located at 35 sites. The area of the suggested methane seepage was estimated to be 40,000 square meters.

Next, the vertical profile of the sea water temperature with its seasonal variability around the knoll was examined in order to verify if methane hydrate exists stably beneath the seafloor of the knoll by use of the JODC data catalogue. It is, however, hard to expect a methane hydrate layer underneath the knoll considering the water temperature at the seafloor in this area. Examination of the vertical profiles of the sea water temperature along the whole Ryukyu Arc also shows that a possible methane hydrate layer is confined to the area with more than 700m in water depth in the fore-arc area.

Keywords: methane hydrate, Kuroshima Knoll

## Hydrogen isotope of hydrate-bound hydrocarbons at Lake Baikal

HACHIKUBO, Akihiro<sup>1\*</sup>; SAKAGAMI, Hiroto<sup>1</sup>; MINAMI, Hirotsugu<sup>1</sup>; YAMASHITA, Satoshi<sup>1</sup>; TAKAHASHI, Nobuo<sup>1</sup>; SHOJI, Hitoshi<sup>1</sup>; KHLYSTOV, Oleg<sup>2</sup>; KALMYCHKOV, Gennadiy<sup>3</sup>; DE BATIST, Marc<sup>4</sup>

<sup>1</sup>Kitami Institute of Technology, <sup>2</sup>Limnological Institute, SB RAS, <sup>3</sup>Vinogradov Institute of Geochemistry, SB RAS, <sup>4</sup>Ghent University

Natural gas hydrates exist in sublacustrine sediments of Lake Baikal. Gas hydrates were first obtained from sub-bottom depths of 121 and 161 m in the Baikal Drilling Project well located at the southern Baikal basin. Recently, MHP (Multi-phase Gas Hydrate Project, 2009-2013) revealed distribution of gas hydrate in sub-bottom sediment at the southern and central Baikal basins. We obtained gas hydrate crystals from more than 25 places, and retrieved hydrate-bound gas onboard. We measured molecular and isotopic compositions of hydrate-bound gas.

According to the  $\delta^{13}\text{C}$ - $\delta\text{D}$  diagram for methane (Whiticar, 1999), high and low methane  $\delta^{13}\text{C}$  values indicate thermogenic and microbial origins, respectively, and methane  $\delta\text{D}$  provides information on methyl-type fermentation or  $\text{CO}_2$  reduction in the microbial field. Kida *et al.* (2006) and Hachikubo *et al.* (2010) reported that hydrate-bound methane of Lake Baikal was microbial origin via methyl-type fermentation, because methane  $\delta\text{D}$  was about -300 ‰. We found heavier methane ( $\delta^{13}\text{C}$  ranged from -50 ‰ to -40 ‰) in the Kukuy Canyon area (central Baikal basin), indicating thermogenic origin. Methane  $\delta\text{D}$  was distributed from -330 ‰ to -270 ‰. Generally,  $\delta\text{D}$  of thermogenic methane of marine gas hydrates is much more heavier (more than -200 ‰). Methane  $\delta\text{D}$  of Lake Baikal gas hydrate seems to be about 100 ‰ smaller than that of marine gas hydrate. Matveeva *et al.* (2003) reported that  $\delta\text{D}$  of the lake bottom water was about -133 ‰. Possibly, methane  $\delta\text{D}$  of hydrate-bound methane derives from  $\delta\text{D}$  of water.

Hachikubo A, Khlystov O, Krylov A, Sakagami H, Minami H, Nunokawa Y, Yamashita S, Takahashi N, Shoji H, Nishio S, Kida M, Ebinuma T, Kalmychkov G, Poort J (2010) Molecular and isotopic characteristics of gas hydrate-bound hydrocarbons in southern and central Lake Baikal. *Geo-Mar Lett* **30**: 321-329. doi:10.1007/s00367-010-0203-1

Kida M, Khlystov O, Zemskaya T, Takahashi N, Minami H, Sakagami H, Krylov A, Hachikubo A, Yamashita S, Shoji H, Poort J, Naudts L (2006) Coexistence of structure I and II gas hydrates in Lake Baikal suggesting gas sources from microbial and thermogenic origin. *Geophys Res Lett* **33**: L24603. doi:10.1029/2006GL028296

Matveeva TV, Mazurenko LL, Soloviev VA, Klerkx J, Kaulio VV, Prasolov EM (2003) Gas hydrate accumulation in the subsurface sediments of Lake Baikal (Eastern Siberia). In: Woodside JM, Garrison RE, Moore JC, Kvenvolden KA (eds) Proc 7th Int Conf Gas in Marine Sediments, 7-11 October 2002, Baku, Azerbaijan. *Geo-Mar Lett* **23(3/4)**: 289-299. doi:10.1007/s00367-003-0144-7.

Whiticar MJ (1999) Carbon and hydrogen isotope systematics of bacterial formation and oxidation of methane. *Chem Geol* **161**: 291-314. doi:10.1016/S0009-2541(99)00092-3

Keywords: gas hydrate, crystallographic structure, Lake Baikal, methane, stable isotope

## Sedimentary environments and pore properties of subseafloor sediments in the eastern margin of Japan Sea

UCHIDA, Takashi<sup>1\*</sup> ; HORIUCHI, Sena<sup>1</sup> ; KATO, Yuki<sup>2</sup> ; MATSUMOTO, Ryo<sup>3</sup>

<sup>1</sup>Faculty of Engineering and Resource Science, Akita University, <sup>2</sup>Graduate School of Frontier Sciences, the University of Tokyo, <sup>3</sup>Organization for the Strategic Laboratory of Research and Intellectual Properties, Meiji University

Sediment samples below the seafloor were retrieved as long as 40 meters at the Umitaka Spur, Joetsu Channel, Toyama Trough, Japan Basin, Nishi Tsugaru and Okushiri Ridge areas in the east margin on Japan Sea. Small amounts of sandy sediment have been retrieved as thin intercalations in Pleistocene and Holocene muddy layers, where trace fossils and strong bioturbations are commonly observed. Those sandy sediments consist of very fine- to fine-grained sands, and are sometimes tuffaceous. These sandy sediments might have been transported approximately around 3 to 30 ka according to the tephra ages, where supplying sediments might have not been abundant due to sea level fluctuation during the Pleistocene ice age.

It is important to clarify the relationship between burial depths and absolute porosities of the argillaceous sediments. Therefore, macroscopic observations and descriptions, measurements of porosities and the pore size distributions, thin-section observations, SEM (scanning electron microscope) observations, and the X-ray diffraction analyses have been performed. They consist of silt- to clay-grained particles, and they sometimes contain very fine- to medium-grained thin sandy layers. Average porosities are 50 % in all study areas, but mean pore sizes in the Nishi Tsugaru are around 1000 nm while 100 nm in the other areas, which tend to decrease as increasing of depths. It is suggested that repacking of the muddy particles dominantly advances by physical compaction in early diagenesis.

They generally contain much opal-A, quartz, feldspar, illite and smectite that do not change definitely with depth, because they are tuffaceous and are suffered only from early diagenesis. By optical and microscopic observations, diatom tests, foraminifers and framboidal pyrites are commonly observed, and, in particular, the shapes of diatom are usually various, dominantly fragmental and infrequently preserved.

The sedimentological properties of subseabottom argillaceous sediments in early diagenesis can be discussed in terms of physical and geochemical aspects such as porosity, permeability, pore size distribution, diagenetic mineral composition as well as microscopic observation. It is remarked that the physical diagenesis proceeds first as repacking of clastic grains due to mechanical compaction, whereas the chemical diagenesis advances very slowly in early diagenesis.

This study was performed as a part of the MH21 Research Consortium on methane hydrate in Japan.

Keywords: hydrate, Japan Sea, pore

## Isotopic and microbial compositions of carbonate nodules from sea bottom sediments in the Japan Sea

MORI, Taiki<sup>1\*</sup> ; KANO, Akihiro<sup>1</sup> ; OKUMURA, Tomoyo<sup>2</sup> ; MATSUMOTO, Ryo<sup>3</sup>

<sup>1</sup>SCS Kyushu University, <sup>2</sup>JAMSTEC, <sup>3</sup>Meiji University

Carbonate precipitates on sea bottom sediments and shallow core in methane seep areas are often associated with methanogens. Anoxic methane oxidization is a particularly important metabolism for carbonate precipitation in terms of raising local alkalinity and supersaturation. We recovered carbonate nodules from sea bottom sediments from Umitaka Spur, Joetsu Knoll and Akita offshore during an expedition for gas hydrate in the Japan Sea in August-October 2013. We investigate microbial metabolisms for carbonate precipitation based on textural observation, isotopic measurement, and gene analysis.

Many specimens appear grapestone textures consisting of aggregated small nodules, which indicate multiple generation of carbonate precipitation. Aragonite needles are commonly observed on outer margin and in pore spaces in the grapestone. Core part of the nodules are often black color due to concentration of organic substance. Isotopic compositions were measured for sub-samples that were micro-drilled from the section of the nodules. Some of the Umitaka specimens exhibit large variation in carbon isotope, which generally decrease from core to margin. Methanogenesis is only accountable microbial processes for the highest values up to +12 permil. This metabolism can separate organic carbon into <sup>13</sup>C-depleted methane and <sup>13</sup>C-enriched carbon dioxide species. On the other hand, nodules from Joetsu and Akita are relatively homogenous and very low (-45 to -60 permil) in carbon isotope. This indicate that carbonate carbon in the nodules was largely originated from methane. Gene analysis for an Umitaka specimen extracts many sulfate reducers, but no methanogens. This specimen was calcified by sulfate reduction of organic matter.

We would like to thank onboard scientists and crews for their kind support during the expedition. We appreciate British Geological Survey for drilling.

Keywords: gas hydrate, carbonate nodule, stable isotope, microbes

## Microstratigraphic studies using UT13 piston cores around methane seep areas, eastern margin of the Japan Sea

OI, Takeshi<sup>1\*</sup>; ISHIHAMA, Saeko<sup>2</sup>; AKIBA, Fumio<sup>3</sup>; NUMANAMI, Hideki<sup>4</sup>; MATSUMOTO, Ryo<sup>1</sup>; HASEGAWA, Shiro<sup>5</sup>

<sup>1</sup>Meiji University, OSRI, <sup>2</sup>Kanagawa Prefectural Museum of Natural History, <sup>3</sup>Diatom Minilab Akiba, Co. Ltd., <sup>4</sup>Tokyo Kasei University, <sup>5</sup>Kumamoto University

### 1. Introduction

Microbiostratigraphy is important for the submarine resources survey to research the chronology and paleoceanography. Furthermore, benthic foraminiferal studies are also useful to clear the environmental impacts caused by the dissociation of subsurface methane hydrate in shallow sediments of the Umitaka Spur and Joetsu Knoll of the Joetsu basin 30 km off Joetsu city, Niigata Prefecture (Matsumoto et al., 2009). It is possible to estimate the age and environments of core sediments in detail, because the Microbiostratigraphy during the past 130 ka could be evident in the giant piston cores recovered by MD179 cruise in June 2010.

In this poster, we introduce the late Quaternary microbiostratigraphy of diatom and foraminifera off Joetsu in the eastern part of the Japan Sea, and applied these results and foraminiferal <sup>14</sup>C dates to the core sediments in the other hydrate areas of the Japan Sea.

### 2. Microbiostratigraphy of diatom and foraminifera off Joetsu

12 foraminiferal biozones (Biozone I to XII in descending order) in the last 32 ka and 8 diatom zones (A-H diatom zones) in the last 130 ka were recognized based on some piston cores off Joetsu and indicate the paleoenvironmental changes of the surface and bottom sea water, respectively (Nakagawa et al., 2009; Akiba et al., 2014).

### 3. UT13 studies

In July 2013, Umitaka-maru sailed to two new areas to delineate the entire sequence of gas hydrate mound in the Oki-Trough and the Mogami-Trough. Piston corer penetrated down to 6-8 mbsf on hydrate mounds and recovered some massive methane hydrate and 13 core sediments. We analyzed microfossil assemblages and <sup>14</sup>C dating of these sediments and estimated each sedimentation rate by comparing with the previous studies.

#### 3-1. Result 1 - Sedimentation rates of Oki Trough

Main core sediments in the Oki Trough have similar sedimentation rates (about 15 cm/kyr) from 3-4 ka to present, but PC1302 reduced top sediments has a higher rate and PC1305 included methane hydrates a relative lower rate. The sediment age upon massive hydrates from the bottom of PC1305 was calculated ca. 40 ka.

#### 3-2. Result 2 - Microbiostratigraphic features in Mogami Trough

Three cores in the Mogami Trough indicate the lack of sediments around LGM because of older <sup>14</sup>C dates and occurrences of the extinct benthic foraminifera, *Epistominella pulchella*. In particular, whole foraminiferal assemblages of PC1311 sediments are characterized by the distributions of *E. pulchella* and poor preserved specimens, whereas mixed the well-preserved subtropical planktonic species. These features might indicate the gas hydrate activities from the deep seafloor.

Keywords: the eastern margin of the Japan Sea, methane hydrate, microbiostratigraphy, stable isotope, sedimentation rate, extinct species

## Deposition process based on foraminiferal stratigraphy

UMEZAKI, Yosuke<sup>1\*</sup>

<sup>1</sup>Graduate School of Science and Tecnology Kumamoto University

There are mound called Joetsu Knoll and Umitaka Spur which was associated with the formation of methane hydrate off the coast of Joetsu city, Niigata Prefecture. There are valley in east side of Joetsu Knoll, there have a very special geographical features. In this area, previous researches recognized 12 foraminiferal biozones and 8 diatom biozones. These are the good stratigraphic indicators in contrast of sediment core. Sediment core I use to study (MD179-3308) collected from the valley. The length of this core is 30.9m and water depth is 1224m. This core recognized 4 diatom biozones and at 5 layers of this core, radiometric age was measured. From these researches, it was estimated that there was a large age gap around 1620cmbsf in the sediment core. In the valley, it is considered that landslides and flows from the shallow occurred. For clarify depositional process and relationship of valley and mound, in this study, foraminifera in this sediment core was analysed.

Around 1620cmbsf in the sediment core, benthic foraminifera association and planktonic foraminifera numbers are changed. It is considered that the layer of 0 ~1620cm have a sedimentary record of about 30,000 years. In this layer, benthic foraminifera associations are similar to previous researches. It is considered that layer of 1620cm~2820cm have a sedimentary record of about 70,000 years ~110,000 years. Benthic foraminifera is alternated crowd in which *Brizarina pacifica* is priority species, and crowd in which *Eilohedra rotunda*, *Islandiella* sp are priority species. In particular, foraminifera in 1700cmbsf is characterized by *Brizarina pacifica* and maximum number of foraminifera.

*Rutherfordoides rotundata* output from 1000 ~1800cmbsf and 2280cmbsf. It is the related species of *Rutherfordoides coronata* which is methane-related species. Therefore, it is considered that sediment of these layers are derived from the methane seep.

Keywords: benthic foraminifera, planktonic foraminifera, foraminiferal number, methane hydrate, Deposition process

## Marine biomarkers deposited on land by the 2011 Tohoku-oki tsunami

SHINOZAKI, Tetsuya<sup>1\*</sup>; FUJINO, Shigehiro<sup>2</sup>; IKEHARA, Minoru<sup>3</sup>; SAWAI, Yuki<sup>4</sup>; TAMURA, Toru<sup>4</sup>; GOTO, Kazuhisa<sup>5</sup>; SUGAWARA, Daisuke<sup>5</sup>; ABE, Tomoya<sup>6</sup>

<sup>1</sup>University of Tsukuba, <sup>2</sup>University of Tsukuba, <sup>3</sup>Kochi University, <sup>4</sup>GSJ, AIST, <sup>5</sup>Tohoku University, <sup>6</sup>Nagoya University

Tsunami deposits, especially sand deposits is generally used for estimating paleotsunami event. Sand deposit is mainly identified as tsunamigenic on the basis of geological, chemical, biological, archaeological, anthropological, geomorphological, and contextual features, especially geological and biological features such as lateral changes in thickness and grain size of deposit, presence of marine-origin microfossils and others have been frequently utilized as identifying proxies. However, these characteristics do not always get preserved, in which case it is difficult to identify paleotsunami deposit. If evidence of seawater inundation can be detected, it became a good criterion for marine source of sand deposits. As a proxy of seawater evidence, in this study, we focused on biomarker which is molecular fossils originated from formerly living organisms. Biomarker has two advantages. One is their high preservation potential. It is confirmed to be stable in geological time scale. Another is the obvious difference between terrigenous and marine biomarkers; To take the *n*-alkane, lower *n*-alkane homologs, notably C<sub>15</sub>, C<sub>17</sub>, and C<sub>19</sub> *n*-alkanes, tend to be predominant in many algae whereas higher *n*-alkane homologs, such as C<sub>27</sub>, C<sub>29</sub>, and C<sub>31</sub>, tend to be predominant in leaf waxes of higher plants. To verify whether marine biomarkers are deposit on land by tsunami inundation, samples of the 2011 Tohoku-oki tsunami deposit and underlying soil were collected at Sendai and Odaka, Northeast Japan.

In Sendai, a 3 cm-thick fine sand deposits was formed by the 2011 tsunami at the top of core, and there was paddy soil beneath the sand deposits. Biomarkers were measured at 1 layer in sand deposits and 7 layers in soil deposits. Short-chain *n*-alkanes (C<sub>16</sub>, C<sub>17</sub>, C<sub>18</sub>, and C<sub>19</sub>) mainly elaborated from algae and fish were occurred only at 5-6 cm depth. It seems that these short-chain *n*-alkanes were penetrated sandy tsunami deposit and concentrated at 5-6 cm depth. In Odaka, sand deposits were found at 8-15 cm and 18-20 cm depth, and there was paddy soil beneath sand deposits. Organic-rich mud deposits (15-18 cm depth) was intercalated between two sand layers. This mud drape was seems to be formed by first wave together with thin sand layer (18-20 cm depth), and then following waves formed thick sand layer (8-15 cm depth). Biomarkers were measured at 1 layer in surface soil deposits, 8 layers in the 2011 tsunami deposits, and 3 layers in underlying soil deposits. Short-chain *n*-alkanes (C<sub>16</sub>, C<sub>17</sub>, C<sub>18</sub>, and C<sub>19</sub>), pristane, and phytane were detected only from 20-21 cm deep. Pristane is predominately elaborated from zooplankton, benthos, and fish, while phytane is predominately elaborated from zooplankton or sediment itself by biological activity. Presence of these hydrocarbons suggests a contribution from marine/aquatic, and this characteristic is similar to the results of Sendai.

Marine origin hydrocarbons, such as short-chain *n*-alkanes, pristane, and phytane, were detected at soil layers below sandy tsunami deposits in both sites. Since no marine biomarkers were presented further deep soil layer in both sites and surface soil layer overlying tsunami deposit in Odaka, it is highly possible that these biomarkers were transported by the tsunami. Each sediment samples were collected more than two years after the tsunami, it means marine biomarkers have been preserved at least two years. Our study present the first evidence for the marine biomarkers detected from the modern tsunami event, and we propose possibility of biomarkers as a proxy of paleotsunami identification.

Keywords: biomarker, hydrocarbon, tsunami deposit, 2011 Tohoku-oki tsunami



## Geochemical identification of the tsunami deposit using machine learning machine learning techniques

KUWATANI, Tatsu<sup>1\*</sup> ; NAGATA, Kenji<sup>2</sup> ; OKADA, Masato<sup>2</sup> ; WATANABE, Takahiro<sup>1</sup> ; OGAWA, Yasumasa<sup>1</sup> ; KOMAI, Takeshi<sup>1</sup> ; TSUCHIYA, Noriyoshi<sup>1</sup>

<sup>1</sup>Graduate school of environmental studies, <sup>2</sup>Graduate school of frontier science

Tsunami deposit is a direct evidence of inundation area of past tsunamis. A large number of publications have been written about the diagnostic signatures and identification criteria for past tsunamis, including sedimentological, micropalaeontological evidences. However their identification is still difficult because all criteria is neither necessary condition nor sufficient condition due to various origin, mechanism and temporal variation of tsunami deposits. Geochemical discrimination is now recognized as other useful proxy which dose not depend on the researcher's subjectivity, especially in the case that other proxies can not be used. Especially, geochemical indicator is suggested to be useful in identification beyond the limit of recognizable sand deposition. In this study, we established the criteria for geochemical discrimination of 2011 Tohoku-oki tsunami deposits and their background marine sediments using machine learning techniques. For 18 analyzed elements, several tens of elemental combinations show the discrimination rates higher than 99%. By applying the criteria to past tsunami deposits in the Sendai Plain, we discuss the validity and effectiveness of the method.

Keywords: tsunami deposit, machine learning, Geochemistry

## Chemical composition of historical tsunami deposits in the Sendai plain and proposal of geochemical discrimination

HOSODA, Norihiro<sup>1\*</sup> ; WATANABE, Takahiro<sup>1</sup> ; TSUCHIYA, Noriyoshi<sup>1</sup> ; YAMASAKI, Shin-ichi<sup>1</sup> ; NAKAMURA, Toshio<sup>2</sup> ; NARA, Fumiko<sup>1</sup> ; OKAMOTO, Atsushi<sup>1</sup> ; HIRANO, Nobuo<sup>1</sup>

<sup>1</sup>Graduate School of Environmental Science, Tohoku University, <sup>2</sup> Center for Chronological Research, Nagoya University

A magnitude 9.0 earthquake and huge tsunami occurred off the Pacific coast of Tohoku area in Northeast Japan. After the 2011 Tohoku earthquake and tsunami, disaster science is much focused to reduce the damage around costal area, and it plays an important role as making the set of guidelines in an emergency. Because Japanese islands are located on the plate boundaries among the Pacific, Eurasian, Philippine Sea and North American plates, large earthquakes and tsunamis have repeatedly occurred during historic and prehistoric times. A huge tsunami more than 10m-height is often accompanied with submarine earthquakes around the Pacific Rim. The 2011 Tohoku tsunami was the one of the most destructive natural disasters. By the effect of that, study on earthquakes and tsunami become more and more significant, and it a major issue of social concern in Tohoku and other areas. After the 2011 Tohoku tsunami, these invasion areas were covered by a huge amount of tsunami deposits more than 10 million tons. In addition, we are able to obtain past tsunami deposits with the age of ~1000-2000 years before present (BP) in the same area using boring corer. In order to make an expecting tsunami invasion map in other areas as soon as possible, we must provide the information about the distribution of past tsunami deposits. However, it is difficult to discriminate the one of tsunami and other events, such as storm and flood. Additionally, we must establish a new technique to detect invisible muddy and thin tsunami deposits. We need historical archives and geological proxy of past tsunami invasion, but it is rare to have both evidences in many cases. Geochemistry is useful techniques to know the source of terrestrial deposits and these weathering processes. Therefore, we tried to apply geochemical techniques in this study.

Keywords: Jogan tsunami sediments, The 2011 Tohoku tsunami, geochemistry

## Scour and deposition by the 2011 Tohoku-oki tsunami at Takata-matsubara in Rikuzentakata City, Japan

TAKASHIMIZU, Yasuhiro<sup>1\*</sup> ; SHIBUYA, Takahiro<sup>2</sup>

<sup>1</sup>Faculty of Education, Niigata University, <sup>2</sup>Graduate school of Education, Niigata University

The behavior of the 2011 Tohoku-oki tsunami at the Takata-matsubara in Rikuzentakata city was reconstructed using sedimentary facies analysis, grain size properties and magnetic fabric were summarized as follows;

- 1) Vertical variations in grain size of the tsunami deposits show ten and several tsunami inflows and outflows of the tsunamis.
- 2) The deposits were mainly formed by backwash of the tsunami based on the paleocurrent analysis using magnetic fabric measurements.
- 3) The tsunami flow over the artificial sea wall and destroyed the sea wall with large scours on ground surface. Following ten and several tsunamis with minor wave height can ran-up in order to destroying the sea wall.

Keywords: tsunami deposits, Rikuzentakata City, shooting flow, hydraulic jump, Takata-matsubara, Seawall

## Traces of the 2011 Tohoku-oki tsunami as seen from the topography and geology in rias coast, Iwate Pref.

SAKAMOTO, Izumi<sup>1\*</sup>; YOKOYAMA, Yuka<sup>1</sup>; YAGI, Masatoshi<sup>1</sup>; IIJIMA, Satsuki<sup>1</sup>; IMURA, Riichiro<sup>1</sup>; NEMOTO, Kenji<sup>1</sup>; KITO, Takeshi<sup>2</sup>; FUJIMAKI, Mikio<sup>3</sup>; FUJIWARA, Yoshihiro<sup>4</sup>; KASAYA, Takafumi<sup>4</sup>

<sup>1</sup>TOKAI Univ., <sup>2</sup>FODECO, <sup>3</sup>COR, <sup>4</sup>JAMSTEC

The recent 2011 Tohoku tsunami strongly affected the coastal area of the Pacific coast of Tohoku. Tokai University with JAMSTEC investigated the Tohoku coastal area as a part of Tohoku Ecosystem-Associated Marine Sciences (TEAMS). We have succeeded in capturing traces of tsunami in various sea-bottom.

The trace in the bottom topography: Many uneven terrain has distributed around 15 ~20m water depth. Many of its terrain is denudation mark, mark denudation of these exhibits an axial direction southeast of Toni-bay case. In the Okirai-bay a distance of approximately 20km from Toni-bay, denudation phenomenon that traces to develop in 15-25m water depth around has been confirmed. This denudation mark is presumed to have been formed by mud flowing toward the sea floor off the coast on the tsunami wave at the time of argument.

The trace in the high-resolution geo-stratigraphic survey: We have defined the A layer between the reflective surface and 1 seafloor. The A layer is located below a few tens of cm seafloor, and is widely distributed. The A layer is equivalent to the unit 1 of core samples described below. Reflecting surface enriched unevenness is also confirmed A layer below, which are estimated to be the traces of past tsunami activity.

The trace in the sea-bottom columnar core section: We estimate that the surface U-1 layer with grading structure (fine sand at the surface and coarse sand with gravel from lower part) of columnar core was the sediment gravity flow caused by the tsunami activity. The U-2 layer with bioturbation structure estimated by the normal bay sediment. There is some sandy layer with 10cm thick in the U-2 layer and also under the U-2 layer. It is estimated that these sandy layer have been formed by the historical tsunami activity.

Keywords: Tsunami deposit, Sanriku coast

## Shallow-marine sedimentary processes of the 2011 Tohoku earthquake tsunami, inferred from sediment c

TAMURA, Toru<sup>1\*</sup> ; SAWAI, Yuki<sup>1</sup> ; SAWAI, Yuki<sup>1</sup> ; NAKASHIMA, Rei<sup>1</sup> ; HARA, Junko<sup>1</sup>

<sup>1</sup>Geological Survey of Japan, AIST

While subaerial tsunami deposits have been much explored in recent years, our knowledge of shallow-marine tsunami sedimentation and its resultant deposits is limited. In August and September 2012, we practiced vibrocore drilling at 44 sites in Sendai Bay off the Pacific coast of northeastern Japan to investigate features of the open-sea shallow-marine deposits of the 2011 Tohoku earthquake tsunami and their variations. The tsunami deposit was inferred in the uppermost part of the cores based on the extent of bioturbation and concentrations of short-lived radionuclides. The preserved tsunami deposit, where identifiable, is typically 10-50 cm thick. Its grain size is basically similar to that of the original sediment at each site, which differs from medium to fine sand in the lower shoreface, through very fine sand to clay in the inner shelf, to poorly-sorted gravel, sand and mud offshore. This suggests the limited extent of cross-shelf sediment transport. Several lower shoreface sites show a yellowish coarse sand layer at the top. This yellowish layer is differentiated from the underlying greenish gray sand, and is possibly composed of beach sand transported by the tsunami backwash. In the inner shelf, the tsunami layer tends to show multiple inverse and normal grading of grain size as known in some of subaerial tsunami deposits. These features may help identify older shallow-marine tsunami deposits although more research in different settings is needed for establishing comprehensive criteria.

## Sediment transport induced by the 2011 Tohoku-oki tsunami: A shallow seafloor survey at southern part of the Sendai Bay

YOSHIKAWA, Shuro<sup>1\*</sup> ; KANAMATSU, Toshiya<sup>1</sup> ; SAKAMOTO, Izumi<sup>2</sup> ; FUJIMAKI, Mikio<sup>3</sup> ; IMURA, Riichirou<sup>2</sup> ; YAGI, Masatoshi<sup>2</sup> ; NEMOTO, Kenji<sup>2</sup> ; GOTO, Kazuhisa<sup>4</sup> ; SAKAGUCHI, Hide<sup>1</sup>

<sup>1</sup>JAMSTEC, <sup>2</sup>Tokai University, <sup>3</sup>Coastal Ocean Research CO., LTD., <sup>4</sup>Tohoku University

After the 2011 Tohoku-Oki earthquake (Mw 9.0), to examine the tsunami-generated sediment transport and topographic change, and inundation area, a large number of investigations have been conducted on land, particularly at the coastal area of Sendai plain (e.g., Goto et al., 2012, 2014). Understanding the linkage of the transport between land and seafloor is also important. In the present study, to examine the influence of the tsunami and offshore sediment transport, high-resolution shallow seismic survey, sampling of surface sediments, vibracoring, and seafloor observation by underwater video camera were conducted on the shallow seafloor at the southern part of the Sendai Bay, northeastern Japan. The present study will help to understand not only modern sedimentary process induced by tsunami but also identification of paleo-tsunami records, because our knowledge of shallow marine tsunami deposits is limited in contrast to the subaerial tsunami deposits.

One of the principal results is as follows. One or two sharp and continuous reflectors are recognized on the sub-bottom profiles in water depths approx. 6-15 m, excluding the area of outcrops in the southern part of the survey area. With decreasing water depth, depth of the reflectors from the seafloor generally increases (up to approx. 1.5 m). A comparison between the seismic profiles and vibracores infers that the sharp reflectors are erosional surface formed during the 2011 tsunami.

Keywords: shallow marine tsunami deposit, 2011 Tohoku-oki tsunami

## Paleo tsunami events determination using radiogenic nuclides

YOKOYAMA, Yusuke<sup>1\*</sup>

<sup>1</sup>Atmosphere and Ocean Research Institute, University of Tokyo

Recent advancement of mass spectrometry enables us to determine timing of past events using trace amounts of geological samples. Accelerator Mass Spectrometry (AMS) and Inductively Coupled Plasma Mass Spectrometry (ICP-MS) are amongst them and long-lived nuclides can be measured precisely. We have been conducted paleo Tsunami studies applying <sup>14</sup>C and U-series dating employing these techniques. Together with geophysical modeling as well as paleo climate proxy data, paleo Tsunami events are clearly reconstructed from these measurements. Also newly developed AMS, single stage AMS, that is dedicated for <sup>14</sup>C measurements can produce large number of data to constrain the timing in different manner. In this presentation, several examples of these studies will be introduced along with perspectives of age determinations of paleo Tsunami events.

Keywords: Radiocarbon, Accelerator Mass Spectrometry, Uranium series, Quaternary, Dating

## Marker-tephras for the chronological study of tsunami deposits along the Pacific coast of Eastern Japan

SODA, Tsutomu<sup>1\*</sup>

<sup>1</sup>Institute of Tephrochronology for Nature and History Co., Ltd.

Tephra are effective markers for chronological studies of tsunami deposits along the Pacific coast of Eastern Japan. Because the information on marker-tephras in the tephra catalog of Japan and its surrounding area (Machida and Arai, 2003) is only basic, this author describes the detailed characteristics of some important tephra for their identifications.

The Kikai-Akahoya ash (K-Ah), one of representative widespread marker-tephras on the Japanese Islands, erupted 7.3 ka from the Kikai Caldera, covering most of the Pacific coastal area of Eastern Japan. Towada-Chuseri tephra (To-Cu, ca.6.0 ka), Towada-a tephra (To-a, 915 A.D.) and Baegdusan-Tomakomai ash (B-Tm, the 10<sup>th</sup> century A.D.) are markers in the northern Tohoku area. To-Cu and To-a cover the southern Tohoku area, as well. Tephra erupted from Numazawa, Asama and Haruna volcanoes are useful in the southern Tohoku area. They are Numazawa Lake tephra (Nm-N, ca.5.0 k.y.BP), Haruna-Futatsudake-Shibukawa tephra (Hr-FA, the early 6<sup>th</sup> century A.D.), Haruna-Futatsudake-Ikaho tephra (Hr-FP, the middle of the 6<sup>th</sup> century A.D.) and Asama-Kasukawa tephra (As-Kk, 1128 A.D.).

Likewise, tephra from Asama and Haruna volcanoes are useful for chronological studies of tsunami deposits in the Kanto area. They are Asama-C tephra (As-C, the latter half of the 3<sup>rd</sup> century A.D.), Hr-FA, Asama-B tephra (As-B, 1108 A.D.) and Asama-A tephra (As-A, 1783 A.D.). Tephra from Fuji, Amagi, Izu-Oshima, Niijima and Kozushima volcanoes are distributed in the southern Kanto area. As a scoriaceous tephra has difficulty in identification, it is also necessary to check its stratigraphic relationships with silicic marker-tephras, archeological and historical data and radiocarbon ages.

Machida, H. and Arai, F. (2003) Atlas of tephra in and around Japan. Unie. Tokyo Press, 336p.

Keywords: tephra, chronology, tsunami deposit, Eastern Japan, Towada-a tephra, Towada-Chuseri tephra



## Modern and possible paleotsunami deposits in Samenoura, Sanriku Coast, and their relation to tsunami source mechanisms

SUGAWARA, Daisuke<sup>1\*</sup> ; NISHIMURA, Yuichi<sup>2</sup> ; GOTO, Kazuhisa<sup>1</sup> ; GOFF, James<sup>3</sup> ; JAFFE, Bruce<sup>5</sup> ; RICHMOND, Bruce<sup>5</sup> ; CHAGUE-GOFF, Catherine<sup>4</sup> ; SZCZUCINSKI, Witold<sup>6</sup> ; YOKOYAMA, Yusuke<sup>7</sup> ; MIYAIRI, Yosuke<sup>7</sup> ; SAWADA, Chikako<sup>7</sup>

<sup>1</sup>Tohoku University, <sup>2</sup>Hokkaido University, <sup>3</sup>University of New South Wales, <sup>4</sup>Australian Nuclear Science and Technology Organisation, <sup>5</sup>U.S. Geological Survey, Pacific Coastal and Marine Science Center, <sup>6</sup>Adam Mickiewicz University in Poznan, <sup>7</sup>Tokyo University

Samenoura is situated in the bay head of a small inlet on the Pacific coast of Oshika Peninsula, one of the nearest places to the epicenter of the 2011 Tohoku-oki Earthquake. According to the Joint Survey Group, wave heights were measured at more than 20 m near the coastline. This area was severely damaged as a result of both co-seismic subsidence and tsunami inundation.

We carried out field surveys of the Tohoku-oki and paleotsunami deposits at Samenoura in March, May and October 2013. Sandy deposits laid down by the Tohoku-oki tsunami were up to 20 cm thick at locations with an elevation greater than 10 m, and were several cm thick within the forest higher up. The tsunami deposit also contained numerous shell fragments and foraminifera. Although some possible sources of the tsunami deposits can be attributed to narrow sandy beaches near the study area, the deposition of such a thick sandy deposit is more or less enigmatic, considering the steep Ria-type coastal topography.

Using a gouge auger and geoslicer, we found at least two sand layers intercalated within muddy sediments. A volcanic ash layer, which corresponds to the AD 915 Towada-a tephra, was also identified from a horizon between these sand layers. The underlying sand layer was most probably laid down by the 869 Jogan earthquake tsunami, one of the large-scale events known to have affected the region. Previous studies of the Jogan tsunami have proposed several possible source models that involve an interplate thrust earthquake. Given that the local bathymetry and topography of Samenoura Bay may be sensitive to the waveform of a large-scale tsunami, paleotsunami deposits found from this area may be the key to determining the source mechanisms of events on the Sanriku Coast.

In this presentation, the possible correlation of the sandy deposits with known paleotsunami events based on detailed radiocarbon dating is discussed. The hydrodynamic character and processes of tsunami sediment erosion and deposition in Samenoura Bay are analyzed using numerical modeling of both interplate and outer-rise earthquake scenarios.

Keywords: tsunami deposit, 2011 Tohoku-oki and 869 Jogan earthquake tsunamis

## Identification and ages of paleotsunami deposits in Sanriku Coast: Trench survey in Koyadori, Iwate Prefecture

ISHIMURA, Daisuke<sup>1\*</sup> ; MIYAUCHI, Takahiro<sup>1</sup> ; ABE, Kohei<sup>2</sup> ; HAYASE, Ryosuke<sup>3</sup> ; OHARA, Keiichi<sup>3</sup>

<sup>1</sup>Chiba Univ. Sci., <sup>2</sup>OYO Co., <sup>3</sup>Institute of Accelerator Analysis Ltd.

We show new geological evidence of some historical tsunami deposits based on many radiocarbon dating and tephra analysis. Firstly, we sought study area matching for paleotsunami research based on geomorphological analysis and field survey, and excavated trench in coastal lowlands in Koyadori, Iwate Prefecture, northeast Japan. In trench, eleven event deposits (E1-E11: E1 is the 2011 Tohoku-oki tsunami deposits) interbedded within peat/peaty sediments were discovered. Thus, we revealed roundness of each event deposits and modern beach and river deposits to deduce the origin of event deposits. Consequently, we correlated tsunami deposits to historical tsunami events; E1: the 2011 Tohoku-oki tsunami, E2: 1896 Meiji Sanriku tsunami, E3: 1611 Keicho Sanriku tsunami, E4: 869 Jogan tsunami, and identified total eleven tsunami deposits during the last 3000-4000 years.

Keywords: tsunami deposits, Sanriku Coast, 2011 Tohoku-oki earthquake, historical tsunami, AD869 Jogan tsunami

## Geological survey of paleotsunamis at Noda Village, Iwate Prefecture, Japan

GOTO, Kazuhisa<sup>1\*</sup>; IJJIMA, Yasutaka<sup>1</sup>; NISHIMURA, Yuichi<sup>2</sup>; SUGAWARA, Daisuke<sup>1</sup>; YOKOYAMA, Yusuke<sup>3</sup>; MIYAIRI, Yosuke<sup>3</sup>; SAWADA, Chicako<sup>3</sup>; NAKAMURA, Yugo<sup>2</sup>

<sup>1</sup>Tohoku University, <sup>2</sup>Hokkaido University, <sup>3</sup>The University of Tokyo

Along the Sanriku coast, pre-historic tsunami record is still poorly understood in contrast to the well-documented historical tsunamis of past 400 years. AD869 Jogan tsunami is one of these cases. The tsunami affected the Sendai Bay area, as tsunami deposits were reported on Sendai and Ishinomaki Plains, but evidence is unsure if the tsunami was also reached along the Sanriku coast. To explore the paleotsunami histories along the Sanriku coast with emphasis on the possible inundation of AD869 event, we conducted field survey along the coast of Noda Village, Iwate Prefecture. Our survey site is now occupied by paddy and the 2011 Tohoku-oki, 1869 Meiji Sanriku and the 1933 Showa Sanriku tsunamis inundated to this site. We took ~3 m long cores and found several gravel and sand deposits in peat buried by surface paddy soil. Considering the continuous distribution of deposits over 0.7 km from the present shoreline and analytical results of grain size and mineral composition, the deposits are likely formed by the tsunami although further investigation is required. Among these tsunami-like layers, a ~10 cm thick gravel layer is deposited below tephra layers. One of the tephra layers is identified as Baitoushan-Tomakomai tephra (B-Tm) that was deposited in early to middle 10th Century. Volcanic glasses that can be identified as Towada-a tephra (To-a) of AD915 also is observed in patches at the similar horizon as B-Tm tephra. Radiocarbon dating results above the gravel layer is consistent with the tephra chronology. These analytical results as well as tsunami numerical modeling result suggest the inundation of potentially large tsunami before early to middle 10th Century along the northern Sanriku coast.

Keywords: tsunami, tsunami deposit, Noda village, Jogan tsunami

## Origin of a tsunami-drifted rock in Raga, Tanohata, Iwate Prefecture, transported by the Meiji Sanriku Tsunami in 1896.

OJI, Tatsuo<sup>1\*</sup> ; OISHI, Masayuki<sup>2</sup>

<sup>1</sup>Nagoya University Museum, <sup>2</sup>Iwate Prefectural Museum

There are two large boulders on the hill of Raga, Tanohata, Iwate Prefecture. They are located at 24 m above sea level, and approximately 350 m from the coastline. Local villagers have told that these two boulders were derived as tsunami-drifted rocks at the time of Meiji Sanriku Tsunami in 1896. The eastside boulder is approximately 2-3 m in length, 2 m in width and at least 1.5 m in height, and it is estimated to weigh approximately 20 t. This boulder consists of calcarenite, containing numerous individuals of *Orbitolina* sp. that is a common large benthic foraminifera of the Lower Cretaceous. *Orbitolina* is found in 'Orbitolina Facies' of the Miyako Group, and it is particularly abundant in the upper and uppermost part of the Hiraiga Formation. This *Orbitolina*-abundant horizon is exposed near the mouth of Raga inlet, just southwest of Hiraname coast. Therefore, this boulder is estimated to be located originally near the mouth of Raga inlet, and it should be transported as long as approximately 500 m by (a) tsunami(s). It is not certain whether this boulder was moved by one tsunami, or stepwisely by multiple tsunamis. On the other hand, another boulder on the west side of the calcarenite boulder consists of conglomerate with rounded and subrounded pebbles of siliceous shale and chert, and this is considered as derived from the lower part of the Tanohata Formation, which is also exposed just on the southeastern slope of the boulder. This boulder is possibly derived from the southeastern hill, and thus it is not considered as a tsunami-derived rock. In Haibe inlet located about 1.2 km south of Raga, many new tsunami-drifted rocks have arrived onshore particularly on the northwestern side of the bay. The concentrated distribution of these rocks are in concordant with the direction of Tsunami current that came from the southeastern direction toward the earthquake epicenter located off Miyagi Prefecture. On the other hand, the tsunami-drifted rock in Raga is located in the west southwest of Raga inlet. Considering that the epicenter of Meiji Sanriku Earthquake was located off Kamaishi, this location reflects that the Tsunami current came from the east.

Keywords: Miyako Group, Orbitolina, tsunami-drifted rock

## Estimation of the magnitude of tsunami earthquakes along Japan Trench -Re-evaluation of the 1677 Enpo Boso-oki tsunami-

YANAGISAWA, Hideaki<sup>1\*</sup> ; GOTO, Kazuhisa<sup>2</sup> ; SUZUKI, Keita<sup>1</sup> ; KANEMARU, Kinuyo<sup>3</sup> ; SUGAWARA, Daisuke<sup>2</sup> ; YANAGISAWA, Hinako<sup>2</sup> ; HASHIMOTO, Kohei<sup>2</sup> ; IWAMOTO, Naoya<sup>4</sup> ; TAKAMORI, Yoshibumi<sup>5</sup>

<sup>1</sup>Tohoku Gakuin University, <sup>2</sup>Tohoku University, <sup>3</sup>Kansai University, <sup>4</sup>Choshi Geopark, <sup>5</sup>Choshi City Board Education

Along the Japan Trench, unusual earthquakes sometimes trigger much larger tsunamis than expected from their seismic waves, which were called "Tsunami earthquake". The Enpo Boso-oki earthquake tsunami on November 4th of 1677 killed more than 500 persons was a so-called "Tsunami earthquake". The magnitude of this earthquake and tsunami has been estimated based on the historical documents which were recorded more than three hundred years ago. However, it is difficult to conduct accurate estimation for the magnitude of the 1677 earthquake and tsunami because the documents include ambiguous and insufficient descriptions. The aim of this study is to determine the magnitude of the 1677 earthquake and tsunami integrating the analysis of historical documents, field survey of tsunami deposit and numerical simulation. From field survey in Choshi city, Chiba prefecture, we found the candidate tsunami deposit in the Kobatke pond. Radiocarbon dating and tephra analysis indicated that the sand deposit was formed between AD1100 and AD1700. Based on these results as well as the interpretation of historical documents, we concluded the sand deposits were formed by the 1677 Enpo boso-oki earthquake tsunami. We further conducted numerical simulation to estimate the magnitude of the earthquake and tsunami and the magnitude of the 1677 earthquake was estimated as  $M_w=8.34$ . This magnitude is equivalent to that of the 1896 Meiji Sanriku earthquake tsunami which is well known as "Tsunami earthquake". Our results would be very important information to understand the magnitude and nature of "Tsunami earthquake" along Japan Trench.

## The assemblages of foraminifera in paleo-tsunami sediments on Ishigaki island

TU, Yoko<sup>1\*</sup> ; ANDO, Masataka<sup>2</sup> ; CHIEN, Chih-wei<sup>4</sup> ; KITAMURA, Akihisa<sup>5</sup> ; SHISHIKURA, Masanobu<sup>6</sup> ; NAKAMURA, Mamoru<sup>7</sup> ; ARASHIRO, Yasuhisa<sup>7</sup>

<sup>1</sup>Department of Natural History Sciences, Hokkaido University, Japan., <sup>2</sup>Center for Integrated Research and Education of Natural Hazards, Shizuoka University, Japan, <sup>3</sup>Institute of Earth Sciences, Academia Sinica, Taiwan., <sup>4</sup>Department of Earth Sciences, National Chen Kung University, Taiwan, <sup>5</sup>Department of Geosciences, Shizuoka University, Japan, <sup>6</sup>Activity Fault and Earthquake Research Center, The National Institute of Advanced Industrial Science, <sup>7</sup>Department of Physics and Earth Sciences, Ryukyu University, Japan

The Ryukyu subduction zone is generally believed to be aseismic because no large thrust earthquake ( $M > 8$ ) has recently occurred; GPS velocity vectors on the islands are parallel but opposite to the relative motion of the oceanic plate. These observations support the idea that the Ryukyu trench is aseismic or unlocked. However, in 1771 a tsunami struck Ishigaki and Miyako islands with the maximum run-up height of 30 m and caused destructive disaster, which implies that a significant earthquake occurred along the Ryukyu subduction zone. According to Nakamura (2009), the source of this event is a tsunami (slow) earthquake near the Ryukyu trench. Moreover, slow-slip events at depths of 30km (Heki and Kataoka, 2009) and very-low frequency earthquakes at shallow depths near the trench axis (Ando et al., 2012) have been identified in the western Ryukyu trench. These findings suggest that the western Ryukyu subduction zone has a potential to generate large thrust earthquakes.

To estimate recurrence intervals and sizes of paleo-tsunamis near the Ryukyu trench, we excavated Holocene deposits at 5 sites on Ishigaki Island during the years of 2011 to 2013. We analyzed the assemblages of foraminifera in the sediments that were transported by tsunamis from the deep seafloor. Most of foraminifera detected from the deposits are benthonic and planktonic foraminifera are rare in all samples at the excavation sites. Species of benthonic foraminifer such as *Calcarina defranciai* (living at 15 to 50 m depths) are dominant in the tsunami deposits compared to the current beach sand. In addition, some mesopelagic species that commonly live at continental shelf depths are also identified from the tsunami sediments. We found that the percentage of mid epipelagic and mesopelagic species in the deposits can provide a significant key to identify paleo-tsunamis. On the western Ishigaki Island, if the population density of these species in a deposit exceeds 10 %, it can be concluded as a tsunami origin, while on the eastern coast if the population density exceeds 20 %, it can be a tsunami deposit because of the bathymetric reasons.

Together with the results of stratigraphic facies and C14 dating data of the above tsunami sediments, we identified three large tsunamis (similar to the 1771 tsunami) in the past 2000-3000 years: in 1771, between 10-11<sup>th</sup> C and between 2000 and 2900 cal. B.P. The average recurrence interval of large earthquake was found to be very long, 500 to 1000-2000 years along the western Ryukyu trench.

Keywords: tsunami sediments, foraminifera, Ryukyu subduction zone, paleo-tsunami, 1771 tsunami

## Tsunami sediment in the Okinawa Island

SHIGA, Shota<sup>1\*</sup>; NAKAMURA, Mamoru<sup>1</sup>; FUJITA, Kazuhiko<sup>1</sup>; ARASHIRO, Yasuhisa<sup>1</sup>; YAMASHIRO, Sakaki<sup>1</sup>; SUNAGA, Naoya<sup>1</sup>; SANA, Tomoko<sup>1</sup>; TAMAKI, Naoyuki<sup>1</sup>

<sup>1</sup>Faculty of Science, University of Ryukyus

The occurrence interval of mega-tsunamis in the south Ryukyu arc was estimated to 200-500 years from the ages of tsunami boulders (Nakata, Kawana 1994, Araoka et al., 2013). The source of 1771 Yaeyama tsunami (Meiwa tsunami), which was the latest mega-tsunami, is interpreted as the M8 class thrust-type earthquake in the Ryukyu trench from the numerical simulation of tsunami. However, past tsunamis have not been found in the central Ryukyu arc because the tsunami boulders were not detected in this area. No tsunami records were documented in the old literatures of central Ryukyu arc. We conducted a tsunami sediment survey in the Okinawa Island to investigate the history of large tsunami on the central Ryukyu Trench. We performed drilling survey from 4 to 15 March 2013 in the Okinawa Island in a collaboration with the coastal disaster prevention section of civil engineering and construction division, the Okinawa Prefectural Office. Survey sites were is Kijoka (Ogimi Village), Teima (Nago), Yaka (Kin Town), Yagi (Nakagusuku Village), Oyama (Ginowan). The sand layers, which have the possibility of tsunami sediments, were found at the cores samples of Teima and Yagi from visual observation. Then, we analyzed the sand layers and their overlying and underlying layers, and compared them with the sand layers. Teima-1 (elevation 4.5m, 0.4km from the coast) is located at the back marshes of the inner part of Oura Bay. We collected five samples at the depth between 1.85m to 1.25m from the surface ground. Yagi1-3 (elevation 2.8-3.1m, 0.1-0.2km from the coast) are located at the coastal lowlands along Nakagusuku. We collected 7 samples at the depths between 0.8m to 4.15m at Yagi-1, 4 samples at the depths between 1.35m to 2.05m at Yagi-2, and 1 sample at the depth of 1.95m at Yagi-3. Furthermore, we sampled modern coastal sands near the survey sites. First, the samples were charged with 10-fold diluted hydrogen peroxide solution after drying completely at the temperature of about 60 degrees. Then samples were washed by the water flow during sieving 63um. After that, the samples were divided to a particle size of five types for using sieve. Foraminifera analysis method was conducted the particle size of 1.00mm ~0.5mm from sample collection. We picked the samples so as to contain over 150 individuals of foraminifera. Next we classified them to dominant species foraminifera and other species. In addition, we compared their foraminifera composition with those of modern coastal sand, and estimated the origin of the sediment. From the core samples of Teima-1, we detected 3 individuals of *Anomalinella* at the depths of 1.55 m and 1.65 m, and 2 individuals of *Calcarina Mayori* at the depth of 1.65 m. This suggests that the sediments at the depths of 1.55 m and 1.65 m were moved from out of the reef because these species live out of the reef. From the core samples of Yagi-1, we detected 2 individuals of *Anomalinella* at the depths of 3.75 m and 3.85 m, and 4 individuals of *Dendritina* and 3 individuals of *Operculina* at the depth of 3.75 m. Since these species live out of the reef, the sediments at the depths of 3.75 m and 3.85 m were moved from out of the reef. Next we detected 4 individuals of *Dendritina* and 4 individuals of *Operculina* at the depth of 1.85 m in the core sample of Yagi-2. As well, we detected 2 individuals of *Dendritina* at the depth of 2.05 m in the core sample of Yagi-2. These suggest that the sediments at the depth of 1.85 m and 2.05 m were moved from the out of the reef. Thus, we found that the species, which live in the out of reef, were included in the core samples of Teima and Yagi. A possible mechanisms to move the sediment from seafloor to land are ocean waves, storm surges, and tsunamis. However, since ocean waves and storm surge are attenuated by the reef, these could not move the sediments from out of the reef. The sediments which contain the species living out of the reef would have been moved by tsunamis.

Keywords: tsunami, tsunami sediment, foraminifera

## Recognition of washover deposits in the Shizuoka Plain, based on analysis of shape of sand grains

KITAMURA, Akihisa<sup>1\*</sup>; OGURA, Kazuki<sup>1</sup>; UBUKATA, Takao<sup>1</sup>

<sup>1</sup>Shizuoka Univ

Three-dimensional morphometric analyses were performed to compare the shape of the sand grains as mentioned below. The surface of the upper part of the sand grain was first scanned to collect the x-, y- and z-coordinates of each point on the grain surface using a Shimadzu OLS4000 confocal laser scanning microscope. The obtained upper surface was connected with its vertically reflected shape to obtain a symmetric closed surface model. The surface model was then converted into a solid model by filling the inside of the surface model with equally spaced points. The axes of sand grains were defined as the principal component axes for the 3D coordinate data of the points consisting of the solid model. The aspect ratios of the sand grain was computed as the square roots of the ratios between eigenvalues of the covariance matrix between the coordinates. The collected coordinate data for the upper surface were normalized for location, orientation, and size so that the centroid of the solid model is placed at the origin, the major axis is placed along the x-axis, and the volume of the solid model is fixed at a constant value. A series of the normalized z-coordinates of individual points was defined as the shape function of the corresponding x- and y-coordinate data and was then decomposed into a 2D domain using a two dimensional Fourier transform. The shape of the sand grain was represented by a set of Fourier amplitudes of each frequency. The angularity was assessed for each grain by the sum of the Fourier amplitudes of the first and higher harmonics divided by the magnitude of the 0th harmonic.

The results of the morphometric analyses clearly indicated that the ratio of the minor axis length to the major axis length well defines the difference in grain shape between beach sands and inferred flood sediments. Most of the flood sediments have smaller aspect ratio (i.e., elongate form) than do most of the beach sands. Scatter plots of the angularity against the aspect ratio for the two sedimentary environments were fairly separated with only slight overlap along the axis of the aspect ratio. Variation in angularity was greater among flood sediments than among beach sands and there was no beach-sand grain with the angularity larger than 7.89. The composition of inferred tsunami deposits seems a mixture of the flood and beach sediments in terms of their grain shape.

Keywords: washover deposits, sedimentary grains, analysis of shape



## Two paleotsunami layers in Kushiro Wetlands and their wide correlation in eastern Hokkaido

NAKAMURA, Yugo<sup>1\*</sup> ; NISHIMURA, Yuichi<sup>1</sup>

<sup>1</sup>Institute of Seismology and Volcanology, Hokkaido University

Two paleotsunami sand layers, Ks-TS1 and Ks-TS2, were identified in peatland in Kushiro, eastern Hokkaido. Ks-TS1 occurs several cm beneath Ko-c2 (AD 1694) and Ta-b (AD 1667) tephtras, and Ks-TS2 occurs 10 cm above B-Tm tephra (ca. 1000 yBP). Thicknesses of these layers are less than 1-3 mm. Particle size of Ks-TS1 is around 2 phi and Ks-TS2 is around 4 phi. They can be identified by their particle size distribution in the precision of 1/16 phi using Morphologi G3. Ks-TS1 is found at the site located about 2120 m from the modern coastline, 5.9 m above the mean sea level, and Ks-TS2 about 1810 m from the modern coastline, 5.7 m above the mean sea level. The actual run-up limit of paleotsunami may exceed these deposition areas.

At present analytical method is not available to correlate paleotsunami layers across distant regions. However, the tsunami layers in Kushiro are likely correlated with paleotsunami layers in other regions in eastern Hokkaido (Urahoro, Kinashibetsu, Onbetsu, Akkeshi, and Nemuro) on the basis of the stratigraphic relationships between the paleotsunami layers, marker tephtras, and peat layers. In Kushiro region, thickness of the peat layer between Ta-b and Ks-TS1 is 16 % of the total peat thickness between Ta-b and B-Tm, and thickness between Ta-b and Ks-TS2 is 81 %. These ratios are similar between Kushiro and other regions, although 10-20 % difference can be seen. According to previous researches, up to eight paleo-tsunami layers in the last 3000 years were identified in eastern Hokkaido. The paleo-tsunami layers in Kushiro are correlated with the last two events and presumed to be the greatest events in the last 3000 years.

Keywords: Paleotsunami deposit, correlation, Precise grain size analysis, Morphologi G3, Hokkaido

## Insight of large tsunami recurrence around the Sea of Japan revealed by surveys of historical and pre-historical tsunami

NISHIMURA, Yuichi<sup>1\*</sup> ; RAZJIGAEVA, Nadya<sup>2</sup> ; GANZEY, Larisa<sup>2</sup> ; GREBENNIKVA, Tatiana<sup>2</sup> ; KAISTRENKO, Viktor<sup>2</sup> ; GORBUNOV, Alexsey<sup>2</sup> ; NAKAMURA, Yugo<sup>1</sup>

<sup>1</sup>Hokkaido University, <sup>2</sup>Far East Branch of Russian Academy of Sciences, Russia

Tsunami deposits provides essential information for assessing tsunami and earthquake hazards in areas where recurrence of tsunamis are not known or poorly recorded. Northern coast of the Sea of Japan is one of these areas. Recent earthquakes such as the 1940 Shakotan-oki, the 1983 Nihonkai-chubu and the 1993 Hokkaido Nansei-oki earthquakes caused severe damage along the coastal communities in SW Hokkaido, Japan, however, the past tsunami in this region are not known. The historical tsunamis inundated not only in the Japanese coast but also along the Primorye coast, Russia, located at the other side of the Sea of Japan. We repeated reconnaissance along the Primorye coast to find the historical and pre-historical tsunami evidences. In the region, there are natural lowlands facing sandy beach that are suitable for tsunami deposit formation and preservation. The surveys were done from 2010 to 2013 as a joint research project with Hokkaido University and the Russian Academy of Science. We could trace sandy or muddy tsunami deposits buried in the peat associated with the modern tsunamis, and also found candidate of tsunami deposits at multiple sites along the coast. The sandy layers include significant amount of marine diatoms. Based on the C14 dating results of peat sandwiching the sandy layers, age of the events are estimated to be ca. 350 BP, 600 BP, 800 BP and 2100 BP. In Kit Bay, the southernmost site in our survey area, B-Tm tephra (ca. 1000 AD) were deposited patchy between the 800 BP and 2100 BP. Most of the paleo-event deposits are traced inland up to a few hundred meters from the present coast and they are distributed at 4-5 m above the sea level. These might be the first evidence for the recurrence of large tsunamis around the Sea of Japan in the past.

Keywords: tsunami deposit, Primorye, Sea of Japan, paleo-tsunami, historical tsunami

## Preliminary study for evidence of tsunami deposits from Holocene sediments along the coastal area of the Wakasa Bay.

YAMAMOTO, Hirofumi<sup>1\*</sup> ; URABE, Atsushi<sup>2</sup> ; SASAKI, Naohiro<sup>1</sup> ; TAKASHIMIZU, Yasuhiro<sup>3</sup> ; KATAOKA, Kyoko S.<sup>2</sup>

<sup>1</sup>Fukui University, <sup>2</sup>NHDR, Niigata University, <sup>3</sup>Niigata University

This study reconstructed the Holocene sedimentary environment and researched the distribution of possible tsunami deposits in the coastal plain along the Wakasa Bay area in Fukui Prefecture.

Around the Wakasa Bay Area, some historical documents suggested the tsunami event of AD 1586 (Tensho Tsunami), but no sedimentary evidence of this event was reported from this area. So, we carried out reconnaissance along the coastal area of the Wakasa Bay to find the natural lowlands facing sandy beach that are suitable for tsunami deposit reservation. For example, at the Sonobe area in Takahama-cho, a low land behind the beach ridges was said to have been a marshes area, and our preliminary study show that this area had shifted from inner bay environments to marshes area about 3000 years ago. At these places, we study the Holocene sediment using the Geoslicer of 5 meters long.

Keywords: Wakasa Bay area, coastal plain, tsunami deposits, Holocene

## Bleaching of K-feldspar grains contained in the tsunami deposits of the 2011 off the Pacific coast of Tohoku Tsunami

HAYASHIZAKI, Ryo<sup>1\*</sup> ; SHIRAI, Masaaki<sup>1</sup>

<sup>1</sup>Tokyo Metropolitan University

Optically stimulated luminescence (OSL) dating is feasible method to obtain depositional age from sediments and then, it is expected to be useful for tsunami deposits dating. However, it is not clear that the degree of sun bleaching during tsunami transport processes. Firstly, bleaching of K-feldspar grains during tsunami transport processes was investigated with post-IR IRSL (pIRIR) dating using the 2011 off the Pacific coast of Tohoku Tsunami deposits. Then, single-grain OSL dating was attempted to obtain accurate equivalent doses of tsunami deposits. Equivalent doses of K-feldspar grains obtained from various sampling locations and positions.

Comparing IRSL and pIRIR equivalent doses which showed different decreasing rates of OSL intensities with the sunlight exposure time, sandy tsunami deposits were hardly exposed sunlight during tsunami transport processes. However, nearly zero equivalent dose of single-grain OSL measurement was often acquired. Probably, these “ zero-dose ” K-feldspar grains had been exposed enough to sunlight before the tsunami. Upper position of one run-up tsunami deposits seemed to be rich in K-feldspar grains suggesting the accurate depositional age.

Keywords: tsunami deposits, Optically Stimulated Luminescence, post-IR IRSL, K-feldspar, sedimentary structure, Fukushima

## Sedimentological features of tsunami deposit caused by the 2011 Tohoku-oki earthquake tsunami

YOSHII, Takumi<sup>1\*</sup> ; HAMADA, Takaomi<sup>1</sup> ; SASAKI, Toshinori<sup>1</sup> ; MATSUYAMA, Masafumi<sup>1</sup> ; TANAKA, Shiro<sup>1</sup> ; ITO, Yuki<sup>1</sup> ; WATANABE, Masakazu<sup>2</sup> ; OKUZAWA, Koichi<sup>3</sup>

<sup>1</sup>Central Research Institute of Electric Power Industry, <sup>2</sup>Ceres, Inc., <sup>3</sup>Obayashi Corporation

In some areas, the inundation distances of the 2011 Tohoku-oki earthquake tsunami was comparable to that of the 869 Jogan tsunami estimated by geological investigations of tsunami deposits. This fact revealed the potential of research of tsunami deposits to speculate the scales of future tsunamis, resulting in strong social demand to detect ancient tsunamis, especially giant tsunamis, using geological studies. Investigation of present tsunami deposits is crucial to understanding sedimentological features of tsunami deposits because the present tsunami deposits can be identified with high reliability and the investigation of the surrounding circumstances is also feasible. In this study, we collected tsunami deposits caused by the 2011 Tohoku-oki earthquake tsunami from 19 areas with different topography. The obtained cores were observed by the unaided eye and by using CT images. In this presentation, we will discuss sedimentological features of these tsunami deposits and relationship with the surrounding circumstances.

Keywords: Tsunami deposit, The 2011 Tohoku-oki earthquake, Tsunami

## Characteristic of tsunami deposit left by 2011 Tohoku earthquake, case study of Toni bay

IJIMA, Satsuki<sup>1\*</sup> ; SAKAMOTO, Izumi<sup>1</sup> ; YOKOYAMA, Yuka<sup>1</sup> ; YAGI, Masatoshi<sup>1</sup> ; IMURA, Riichiro<sup>1</sup> ; NEMOTO, Kenji<sup>1</sup> ; FUJIMAKI, Mikio<sup>2</sup> ; FUJIWARA, Yoshihiro<sup>3</sup> ; KASAYA, Takafumi<sup>3</sup>

<sup>1</sup>Tokai University, <sup>2</sup>COR, <sup>3</sup>JAMSTEC

The recent 2011 Tohoku tsunami strongly affected the coastal area of the Pacific coast of Tohoku. The result of onshore features for tsunami impact is well researched, but offshore is only a few researches.

In this presentation, we will show about characteristic of tsunami deposit left by 2011 Tohoku earthquake, case study of Toni bay. We researched about tsunami deposit using acoustic equipments (Multi beam echo sounder ; MBES, Sub bottom profiler ; SBP) and Vibration core sampler (VCS).

The first of all, as the characteristic of submarine topography was sectionalized to 4 areas from topography profile of the valley axis direction.

Second, SBP data was seen signature reflecting surface (40-100cm down from seabed), and it was able to track at the wide area. Thickness of this reflecting surface and seabed were estimate 25-110cm in this bay. This thickness corresponded with the characteristic of the submarine topography.

Moreover, columnar sample of 13T\_V\_2 (water depth 14 m) could be divided into U1 (sand), U2 (mud), and the U3 (gravel bed). Sand to silt sediments layer with grading (fine sand to gravel) structure observed at the U1. We assume this U1 is 2011 tsunami deposit. The boundary of between U1 and 2 has continuity reflecting surface by SBP data and confirm distribution of this reflecting surface and thickness.

Finally, we were able to estimate tsunami deposit distributed with thickness approximately 25-110cm, and high thickness was distributed to the valley axis.

Keywords: Tsunami deposit, Sanriku Coast

## Characteristic of tsunami deposit left by 2011 Tohoku earthquake, case study of Hirota bay

YOKOYAMA, Yuka<sup>1\*</sup> ; SAKAMOTO, Izumi<sup>1</sup> ; YAGI, Masatoshi<sup>1</sup> ; IMURA, Riichiro<sup>1</sup> ; IJIMA, Satsuki<sup>1</sup> ; KANEI, Tatsuki<sup>1</sup> ; NEMOTO, Kenji<sup>1</sup> ; KITO, Takeshi<sup>2</sup> ; FUJIMAKI, Mikio<sup>3</sup> ; FUJIWARA, Yoshihiro<sup>4</sup> ; KASAYA, Takafumi<sup>4</sup>

<sup>1</sup>Tokai University, <sup>2</sup>FODECO, <sup>3</sup>COR, <sup>4</sup>JAMSTEC

The recent 2011Tohoku tsunami strongly affected the coastal area of the Pacific coast of Tohoku. The study of onshore features for tsunami impact is well researched, but offshore is only a few researches. In this presentation, we will show about characteristic of tsunami deposit left by 2011Tohoku earthquake at Hirota bay using by Sub bottom profiler (SBP) and Vibration core sampler (VCS).

We took the total 17sites columnar core (2012:5sites, 2013:12sites) at water depth 8-25 m. The columnar cores were able to sectionalize to 2 units from lithofacies. Unit-1 consists of sand layer and Unit-2 consists of muddy sediment.

Unit-1 was sand to silt sediments layer with grading (fine to very coarse consists gravel and shell fragments) and lamination, and has forms the erosion surface with the lower layer. We assume that denudation is boundary of previous or after tsunami sediment and upper layer (Unit-1) is 2011tsunami deposit. And, Unit-1 was able to sectionalize to some subunits (Unit1a-1e) by grain size analysis and soft X-ray photo.

Unit-2 was massive sediments with fine sand to silt layer characterized by bioturbation. We assume this unit is normal sediment in this bay. And, some columnar cores have Unit-3(underlying layer of Unit-2) that has similar characteristics of Unit-1.

We estimate the 2011tsunami deposit distribution with thickness approximately 20-50 cm, and high thickness area was valley axis and estuarine region, and those area have sedimentation axis each other (NNW-SSE and NW-SE), and join together at offshore area (around 20m). So, tsunami deposits become thicker by overlap with a few tsunami deposits at offshore area.

Keywords: Tsunami deposit, Sanriku coast

## Characteristic of tsunami origin submarine topography -Case study of Toni Bay and Okirai Bay

YAGI, Masatoshi<sup>1\*</sup> ; SAKAMOTO, Izumi<sup>1</sup> ; YOKOYAMA, Yuka<sup>1</sup> ; MIZUNO, Ren<sup>1</sup> ; IIJIMA, Satsuki<sup>1</sup> ; NEMOTO, Kenji<sup>1</sup> ; FUJIMAKI, Mikio<sup>2</sup> ; FUJIWARA, Yoshihiro<sup>3</sup> ; KASAYA, Takafumi<sup>3</sup>

<sup>1</sup>School of Marine Science and Technology, Tokai University, <sup>2</sup>COR, <sup>3</sup>JAMSTEC

The recent 2011 Tohoku tsunami strongly affected the coastal area of the Pacific coast of Tohoku. Toni Bay located south of Kamaishi city and open toward east. Also Okirai bay open toward east. Tokai University started survey there to confirm effect of Tsunami in 2012

Survey of first year, we make extensively submarine topography. As a result, anomaly topography was observed at Toni Bay (depth of 20-25m) and Okirai (depth of 15-20m). Transparent layer with poor internal reflection was observed as the surface layer within the anomaly topography by Sub Bottom Profiler (SBP). Characteristic of columnar core have grading structure (fine to coarse) of sand sediment and erosion structure between sand sediment and clay sediment. It was guessed that erosion structure was made by turbidity current by tsunami activity. For the above reason, estimated anomaly topography is Tsunami origin topography. So we survey around anomaly topography area more closely in 2013. Describe below the character of Toni Bay and Okirai Bay.

[Toni Bay]

In this research area, submarine topography can be divided into three: 1)gentle slope (0.9 degrees) at depth of 15-22m, 2)planation surface at depth of 22-24m, 3)gentle slope at depth of 24m or more. On the 1)-3), these are a lot of protuberance has distributed. Around the protuberance, current marks like a fan or delta shape extend to toward offshore. And groove mark also observed. And we assume this tsunami origin submarine topography have control by protuberance in this way.

[Okirai Bay]

In this research area, topography can be divided into three: 1)gentle slope (1 degrees) at depth of 8.5-17.5m, 2)planation surface at depth of 17.5-19m, 3)gentle slope at depth of 19.5m or more. On the 1), these are a lot of protuberance has distributed. Some tool mark that is cause of protuberance distribute similar to Toni bay, but most of current mark show scour mark.

Tsunami origin submarine topography has almost same character (ex. Water depth) at both bays. But formation factor is different from Toni and OKirai bay.

Keywords: Tsunami orijin submarine topography, Toni Bay, Okirai Bay, Current mark



## Relationship between the inundation limit and the maximum extent of the sandy tsunami deposit in Sendai Bay coasts

ABE, Tomoya<sup>1\*</sup> ; GOTO, Kazuhisa<sup>2</sup> ; SUGAWARA, Daisuke<sup>2</sup>

<sup>1</sup>Department of Geography, Nagoya University, <sup>2</sup>IRIDEs, Tohoku University

Maximum landward extent of the sandy tsunami deposits can be regarded as the minimum inundation limit. Before the 2011 Tohoku-oki tsunami, recent post-tsunami field surveys along low-lying coastlines showed that sandy tsunami deposits commonly extend to approximately over 90% of the actual inundation limit (MacInnes et al., 2009). On the other hand, after the 2011 Tohoku-oki tsunami, some researches of the 2011 tsunami pointed out that the significant gap (0.6-2.0 km) between the inundation limit and the maximum landward extent of the sandy tsunami deposit where the inundation distance was more than 2.5-3.0 km (Goto et al., 2011; Abe et al., 2012; Shishikura et al., 2012). However, it is uncertain why the gap appeared. This study focuses on the relationship between the maximum extent of sandy tsunami deposits and inundation limit of the 2011 Tohoku-oki tsunami.

Inundation limits of the Tohoku-oki tsunami were assessed over 15 shore-normal transects in the Sendai Bay coast. Inundation distances of the 15 transects were found to range from 0.60 to 5.07 km. The maximum limit of the sand layer extended to 2.3-3.0 km (55-74% of the inundation distance) along 6 transects in the wide coastal plain in the northern-middle part of the Sendai Plain. Absence of the sandy tsunami deposits over 3.0 km inland may explained by the limitation of the sand supply from sand beach and sand dune.

Keywords: 2011 Tohoku-oki tsunami, Sendai Bay coast, Inundation limit, Maximum extent of sandy tsunami deposit

## Historical tsunami deposits in Numanohama on the Sanriku coast, Japan

GOTO, Tomoko<sup>1\*</sup>; SATAKE, Kenji<sup>2</sup>; SUGAI, Toshihiko<sup>1</sup>; ISHIBE, Takeo<sup>2</sup>; HARADA, Tomoya<sup>3</sup>; MUROTANI, Satoko<sup>2</sup>

<sup>1</sup>GSFS, the University of Tokyo, <sup>2</sup>ERI, the University of Tokyo, <sup>3</sup>CIDIR/ERI, the University of Tokyo

We conducted tsunami deposit survey in a small valley along the Sanriku coast, Japan, just north of Taro (Miyako city, Iwate prefecture), where the 2011 tsunami heights from the Tohoku earthquake ranged from 17 to 34 m. We identified six tsunami deposits during the recent 500 yrs from the 3-m long Geo-slicer sample. The uppermost one is located on or just below the ground surface and probably from the 2011 Tohoku earthquake. The <sup>210</sup>Pb and <sup>137</sup>Cs dating analyses indicated that the 2<sup>nd</sup> to 4<sup>th</sup> uppermost tsunami deposits can be correlated with historical tsunamis: the 1960 Chilean tsunami, the 1933 and 1896 Sanriku tsunamis. According to Japanese historical documents, other candidate tsunamis since the 15<sup>th</sup> century are from the 1793 Miyagi-oki earthquake, the 1763 and 1677 Aomori-oki earthquakes, the 1677 Boso-oki earthquake, and the 1611 Sanriku earthquake. Other trans-Pacific tsunamis includes the 1700 Cascadia tsunamis severe damage along the Sanriku coast and these tsunami deposits may be also preserved.

After the 2011 Tohoku earthquake, many surveys for tsunami deposits have been conducted in Sendai plain (Goto *et al.*, 2011, Marine Geology; Shishikura *et al.*, 2012, Annual Report on Active Fault and Paleoequake Researches). There are few reports of tsunami deposit studies along the Sanriku coast. Furthermore, depositional ages of many identified tsunami traces along the Sanriku coast were estimated to be several thousand years before present. The reasons for absence of recent tsunami deposits include that the Sanriku coast is a ria coast characterized by sawtooth-shaped coastline. Because of the steep-sloped valleys, alluvial deposits are very limited and tsunami traces are difficult to be preserved. Around the survey site, however, a marsh is separated from open sea by a beach ridge of ~ 4m high. In this marsh, well-decomposed peat has been developed. The sand deposits were brought by large tsunamis over the beach ridge and preserved in the marsh peat. Our study is the rare case that the geological evidence of recent historical tsunamis was continuously identified.

To identify tsunami deposits, we sketched the sedimentary structure, measured the distribution of grain sizes, and analyzed the microfossils. Depositional ages of tsunami deposits were estimated on the basis of radiocarbon (AMS) dating and <sup>210</sup>Pb, <sup>137</sup>Cs analysis. The <sup>210</sup>Pb dating is useful to determine the depositional rate during the recent 100 years because of its short decay time (the half life time is 22.3 year). The <sup>137</sup>Cs dating is useful to judge whether the depositional ages are before or after the start of atmospheric nuclear experiments in AD 1954.

Peat and sand layers are alternated with their thickness of several centimeters to several tens centimeters. Each sand layer consists of beach pebble and sand or rock pieces from host rock in this area. The sand layers have structure characteristic to tsunami deposit: erosional contact, alternation of normal- and inverse-grading, lamination and thin mud layer sandwiched between two sand layers. The sand layer can be traced continuously along the landward transect. Abundant marine microfossils in the sand layers indicate that the sea water flow into the marsh with the tsunami sand.

The <sup>14</sup>C result shows that peat at around 3 m depth deposited after the 15<sup>th</sup> century. The <sup>210</sup>Pb decay curve indicates that the deposition ages of the upper four tsunami deposit layers are during recent 100 yrs. The 2<sup>nd</sup> uppermost tsunami deposit can be correlated with the 1960 Chilean tsunami because <sup>137</sup>Cs was detected down to this layer.

### Acknowledgment

We thank Kazuomi Hirakawa and Javed N. Malik for giving useful comments and suggestions in the field. We also thank Jun Muragishi, Ryutaro Naruhashi, Satoshi Kusumoto, Akira Takigawa, Tsuyoshi Yamaichi and Ravi K. Parabhat for helping the field survey.

Keywords: Tsunami deposit, Sanriku coast

## A Study of Paleo-Tsunami along the Coastal Area of Akita Prefecture, the eastern margin of Japan Sea

KAMATAKI, Takanobu<sup>1\*</sup> ; HOSOYA, Takashi<sup>2</sup> ; KUROSAWA, Hideki<sup>3</sup>

<sup>1</sup>Akita University, <sup>2</sup>Chuo Kaihatsu Corporation, <sup>3</sup>OYO Corporation

Tsunami is the most destructive natural disaster on the coastal area. North-eastern Japan along the Japan Sea has been suffered by tsunamis, such as the 1833, 1983, and 1993 tsunamis. Recently, tsunami deposits have been reported from various areas and environments in Japan. However, paleo-seismological study based on the tsunami deposits has not been reported from along the coastal area of Akita Prefecture. We report a study of paleo-tsunami along the coastal area of Akita Prefecture. These results will be presented in this session.

Keywords: tsunami deposit, paleo-tsunami, eastern margin of Japan Sea, Akita Prefecture

## Paleoenvironmental changes and tectonic movements reconstructed from diatoms in Tokushima, during the last 4000 years

CHIBA, Takashi<sup>1\*</sup> ; FUJINO, Shigehiro<sup>1</sup> ; KOBORI, Emmy<sup>2</sup>

<sup>1</sup>Faculty of Life and Environmental Sciences University of Tsukuba, <sup>2</sup>College of Geoscience, School of Life and Environmental Sciences, University of Tsukuba

The average recurrence interval of the interplate earthquakes along the Nankai Trough is estimated from many historical records and archaeological data (Sangawa 2008). However, the studies of tectonic movement related to Nankai earthquakes is still limited (Maemoku 1989, Shishikura et al. 2008).

Yuki city, Tokushima prefecture, which located in north part of the Nankai Trough, has been subsided and many tsunamis attacked along the coast of the Shikoku islands accompanied by the previous Nankai earthquakes. Therefore, some historical documents and memorial monuments written about the past Nankai earthquakes and tsunamis remain in this city.

In order to obtain the geological evidences of tectonic movements and tsunami deposits, we conducted a 7m long core drilling at a small marsh behind a barrier spit in Tainohama of Minami city nearly Yuki city. The core includes more than 12 sand layers in organic-rich muddy sedimentary succession up to 5 m depth in this core. And we analyzed fossil diatoms from the core.

The diatom assemblages included in the peat and peaty mud deposits were predominated by fresh and brackish water species, especially *Pseudostaurosira brevistriata*, *Pseudostaurosira subsalina*, *Staurosirella pinnata*, *Tabellaria fenestrata*. *Pinnularia* spp. and *Eunotia* spp. are also dominated. In contrast to the above mentioned sand layers, brackish water and marine species, especially *Diploneis smithii*, *Mastogloia recta* were increased. The diatom assemblages from the organic rich muddy sediments and radiocarbon ages indicates that freshwater marsh or saltmarsh formed in this region during at least the past 4000 years. On the other hand, the diatoms from the sandy layers indicates that salinity of environments when the layers were formed was higher than freshwater or salt marsh. The diatom assemblage suggest that the sand layers were transported from seaside by past tsunamis. On the other hand, changes of diatom assemblages in the muddy sediments show increase or a decrease of freshwater species, suggesting a paleo coastal environment changes due to past earthquakes along the Nankai Trough.

Keywords: Nankai trough, Tsunami deposit, Tectonic movement, Pleo coastal environment, Diatom

## Study of tsunami deposits along west coastal area of Kagoshima Prefecture, Japan

OSHIMA, Akihiro<sup>1\*</sup> ; HARAGUCHI, Tsuyoshi<sup>2</sup> ; TAJIRI, Yuuta<sup>3</sup>

<sup>1</sup>West Japan Engineering Consultants, Inc., <sup>2</sup>Osaka City University, <sup>3</sup>Kyushu Electric Power Co., Inc.

In the west coast of the Kyushu district, there is no plate boundary in the front, and there is few record of an earthquake and tsunami. There are little investigations and researches of tsunami deposits in this area compared with East Coast facing the Pacific Ocean. However, reexamination of the disaster prevention planning in a coastal area is advanced by the occurrence of the 2011 off the Pacific coast of Tohoku Earthquake, and it is necessary to expand the data about the past tsunami history.

We have investigated the literature about records of the disasters of tsunami, and observed drilling core. We read aerial photos and topographical maps, and classified topography such as beach ridge, sand dune, backswamp. Based on the geographical classifications, we confirmed geographical features and existence of reclaimed land, and determined the survey sites. Drilling cores were taken in ten sites along the west coastal areas of Kagoshima Prefecture. In order to clarify lateral continuity of sediments, several cores were taken at each site. In consideration of sea level change, we collected sediments after about 6,000-7,000 years ago.

We acquired X-rays CT images to visualize internal structure of sediment three-dimensionally without destroying core. After having photographed X-rays CT image, we divided the core into half in lengthwise direction and observed the surface. Sediments are dated using radiocarbon dating and tephrochronology.

Some event deposits are identified in the drilling core taken from Gumizaki site, Nakayama site and Hashima site. Ages of these event deposits are around 7,000 cal BP and 9,500 cal BP (Gumizaki site), 3,500-2,500 cal BP (Nakayama site). However, these event deposits are not defined in other sites. These event deposits were possibly made by local event.

We found the layer including volcanic glass derived from the Kikai-Akahoya tephra in drilling core which were taken from Gumizaki site. The layer was possibly carried by the event accompanied with explosion of Kikai caldera.

In this presentation, we discuss the depositional environmental changes and the origin of event deposits by analysis of micro-fossil and detail observation of cores.

Keywords: tsunami deposits, event deposits, Kagoshima Prefecture

## Tsunami deposits in eastern coast area of Ishigaki Island, Japan.

KITAMURA, Akihisa<sup>1\*</sup>; ANDO, Masataka<sup>1</sup>; TU, Yoko<sup>4</sup>; OHASHI, Yoko<sup>1</sup>; NAKAMURA, Mamoru<sup>2</sup>; MIYAIRI, Yosuke<sup>3</sup>; YOKOYAMA, Yusuke<sup>3</sup>; SHIGA, Shota<sup>2</sup>; IKUTA, Ryoya<sup>1</sup>

<sup>1</sup>Shizuoka University, <sup>2</sup>Ryukyu University, <sup>3</sup>The University of Tokyo, <sup>4</sup>Institute of Earth Sciences, Academia Sinica

We found two tsunami deposits in eastern coast area of Ishigaki Island, Japan. The tsunami deposits contain many pebble-sized bioclasts such as coral fragments and mollusks, and clay rip-up clasts comprising material from the underlying soil. These deposits have erosive basement and fine upward. These layers thin abruptly at the landward margins, and fine inland. The altitude of the landward end of the lower and upper tsunami deposits attain up to 6 and 8 m, respectively. We referred to as deposits T-II and T-I in order of ascending stratigraphic position. Radiocarbon ages of excellent preserved and articulated marine bivalves mean that T-I and T-II were caused by the AD 1771 Meiwa tsunami and by tsunami at 740-500 cal. yrs BP (AD 1210-1450), respectively. It is noteworthy that abundant fragments of coral and molluscs remains are found from the debris flow deposit below T-II. Radiocarbon ages suggest these fragments were transported up to 8 m elevation by tsunami between 2490-2240 and 930-620 cal. yrs BP.

Keywords: tsunami deposits, Ishigaki Island

## The use of benthic foraminifera within tsunami sediments

MAMO, Briony<sup>1\*</sup> ; TOYOFUKU, Takashi<sup>1</sup>

<sup>1</sup>Japan Agency for Marine and Earth Science and Technology

Tsunami hazard assessment begins with a compilation of past events that have affected a specific location. Given the inherent limitations of historical archives, the geological record has the potential to provide an independent dataset useful for establishing a richer, chronologically deeper time series of past events. Recent geological studies of tsunami are helping to improve our understanding of the nature and character of tsunami sediments. Wherever possible, researchers should be increasingly working to improve the research 'tool kit' available to identify past and analyse modern tsunami events. Marine, benthic foraminifera (single celled heterotrophic protists) have often been reported as present within tsunami-deposited sediments but in reality, little information about environmental conditions, and by analogy, the tsunami that deposited them, has been reported even though foraminifera have an enormous capacity to provide meaningful palaeo-environmental data. In light of more recent tsunami events, the use of foraminifera has increased yet their full potential in this capacity is still often not frequently utilised. We discuss the potential use of foraminifera within tsunami research using results from specific case studies from Japan, south Asia, North America, Europe, the UK and New Zealand. We present an updated review in the gaps in our understanding on this topic area and reassert models for 'better' practice where possible, to assist researchers who examine foraminiferal assemblages within tsunami geology.

Keywords: Tsunami, Foraminifera, Benthic, Tsunami deposit

## Measuring the relative humidity within an error of 0.1% by Arduino

MATSUO, Ryo<sup>1\*</sup> ; SAKAI, Satoshi<sup>1</sup>

<sup>1</sup>Graduate School of Human and Environmental Studies, Kyoto University

It is said that the forest is cooler than the city. We measure the temperature and relative humidity at Kyoto University and Mt.Yoshida to find what causes the difference.

We used humidity and temperature sensor IC within an error of 0.1 percent.

We found that always forest is cooler and wetter than city. However the latent heat of vaporization of water did not cool the air on a day change.

Keywords: relative humidity, tempature, measure, Arduino, Forest and City



## Spontaneous rotation of a block of ice on a flat surface of a warm metal column

TANAKA, Masashi<sup>1\*</sup> ; HOHOKABE, Hirotaka<sup>1</sup> ; YOSHIDA, Shigeo<sup>2</sup> ; NAKAJIMA, Kensuke<sup>2</sup>

<sup>1</sup>Graduate School of Science, Kyushu University, <sup>2</sup>Faculty of Science, Kyushu University

### Summary

We have discovered that a block of ice placed on a flat surface of a warm brass column rotates slowly without any external mechanical driving force.

### Description of the Phenomenon

A column of brass, whose radius and height are 8cm and 16cm, respectively, is placed with its flat surface set horizontally. After it is warmed at least to the room temperature, a flat bottomed block of home-made ice, whose radius and height are 10cm and 4cm, respectively, is placed on the flat surface of the brass column. As the block of ice melts, it begins to rotate about the vertical axis spontaneously. The direction of the rotation does not change by itself. However, it reverses instantaneously if we gently tap the ice block to the opposite direction. The rotation period is typically about 20 seconds. The rotation stops when the brass column cools or when the ice block melts and the brass surface becomes exposed.

### The Importance of Bubbles between the Ice and the Brass Surface

If we use a block of factory-made ice which contains no bubbles, the ice does not rotate. However, if we drill non-through holes on the bottom surface of the ice block so that air bubbles shall be supplied between the ice and brass surface as the ice block melts, the ice rotates. The behavior of the air bubbles observed when the ice rotates and that observed when the ice rotation is blocked are quite different. When the ice rotates, the air bubbles tend to elongate radially and are nearly stationary relative to the brass surface. When the ice is anchored and does not rotate, the air bubbles flow outward, deforming and moving randomly. The observed behaviors above imply a crucial role played by the bubbles in the physics of this phenomenon.

### The Importance of Heat Supply

We measured temperature distribution within the brass column, and found a strong positive correlation between the vertical temperature difference in the column and the angular velocity of the ice rotation. We also conducted a similar experiment using a column of stainless steel, whose thermal conductivity is considerably smaller than brass, the rotation period tends to be quite longer. These observations imply that the flux of heat supplied by the heat conduction in the column of metal is crucial to the emergence of the phenomenon.

### Future Directions

Presently, we have no concrete idea on the dynamics of the phenomenon, even though the strong relationship between the heat supply and the angular velocity suggests that the phenomenon may be interpreted as a kind of heat engine. In the near future, we will conduct more experiments with parameters being better controlled, and with the results of such additional experiments, we will investigate physics of the phenomenon from various aspects.

Keywords: bubble, ice, rotation, heat engine, phase change, spontaneous motion

## Regimes of solutions of an axisymmetric flow in a cylindrical tank with a rotating bottom

IGA, Keita<sup>1\*</sup>

<sup>1</sup>AORI, The University of Tokyo

Non-axisymmetric flows are often observed even in axisymmetric environments in the terrestrial and planetary atmospheres. Such a non-axisymmetry is realized in a simple laboratory experiment using a cylindrical container which is filled with water driven by a rapidly-rotating disk at the bottom. We have been reported on the results of the experiments. When we investigate the mechanism of these phenomena, the solution of the axisymmetric flow realized under this condition is necessary, and we reported last year the expression of the analytical solution obtained using boundary layer theories.

We investigated the features of this analytical solution precisely and extracted some features related to its stability. Applying the solution to the situation with water free surface, we can classify the realized axisymmetric flow into three regimes: (i) Cases where all part of the bottom disk is covered with water and it is divided into inner rigid-body rotation region and outer region with constant angular momentum (ii) Cases where the water exposes the center part of the bottom disk air and the water is divided into inner rigid-body rotation region and outer region with constant angular momentum, and (iii) Cases where the water exposes the center part of the bottom disk air and all the water keeps constant angular momentum. Applying the analytical solution, we elucidated the parameter dependence of the transition between these regimes. Each regime has different characteristic waves, which affects crucially the stability of the flow.

Moreover, in the boundary layer along the side wall, transverse velocity distribution has a jet like structure, which forms negative vorticity gradient region. It is also an important factor which may cause critical layer instability.

Keywords: rotating flow, symmetry breaking, boundary layer, axisymmetric flow, stability

## Benchmark experiments for Venus AGCM: sensitivities to model and astronomical parameters

YAMAMOTO, Masaru<sup>1\*</sup> ; TAKAHASHI, Masaaki<sup>2</sup>

<sup>1</sup>Kyushu University, <sup>2</sup>University of Tokyo

Benchmark experiments and inter-comparisons of atmospheric general circulation models (AGCMs) have been conducted in the climate and Geophysical Fluid Dynamics (GFD) communities. Recently, the AGCM inter-comparisons are extended to Venus and hot extrasolar planets. The ISSI inter-comparison project of Venus AGCM (Lebonnois et al. 2013) shows that there are large differences among the models under the same Venus-like condition, and some model parameters influence the general circulation structures. At the present stage, in the inter-comparisons project, the wave analyses have yet to be fully conducted. For Venus' atmospheric modeling, we need to investigate sensitivity to model parameter (such as resolution), in order to understand the numerical properties of the AGCM and to confirm the model results. In terms of GFD, sensitivity to astronomical parameter (such as planetary rotation) is interesting in profoundly understanding the dynamics of superrotation in a mimic slowly rotating planet, which is represented by the base simulation in the inter-comparison. By using the widely-used benchmark, we can easily compare with previous models. In the present study, the base simulation of the ISSI project is applied to a MIROC AGCM for checking the validity of the Venus model, and is extend to the sensitivity experiments for model resolution (T21, T42, T63, and T106) and planetary rotation (Venus, Titan, and Earth), in which the general circulations and waves are analyzed. In the Venus case, as the model resolution is increased, the total angular momentum of the whole atmosphere becomes larger, although the cloud-top superrotation weakens. This indicates that the high-resolution contributes to the accumulation of the angular momentum in the lower atmosphere. The eddy momentum and heat fluxes in the lower atmosphere are also sensitive to the horizontal resolution. Associated with the eddy heat flux, the indirect circulation is also influenced by the resolution. In T42 and higher resolution experiments, the high-latitude jet and polar indirect circulation are extended to the lower atmosphere. The lower-atmospheric high-latitude jet induces large equatorward eddy angular momentum fluxes. In this presentation, we discuss the sensitivities to model resolution and planetary rotation, based on the transformed Euler mean and Eliassen-Palm flux analyses, which are useful even for slowly rotating planet with very small Coriolis force (although they are not widely used in atmospheric researches of Venus).

## Relationship between structure and replacement of concentric eyewalls in idealized tropical cyclones

TSUJINO, Satoki<sup>1\*</sup> ; TSUBOKI, Kazuhisa<sup>1</sup>

<sup>1</sup>HyARC, Nagoya University

Eyewall is a ring of convective clouds that encircles the eye of a tropical cyclone (TC) such as typhoon and hurricane. TC occasionally has some eyewalls which are called as concentric eyewalls. Once concentric eyewalls are formed, eyewall replacement often occurs. The eyewall replacement is a process that the inner eyewall gradually decays and the outer eyewall moves into the position of the inner (old) eyewall. The wind speed of TC rapidly varies during the replacement (Willoughby, 1987). However, the eyewall replacement does not always occur even if concentric eyewalls are formed and the process of eyewall replacement is not fully known. Tsujino and Tsuboki (2013; the Fall Meeting of the Meteorological Society of Japan) indicated that, on the basis of some analyses of Typhoon Bolaven (2012), the vertical flow of the outer eyewall is weaker than that of the inner eyewall and the outer eyewall tilts relative to the inner eyewall in the long-lived concentric eyewalls. Therefore, we suspect that the eyewall replacement is related to the structure of the concentric eyewalls of TC.

In this study, we investigate the relationship between structure and replacement of concentric eyewalls in some idealized TCs. We conduct some parameter experiments for structure of concentric eyewalls in TC, using the Cloud Resolving Storm Simulator (CReSS; Cloud Resolving Storm Simulator, Tsuboki and Sakakibara, 2007) which is a three-dimensional, nonhydrostatic model. And we investigate the structure of concentric eyewalls in these experiments. In our experiments, the initial wind field was axisymmetric and cyclonic vortex, which is hydrostatic and gradient wind. This wind field was based on the eq. (2) and (3) of Terwey and Montgomery (2008, hereafter TM08). The initial thermodynamic field was given by Jordan (1958; hereafter J58). The horizontal grid spacing was 2 km. The number of vertical grids was 45 and the vertical grid interval on the lowest layer was 100 m. The calculating domain had 2000 km x 2000 km x 22.5 km. The simulation time for each experiment was 500 hour. For each experiment, SST value was constant, horizontally uniformed and did not change during the simulation. We considered that structure of concentric eyewalls varies with the radial profile of the tangential wind of TC, on the basis of TM08. Therefore we conducted some parameter experiments for SST and vertical instability in the atmosphere. Because these parameters are sensitive for the maximum tangential wind of TC (Rotunno and Emanuel, 1987). We had four experiments: (1) SST = 301 K, thermodynamic field was J58, (2) SST = 302 K, thermodynamic field was J58, (3) SST = 302 K, thermodynamic field was J58 + 3 K, (4) SST = 300 K, thermodynamic field was J58 + 1 K. Here " J58 + 3 K " means that 3 K was uniformly added to the potential temperature profile of J58, and " J58 + 1 K " was the same of " J58 + 3 K " but except for the added value of 1 K. We named experiments of (1) - (4) as " CTL " , " S302 " , " ST302 " , " ST300 " , respectively.

In CTL and S302, eyewall replacements occurred on several occasions during the last 100 hours. On the other hand, in ST302, clear concentric eyewalls were formed. However, eyewall replacement did not occur over 500 hours. In ST300, concentric eyewall was not formed. In CTL and S302, the outward slope associated with height of the outer eyewall was similar to that of the inner eyewall. Moreover, the vertical wind speed in the outer eyewall was comparable with that in the inner eyewall. The other hand, in ST302, the outward slope of the outer eyewall was more gradual than that of the inner eyewall. For the vertical wind speed, it was weaker than that of the inner eyewall. These characters is also indicated in the simulated Typhoon Bolaven (2012) of Tsujino and Tsuboki (2013). Thus, we think that the occurrence of eyewall replacement is related to the similar extent of the slope between the inner and outer eyewall associated with height.

Keywords: tropical cyclone, concentric eyewall, eyewall replacement, vortex dynamics

## Mechanism of vortex movement in environmental vorticity gradient and its estimation

YAMADA, Kao<sup>1\*</sup> ; IGA, Keita<sup>1</sup>

<sup>1</sup>AORI, The University of Tokyo

Yamazaki and Itoh(2013) proposed SAM(selective absorption mechanism) as the maintenance mechanism of the blocking which is known as quasi-steady state of the atmosphere. The essence of SAM is vortex-vortex interaction and the blocking can subsist for a prolonged period by absorbing eddies of the same polarity. The movement of tropical cyclones and mid-latitude cyclones have also been investigated by vortex-vortex interaction (e.g. Fiorino and Elsberry, 1989; Oruba et al., 2012). Also, it has been indicated that the key parameters of vortex movement are the absolute vorticity gradient of the environment, the radius of vortex and its strength (e.g. DeMaria, 1985; Chan and Williams, 1987), but these researches remain at a posteriori argument of the results of the numerical simulations. In this study, we conducted numerical simulations using variety of combinations of these parameters by means of two-dimensional nondivergent barotropic model. Besides, we investigated the mechanism of the vortex movement by vortex-vortex interaction and evaluated it quantitatively.

It was found that the time-development of the vortex movement is divided into two periods with different features: the acceleration regime at the initial stage and the vortex pair translation regime with quasi-steady movement. In each regime, the vortex excites characteristic vorticity field around it and the vortex movement showed different dependence on the parameters. While the vortex slightly rotates and deforms the background field in the acceleration regime, another prolonged vortex with opposite sign appears in the eastside of the original vortex in the vortex pair translation regime.

In the acceleration regime, we evaluated the acceleration by applying directly the concept of SAM and obtained the results that the movement velocity is proportional to the product of the absolute vorticity gradient, the circulation of the vortex and the elapsed time. In the vortex pair translation regime, the velocity of the vortex movement can be evaluated by a few number of the parameters which characterize the counterrotating vortex beside, considering the mechanism of the vortex pair propagation. As a result, it is shown that the velocity is proportional to the product of the two-thirds power of the circulation of the vortex and the one third power of the planetary vorticity gradient. These estimations represent the dependence of the each-period velocity on the parameters well, and we succeeded in clarification of the physical effect on the vortex movement by the parameters and estimation of the vortex displacement.

We evaluated these parameters of the experiments for the effective beta and revealed that the difference of the influence of the planetary vorticity gradient and the relative vorticity gradient on the vortex movements results in the shear of the background flow, which has not clearly shown by previous researches.

Keywords: vortex

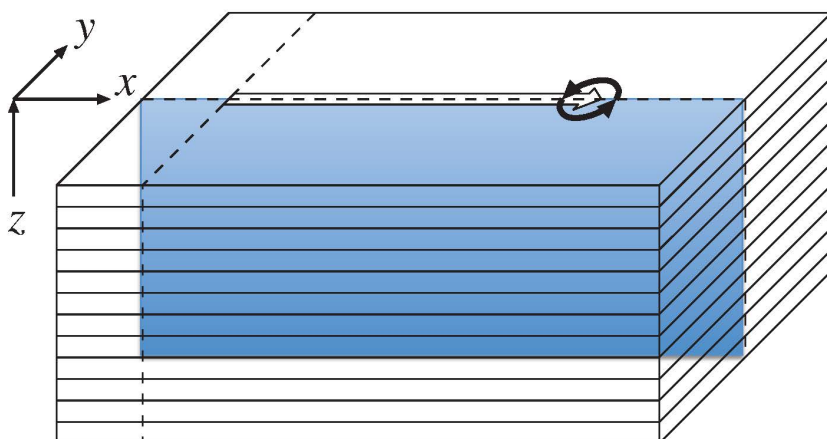
## A phase-independent expression for the energy flux associated with inertia-gravity waves

AIKI, Hidenori<sup>1\*</sup>

<sup>1</sup>Japan Agency for Marine-Earth Science and Technology

For diagnosing the effect of stationary Rossby waves on atmospheric circulation, a phase-independent expression for the wave activity flux has been developed by Takaya and Nakamura (2001) using quasigeostrophic equations. On the other hand, concerning inertia-gravity waves, a phase-expression has not been derived in previous studies. Recently we have developed a phase-independent expression for both the energy flux and the pseudo momentum flux associated with inertial-gravity waves. We have investigated the performance of the new expression using high-resolution simulations for internal waves in the ocean, such as internal gravity waves generated by a moving storm (figure) as well as tidal internal waves in JCOPE-T. The new expression for the energy flux may be used to reduce a noise associated with sampling errors in a model output, while the new expression for the pseudomomentum flux may be used for the diagnosis of mountain waves.

Keywords: inertia-gravity waves, energy flux, phase dependency



## A mechanistic model of double-diffusive intrusions

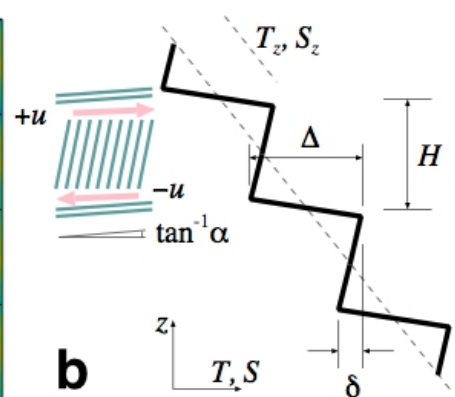
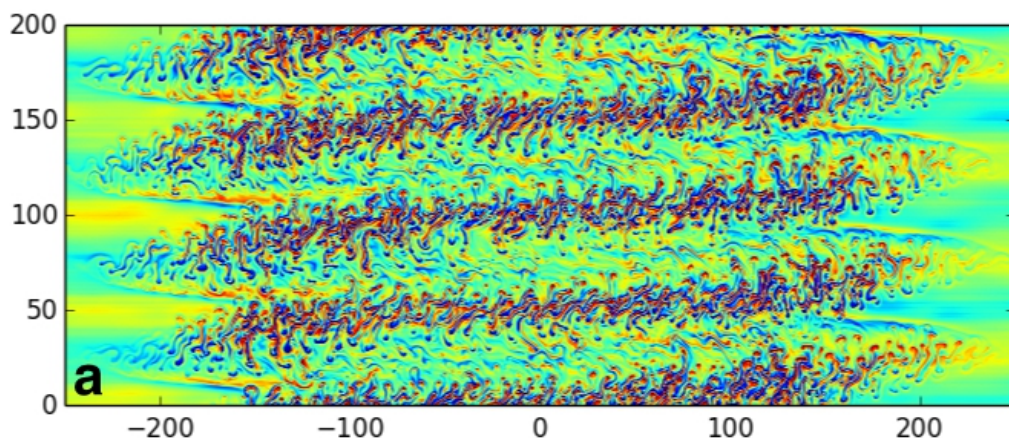
NOGUCHI, Takashi<sup>1\*</sup>

<sup>1</sup>Graduate School of Engineering, Kyoto University

Dynamical structure of double-diffusive interleaving at a density-compensating thermohaline front is investigated. Numerical simulations successfully reproduced a series of sloped intrusive motions (fig. a). It is revealed that the finger convection and its collective vertical buoyancy transport drastically changes the inner structure of the layers as well as the slope of the intrusion layers. To understand the dynamical balance of the motions in layers, a mechanistic model of intrusive layers was devised for an idealised configuration in which a unit layer repeats in vertical direction (fig. b). Transports of heat and salt by small-scale convective motions are parameterised in terms of large-scale quantities. Balances between parameterised transports yielded results qualitatively consistent with that of the numerical simulations.

Acknowledgements: This work was supported by JSPS Grant-in-Aid for Young Scientists B 23740354.

Keywords: double-diffusive convection, lateral mixing



## Low-frequency internal waves in Shiozu Bay, Lake Biwa: A numerical approach

AUGER, Guillaume<sup>1\*</sup> ; NAGAI, Takeyoshi<sup>2</sup> ; YAMAZAKI, Hidekatsu<sup>2</sup>

<sup>1</sup>Department of Civil Engineering, Ritsumeikan, <sup>2</sup>Department of Ocean Science, TUMSAT

In this study, we present results from the three-dimensional unstructured numerical simulator SUNTANS, used to understand the dynamics of the low-frequency internal wave field inside Shiozu Bay, a bay in the Northern part of Lake Biwa. Initial conditions for a fine-scale grid were generated in using a coarse grid with measured heat fluxes and wind stress. After being compared against observational data, the simulation reproduced consistently the low-frequency internal wave field, (similar frequencies and waves features). Based on the analysis of integrated potential energy and integrated dissipated energy time series, this study shows that the low-frequency internal wave field that enters Shiozu Bay does not either completely dissipate or break. Moreover isotherm elevation associated to the internal the first horizontal mode and first vertical mode Kelvin wave highlights the cyclonic rotation pattern, which is characteristic of the Kelvin wave, within the bay. This result shows that the part of the Kelvin wave entering the bay goes in and out. Moreover the dynamic of the internal wave field within the bay displays an peculiar process at the narrowing of the bay. At the contraction of the bay, the flow speeds up and deep isotherms deepen further. These two processes generated turbulence by shear and strain; according to the turbulence model (Mellor and Yamada, 1982) turbulent kinetic dissipation rate reached  $10^{-6} \text{ W kg}^{-1}$ , occurring during the trough phase of the internal wave field. Additionally the occurrence of these enhanced turbulent events appears to depend on the amount of energy detained by the low frequency internal wave. When the internal wave field was energized by the wind the turbulent events were enhanced. Such events could modify the long-term distribution of material in the lake.

Keywords: wind forcing, internal waves, contraction, strain



## Anomalous wave dispersion of distant tsunamis in a coupled system between the self-gravitating elastic Earth and ocean

WATADA, Shingo<sup>1\*</sup>

<sup>1</sup>Earthquake Research Institute, University of Tokyo

Traveltime delay and waveform dispersion of distant tsunamis that propagated over the Pacific after the 2010 Chilean and 2011 Tohoku-Oki earthquake can be understood as a propagating wave in a unified gravitationally and elastically coupled system between the solid Earth and ocean.

Keywords: Tsunami propagation delay, Tsunami phase velocity measurements, Tsunami waveform dispersion, Tsunami initial phase with reversed polarity, Tsunami precursor, DART tsunami records from the 2010 Tohoku?Oki earthquake and

## On the vigor of mantle convection and stagnant lid formation in super-Earths

MIYAGOSHI, Takehiro<sup>1\*</sup>; KAMEYAMA, Masanori<sup>2</sup>; OGAWA, Masaki<sup>3</sup>

<sup>1</sup>JAMSTEC, <sup>2</sup>Ehime University, <sup>3</sup>University of Tokyo

Super-Earths are extra-solar terrestrial planets which have large sizes and masses (up to about ten times the Earth's mass). Understanding mantle convection in super-Earths is a key to clarifying their evolution, surface environment, and habitability. In large super-Earths, the mantle depth far exceeds the thermal scale height, and adiabatic compression strongly influences super-Earths' mantle convection in contrast to the Earth's one. In this paper, we present numerical models of mantle convection in super-Earths with high compressibility, high Rayleigh number, temperature-dependent viscosity and depth-dependent thermal expansivity.

Thermal convection of compressible infinite Prandtl number fluid is solved in a rectangular box under anelastic approximation by the ACuTEMAN (Kameyama et al. 2005). The model of the super-Earths includes depth-dependent thermal expansivity and density, as well as a strong temperature-dependence of viscosity. We assume the mass of the planet is ten times the Earth's. The Rayleigh number defined with the viscosity at the core-mantle boundary (CMB)  $Ra$  is  $1E10$ . A viscosity contrast  $r$  up to  $1E7$  arises between the CMB and the surface owing to the temperature-dependence of viscosity. The employed grid number is 1024 (horizontal) and 256 (vertical).

We identified the stagnant lid regime in the model of super-Earths. When the viscosity contrast  $r$  is larger than about  $1E6$ , a stagnant lid of highly viscous fluid is formed along the surface. The lid hardly moves and is not involved in the convection, as has been observed earlier for the Boussinesq model of the Earth's mantle convection (Kameyama and Ogawa, 2000). The lithosphere is as thick as about thirty percent of the depth of the whole mantle, and the Nusselt number is about three at  $r=1E7$  and  $Ra = 1E10$ . This value is comparable to that of the Earth's model at the same  $r$  but at much lower  $Ra$  of  $6E6$  (Kameyama and Ogawa, 2000). The lithosphere is much thicker than has been expected earlier for super-Earths (e.g., Valencia et al. 2007), and the thick lithosphere is likely to affect the possibility of plate tectonics at the surface of super-Earths. The strong effect of adiabatic compression also affects the dynamics of hot plumes that ascend from the CMB when the temperature-dependence of the viscosity is strong: At  $r > \sim 1E3$ , hot plumes from the CMB are strongly suppressed. They do not ascend to the surface of the planet. The overall pattern of convective circulation in the mantle is, therefore, dominated by the cold plumes that descend from the lithosphere to the CMB. The low efficiency of heat transport by the mild convection would strongly affect the evolution history of super-Earths, and is likely to weaken the core convection, and thus, the magnetic field of super-Earths.

Keywords: super-Earths, mantle convection

## Heater size effect on generation of thermal plumes

KUMAGAI, Ichiro<sup>1\*</sup> ; YAMAGISHI, Yasuko<sup>2</sup>

<sup>1</sup>Meisei University, <sup>2</sup>IFREE, JAMSTEC

Mantle plumes from the CMB experience a filtering effect by the endothermic phase change at the 660-km phase transition. Fluid dynamics predicts that the hot mantle plumes stagnate at and locally heat the upper-lower mantle boundary, which causes generation of the secondary plumes in the upper mantle, and hence hotspots volcanic activities on the surface. To understand the effects of heater size on the plumes generation, we have experimentally investigated the behaviors of thermally buoyant plumes generated from a localized heat source (circular plate heater) using quantitative visualization techniques of temperature (TLC) and velocity (PIV) fields. Scaling laws for their ascent velocity and spacing of the plumes are experimentally determined. We also estimate the onset time of the secondary plumes in the upper mantle which depends on local characteristics of the thermal boundary layer developing at the upper-lower mantle boundary.

Keywords: plume, mantle, fluid dynamics, experiment

## Waves and linear stability of magnetoconvection in a rotating cylindrical annulus

HORI, Kumiko<sup>1\*</sup> ; TAKEHIRO, Shin-ichi<sup>2</sup> ; SHIMIZU, Hisayoshi<sup>1</sup>

<sup>1</sup>Earthquake Research Institute, University of Tokyo, <sup>2</sup>Research Institute for Mathematical Sciences, Kyoto University

Magnetohydrodynamic waves in a rapidly rotating planetary core can cause the magnetic secular variation. To strengthen our understanding of the physical basis of such waves, we revisit the linear stability analyses of thermal convection in a quasi-geostrophic rotating cylindrical annulus with an applied toroidal magnetic field, and we extend the investigation of the oscillatory modes to a broader range of the parameters. Particular attention is paid to influence of thermal boundary conditions, either fixed temperature or heat-flux conditions.

While the non-dissipative approximation yields a slow wave propagating retrograde (westward), termed as a Magnetic-Coriolis/Magnetic-Coriolis-Archimedes (MC/MAC) Rossby wave, dissipative effects produce a variety of waves. When magnetic diffusion is much stronger than thermal diffusion, this can cause a very slow wave propagating prograde (eastward). Retrograde-travelling slow waves appear when magnetic diffusion is weaker. Emergence of the slow modes allows convection to occur at lower critical Rayleigh numbers than in the nonmagnetic case. When the magnetic diffusion is strong, the onset of the convection occurs with the prograde-propagating slow wave, whereas when it is weak, a slow MC mode conducts the critical convection.

Fixed heat-flux boundary conditions have profound effects on the marginal curves, which monotonically increase with the horizontal wavenumber, and lead to larger length scales at the onset of the convection, provided there is sufficient field strength that the Lorentz force is balanced with the Coriolis force. The effect, however, becomes less clear as the magnetic diffusion is weakened and various magnetohydrodynamic waves emerge.

## Investigation of cell patterns on a rotating convection by ultrasonic velocity profile measurements

FUJITA, Kodai<sup>1\*</sup> ; TASAKA, Yuji<sup>1</sup> ; MURAI, Yuichi<sup>1</sup> ; OISHI, Yoshihiko<sup>1</sup> ; YANAGISAWA, Takatoshi<sup>2</sup>

<sup>1</sup>Hokkaido University, <sup>2</sup>IFREE JAMSTEC

Rayleigh-Benard convection is the well-known topic as fundamental system in fluid dynamics. In particular, the effect of rotating field on the convection is one of essential piece for geophysics. The influence of centrifugal force and Coriolis force on convection pattern formation was experimentally showed by Rossby (1969). The flow structure of Rayleigh-Benard convection in a rotating field is described by Rayleigh number (Ra), Taylor number (Ta) and Prandtl number (Pr). Especially, it is important to study the behavior of low Pr fluid like liquid metals, because this knowledge helps to understand the dynamics of metallic cores in planets. In low Pr fluids, the flow regimes dramatically changes in comparison with ordinal fluid with  $Pr > 1$ . For example, Rayleigh-Benard convections in a liquid metal layer easily take transition to turbulent state. Generally, adding rotating field stabilizes the flow. On the other hand, flows of low Pr fluids with background rotation are expected to become oscillatory and irregular motion near the marginal stability conditions. These characteristics of low Pr fluids, however, have not been studied experimentally so much, because it is impossible to capture the convection patterns of liquid metal flows optically. To solve this problem, the authors adopt Ultrasonic Velocity Profile (UVP) method to visualize convective flow of liquid metal in a rotating field. As the data set of UVP measurement is one-dimensional velocity distribution, it is difficult to guess flow fields of convection from only a result of UVP without any criterion of translation. In this study, as preparations for liquid metal experiments, we performed two different visualizations using optics and ultrasound on ordinal transparent fluid, water ( $Pr = 7$ ), to understand flow field from spatio-temporal velocity distribution obtained by UVP. Optical visualization provides path line images for the comparison. In addition, we purpose to take the knowledge about spatio-temporal velocity distribution of high Pr contrasted with low Pr.

Experiments were performed on a rotating table. The vessel of fluid layer has a square geometry, which aspect ratio is seven. The bottom of fluid layer was heated by electrical heating and the upper surface was cooled by circulating water through flow channel made of glass plate. Optical visualization images were obtained from a horizontal section of the fluid layer. An ultrasonic transducer for UVP measurement was mounted horizontally on the side wall of fluid layer.

The path line showed many small round convective cells in the fluid layer, and it represented that the size of cells become smaller as Ta takes larger. In addition, the size of cell and cell motions were also detected by spatio-temporal velocity distributions acquired by UVP. For example, cells moved in certain direction and passed over measurement line of transducer. Staying time of cell on the line was observed and means speed of cells moving. As Ta gets larger, it was found that the speed of each cell motion became slower. The cell diameter was calculated from velocity data. When cells stay next to each other, there is 0 mm/s on cells boundaries in spatial velocity distribution at the time. We defined distances between neighboring cells on the spatial line respectively as scales of cell size. Then we extracted all distances from spatio-temporal distribution and calculated the expected value of these. The expected value represents dominant cell diameter. We confirmed that the cell size on the distribution roughly corresponds to that on the path line. Thereby we obtained information of convective cell from only UVP data.

Keywords: Rayleigh Benard convection, Rotating field, Flow pattern

## Roll convection in a liquid metal layer subject to a horizontal magnetic field

TASAKA, Yuji<sup>1\*</sup> ; IGAKI, Kazuto<sup>1</sup> ; YANAGISAWA, Takatoshi<sup>2</sup> ; ECKERT, Sven<sup>3</sup> ; MURAI, Yuichi<sup>1</sup>

<sup>1</sup>Faculty of Engineering, Hokkaido University, <sup>2</sup>JAMSTEC, <sup>3</sup>Helmholtz center at Dresden-Rossendorf

Recent investigations using ultrasonic velocity profiling (UVP) on Rayleigh-Benard convection in a liquid metal layer under horizontal magnetic field gave good understanding for typical temperature fluctuations shown in previous studies (Yanagisawa, et al., 2013). For example, regime transition against variations of Rayleigh number (Ra) and Chandrasekhar number (Q), variation of the roll number and spontaneous, random flow reversal that consists of spontaneous transition between two modes having different number of rolls, mainly  $N = 4$  and  $5$ . This flow reversal may be due to non-integer number of stable wave number in corresponding conditions of Ra and Q. The rolls can take only integer number even though the stable wave number determined by flow instability is, for example,  $N = 4.3$ . In this case the dominant condition is  $N = 4$ , and it is sometime modified into  $N = 5$  due to external noise. However,  $N = 5$  is not stable, and thus Skewed varicose instability occurs to restore  $N$  into  $4$ . Time average of instantaneous  $N$  may correspond to stable wave number for the corresponding conditions.

This study aims to widen the flow regimes into larger Ra and larger Q by one order to clarify the influence of strong magnetic field: Past studies predict that the strong magnetic field greatly modifies the critical Rayleigh number at the onset of the convection. Experiments were done in Helmholtz center at Dresden-Rossendorf (HZDR) to utilize strong magnetic field generator that can provide quasi uniform magnetic field with 30 mT in the intensity. The test fluid layer is almost same with our previous study (Yanagisawa, et al., 2013) and its main aspects are, 5 in aspect ratio, 40 mm in height and sandwiched between copper plates for cooling at top and heating at bottom. The obtained regime diagram shows that the fraction rule on Ra/Q determining the regimes is still almost valid in the widen region of Ra and Q. But the number of rolls is slightly modified from expectations by the rule. Also we observed "regular" flow reversals instead of random one. This may be due to stable number of rolls larger than  $N = 4.5$  and aspect ratio of the vessel, 5. The dominant roll number also depends on the side boundary of the vessel. Velocity profiles parallel to the roll axes clarified three dimensional motion during the regular flow reversals.

Keywords: Rayleigh-Benard convection, Liquid metal, Magnetic field, Convection pattern

## Flow reversals in liquid metal convection by the skewed-varicose instability

YANAGISAWA, Takatoshi<sup>1\*</sup> ; SAKURABA, Ataru<sup>2</sup> ; HAMANO, Yozo<sup>1</sup>

<sup>1</sup>IFREE, JAMSTEC, <sup>2</sup>School of Science, Univ. Tokyo

The natures of turbulence and large-scale flow pattern in the outer core are controlled by the magnetic field. It is important to know the basic behavior of flow in relation to the magnetic field, for understanding the flow patterns observed in real Earth and core dynamo simulations. By recent laboratory experiments of Rayleigh-Benard convection with liquid gallium, a regime diagram of convection patterns was established under various intensities of a uniform horizontal magnetic field for a wide square geometry (Yanagisawa et al. 2013, PRE). Five flow regimes are recognized; (I) fluctuating large-scale pattern without roll, (II) weakly constrained roll with fluctuations, (III) continuous oscillation of roll, (IV) repetition of roll number transitions with random reversals of the flow direction, and (V) steady 2-D rolls. In these, regime (IV) with flow reversals is the most interesting behavior. Flow reversals have been observed so far in narrow vessels with small aspect ratio, and the proposed processes for reversals are reorientation and cessation. Experiments with liquid metal under horizontal magnetic field suggest the existence of new type of reversal, via the skewed-varicose instability.

We performed numerical simulations of magnetoconvection in a same setting as the experiment with no-slip velocity boundary conditions. Both the Prandtl number and magnetic Prandtl number of the working fluid are set small to simulate liquid metals. Our numerical result successfully reproduced all regimes that observed in the experiments. The process of flow reversal is illuminated by the simulation. Axis of roll is skewed with a roll shrinking, and the number of rolls is reduced. In case the reduced roll number structure is not fit the vessel, new small circulation grows to a roll again, and then reversed flow state is established. The process repeats with irregular time interval. It works in 3-dimensional geometry, and should play important role in various flow systems.

Keywords: thermal convection, liquid metal, flow reversal

## Spectrum of internal waves in bounded domains of the Atmosphere and the Ocean

GINIATOULLINE, Andrei<sup>1\*</sup>

<sup>1</sup>Department of Mathematics, Los Andes University, Bogota, Colombia, South America

We consider the spectral properties of internal waves for three-dimensional compressible rotating exponentially stratified fluid. This model describes the flows in the Atmosphere and the Ocean which include simultaneously the rotation of the Earth over the vertical axis, and the non-homogeneous initial stratification of density caused by the gravitational force. We obtain theoretical results for the spectrum of the resulting internal waves in terms of its structure, localization, and its possible usage in computational algorithms. The applications of the spectral properties of such internal waves can be found, in particular, in the models of the resonance effect. We consider both the general case of bounded domains, and the explicit results of some particular domains, such as cubes and cylinders.

**Keywords:** computational fluid dynamics, compressible fluid, rotating stratified fluid, essential spectrum, internal waves, fluid dynamics of the Atmosphere and the Ocean



## Relationship between the Kamiaso unit and the Nabi unit in the Mino terrane of the Mino-Seki area, Gifu Prefecture

KITAGAWA, Yusuke<sup>1\*</sup> ; MATSUOKA, Atsushi<sup>2</sup>

<sup>1</sup>Graduate School of Science and Technology, Environmental Science and Technology, Earth Science, Niiga, <sup>2</sup>Department of Geology, Faculty of Science, Niigata University

The Mino terrane, one of the disrupted terranes in central Japan, is divided into several tectonostratigraphic units on the basis of composition, fabric and age. However, there is a problem that these data are biased, because detailed studies have been conducted only in limited areas. The Mino-Seki area of the central part in Gifu Prefecture is one of such area. According to Wakita (1988b), this area is occupied by the Kamiaso unit characterized by repeating coherent chert-clastic sequences and the Nabi unit characterized by broken formation composed of sandstone / mudstone and melange. The Wadano Conglomerate (Kanuma, 1956), characterized by breccias of chert, siliceous claystone, limestone and basaltic rocks, is also distributed in the study area. Here, I will discuss relationship between the Kamiaso unit and the Nabi unit in the Mino terrane.

As a result of a detailed field work, accretionary complexes in the Mino-Seki area are divided into a coherent unit (Kamiaso unit), melange unit (Nabi unit) and the Wadano Conglomerate. The Kamiaso unit is characterized by a tectonic pile composed of chert-clastic sequences that retain the oceanic plate stratigraphy. Chert samples yield Middle Triassic to Early Jurassic radiolarians, while mudstone samples yield Early Bathonian radiolarians. The Nabi unit includes melange and alternating beds of chert and siliceous micrite. There are also differences in the lithology of chert. Black chert with weathered red surface is commonly found in the Nabi unit especially along the Nagara River. These lithofacies generally are not recognized in the Kamiaso unit. Chert samples yield Middle Triassic to Early Jurassic radiolarians, while siliceous mudstone samples yield Middle Jurassic radiolarians. A chert sample in alternating beds of chert and siliceous micrite yields of Late Triassic radiolarians. Igo and Koike (1975) reported Late Norian conodonts from a limestone sample in alternating beds of chert and limestone. The Wadano Conglomerate consists mainly of conglomerate and massive sandstone. It is characterized by blocks of basaltic rock chert, siliceous claystone, and limestone. The Upper Triassic siliceous micrite-chert facies of the Nabi unit differs in containing siliceous micrite from the coeval chert of the Kamiaso unit. This relationship has already been pointed out by Sano et al. (2010).

Keywords: Mino terrane, Kamiaso unit, accretionary complex, chert-clastic sequence, radiolaria

## Recognition of the Olenekian-Anisian Boundary Sequence from Ogama, Ashio Belt

MUTO, Shun<sup>1\*</sup>; TAKAHASHI, Satoshi<sup>1</sup>; YAMAKITA, Satoshi<sup>2</sup>; SUZUKI, Noritoshi<sup>3</sup>; AITA, Yoshiaki<sup>4</sup>

<sup>1</sup>Department of Earth and Planetary Science, Graduate School of Science, The University of Tokyo, <sup>2</sup>Department of Earth Sciences, Faculty of Education and Culture, University of Miyazaki, <sup>3</sup>Institute of Geology and Paleontology, Graduate school of Science, Tohoku University, <sup>4</sup>Geology Lab, Faculty of Agriculture, Utsunomiya University

Pre-Jurassic pelagic sedimentary sequences are known to have accumulated in the pelagic Panthalassa over millions of years (Matsuda and Isozaki, 1991; Ando et al., 2001). These pelagic sequences are considered to preserve environmental record of the pelagic Panthalassa. However, spatial variations of pelagic sequences are not fully understood, due to the scarcity of well-preserved sequences. In order to face this problem, this study reconstructed the stratigraphic sequence ranging from Lower to Middle Triassic with high resolution at the Ogama section of the Ashio Belt, which is located in Tochigi, Japan (Kamata, 1996; Kamata 1997).

The section consists of three parts, which occur in separate outcrops; Og-A section, Og-B section and Og-C section. The boundaries of these outcrops were not directly observed, but the major difference in lithology suggests that these outcrops are in contact with faults. The Og-A section consists of approximately 2.5 m thick black claystone overlain by bedded chert. The Og-B section consists of alternating claystone and chert. Claystone in the Og-B section has two types: black claystone and grey siliceous claystone. The Og-C section consists entirely of bedded chert. Components of bedded chert are 1 to 10 cm thick chert beds and 2 to 25 mm thick intercalated claystone beds.

Age diagnostic conodonts were recovered from the Og-B section. Spathian conodonts indicating the *Triassospathodus homeri* zone (*Neospathodus homeri* zone; Koike, 1981), early Anisian conodonts indicating the *Chiosella timorensis* zone (*Neogondolella timorensis* zone; Koike, 1981), Middle Anisian conodonts indicating the *Neogondolella bulgarica* zone (Koike, 1981) were recovered. Radiolarian fossils were recovered from the Og-C section. Early-middle Anisian radiolarian *Triassocampe eruca* (Sugiyama, 1997) and late Anisian radiolarian *Triassocampe coronata* (Bragin) group were recovered.

The reconstructed stratigraphic sequence spans from upper Spathian of Lower Triassic to upper Anisian of Middle Triassic. The Spathian-Anisian boundary determined by the first occurrence of conodont *Ch. timorensis* is placed at the lower part of the Og-B section. The Lower to Middle Triassic pelagic sequence of the Ogama section has two important characteristics. One is the lithofacies change from claystone dominant facies of upper Spathian to bedded chert facies of middle Anisian. The other is the 4 m thick interval of black claystone and black chert, which spans from uppermost Spathian to lower Anisian.

Lower to Middle Triassic pelagic sequences are also exposed in other Jurassic accretionary complexes. A particularly well-studied sequence belongs to the Mino Belt, and is situated in the Inuyama area, Gifu, Japan. This area has been the target of intensive biostratigraphical examinations (Sugiyama, 1997; Yao and Kuwahara, 1997) and cyclostratigraphical researches (Ikeda et al., 2010). The comparison of the two pelagic sequences from the Ashio Belt and the Mino Belt revealed the common general trend of increasing chert content within the lower to middle Anisian interval. However, it is also noteworthy that the interval consisting of black claystone and black chert is remarkably thicker in the Ogama section than in the Inuyama area. Takahashi et al. (2009) indicated the uppermost Spathian interval consisting of black claystone and black chert in the Inuyama area is the result of an oceanic anoxia. The thicker interval at Ogama section may represent longer duration of this event, or a greater sedimentation rate during the event, at the depositional setting than that of Inuyama area. Further correlations by biostratigraphy and carbon isotope stratigraphy are required to compare the onset and offset timing of this event in both depositional settings. The comparison of timing between the two sections may reveal the cause of this regional difference in pelagic sequences.

Keywords: Ogama section, Ashio Belt, Olenekian-Anisian Boundary, Conodont, Radiolarian, Equatorial Panthalassa

## Upper Triassic conodont, ammonoid, and radiolarian biostratigraphy in a pelagic sequence of Japan

YAMASHITA, Daisuke<sup>1\*</sup> ; YASUDA, Chika<sup>2</sup> ; SATO, Honami<sup>3</sup> ; ONOUE, Tetsuji<sup>4</sup>

<sup>1</sup>Earth and Environmental Sciences, Graduate School of Science and Engineering, Kagoshima University, <sup>2</sup>INPEX Corporation, <sup>3</sup>Graduate School of Earth and Planetary Sciences, Kyushu University, <sup>4</sup>Earth and Environmental Sciences, Graduate School of Science and Technology, Kumamoto University

The chronology for the Triassic pelagic deposits in the Panthalassa Ocean is based on the radiolarian zonation, which is well studied in the Middle and Upper Triassic bedded chert successions in the Japanese accretionary complex. Although accurate calibration for the chronostratigraphic stages and substages are established basically by means of ammonites and conodonts, most of the Japanese radiolarian zones were calibrated through correlation with zonal schemes in other regions, and have not been calibrated with ammonoid and conodont biostratigraphy. Here we present the results of Late Triassic (Carnian-early Norian) conodont biostratigraphy from the two pelagic sections in the Jurassic accretionary complex of southwest Japan. Samples for this study were collected from the Sakahogi section of a bedded chert sequence in central Japan and the Nakijin Formation of a pelagic limestone sequence in the northern tip of the Okinawa Island. We found 56 platform conodonts from 36 samples in the Sakahogi section, where the radiolarian biostratigraphy have previously been investigated. The biostratigraphy of the Carnian-Norian sequence of the Nakijin Formation is based primarily on ammonites, since the rare occurrence of conodonts minimizes the stratigraphic potential of these groups. However, our study revealed that the clastic limestones intercalated within the Nakijin Formation contain rich conodonts assemblages. Based on detailed study of the conodont biostratigraphy from the interval of the Carnian and the early Norian in the Sakahogi section and the Nakijin Formation, three conodont zones are recognized in ascending order as follows: lower Carnian *Paragondolella praelindae* - *Metapolygnathus polygnathiformis* zone, upper Carnian *Metapolygnathus lindae* - *Metapolygnathus primitius* zone, and lower Norian *Epigondolella quadrata* zone. This result is consistent with the presence of the lower to upper Carnian ammonites assemblages in the Nakijin Formation.

Keywords: Late Triassic, Carnian to early Norian, conodont, ammonoid, and radiolarian biostratigraphy, Sambosan Terrane, Mino Terrane, Panthalassa Ocean

## Toward reconstruction of oceanic plate paleogeography in the NW Pacific: a subject from the NE Japan arc.

UEDA, Hayato<sup>1\*</sup> ; KIMURA, Sho<sup>1</sup> ; ORIHASHI, Yuji<sup>2</sup>

<sup>1</sup>Hirosaki Univ., <sup>2</sup>ERI, Univ. Tokyo

Spatial distribution of oceanic plates in the Mesozoic NW Pacific has been indirectly assumed extrapolating from magnetic anomalies tracked back to the mid-Pacific. However, common occurrences of suprasubduction ophiolites and arc terranes, existence of the Philippine Sea plate originated in the Jurassic, and lower mantle tomography suggesting remnants of subducted slab in the mid-Pacific all imply that plates occupied NW Pacific were distinct from those in the middle to east Pacific in the Mesozoic. To test this possibility, it is important to reconstruct oceanic plates from geology and chronology of accretionary complexes and ophiolites independently from the traditional methods based on magnetic anomaly. Here we present a subject for the oceanic plate reconstruction raised from NE Japan.

In this study, we determined U-Pb ages of zircons extracted from a tuff bed in a coherent clastic sequence of the Cape Shiriya accretionary complex (Shimokita Peninsula) at the northeastern tip of the North Kitakami belt. These zircons yielded a mean age of ca. 130 Ma (about Hauterivian / Barremian boundary). Almost identical ages were also obtained from the youngest zircon grains in sandstone. The 130 Ma age is concurrent with (a) Trench sedimentation in the Idonnappu accretionary zone, (b) high-P/T metamorphism in the Kamuikotan zone, and (c) island arc volcanism in the upper Sorachi Group, all in the central Hokkaido far in the east. A shift of the NE Japan trench from the North Kitakami belt to central Hokkaido has been assumed, with contemporaneous onset of arc volcanism in central Hokkaido. However, our result implies dual subduction in the both areas at 130 Ma. If this hypothesis stands, arc-trench system in central Hokkaido could have formed not along the Eurasian continental margin but belonging to another plate.

We also dated a diorite dike as a member of microdiorites, which commonly occur associated with serpentinites in central Hokkaido. These rocks have been attributed to Cretaceous arc magmatism based on chemistry and K-Ar ages. The diorite sample yielded a 160 Ma zircon U-Pb age of Late Jurassic, within the period of trench accretion in the North Kitakami belt. This age thus also suggest the hypothesis of dual subduction, where arc activity occurred outside the trench of Eurasian continental margin.

NE Japan has been held other problems difficult to be explained by simple, single subduction schemes. For example, adakite magmatism (suggesting slab melting) in the Kitakami mountains occurred contemporaneously with lawsonite-blueschist metamorphism (suggesting very cold subduction) in the Kamuikotan zone. Our new age data encourages to test possibilities that another subduction zone existed in the NW Pacific distinct from Eurasian active continental margin at least during Late Jurassic to middle Early Cretaceous.

Keywords: Pacific, oceanic plate paleogeography, zircon, U-Pb age, accretionary complex, ophiolite

## Philippine sea plate motion since the Pleistocene viewed from deformed conglomerates of the Ashigara group

KOBAYASHI, Kenta<sup>1\*</sup>

<sup>1</sup>Dep. Geol., Fac. Sci., Niigata Univ.

On the northern convergence border of the Philippine Sea plate, Pleistocene Ashigara group (1.6-0.5Ma) filled a trough. Miocene Tanzawa group is distributed on the north side, and both are bounded with the Kannawa fault system. The Kannawa fault system is divided into the Kannawa fault (E-W direction, dextral sense) of the narrow sense, Hisari fault system (NE-SW, sinistral-normal), Nakatsugawa fault system (NW-SE, dextral-reverse), Shiozawa fault system (NE-SW, sinistral-reverse), etc. The Shiozawa formation (conglomerates) which is the high-end strata of the Ashigara group is distributed over the southeastern side of the Shiozawa fault. Parts of the conglomerates are deformed remarkably. These deformation zones are divided into six types (P-R1 cataclasite: A, B, C; fault gouge: Dr, Dg, Db) based on the fault rock property, shear sense, cutting relations. The cataclasites are distributed over the range of 600m from the Shiozawa fault. The shear sense is reverse fault mainly, but shows sinistral in a part of the B and Db type. Quartz grain becomes fine fragment by crush, and biotite does basal slip, it is thought that this cataclasite was formed under environment of 150-300 oC, and 5-10km in depth. The influence of the subducting Philippine Sea plate might have increased. In addition, the moving direction was not constant, northwest and north might be mixed in the Pleistocene age.

Keywords: Kanagawa Prefecture, Ashigara group, Shiozawa formation, cataclasite, fault gouge, Philippine sea plate

## Radiolarian morphology as a proxy for reconstructing pelagic environments: problem and perspective

MATSUOKA, Atsushi<sup>1\*</sup>

<sup>1</sup>Niigata University

Late Paleozoic and Mesozoic radiolarian cherts are widely distributed within accretionary complexes in the Circum-Pacific and Alps-Himalaya orogenic belts. These cherts are materials for reconstructing the paleoenvironment of the Panthalassa and the Tethys. Many proxies have been developed to elucidate the environment of the past pelagic realm. Species diversity in radiolarian assemblages is expected to be one of proxies for monitoring paleoenvironmental change. However, the species concept of radiolarians is not always consistent throughout the Phanerozoic time. This makes a serious problem to use radiolarian diversity for elucidating environmental fluctuations. This paper documents the present status of taxonomy for Mesozoic and recent radiolarians. Detailed morphological analysis of radiolarian tests and the understanding of the morphogenesis through culture work are clues toward reconstructing pelagic environments in the past oceans.

Keywords: radiolarians, taxonomy, species concept, morphological diversity, pelagic realm

## Lifestyle of adherent benthic foraminifers in the open ocean based on stable of isotope records

KIMOTO, Katsunori<sup>2</sup> ; HASEGAWA, Shiro<sup>1\*</sup> ; NAMIKAWA, Hiroshi<sup>3</sup> ; KITAMURA, Minoru<sup>1</sup> ; KAWAKAMI, Hajime<sup>1</sup> ; HONDA, Makio<sup>1</sup>

<sup>1</sup>Japan Agency for Marine-Earth Science and Technology, <sup>2</sup>Kumamoto University, <sup>3</sup>National Museum of Nature and Science, Tokyo

Colonization of new habitat of benthic foraminifers is related to their diversion, survival strategies and evolutions. However their dispersal mechanisms are not well documented and still poorly understood. Last year, we reported a new lifestyle of neritic benthic foraminifera: They had lived on the stems of hydrozoan attaching to observational moorings in the Pacific Ocean. This is a new insight of dispersal strategy of benthic foraminifera to the open ocean. However there are no evidences whether benthic foraminifera developed their calcareous shells in the water column or not. Here we report the new evidences of benthic foraminiferal lifestyles based on micropaleontological and geochemical methods.

Physical and biogeochemical observational mooring systems (POPSS & Sediment trap) were deployed on July, 2012 at the Station S1 (30N, 145E, water depth: 5,900m). Moored periods were from July 2012 to July 2013 (1 year). Hydrozoan attaching on the both mooring systems were observed at the surface of the winch, sensor buoy, sediment trap and float at shallower depths (~200 m) and we could not observed hydrozoan at the 500 m water sediment trap. More than 300 individuals of benthic foraminifers attached of the surface of hydrozoan body. At least, fourteen living benthic foraminifers were identified under the microscope and faunal assemblages were basically same (calcareous, agglutinated, and sessile) with that of previous year. We performed the stable isotope analysis for these calcareous specimens including some porcellanic benthic and planktic foraminifera. As the results, oxygen and carbon isotopes of calcareous benthic foraminifera showed remarkably lighter and heavier values than planktic foraminifera, respectively. It suggested that calcareous benthic foraminifera in this study built their calcareous shells at shallower water depth than planktic species.

Keywords: adherent benthic foraminifera, Stable isotopes, Lifestyle, Hydrozoan

## Comparison between morphological dissimilarity and morphological richness

UBUKATA, Takao<sup>1\*</sup>

<sup>1</sup>Shizuoka University

Morphological disparity, another look at biodiversity, has recently attracted attention of paleontologists in the context of mass extinction and recovery. The measure of disparity has commonly been based on morphological dissimilarity between objects, e.g., sum of variance, mean pairwise distance, range of variation etc. It is widely known that this sort of disparity is robust against sample size and is not seriously affected by a nonselective extinction, whereas selective extinctions should readily reduce the disparity. On the other hand, another aspect of disparity is morphological richness, which is assessed through compilations of the number of character states; e.g., number of pairwise character-state combinations and number of morphospace divisions occupied by observation. Unlike the morphological dissimilarity, the morphological richness appears to be fairly sensitive to nonselective extinctions as well as to selective ones.

The comparison among the diversity measures based on the morphometric data obtained from the ammonoids revealed that the patterns of disparity change were totally different between dissimilarity and richness, while comparison within the same categories tended to indicate a consistent result. This result suggests that comparison between morphological dissimilarity and morphological richness provides a powerful tool to assess the selectivity of an extinction event.

Keywords: disparity, biodiversity, morphological dissimilarity, morphological richness



## Is the growth hiatus of ferromanganese crusts a local or global event?

NOZAKI, Tatsuo<sup>1\*</sup> ; GOTO, Kosuke T.<sup>2</sup> ; TOKUMARU, Ayaka<sup>3</sup> ; TAKAYA, Yutaro<sup>4</sup> ; SUZUKI, Katsuhiko<sup>1</sup> ; CHANG, Qing<sup>1</sup> ; KIMURA, Jun-ichi<sup>1</sup> ; KATO, Yasuhiro<sup>4</sup> ; SHIMODA, Gen<sup>2</sup> ; TOYOFUKU, Takashi<sup>5</sup> ; USUI, Akira<sup>6</sup> ; URABE, Tetsuro<sup>3</sup>

<sup>1</sup>JAMSTEC/IFREE, <sup>2</sup>AIST/GSJ, <sup>3</sup>Univ. of Tokyo, <sup>4</sup>Univ. of Tokyo, <sup>5</sup>JAMSTEC/BIOGEOS, <sup>6</sup>Kochi Univ.

Recent applications of an Os isotope dating method revealed that some ferromanganese crusts collected from the Pacific Ocean might have experienced the growth hiatus. However, it is still controversial whether this growth hiatus was a local or global event. In the present study, we discuss the geological trigger of this growth hiatus based on our results of the Os isotope dating on various ferromanganese crust samples collected from Northwestern Pacific, South Atlantic Oceans and Philippine Sea.

Keywords: ferromanganese crust, Os isotope, geochemistry, growth hiatus, paleoceanography

## Sedimentation rate of the end-Permian to earliest Triassic black claystone strata in the Panthalassic deep-sea

TAKAHASHI, Satoshi<sup>1\*</sup> ; YAMAGUCHI, Asuka<sup>2</sup> ; YAMAKITA, Satoshi<sup>3</sup> ; MIZUTANI, Akane<sup>1</sup> ; ISHIDA, Jun<sup>1</sup> ; YAMAMOTO, Shinji<sup>1</sup> ; IKEDA, Masayuki<sup>4</sup> ; OZAKI, Kazumi<sup>2</sup> ; TADA, Ryuji<sup>1</sup>

<sup>1</sup>Department of Earth and Planetary Science, the University of Tokyo, <sup>2</sup>Atmosphere and Ocean Research Institute, the University of Tokyo, <sup>3</sup>Department of Earth Science, Faculty of Culture, Miyazaki University, <sup>4</sup>Department of Earth Sciences, Graduate School of Science and Engineering, Ehime University

The greatest mass extinction occurred at the end-Permian, its aftermath continued during following Early Triassic. This period, especially interval between the end-Permian and Induan is characterized by occurrences of the black claystone in the pelagic deep-sea depositional area where now locate in Japan and western North America etc. This black claystone generally contains high organic matter and few silicic fossils, in contrast that bedded chert before the mass extinction event has few organic matter and abundant radiolarian tests. Detailed background of this black claystone has not been fully understood due to the scarcity of well-preserved lithologic sequences. Herein, we show preliminary achievement on continuous black claystone strata based on the one of most continuous Permian-Triassic Boundary section (Akkamori-2 section; Takahashi et al., 2009).

We polished the outcrops of the study section using hand grinders with diamond-blades and diamond-polishing pad for observation of sedimentary facies and structures. Observing the outcrop, structural geology examination was conducted (See Yamaguchi et al. in this session). Using their results, we divided the outcrop into 20 subsections that preserve continuous lithologic stratigraphy. Then, high-resolution lithologic column was reconstructed from these subsections.

After careful observation on the polished surface of the outcrop, we found many key bed layers. For instances, dolomitic layers, light and dark grey colored siliceous claystone interbedded within black claystone, and alternations of black and grey colored claystones. Using these key beds, we correlated the lithologic columns from each subsection. In the case of that useful key beds were not found, we simply built the columns up, because no duplication of strata was recognized. After these processes, totally ca. 10 m thick lithologic column of black claystone was reconstructed. Its lower most horizon accords to carbon isotopic negative excursion (Takahashi et al., 2010) coinciding with the main mass extinction event, ca. 252.2 Ma (U-Pb dating by Shen et al., 2011). Meanwhile, in the thick grey-color siliceous claystone horizon from uppermost part of the strata, conodont fossils of *Neospathodus waageni* and *Eurygnathodus costatus* were recovered. This combination indicates lowest Smithian. After interpolation by Geologic Time Scale 2012 (Gradstein et al., 2012), beginning of Smithian (end of Induan) is ca. 250.0 Ma. Using these absolute ages, sedimentation rate of black claystone is calculated 4.34mm/kyr (= 10000 mm /2300 kyr). This calculation is still comprehensive. Also, we can calculate the sedimentation rate in another way using the earliest Triassic conodont occurrence of *Hindeodus parvus* in the 7.5 m above the base of black claystone. The first occurrence horizon is estimated to be 252.3Ma in the type section of Permian-Triassic Boundary (Shen et al., 2011). The calculated sedimentation rate of black claystone in this way is 7.5 mm/kyr (750 mm/100 kyr). As the fossil age is uncertain between the basal 7.5 m interval, this is a maximum estimation. These two results of sedimentation rate indicate that the black claystone beds were accumulated in several millimetres per a thousand year. This rate is in similar class of sedimentation rate of radiolarian chert deposited before and after the black claystone deposition. In fact, recent study of Ikeda et al. (2010) concluded several centimetres thick one chert-clay couplet accords about 20 kyr. The sedimentation rate of the black claystone as similar as silicic fossil rich bedded chert before mass extinction event implies that some materials increased into the pelagic deep-sea at and after the extinction event instead of significantly decreased radiolarian tests (Takahashi et al., 2009). Possible materials are terrigenous clastic material (Algeo and Twitchett, 2009; Sakuma et al., 2012) and very fine silicic biotic crust (such as silicic sponges).

Keywords: Permian, Triassic, pelagic deepsea, black claystone, mass extinction

## Stratigraphy and formation process of Late Cretaceous pelagic sediments in the Wadi Hilti area of the Oman Ophiolite

AGUI, Yumi<sup>1\*</sup> ; HARA, Kousuke<sup>1</sup> ; KURIHARA, Toshiyuki<sup>1</sup>

<sup>1</sup>Graduate School of Science and Technology, Niigata University

The Oman Ophiolite consists of mantle peridotites, gabbros, a sheeted dyke complex, and basaltic lavas. The extrusive rocks have been subdivided into three volcanic units: the V1 lava with the N-MORB signature, the V2 lava formed by intra-oceanic volcanism, and the V3 lava generated by intra-plate seamount magmatism (Ernewein et al., 1988). Pelagic sediments commonly occur at the boundaries between these volcanic units. Thick sediments upon the V1 lava in the Wadi Jizzi area are subdivided into the Suhaylah and Zabyat formations; the former is composed of metalliferous and fine-grained pelagic sediments of Cenomanian-Santonian? age, and the latter consists of conglomerate derived mainly from a collapsed oceanic crust during the thrusting stage (Fleet and Robertson, 1980; Tippit et al., 1981; Woodcock and Robertson, 1982; Robertson and Woodcock, 1983).

The V2 and V3 lavas are widely distributed in the Wadi Hilti area, about 25 km west of Sohar, northern Oman Mountains. Recently, the eruption and emplacement mechanism of the V3 lava has been studied by Umino (2012). Pelagic sediments, about 50 m thick at a maximum, overlie the V2 lava and are covered by the V3 lava. The sediments also occur on and within the V3 lava. Based on our field examination for several sections in the Wadi Hilti area, the stratigraphy of the pelagic sediments on the V2 lava consists of metalliferous sediments, micritic limestone, red mudstone, conglomerate, V3 lava, and siliceous mudstone, in ascending order. We first found conglomerate containing gravels of lavas and pelagic cherts from this area. From fine-grained pelagic sediments on the V2 and V3 lavas, we obtained *Rhopalosyringium scissum* O'Dogherty and *Hemicryptocapsa polyhedra* Dumitrica that can be assigned to a Turonian age (O'Dogherty, 1994). In addition, *Rhopalosyringium petilum* (Foreman) and *Guttacapsa biacta* (Squinabol) were recovered from a block of siliceous mudstone probably within the conglomerate. According to O'Dogherty (1994), the co-occurrence of these species is restricted to be middle to late Cenomanian.

Based on these age assignments, the fine-grained pelagic sediments on the V2 lava (metalliferous sediments, micritic limestone, and red mudstone) in the Wadi Hilti area can be correlated with the Turonian part of the Suhaylah Formation in the Wadi Jizzi area. This reveals that the activity of the V2 lava was terminated in Turonian. The conglomerate and the siliceous mudstone on the V3 lava are correlated with the Zabyat Formation, indicating that the eruption of the V3 lava occurred in Turonian. These age constraints for basaltic extrusive rocks imply that the tectonic setting from subduction to oceanic-thrusting changed rapidly in a short period of Turonian time.

Keywords: Oman Ophiolite, pelagic sediments

## Stratigraphy and radiolarian age of the Zabyat Formation at Lasail section in the Wadi Jizzi area, Oman Ophiolite

HAYASHI, Rina<sup>1</sup> ; HARA, Kousuke<sup>2</sup> ; KURIHARA, Toshiyuki<sup>2\*</sup>

<sup>1</sup>Department of Geology, Faculty of Science, Niigata University, <sup>2</sup>Graduate School of Science and Technology, Niigata University

The Oman Ophiolite consists of mantle peridotites, gabbros, a sheeted dyke complex, and extrusive lavas overlain by pelagic sediments. The basaltic extrusive rocks have been subdivided into three volcanic units (the V1, V2, and V3 lavas) (Ernewein et al., 1988). The overlying pelagic sediments, named the Suhaylah Formation, consist of metalliferous and fine-grained calcareous sediments of Cenomanian-Santonian? age (Fleet and Robertson, 1980; Tippit et al., 1981). The Zabyat Formation, which covers conformably the Suhaylah Formation, is composed of conglomerate derived mainly from a collapsed oceanic crust during the thrusting stage (Woodcock and Robertson, 1982; Robertson and Woodcock, 1983). Although Robertson and Woodcock (1983) investigated the sedimentation process of this formation, they did not study the biostratigraphic age of fine-grained sediments intercalated with conglomerate at Lasail section in the Wadi Jizzi area.

At Lasail section, the stratigraphy of the Zabyat Formation consists of the lower conglomerate interbedded with micritic limestone and red mudstone and the upper red mudstone and siliceous mudstone. The micritic limestone of the lower part contains *Alievium superbum* and *Rhopalosyringium scissum*, indicating Turonian in age (O'Doghterty, 1994). From the red mudstone of the upper part, we obtained *Pseudoaulophacus lenticularis*, *Pseudoaulophacus praefloresensis*, and *Theocampe salillum*. The occurrence of these species assigns the upper part of the Zabyat Formation to Coniacian (Pessagno, 1976; Bandini et al., 2008). Our biostratigraphic result of the Zabyat Formation, taken together with that of the Suhaylah Formation, shows that the change of the tectonic setting from mid-ocean ridge through subduction zone to oceanic thrusting occurred in a short period (c.a. 4 m.y.) of latest Cenomanian to Coniacian time.

Keywords: Oman Ophiolite, pelagic sediments

## Deformational features of Permian-Triassic boundary preserved within an on-land accretionary complex

YAMAGUCHI, Asuka<sup>1\*</sup> ; TAKAHASHI, Satoshi<sup>2</sup> ; YAMAKITA, Satoshi<sup>3</sup>

<sup>1</sup>Atmosphere and Ocean Research Institute, the University of Tokyo, <sup>2</sup>Department of Earth and Planetary Science, the University of Tokyo, <sup>3</sup>Faculty of Education and Culture, University of Miyazaki

Pelagic siliceous sediment covering on oceanic crust is one of the components in subduction plate boundaries where old oceanic plate subduct. Its mechanical, frictional and fluid transport properties are key to understand faulting and earthquake mechanics in such settings (Kimura et al., 2012; Yamaguchi et al., this meeting). Plate boundary deformations are strongly affected by inhomogeneity of incoming sediments: in the case of Jurassic accretionary complex in Japan (Mino-Tanba belt), siliceous/black claystone at Permian-Triassic boundary horizon within bedded chert functioned as plate boundary decollement, and only Triassic-Jurassic chert is preserved in the complex, whereas Carboniferous-Permian chert is lacking (Nakae, 1993). However, few outcrops in the Jurassic accretionary complex comprise continuous sections across Permian-Triassic boundary. To understand the limitation of lithology-controlled deformations, we investigated structural analysis of the Permian-Triassic boundary section in the North Kitakami Belt (Akkamori-2 section; Takahashi et al., 2009), where the most continuous Permian-Triassic boundary is observed.

Permian gray-color siliceous claystone to Triassic gray-color siliceous claystone through black claystone is successively observed in this outcrop (lithology detail: see Takahashi et al., this session). Orientations of 36 bedding dips, 90 low-angle cleavages, 17 high-angle cleavages, and 22 faults are measured from the outcrop. Strikes of bedding and low-angle cleavage vary NW-SE to NE-SW, gently dip eastward. Faults have two populations: one is subparallel to bedding and low-angle cleavage; the other is dipping gently to the north. Shear sense of the faults is unclear because of the lack of shear sense indicators due to intense development of overprinting high-angle cleavage.

In contrast to the scattered orientations of low-angle cleavage, strike of high-angle cleavage is limited to N40-70E with sub-vertical dip. The high-angle cleavages are recognized as axial plane cleavage of map-scale Hiraniwa-dake Syncline (Sugimoto, 1974) striking NW-SE and plunging southeastward, since the studied section is located nearby the axis of the syncline. Orientations of bedding, low-angle cleavage, and fault would be also rotated by secondary-order outcrop-scale open folds.

Hiraniwa-dake syncline involves several chert-clastics sequences in this region (Ehiro, 2008). Substrating fold-related deformations, bedding-parallel cleavages and low-angle faults (likely to be thrust) are only initial deformations observed in the studied outcrop. Those deformational features are also typical in off-scraped and underthrust accretionary complex (Kimura and Hori, 1993, Raimbourg et al., 2009). Lack of intense deformation in the black claystone suggests that not only lithology-controlled physical properties but other factors (e.g. topographic and thermal effects) would be also important to constrain the position where decollement develops.

Keywords: Permian-Triassic Boundary, subduction zone, accretionary complex, Deformation structure

## Magnetosphere-Ionosphere coupling events and Atmospheric electricity at Syowa station, Antarctica

MINAMOTO, Yasuhiro<sup>1\*</sup> ; KADOKURA, Akira<sup>2</sup> ; KAMOGAWA, Masashi<sup>3</sup>

<sup>1</sup>Kakioka Magnetic Observatory, Japan Meteorological Agency, <sup>2</sup>National Institute of Polar Research, <sup>3</sup>Department of Physics, Tokyo Gakugei University

At Syowa Station(69.0S, 39.6E), located on East Ongul Island near the continent of Antarctica, atmospheric electric field observation has been carried out with an electric field mill. We extracted 'fair-weather' electric field data over six years, from 2006 to 2012. We considered the 'fair-weather' electric field data and Geomagnetic field by comparison, and found an event which suggests variations of electricity in ionosphere caused by magnetosphere-ionosphere coupling. In this presentation, we will show atmospheric electric field, aurora activity, HF radar, etc. during the event, and discuss the influence of Solar-Terrestrial environment on atmospheric electricity.

Keywords: fair-weather, Antarctica, atmospheric electricity, Magnetosphere-Ionosphere coupling, global circuit

## Changes in atmospheric electricity over about eighty years

HIRAHARA, Hideyuki<sup>1\*</sup> ; MINAMOTO, Yasuhiro<sup>1</sup>

<sup>1</sup>Kakioka Magnetic Observatory

The Japan Meteorological Agency has observed atmospheric electric field at Kakioka magnetic observatory (KMO) since 1929. This observation has been carried out by a water-dropper instrument without replacing. Meteorological observations at KMO stopped in 1997, and fair-weather days of atmospheric electricity have been extracted from data of atmospheric electricity itself and precipitations. We extracted clear weather days with weather satellite images and all-sky photos at KMO, and derived diurnal variation of the atmospheric electric field in calm days. In this presentation, we will show the diurnal curve at present and past, from 1931 to 1935, and discuss changes in atmospheric electricity over about eighty years.

Keywords: atmospheric electricity, diurnal variation, fair weather, water dropper, cloud grid information

## Snow electrification observed at Memanbetsu

KAMOGAWA, Masashi<sup>1\*</sup> ; KADOKURA, Akira<sup>2</sup> ; MINAMOTO, Yasuhiro<sup>3</sup> ; SATO, Mitsuteru<sup>4</sup> ; SAITO, Shogen<sup>1</sup>

<sup>1</sup>Dpt. of Phys., Tokyo Gakugei Univ., <sup>2</sup>National Institute of Polar Research, <sup>3</sup>Kakioka Magnetic Observatory, Japan Meteorological Agency, <sup>4</sup>Department of Cosmoscience, Hokkaido University

We investigate the snow electrification observed at Memanbetsu. In this presentation, we report a preliminary analysis of atmospheric data observed in Memanbetsu.

Keywords: Atmospheric electric field, Snow electrification



## Spatio-temporal characteristics of subionospheric perturbations associated with annular solar eclipse

INUI, Daiki<sup>1\*</sup> ; HOBARA, Yasuhide<sup>1</sup>

<sup>1</sup>Graduate School of Informatics and Communication Eng., The University of Electro-Communications

In this paper, we analyse UEC's VLF/LF transmitter observation network data associated with annular solar eclipse in 2012. Clear temporal dependences of the VLF amplitude are observed by various transmitter-receiver paths. Numerical computations of VLF/LF signals with the ionospheric perturbations due to the solar eclipse are carried out by using 2D-FDTD method. As a result, temporal variations of the VLF/LF amplitude are in rather good agreement with those from the numerical modeling.

Keywords: Annular solar eclipse, Ionospheric perturbations, VLF radio waves, FDTD method

## Electrical characteristics of the lightning discharges generating long-recovery VLF events

YAMASHITA, Junpei<sup>1\*</sup> ; HOBARA, Yasuhide<sup>1</sup>

<sup>1</sup>Graduate School of Informatics and Communication Eng., The University of Electro-Communications

In this paper, we focus on the special type of early/fast VLF event so-called long-recovery VLF event to study its generation mechanism. We identify many long-recovery VLF events by using UEC's VLF/LF transmitter signal receiving network. Electrical properties of causative lightning discharges of the long-recovery events are presented based on both the peak current and electrical charge moment changes by the ELF waveform observations.

Keywords: long-recovery event, ionospheric perturbations, charge moment, early/fast event, lightning discharge

## Signature of subionospheric LF wave perturbations associated by Hokuriku winter lightning observed at the Zao station

MORINAGA, Yosuke<sup>1\*</sup> ; TSUCHIYA, Fuminori<sup>1</sup> ; OBARA, Takahiro<sup>1</sup> ; MISAWA, Hiroaki<sup>1</sup>

<sup>1</sup>Planetary Plasma and Atmospheric Research Center, Tohoku University

Intense electromagnetic pulses (EMP) radiated from lightning discharge could cause heating and ionization and alter the conductivity in the ionospheric D-region. Quasi-electrostatic fields (QE Fields) which are generated due to the removal of electric charge could also affect it. The purpose of this study is to reveal influence of the lightning on the lower ionosphere and its dependence on properties of lightning discharges. The VLF/LF signature of subionospheric perturbations associated with winter lightning in the Sea of Japan (around Hokuriku) has been observed during December 16-31, 2009. LF (60kHz) radio observation was made at Zao (Miyagi) for Haganeyama JJY transmitter (border between Saga and Fukuoka) whose great circle path (GCP) passes over the coast area of Hokuriku. The amplitude and phase of the JJY signal are recorded every 0.1 seconds. In addition to the subionospheric LF observation, lightning locations are determined by a lightning location network (WWLLN). The number of total lightning event identified in the area of 35-37 degrees N and 134-137 degrees E is 1002. Based on the LF observation, subionospheric perturbations which occur immediately after the causative lightning (early event) were detected. The number of the total detection of the early event in the selected area is 72. Early events identified will be compared with peak current and charge moment of the causative lightning which are derived from LF and ELF waveform observations, respectively, to investigate the relation between early event properties and magnitude of EMP and QE fields.

Keywords: lightning, subionospheric perturbations, electromagnetic pulses, quasi-electrostatic fields

## Generating position identification of high-energy radiation associated with the summer thundercloud

SHOJI, Tomomi<sup>1\*</sup> ; SAITO, Shogen<sup>1</sup> ; KAMOGAWA, Masashi<sup>1</sup> ; TORII, Tatsuo<sup>2</sup>

<sup>1</sup>Dpt. of Phys., Tokyo Gakugei Univ., <sup>2</sup>Japan Atomic Energy Agency

We perform the observation on the Fuji mountaintop in the summer from 2008 to elucidate mechanism of the high energy radiation of the thundercloud origin. This presentation is the result of observation in 2013.

Keywords: thundercloud, high-energy radiation, Mt. Fuji

## Development of broadband lightning monitoring system and its application

YOSHIDA, Satoru<sup>1\*</sup> ; WU, Ting<sup>2</sup> ; USHIO, Tomoo<sup>2</sup> ; KENICHI, Kusunoki<sup>1</sup>

<sup>1</sup>Meteorological Research Institute, <sup>2</sup>Graduate school of Engineering, Osaka University

We have been designing and developing Broadband Observation network for Lightning and Thunderstorm (BOLT) in Kinki area to study lightning discharges and thunderstorms. The BOLT consists of 11 sensors which detect LF radiation from lightning discharge and locate emission sources in 3D. We have been developing both hardware and algorithm to locate lightning so that the BOLT produces detail progression of lightning discharges, including stepped leader and negative recoil leader in negative charge region. In this presentation, we show clear 3D BOLT images of lightning discharges and compare the results with VHF source locations.

Keywords: lightning discharge, thundercloud monitoring, remote sensing

## Simultaneous observations of VHF waves and optical emissions for lightning from the International Space Station

KIKUCHI, Hiroshi<sup>1\*</sup> ; MORIMOTO, Takeshi<sup>2</sup> ; USHIO, Tomoo<sup>1</sup> ; SATO, Mitsuteru<sup>3</sup> ; YAMAZAKI, Atsushi<sup>4</sup> ; SUZUKI, Makoto<sup>4</sup>

<sup>1</sup>Osaka University, <sup>2</sup>Kinki University, <sup>3</sup>Hokkaido University, <sup>4</sup>Japan Aerospace eXploration Agency

Since November 2012, Global Lightning and sprIte MeaSurementS (GLIMS) mission has been conducted on Exposed Facility of Japanese Experiment Module (JEM-EF) of the international space station (ISS) which is orbiting the earth at an altitude 400 km. The VHF broadband digital interferometer (VITF) attached on JEM-EF is designed to estimate the direction of arrival of electromagnetic waves. The VITF has th bandwidth from 70 MHz to 100 MHz. The VITF consists of two antennas, band-pass filters, amplifiers, and 2-channel-AD-converter. The electromagnetic radiations from lightning discharges received by the antennas are digitized by the AD converter synchronizing with another channel through the filters and the amplifiers. The band-pass filter and the amplifier of the VITF are exactly the same as the ones of the VHF sensor on Mado-1 satellite. The basic specification and most of devices in the AD converter of VITF.

In previous study, the Array of Low Energy X-ray Imaging Sensors (ALEXIS) satellite (1993) had a high-speed VHF receiver/digitizer (Blackbeard) for studying the effect of lightning and electromagnetic impulse from lightning and other man-made noise, which means TV and FM carrier interference. Furthermore, the Blackbeard reported the unique characteristics of VHF waves radiated from lightning known as transionospheric pulse pairs (TIPP). In 1997, the Fast On-orbit Rapid Recording of Transient Events (FORTE) satellite recorded many VHF pulses associated with lightning discharges.

The observation results of the VITF of the JEM-GLIMS mission were described. As a case study, the lightning event captured by the two optical sensors (photometers and CMOS sensor) was analyzed. In these events, the waveform data of VITF were used to estimate the arrival direction of EM waves. There are two methodologies which are the interferometry technic and the group delay characteristic of EM waves. We compared the results of direction of arrival estimation with CMOS sensor data. The results agreed with the position of the lightning emission captured by the CMOS sensor. We also compared the results of VITF with that of the photometers in order to find the temporal relationship. The results indicated that the frequency of the VHF radiations recorded with the VITF had a positive relationship with optical waveform captured with the photometers.

Keywords: lightning, radio wave propagation, VHF waves

## Magnetotelluric measurements of volcanic lightning at Sakurajima, Japan

AIZAWA, Koki<sup>1\*</sup> ; YOKOO, Akihiko<sup>2</sup>

<sup>1</sup>Institute of Seismology and Volcanology, Kyushu University, <sup>2</sup>Aso Volcanological Laboratory, Kyoto University

Magnetotelluric (MT) method uses the natural electromagnetic (EM) field variation to image subsurface resistivity structure, and usually involves measuring two horizontal electric field components ( $E_x$  and  $E_y$ ) and three magnetic field components ( $B_x$ ,  $B_y$ , and  $B_z$ ) at the Earth's surface, where the subscripts  $x$  and  $y$  indicate the N-S and E-W directions, respectively. In the MT data recorded 3 km away from the active crater of Sakurajima volcano, pulse-like signals that synchronize with the volcanic lightning are frequently observed within 3 minutes from the eruption onset (Aizawa et al. 2010). However the sampling rate on that paper was so low as 15 Hz that the physical properties of volcanic lightning, such as waveform of EM radiation, amplitude of electric current, and its duration, were not investigated.

In the presentation, we show the result from the temporal MT observation with the sampling rate of 65 kHz. The MT data were recorded at two sites approximately 3km away from the active crater between October 27 and November 6, 2013. The preliminary analysis shows the following features of volcanic lightning;

(1) There are two types of discharges. One is the assemblage of several pulses. Another is the EM burst that continues several ms.

(2) The duration of each pulse in the assemblage type is short as a few tens of micro seconds, but its amplitude is far strong than that of EM burst.

(3) Regarding the discharges of the pulse type, there are examples that the first discharge is weaker than the second and third discharges.

The points of (1) and (2) are similar to the lightning in the thundercloud. However, its duration is approximately  $1/10 \sim 1/100$  of that of thundercloud. In addition, we will show the data of physical unit (mv/Km and nT) which was recovered by incorporating the frequency response of the logger and induction coil, and will closely investigate the relationship between MT signals and the corresponding lighting movie. In addition, the 32 Hz MT data since December 2011 will be presented.

### References

Aizawa, K., A. Yokoo, W. Kanda, Y. Ogawa, and M. Iguchi (2010), Magnetotelluric pulses generated by volcanic lightning at Sakurajima volcano, Japan, *Geophysical Research Letters*, 37, L17301, doi:10.1029/2010GL044208.

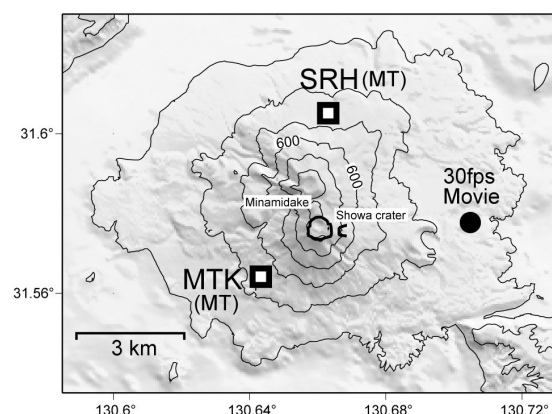


Fig.1

## Pressure field of a tornado observed by POTEKA project

KOBAYASHI, Fumiaki<sup>1\*</sup> ; NOROSE, Keiko<sup>1</sup> ; KURE, Hirotaka<sup>2</sup> ; MORITA, Toshiaki<sup>2</sup>

<sup>1</sup>Dep. Geoscience National Defense Academy, <sup>2</sup>Meisei Electric co.,ltd

A tornado event, which occurred in Midori city Gunma prefecture on 16 September 2013, was observed by the fine-mesh surface weather station network named as POTEKA. The pressure field around the tornado revealed the pressure dip pattern at the time of the wind damage and useful for the judgement of the cause of wind damage.

Keywords: surface weather station, tornado, downburst, gust front



## Discrimination between downburst and gust-front by the surface dense observation network POTEKA

NOROSE, Keiko<sup>1\*</sup> ; KOBAYASHI, Fumiaki<sup>1</sup> ; KURE, Hirotaka<sup>2</sup> ; MORITA, Toshiaki<sup>2</sup>

<sup>1</sup>National Defense Academy, <sup>2</sup>Meisei Electric

On the evening of 11 August 2013, a severe thunderstorm passed over the Takasaki and Maebashi city, Gunma prefecture, and produced gusty wind damages. The change of surface weather elements was recorded by dense observation POTEKA when gust occurred. In this study, we follow the development and propagation of gust-front and downburst through the analysis of features of pressure field observed by POTEKA. The result of this analysis reveals that the reason of gust caused damages in Maebashi city is downburst.

## Doppler Observation of Cumulonimbus Turret Generation by 95GHz Cloud Radar in Boso Peninsula on 30 August 2012

KASHIWAYANAGI, Taro<sup>1\*</sup> ; KOBAYASHI, Fumiaki<sup>2</sup> ; OKUBO, Takumi<sup>2</sup> ; YAMAJI, Mika<sup>2</sup> ; TAKANO, Toshiaki<sup>3</sup> ; TAKAMURA, Tamio<sup>4</sup>

<sup>1</sup>Center for Environmental Remote Sensing, Chiba University/Japan Radio Co., Ltd., <sup>2</sup>National Defense Academy, <sup>3</sup>Graduate School of Engineering, Chiba University, <sup>4</sup>Center for Environmental Remote Sensing, Chiba University

Simultaneous observations of cumulonimbus turrets using a 95GHz W-band cloud radar, an X-Band radar, the MTSAT-1R rapid scan and photogrammetry were held during the summer in 2012 in Kanto Region, Japan to understand the convection initiation and the structure of cumulonimbus turrets. During these observations, the cloud radar was installed in the middle of Boso Peninsula, where cumuli and cumulonimbi frequently generate in mid-summer season.

Cumulonimbus turrets were developed above the W-band cloud radar after 12:30 on 30 August 2012. The turrets continued development and degeneration for two hours above the radar. In a previous study, we have shown the Doppler analysis by X-band radar which indicated convergence of horizontal winds below 1.5 km around the cloud radar site at the initiation of the first cumulonimbus turret generation.

In this presentation, we show the vertical Doppler analysis result of the cloud radar at the initiation of the cumulonimbus turret generation. The result indicates the existence of a strong updraft of over 6 m/s at the initiation of the first cumulonimbus turret generation.

Keywords: cumulonimbus, turret, cloud radar, Doppler

## Surface Temperature and Pressure Distributions of Downburst captured by High Dense Ground Observation Network "POTEKA"

KOJIMA, Shinya<sup>1\*</sup> ; SATO, Kae<sup>1</sup> ; MAEDA, Ryota<sup>1</sup> ; KURE, Hiroataka<sup>1</sup> ; YADA, Takuya<sup>1</sup> ; MORITA, Toshiaki<sup>1</sup> ; IWASAKI, Hiroyuki<sup>2</sup>

<sup>1</sup>Meisei Electric co., ltd, <sup>2</sup>Faculty of Education, Gunma University

Meisei developed low-cost compact weather sensor (POTEKA Sta., hereinafter referred to as the POTEKA), which can measure temperature, relative humidity, pressure, sunlight, and rain detection per one minute and achieve higher density weather observation system economically. We installed economical and high dense ground observation network (total 55 stations, 1.5~4 km-mesh) in Gunma, Japan. This paper presents observation of wind gust phenomena around Takasaki city and Maebashi city on 11 August 2013.

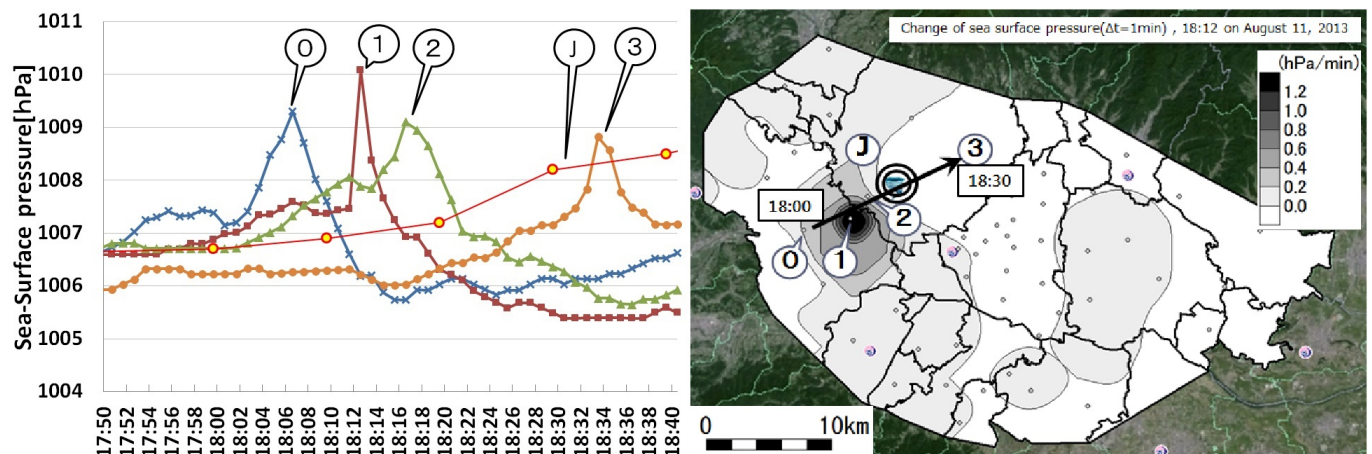
The wind gust occurred from Takasaki thru Maebashi city around 18:00 JST and caused damages to private houses. Temperature changes obtained from POTEKA network show that surface temperature dropped by up to 13.9 deg. C in 12 minutes.

The following figure exhibits the change of sea surface pressure calculated from POTEKA around the gust pathway reported by JMA (Maebashi). Although pressure at Maebashi station increased gradually with 10 minutes resolution, pressure jumps of 1-2 hPa were recorded at POTEKA with one minute resolution, indicating that the temporal high pressure was caused by downburst downflow. Beside, two pressure jump can be found at some stations. The first and second jumps are coincided with gust fronts and down flow of downburst, respectively (Discrimination between downburst and gust-front by the surface dense observation network POTEKA).

Local weather observation network consisting of POTEKA succeeded in capturing the change of surface pressure caused by gust wind phenomena with unprecedented spatio-temporal resolution, which enables us not only to distinguish between gust fronts and downbursts but also to detect such wind phenomena earlier.

Acknowledgments: The authors would like to thank SANDEN Corporation, SAVE ON, and Board of Education of Isesaki city for support POTEKA project.

Keywords: high dense ground observation network, Downburst, Gust fronts



## Preliminary Reports of Summer Sprite Observation Campaign at Summit of Mt. Fuji, Japan

SUZUKI, Yuko<sup>1\*</sup> ; SUZUKI, Tomoyuki<sup>1</sup> ; KAMOGAWA, Masashi<sup>1</sup>

<sup>1</sup>Dpt. of Phys., Tokyo Gakugei Univ

Many investigations of transient luminous events (TLEs) such as sprites and elves have been carried out since the 1990s. However, there are still unsolved issues like the morphologies of sprites. One of approach to investigate this issue is statistical study with collecting many events. In this study, we report a preliminary result of a mountain observation which enables us to observe the TLEs for a long term at the fixed point. The mountain observation was conducted at the summit of Mt. Fuji (3776 meter altitude), Japan, which enables us to detect the TLEs above off the coast of Boso peninsula, Chiba, Japan and the coast of Japan Sea which a large number of summer TLEs and the winter TLEs due to energetic positive cloud-to-lightning occurs. In particular, the altitude of the summit is located over the summer cloud covering the wide regions, so that the distant TLEs can be observed and low pressure and clean air yield better color images of TLEs. Moreover, the lower cost operation is possible, comparing with than the aerial and balloon measurement.

In the summer of 2013, we detected several events of TLEs with sensitive black-and-white CCD cameras at the fixed point for one month and with the color single-lens reflex camera. We will show the detailed analysis in the presentation. Such a mountain observation gives us a high chance to detect low-altitude blue-jets and starters and a 360-degree view from the isolated mountain, Mt. Fuji, also gives us a high chance to detect a number of TLEs. In this presentation, we show the results of sprite images taken at the summit of Mt. Fuji on Aug. 2, 2014.

Keywords: Sprite, Lightning, TLEs

## Development of polarimetric 2-D phased array weather radar using minimum mean square error method

KIKUCHI, Hiroshi<sup>1\*</sup> ; WU, Ting<sup>1</sup> ; USHIO, Tomoo<sup>1</sup> ; SHANG, Jin<sup>1</sup> ; KIM, Gwan<sup>1</sup> ; GOTO, Hideto<sup>2</sup> ; MIZUTANI, Humihiko<sup>2</sup>

<sup>1</sup>Osaka University, <sup>2</sup>Toshiba

We have been developing a polarimetric 2-D phased array weather radar which detects small scale phenomena such as tornadoes and downbursts. In this paper, we compare Beam Former method (BF), which is a conventional method in Digital Beam Forming signal processing of array antenna, with Minimum Mean Square Error method (MMSE), which is our proposed method, and discuss simulation results estimated by each method. In BF, antenna pattern is uniform and unique in the radar system, and its sidelobe level is high. As a result, if there are obstacles, for example high building, or very heavy rain area, the observation results of array antenna is imprecision in the region near them. In contrast, we can turn the null-point to interference wave direction at the same time we turn the mainlobe to the desired signal direction in MMSE.

Keywords: phased array radar, MMSE

## Metal Flux of Ferromanganese from Northwest and Equatorial Pacific

HISAAKI, Sato<sup>1\*</sup> ; USUI, Akira<sup>1</sup> ; NAKASATO, Yoshio<sup>1</sup> ; NISHI, Keisuke<sup>1</sup> ; IAN, Graham<sup>2</sup>

<sup>1</sup>Department of Integrated Arts and Sciences, Kochi university, <sup>2</sup>GNS science

The hydrogenetic ferromanganese crust is a slowly-growing chemical sedimentary rock composed iron and manganese oxides, with minor heavy metal elements, for example, Co, Ni, Pt, and REEs. We selected some seamounts on the Pacific plate and equatorial seamount for two typical model areas. We carried out occurrence observation of the crusts in a slope of the seamounts at water depths of 1000m to 3000m continually with high-vision camera equipped with ROV, and took intact and unbroken samples with the manipulator at Takuyo-5th seamount. We described substrate rocks, mineralogy and chemistry, and microstructures on fine-microscopic scales with radiometric dating (I. Graham, GNS).

The chemical analysis and calculation of metal flux indicated that, the Mn, the major component has concentrated continuously and fairly constantly in all areas and the depths, while the accumulation of Co depends mainly on water depth. On the other hand, elements which are of clastic origin including Fe and Al greatly reflect the distance from the continental source. Thus the hydrogenetic ferromanganese crusts are probably regarded as useful paleoceanographic archive.

Keywords: ferromanganese crusts, metal flux, northwest pacific, equatorial pacific

## Comparing rare earth elements in the surface layers of ferromanganese crusts and ambient seawater from the Takuyo Daigo

TOKUMARU, Ayaka<sup>1\*</sup> ; ZHU, Yanbei<sup>2</sup> ; NOZAKI, Tatsuo<sup>3</sup> ; TAKAYA, Yutaro<sup>4</sup> ; GOTO, Kosuke T.<sup>5</sup> ; SUZUKI, Katsuhiko<sup>3</sup> ; CHANG, Qing<sup>3</sup> ; KIMURA, Jun-ichi<sup>3</sup> ; KATO, Yasuhiro<sup>4</sup> ; USUI, Akira<sup>6</sup> ; URABE, Tetsuro<sup>7</sup> ; SUZUKI, Yohey<sup>1</sup>

<sup>1</sup>Dept. Earth Planet., Univ., Tokyo, <sup>2</sup>NIST/AIST, <sup>3</sup>IFREE/JAMSTEC, <sup>4</sup>Dept. System Innovation, Univ. of Tokyo, <sup>5</sup>GSJ/AIST, <sup>6</sup>Natural Sciences Cluster, Kochi Univ., <sup>7</sup>JMEC

Hydrogenetic ferromanganese (Fe-Mn) crusts are strongly enriched relative to the Earth's lithosphere in many rare and precious metals, including Co, Te, Mo, Bi, Pt, W, Zr, Nb, Y, and rare earth elements (REEs) (e.g. Hein et al., 2013). Accumulation of these trace metals from seawater is generally controlled by sorption (Koschinsky and Halbach, 1995; Koschinsky and Hein, 2003). REEs, except for Ce, behave as a dissolved trivalent cation in seawater and concentrated in the solid phase by adsorption (Nakada et al., 2013). Although a set of REE concentrations in Fe-Mn crusts is frequently used as a proxy to distinguish formation processes (e.g. Usui and Someya, 1997; Hein et al., 2000), it is not certain if REE concentrations in Fe-Mn crusts are correlated to those in surrounding seawater. In order to verify the correlation, REE concentrations in the outermost surface of Fe-Mn crusts and the surrounding seawater were directly compared at various depths (957-2987 m) on the Takuyo Daigo Seamount. We normalized the REE concentrations in the outermost surface of Fe-Mn crusts with its formation age, as the relative age of Fe-Mn crusts can be determined using osmium isotopic ratio (e.g. Klemm et al., 2005; 2008). For measurement of REE concentrations in seawater, inductively coupled plasma mass spectrometry (ICP-MS) was applied and solid phase extraction (SPE) techniques using chelating resins were conducted as pretreatment (Zhu et al., 2013). In this study, we compare depth profiles of the normalized REE concentrations in the outermost surface of Fe-Mn crusts and the REE concentrations in surrounding seawater.

Keywords: ferromanganese crust, seawater, Os isotope, rare earth elements, geochemistry

## Iron isotopic composition of seawater recorded in ferromanganese deposits

YAMAOKA, Kyoko<sup>1\*</sup> ; BORROK, David<sup>2</sup> ; USUI, Akira<sup>3</sup>

<sup>1</sup>Geological Survey of Japan, AIST, <sup>2</sup>Univ. of Louisiana, <sup>3</sup>Kochi Univ.

Iron isotopic composition of marine ferromanganese deposits could be a useful tool to understand the biogeochemical cycle of iron in the ocean. In this study, we measured the iron isotopic compositions ( $\delta^{56}\text{Fe}$  relative to IRMM-14) of hydrogenetic and diagenetic ferromanganese deposits from the Pacific Ocean (1400-6000 m water depth). The hydrogenetic ferromanganese crusts and nodules had a consistent average Fe isotopic composition of  $-0.32 \pm 0.12$  ‰ (2SD). The consistent  $\delta^{56}\text{Fe}$  values imply homogenous Fe isotopic composition of modern deep seawater in the central to northwestern Pacific. Despite differences in mineralogy and chemistry, the  $\delta^{56}\text{Fe}$  values of diagenetic nodules ( $-0.34$  to  $-0.20$  ‰) were indistinguishable from those of hydrogenetic origin. These observations suggest that dissolution and re-precipitation of Fe in sediments resulted in no significant Fe isotope fractionation. These values are apparently lower than the  $\delta^{56}\text{Fe}$  values of seawater from  $<900$  m in the central Pacific ranging from  $+0.01$  to  $+0.58$  ‰ (Radic et al., 2011), implying that deep water is enriched in isotopically light iron. We also reconstructed the temporal variations of iron isotopic compositions in three hydrogenetic ferromanganese crusts from different water depths (1440, 2239, 2987 m) in the northwest Pacific. Regardless of water depth, the  $\delta^{56}\text{Fe}$  values of these crusts showed essentially constant ( $-0.31 \pm 0.13$  ‰, 2SD) throughout the past  $\sim 20$  Ma. This is remarkably consistent with the constant iron isotopic compositions of ferromanganese crust ( $-0.31 \pm 0.10$  ‰, 2SD) in the central Pacific over the last 10 Ma (Chu et al., 2006). Thus, it is suggested that the Pacific deep water has remained constant in iron isotopic composition for long time scale.

Keywords: iron isotope, ferromanganese crust



## Fractionation of Hafnium-Zirconium in ferromanganese crusts

INOUE, Minami<sup>1</sup> ; SAKAGUCHI, Aya<sup>1\*</sup> ; KASHIWABARA, Teruhiko<sup>2</sup> ; USUI, Akira<sup>3</sup> ; TAKAHASHI, Yoshio<sup>1</sup>

<sup>1</sup>Hiroshima Univ., <sup>2</sup>JAMSTEC, <sup>3</sup>Kochi Univ.

The couples of High Field Strength elements (HFS elements), e.g. Zirconium (Zr)-Hafnium (Hf) and Niobium (Nb)-Tantalum (Ta), are called Twin-element due to the consistency of their valences and ionic-radii in the environment. As a consequence, these couples must show uniform ratio, which is theoretically same as that of chondrite meteorite. However, the significant fractionations among HFS elements in natural samples have been found, and it was proposed as enigma of Zr-Hf and Nb-Ta fractionation (Niu et al. 2012). The large fractionation of these elemental couples has also been found in the ferromanganese crust (FMC) (Bau 1996). In this study, we attempted to clarify the accumulation mechanism of HFS elements in FMCs with some methods including X-ray absorption fine structure (XAFS) technique for synthesised and natural samples to serve as an aid to approach to this enigma.

Six FMC samples were collected from the Takuyo-Daigo and Ryusei seamounts, from 950 m (summit) to 3000 m water depth, with hyper-dolphin (remotely operated vehicle) equipped with live video camera and manipulators. Near urface layer (less than 1 mm) of all FMC was analysed with XRD and XAFS to confirm the mineral composition and speciation of Zr together with chemical reagents, Zr minerals and rock samples as standard materials. The concentrations of Zr and Hf in these samples were also measured by ICP-MS after appropriate treatments. Furthermore, to serve as an aid to clarify the fractionation mechanism between Zr and Hf in FMCs, distribution coefficients (Kd) and chemical states were determined through the co-precipitation experiments of Hf and Zr with ferrihydrite and  $\delta$ -MnO<sub>2</sub>. To analyse the chemical states on the solid phase, XAFS was employed.

The major mineral composition of Fe and Mn had no significant variation with the water depth of these seamounts. The concentrations of Zr and Hf were increased with depth, and their ratios were varied without showing any trends. However, these ratios were totally fractionated from that in the seawater (Firdaus et al., 2011). For all samples, Hf was enriched in FMC compared to Zr. The chemical state of Zr in FMCs through the depth showed, 1) coprecipitation with ferrihydrite, 2) coprecipitation with  $\delta$ -MnO<sub>2</sub>, and 3) basalt-like composition, and the rate of basalt-like composition of Zr was increased with water depth. The concentrations of Zr in the fraction between ferrihydrite and  $\delta$ -MnO<sub>2</sub> were uniform through with the depth. Furthermore, the concentration of Zr in these fraction was also uniform, that is, the increased-concentration of Zr in the samples from deeper seamounts could be explained by the increase in basalt-like fraction. From the results of co-precipitation experiments of Zr and Hf with ferrihydrite and  $\delta$ -MnO<sub>2</sub>, it was found that the Hf-DFO was more precipitated compared with Zr-DFO. In this case, the bond length of Hf-O was significantly shorter than that of Zr-O.

Keywords: Zirconium, Hafnium, Ferromanganese crust

## Paleoceanographic Record on the Dual Structure of Hydrogenetic Ferromanganese Crusts

NISHI, Keisuke<sup>1\*</sup> ; USUI, Akira<sup>1</sup> ; NAKASATO, Yoshio<sup>1</sup> ; HISAAKI, Sato<sup>1</sup> ; IAN, Graham<sup>2</sup> ; YAMAOKA, Kyoko<sup>3</sup> ; GOTO, Kosuke T.<sup>3</sup>

<sup>1</sup>Kochi University, <sup>2</sup>The Institute of Geological and Nuclear Science, <sup>3</sup>National Institute of Advanced Industrial Science and Technology

Most Hydrogenetic ferromanganese crusts in the Pacific consist of two growth generations: a phosphatized older growth generation and a non-phosphatized growth generation. This study attempts some detail analyses such as macroscopy, microscopy, chemistry, mineralogy, age and growth rate determination to consider how the dual structures are formed. As a result of age growth rate determinations supported by GNS, the boundary of two growth generations concentrates approximately 15-10 Ma regardless of water depth and region. In the middle to late Miocene, the climate was prominently cold by Antarctic glaciation. As a result, a phosphogenesis of ferromanganese crusts may have occurred because the dissolves phosphate rich and oxygen rich deep water were redistributed to the intermediate water depths by upwelling at the seamounts.

Keywords: ferromanganese crust, marine environment, pacific, seamount

## Proposed valid description of ferromanganese crusts and the significance of this method

NAKASATO, Yoshio<sup>1\*</sup> ; USUI, Akira<sup>1</sup> ; HISAAKI, Sato<sup>1</sup> ; NISHI, Keisuke<sup>1</sup> ; GOTO, Kosuke T.<sup>2</sup>

<sup>1</sup>Department of Integrated Arts and Sciences, Kochi University, <sup>2</sup>Geological Survey of Japan

This study shows valid description of ferromanganese crusts for acid solution method. Before this, we used some detail analyses such as chemistry, mineralogy and microscopy. This method can extract the dissolution fragments from ferromanganese crusts and is more useful than the method used up, until now. The fragments consists of several kinds of minerals, for example, quartz, magnetite and clay mineral. These fragments, possibly, can be classified into detrital, biogenetic, volcanic and hydroge-netic origins.

Keywords: Ferromanganese crusts, Microstratigraphy, Paleoceanography

## Comparative analysis of microbial community on hydrogenetic ferro-manganese crusts from North-West Pacific Ocean

NITAHARA, Shota<sup>1\*</sup> ; KATO, Shingo<sup>2</sup> ; YAMAGISHI, Akihiko<sup>1</sup>

<sup>1</sup>Tokyo University of Pharmacy and Life Sciences, <sup>2</sup>RIKEN

Ferro-manganese crust (Mn crusts) is rock covered with iron and manganese oxides, and present on the boundary layer between hydrosphere and lithosphere. Mn crusts grow with sedimentation of these oxides from seawater. Growth rate is 1-10 mm/Myr, estimated by radiometric dating and magnetic stratigraphy (Usui and Someya, 1997). Mn crust is widely distributed on outcrop of seamount and sea plateau with slow sedimentation rate.

Mn crust contains several metals (ex. Cu, Co, Ni, Pt and Rare Earth Element etc. Hein, 2000). Considering content of rare metals and rare earth element, and abundance of Mn crust on seafloor, it is expected to use of Mn crust as a resource.

Our knowledge about microbes on surface and inside of Mn crust is limited. We analyzed the microbial community on the surface of Mn crust from Takuyo-Daigo Seamount at the depth of 2991 m. We show that high abundance of microbes and highly diversified microbial community on the surface of Mn crust and microbial community on Mn crust is different from that of sediment or seawater (Nitahara et al., 2011). However, it is not clear that these characteristics are general between Mn crust on different area or different depth. So we collected and analyzed Mn crust from several seamounts including Takuyo-Daigo seamount using 16S rRNA gene phylogeny.

We compared microbial communities of Mn crust from Takuyo-Daigo seamount and Ryusei seamount, there is a little difference. Comparative analysis between Mn crust, sediment and seawater from Takuyo-Daigo seamount and Ryusei seamount shows that microbial community composition of Mn crust and sediment are similar, while that of seawater is different from that of Mn crust and seawater.

In this presentation, in addition to Takuyo-Daigo seamount and Ryusei seamount, we will discuss about comparative analysis including Mn crust from Daito Ridge and Ogasawara sea plateau.

Hein, J.R.K., A.; Bau, M.; Manheim, F.T.; Kang, J.-K.; Roberts, L. (2000) Cobalt-rich ferromanganese crusts in the Pacific. In Handbook of marine mineral deposits. Cronan, D. (ed): Boca Raton: CRC Press, pp. 2-279.

Nitahara, S., Kato, S., Urabe, T., Usui, A., and Yamagishi, A. (2011) Molecular characterization of the microbial community in hydrogenetic ferromanganese crusts of the Takuyo-Daigo Seamount, northwest Pacific. FEMS Microbiol Lett 321: 121-129.

Usui, A., and Someya, M. (1997) Distribution and composition of marine hydrogenetic and hydrothermal manganese deposits in the northwest Pacific. Geological Society, London, Special Publications 119: 177-198.

## On-site deposition and exposure experiments at a low-temperature hydrothermal area

USUI, Akira<sup>1\*</sup> ; HINO, Hikari<sup>1</sup> ; SUZUKI, Yohey<sup>2</sup> ; YAMAOKA, Kyoko<sup>3</sup> ; OKAMURA, Kei<sup>4</sup>

<sup>1</sup>Kochi University, <sup>2</sup>Earth & Planetary Sciences, Univ. Tokyo, <sup>3</sup>Geological Survey of Japan, AIST, Tsukuba, <sup>4</sup>Kochi Core Center, Kochi University

An on-site deposition and on-site adsorption experiments were carried out at a possible hydrothermal area in the Izu-Bonin arc, NW Pacific. The mineralogical and chemical analyses on the exposed glass, ceramics and on the artificial busserite samples suggested a new precipitation during 12 years and positive accumulation of some transitional metals. This finding was the first evidence of modern active precipitation of manganese oxide from normal sea water/ hydrothermal waters in the ocean floors.

Keywords: low-temperature hydrothermal activity, bayonaise hill, manganese mineral, busserite, todorokite, adsorption

## Uranium isotope composition in ferromanganese crusts: Implications for the paleoredox proxy

GOTO, Kosuke T.<sup>1\*</sup> ; ANBAR, Ariel D.<sup>2</sup> ; GORDON, Gwyneth W.<sup>2</sup> ; ROMANIELLO, Stephen J.<sup>2</sup> ; SHIMODA, Gen<sup>1</sup> ; TAKAYA, Yutaro<sup>3</sup> ; TOKUMARU, Ayaka<sup>3</sup> ; NOZAKI, Tatsuo<sup>4</sup> ; SUZUKI, Katsuhiko<sup>4</sup> ; MACHIDA, Shiki<sup>5</sup> ; HANYU, Takeshi<sup>4</sup> ; USUI, Akira<sup>6</sup>

<sup>1</sup>GSJ, AIST, <sup>2</sup>Arizona state University, <sup>3</sup>The University of Tokyo, <sup>4</sup>JAMSTEC, <sup>5</sup>Waseda University, <sup>6</sup>Kochi University

Variations of the  $^{238}\text{U}/^{235}\text{U}$  ratio ( $d^{238}\text{U}$ ) in sedimentary rocks have been proposed as a possible proxy for decoding the paleo-oceanic redox conditions, although the marine U isotope system is not fully understood (Stirling et al., 2007 GCA; Weyer et al., 2008 EPSL).

Here we investigate the spatial variation of  $d^{238}\text{U}$  in modern ferromanganese crusts by analyzing U isotopes in the surface layer (0-3 mm depth) of 19 samples collected from 6 seamounts in the Pacific Ocean. The  $d^{238}\text{U}$  values in the surface layers show little variation and range from -0.59 to -0.69 permil. The uniformity of  $d^{238}\text{U}$  values is consistent with the long residence time of U in modern seawater (Dunk et al., 2002 Chem. Geol.), although the  $d^{238}\text{U}$  values are lighter than that of present-day seawater by  $\sim 0.24$  permil (Stirling et al., 2007 GCA; Weyer et al., 2008 EPSL). The light  $d^{238}\text{U}$  is consistent with the isotope offset found during the adsorption experiment of U to birnessite (Brennecke et al., 2011 ES&T). Our results suggest that removal of lighter U from seawater to ferromanganese crusts is responsible for the second largest uranium isotopic fractionation in the modern marine system and could provide a source of heavy U to seawater.

Depth profiles of U isotopes ( $d^{234}\text{U}$  and  $d^{238}\text{U}$ ) in two ferromanganese crusts were investigated to reconstruct the evolution of oceanic redox state during the Cenozoic. The depth profiles of  $d^{238}\text{U}$  show very limited ranges, and have similar values with those of the surface layer samples. The absence of any resolvable variations in the  $d^{238}\text{U}$  depth profiles suggests that the relative proportions of oxic and reducing uranium sinks have not varied significantly over the past 40 Myr. However, the  $d^{234}\text{U}$  depth profiles in the same samples suggest the possible U redistribution after deposition. Therefore, the  $d^{238}\text{U}$  values may have been overprinted by secondary mobilization with pore-water or seawater. These results suggest that careful evaluation of secondary disturbance is required before applying chemical and isotope depth profiles of ferromanganese crusts to understand paleocean environmental changes.

To assess the potential effect of U removal by Mn oxides on seawater  $d^{238}\text{U}$ , we calculated the seawater  $d^{238}\text{U}$  under different fractions of U removal by Mn oxides using a simple isotope balance model. This calculation suggests that seawater  $d^{238}\text{U}$  could have varied significantly throughout the Earth's history along with the changes of the Mn oxides accumulation rate.

Keywords: Uranium,  $^{238}\text{U}/^{235}\text{U}$ ,  $^{234}\text{U}/^{238}\text{U}$ , paleoredox, ferromanganese crust, isotope geochemistry

## Amplification of induced current due to complicated resistivity structure in the earth

GOTO, Tada-nori<sup>1\*</sup>

<sup>1</sup>Graduate School of Engineering, Kyoto University

Abrupt changes of geomagnetic field can make large induced electric current on the earth, and yield damages to pipelines, cables and other architectures. For understanding the phenomena and future risks, explorations of sub-surface resistivity structure are necessary because the heterogeneous resistivity structure in the crust and mantle amplifies the induced electrical current locally. The hazard prediction based on the homogeneous earth may result in the under-estimation. Here, I introduce possible cases of induced current near the coastal areas, based on two-dimensional (2D) and three-dimensional (3D) earth structure including the sea layer. My study is based on the numerical forward calculation of induced electric field in the earth. The former case comes from 2D forward simulation. In this case, the straightly elongated coastal line is assumed, and various sub-surface and sub-seafloor resistivity structures are imposed. The numerical results suggest that the amplitude of induced current becomes about 6 times larger than the homogeneous earth without the sea layer. The width of affected land zone is about 20 km from the coast line. In the second case, the 3D forward modeling is employed to express the complicated coastal line and bathymetry. As a result, the amplitude goes double at the cape zones. These phenomena come from the boundary charge along the coastal area. I conclude that electrical structure around the coast line (not only below the land, but also below the seafloor) should be focused for the huge induce current.

Keywords: Geomagnetic field, Induced current, Land-Ocean interaction, resistivity

## A Numerical Simulation of the Geomagnetically Induced Electric Field with the Three-Dimensional Resistivity Model

ENDO, Arata<sup>1\*</sup> ; FUJITA, Shigeru<sup>2</sup> ; FUJII, Ikuko<sup>3</sup>

<sup>1</sup>Japan Meteorological Agency, <sup>2</sup>Meteorological College, <sup>3</sup>Magnetic Observatory

The Geomagnetically induced current (GIC) sometimes causes power-line failure in the geomagnetically high-latitude regions like Canada and Sweden. On the other hand, it has been regarded that Japan is free from this danger because it is located in the lower-latitude region. However, this assumption may not be valid when an extremely severe space weather event happens. In addition, as the GIC and the induced electric field are strongly controlled by non-uniform distribution of the Earth's electric resistivity, we need to evaluate these values taking the non-uniform distribution into account. It is noted that there has been no works about it. In this talk, we will present the geomagnetically induced electric field based on the modeled electric resistivity distribution by using a numerical code applicable to the three-dimensional induction problems. As the results, there are large anomalies in the intensity of the electric field in Japan.

Keywords: Geomagnetically Induced Current, SC, resistivity, conductivity, magnetic storm



## Simultaneous inversion of temporal magnetotelluric signal change and conductivity structure using the time domain simula

IMAMURA, Naoto<sup>1\*</sup> ; SCHULTZ, Adam<sup>2</sup> ; GOTO, Tada-nori<sup>1</sup> ; TAKEKAWA, Junichi<sup>1</sup> ; MIKADA, Hitoshi<sup>1</sup>

<sup>1</sup>Graduate School of Engineering, Kyoto University, <sup>2</sup>Oregon State University

Magnetotelluric method is mainly used for estimation of subsurface resistivity structure. However, the time-domain analysis of source field is normally omitted, although its estimation should be included at the cases such as in the high-latitude zones or on the global scale. In previous research, simultaneous inversion is proposed to estimate both magnetotelluric signal and resistivity structure in the earth. Koch and Kuvshinov (2013) proposed inversion algorithm that iteratively estimates magnetotelluric signal and resistivity structure, although this inversion method cannot determine both unknowns in a seamless manner. In this study, we developed simultaneous inversion that can determine both unknowns at the same time. Because magnetotelluric signal is considered non-stationary time series, we try a direct inversion of time-domain electromagnetic field, not in the frequency -domain. It has a chance to give higher accuracy than the frequency domain inversion.

Our new inversion results applied to the synthetic model suggested that we could estimate both magnetotelluric signal and resistivity structure properly even under the condition of noise contamination in the observed data. Moreover, when the time domain and frequency domain inversions are applied to same synthetic time series, the result using time domain inversion has higher resolving capability than result using the frequency domain inversion.

Keywords: Magnetotelluric method, Time domain modelling, Simultaneous inversion

## Geoelectric Field at Kakioka, Kanoya, and Memambetsu

FUJII, Ikuko<sup>1\*</sup>

<sup>1</sup>Kakioka Magnetic Observatory, JMA

Kakioka Magnetic Observatory, Japan Meteorological Agency (JMA) has continuously observed the geoelectric field at Kakioka, Kanoya, and Memambetsu for decades. I checked the JMA collection of the geoelectric field from a view point of applicability to studies on the geomagnetically induced current (GIC).

Two horizontal components (northward and eastward components) of the geoelectric field are obtained on the geographical coordinates at the three sites by measuring voltage differences between two pairs of electrodes. Details of the measurements such as locations and materials of the electrodes, baseline lengths, sampling intervals, and filtering responses of the systems differ time to time giving fluctuations on data quality.

I picked up a 11-year data segment ranging from Jan 1, 2000 to investigate the characteristics of the geoelectric field obtained by JMA.

It turned out that the geoelectric fields at three sites were unstable on the long-term basis because the baseline lengths are as short as a few hundred meters and the instability of the electrodes are relatively noticeable. However, the electric field highly correlates with the geomagnetic field at periods from 100 sec to 1 day at any of three sites, suggesting the geoelectric field induced by a change of the geomagnetic field is successfully obtained at least on the short-term basis. Amplitudes of the geoelectric field are different among the sites. For instance, the eastward component of the field is about 10 times larger than the other at Kakioka, while the northward component is larger than the other at Memambetsu.

The MT response was computed at the three sites to evaluate the signal and infer effects of electrical conductivity structures. A robust procedure BIRRP (Chave and Thomson, 2004) was applied to 0.1 sec, 1 sec and 1min values of the geoelectric and geomagnetic fields at large-scale geomagnetic storms in 2003 and 2004 to estimate the MT response at periods shorter than 10000 sec. Since the 0.1 and 1 sec values of the geoelectric and geomagnetic fields are affected by system filters, shortest periods were not able to be included into the response estimation even after corrections of the filters were made. As for that at periods longer than 10000 sec, I verified a procedure to decompose a time series by Fujii and Kanda (2008) so that a noisy data set can be treated. Then, a trend with step-like anomalies and outliers were estimated from a 11-year segment of 1 hour values of the geoelectric field. Then, the MT response was estimated from the geoelectric field with the trend and outliers removed. In the end, the MT response was obtained at periods from several sec to 12 days. If this response is converted into the time domain by convolution, filter coefficients to estimate the geoelectric field from the geomagnetic field will be obtained.

Effects of local small-scale structures on the MT response were checked as a next step. The  $Z_{yx}$  at Kakioka shows an unusually high value ( $\sim 1000$  ohm m) even at a period of 10days and the comparison with the C value by Fujii and Schultz (2002) suggests it is about 100 times amplified by the local small-scale structures.

Yanagihara and Yokouchi (1965) explained a biased distribution of the electric field at a short frequency range at Kakioka by heterogeneities of a near surface structure. If these affects even at very long periods, use of the geoelectric field at Kakioka for GIC or induction studies should be done with a certain caution.

The electric field at three sites basically reflects the induction as it is supposed to be, although the measurement system and procedure can be verified so that data of higher quality are obtained.

Keywords: geoelectric field, induction, geomagnetically induced current, MT response

## Magnetotelluric method and the source field with finite wave number

OGAWA, Yasuo<sup>1\*</sup>

<sup>1</sup>Volcanic Fluid Research Center, Tokyo Institute of Technology

Magnetotelluric method is now widely used for mapping the crustal and upper mantle structure in three-dimensions. In magnetotelluric method, we normally assume the source field as a plane wave. However, if the source field has a finite wave length, the impedances (apparent resistivity, and impedance phase) and the geomagnetic transfer functions will be affected. In a simple case with uniform earth where the source field has a wave number is considered. The apparent resistivity inferred from the impedance (ratio of horizontal electric field to the orthogonal horizontal magnetic field), by assuming a plane wave source will be biased downward and impedance phase will be biased upward. Also the geomagnetic transfer function will have phase of  $\pi/4$ , even without any lateral heterogeneity.

Some magnetotelluric studies at the high latitude and under the magnetic equator will be reviewed.

Keywords: magnetotelluric method, source field

## Electromagnetically coupled system between non-uniformly and anisotropically conducting inner earth and upper atmosphere

YOSHIKAWA, Akimasa<sup>1\*</sup>

<sup>1</sup>International Center for Space Science and Education, Kyushu University

Electromagnetically coupled system between upper atmosphere and inner earth, is discussed. It is well known that upper atmosphere and inner earth system is electromagnetically coupled across very small conducting atmospheric region, which means 'primary' induced electric field produced by the mutual coupling is almost inductive (divergence free). However if the conductivity distribution is inhomogeneous, 'secondary' polarization (curl-free) electric field can be produced at the region of conductivity gradient. In the ionosphere, non-uniform Hall conductivity distribution induces the Hall polarization field, which becomes cause of current concentration and potential deformation by the Cowling effect. Formation of Cowling channel is one of the most important and peculiar nature of weakly ionized system under strongly background magnetic field distribution.

In this presentation, we will introduce basic feature of electrodynamics at the non-uniform and anisotropically conducting ionosphere, and will discuss a possible electromagnetic coupling mechanism when the telluric conductivity distribution is non-uniform and anisotropic.

Keywords: ionospheric current, telluric current, electromagnetically coupled system

## The distribution of the internal geomagnetic field during a magnetic storm

IWASHITA, Kodai<sup>1\*</sup> ; TOH, Hiroaki<sup>2</sup>

<sup>1</sup>Graduate School of Science, Kyoto University, <sup>2</sup>Data Analysis Center for Geomagnetism and Space Magnetism,

We calculated the Gauss coefficients of magnetic potential and estimated the current in the earth during a magnetic storm.

There are two kinds of magnetic storms. One is sudden. The other is synchronized to the sun's rotation period. How does the earth react to such a strong disturbance of external magnetic field?

We quantitatively estimated the induced current in the earth which had reacted to the large change of magnetic field like a strong magnetic storm, using a spherical harmonic expansion and a three dimensional forward calculation code. With a spherical harmonic expansion, we used geomagnetic data of the surface of the earth and calculated the internal and external geomagnetic field. With a three dimensional forward calculation code, we used the time variation of the external Gauss coefficients calculated by the spherical harmonic expansion and visualized and quantified the induced current in the earth during a magnetic storm.

We expect that we estimate the electric conductivity of the earth with the internal Gauss coefficient to the external Gauss coefficients ratio as a development of this study.

Keywords: induced current, magnetic storm

## Why did the Carrington storm recover very rapidly?

KEIKA, Kunihiro<sup>1\*</sup>; EBIHARA, Yusuke<sup>2</sup>; KATAOKA, Ryuho<sup>3</sup>

<sup>1</sup>Solar-Terrestrial Environment Laboratory, Nagoya University, <sup>2</sup>Research Institute for Sustainable Humanosphere, Kyoto University, <sup>3</sup>National Institute of Polar Research

Intense geomagnetic storms are accompanied by rapid recovery, as represented by a quick increase of the Dst index after its minimum. As far as the geomagnetic storms that we have observed since the early 20th century, the more intense storms experienced the more rapid recovery. The Carrington event on 2 September 1859 also experienced an extremely rapid recovery ( $>1000$  nT/h at Bombay, India;  $>300$  nT/h with 1-hour average data). At least three major processes that occur in the Earth's inner magnetosphere are proposed to explain such rapid recovery: (1) the neutralization of energetic  $O^+$  ions through charge exchange, (2) flow-out of energetic ions to the interplanetary field, and (3) loss of energetic ions into the atmosphere through pitch-angle scattering due to interactions with electromagnetic ion cyclotron (EMIC) waves. In addition, a sudden increase in the solar wind dynamic pressure around the storm maximum could cause a quicker recovery.

In this talk, we focus on intense magnetic storms with the Dst minimum smaller than  $-200$  nT for which solar wind data are available. We first examine whether the rapid recovery can be explained by an ion flow-out effect associated with sudden changes of solar wind density, by modifying the empirical Burton's equation. We also estimate the amount of energetic  $O^+$  ions, the spatial extent of EMIC wave active regions, and the increase rate of the solar wind dynamic pressure that could be required to reproduce the storm rapid recovery. In addition, we discuss how quickly the geomagnetic field could change during the recovery of an extremely intense storm such as the Carrington event.

**Keywords:** The Carrington event, Geomagnetically induced currents (GICs), Ring current, Magnetopause current, Interplanetary shocks, Coronal mass ejections (CMEs)

## Consideration of geomagnetically induced currents — a case of geomagnetic sudden commencement(SC)

ARAKI, Tohru<sup>1\*</sup> ; SHINBORI, Atsuki<sup>2</sup>

<sup>1</sup>Polar Research Institute of China, <sup>2</sup>RISH, Kyoto University

Siscoe et al.(1968) assumed a relationship between the SC amplitude,  $dH$ , and solar wind dynamic pressure,  $P_d$ , as  $dH = fgk d(P_d)^{0.5}$  and experimentally determined the proportional constant,  $k$ . Here  $f$  is a constant associated with the solar wind-magnetosphere interaction and  $g$  shows effects of currents induced in the Earth. This constant  $g$  has been traditionally taken as 1.5 without detailed check of its meaning for a long time. Here we make a physical consideration on it based upon the present SC model.

The disturbance field of SC,  $D_{sc}$ , is expressed as  $D_{sc} = DL + DP_{pi} + DP_{mi}$ .

Here,  $DL$  is caused by the magnetopause current (MC) enhanced during sudden compression of the magnetosphere and dominant in low latitudes on the ground.  $DP$  is produced by field-aligned currents (FAC) and FAC-produced ionospheric currents (IC) and larger in the higher latitude region.

The  $DP$  shows a two pulse structure where the first pulse is called  $pi$  (preliminary impulse) and the following pulse is denoted as  $mi$  (main impulse). Thus we have to assume 3 current sources in the consideration of induction effects of SC.

The magnetopause current, MC induces currents both in the ionosphere and Earth. As the induced ionospheric current reduces the amplitude of SC on the ground while the earth currents enhance it, induction current effects will be small for the  $DL$  field. Ionospheric currents causing the  $DP$  field induces currents only in the Earth which enhances the  $DP$  field on the ground.

The LT variation of SC amplitude shows the maximum in the D-component and minimum in the H-component around 8h LT in low and middle latitudes. On the other hand, calculation of a global distribution of ionospheric currents produced by a pair of FACs shows that the current direction is in north-south near 8h LT. This means that the H-component amplitude of SC observed near 8h LT consists of only the  $DL$  field which is less affected by induction effects..

Keywords: sudden commencement, induced current, ionospheric current,, magnetopause current, DL/DP-field

## Quasi-periodic DP2 fluctuations in the geomagnetically induced currents

KIKUCHI, Takashi<sup>1\*</sup> ; WATARI, Shinichi<sup>2</sup> ; HASHIMOTO, Kumiko<sup>3</sup> ; EBIHARA, Yusuke<sup>4</sup>

<sup>1</sup>Solar-Terrestrial Environment Laboratory, <sup>2</sup>National Institute of Information and Communications Technology, <sup>3</sup>Kibi International University, <sup>4</sup>Research Institute for Sustainable Humanosphere

The geomagnetically induced current (GIC) has been attributed to the time change in the Bx component of the ground magnetic field. However, the GIC was found to be well correlated with By component at mid latitudes [e.g., Watari et al., Space Weather 2009]. Braendlein et al., JGR 2012] reported that the GIC has diurnal and seasonal variations, and suggested that the GIC could be a return current of the ionospheric currents via the wave front of the TM0 mode waves in the Earth-ionosphere waveguide [Kikuchi and Araki, JATP 1979]. We analyzed the quasi-periodic fluctuations in the GIC recorded in Hokkaido on December 14 2006, which accompany the DP2 fluctuations in the equatorial electrojet (EEJ) and D-component magnetic field at midlatitudes. We found that the GIC is well correlated with the EEJ as well as the midlatitude D-components. We suggest that the midlatitude GIC is a part of the magnetosphere-ionosphere-ground (MIG) circuit currents [Kikuchi, JGR 2014], and therefore, the GIC is the return current of the ionospheric currents via the wave front of the TM0 mode waves.

Keywords: midlatitude geomagnetically induced current, midlatitude D-component magnetic field, equatorial electrojet, TM0 Earth-ionosphere waveguide mode



## Statistical properties of superflares on solar-type stars

MAEHARA, Hiroyuki<sup>1\*</sup>; SHIBAYAMA, Takuya<sup>2</sup>; NOTSU, Yuta<sup>2</sup>; NOTSU, Shota<sup>2</sup>; HONDA, Satoshi<sup>3</sup>; NOGAMI, Daisaku<sup>2</sup>; SHIBATA, Kazunari<sup>2</sup>

<sup>1</sup>University of Tokyo, <sup>2</sup>Kyoto University, <sup>3</sup>University of Hyogo

Solar-flares are energetic explosions in the solar atmosphere. The energy released by a solar flare is typically of the order of  $10^{29}$  -  $10^{32}$  erg. Recent high-precision photometry from space shows that "superflares", which are 10-10000 times more energetic

than the largest solar-flares, occur on Sun-like stars (slowly rotating G-type main sequence stars).

We present recent results on superflares on solar-type stars using the high time-resolution data. We search for superflares from the short-cadence data (time resolution: 1 min) of about 1300 solar-type stars observed with the Kepler space telescope and found about 150 superflares on 20 stars. The energy of detected flares ranges from  $10^{33}$  to  $10^{35}$  erg, which is equivalent to that of X100 - X10000 class solar flares. These superflare data, combined with the previous results from the low time-resolution data (1547 superflares on 279 solar-type stars), indicate that the occurrence frequency distribution of superflares can be fitted in the energy range  $>10^{33}$  erg by a simple power-law function with the index of about -2. Moreover, the frequency distribution of superflares on Sun-like stars and that of solar flares are roughly on the same power-law line. The average occurrence frequency of superflares with energy of  $10^{33}$  erg (X100 class) is about once in 100 years and that of superflares with energy of  $10^{34}$  erg (X1000 class) is about once in 1000 years. The duration of superflares depends on the total energy released by superflares. Larger flares tend to have longer duration time. The duration of superflares is proportional to the 1/3 power of the flare energy. This correlation between energy and duration of superflares on solar-type stars is similar to that of solar flares. These results suggest that statistical properties of superflares on solar-type stars is basically the same as those of solar flares.

Keywords: superflare, solar flare

## Extreme value statistics analysis of the auroral electrojet indices

NAKAMURA, Masao<sup>1\*</sup>; YONEDA, Asato<sup>1</sup>; TSUBOUCHI, Ken<sup>2</sup>

<sup>1</sup>Osaka Prefecture University, <sup>2</sup>Tokyo Institute of Technology

The worst space environment phenomena have a possibility of damaging electric transmission grids due to large induced currents on the earth and causing satellite anomalies due to increased high energy plasma on satellite orbits. Therefore a statistical study of the worst substorm events is important. For the study, we utilize extreme value statistics, which focus on the statistical behavior in the tail of a distribution. We analyze the one-minute values of the auroral indices (AE, AU, AL) in 1996-2012. These indices are derived from geomagnetic variations in the horizontal component observed at twelve observatories along the auroral zone in the northern hemisphere. The AU and AL indices are the uppermost and lowermost envelopes of the superposed horizontal component perturbations, and are thought to represent the maximum eastward and westward electrojet currents over the auroral zone, respectively. The AE index is defined by the separation between the upper and lower envelopes ( $AE=AU-AL$ ) and commonly used as an index of the aurora activity. As a result of the analysis, we can estimate the upper limit of AU and the lower limit of AL, which suggests the maximum strengths of the eastward and westward electrojet currents. However, it is found that the AE index is not suitable for the extreme value statistics analysis, because it is a combined index. The largest values of AE are not generated by a single process and do not show a simple extreme value distribution.

Keywords: Auroral electrojet index, Extreme value statistics

## Statistical estimations of geomagnetic disturbances at Kakioka, Memambetsu and Kanoya

MINAMOTO, Yasuhiro<sup>1\*</sup> ; FUJITA, Shigeru<sup>2</sup> ; OOGI, Junpei<sup>1</sup> ; HARA, Masahiro<sup>1</sup>

<sup>1</sup>Kakioka Magnetic Observatory, Japan Meteorological Agency, <sup>2</sup>Meteorological College, Japan Meteorological Agency

We investigated scale of geomagnetic disturbances which can cause extremely large geomagnetically induced current with record of geomagnetic phenomena by The Japan Meteorological Agency with statistical analyses. In this presentation, we will show the following items,

1. an estimation of the scale of millennium magnetic storm calculated from 1932 cases of observations at Kakioka magnetic observatory.
2. estimations of the scale of millennium storm sudden commencements and sudden impulses calculated from 2848, 2408 and 2257 cases of observations at Kakioka, Memambetsu and Kanoya respectively.
3. probable geomagnetic disturbances suggested from one-minutes data of geomagnetic field at Kakioka, Memambetsu and Kanoya over about thirty years.

Keywords: magnetic storm, sudden impulse, storm sudden commencement, statistics, magnetic observatory

## Analysis of geomagnetically induced current measured in Japan

WATARI, Shinichi<sup>1\*</sup>

<sup>1</sup>National Institute of Informaton and Communications Technology

It is known that there is a possibility of failure of power grids caused by geomagnetically induced currents associated with intense geomagnetic storms. It is believed that effect of GIC is small in Japan because Japan locates low geomagnetic latitude comparing with its geographical latitude. Damage of transformer is reported from the Republic of South Africa associated with the October, 2003 storm. The Republic of South Africa locates in similar geomagnetic latitude with that of Japan. We made GIC measurements of a transformer of the Memanbetsu substation between 2005 and 2007. Those data are compared with geoelectric data observed by the Memanbetsu geomagnetic observatory of Japan Meteorological Agency. We estimated GICs associated with past intense geomagnetic storms using the geoelectric field data based on the result of the comparison. The result of our analysis will be reported.

Keywords: Geomagnetically Induced Current, geomagnetic storm, earth current, power grids, space weather

## Global MHD simulation of the magnetospheric response to large and sudden enhancement of the solar wind dynamic pressure

KUBOTA, Yasubumi<sup>1\*</sup> ; KATAOKA, Ryuho<sup>2</sup> ; DEN, Mitsue<sup>1</sup> ; TANAKA, Takashi<sup>3</sup> ; NAGATSUMA, Tsutomu<sup>1</sup> ; FUJITA, Shigeru<sup>4</sup>

<sup>1</sup>NICT, <sup>2</sup>NIPR, <sup>3</sup>Kyushu University, <sup>4</sup>Meteorological College

A large and sudden enhancement of the dynamic pressure in the solar wind generates a geomagnetic sudden commencement (SC). The magnetic field variation of SC at auroral latitudes shows a bipolar change which consists of preliminary impulse (PI) and main impulse (MI). Fujita et al. [2003a, 2003b] reproduced the PI/MI magnetic field variation using a magnetosphere-ionosphere coupling simulation and clarified the fundamental mechanisms. Interestingly, Araki et al. [1997] reported an anomalously large-amplitude SC of more than 200 nT with an unusually spiky waveform at low latitude, which occurred when the magnetopause was pushed inside geostationary orbit. Such a super SC is the target of this study. We investigate the large-amplitude SC at auroral latitudes when a large solar wind dynamic pressure impinges on the magnetosphere using a newly developed magnetosphere-ionosphere coupling simulation which has advanced robustness. We simulate two SC events of dynamic pressure enhancement of 16 times larger than the standard value, caused by the density enhancement and velocity enhancement, respectively. As an initial result of the comparison with the SC events, it is found that magnetic field variation of PI/MI is larger and sharper in the case of velocity rise than the case of density rise. It is therefore suggested that high-speed solar wind may be needed to create large and sharp SC. It is also found that a magnetic field variation similar to so-called Psc appears after PI/MI only in the case of velocity rise. When the high-speed solar wind impinges on magnetosphere, vortices are repeatedly formed at the equatorial magnetopause, probably due to the K-H instability. It seems that the high pressure of the vortices play an essential role as a current generator to drive the field-aligned currents and the magnetic field oscillation. In this presentation, we discuss the mechanisms of super SC in more detail, combining the other interesting simulation results.

## Radiations of earthquake-excited electromagnetic waves from the ground

TSUTSUI, Minoru<sup>1\*</sup>

<sup>1</sup>Kyoto Sangyo University

We have been observing electromagnetic (EM) pluses excited by earthquakes, using tri-axial electromagnetic sensor system installed in a borehole of 100 m in depth in the campus of Kyoto Sangyo University. During the period of 13 months from December 20, 2011 to March 26, 2013, we had nineteen earthquakes with magnitude of  $M > 2$  occurred around our EM observation site. They were within a circle of radius of 40 km centered at the EM observation site. We have confirmed detections of clear EM pulses for thirteen earthquakes among them. Seismic intensities at the EM observation site by these earthquakes were mostly 1 or less. From March, 2013, we added EM measurement above the ground. Furthermore, we began to capture waveforms of EM pulses in the borehole and above the ground and of seismic waves installed near the borehole simultaneously. Then we have confirmed that the detected EM waves were co-seismic ones readily generated by piezo-electric effect in earth's crusts [1].

Figure 1(a) shows a waveform of seismic wave detected at the EM observation site when an earthquake of M3.0 occurred at 10 km depth and at 5.4 km north of the EM observation site at 03:57 Dec. 2013, and (b) shows a waveform of magnetic  $H_{ew}$  components of the EM pulse detected in the borehole. Figure 1(c) also shows a waveform of  $H_{ew}$  component of the EM pulses detected above the ground where is on a hill of 60 m at about 600 m south-east of the EM observation site, in which the waveform have delayed 0.257 sec from that measured in the borehole. Therefore, this result shows clear evidence that earthquake-excited EM pulse has been radiated from the ground. We had another evidence of EM pulse radiation out of the ground surface when a large earthquake (M6.3) occurred at 14.8 km depth and at 130 km south-west of the EM observation site, in which earthquake-excited EM pulse was detected above the ground of the EM observation site in the campus. In that case, EM pulse was detected above the ground at 13.063 sec prior the detection in the borehole.

Next step is to detect and confirm EM pulses radiated at the occurrence of earthquakes. The final destination is to detect EM pulses radiated before earthquakes. For these purposes, we need to accomplish measurements of EM pulses in deeper earth (at about 1 km depth) after improving the sensitivity of the EM sensors.

[1] M. Tsutsui, submitted to IEEE Geoscience, Letters, 2014.

Keywords: seismic wave, electromagnetic wave, observations above and under ground, EM wave radiation from the ground

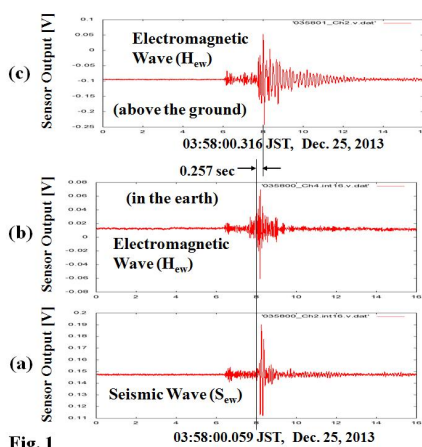


Fig. 1

## A statistical study for relationship between anomalous transmission of VHF band radio waves and earthquakes at Hidaka

MORITA, Shou<sup>1\*</sup> ; MOGI, Toru<sup>1</sup>

<sup>1</sup>Institute of Seismology and Volcanology, Hokkaido University

Electromagnetic phenomena precursors to earthquakes, such as variations of geo-electric current, total electron contents in the ionosphere and anomalous transmission of radio waves, have been observed (ex. Hayakawa, 1996). The statistical relationship between such anomalies and an earthquake has investigated statistically (Liu et al., 2011; Orihara et al., 2012).

Anomalous transmission of VHF-band radio wave beyond the line-of-sight has been investigated by many researchers (Kushida and Kushida, 2002), and anomalous FM broadcasting wave (VHF range) has observed close to the epicenter of impending (Moriya et al., 2010). Radio waves transmitted from a given FM radio station are considered to be scattered, such that they could be received by an observation station beyond the line of sight. A quantitative correlation between total duration of scattered wave transmission and the magnitude, or maximum seismic intensity has been proposed (Moriya et al., 2010).

Nevertheless, a statistical relation between the anomalies transmission in VHF-band and impending earthquakes has not been investigated yet. We carried out statistical consideration by using the anomalous transmission data documented by Hokkaido University, and discuss the significance of this relation in this study.

The anomalous VHF-band radio wave data used in this research was observed at the Erimo observatory in Hidakra area from June 1st 2012 to December 31th, 2013. To judge anomalous data, we refer to the statistical method proposed by Liu et al. (2011) that they had used to detect abnormal signals of GPS TEC (total electron content) variations. We adopt a certain standard from median of observed data, and we identified anomalies if data beyond the standard value over 10 minutes.

As a result, some earthquakes were observed precursory anomalous radio propagation, but others are not observed a precursory anomaly. If we set the standard values strictly, the numbers of misdetections are decreased.

Big noises are found because of the appearance of a sporadic E layer in the ionosphere and so on especially in summer. We have to overcome the problem that how to remove such noises.

The earthquakes that we have chosen as targets were magnitude is more than 4.0 and the distance from Erimo observatory is less than 50km as the first trial.

We will investigate the statistical method in many conditions such as duration time, threshold of anomaly, magnitude, hypocenter distance etc and also discuss reasonable method to remove big noise. After that, we need to discuss probability of prediction using the relation between the occurrence of earthquake and anomalous transmission of radio wave propagation.

Keywords: ionosphere, anomalous transmission, relation with earthquakes

## Preseismic geomagnetic deflection synchronized with GPS-TEC enhancement 2011 Tohoku-Oki earthquake

HEKI, Kosuke<sup>1\*</sup>

<sup>1</sup>Toyama Industrial Technology Center

The GPS-TEC enhancement starting 40 minutes before the 2011 Tohoku-Oki earthquake has been observed (Heki, GRL, 2011). The geomagnetic declination change was confirmed nearby the fracture zone, at Easashi (ESA), Mizusawa (MIZ) by GSI and at Kakioka (KAK), Kanozan (KNZ) by JMA in respect to Kanoya (KNY) in synchronization with the GPS-TEC anomaly (Heki & Enomoto, JGR, 2013). These anomalies satisfy the criteria of earthquake precursor candidate (Wyss, AGU, 1991).

The magnetic declination; the difference between the direction of the horizontal components H of the Earth's magnetic field and the magnetic north is normally 6.9 degree westward (= -415.7 arc min) from true north at the ESA site, but, as seen in the Figure,  $\Delta D$  ([ESA]-[KNY]) gradually changes to the positive direction (eastward) starting from 40 minutes to the maximum  $\Delta D$  value of  $\Delta D = +0.32$  arc min (=  $9.31 \times 10^{-5}$  rad) just before the main shock. This change should be affected by generation of preseismic magnetic field  $\Delta B$ . As  $\Delta D$  is small, we can approximate the relationship between  $\Delta H$ ,  $\Delta D$  and  $\Delta B$  as shown in an insert of the Figure; i.e.

$$\Delta B \approx \mu_0 \mathbf{I} \sin \theta \frac{w_c t^*}{4\pi R^2}$$

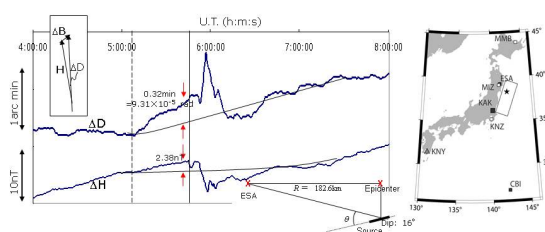
The amount of H is normally 29037 nT at ESA. The  $\Delta B$  is then  $29037 \text{ nT} \times 9.31 \times 10^{-5} \text{ rad} = 2.70 \text{ nT}$ , which is in agreement with the observed preseismic variation of  $\Delta H$  (2.38 nT) as seen in the Figure.

The preseismic geomagnetic field  $|\Delta B|$ , resulting from the time-varying current at the earthquake nucleus zone by Biot-Savart's law, is expressed, by assuming the time-varying source current element of the length  $w_c t^*$ , as:

$$\Delta B = \mu_0 \mathbf{I} \sin \theta \frac{w_c t^*}{4\pi R^2},$$

where  $\mu_0$  is the permittivity of free space,  $\mathbf{I}$  is the pressure-impressed current, which is 170kA in the Tohoku-Oki earthquake (Enomoto & Heki, GJI, submitted),  $\theta$  is an angle shown in the Figure,  $w_c$  is the earthquake nucleation size,  $t^*$  is the normalized preseismic time duration, R is the distance between observation site from the epicenter. The present model of the above equation at  $t^*=1$  gives  $\Delta B = 1.78 \text{ nT}$  with  $R = 181 \text{ km}$ : distance between the ESA and the epicenter of which the agreement with the observed value of 2.38 nT is rather well.

Keywords: Tohoku-Oki earthquake, Precursor phenomena, Geomagnetic, Declination, GPS-TEC, Modelling





## Preseismic ionospheric electron enhancements, revisited : Discrimination from TID and interfrequency receiver bias estim

HEKI, Kosuke<sup>1\*</sup>

<sup>1</sup>Dept. Natural History Sci., Hokkaido University

Possible enhancement of ionospheric Total Electron Content (TEC) immediately before the 2011 Tohoku-oki earthquake (Mw9.0) has been reported by Heki [2011]. Later, Kamogawa and Kakinami [2013] attributed the enhancement to an artifact falsely detected by the combined effect of the highly variable TEC under active geomagnetic condition and the occurrence of a tsunamigenic ionospheric hole [Kakinami et al., 2012]. Recently, Heki and Enomoto [2013] showed that preseismic TEC increase did occur by studying vertical TEC (VTEC) rather than slant TEC (STEC) before and after the 2011 Tohoku-oki earthquake and by comparing them with other geophysical data including the electron density profile from radio occultation, foEs at the Kokubunji ionosonde, and geomagnetic declination changes. In this paper, I focus on a few remaining problems in preseismic TEC enhancement, i.e. (1) possibility to discriminate preseismic TEC anomalies from space-weather origin TEC changes represented by the large-scale traveling ionospheric disturbances (LSTID), (2) estimation of site-specific inter-frequency biases for stations outside Japan, (3) possible difference of amplitudes of preseismic TEC anomalies between mid-latitude and equatorial regions, and (4) comparison between the TEC drops occurring ~10 minutes after earthquakes with preseismic enhancements.

### References

- Cahyadi, M. N. and K. Heki, Ionospheric disturbances of the 2007 Bengkulu and the 2005 Nias earthquakes, Sumatra, observed with a regional GPS network, *J. Geophys. Res.*, 118, 1-11, doi:10.1002/jgra50208, 2013.
- Heki, K., Ionospheric electron enhancement preceding the 2011 Tohoku-Oki earthquake, *Geophys. Res. Lett.*, 38, L17312, doi:10.1029/2011GL047908, 2011.
- Heki, K. and Y. Enomoto, Preseismic ionospheric electron enhancements revisited, *J. Geophys. Res.*, 118, 6618-6626, doi:10.1002/jgra.50578, 2013.
- Kakinami, Y., M. Kamogawa, Y. Tanioka, S. Watanabe, A. R. Gusman, J.-Y. Liu, Y. Watanabe, and T. Mogi, Tsunamigenic ionospheric hole, *Geophys. Res. Lett.* 39, L00G27, doi:10.1029/2011GL050159, 2012.
- Kamogawa, M. and Y. Kakinami, Is an ionospheric electron enhancement preceding the 2011 Tohoku-oki earthquake a precursor?, *J. Geophys. Res.*, 118, 1-4, doi:10.1002/jgra.50118, 2013.
- Maeda, J. and K. Heki, Two-dimensional observations of mid-latitude sporadic-E irregularities with a dense GPS array in Japan, *Radio Sci.*, 49, 1-8, doi:10.1002/2013RS005295, 2014.

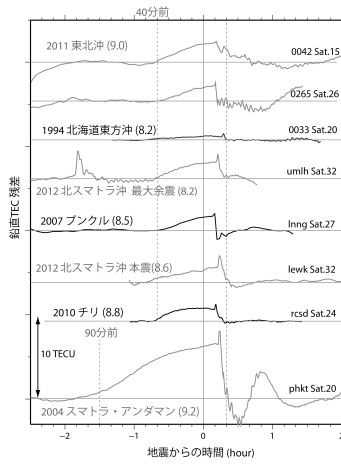
(Figure caption) Residual vertical TEC time series for seven large earthquakes for which precursory TEC enhancements have been observed. Below the two examples of the 2011 Tohoku-oki earthquake, the rest (six) of the events are arranged by their moment magnitudes. Distinct trend changes seem to occur about 40 minutes before the earthquake. In some cases, they are cancelled by sudden drops 10 minutes after the earthquakes (e.g. 2007 Bengkulu, 2004 Sumatra-Andaman). In other cases, they decay gradually with a timescale of 20 minutes or so (e.g. 2012 North Sumatra earthquakes). Site names and satellite PRN numbers are given at the right end of the time series.

Keywords: GNSS, GPS, ionosphere, earthquake, precursor, TEC

MIS29-04

Room:313

Time:April 29 15:00-15:15



---

MIS29-05

Room:313

Time:April 29 15:15-15:30

## A Decision Process of the Observation and Research Program of Earthquakes and Volcanoes

KODAMA, Tetsuya<sup>1\*</sup>

<sup>1</sup>Tetsuya KODAMA

A Decision Process of the Observation and Research Program of Earthquakes and Volcanoes for Contribution to the Reduction of Disaster will be presented.

Keywords: Subdivision on Geodesy and Geophysics, Earthquake and Volcanoes Subcommittee, Next Research Program Review Committee

## New coordination program of next "earthquake prediction research" based on the electromagnetic methods

NAGAO, Toshiyasu<sup>1\*</sup> ; KODAMA, Tetsuya<sup>2</sup>

<sup>1</sup>Earthquake Prediction Research Center, Tokai University, <sup>2</sup>JAXA

FY 2013 is the final year of the current five years program called the University's earthquake prediction research study. During the current program, devastating Tohoku earthquake occurred in 2011. Therefore extensive revision is requested by the evaluation committee. Unfortunately, the short-term prediction research is not on the map among the current program. We believe that the most important issue in the prediction is the short-term prediction. Therefore, for the next five years' program we proposed and adopted the unified project based on the electromagnetic methods, which includes Tokai University, Hokkaido University, Earthquake Research Institute, Kyushu University and so on. This really needs close coordination of the SEMS community. In the presentation, we would like to present the outline of impending research plan and tactics.

Keywords: Earthquake Prediction, Electromagnetics, VLF, VHF

## Review of seismo-electromagnetics and earthquake predictology

HAYAKAWA, Masashi<sup>1\*</sup>

<sup>1</sup>University of Electro-Communications

This paper consists of a few parts. The 1st part deals with the review of electromagnetic precursors to the 2011 Japan earthquake (EQ). The 2nd part is based on the general review of seismo-electromagnetics, and the 3rd, the proposal of a new science field of EQ predictology. In the 1st paper we present our own results on electromagnetic precursors to the 2011 EQ, including (1) subionospheric VLF/LF propagation anomaly, (2) ULF (ultra-low-frequency) magnetic field depression, and (3) atmospheric VLF/ELF radiation. The 2nd part deals with the present situation of seismo-electromagnetics (DC geoelectric measurement, ULF emissions, atmospheric effect and ionospheric effects), in which the ionospheric precursor has already been found to be statistically correlated with EQs based on long-term data. Finally, by using such EQ precursors we are ready to perform the short-term EQ prediction and to propose a new science field of EQ predictology.

Keywords: Earthquake precursors, Earthquake predictology

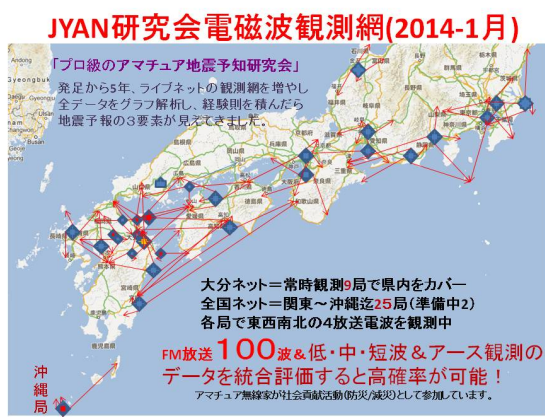
## Let's make use of foretelling an earthquake information.

KUNIHURO, Hidemitsu<sup>1\*</sup>

<sup>1</sup>JYAN meeting for the study

**The observation information of 1 JYAN meeting for the study** (a foretelling an earthquake amateur net = volunteer group)

(1) Our society for the study performs the NET observation of the FM broadcasting electric-wave, but recorded a decisive harbinger by Awajishima earthquake in last April, and elsewhere much observation records are accumulated, and act for high-reliability as a law learned by experience of the earthquakes. When I could go ahead through the high-reliability in three kinds of observation networks such as the low inside, all frequency to the short wave zone, FM broadcast 100, observation of the ground electromagnetism, and the (2) JYAN meeting for the study collated each observation result, I understood a correlative thing. (3) A great variety of seismometry is carried out, and we demand the collection and feedback of the information there, and can go ahead through the preparations for an exhibition of the observation information nationwide. **I announce the electromagnetism observation to contribute to the mechanism elucidation of 2 earthquakes.** (1) The electric wave propagation change (3) others which appear for several months of the electromagnetism change (2) earthquake that appeared before an earthquake. The cause that **3 "foretelling an earthquake information" is not valid?** (1) When "the foretelling an earthquake is very difficult", the Japanese Seismological Society of Japan announced it, but do not progress before can announce the foresight information of the earthquake, and therefore cannot start the yet most recent "foretelling an earthquake information". (2) If earthquake information is accompanied with a panic and information responsibility, and the information of the major earthquake is announced, a panic is worried about ahead of an earthquake, and if earthquake information is wrong again, is asked the responsibility, and, therefore, cannot be involved in administration and the media either. **4 problems and good solution?** (1) It is necessary let the advancement of the observation technology is necessary, and the promising field of the foretelling an earthquake observe it with enough studies with the earthquake study that the accuracy of the earthquake forecast is necessary for foretelling an earthquake to becoming it there, and to plan the advancement of the foresight technology, and knowledge and the cooperation of the field of extensive arts and sciences let all integrates scientific study or observation information because necessary, and visualize it, and the earthquake study plans the development of the new technology again. (2) Is a panic and information responsibility, but if wake up a large panic in little information, and the warning information of the earthquake cooperates with the media there, and the commuter rush of the city just announces the observation information of the earthquake in the same way as typhoon information because daily life is an abnormal situation, and change it to use earthquake information by a self-judgment anytime, the panic is controlled, and do not have the responsibility problem besides now. **To convey the earthquake forecast that 5 is ideal for** If it is with more right seismometry information if it establishes a seismometry center (a tentative name) to make environment let unify all observation information, and to be able to give synthetic judgment to do earthquake information precisely because necessary, and let unify a study and observation information, and feed back information again necessary for each observation spot., and may start the earthquake forecast that the nation can rely on, and there are administration and cooperation of the media, may change in the country more reliable safely.



### 3-D visualization of the preseismic ionospheric anomalies

HIROOKA, Shinji<sup>1\*</sup> ; HATTORI, Katsumi<sup>1</sup> ; ICHIKAWA, Takashi<sup>1</sup>

<sup>1</sup>Graduate School of Sci., Chiba Univ.

The ionospheric anomalies possibly associated with large earthquakes have been reported by many researchers. However, a physical mechanism of pre-seismic ionospheric anomalies has not been clarified. To understand the mechanism, monitoring of three-dimensional distributions of ionospheric electron density is considered to be effective. In this study, to investigate the three-dimensional structure of ionospheric electron density prior to large earthquake, the Neural Network based tomographic approach is adapted to GEONET and ionosonde data. In the case of the 2011 Off the Pacific Coast of Tohoku Earthquake (Mw9.0), the significant enhancements are found in Total Electron Content (TEC) investigation, 1, 3-4 days prior to the earthquake. Especially, TEC increase of 3 days prior to the earthquake was remarkable. As a result of tomographic analysis, the reconstructed distribution of electron density was decreased above the epicenter around 250 km altitude (below the hmF2 altitude) in comparison with 15 days backward median distribution. Meanwhile, we found the electron density enhancement above hmF2 altitude. Moreover, the similar structures were found in many other earthquake occurred in Japan. Especially, in the case of long-term GIM-TEC anomalies (10 hours per day and over) were found, the similar structure was detected at a high rate (85%). Details will be shown in the presentation.

Keywords: Ionospheric tomography, GPS-TEC, Preseismic ionospheric anomaly

## Study on lithosphere-atmosphere-ionosphere coupling inferred from the data of GPS surface displacement and ionospheric pe

HOBARA, Yasuhide<sup>1\*</sup> ; MIYAKE, Risa<sup>1</sup> ; CHEN, Chieh-hung<sup>2</sup>

<sup>1</sup>Graduate School of Information and Engineering Department of Communication Engineering and Informati, <sup>2</sup>Institute of Earth Sciences, Academia Sinica, Taiwan

Various scenarios of coupling mechanisms between the major seismic activities on the ground and overlaying ionosphere have been proposed, experimental evidence has not been observed clearly. In this paper we analyze long-term data from ground movement and ionospheric anomalies in relation with major earthquakes occurred around Japan. In association with major earthquakes, anomalous surface displacements are observed by dens GPS network whilst lower ionospheric perturbations are identified by continuous measurement of VLF/LF transmitter signals. As a result, we found that the ionospheric anomalies are observed preferably associated with the thrust type earthquakes. GPS surface displacements tend to occur in association with any types of earthquakes.

Keywords: ionospheric perturbations, GPS surface displacement, lithosphere-atmosphere-ionosphere coupling, earthquake



## Precursor Ionization Anomaly (PIA) caused by earthquake electric field- with and without natural eastward electric field

OYAMA, Koichiro<sup>1\*</sup> ; KAKINAMI, Yoshihiro<sup>2</sup>

<sup>1</sup>Plasma and Space Science Center, National Cheng Kung University, Taiwan, <sup>2</sup>School of Systems Engineering, Kochi University of Technology

In the low/midlatitude ionosphere, feature which is similar to Equator Ionization anomaly (EIA) is produced about 5 days before large earthquake (Oyama et al., 2010). The phenomenon was found by using the data obtained by US satellite DE-2, which was in orbit during 1981-1982. We named this phenomenon Precursor Ionization Anomaly (PIA). To find the PIA, satellite altitude should be below 400 Km. PIA seems to show different feature depending on the magnitude of electric field associated with earthquake, distance from the magnetic equator, and the height of the ionosphere to be studied. Depending on the magnitude of the earthquake electric field, and the height to be measured, the electron density shows the minimum or the peak. PIA is also influenced by natural electric field. When EIA exists, two minima of the electron density appear; one is caused by natural eastward E field, another by earthquake electric field. sometimes three minima appear. Here we present two cases: 1. PIA under the existence of natural eastward electric field. 2. PIA without/or weak natural eastward electric field. We stress here that constellation of small satellites will provide a breakthrough for precursor study of large earthquake.

Keywords: Earthquake, electric field, plasma density, fountain effect

## Mission Analysis of Micro-Satellite for Earthquake Precursor Study

SUTO, Yushi<sup>1\*</sup> ; NAKAMURA, Maho<sup>1</sup> ; KAMOGAWA, Masashi<sup>1</sup>

<sup>1</sup>Dpt. of Phys., Tokyo Gakugei Univ.

A mitigation of the disasters attributed to mega-earthquake should be prioritized for saving human lives. In order to promote earthquake prediction, we take particular notice of one of plausible ionospheric precursors, the decrease of VLF electromagnetic wave intensity. Then we statistically verify such a precursor associated with world-wide large earthquakes, and finally conclude whether earthquakes are predicable or not. For this purpose, a dedicated satellite with 2.5- year operation is proposed.

Keywords: Earthquake, Ionospheric Precursors, Micro-Satellite

## Satelite orbit of detecting Ionospheric Earthquake Precursor

TOGO, Shoho<sup>1\*</sup> ; SUTO, Yushi<sup>1</sup> ; KAMOGAWA, Masashi<sup>1</sup>

<sup>1</sup>Dpt. of Phys., Tokyo Gakugei Univ.

In general, it is difficult to show a statistical correlation between the precursor and the large earthquake, because of infrequent occurrences of the large earthquake. In particular, to prove the causation required by the identification criteria 5 needs a number of much larger earthquakes, which are further less number according to Gutenberg- Richter relation. In addition, the events of earthquakes in the ocean and far from the ground observation site might be undetectable. Supposing that a number of precursors are detectable on the ground-based station, it might take the long term of thousand years. Theses plausible atmospheric-ionospheric precursors last for a few hours to a few days before the mainshock. Therefore, some of precursors are detectable by satellites because the orbit sampling of satellite is less than the duration of the precursors. Moreover, the satellite observation can cover the whole of a region of active seismicity, when the inclination of satellite is more than 60 degrees. In this presentation, we propose ideal orbits of dedicated satellite for this study.

Keywords: Earthquake, Ionosphere, Satellite

## Investigation of "positive hole excitation" for stressed igneous rocks with a control of water content

OSADA, Akira<sup>1\*</sup> ; YAMANAKA, Chihiro<sup>1</sup>

<sup>1</sup>Graduate School of Science, Osaka University

Piezo electric effects, positive hole excitation for stressed igneous rocks and streaming potential have been considered possible mechanisms that explain pre-seismic electric signals. Especially, positive hole excitation, (Freund et al. 2006), explains long-term anomalous electromagnetic signals and telluric current signals observed for a long distance, therefore attracts a lot of attention.

To clarify the mechanism of pre-seismic electric signals, we performed following experiments for stressed igneous rocks with saturated by water. Samples of granite and gabbro sized  $3 \times 3 \times 10$ cm. Then, the samples were loaded from 1.08MPa to 5.45MPa, with recording of water content. Current-flows from -40pA to -20pA and around -1.5nA were observed for granite and gabbro samples respectively, while any current changes were not observed from bone-dry rocks. These results indicate that pore water is closely tied to current changes. Samples with different size were also tested. The values of current-flow agree well with results of observation of pre-seismic anomalous telluric current signals in Kozu-shima Island (Orihara et al. 2012), assuming the resistivity 10-1000 $\Omega$ m.

### Reference

- 1) F.T.Freund, A.Takeuchi, B.W.S.Lau, 'Electric currents streaming out of stressed igneous rock - A step towards understanding pre-earthquake low frequency EM emissions', *Physics and Chemistry of the Earth* 31. pp.389-396. (2006)
- 2) Y.Orihara, M.Kamogawa, T.Nagao, S.Uyeda, 'Preseismic anomalous telluric current signals observed in Kozu-shima Island, Japan', *Proceedings of the National Academy of Sciences* Vol.109 No.47 pp.19125-19128. (2012)

Keywords: Seismic electric signals, Streaming potential, Positive hole excitation, Igneous rocks

## Analysis of geomagnetic diurnal variations at Esashi station from 1997~2012

ASHIDA, Ryo<sup>1\*</sup> ; HATTORI, Katsumi<sup>1</sup> ; HAN, Peng<sup>1</sup> ; FEBRIANI, Febty<sup>1</sup> ; YOSHINO, Chie<sup>1</sup>

<sup>1</sup>Graduate School of Science, Chiba University

There have been many reports on ultra-low-frequency (ULF) electromagnetic phenomena associated with earthquakes in a very wide frequency range. In this study, unusual behaviors of geomagnetic diurnal variations prior to the 2011 off the Pacific coast of Tohoku earthquake (Mw9.0) have been reported. Ratios of diurnal variation range between the target station Esashi (ESA) which is about 135 km from the epicenter and the remote reference station Kakioka (KAK) have been computed. The results showed that there had been clear anomalies exceeding the statistical threshold in the vertical component about 2 months before the mega event. These anomalies are unique over a 16 years background. The original records of geomagnetic fields of the ESA station also exhibited continuous anomalous behaviors for about 10 days in the vertical component from Jan.3, 2011-Jan.13, 2011, about two months prior to the Mw 9.0 earthquake. During the same period, other independent geophysical parameters such as seismicity and crustal deformation also show clear unusual changes, which suggests these anomalies might be related with the mega event.

Keywords: ULF seismo-magnetic phenomena, earthquake, geomagnetic diurnal variations

## Identification of seismo - ionospheric signatures by using amplitude and phase information of VLF/LF transmitter waves

TATSUTA, Kenshin<sup>1\*</sup> ; HOBARA, Yasuhide<sup>1</sup>

<sup>1</sup>Graduate School of Informatics and Communication Eng. , The University of Electro-Communications

In this paper, we analyse the VLF/LF transmitter signals in association with major seismic activities over Japan. Particular attention is paid to phase in addition to amplitude information of the VLF/LF signals. As a result, significant change both in the phase and amplitude are identified as an anomaly of seismo - ionospheric signatures. Moreover, the results of numerical analysis of VLF/LF transmitter waves in the earth - ionosphere waveguide by using FDTD method are in good agreement with the experimental results. We conclude that simultaneous use of amplitude and phase information of VLF/LF signal will be useful to identify the special scale of seismo - ionospheric anomalies.

Keywords: seismo - ionospheric perturbation, FDTD method, VLF/LF transmitter, earthquake

## Ionospheric Anomaly as an Earthquake Precursor : Statistical Study during 1998-2012 around Japan

KUNIMITSU, Mayuka<sup>2\*</sup> ; HATTORI, Katsumi<sup>3</sup> ; HAN, Peng<sup>3</sup> ; LIU, Jann-yenq<sup>1</sup>

<sup>1</sup>Faculty of science, Chiba University, <sup>2</sup>Graduate School of Science, Chiba University, <sup>3</sup>Institute of Space Science, National Central University, Taiwan

Many anomalous electromagnetic phenomena possibly associated with large earthquakes have been reported. TEC (Total Electron Contents) anomaly is one of the most promising phenomena preceding large earthquakes. We investigated statistically TEC anomalies before large earthquakes around Japan region during 1998-2012. In this study, superposed epoch analysis (SEA) and Molchan's error diagram (MED) analysis have been taken to investigate correlation and predictability in the statistical manner. The results of SEA show that positive anomaly 1-5 days before the large earthquake ( $M \geq 6.0$  and depth  $\leq 40$  km) is significant. The results of MED analysis indicate the some gain against the random estimation (Poisson model). That is, the prediction using TEC anomaly around Japan is not random and has an information. The details will be given in the presentation.

## Detection of thermal anomaly associated with Earthquake from MODIS data

TSUTSUMI, Rika<sup>1\*</sup>

<sup>1</sup>Chiba University

It is a critical issue to mitigate of disasters including earthquake. And it is required to develop of technique to monitor and predict major earthquakes. Therefore, the purpose of this study is to develop an adequate algorithm to detect LST (Land Surface Temperature) anomalies related to earthquakes using MODIS (Moderate Resolution Imaging Spectroradiometer) infrared sensor onboard Terra/Arqua satellite.

We investigate spatial-time changes in LST in the statistical way. In order to detect only hotspots related to earthquakes without faints, the developed algorithm investigates the difference temperature behavior between a target point and spatial average, and we get spatial difference of brightness temperature( $\Delta T$ ). In order to evaluate the temporal singularity of  $\Delta T$ , we calculate the following equation.

$$R = (\Delta T(x,y,t) - \text{ave}(x,y)) / \sigma(x,y)$$

where  $\text{ave}(x,y)$  is multi year plus minus 15 days moving average. And  $\sigma(x,y)$  is multi year plus minus 15 days moving standard deviation.

We detect LST anomaly 8 days before L'Aquila earthquake. And it continued for several hours. This result represents that it has potential for monitoring/predicting major earthquakes to develop algorithms to detect thermal anomalies using MODIS data.

Keywords: MODIS, Earthquake, L'Aquila, thermal anomaly



## diatom assemblages in INW2012 drilling cores from Lake Inawashiro , Tohoku, Japan

HIROSE, Kotaro<sup>1\*</sup> ; NAGAHASHI, Yoshitaka<sup>1</sup>

<sup>1</sup>Fukushima University

Inawashiro-ko Formation is named by a 28.13m sediment core taken from Lake Inawashiro-ko, Fukushima Prefecture, Japan. Stratigraphy and facies analysis combined with tephra and AMS radiocarbon dating were carried out on INW-2012. The Inawashiro-ko Formation are divided into three stratigraphic units: the Lower part (37.17-26.60m) consisted by medium sand-sandy silt (vertically varied in grain size) with granule and wood fragments, the Middle part (26.60-24.89m) consisted by very fine sand-silt with upper level grain refinement, and the Upper part (24.89-0.00m) consisted by dense alternation of brighter and darker clay layers including fallout tephra and Lahars by sediment gravity flow. Each unit are formed by fluvial basin before the form of the lake, early stage of the lake, lake with deep water as present, respectively. <sup>14</sup>C dating indicate that Lake Inawashiro-ko is formed 42 cal k BP, and characteristic dense alternation of brighter and darker clay layers deposit continuously except for the most early stage of the Lake. The sedimentation rate in the upper part is 0.3-1.0(mm/yr). Additionally, We report the temporal variation of diatom assemblage and its relation to water environment in the past 2000 years from upper 2.00m of IN2012.

Keywords: Lake Inawashiro-ko, lacustrine sediment core, stratigraphy, diatom assemblage, late Pleistocene, <sup>14</sup>C dating

## Two different types of regime shift appeared in a 2900-yr record of Japanese sardine abundance

KUWAE, Michinobu<sup>2\*</sup> ; YAMAMOTO, Masanobu<sup>2</sup> ; SUGIMOTO, Takashige<sup>3</sup> ; TAKEOKA, Hidetaka<sup>1</sup>

<sup>1</sup>CMES, Ehime Univ., <sup>2</sup>Faculty of Environmental Earth Science, Hokkaido Univ., <sup>3</sup>Institute of Civilization, Tokai University,

Regime shift, revealed in climates and marine ecosystem, is one of key dynamics to predict rapid changes in marine ecosystems and fisheries resources for decades. The regime shift is defined as a relatively rapid change (occurring within a year or two) from one decadal-scale period of a persistent state (regime) to another decadal-scale period of a persistent state (Minobe 1997; King 2005). In the Pacific it has been detected in Pacific Decadal Oscillation (PDO) (Mantua et al., 1997) and species replacement between anchovy and sardine (Lluch-Belda et al., 1989). There is so far no sufficient evidence of how regime shift changes in its feature on longer timescales because of paucity of long-term high-resolution marine records in the Pacific. Here we present a 2900-year record of ecosystem regime shift in the western North Pacific using Japanese sardine abundance which can be reconstructed from fossil scales in the coastal marine sediments; timing of decreases and increases in the abundance can be used as an index of regime shift. Sardine abundance showed two different types of regime shift in the time series. One is a regime shift similar to that previously detected in the 20th century, which repeatedly occurs on interdecadal timescales. The other is a regime shift in relation to centennial-scale variability in sardine abundance, which could be followed by a centennial-scale low or high abundance period characterized by respective small or large amplitudes of decadal variations in abundance. Our estimation suggests that the maximum abundance is depleted one-quarter to one-tenth of that in the sardine regime in 1980s. Similar patterns of the latter regime shift are revealed in the time series of sardine abundance off California (Baumgartner et al., 1992) and Chile (Valdes et al. 2008), PDO index reconstructed from North America (Macdonald and Case 2005), and abnormal snow index in East Asia (Chu et al., 2008). This indicates that the latter regime shifts that we found are associated with those of marine ecosystems and climate over the Pacific. The recent high sardine abundance period lasted 200 years in the Pacific, suggesting transition to next centennial low abundance period in the near future. Careful examinations on whether the latest regime shift in 1990s is the case of the latter regime shift are important for the long-term prediction of climate and fisheries resources.

Keywords: regime shift, marine ecosystem, sardine fossil scale record, Pacific, Beppu Bay

## Modern changes of sedimentary environments in the brackish Lake Shinji, the east part of Shimane prefecture, Japan

SETO, Koji<sup>1\*</sup> ; IKEDA, Hiroko<sup>2</sup> ; YAMAGUCHI, Keiko<sup>3</sup> ; KURATA, Kengo<sup>3</sup>

<sup>1</sup>ReCCLE, Shimane Univ., <sup>2</sup>Geoscience, Shimane Univ., <sup>3</sup>Life and Environmental Science, Shimane Univ.

Lake Shinji is oligohaline brackish lake in the east part of Shimane prefecture. Area of Lake Shinji is 79.1km<sup>2</sup>, water depth shows less than 6m. The water column of Lake Shinji is divided into oligohaline surface water, mesohaline pycnocline, and mesohaline bottom water.

In recent years, Lake Shinji is observed environmental events such as Cyanobacterial water bloom, anomaly overgrowth of aquatic plants, decrease in the catch of Corbicula and so on. The purpose of this study is to reveal the changes in the sedimentary environment by using the comparison with the spatial investigation of surface sediments in 2006 and 2013 and the result of monitoring since 2010 in Lake Shinji.

The surface sediments in Lake Shinji in 2006 are sandy deposits shallower than 3.5m in water depth, but are muddy deposits deeper than its depth. Mean grain size of surface sediments deeper than 3.5m tend to be fine-grained with water depth, and shows 7.5 phi in deepest site. In shallower than 3.5m, many surface sediments shows fine to medium sand around 2 phi. Total organic carbon (TOC) contents of surface sediments was less than 4%. TOC contents shows high positive correlation coefficient 0.85 with mean grain size. This is suggested that the spatial distribution of TOC contents depend on grain size. Total Sulfur (TS) contents of surface sediments were less than 1 %, and tend to be decreased with water depth. However, TS contents were less than 0.2 % shallower than 4.5m. In deeper than its depth, TS contents decreases dramatically.

The surface sediments in Lake Shinji in 2013 are sandy deposits shallower than 3.5m in water depth, but are muddy deposits deeper than its depth. Mean grain size in 2013 was similar to the 2006. TOC contents of surface sediments were 6 to 8 %. TS contents were less than 2 %. TS contents were less than 0.2 % shallower than 3.0m. This depth is shallow clearly than in 2006.

TOC contents in monitoring site from 2010 to 2013 fluctuated greatly in the range of 4% to 10%. TOC contents shows low values in summer season, and high values in winter season. It is considered that the fluctuation of TOC contents is caused by the dilution effect of inorganic sediment due to rainfall in the summer. In addition, TOC contents tend to increase from 2010 to 2013. TS contents fluctuated greatly in the range of 0.5 % to 2.0 %. TOC contents shows high values in summer season, and low values in winter season, and tend to increase from 2010 to 2013 as with the TOC contents. This is suggested that the increase of TS contents is caused by the inflow of mesohaline water and the decrease of dissolved oxygen in bottom water.

From the results of these, surface sediments and bottom water environments in Lake Shinji are a distinct change during term from 2006 to 2013. We are thinking that some of this cause.

Keywords: Lake Shinji, Surface sediments, Total organic carbon contents, Total Sulfur contents, Grain size analysis

## Provenances of detrital materials in the Lake Suigetsu sediment and quantitative evaluation of their mixing ratio

SUZUKI, Yoshiaki<sup>1\*</sup>; TADA, Ryuji<sup>1</sup>; NAKAGAWA, Takeshi<sup>2</sup>; NAGASHIMA, Kana<sup>3</sup>; HARAGUCHI, Tsuyoshi<sup>4</sup>; GOTANDA, Katsuya<sup>5</sup>; IRINO, Tomohisa<sup>6</sup>; SUGISAKI, Saiko<sup>1</sup>; SG12/06, Project members<sup>7</sup>

<sup>1</sup>Univ. Tokyo, <sup>2</sup>Univ. Newcastle, <sup>3</sup>JAMSTEC, <sup>4</sup>Osaka City University, <sup>5</sup>Chiba University of Commerce, <sup>6</sup>Hokkaido University, <sup>7</sup>SG12/06 Project

Lake Suigetsu, central Japan, is characterized by annually laminated sediment, and extremely high resolution and precise age-depth model was established using drilled cores retrieved on 1993 and 2006. For this reason, Lake Suigetsu sediment is ideal subject of high resolution and precise paleo-climate reconstruction. Detrital material accumulated in Lake Suigetsu is thought to have 3 provenances with 3 different transport paths. One is eolian dust transported by wind from Asian continent. Second is detrital material transported by small rivers from surrounding slopes. Third is suspended sediment supplied from Hasu River and transported through Lake Mikata, which is connected to Lake Suigetsu with shallow channel. Mechanism and flux of detrital materials from these 3 sources could be controlled by the behavior of westerly jet, slope failure due to flood and/or earthquake, and rainfall and erosional process within the drainage area. Therefore, if we could reconstruct the flux of detrital materials from each provenance, we could gain detailed information on histories of paleo-climate and disasters.

In this study, we did factor analysis of chemical composition of detrital fraction extracted from the sediment by chemical treatment. Each end-member extracted by factor analysis was characterized with respect to mineral composition, color, and grain-size distribution. We compared these characteristics with samples taken from probable sources and from event layers in the sediment, and tried to re-construct the flux change of each detrital component.

Keywords: Lake Suigetsu, Deglaciation, Holocene, Factor analysis, Multi-regression analysis

## Wetter condition during the Heinrich Event 1? deduced from detrital flux and provenance records from Lake Suigetsu

NAGASHIMA, Kana<sup>1\*</sup> ; NAKAGAWA, Takeshi<sup>2</sup> ; SUZUKI, Yoshiaki<sup>3</sup> ; TADA, Ryuji<sup>3</sup> ; HORIUCHI, Daishi<sup>4</sup> ; SUGISAKI, Saiko<sup>3</sup> ; GOTANDA, Katsuya<sup>5</sup> ; HARAGUCHI, Tsuyoshi<sup>6</sup> ; SG06/12, Project member<sup>7</sup>

<sup>1</sup>JAMSTEC RIGC, <sup>2</sup>University of Newcastle, <sup>3</sup>The University of Tokyo, <sup>4</sup>Japan Coast Guard, <sup>5</sup>Chiba University of Commerce, <sup>6</sup>Osaka City University, <sup>7</sup><http://www.suigetsu.org>

Stalagmites in Chinese caves, loess/paleosol sequence of the Chinese Loess Plateau, and lacustrine sediments in Asian countries are favorable to monitor the past changes in East Asian summer monsoon (EASM). However, not much is known about EASM spatial changes during the last deglaciation mostly due to the large uncertainty in the chronologies of the lacustrine and loess/paleosol sediments.

Lake Suigetsu in Central Japan is known for the varved sediments which cover at least last 70 kyr. Recently, accurate age model is established for SG06 core based on varve counting and more than 800 radiocarbon dates (e.g., Ramsey et al., 2012; Staff et al., 2013). Here we examine the precipitation changes in Central Japan during the last deglaciation from the flux and provenance changes of the detrital materials found in the SG06 core sediment.

We analysed flux of detrital materials for the last glacial part of the SG06 core (1402-1810 cm interval of the SG06 composite depth) with 1 cm resolution (corresponding to 7-13 yrs) and estimated provenance of the detrital materials using chemical and mineral compositions, grain sizes, and electron spin resonance intensity and crystallinity of the quartz. The reconstructed flux of detrital materials are characterized by the millennial-scale increases exceeding 12 mg/cm<sup>2</sup>/yr at 16,600-14,800 and 13,700-12,800 SG06<sub>2012</sub> yr BP and short-lived (decadal to centennial) episodes of higher flux repeated more than thirty times throughout the deglaciation interval.

The grain size, color, chemical composition, and crystallinity of quartz records suggest that the increase of the detrital materials during 16,600-14,800 SG06<sub>2012</sub> yr BP was mainly due to increase of suspended particles supplied from Hasu river through Lake Mikata, that is located immediately upstream of Lake Suigetsu and trapping most of coarse detrital grains. In contrast, the increase of detrital materials during 13,700-12,800 SG06<sub>2012</sub> yr BP likely reflects local slope erosion around the lake and partly the long-distance aeolian transport from the Asian deserts. Our result suggests the wetter condition in Central Japan during the Heinrich Event 1 in contrast to the dry condition in Yangtze River Basin, China, according to the  $\delta^{18}O$  stalagmite record (Wang et al., 2001).

Keywords: Lake Suigetsu, Heinrich Event, East Asian Summer Monsoon, detrital material, quartz

## Variation of very fine grained elemental carbon deposition to the Rebun Island, Hokkaido, during the last 5 ky

NAKAI, Yoshie<sup>1\*</sup> ; IRINO, Tomohisa<sup>1</sup> ; YAMAMOTO, Masanobu<sup>1</sup> ; MIYAZAKI, Yuzo<sup>1</sup> ; KAWAMURA, Kimitaka<sup>1</sup> ; YAMADA, Kazuyoshi<sup>2</sup> ; YONENOBU, Hitoshi<sup>3</sup>

<sup>1</sup>Hokkaido University, <sup>2</sup>Waseda University, <sup>3</sup>Naruto University of Education

Elemental carbon (EC) is a combustion product which is composed of rich C and depleted O, H, S, N. Biomass burning is major source of Pre-industrial EC, while fossil fuel burning has been the most important source since the 18th century. Black carbon (BC) transferred in the atmosphere as aerosols, including EC have a great impact on the climate. EC is also the second strongest contributor to global warming, and has effect to darken snow and ice surface. On the other hand, aerosols including EC have also negative effect on radiative forcing, which lead cooling. Although it is difficult to evaluate the net EC effect on climate, it is necessary to discriminate EC produced by fossil fuel burning from those from biomass burning. EC is not a single chemical compound, but it can be classified into two types, char and soot. Char is produced by pyrolysis, while soot is formed via gas-to-particle conversion. The char particles which are countable under microscope are called charcoal. There are many researches to reconstruct paleo-fire by counting charcoal, and in the late Holocene, the fire sometimes synchronized with human activity. Therefore, it is very important to understand the past EC variation to examine the relationship between climate change and history of human.

There are some methods for analysis of EC, and in this study, we use the method called thermal optical reflectance (TOR)-method. This method is principally used to analyze EC/OC in aerosols, where we can evaluate an interference of pyrolyzed OC produced during the temperature rise under He atmosphere by measuring the transmittance of near-infrared laser. In order to apply TOR-method to analysis of sediment, we examined thermograms for sucrose, fulvic acid, humic acid, and fullerene in advance. As a result, we confirmed that carbon fraction decomposed at 700-850 °C under O<sub>2</sub> atmosphere can be regarded as an EC.

The sediment sample we used was collected from the Kusyu Lake in the Rebun Island. We established the stratigraphy of the sediment core of 20 m long as well as the sedimentation rate of the surface sediment. From variation of the ratio of coarse/fine particles down to 12 m depth, the sedimentary environment would be changed from marine to fresh water at 600 cm. We analyzed EC/OC both for coarse and fine particles for 0-600 cm interval. The result shows that the variation of EC in coarse particle reflects local variation, while the EC in the fine fraction reflects local and/or distal variation. The local biomass burning increased at 521 cm. The influence of distal EC variability was larger in the interval of >217 cm, with the maximum at 217 cm and the minimum at 263 cm. The long-distance transportation of EC could be influenced not only by increase and decrease of supply from biomass burning but also by the variation of wind pathway which transports distant EC.

Keywords: elemental carbon, biomass burning, Holocene, Rebun Island

## Chronological study on widespread tephras for the past 50,000 years in and around Japanese Islands

OKUNO, Mitsuru<sup>1\*</sup> ; TORII, Masayuki<sup>2</sup> ; NAKAMURA, Toshio<sup>3</sup>

<sup>1</sup>Fac. Sci., Fukuoka Univ., <sup>2</sup>Grad. Sch., Sci. Tech., Kumamoto Univ., <sup>3</sup>CCR, Nagoya Univ.

After discovery of Aira Tn (AT) tephra, many widespread tephras have been recognized. The tephra for the past 50,000 years can be dated by the radiocarbon (<sup>14</sup>C) age determination. All <sup>14</sup>C dates for tephras after Spfa-1 can be calibrated to a calendar year using calibration dataset "IntCal13". On the other hand, the stratigraphy and the age of tephras intercalated with core sample from marine and lake have been made highly precise. In this presentation, we review the chronological research on widespread tephras for the past 50,000 years, and then present its perspective

Keywords: widespread tephra, radiocarbon dating

---

MIS30-08

Room:501

Time:April 28 11:00-11:30

## The door that the IntCal13 and Suigetsu dataset opened for us all

NAKAGAWA, Takeshi<sup>1\*</sup> ; SUIGETSU 2006, Project members<sup>1</sup>

<sup>1</sup>Department of Geography, Newcastle University (UK)

See the Japanese abstract (the presentation will be in Japanese)

Keywords: IntCal13, Radiocarbon dating, Radiocarbon calibration, varved sediment, climate change, age-based correlation



## A new high resolution dating method using tree-ring cellulose oxygen isotope ratio

NAKATSUKA, Takeshi<sup>1\*</sup> ; SANO, Masaki<sup>1</sup> ; XU, Chenxi<sup>1</sup> ; KIMURA, Katsuhiko<sup>2</sup>

<sup>1</sup>Research Institute for Humanity and Nature, <sup>2</sup>Fukushima University

### Introduction

Dendrochronology is the most accurate dating method by comparing of inter-annual variations in tree-ring width of wood samples from sedimentary layers, archaeological remains or old architectures against the predated standard ring width variations. Master chronologies of tree-ring width, necessary to be built for each region and species, have been established all over world. Some of them based on many living and buried trees cover the whole Holocene in Northern Europe and New Zealand. Tree rings contain other parameters than ring width, applicable for dendrochronological dating. Oxygen isotope ratio (d18O) of cellulose is one of them. Here, we demonstrate merits, methods and problems of the tree-ring d18O chronology in details.

### Merits of tree-ring cellulose d18O chronology

Because tree-ring cellulose d18O is controlled solely by two meteorological factors, precipitation d18O and relative humidity, its inter-annual variation is usually independent from ecophysiological conditions of each tree. As the result, highly correlated tree-ring cellulose d18O variations between different trees ensure high success rate of dating. Moreover, the master chronology of tree-ring cellulose d18O built on cedar and cypress trees can be applied to date wood samples from all other tree species living in the same region and period. Therefore, many tree-ring d18O chronologies are now being created very rapidly all over Japan during the late Holocene, and the established tree-ring cellulose d18O chronologies have been applied for dating of various natural and artificial wood samples to promote new inter-disciplinary studies in both natural and human sciences.

### Methods in tree-ring cellulose d18O chronology

There are two important progresses in analytical method behind the emergence of tree-ring d18O chronology. One is the combined instrument of a pyrolysis-type elemental analyzer and an isotope ratio mass spectrometer. The other is "plate method for cellulose extraction" from tree ring samples. Before 2000AD, it was extremely difficult to measure d18O of organic matter because combustion of samples to gases inevitably causes terrible oxygen contamination. The development of an instrument, which converts organic oxygen to CO without any oxidant at 1400 degree C and transfer the CO to mass spectrometer directly, solved the question how to measure d18O in huge numbers of tree ring cellulose. So far, cellulose extraction from many tree ring samples has been too time-consuming and labor-intensive to meet the huge number of samples in dendrochronological purposes. In 2010, we have developed a new method to extract cellulose directly from thin wood plates with hundreds of rings, which enabled us to start the tree-ring cellulose d18O chronology at last.

### Perspectives of tree-ring cellulose d18O chronology

Although it is much more time-consuming to analyze tree-ring cellulose d18O than to measure tree ring width, we have accumulated many tree-ring d18O data from various kinds of samples and obtained many essential knowledge. While some data have successfully dated important archaeological remains, new problems have also emerged. Here, we show those problems and discuss future perspective of the tree-ring d18O chronology. <Tree Species>There are usually high correlations in tree-ring d18O time series between conifer and deciduous hardwood. But, evergreen hardwood may be somewhat different due to the longer photosynthetic season. <Spatial Correlation>Tree-ring d18O chronology in central Japan is coincident with those in western Japan, reflecting inter-annual changes of stationary rain band (Baiu front) activity in early summer. However, tree-ring d18O time series on Japan Sea side sometimes becomes complicated due to effect of heavy snow cover. <Analytical Method>"Plate method" sometimes destroys ring boundary of buried wood, so that it is necessary to further improve cellulose extraction procedure.

Keywords: tree ring, cellulose, oxygen isotope ratio, dendrochronology

## Calcareous nodules for sea floor paleothermometry

HASEGAWA, Takashi<sup>1\*</sup>; KOBIYAMA, Yosuke<sup>2</sup>; YONEZAWA, Shunsuke<sup>2</sup>; SUZUKI, Takaaki<sup>4</sup>; JENKINS, Robert<sup>1</sup>; MORI, Takami<sup>3</sup>

<sup>1</sup>College of Natural Science and Engineering, Kanazawa University, <sup>2</sup>Graduate School of Natural Science and Technology, Kanazawa University, <sup>3</sup>Kanazawa University (currently Marine Work Japan), <sup>4</sup>Kanazawa University (currently Itochu Oil Exp. Co. Ltd.)

Paleothermometry is one of the most important proxies for paleoceanographers. Benthic foraminifers have been used for reconstructing paleotemperature on the bottom of the sea. They are excellent materials for calcareous ooze, while mudstone sequences shows lots of difficulty to apply this technique for terrigenous sediments distributed around Pacific. Calcareous nodules are commonly observed in mudstone sequences, however, no study discussed potential paleothermometry based on calcareous nodules. It might supplements the role of benthic foraminifers. We described occurrences at outcrops, general configurations including their cut sections, analyzed carbon content, total organic carbon, and carbon and oxygen isotopes of nodules collected from Cretaceous strata of several regions in Hokkaido including the Haboro area.

Structure suggesting consolidation just below the sea floor includes burrows that eject calcareous material from nodule. Nodules consolidated associated with anaerobic oxidation of methane with sulfate reduction appear to be just-below-the-sea-bottom origin. Such nodules show the exactly same oxygen isotope values with that of benthic foraminifers. A bivalve fossil found on one of the methane seep nodules preserved aragonite of the shell and yielded close oxygen isotope temperature with that of host nodule.

Carbonate content and oxygen isotope values had positive relation suggesting carbonate content was controlled by the depth of nodule production. Nodules with lower carbonate content (<50%) exclusively show low oxygen isotope values and inappropriate for the sea bottom paleothermometry.

Study on nodules from the Haboro area showed that selections in front of outcrops and at laboratory enable us to select "high quality nodules" for oxygen isotope paleothermometry. As it is simple procedure, large numbers of analyses are available. The cross-plot of these data can emerge "upper limit line" of oxygen isotope values. The paleotemperature based on that value could provide reliable temperature for the sea bottom. On the other hand, nodules with similar condition from the Oyubari area appeared to be recrystallized and inappropriate for paleothermometry. It might be derived from the difference of burial depth between sediments of the Haboro and Oyubari areas. Even if it was originally consolidated near the bottom of the sea, strong compaction during burial would have caused permeation of pore water into the nodule. Carbon dioxide or bicarbonate ions derived from decomposed organic matter would have caused recrystallization of calcite with oxygen isotopes as low as -10 permil in the nodule.

Keywords: nodules, paleothermometry, oxygen isotope

## Identification of single pollen grains found in a glacier using a whole genome amplification method

NAKAZAWA, Fumio<sup>1\*</sup> ; SUYAMA, Yoshihisa<sup>2</sup> ; IMURA, Satoshi<sup>1</sup> ; MOTOYAMA, Hideaki<sup>1</sup>

<sup>1</sup>National Institute of Polar Research, <sup>2</sup>Tohoku University

Pollen taxon in sediment samples can be identified by analyzing pollen morphology. Identification of related species based on pollen morphology is difficult and is limited primarily to genus or family. Because many pollen grains in glaciers contain protoplasm, genetic information of pollen grains should enable identification of plant taxa below the genus level. The present study attempted to analyze the DNA of *Pinus* pollen grains collected from subsurface snow layers on the Belukha Glacier in the Altai Mountains of Russia in the summer of 2003 in order to identify them. *Pinus* is a taxon with approximately 111 recognized species in two subgenera, four sections and 11 subsections. Each *Pinus* pollen grain was amplified using a whole genome amplification method, and some regions of chloroplast genome were sequenced. As a result, each pollen grain was identified at subsection level and was narrowed down to around 10 species.

Keywords: glacier, ice core, pollen analysis, *Pinus*, DNA, WGA

## Dissolution process of *G. bulloides* shell observed by X-ray CT based on dissolution experiment

IWASAKI, Shinya<sup>1\*</sup> ; KIMOTO, Katsunori<sup>2</sup> ; SASAKI, Osamu<sup>3</sup> ; KANO, Harumasa<sup>3</sup> ; HONDA, Makio<sup>2</sup> ; OKAZAKI, Yusuke<sup>1</sup>

<sup>1</sup>Graduate School of Sciences, Kyushu University, <sup>2</sup>Japan Agency for Marine-Earth Science and Technology, <sup>3</sup>Tohoku University Museum

We performed nine-day dissolution experiments with shells of the planktic foraminifera *Globigerina bulloides* at a pH of  $6.7 \pm 0.1$  in water undersaturated with respect to calcite. *Globigerina bulloides* shells were collected from sediment trap samples in the western subarctic Pacific. The process of dissolution of the shells was quantitatively evaluated with observations made with X-ray micro-computed tomography (CT). On the basis of these observations, we divided the shell structures of *G. bulloides* shells into three categories: early-developed calcite formed during the juvenile stage, inner calcite, and outer calcite. The early-developed and inner calcites had low CT numbers (low density) and were sensitive to dissolution. In contrast, the outer calcite had high CT numbers (high density) and resisted dissolution. Both the mode and frequencies of the CT numbers of *G. bulloides* shells decreased as dissolution progressed. Temporal changes of the histogram of CT numbers as the shells dissolved were quantified in terms of the percentage of calcite volume accounted for by low-density calcite (%low-CT-number calcite volume). There was a linear relationship ( $R^2 = 0.62$ ) between the volume ratio of low-density calcite and shell weight loss. This relationship indicates that shell weight loss can be estimated from the CT number distribution, regardless of the initial condition of the shell, such as size or thickness. We suggest that the X-ray micro-CT method may be used to estimate the extent of foraminiferal shell dissolution with respect to effects on internal structure and shell density.

Keywords: carbonate, planktic foraminifera, X-ray CT, shell weight, shell density, dissolution index

## Relationship between modern speleothem formation and surface weather in an Asian tropical cave

HASEGAWA, Wataru<sup>1\*</sup> ; WATANABE, Yumiko<sup>1</sup> ; MATSUOKA, Hiroshige<sup>1</sup> ; OHSAWA, Shinji<sup>2</sup> ; TAGAMI, Takahiro<sup>1</sup>

<sup>1</sup>Earth and Planetary Sciences, Graduate school of Science, Kyoto Univ., <sup>2</sup>Geophysics, Graduate school of Science, Kyoto Univ.

### Introduction

For precise climate prediction, it is necessary to reconstruct high time and space resolution paleo-climate (especially past 2000 years) from paleo-climate proxies and assimilate the result to climate model. Tropical Asia, including Indonesia, is well affected by El Nino Southern Oscillation (ENSO). The ENSO does not only directly affect on precipitation in tropical Asia, but also indirectly on middle and high latitude climate through teleconnection [1]. In Indonesia, Watanabe et al. [2] suggested inverse-correlation between  $\delta^{18}\text{O}$  and  $\delta^{13}\text{C}$  in speleothems and instrumental precipitation. However, relationship between modern speleothem formation and surface weather is not revealed clearly.

Therefore, the cave monitoring program, which included cave air temperature, relative humidity, airflow current, air  $\text{CO}_2$  concentration monitoring and  $\delta^{18}\text{O}$  and  $\delta^{13}\text{C}$  analysis of dripwater and farmed speleothems, was initiated from 2011 in Petruk Cave (Central Java, Indonesia) in order to study the recording mechanism of precipitation variation into the  $\delta^{18}\text{O}$  and  $\delta^{13}\text{C}$  fluctuation in speleothems.

### Result and Discussion

Air  $\text{CO}_2$  concentration in Petruk Cave is fluctuated daily and seasonally until over 100 m deep site from the entrance.

It is revealed that cave air  $\text{CO}_2$  concentration may be a significant factor that controls stable isotope value in speleothems, because temperature, humidity and drip rate in Petruk cave are nearly stable.

A scenario of precipitation recording is as follows: (1) surface rainfall cools outside air temperature; (2) cave airflow direction is inverted; (3) outside fresh air flows into the cave and air  $\text{CO}_2$  concentration is dropped; (4)  $\text{pCO}_2$  difference between cave air and dripwater becomes higher and calcite precipitation is promoted; (5)  $\delta^{18}\text{O}$  and  $\delta^{13}\text{C}$  in dripwaters and speleothems are decreased.

In addition to above discussion, we will show you  $\delta^{18}\text{O}$  and  $\delta^{13}\text{C}$  values in dripwaters and farmed speleothems and confirm the scenario by these data.

[1] Hastenrath (1991) Climate dynamics of the tropics. [2] Watanabe et al. (2010) Palaeogeography, Palaeoclimatology, Palaeoecology 293, 90-97.

Keywords: cave monitoring, speleothem, isotope, paleo-climate

## Millennial changes recorded in a stalagmite from central Gifu, Japan

SONE, Tomomi<sup>1</sup> ; KANO, Akihiro<sup>1\*</sup> ; MORI, Taiki<sup>1</sup> ; OKUMURA, Tomoyo<sup>2</sup>

<sup>1</sup>SCS Kyushu University, <sup>2</sup>JAMSTEC

A 13-cm-long stalagmite collected from Gujyo City (central Gifu Prefecture) was formed from Marine isotopic stage 3 (MIS-3) to mid-Holocene. The stalagmite is divided into the lower and upper parts by a long-time hiatus during the Last Glacial time. Textural difference appears between the homogenous and transparent upper part and the dark-colored lower part. Oxygen isotopic values are also different; the values of the lower part are 0.5-1.0 permil higher than the values of the upper part. This difference is comparable to one that has been reported from stalagmites in south China, revealing that the Gifu stalagmite was formed under the influence from East Asian summer monsoon.

The most prominent feature of this stalagmite is cyclic changes of ~1 cm intervals in the lower stalagmite. Assuming that the lower part had grown continuous with a uniform rate, it includes a period from 56-35 ka. Eight cyclic changes could coincide to the dark layers in deep-sea sediments from the Japan Sea, which are likely associated with Dansgaard-Oeschger (D-O) events. In each cycle, the stalagmite increases transparency to the upward, and suddenly becomes darker at the base of the upper cycle. Similarly, oxygen isotopic values gradually increase in each cycle and rapidly decrease at the base of the upper cycle.

Millennial changes in the Gifu stalagmite indicate D-O cycles, and further records regular intervals that cannot be seen in the Greenland ice sheet. Records of the lower stalagmite support the global extension of D-O events, and suggest that D-O cycles were not necessary originated from the phenomena in North Atlantic. Assuming that the oxygen isotopic values reflect precipitation intensity, it became dry during a gradual cooling period and shifted wet with an abrupt warming.

U-Th dating was performed in National Taiwan University under the guidance of Prof. C.C. Shen.

Keywords: stalagmite, oxygen isotope, late Pleistocene

## Changes in precipitation over the last 2000 yrs recorded in a stalagmite and famine and disaster records in Iwate Pref.

KATO, Hirokazu<sup>1\*</sup> ; YAMADA, Tsutomu<sup>1</sup>

<sup>1</sup>Graduate School of Science, Tohoku University

Stalagmites are excellent archives of terrestrial paleoclimate information. Some of them are formed in caves near the noosphere and may have recorded past climatic changes influenced human activity. Stable oxygen isotopic compositions of stalagmites especially have been utilized in many paleoclimate studies. However, many factors controlling stalagmite oxygen isotopic composition are known and the degrees of their influence varied from region to region. It is not easy to specify the main controlling factor in Northeast Japan, because the climate is influenced by the East Asian Monsoon and surrounding continental and oceanic air masses struggling with each other. Therefore stalagmite climatic studies is not advanced in this region.

We collected growing stalagmite UT-A from Uchimagi-do Cave, Iwate Prefecture, Northeast Japan. UT-A is 25 cm in height and obvious annual growth layers are found entirely under UV light. The age model of UT-A was based on these growth bands and it revealed that the mean growth rate is 0.12 mm/year and the stalagmite has continuously grown over the last 2000 years. In order to specify the major factor controlling isotopic composition of UT-A, we analyzed changes in annual layer thickness and oxygen isotopic composition of the uppermost part of UT-A and examined the correlations between these changes and weather around the cave over the last 30 years. As the changes in  $d^{18}O$  correlates well with the growth rates and amount of precipitation, the oxygen isotopic profiles of UT-A could be interpreted as a proxy of precipitation change over the last 2000 years. The past precipitation deduced from oxygen isotopic composition of UT-A has a 100-200-year cycle and synchronized with famine and disaster caused by excess and lack of precipitation in regional historical records (e.g. Nihon'yanagi, 1968MS). Thus oxygen isotopic composition of stalagmites in Northeast Japan could be a good proxy of past precipitation and we can reconstruct past precipitation and possible famine and disaster events in prehistoric times. Moreover, we may be able to forecast the near future precipitation change in this region by the cyclic fluctuation.

### Reference

Nihon'yanagi, S., 1968MS. *Small history of famines in Nanbu-Hachinohe Han in the Thousand Years* (in Japanese). Aomori.

Keywords: stalagmite,  $d^{18}O$ , precipitation, famine and disaster records, Uchimagi-do Cave, Iwate Prefecture

## Skeletal records in a long-lived *Porites* coral from Okinoerabu-jima, Ryukyu Islands

ASAMI, Ryuji<sup>1\*</sup> ; TAMASHIRO, Shota<sup>1</sup> ; TSUCHIYA, Maika<sup>1</sup> ; KAWAKAMI, Saya<sup>1</sup> ; MURAYAMA, Masafumi<sup>2</sup> ; IRYU, Yasufumi<sup>3</sup>

<sup>1</sup>University of the Ryukyus, <sup>2</sup>Kochi University, <sup>3</sup>Tohoku University

Tropical and subtropical ocean-atmosphere interactions play a significant role in global climate changes on seasonal, interannual and decadal timescales. Knowledge of past ocean variability is crucial for understanding and modeling current and future climate. However, spatial and temporal instrumental time series from tropical and subtropical oceans before 1950 are quite limited. There is, therefore, a strong need for high-resolution paleoclimate proxies such as corals and sclerosponges from the oceans that extend beyond the instrumental data.

Massive *Porites* corals, living in shallow waters of the tropical to subtropical oceans, precipitate annually banded aragonite skeletons. These colonies provide robust chronological control and allow sub-sampling at monthly-to-seasonal resolution. Oxygen isotope composition of coral skeleton reflects variations in sea surface temperature and seawater oxygen isotope composition (salinity) with the latter being closely related to the precipitation-evaporation balance at sea surface and changes in water mass transport (e.g., Gagan et al., 1998). Long-lived corals are an excellent archive for documenting high temporal resolved time series of thermal and hydrologic changes at sea surface for the last several centuries (e.g., Quinn et al., 1998). Nevertheless, there are a few published long coral records of more than 100 years in the tropical northwestern Pacific (Guam: Asami et al., 2005; Ogasawara: Felis et al., 2009; Ishigaki: Mishima et al., 2010).

We collected a 4.5-m-long skeleton core from a modern *Porites* coral colony in Okinoerabu-jima, Ryukyu Islands on October 2011. Our continuous observational data at the coral living site for the years 2009-2011 are consistent with gridded sea surface temperature and salinity products, suggesting that the site is exposed directly to open sea surface conditions. X-ray images of the coral skeleton showed well-developed annual density bands for the last several centuries. Here we present monthly-to-bimonthly resolved oxygen and carbon isotope composition time series from the coral skeleton to reconstruct secular trend of oceanographic changes before and after the Industrial Revolution. Along with previously published long coral records, our coral-based climate reconstruction will document spatial changes in thermal and hydrologic conditions in the northwestern Pacific for the last several centuries.

**Keywords:** coral skeleton, oxygen isotope composition, carbon isotope composition, paleo-temperature, paleo-salinity, Ryukyu Islands



## Particle flux and paleoceanographic studies in the subarctic Pacific and the Arctic Ocean

TAKAHASHI, Kozo<sup>1\*</sup>

<sup>1</sup>Hokusei Gakuen University

Particle flux studies employing time-series sediment traps have been very useful in obtaining novel knowledge concerning the environmental conditions in ever changing upper water columns of the subarctic Pacific since there had essentially been no such information available prior to our attempt. We employed T/S Oshoro-maru of the Hokkaido University in deploying the sediment traps in two remote areas of the subarctic Pacific during 1989-2010, for >20 years: one in the pelagic central subarctic Pacific (49.5 degree N, 174 degree E) and the other at a hemipelagic site of the Aleutian Basin of the Bering Sea (53.5 degree N, 177 degree E). Major biogenic particles in the flues include siliceous shells such as diatoms, radiolarians, and silicoflagellates as well as carbonate shells such as coccolithophores, foraminifers.

These shell-bearing plankton particles are useful in identifying detailed environmental conditions concerning seasonal and inter-annual changes. In particular, the effectiveness of biological pumps has been clarified, showing uptake of atmospheric CO<sub>2</sub> into the upper water columns at a different extent depending of the sites for the first time. Another important aspect of the biogenic particles is initial fossilization process during the settling phase in the water column, which also will be discussed.

Furthermore, application of what had been learnt from the particle flux studies to the sediment records of the past climate changes has been quite a challenge, but rewarding. Integrated Ocean Drilling Program (IODP) Expedition 302 (Arctic Coring Expedition: ACEX) in the vicinity of the North Pole at 88 degree N on the Lomonosov Ridge provided an opportunity of studying the middle Eocene environmental conditions of the paleo-Arctic. The conditions revealed for the first time mainly by siliceous microfossils such as diatoms, silicoflagellates, ebridians and chrysophytes are: fresh water at the top, brackish water next within the euphotic layer, and salty marine water supplied from the outside palegic realm. Another important aspect of the paleoceanographic exploration had been focused on the Bering Sea as IODP Expedition 323, for which the author proposed during the ODP era and materialized during the IODP era after 14 years of drilling preparation effort. The successful drilling down to ca. 5 Ma led to novel knowledge of many aspects such as evolution of sea-ice, the linkages both to the Pacific Ocean and the Arctic Ocean through the Beringian gateway. The Bering Sea drilling data linking to the intensification of the Northern Hemisphere Glaciation (NHG) ca. 2.7 Ma as well as the Mid-Pleistocene Transition (MPT) during 1.2-0.8 Ma are of extremely of interest and will be discussed in details.

Keywords: particle flux, Bering Sea, Arctic Ocean, Northern Hemisphere glaciation, Oceanic gateway

## Calcareous nanoplanktons and nanofossils as useful tools for paleoceanography

OKADA, Hisatake<sup>1\*</sup>

<sup>1</sup>Hokkaido University

Microfossils are useful tools for paleoceanographic studies in two ways: age identification by detailed biostratigraphy, and reconstruction of sea state such as water temperature, productivity and dynamic properties of water mass. Needless to say, calcareous nanofossils are powerful age-diagnostic tool for oceanic sediments, but because of their minute size, its usefulness for oxygen and carbon isotopic analysis are limited. On the other hand, the unique existence of *Florisphaera profunda*, a deep photic-zone dweller, provide an useful method for paleoproductivity and dynamic analysis of water column. By the way, new discoveries or break through in any disciplines are often resulted from unexpected encounters or conversations between researchers. Personal relationships are also very important factor to progress career and to accomplish scientific achievement for young scientists. Utilizing this opportunity, I will summarize major points for paleoceanographic applications of calcareous nanofossils, and also, I will explain my own experiences of various encounters that resulted fruitful scientific achievements.

Keywords: paleoceanography, calcareous nanofossils, biostratigraphy, water dynamics, lower photic-zone

## Mechanism of ice age cycle and paleoclimate modeling

ABE-OUCHI, Ayako<sup>1\*</sup>

<sup>1</sup>University of Tokyo (AORI) and JAMSTEC

The 100-kyr cycle of the waxing and waning of the large Northern Hemisphere ice sheets and fast termination of the glacial cycles are the prominent pattern known from paleoceanographic records which can not be explained by the summer insolation proposed by the Milankovitch theory alone. Conceptual models imposing a threshold for the terminations by a large size of the ice sheet and/or large insolation can reproduce the patterns of glacial cycles, however, a physical explanation was not given. Here we simulated the past seven glacial cycles successfully with an ice sheet model in combination with a general circulation model imposing the time series of insolation and atmospheric CO<sub>2</sub>. The response of climate to ice sheet, greenhouse gases and orbital forcings is examined with high resolution. The stationary wave feedback of ice sheet is also taken into account. Our model reproduces 100-kyr periodicity of the glacial cycles even with the astronomical forcing alone under a certain range of CO<sub>2</sub> level for the case of North America ice sheet. We show that the threshold which leads to the termination of the glacial cycle is governed by how the ice sheet responds to a given insolation. The characteristics of how the ice sheet responds to external forcing strongly depends on the climatic condition, such as the north-south temperature gradient and the topographic condition for each continent.

Keywords: climate, paleoclimate

## Cretaceous-Paleogene stratigraphy in Northwest Pacific and its significance for paleoenvironmental study

NISHI, Hiroshi<sup>1\*</sup> ; TAKASHIMA, Reishi<sup>1</sup> ; YAMANAKA, Toshiro<sup>2</sup> ; ORIHASHI, Yuji<sup>3</sup> ; HAYASHI, Kei-ichi<sup>4</sup> ; KANETSUNA, Masaya<sup>1</sup>

<sup>1</sup>Tohoku University, <sup>2</sup>Okayama University, <sup>3</sup>The University of Tokyo, <sup>4</sup>Geological Survey of Hokkaido

The Cretaceous – Paleogene period is known as the latest Greenhouse climate in the history of earth. In order to understand ocean – climate system during past Greenhouse climate, numerous attempt has long been made for the marine sequences in the Atlantic and Southern oceans and the Tethyas Sea. The Pacific Ocean was the outstandingly largest ocean during Cretaceous – Paleogene, and it may have played important roles in Earth's ocean – climate system. Despite its importance, very little work has been done to establish detailed paleo-oceanographic changes during Cretaceous – Paleogene. This is largely because most of the Cretaceous – Paleogene Pacific oceanic crusts have subducted under continents, and bad recoveries of Cretaceous – Paleogene sediments of the ODP and DSDP cores from the Pacific sites have prevented researchers from studying paleoenvironmental changes of the Pacific Ocean.

First, we establish the detailed integrated stratigraphy (planktic foraminiferal and dinoflagellate cyst biostratigraphy, carbon isotope stratigraphy and U-Pb dating of tuff beds) of the Cretaceous – Paleogene marine sequences exposed in Hokkaido Japan because the resolution of international stratigraphic correlation of these strata is not enough to identify important climatic and/or extinction events such as the OAEs, K/Pg, PETM and others. The strata used in this study is as follows; the Yezo Group (early Aptian – early Campanian: 125 – 75 Ma), the Nemuro Group (Campanian?– early Eocene: 75?– 53 Ma), the Poronai Formation (late Eocene: 42 – 35 Ma) and the Onbetsu Formation (late Eocene – early Oligocene: 34 – 32 Ma). Our integrated stratigraphy enables to identify the exact horizons of following climatic and extinction events. The Cretaceous Oceanic Anoxic Events (OAEs) of the OAE1a (125.5 – 124 Ma), Leenhardt Level of OAE1b (110 Ma), OAE1c (107 Ma), OAE1d (101 Ma), OAE 2(94 – 93.5 Ma) are identified in the Yezo Group exposed in Oyubari and Tomamae areas. Although no so-called black shales were found in these horizons, evidences of oxygen depletion were identified from the most of these horizon based on the analyses of benthic foraminifera, degree of pyritization and sedimentary structure such as degree of bioturbation. The horizons of the K/Pg (66 Ma) and PETM (Paleocene Eocene Thermal Maximum; 56 Ma) in the Nemuro Group and Late Eocene Warming (37 Ma) in the Poronai Formation exhibit no obvious differences in lithology. Especially, the strata across the K/Pg boundary in the Shiranuka Hill consists of massive mudstone and a few intercalations of thin felsic tuff and turbidite sandstone. The middle – late Eocene cooling (40 – 39 Ma) is characterized by abundant occurrences of glendonites and buliminids (benthic foraminifera) in the middle part of the Poronai Formation, which indicates that cooling and eutrophication of surface water occurred in the northwest Pacific. The prominent positive excursion of oxygen isotope around Eocene/Oligocene boundary (34 – 33.6 Ma) is placed at the top of the Urahoro Group. The overlying Onbetsu Formation includes Oi-1a and Oi-1b of early Oligocene. Flood occurrence of buliminids in the lower part of the Onbetsu Formation suggest that surface water eutrophication occurred in response to global cooling after the Oi-1 glaciation.

The horizons of climatic and extinction in Hokkaido have continuous outcrop without significant hiatus and faults. High resolution analyses of these horizons will improve our understanding of climatic and environmental changes in northwest Pacific during the latest greenhouse period.

Keywords: Cretaceous, Paleogene

## Milankovitch forcing and carbon cycle during the Toarcian Oceanic Anoxic event

IKEDA, Masayuki<sup>1</sup> ; HORI, S., Rie<sup>1\*</sup> ; IKEHARA, Minoru<sup>2</sup>

<sup>1</sup>Department of Earth Science, Faculty of Science, Ehime University, <sup>2</sup>Center for Advanced Marine Core Research, Kochi University

One of the most profound environmental changes in the Mesozoic took place during Toarcian (Early Jurassic), including oceanic anoxia (Toarcian Oceanic Anoxic Event; T-OAE). The T-OAE is characterized by negative carbon isotope excursion (CIE) of up to ~8 ‰. The T-OAE is considered to have resulted from the release of CO<sub>2</sub> by Karoo-Ferrar volcanism and possible methane hydrate dissociation. However, the origin of these perturbations remains strongly debated, primarily due to lack of radiometric age constraints across the T-OAE (e.g. Palfy and Smith, 2000; Kemp et al., 2005, 2011; Suan et al., 2008).

Here we present the orbitally-tuned bio-, and  $\delta^{13}\text{C}_{org}$  stratigraphy of the Lower Jurassic deep-sea bedded chert sequence at the Katsuyama-Sakahogi section, in the Inuyama area, central Japan, which covers the T-OAE (Ikeda and Tada, 2013; Ikeda and Hori, in review). The sedimentary rhythms of the bedded chert display a full range of climatic precession related cycles; ~20 kyr cycle as a chert-shale couplet and ~100 kyr, 405 kyr, ~2000 to 4000 kyr cycles as chert bed thickness variations (Ikeda et al., 2010; Ikeda and Tada, 2013). Chert-shale cycles and variations in chert bed thickness are interpreted as resulted from changes in the burial rate of biogenic silica (Hori et al., 1993).

By using 405-kyr eccentricity cycle of constant and stable periodicity (Laskar et al., 2004) observed in the Inuyama bedded chert, we established the astronomical time scale (ATS) by counting 405 kyr cycle (~20 bed cycle; Ikeda and Tada, 2013). Then, this ATS is anchored at the end-Triassic radiolarian extinction level of which age is estimated as  $201.4 \pm 0.2$  Ma based on projection of the U-Pb date measured at the Pucara section, Peru, using the conodont and radiolarian biostratigraphy (e.g. Carter and Hori, 2005; Schoene et al., 2010; Ikeda and Tada, 2013).

This astronomical time scale suggests the absolute ages of the T-OAEs. The timing of two black bedded chert intervals (T-OAEs 1 and 2) and the negative CIE of ~5 ‰ are within the time interval of radiometric ages from the Karoo-Ferrar Lips (Svencen et al., 2007; Jourdan et al., 2008). This result supports the volcanic degassing origin of these carbon cycle perturbations (Palfy and Smith, 2000; Suan et al., 2008).

The termination of black shale deposition occurred at the minimum of 40 kyr obliquity and 100 kyr and 405 kyr eccentricity cycles. These temporal relations imply the possible impacts of these orbital forcing on the stabilization of carbon cycle perturbation through Earth system dynamics, such as weathering and nutrient cycles.

Keywords: Milankovitch cycle, carbon cycle, volcanism, silica cycle, hydrological cycle

## Paleoceanographic evolution of Miocene to Pliocene mud sea in the Ryukyus based on calcareous nannofossil assemblages

IMAI, Ryo<sup>1\*</sup> ; SATO, Tokiyuki<sup>2</sup> ; IRYU, Yasufumi<sup>1</sup>

<sup>1</sup>Institute of Geology and Paleontology, Graduate School of Science, Tohoku University, <sup>2</sup>Institute of Applied Earth Sciences, Faculty of Engineering and Resource Science, Akita University

The Cenozoic sedimentary succession in Okinawa-jima, including the upper Miocene to Pleistocene siliciclastic deposits (Shimajiri Group) and the Pleistocene reef to shelf deposits (Ryukyu Group), suggests a drastic paleoceanographic change from a mud sea to a coral sea. To delineate the paleoceanographic evolution of the mud sea, we quantified the stratigraphic distribution of the calcareous nannofossil assemblages from the Shimajiri Group in a 2119.49 m-deep well (Nanjo R1 Exploratory Well) drilled in southern Okinawa-jima (Ryukyu Islands, southwestern Japan). Four late Miocene and Pliocene datum planes were found in the studied interval. The calcareous nannofossil assemblages suggest the existence of oligotrophic conditions between 5.3 and >8.3 Ma followed by eutrophic conditions and a return to oligotrophic conditions at 3.5 Ma. Micropaleontological evidence suggests that these oceanographic changes were likely caused by local tectonic movement (shallowing of the sedimentary basin in which the Shimajiri Group was deposited). We will report calcareous nannofossil records from two exploratory wells drilled in southern Okinawa-jima in 2013 – 2014 as well.

Keywords: calcareous nannofossil, Miocene, Pliocene, Ryukyu Islands

## East Antarctic deglaciation and the link to global cooling since the Pliocene

SUGANUMA, Yusuke<sup>1\*</sup> ; MIURA, Hideki<sup>1</sup> ; ZONDERVAN, Albert<sup>3</sup> ; OKUNO, Jun'ichi<sup>2</sup>

<sup>1</sup>National Institute of Polar Research, <sup>2</sup>JAMSTEC, <sup>3</sup>GNS, Science

Reconstructing past variability of the Antarctic ice sheets is essential to understand their stability and to anticipate their contribution to sea level change as a result of future climate change in a high-CO<sub>2</sub> world. Recent studies have reported a significant decrease in thickness of the East Antarctic Ice Sheet (EAIS) during the last several million years. However, the geographical extent of this decrease and subsequent isostatic rebound remain uncertain and a topic of debate. In this study, we reconstruct magnitude and timing of ice sheet retreat at the Sor Rondane Mountains in Dronning Maud Land, East Antarctica, based on detailed geomorphological survey, cosmogenic exposure dating, and glacial isostatic adjustment modeling. Three distinct deglaciation phases since Pliocene for this sector of the EAIS are identified, based on rock weathering and <sup>10</sup>Be surface exposure data. We estimate that during the Plio-Pleistocene the ice sheet thinned by at least 500 m. This thinning is attributed to the reorganization of Southern Ocean circulation associated with the global cooling into the Pleistocene, which reduced the transport of moisture from the Southern Ocean to the interior of EAIS. The data also show since the Last Glacial Maximum the ice surface has lowered less than ca.50 m and probably started after ca. 14 ka. This suggests that the EAIS in Dronning Maud Land is unlikely to have been a major contributor to postglacial sea-level rise and Meltwater pulse 1A.

## Past 2 Myr Radiolarian Assemblages and Paleoceanographic Changes off the Southwestern Japan (IODP Site C0001)

MATSUZAKI, Kenji M.<sup>1\*</sup> ; NISHI, Hiroshi<sup>1</sup> ; SUZUKI, Noritoshi<sup>2</sup> ; HAYASHI, Hiroki<sup>3</sup> ; IKEHARA, Minoru<sup>4</sup> ; GYAWALI, Babu R.<sup>2</sup> ; TAKASHIMA, Reishi<sup>1</sup>

<sup>1</sup>The Center for Academic Resources and Archives, Tohoku University Museum, Tohoku University (Japan), <sup>2</sup>Institute of Geology and Paleontology, Graduate School of Science, Tohoku University (Japan), <sup>3</sup>Interdisciplinary Faculty of Science and Engineering, Shimane University (Japan), <sup>4</sup>Center for Advanced Marine Core Research, Kochi University (Japan)

The effects of Quaternary paleoceanographic events on the Kuroshio Current off the southwestern Japan, including the mid-Pleistocene Transition (MPT) (1,200?700 ka) and the mid-Brunhes event (MBE) (400?300 ka), are poorly documented at this time because of a lack of long core recovering the MBE and the MPT. In this context, this study aims to establish paleoceanography of this region since the Early Pleistocene, using radiolarian assemblages as paleoceanographical proxy. The Holes C0001E and F, drilled by the R/V Chikyu during IODP Expedition 315 at a depth of 2198 m in the Shikoku Basin off the Kii Peninsula on the slope of the Nankai accretionary prism (southern Japan) are used in this study. The upper 190 m LSF sediments cover the Quaternary based on the shipboard results, the dominant lithology consisted of greenish-gray to grayish-green mud. The age model of Site C0001 is based on calcareous nannofossils datums, planktic foraminifers datums, radiolarians datums and *Globorotalia inflata* oxygen isotope stratigraphy. In this study, 240 samples of 20 cc, covering the Early to Middle Pleistocene, were used for radiolarian faunal analysis. The examination of the polycystine radiolarians was performed using an optical microscope at a magnification of 100?400x. In each sample, 400 to 1000 polycystine radiolarians were identified. The radiolarian-based sea surface temperature (rSST) was estimated using a Modern Analogue Technique (MAT). Several warming event is recorded during the Early Pleistocene. However, the strongest warming event is recorded during the MPT, where the subtropical fauna abundances increased consequently.

Keywords: Pleistocene, Paleoceanography, Mid Pleistocene Transition, Radiolarian



## Sea-ice conditions in the Okhotsk Sea during the last 550 kyr deduced from environmental magnetism

YAMAZAKI, Toshitsugu<sup>1\*</sup> ; INOUE, Seiko<sup>2</sup> ; SHIMONO, Takaya<sup>2</sup> ; SAKAMOTO, Tatsuhiko<sup>3</sup> ; SAKAI, Saburo<sup>4</sup>

<sup>1</sup>AORI, University of Tokyo, <sup>2</sup>Tsukuba University, <sup>3</sup>Mie University, <sup>4</sup>JAMSTEC

Reconstructing past sea-ice conditions in the Okhotsk Sea is important because sea-ice conditions vary in response to global climate changes, which in turn may affect global ocean circulation through intermediate water mass formation. We conducted an environmental magnetic study of six cores from three stations in the central Okhotsk Sea to better understand temporal and spatial sea-ice variations. Inter-core correlations and age estimations are based mainly on geomagnetic paleointensity; an oxygen-isotope stratigraphy is available for one station. Magnetic susceptibility (MS) minima are accompanied by maxima in color  $b^*$ , the ratio of the anhysteretic remanent magnetization susceptibility to saturation isothermal remanent magnetization ( $k_{ARM}/SIRM$ ), and the S-ratio, which indicates a higher proportion of biogenic to terrigenous magnetic components. This reflects enhanced ocean productivity. First-order reversal curve diagrams and IRM component analyses support the dominance of biogenic magnetite at MS minima. In contrast, color  $b^*$ ,  $k_{ARM}/SIRM$ , and S-ratio values are low when MS is high, which indicates an increased proportion of the terrigenous component that was probably transported as ice-rafted debris (IRD). For the southern two stations, IRD accumulation increased in glacial and deglacial periods, which implies mobile sea-ice conditions even in full glacials. This was succeeded by extremely enhanced ocean productivity in early interglacials, which suggests nearly ice-free conditions. For the northernmost station, on the other hand, IRD accumulation was low in glacials and increased in early interglacials, which indicates perennial sea-ice coverage with little mobility in glacials. Succeeding ocean-productivity enhancement was delayed compared to the southern stations.

Keywords: Okhotsk Sea, paleoceanography, environmental magnetism, sea ice, IRD

## Pliocene and Pleistocene paleoceanography in the northwestern Pacific and the Bering Sea based on diatom analyses

KATO, Yuji<sup>1\*</sup> ; ONODERA, Jonaotaro<sup>2</sup> ; SUTO, Itsuki<sup>1</sup> ; TERAISHI, Akihito<sup>3</sup> ; TAKAHASHI, Kozo<sup>4</sup>

<sup>1</sup>Graduate School of Environmental Studies, Nagoya University, <sup>2</sup>Research Institute for Global Change, JAMSTEC, <sup>3</sup>NTT COMWARE Co, Ltd., <sup>4</sup>School of Social Welfare, Hokusei Gakuen University

Late Pliocene-Pleistocene fossil diatom assemblages from Ocean Drilling Program (ODP) Leg 145 Hole 884B in the western Subarctic North Pacific were investigated and the paleoceanographic records were compared with those at Integrated Ocean Drilling Program (IODP) Expedition 323 Holes U1341B and U1343E in the Bering Sea for an interval of 2.5-0 Ma.

As the results, in Hole 884B, five diatom zones, from the *Neodenticula koizumii*-*N. kamtschatica* Zone to the *N. seminae* Zone, were identified. The cold-water indicators from Hole 884B, which represented high abundances throughout the interval, suggest the cold environmental conditions analogous to the modern sea-surface conditions in the western subarctic Pacific. The drastic decrease of the temperate-water species at ca. 2.2 Ma is related to a rapid cooling event at ~2 Ma. Sporadic appearances of sea-ice related species from ca. 2.3 Ma and a slight increase of neritic species observed at ca. 2.0 Ma may be reflection of a series of the Northern Hemisphere Glaciation (NHG) events. Slightly higher abundances of the sea-ice related species at 1.0-0.8 and 0.4 Ma and those of the neritic species at 2.0, 1.8, 1.2, and 0.9 Ma are likely to correspond to the southward advance of the subarctic front and drop in sea-surface temperature mentioned by Sancetta and Silvestri (1986).

The age differences of the distinct decreases of temperate-water species recognized at ca. 1.9 Ma for Hole U1343E, ca. 2.1 Ma for Hole U1341B and ca. 2.2 Ma for Hole 884B indicate that the East Kamchatka Current in the Western Subarctic Gyre was strengthened and the westward advection of the Alaskan Stream was weakened at ca. 2.2 Ma. In the Bering Sea, the limited input of temperate waters via the Near Strait resulted as a decrease of warm water supply to the region around Site U1341 at ca. 2.1 Ma, while the eastern Bering slope region had been still affected by the warm water masses advected from the Amchtka and Amukta Passes. Further global cooling might have restricted the continuous warm water supply to the Bering slope region around Site U1343 at ca. 1.9 Ma.

Keywords: diatom, paleoceanography, subarctic Pacific, Bering Sea, IODP Expedition 323, ODP Leg 145

## Millennial-scale rock-magnetic variation indicating instability of North Atlantic environments during MIS 100

OHNO, Masao<sup>1\*</sup> ; SATO, Masahiko<sup>1</sup> ; HAYASHI, Tatsuya<sup>2</sup> ; KUWAHARA, Yoshihiro<sup>1</sup> ; KITA, Itsuro<sup>1</sup>

<sup>1</sup>Graduate School of Integrated Sciences for Global Society, <sup>2</sup>Mifune Dinosaur Museum

Ocean thermohaline circulation (THC) plays an important role in global climate change linked with continental ice sheets. To clarify the variation of ocean THC in the early stage of glaciations in the northern hemisphere, we studied a deep-sea sediment core with high sedimentation rate recovered at IODP Site U1314 in the North Atlantic. Rock magnetic study of the sediments during marine oxygen isotope stage (MIS) 100 indicated links between the millennial-scale variability in deep water circulation and iceberg discharge. The observed abrupt decreases of magnetic coercivity associated with ice-rafted debris (IRD) are interpreted to be reduced transport of high-coercivity material from Icelandic source indicating reduced formation of North Atlantic Deep Water (NADW). In these periods, a current from the south, Lower Deep Water, transports sediments with low magnetic coercivity contributed by coarse grained magnetite of continental sources. Repetition of vigorous and weakened NADW production linked to IRD was observed during MIS 100 in a similar manner to that in the last glacial suggests that the regime of climate change in the millennial-scale was already established in the early stage of glaciations in the northern hemisphere.

Keywords: rock magnetism, thermohaline circulation, North Atlantic Deep Water, Ice rafted debris

## Paleoceanographic reconstruction of the Holocene Arctic Chukchi Sea using fossil diatoms

KONNO, Susumu<sup>1\*</sup> ; JORDAN, R. W.<sup>2</sup>

<sup>1</sup>Graduate School of Sciences, Kyushu University, <sup>2</sup>Faculty of Science, Yamagata University

The Chukchi Sea, in the Arctic Ocean, receives the warm outflowing waters of the Bering Sea. These waters are one of the causes of Arctic sea ice decline, and change their flow according to the sea ice distribution in the Chukchi Sea. Sea ice in the global climate system has a significant impact on the global environment (e.g., atmospheric circulation, biological production and ocean circulation), due to the albedo effect, maintenance of low temperatures, and high salinity bottom waters. Therefore, the reconstruction of the past sea ice history of the Chukchi Sea is important in understanding the climate system of the Arctic Ocean as well as the global climate system. However, piston cores previously obtained from the Chukchi Sea were too short and/or contained few or no microfossils, making detailed paleoenvironmental analyses and age determinations difficult.

I started working on the diatom analysis of sediment cores taken during the HLY0501 cruise of the United States Coast Guard icebreaker cutter "Healy" in 2005. They took 8 sediment cores, although diatoms were not obtained at six of the sites. So here I show the diatom analysis results from the remaining two cores (cores 5 and 8).

Keywords: Chukchi Sea, Diatom, Holocene

## Thermal threshold of the Atlantic meridional overturning circulation as a trigger for glacial abrupt climate changes

OKA, Akira<sup>1\*</sup> ; ABE-OUCHI, Ayako<sup>1</sup> ; YOKOYAMA, Yusuke<sup>1</sup> ; KAWAMURA, Kenji<sup>2</sup> ; HASUMI, Hiroyasu<sup>1</sup>

<sup>1</sup>Atmosphere and Ocean Research Institute, University of Tokyo, <sup>2</sup>National Institute of Polar Research

Abrupt climate changes known as Dansgaard-Oeschger events (DO events) took place frequently during glacial climate. Geological evidences support the idea that changes of the Atlantic meridional overturning circulation (AMOC) are related to these events, but question on what triggers the AMOC changes remains unsolved. Although most studies have regarded freshwater flux from melting ice sheet as a cause of the AMOC changes, we recently identified the existence of the thermal threshold of the AMOC during glacial climate. Here, from the results of numerical simulations about the glacial AMOC, we report that the thermal threshold of the AMOC serves as a triggering mechanism of DO events. We investigated the structure of the thermal threshold in glacial climate by conducting ocean general circulation model simulations under various thermal conditions in which degrees of sea surface cooling are systematically changed separately or simultaneously in northern and southern hemispheres. The results suggest that the threshold is located near the condition under which the climate is slightly warmer than the coldest glacial conditions. We also found that the amplitude of AMOC changes in crossing the threshold depends on thermal conditions in northern and southern hemispheres. The most prominent threshold is identified where the southern hemisphere is somewhat warmer than the coldest glacial conditions. It is also demonstrated that gradual warming in the southern hemisphere from the colder glacial climate leads to crossing this threshold and can cause significant strengthening of AMOC. Our results indicate that the thermal threshold could be a triggering mechanism of DO events, especially for those accompanying the gradual warming of southern hemisphere before their abrupt warming in northern hemisphere.

## Role of Southern Ocean stratification in glacial atmospheric CO<sub>2</sub> reduction

KOBAYASHI, Hidetaka<sup>1\*</sup> ; OKA, Akira<sup>1</sup>

<sup>1</sup>Atmosphere and Ocean Research Institute, The University of Tokyo

The global temperatures and atmospheric carbon dioxide (pCO<sub>2</sub>) concentrations varied during the last 800 thousand years. During the glacial times, such as Last Glacial Maximum (LGM), the atmospheric partial pressure of carbon dioxide (pCO<sub>2</sub>) was about 80-100ppmv lower than interglacial times, such as Holocene. Compared to interglacial conditions, terrestrial carbon stocks were reduced during glacial conditions. Marine carbon cycles must have been the main driver for lowering atmospheric pCO<sub>2</sub> during ice ages. A number of candidate mechanisms to explain the reduction in glacial atmospheric pCO<sub>2</sub> have been proposed. However, they failed to explain full amplitude of 80-100ppmv reduction. Based on paleo-proxy reconstructions,  $\delta^{13}\text{C}$  gradient between surface and deep ocean was larger than today, suggesting that the glacial ocean circulation state was different from today. In the deep glacial Southern Ocean, very saline water was identified from paleo proxy data. Moreover, radiocarbon record showed the existence of radiocarbon-depleted old waters in glacial ages. One hypothesis that has been proposed to explain the glacial atmospheric pCO<sub>2</sub> is the isolated reservoir hypothesis: a carbon-rich, radiocarbon-depleted water mass was isolated from the atmosphere during the glacial periods. The stratification of the Southern Ocean water column may have contributed to a reduction of atmospheric pCO<sub>2</sub>.

In this study preindustrial and LGM marine carbon cycle sensitivity experiments are conducted to estimate a role of stratification in glacial Southern Ocean quantitatively, by using an ocean general circulation model (OGCM). In the control case, atmospheric pCO<sub>2</sub> between Modern case and LGM case is about 44ppmv, which was comparable to previous AOGCM study. However, LGM case cannot explain the saline glacial Southern Ocean.

Previous study using intermediate complexity models suggested that glacial atmospheric pCO<sub>2</sub> and  $\delta^{13}\text{C}$  distribution can be reproduced by considering brine induced stratification.

Therefore, we also consider the effect of brine induced stratification. We partly succeeded in reproducing the saline glacial South Atlantic Ocean by imposing body forcing near the bottom in the Weddell Sea, Ross Sea and Eastern Antarctica, whereas saline glacial Southern Ocean resulted in increased northward flow of AABW and increased atmospheric pCO<sub>2</sub>. Additionally, we used stratification-dependent vertical eddy diffusivity parameterization suggested by Gargett (1984) to discuss changes in vertical eddy diffusivity in Southern Ocean. Contrary to our expectation, vertical eddy diffusivity in high latitude becomes very higher under glacial conditions, and sequestered carbon in deep ocean was released into the atmosphere and resulted in higher atmospheric pCO<sub>2</sub>.

Finally, very stratified Southern Ocean achieved by extremely small vertical eddy diffusivity also cannot reduce glacial atmospheric pCO<sub>2</sub>. Other processes, which are not taken into account in our study may be important to reproduce the glacial condition.

Keywords: ocean carbon cycle, Last Glacial Maximum, Southern Ocean, Ocean general circulation model

## A tree-ring oxygen isotope chronology from Yakushima Island and its dendroclimatic potential

SANO, Masaki<sup>1\*</sup> ; YASUE, Koh<sup>2</sup> ; KIMURA, Katsuhiko<sup>3</sup> ; NAKATSUKA, Takeshi<sup>1</sup>

<sup>1</sup>Research Institute for Humanity and Nature, <sup>2</sup>Shinshu University, <sup>3</sup>Fukushima University

Recent progress in isotope dendroclimatology showed that tree-ring oxygen isotopes are a promising proxy to reconstruct past precipitation and/or relative humidity. In the present study, we developed a 300-year tree-ring oxygen isotope chronology using Japanese cedar (*Cryptomeria japonica*) growing in Yakushima Island, southern Japan, and explored its dendroclimatic potential. Two tree samples that were crossdated by visually matching ring-width variations were used for oxygen isotopic analysis. The resulting oxygen isotope series for the period 1700-2009 C.E. were highly correlated with each other ( $r = 0.68$ ), indicating that common signals related to local climate are preserved in these data. Both the delta-18O series were individually normalized to have zero mean and unit variance, and the resulting series were averaged to build the final chronology. Response analysis with monthly climatic records (temperature, precipitation and relative humidity) from the Kagoshima station revealed that tree-ring delta-18O was primarily controlled by relative humidity and precipitation in the summer season (May-September). Perhaps the most striking feature of the delta-18O chronology is a significant increasing trend over the 20th century, indicating a decrease in summer relative humidity in the study region. We will present an extended version of the tree-ring delta-18O chronology over the past 1000 years or so.

Keywords: tree ring, oxygen isotope ratios, Yakushima Island, monsoon

## Assessment of Sungkai tree-ring $\delta^{18}\text{O}$ proxy for paleoclimate reconstruction

HARADA, Mao<sup>1\*</sup>; WATANABE, Yumiko<sup>1</sup>; NAKATSUKA, Takeshi<sup>2</sup>; TAZURU, Suyako<sup>3</sup>; HORIKAWA, Yoshiki<sup>3</sup>; BAMBANG, Subiyanto<sup>4</sup>; SUGIYAMA, Junji<sup>3</sup>; TSUDA, Toshitaka<sup>3</sup>; TAGAMI, Takahiro<sup>1</sup>

<sup>1</sup>Graduate School of Science, Kyoto University, <sup>2</sup>Graduate School of Environmental Studies, <sup>3</sup>Research Institute for Sustainable Humanosphere, Kyoto University, <sup>4</sup>Indonesian Institute of Sciences

We measured annual  $\delta^{18}\text{O}$  variations of two sungkai trees that were collected in the same area as previous study, in order to assess the reproducibility of sungkai  $\delta^{18}\text{O}$  as paleoclimate proxies. Two sungkai  $\delta^{18}\text{O}$  variations has a significant correlation ( $r = 0.80$ ;  $P < 0.001$ ) with each other and also with the previous analysis, suggesting that  $\delta^{18}\text{O}$  values of sungkai are affected by external climatic factors. The annual  $\delta^{18}\text{O}$  of SungkaiNAN7 has significant, positive correlations with temperature, sunlight hours and air pressure whereas it has significant, negative correlations with relative humidity and SOI. Moreover, the seasonal  $\delta^{18}\text{O}$  variation acquired during severe drought of 1997-98 El Nino event shows that the maximum  $\delta^{18}\text{O}$  value around 1997 latewood corresponds to rainfall/relative humidity minimum and temperature/sunlight hours/air pressure maximum with a significant time lag.

Keywords: tree ring, cellulose, stable isotope geochemistry, tropics, paleoclimate



## Characteristics of ESR and TL of natural quartz from river bed sediments

SHIMADA, Aiko<sup>1\*</sup>; TOYODA, Shin<sup>2</sup>; TAKADA, Masashi<sup>1</sup>

<sup>1</sup>Application Support Team, JEOL RESONANCE Inc., <sup>2</sup>Department of Applied Physics, Okayama University of Science, <sup>3</sup>Department of History, Sociology and Geography, Faculty of Letters, Nara Women's University

The sediment provenance would give important information on the erosion processes, uplift of the mountains and so on, suggesting the environments at the time of sediment transportation. The sediment is made of fine grains such as sand and silt. When a new procedure for clarifying provenance of such sediments is established, it will be useful to elucidate the provenance of sediments in the geohistorical environments, which may occasionally be related to stream piracy, regional tectonic setting and/or the environment changes of the hinterland.

There have been already some Electron Spin Resonance (ESR) and luminescence studies on sediment provenance. The intensity of the E<sub>1</sub>' center in quartz is shown to be a useful parameter to investigate the provenance of aeolian dust as well as of sediments [1][2]. The crystallinity index (CI) in combination with ESR is employed to discriminate two different sources of eolian dust in the sediment core taken from the Japan Sea [3]. Quartz of four distinct origins can be distinguished using impurity (Al, Ti-Li, Ti-H, Ge) centers observed after beta irradiation [4]. Shimada and Takada (2008) and Shimada et al. (2013) also show that the Al, Ti-Li and E<sub>1</sub>' center signal intensities from the natural quartz are useful to distinguish the sediment provenance [5][6]. Volcanic quartz is reported to emit stronger red thermoluminescence (TL) than blue one whereas plutonic quartz does vice versa [7]. Quartz of eolian origin transported from China can be distinguished from volcanic quartz originated in Japanese tephra by looking at TL color of quartz grains [8].

In this study, we report the characteristics of ESR and TL of quartz taken from present river bed sediments, to discuss the possibilities of identifying sediment provenance.

[1] Naruse T, Ono Y, Hirakawa K, Okashita M, and Ikeya M, 1997. Source areas of eolian dust quartz in East Asia: a tentative reconstruction of prevailing winds in isotope stage 2 using electron spin resonance. *Geographical review of Japan* 70A-1, 15-27.

[2] Toyoda S and Naruse T, 2002. Eolian Dust from Asia Deserts to Japanese Island since the last Glacial Maximum: the Basis for the ESR Method, *Japan Geomorphological union* 23-5, 811-820.

[3] Nagashima K, Tada R, Tani A, Toyoda S, Sun Y, and Isozaki Y, 2007. Contribution of aeolian dust in Japan Sea sediments estimated from ESR signal intensity and crystallinity of quartz. *Geochemistry, Geophysics, Geosystems*, doi:10.1029/2006GC001364.

[4] Duttinea M, Villeneuve G, Bechtela F, Demazeaub G, 2002. Caracterisation par resonance paramagnetique electronique (RPE) de quartz naturels issus de differentes sources. *C.R.Geoscience* 334, 949-955.

[5] Shimada A and Takada M, 2008. Characteristics of Electron Spin Resonance (ESR) signals in quartz from igneous rock samples: a clue to sediment provenance. *Annual Reports of Graduate School of Humanities and Sciences*, 23, 187-195.

[6] Shimada A, Takada M and Toyoda S, 2013. Characteristics of ESR signals and TLCLs of quartz included in various source rocks and sediments in Japan: A clue to sediment provenance. *Geochronometria*, 40, Issue 4, 334-340.

[7] Hashimoto T, Koyanagi A, Yokosaka K, Hayashi Y and Sotobayashi T, 1986. Thermoluminescence color images from quartz of beach sands. *Geochemical journal* 20, 111-118.

[8] Ganzawa Y, Watanabe Y, Osanai F and Hashimoto T, 1997. TL color images from quartzes of loess and tephra in China and Japan, *Radiation Measurements* 27, 383-388.

Keywords: Electron Spin Resonance, Sediments provenance, Quartz, Sediments, Thermoluminescence, River bed sediments

## A chronostratigraphic study of the upper Anno formation, in the Awa group

HANEDA, Yuuki<sup>1\*</sup>

<sup>1</sup>Ibaraki University

We took oriented mini-core samples for paleomagnetic and rockmagnetic measurements at 79 sites and rock samples to extract fossil foraminifera from sites from the upper Anno formation distributed along the Shikoma river. We carried out rock magnetic, paleomagnetic, oxygen isotopic and carbon isotopic measurements.

Magnetic carrier was interpreted as pseudo-single domain magnetites based on the results of hysteresis and thermal demagnetization, thermomagnetic analyses.

We carried out analysis of principal component to results from the thermal demagnetization and extracted Characteristic Remanent Magnetizations (ChRMs). In the result, a relatively short reversed polarity zone found in the previous study is defined as the Mammoth subchronozone.

We obtained an oxygen isotopic curve from the result of isotopic measurements which is correlatable with the LR04 oxygen isotopic standard curve (Lisiecki & Raymo, 2005). Then we detected 6 tie points to establish an age model for this sequence

Keywords: paleomagnetic stratigraphy, oxygen isotopic stratigraphy, chronostratigraphy

## Palaeoclimatic analysis for 600 ka based on the TOC contents of MD01-2407 core from the Oki Ridge, Japan Sea

TAKIZAWA, Yuko<sup>1\*</sup> ; YAMAMOTO, Hiroki<sup>3</sup> ; HAYASHIDA, Akira<sup>4</sup> ; KUMON, Fujio<sup>2</sup>

<sup>1</sup>Graduate school of Science and Technology, Shinshu University, <sup>2</sup>Faculty of Science, Shinshu University, <sup>3</sup>a former student of Faculty of Science, Shinshu University, <sup>4</sup>Faculty of Science and Engineering, Doshisha University

We have measured total organic carbon (TOC) and total nitrogen (TN) contents of a sediment core, MD01-2407 (932 m depth, 55.28 m length), at 2 cm interval. This core was taken from the Oki ridge at the southern part of the Japan Sea in AD 2001. We used the age model which shows age-depth relation for MD01-2407 core proposed by Kido et al. (2007). This age model used 6 marker tephra layers, 7 <sup>14</sup>C dates, 3 TL layers and 14 delta <sup>18</sup>O events. This core covers the past 670 kyr.

TOC content is generally high in MIS 15, 13, 11, 9, 7, 5, 3 and 1 (about 1.5 - 5.0 %), and low in MIS 16, 14, 12, 10, 8, 6, 4 and 2 (about 0.8 - 1.2 %). This fluctuation pattern is very similar to the marine oxygen isotope curve LR04. TN content shows similar fluctuation with TOC. C/N ratio is constantly 9 - 10, suggesting that TOC is originated mainly from marine planktons. Temporal change of TOC of the sediment can reflect the change of biological productivity in the Japan Sea (Oba and Akasaka, 1990), which may be controlled climate change. This is an excellent record of paleoclimate over Middle and Late Pleistocene in the middle latitude region.

Keywords: TOC, TN, Japan Sea, MD01-2407

## A standard local chronology of late Quaternary based on the TOC profiles of the sediment cores from the Japan Sea

URABE, Tasuku<sup>1\*</sup> ; KUMON, Fujio<sup>2</sup>

<sup>1</sup>Faculty of Science, Shinshu University, <sup>2</sup>Department of Environmental Sciences, Faculty of Science, Shinshu University

The TOC content was measured for the late Quaternary sediments of the Japan Sea with high time resolution (ca. 100 yrs interval), and show the good similarity to the delta  $^{18}\text{O}$  curve of NGRIP not only in the orbital scale but also the D-O cycle scale (Urabe et al., 2013). In this study, we use TOC profile of the MD179-3312 core from the Japan Sea, and we align the TOC profile to the delta  $^{18}\text{O}$  in NGRIP using signal matching, the Match protocol (Lisiecki and Lisiecki, 2002). Before this matching process, there were ca. 4000 years gaps in maxima between both signals, and the gaps are variable. Based on the matched TOC profile, we calculated the ages of TOC peaks, and we proposed a new age of TL layers recognized in MD179-3312 (Kakuwa et al., 2013) on the basis of the matched chronology.

Recently, detailed TOC profiles of the sediment cores were reported from several sites in the Japan Sea, and they show very similar profiles. Therefore, we tried to compile the TOC profiles, using the same match protocol. The matched MD179-3312 profile mentioned above is used as a tentative standard, and TOC profiles of three sediment cores, namely MD179-3304 off Joetsu, MD01-2407 at Oki bank and MD01-2408 off Akita were matched to the tentative standard. This compiled TOC curve (TOC<sub>JSCOM</sub>; Japan Sea TOC compile) has a reliability due to averaging the four cores data. This TOC<sub>JSCOM</sub> have a good similarity with the TOC profiles from lake sediments in Japan. When we compared the TOC<sub>JSCOM</sub> with the delta  $^{18}\text{O}$  of stalagmites from the Hulu/Sanbao caves in the south of China (Wang et al., 2001, 2008), we found the improved chronological correspondence between both proxies in MIS 1/2 boundary, lower MIS 3, 4, 5.1, and 5.2. The difference of the trends is recognized in MIS 5.5, and a part of this discordance is due to the local environmental condition of the Japan Sea.

Keywords: Late Quaternary, Japan Sea, TOC, Chronology

## A Long-term pollen record of the C9001C core from the deep-sea bottom, off Shimokita peninsula, northeastern Japan

SUGAYA, Manami<sup>1\*</sup> ; OKUDA, Masaaki<sup>2</sup> ; OKADA, Makoto<sup>1</sup>

<sup>1</sup>Ibaraki University, <sup>2</sup>Natural History Museum and Institute of Chiba

We used a pollen analysis method for a deep-sea core to reconstruct paleoclimatic changes with the Milankovitch time scale.

In this study, we obtained a continuous pollen record and reconstructed paleovegetation and paleoclimate changes for the past several kyrs from the C9001C core, drilled from off Shimokita Peninsula.

We have applied the Modern Analogue Method to obtain a quantitative paleochimate reconstruction. In the results, a positive correlation has shown on between the paleotemperature parameter and the glacial - interglacial cycle. On the other hands, the summer precipitation parameter matches with the precession cycles but not with the glacial - interglacial cycles. The annual temperature parameter variability show strong negative correlation. These results are support hypothesis of the East Asia monsoon fluctuation mechanism

Keywords: pollen, monsoon, marine core

## Carbon and oxygen stable isotope records of benthic foraminiferal shells at DSDP Site 296

OKAZAKI, Yusuke<sup>1\*</sup> ; YAMAMOTO, Madoka<sup>1</sup> ; KAWAGATA, Shungo<sup>2</sup> ; IKEHARA, Minoru<sup>3</sup>

<sup>1</sup>Kyushu University, <sup>2</sup>Yokohama National University, <sup>3</sup>Kochi University

Carbon and oxygen stable isotope records of benthic foraminifera at DSDP Site 296 (2920 m water depth) from the Kyushu-Palau Ridge were measured. Sediment samples for upper 300 m of DSDP Site 296 were taken at every ~2 m and freeze-dried and washed on a 63 micro m mesh sieve and dried in an oven at 40 degree C. The dry samples were sieved through a mesh with 250 micro m opening. Two epifauna species, *Cibicides wuellerstorfi* and *Cibicidoides mundulus* were picked for isotope measurements. The foraminiferal shells were cleaned by soaking them in 99.5% methyl alcohol, followed by ultrasonication until all chambers were open. After confirming that all dirt had been removed, we washed the shells in Milli-Q water and dried them in an oven at 40 degree C. The dried samples were analyzed using IsoPrime mass spectrometry (Center for Advanced Marine Core Research, Kochi University). Analyses were calibrated to the CO-1, and the average analytical errors for delta 13C and delta 18O were less than 0.03 permil and 0.10 permil, respectively.

Age model of DSDP Site 296 is established by planktic foraminiferal and calcareous nannoplankton stratigraphy (Elias, 1975; Ujiie, 1975). Continuous stable isotope records except for a stratigraphic gap at ~250 mbsf are obtained for the past 20 Myrs. These records are basically consistent with those by Zachos et al. (2001).

Keywords: North Pacific, Benthic foraminifera, Stable isotope, Miocene, Pliocene

## A Southern Ocean trigger for Northwest Pacific ventilation during the Holocene?

RELLA, Stephan<sup>1</sup> ; UCHIDA, Masao<sup>1\*</sup>

<sup>1</sup>National Institute for Environmental Studies

Holocene ocean circulation is poorly understood due to sparsity of dateable marine archives with submillennial-scale resolution. Here we present a record of mid-depth water radiocarbon contents in the Northwest (NW) Pacific Ocean over the last 12,000 years, which shows remarkable millennial-scale variations relative to changes in atmospheric radiocarbon inventory. Apparent decoupling of these variations from regional ventilation and mixing processes leads us to the suggestion that the mid-depth NW Pacific may have responded to changes in Southern Ocean overturning forced by latitudinal displacements of the southern westerly winds. By inference, a tendency of in-phase related North Atlantic and Southern Ocean overturning would argue against the development of a steady bipolar seesaw regime during the Holocene. This study was also published in Scientific Reports.

Keywords: Holocene, Northwest Pacific, Radiocarbon, Southern Ocean overturning, Southern westerly winds

## Multiple early Eocene hyperthermals reconstructed from the Indian Ocean deep-sea sediments

YASUKAWA, Kazutaka<sup>1\*</sup> ; NAKAMURA, Kentaro<sup>1</sup> ; KATO, Yasuhiro<sup>2</sup> ; IKEHARA, Minoru<sup>3</sup>

<sup>1</sup>Sys. Innovation, Univ. of Tokyo, <sup>2</sup>FR CER, Univ. of Tokyo, <sup>3</sup>Center for Advanced Marine Core Research, Kochi Univ.

From the late Paleocene to the early Eocene (ca. 56 Ma), an extreme global warming by 5-8 °C occurred within several thousand years, which is termed as the Paleocene-Eocene Thermal Maximum (PETM). The PETM is known to accompany severe ocean acidification and a prominent negative carbon isotope excursion in both marine and terrestrial environments, which indicate a massive and rapid injection of isotopically light (<sup>12</sup>C-enriched) greenhouse gas into the ocean-atmosphere system. Recently, additional PETM-like global warming events (called as "hyperthermals") have also been identified during the early Eocene period of ca. 56-52 Ma [2]. As is the case with the PETM, the early Eocene hyperthermals also accompanied rapid and pronounced negative carbon isotope excursions. Besides, the hyperthermals appear to be in phase with the oscillations in the eccentricity of Earth's orbit [2, 3], which suggests that the orbital forcing affected to earth's climate and global carbon cycle even in the warmer Earth without large continental ice sheet during this period.

Geologic records of the hyperthermals have so far been reported from all over the world (e.g., the Pacific, the Atlantic, the Arctic, Europe and North America). The Indian Ocean, however, is the exception where only few published data are available for reconstruction of the hyperthermals and thus, the global extent of the hyperthermals remains uncertain. Here, we analyzed  $\delta^{13}\text{C}$ ,  $\delta^{18}\text{O}$  and  $\text{CaCO}_3$  contents of 376 bulk sediment samples taken from four DSDP/ODP cores (DSDP Site 213, DSDP Site 259, ODP Site 738C, ODP Site 752). The analytical results show that sediments from Site 738C and Site 752 contain multiple negative carbon and oxygen isotope excursions and reductions of carbonate contents, which appear to corresponding to the PETM and the early Eocene hyperthermals. Observed hyperthermals from the both sites are inferred to be H1 (Eocene Thermal maximum 2; ETM2)/H2 and I1/I2 events [3]. The observed carbon isotope excursions of ETM2 event ( $\sim -1$  ‰ at Site 752 and  $\sim -0.5$  ‰ at Site 738C) and I1 event ( $\sim -0.6$  ‰ at both sites) are comparable with those reported from the other regions, such as the Pacific and the Atlantic Oceans. Our results strongly suggest that the hyperthermals in the early Eocene period were a global event including the Indian Ocean.

### – References –

- [1] McInerney and Wing (2011) *Annu. Rev. Earth Planet. Sci.*, 39, 489-516.
- [2] Zachos et al. (2010) *Earth Planet. Sci. Lett.*, 299, 242-249.
- [3] Cramer et al. (2003) *Paleoceanography*, 18, 1097. doi: 10.1029/2003PA000909.

Keywords: deep-sea sediment, Indian Ocean, climate change, hyperthermals



## Preliminary analyses on a LGM simulation using MIROC-ESM :climate and dust aerosol representation

OHGAI, Rumi<sup>1\*</sup> ; ABE-OUCHI, Ayako<sup>2</sup> ; TAKEMURA, Toshihiko<sup>3</sup> ; SUEYOSHI, Tetsuo<sup>1</sup> ; WATANABE, Shingo<sup>1</sup> ; HAJIMA, Tomohiro<sup>1</sup> ; O'ISHI, Ryouta<sup>4</sup> ; OKAJIMA, Hideki<sup>1</sup> ; SAITO, Fuyuki<sup>1</sup> ; CHIKAMOTO, Megumi<sup>5</sup> ; KAWAMIYA, Michio<sup>1</sup>

<sup>1</sup>JAMSTEC, <sup>2</sup>AORI, U. Tokyo, <sup>3</sup>Kyusyu U., <sup>4</sup>NIPR, <sup>5</sup>IPRC, U. Hawaii

Future Projection using Earth System Model (ESM) is an important contribution for Intergovernmental Panel on Climate Change Assessment Report 5 (IPCC AR5) from the modelling studies. Therefore, it is important to investigate ability of models and improve them. Especially, Last Glacial Maximum (LGM, 21,000 years before present) is recognized as a benchmarking period because it is the coldest time during relatively recent past. We report the preliminary analyses on climate and dust aerosol representation of the LGM experiment using an ESM, MIROC-ESM (Watanabe et al. 2011).

MIROC-ESM which contributed to IPCC AR5 was used for the study. The resolution of the Atmosphere General Circulation Model is T42 with 80 layers for the vertical levels and the resolution of the Ocean General Circulation Model part is about 1° with 44 vertical levels. An aerosol module SPRINTARS (Takemura et al. 2000, 2002, 2005) is calculated online.

Following the protocol of Coupled Model Intercomparison Project phase 5, we performed two experiments. One experiment is called PI, which corresponds to pre-industrial time, i.e., 1850 A.D. The other is called LGM, which is supposed to represent climate at LGM (Sueyoshi et al. 2013). The differences of the boundary condition from PI are lower greenhouse gases, the orbit of the Earth and the topography (ice sheets and sea level drop).

The climate of PI is reasonably well represented as a state-of-the-art model (Watanabe et al. 2011). The sea surface temperature drop at LGM is reasonably comparable with MARGO dataset (MARGO project members 2009). However the 7 to 10 °C temperature drop suggested by the Antarctic ice cores (Stenni et al. 2010, Uemura et al. 2012) is reasonably represented, the 21 to 25 °C cooling suggested by the Greenland ice cores (Cuffey et al. 1995, Jonsen et al. 1995, Dahl-Jensen et al. 1998) is not enough simulated in the model. The modelled net cooling over the Greenland summit is about 15 °C. Tackling this defect is important to improve future projection. One of the conceivable reasons is the problem on representing enhancement of mineral dust aerosol in the model, which has been pointed out in IPCC AR5. We have compared the modeled dust amount with a dataset called DIRTMAP (Kohfeld and Harrison 2001). As a result, there are problems on the representation of dust over the Greenland both for PI and LGM. In the LGM experiment, the plant functional types (PFT) are basically unchanged from PI. Taking into account the change of PFT may lead more dust generation at LGM and enhance the cooling. The Antarctic dust is significantly lower than the dataset at LGM. The dust emission from Patagonia, the major dust source of the Antarctic ice core, is too low in the LGM experiment. This seems to be caused by too high soil moisture. The precipitation over Patagonia is already too high in the PI. Improving the PI precipitation amount may also affect the LGM precipitation amount and improve the soil moisture conditions.

We present the preliminary analyses on the dust at LGM using MIROC-ESM. As a result, there is a difficulty on representation of the dust enhancement over the ice sheets. Further improvements of the model, for example, taking into account the PFT change or better representation of the precipitation at PI may work to better representation of dust amount/distribution at LGM. Over the Antarctica, the cooling at LGM is expressed in the model but the dust amount is far from the estimation of the ice core data, i.e., the current simulated cooling may be a result of wrong reasons. We are going to improve the processes of the dust emission and investigate deposition procedures and estimation of radiative forcing.

Keywords: LGM, dust, climate sensitivity, Earth System Model

MIS30-P12

Room:Poster

Time:April 28 18:15-19:30

## A 3.3-kyr record of environmental changes in Asian continental interior by Lake Baikal core analysis

IKEDA, Hisashi<sup>1\*</sup> ; MURAKAMI, Takuma<sup>2</sup> ; KATSUTA, Nagayoshi<sup>3</sup>

<sup>1</sup>Graduate School of Education, Gifu University, <sup>2</sup>Japan Atomic Energy Agency, <sup>3</sup>Faculty of Education, Gifu University

We report chemical analysis (TOC, TN, TS, BioSi, and etc) of Lake Baikal sediment.

## Observation of stalagmite laminae for paleoclimate reconstruction at Taga Mine Cave, Shiga Prefecture, Japan

HISAMOCHI, Ryo<sup>1\*</sup> ; WATANABE, Yumiko<sup>1</sup> ; ABE, Yuji<sup>2</sup> ; TAGAMI, Takahiro<sup>1</sup>

<sup>1</sup>Graduate School of Science, Kyoto University, <sup>2</sup>Taga Town Museum

A lot of studies on paleoclimate reconstruction using stalagmites have been done all over the world. However, there are only a few stalagmite paleoclimate researches in Japan. In this study, we observe laminae of stalagmites collected at Taga Mine Cave, Shiga Prefecture, Japan (TAGA3, TAGA5, TAGA7, TAGA11, TAGA12) for paleoclimate reconstruction.

Stalagmite paleoclimate reconstruction has a potential to get high-resolution (annual~decadal) age proxy data, if stalagmite samples have annual laminae. However, some stalagmites have a few types of laminae within a sample (Baker et.al,2008). In this case, it is important to elucidate which types of laminae is annual.

When we observe the thin section of our samples by microscope, all samples show laminae. These laminae consist of natural organic matters because of fluorescent by UV excitation (Baker et.al,2008). Laminae interval is variable from several  $\mu\text{m}$  to a few hundred  $\mu\text{m}$ . Laminae of our samples are similar to the one from China and Turkey (Tan et.al,2006 , Baker et.al,2008).

Especially, sample TAGA3 has more obvious laminae than the other samples, but has the laminae which looks like sub-annual or supra-annual laminae reported in China (Tan et.al,2006). In addition, laminae are wavy in some parts of TAGA3. If we can distinguish annual laminae by U-Th age and find the feature of annual laminae, we will get high-resolution paleoclimate proxy data.

Keywords: stalagmite, laminae, paleoclimate

## New age model of off Takashima drilling sediment

INOUCHI, Yoshio<sup>1\*</sup> ; YAMADA, Kazuyoshi<sup>1</sup> ; OKAMURA, Makoto<sup>2</sup> ; MATSUOKA, Hiromi<sup>2</sup> ; SATOGUCHI, Yasuhumi<sup>3</sup> ; HAYASHI, Ryouma<sup>3</sup> ; KUMON, Fujio<sup>4</sup> ; MATSUHISA, Koki<sup>5</sup> ; OKADA, Ryouyuke<sup>5</sup> ; KAWASHIMA, Shouhei<sup>5</sup>

<sup>1</sup>Faculty of Human Sciences, Waseda University, <sup>2</sup>Faculty of Science, Kochi University, <sup>3</sup>Lake Biwa Museum, <sup>4</sup>Faculty of Science, Shinshu University, <sup>5</sup>School of Human Sciences, Waseda University

Several kinds of studies have been carried out regarding Off Takashima drilling core in Lake Biwa, Japan and a lot of achievements have been reported. In recent years, we have been carrying out chemical analysis on biogenic silica content of cored sediment with high time resolution. However, there have been some age problems regarding uppermost part of the core, namely the last 45 k years. In order to solve the age model problem, we carried out piston core sampling near the Off Takashima drilling site in 2012. About 30 carbon-14 data have been obtained. In addition to well-known wide spread tephra dates, these C-14 dates are converted into new age model. Correlation between Off Takashima drilling core and newly obtained piston core sediment enabled to establish new Off Takashima age model. Last year we reported tentative correlation based on water content profile of both cores. This time, we analyzed grain size, total organic carbon content and total nitrogen content of piston core sediment and compared with those of Off Takashima drilling core. Based on total organic carbon content, correlation between two cores and age model of Off Takashima drilling core are improved greatly.

Keywords: Lake Biwa, sediment, paleoenvironment, age model

## Climate change history of the last 45ka of Lake Biwa based on grain size and TOC, TN of BWK12-2 piston core

MATSUHISA, Koki<sup>2\*</sup> ; MATSUNOSHITA, Kouji<sup>2</sup> ; OKADA, Ryosuke<sup>2</sup> ; KAWASHIMA, Shyohei<sup>2</sup> ; YAMADA, Kazuyoshi<sup>1</sup> ; INOUCHI, Yoshio<sup>1</sup> ; KUMON, Fujio<sup>3</sup> ; OKAMURA, Makoto<sup>4</sup> ; MATSUOKA, Hiromi<sup>4</sup> ; SATOGUCHI, Yasufumi<sup>5</sup> ; HAYASHI, Ryoma<sup>5</sup>

<sup>1</sup>Faculty of Human Sciences, Waseda University, <sup>2</sup>School of Human Sciences, Waseda University, <sup>3</sup>Department of Environmental Sciences, Faculty of Science, Shinshu University, <sup>4</sup>Faculty of Science, Kochi University, <sup>5</sup>Lake Biwa Museum

Based on newly established age model of BWK12-2 piston core sediment, obtained near the Off Takashima drilling station in Lake Biwa, Japan and with about 30 C-14 dates and well dated wide spread tephra, we analyzed grain size and total organic carbon (TOC) and total nitrogen (TN) contents of the sediment. Analyzing interval of those sediments were, 4cm to grain size and 2cm to TOC and TN whose time resolutions were 30 to 120 years and 15 to 60years respectively. Comparison with Marine Isotope Stage profile shows distinct resemblance to MIS1, however, difference between MIS2 and MIS3 is not clear. On the other hand, abrupt cooling events, such as Heinrich events and Younger Dryas, are clearly recognized. Abrupt warming, such as Dansgaard Oeschger events are not clearly recognized.

Keywords: Lake Biwa, sediment, paleo climate, grain size, TOC, TN

## Late Holocene change in lacustrine environment inferred from diatom fossil analysis of lake bed core

SATO, Yoshiki<sup>1\*</sup> ; MATSUOKA, Hiromi<sup>2</sup> ; OKAMURA, Makoto<sup>3</sup> ; KASHIMA, Kaoru<sup>4</sup>

<sup>1</sup>Faculty of Science, Kyushu University, <sup>2</sup>Faculty of Science, Kochi University, <sup>3</sup>Science Research Center, Kochi University, <sup>4</sup>Faculty of Science, Kyushu University

Detail diatom fossils analysis of a lake bed core provided successive reconstruction of lacustrine environmental change after ca. 4700 cal BP in the Lake Hamana, central Japan, with high temporal resolution. In addition, two suspected thin layers as some kind of event deposits were recognized based on allochthonous sediments and/or diatom fossils.

Lake Hamana is a coastal brackish lake located along the Enshu-nada coast. Ikeya *et al.* (1990) performed numerous geological and paleontological analyses on lake bed sediments and reconstructed roughly the Holocene lacustrine environment and geomorphological development of the lake. According to them, after sea area had expanded landward associated with the Jomon Transgression, an inner bay and a fresh water lake occurred at a relatively stable sea-level condition. Furthermore, Morita *et al.* (1998) suggested that fresh water and brackish water conditions had been formed alternately during the Late Holocene, which indicating geomorphological changes presumably caused by some mega thrust earthquakes occurred in the Nankai trough. However, lower temporal resolution made impossible them to clarify detail lacustrine environmental changes.

In order to reconstruct detail lacustrine environmental change of the Lake Hamana during the Late Holocene, diatom fossil assemblages of the 350 cm-long lake bed core were investigated. The core sediments consisted of muddy deposits mainly including a thin sandy layer and two obvious tephra layers. The refractive index of volcanic ashes and core stratigraphy indicated that the lower tephra layer was the Amagi-Kawagodaira pumice (Kg, 3126-3145 cal BP, Machida and Arai, 2003) and the upper one was the Fuji-Osawa scoria (Os, 2.5-2.8 ka, Machida and Arai, 2003). The age model of the core was reconstructed based on the tephra layers and seven radiocarbon ages.

Six diatom zones were identified based on major species composition changes in the diatom assemblages. Stepwise development of the lacustrine environment in the Lake Hamana was suggested as below: Vigorous seawater inflow inferred by marine diatoms (Stage I, 4600-4700 cal BP); A closed inner bay environment with laminated sediments due to formation of sand barriers (Stage II, 4500-4600 cal BP); A circulative brackish lacustrine environment by active mixture of riverine fresh water with enhanced inflow of seawater since 3500 cal BP (Stage III, 2650-4500 cal BP); Gradual salinity decrease of the lake water by reduced seawater inflow (Stage IV, 2250-2650 cal BP); Lake water from brackish to fresh since 2250 cal BP with intermittent salinity increase in the middle of this period, water depth of the lake getting deeper (Stage V, 1498 AD-2250 cal BP); Re-development of an inner bay environment after the Meio earthquake in 1498 AD with temporal salinity increase during 1600 AD to 1750 AD (Stage VI, after 1498 AD).

Additionally, two possible event layers (A and B layer in ascending order) were found. The A layer, during 321-322 cm depth, was characterized by exceptionally high percentage of *Plagiogramma* sp. This temporal abundance accompanying increases of *Thalassiosira* sp. and *Thalassionema nitzschioides* indicates an abrupt environmental change and/or an allochthonous sediments supply. Nevertheless, it is difficult to specify the cause of this layer because the habitat of *Plagiogramma* sp. is still unknown. On the other hand, the B layer was corresponding to the thin sand layer in the range of 285-288 cm depth showed short-term abundance of fresh water diatom species. This indicates that relative coarse sediments supplied abruptly from fresh water environment, ponds and/or marshes, around the lake to the central part of the lake.

### Reference

Ikeya, N. *et al.* 1990. Mem. Geol. Soc. Japan 36, 129-150.

Morita, H. *et al.* 1998. Laguna 5, 47-53.

Machida, H. and Arai, F. 2003. Atlas of Tephra in and around Japan. University of Tokyo Press. 337p.

Keywords: LakeHamana, lacustrine environment, coastal lagoon, diatom fossil, 1498 Meio earthquake, Holocene

## Reconstruction of the Last glacial to Holocene climate changes in Shaamar loess-paleosol succession, northern Mongolia

ORKHONSELENGE, Aleksandr<sup>1</sup> ; HASEGAWA, Hitoshi<sup>2\*</sup>

<sup>1</sup>School of Geography and Geology, National University of Mongolia, <sup>2</sup>Nagoya University Museum

Two atmospheric circulation systems, the mid-latitude Westerlies and the Asian monsoon, play key roles in northern-hemisphere climatic changes. However, the variability of the Westerlies in mid-latitude Asia and their relationship to the Asian summer and winter monsoon remain unclear. We examined the variations in the grain size and elemental composition from the 30 m long loess-paleosol succession in Shaamar area, northern Mongolia, which could be recorded the interplay of the Westerlies and Asian winter monsoon for the last 30 k.y. We then compared our results with the multi-proxy paleoclimate records (e.g., eolian grain sizes, lake levels, pollen assemblages) of the Asian summer and winter monsoon regions and the Westerlies affected region.

According to the compiled data of the Wang and Feng (2013), the Holocene climatic variation patterns (mainly from lake levels and pollen records) in Asia are categorized into 4 characteristic regions, such as the Summer monsoon region (southern and northeastern China), Westerlies affected region (northwestern China), Winter monsoon region (southern Siberia), and Mixture of westerlies and winter monsoon affected region (Mongolia). Specifically, summer monsoon region is characterized by dry earliest Holocene (12-11 ka), humid early to middle Holocene (11-6 ka), and the moderate-humid late Holocene (last 6 ka), corresponding to the Northern hemisphere summer insolation changes. Westerlies affected region is characterized by dry early Holocene (12-8 ka) and humid middle to late Holocene (last 8 ka). Winter monsoon region is characterized by the humid early Holocene (12-8 ka) and dry middle to late Holocene (last 8 ka). On the other hand, Mongolian records (e.g., Lake Khuvsgul, Lake Gun Nuur) demonstrate humid early Holocene (12-9 ka), dry middle Holocene (9-5 ka), and humid late Holocene (last 5 ka), which seems mixture of westerlies and winter monsoon affected region.

Shaamar loess-paleosol succession record is characterized by the humid early Holocene (12-8 ka) and dry middle to late Holocene (last 8 ka), similar to the winter monsoon region in southern Siberia. Thus, it is suggested that the eolian sediment record in Shaamar could be affected more strongly by winter monsoon influence, although Shaamar section is located closely to the mixture of westerlies and winter monsoon affected region (e.g., Lake Khuvsgul and Lake Gun Nuur). Except for the Chinese Loess Plateau, Shaamar loess-paleosol succession is only the continuous eolian sediment record in mid-latitude Asia. Thus, Shaamar loess-paleosol succession should provide us rare glimpse for understanding the interplay of westerlies and winter monsoon in Asian mid-latitude. We will further examine the Last glacial records of the Shaamar loess-paleosol succession and compare with other records of the Asian summer and winter monsoon regions and the Westerlies affected region.

Keywords: Mongolia, Loess-paleosol succession, Westerlies, Winter monsoon, Holocene, LGM

## Reconstruction paleoenvironment by using diatom fossil assemblage analysis in Imuta-ike wetland, Satsumesendai, Kagoshim

GOTO, Daichi<sup>1\*</sup>; KASHIMA, Kaoru<sup>1</sup>; YAMADA, Kazuyoshi<sup>2</sup>; HARAGUCHI, Tsuyoshi<sup>3</sup>; IMURA, Ryusuke<sup>5</sup>; YONENOBU, Hitoshi<sup>4</sup>

<sup>1</sup>Department of Earth and Planetary Sciences, Faculty of Sciences, Kyushu University, <sup>2</sup>School of Human Sciences, Waseda University, <sup>3</sup>Department of Geosciences, Graduate School of Science, Osaka City University, <sup>4</sup>Graduate School of Education, Naruto University of Education, <sup>5</sup>Graduate School of Science and Engineering, Kagoshima University

Paleoenvironmental reconstruction, using diatom assemblage analysis have been carried out in Imuta-ike, Satsumasendai, Kagoshima, Japan. In this site, there are deposit peat layer which is rare in west Japan, 6 visible tephra layer and 2.5m depth laminated layer. Boring survey conducted center of Imuta-ike at Feb. 2011, we was able to got 25m depth core. It can be traced back to 30,000 years past, can be reconstructed until modern environment from ice age. Following environment changes are reconstructed. Since about 30,000 years ago, peat and silt continuously has deposited, but accumulate speed has changed.

About 30,000 yr BP to 23,400 yr BP, we can't reconstruct detail environment change, because of the small number of diatom. About 23,400 yr BP to 13,600 yr BP, inflow river has been existed. And edge of the lake, moor has been formed. About 13,600 yr BP to 10,800 yr BP, moor became land, then pH rose. About 10,800 yr BP to 4,600 yr BP, it starts the postglacial age, increase precipitation and water level was rose. After K-Ah, tephra deposited the lake and water depth was shallow. About 4,600 yr BP to 1,500 yr BP, those days was dystrophic lake and it started to form wet land in west side of the lake. About 1,500 yr BP to present, it continues aggradation, water depth has been shallow. It progresses wet land formation so that water pH was dropped.

Keywords: diatom, Holocene, climatic change, pH change, volcanic stratigraphy, annually laminated lake deposit



## Reconstruction of Paleo-environment at coastal lakes along the Soya Coast, Antarctica, using fossil diatom assemblages

KANG, Ijin<sup>1\*</sup> ; KASHIMA, Kaoru<sup>2</sup> ; SETO, Koji<sup>3</sup> ; TANI, Yukinori<sup>4</sup> ; MATSUMOTO, Genki I.<sup>5</sup>

<sup>1</sup>Department of Earth and Planetary Sciences, Graduate School of Sciences, Kyushu University, <sup>2</sup>Department of Earth and Planetary Sciences, Graduate School of Sciences, Kyushu University, <sup>3</sup>Research Center for Coastal Lagoon Environments, Shimane University, <sup>4</sup>Institute of Environmental Sciences, University of Shizuoka, <sup>5</sup>School of Social Information Studies, Otsuma Women's University

Soya Coast, located at East Antarctica distribute wide ice-free areas such as Langhovde, Skarvsnes, Skallen and Rundvagshetta. The research areas of this study are five lakes in the ice-free coast as follows; Lake Nurume-ike and Lake Yukidori-ike at Langhovde, Lake Oyako-ike at Skarvsnes and Lake Maruwan-minami-ike and Lake Maruwan-oike at Rundvagshetta.

Matsumoto et al.2014 described the Holocene paleo-limnological changes at Lake Oyako-ike. They described soft-x-ray analysis, carbon 14 dating, elemental analyses, Chlorophyll compounds and carotenoids, and algae and cyanobacteria analyses. The paleo-environment of the lake shifted from the open coastal environment, through stratified saline lake, and then to high productive fresh water lake during these two thousand years. They presume that these environmental changes have been affected by isostatic uplift by retreating continental glaciers.

Diatom fossil assemblages at the lake deposit (Ok4C-1) divided into five assemblages zones, from Zone 1 to Zone 5 to upward. The dominated species of each zone is as follows. Zone 1:*Paralia sulcata*, marine species, Zone 2:*Staurosira construens*, Zone3:*Tryblionella littoralis*, marine species, Zone4:*Chamaepinnularia cymatopleura*, brackish species and Zone 5:*Amphora oligotraphent* *Navicula gregaria*, *Diadsmis* spp., freshwater species. The shifts of diatom assemblages presumed the lake water environment shifted from coastal marine environment through freshwater lake environment. This result was fitted to the results of the previous study. Now, we are analyzing other four lake sediment cores.

Keywords: Antarctic coastal lakes, paleolimnology, diatom, the Holocene, Sediment core

## Holocene climate changes detected in the bottom sediments of the glacier lake, southern Peru

YAMADA, Kazuyoshi<sup>1\*</sup> ; SHINOZUKA, Yoshitsugu<sup>2</sup> ; SETO, Koji<sup>3</sup> ; HARAGUCHI, Tsuyoshi<sup>4</sup> ; YONENOBU, Hitoshi<sup>5</sup>

<sup>1</sup>Waseda University, <sup>2</sup>Hokkaido University, <sup>3</sup>Shimane University, <sup>4</sup>Osaka City University, <sup>5</sup>Naruto University of Education

We attempt to reconstruct climate changes during the Holocene by using a glacier lake on the southern Peru. For this, we had undertaken field investigation as echo sounding and piston coring at Lake Yauriuri, which is 130 km apart from Nazca city. The lake is one of typical glacier lake at height of 4,384 m. By the seismic record of the lake bottom from echo sounding, it is identified that 10-m thick mud layer with the intercalated fine sand layers on the bedrocks. And, two sediment cores were taken from the southwestern point at 50 m in water depth. The length of the cores is 50, and 170 cm, respectively. Lithology of the sediment shows that almost homogenous dark grey slit with two thin brownish flood-origin layers. We have analyzed physical properties, magnetic susceptibility, color reflectance, chemical compounds by XRF, CNS and ICP-AES with multiple radiocarbon dating for the whole core section. Our results indicated abrupt changes of S and Ti contents at 4,000 and 7,000 cal BP, suggesting that past lake level fluctuation and precipitation over the last 11,000 years caused by climate changes. These past environmental variations in Lake Yauriuri may have the similar pattern with other records in inland area of Peru as well as off shore Peruvian marine records.

Keywords: Peru, Laguna YauriUri, climate change, Nazca Culture

## Extensions of RCP2.6/4.5 with zero emission after 2100: as 2K/3K stabilization scenarios for MIROC-ESM

TACHIIRI, Kaoru<sup>1\*</sup> ; HAJIMA, Tomohiro<sup>1</sup> ; KAWAMIYA, Michio<sup>1</sup>

<sup>1</sup>Japan Agency for Marine-Earth Science and Technology

Focusing that MIROC-ESM (an earth system model, no atmospheric chemistry version) output around 2K/3K rise in global mean surface air temperature in 2100 with the Representative Concentration Pathways (RCP) 2.6 and 4.5, we extend the experiments with zero-emission after 2100, as 2K/3K stabilization scenarios for the model. As MIROC-ESM is a "pessimistic" (with high climate sensitivity and small ecosystem carbon uptake) model, stabilization for this model means large chance of stabilization for many other models. The experiment, with fixed land use and other non-CO<sub>2</sub> forcing after 2100, is designed to 2300, and we are now just after 2200.

In the 2K stabilization scenario, RCP2.6 followed with zero emission, temperature rise from the pre-industrial state (PI) is slightly over 2K in 2100, and slowly decreased after the zero-emission period starts, and is just below 2K at 2200. Atmospheric CO<sub>2</sub> concentration (pCO<sub>2</sub>) is 421ppm at 2100 and around 400ppm at 2200. On the other hand, in the 3K stabilization scenario, RCP4.5 followed with zero emission, temperature rise from PI is just over 3K, and then decreased after that slightly more rapidly than 2K stabilization scenario and is around 2.8K at 2200. pCO<sub>2</sub> is 540ppm at 2100 and just below 500ppm at 2200.

Looking at air temperature after stabilization (i.e., 2100), the 2K stabilization scenario have temperature rise in and around Antarctica, in Siberia and in Greenland, and decrease in Amazon and in northern lands. The 3K stabilization scenario has similar pattern, but with relatively small rise in and around Antarctica, and no significant increase in Greenland. Some increase in Siberia, and with significant decrease in Arctic Sea. Precipitation decreases in Western Pacific and increases in a part of Eastern Pacific and around Indian Ocean for 2K stabilization scenario. For 3K stabilization scenario, precipitation is decreased in some areas in southern Pacific.

Keywords: Representative Concentration Pathways, zero emission, stabilization, Earth system model

## Parallel and integrated processes of climate-impact-socioeconomics for climate research

EMORI, Seita<sup>1\*</sup>

<sup>1</sup>National Institute for Environmental Studies

The need to take mitigation measures in order to hold the increase in global average temperature below 2 degree C above pre-industrial levels are recognized in international negotiations of the United Nations Framework Convention on Climate Change (UNFCCC). According to the fifth assessment report (AR5) by the Working Group (WG) I of Intergovernmental Panel on Climate Change (IPCC) which was published last September, attaining the temperature goal with a probability of 50% will require cumulative CO<sub>2</sub> emissions from all anthropogenic sources to stay approximately 300 GtC from the present. If the current level of anthropogenic CO<sub>2</sub> emission, 10 GtC yr<sup>-1</sup>, continues, the cumulative emissions will reach this upper limit in only 30 years. If we will seriously pursue the goal of temperature increase below 2 degree C, global CO<sub>2</sub> emission should be turned to decline as soon as possible, and to be reduced at nearly zero by around the end of this century.

A great deal of research on climate change impacts and mitigation measures exist; however, large uncertainties remain in their overall pictures. So far, nobody can grasp clearly risks for human society and ecosystem associated with global warming exceeding "2 degree C", and risks for socioeconomics due to severe emission reductions of greenhouse gases. Furthermore, the risks will be realized in different ways by country, region, generation, and social attribution, and therefore, either if no specific response measures are conducted or if strong measures are conducted, a part of people in the world will have benefits and another part of people will make a loss. Climate change impact is not just an issue on benefits and losses of each person; but it relates to issues how we feel distress on risks for ecosystem, developing countries, and future generations. It relates to different value judgment among people.

Climate research plays a role to provide scientific information to help the societal decision making process of such an uncertain, complex and ambiguous risk problem. To pursue it, there has been a serious international activity to promote interaction across the three research communities, that is, climate, impact and socioeconomics (corresponding to the WG I, II and III of IPCC, respectively). I will look back the idea of parallel and integrated processes of the three research communities, that was attempted during the discussion of Representative Concentration Pathways (RCP) around 2010, from the present where IPCC AR5 was released, and discuss its progress and future prospects.

## Development of the climate model MIROC and initialization system using LETKF for the next IPCC report

TATEBE, Hiroaki<sup>1\*</sup> ; OGURA, Tomoo<sup>2</sup> ; WATANABE, Shingo<sup>1</sup> ; WATANABE, Masahiro<sup>3</sup> ; SUZUKI, Tatsuo<sup>1</sup> ; KOMURO, Yoshiki<sup>1</sup> ; NITTA, Tomoko<sup>3</sup> ; O'ISHI, Ryouta<sup>3</sup> ; TAKATA, Kumiko<sup>5</sup> ; KOYAMA, Hiroshi<sup>1</sup> ; ISHII, Masayoshi<sup>4</sup> ; KIMOTO, Masahide<sup>3</sup>

<sup>1</sup>RIGC, JAMSTEC, <sup>2</sup>NIES, <sup>3</sup>AORI, Univ. of Tokyo, <sup>4</sup>MRI, JMA, <sup>5</sup>NIPR

We have been updating the climate model MIROC and developing a data assimilation and initialization system based on the local ensemble transform Kalman filter (LETKF) for reconstructing global centennial climate, understanding of mechanisms of climatic periodic changes, regime shifts, and extreme events, and improving skills in seasonal-to-decadal climate predictions. For the previous fifth assessment report of IPCC-AR5, decadal climate forecasts and retrospective predictions taking into account both of the global warming due to increase of anthropogenic green house gases and intrinsic variability of the climate system were performed using a series of MIROC with various resolutions and physics. As a result, for example, the mid-latitude SST signals in the North Pacific associated with the Pacific decadal oscillations, the abrupt stepwise climate shift occurred in the late 1990s, and the tropical cyclone activity over the western North Pacific are suggested to be predictable for a few to several years. After the experiments for IPCC-AR5, we additionally performed retrospective climate predictions on seasonal-to-interannual timescales focusing ENSO. Prediction skill of the equatorial SST in MIROC is as high as those in climate models of operational centers over the world. However, because MIROC has remarkable systematic climate biases of stronger equatorial trade winds and resultant deeper thermocline, more subtropical clouds in the lower troposphere and relating colder SST, weaker mid-latitude westerly jets, warmer SST and larger precipitations around Antarctica than observations, so-called anomaly assimilation technique is used in initializing the climate model, and thus the seamless climate predictions cannot be performed by the present system. Therefore, our modeling group is devoting effort to reduce the model biases and to realize the seamless predictions by MIROC based on full field assimilation. In my talk, recent update of MIROC will be introduced along with preliminary results from a newly developing initialization system.

Keywords: climate model, initialization, seamless climate prediction

## Climate projections using high-resolution MRI-AGCM

MIZUTA, Ryo<sup>1\*</sup> ; OSE, Tomoaki<sup>1</sup> ; MURAKAMI, Hiroyuki<sup>2</sup> ; ARAKAWA, Osamu<sup>3</sup> ; YOSHIDA, Kohei<sup>1</sup> ; NAKAEGAWA, Toshiyuki<sup>1</sup>

<sup>1</sup>Meteorological Research Institute, <sup>2</sup>International Pacific Research Center, <sup>3</sup>University of Tsukuba

A high-resolution atmospheric general circulation model of the Meteorological Research Institute (MRI-AGCM), with a horizontal grid size of about 20 km, have been developed, and applied to climate projections for extreme weather events such as tropical cyclones and heavy precipitation. Given the observational sea-surface temperature (SST) as the lower boundary condition, the model can simulate not only global-scale climate of temperature and precipitation, but also climatic characteristics of small-scale phenomena such as geographical distribution and intensity of tropical cyclones, and seasonal march of the East Asian monsoon.

Under the KAKUSHIN program (2007-2012; sponsored by MEXT), giving SST changes from atmosphere-ocean coupled models, time-slice experiments with this model have been performed to investigate detailed and localized changes as a consequence of global warming. The uncertainty of the change has been also evaluated, using many ensemble experiments with 60 km version of the model. The simulation results has been used for many purposes, including impact accessments of disasters, water resources, and agriculture, as well as analyses from meteorological point of view. The results has been also provided to the researchers worldwide, for the researches of regional climate changes of their own countries. Over Japan area, dynamical downscaling experiments have been performed using a regional climate model with horizontal grid sizes of 5km and 2km.

Under the SOUSEI program (2012-2017; sponsored by MEXT), in order to evaluate and reduce the uncertainty of the climate projections, ensemble experiments with the 20-km model with different geographical patterns of SST changes are being performed, using results of CMIP5 coupled models.

Keywords: global warming, atmospheric general circulation model

---

MIS31-05

Room:511

Time:May 2 10:00-10:15

## Earth system modeling - a brief history and future direction

WATANABE, Shingo<sup>1\*</sup>

<sup>1</sup>JAMSTEC

A brief history of Earth system modeling will be outlined, and its future direction will be discussed.

Keywords: Earth system model

## Findings in climate change and global carbon cycle from model inter-comparison analyses

HAJIMA, Tomohiro<sup>1\*</sup>

<sup>1</sup>Japan Agency for Marine-Earth Science and Technology

Interactions between climate and carbon cycle are essential for making long-term climate projection, since some part of carbon cycle processes in land and ocean display slow responses to environmental change in a longer timescale, with giving feedbacks on climate. Climate-carbon cycle models, sometimes referred as "Earth system models (ESMs)", have been developed and utilized for the long-term climate projection. Recent model inter-comparison analyses have revealed some problems in the models, and provided new findings on climate-carbon cycle relationships. For example, a new index "TCRE" is introduced in the latest IPCC report. This index can capture the entire response of global climate-carbon cycle system to anthropogenic CO<sub>2</sub> emission, with suggesting some useful political messages. In this presentation, new findings on climate-carbon cycle system such as TCRE will be reviewed, based on the results from model inter-comparison analyses.



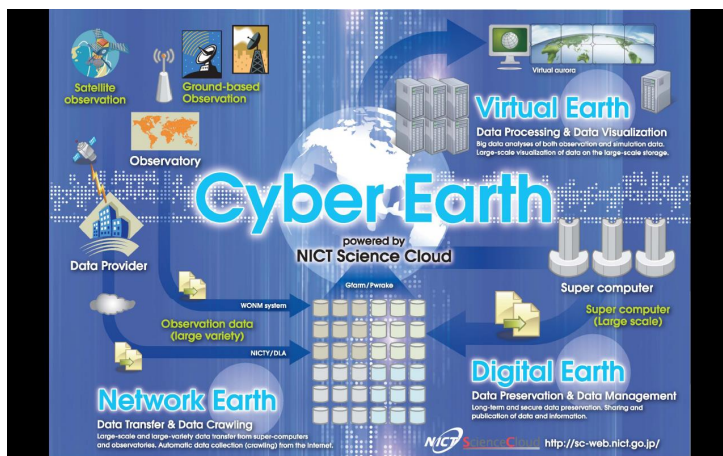
## Cyber Earth: A new technical approach for global studies of Earth

MURATA, Ken T.<sup>1\*</sup>

<sup>1</sup>NICT

In the present paper, the author proposed a concept of the Cyber Earth as a basic approach for the global understanding of the Earth system. In order for our global understandings from a variety of observation and simulation data of Earth sciences, we need a methodology to analyze huge size of big science data. The Cyber Earth is a concept to declare that, for our global understandings, mash-up of information and communication technologies for big data plays an important role. This concept is based on several technological ideas, such as data centric/intensive science, the fourth paradigm, science cloud, big-data science. All of the data, observation data and simulation data, are once transferred and stored on a science cloud system. Data preservation and data stewardship is important since most of the data is so precious that they are never observed again at the observed time and location. Big data processing, including visualization, is also important. The data processing must be applicable for any types of digital data from either Earth observation or simulation. Integrated data processing technology for such variety of data type is preferable.

The Cyber Earth is composed of three methodologies; the Network Earth, the Digital Earth and the Virtual Earth. The Network Earth is a concept that role of network is important for data transfer and collection to the cloud. For global monitoring we often build up global observatories on the Earth. Integrated operations and easy management of the remote sites are significant for labor-saving. The Digital Earth is a concept that long-term data preservation is one of the most expected functions to a science cloud. Data files must be saved and managed under DR (disaster recovery) environment. Easy data publication should be functionally synchronized with data preservation. The Virtual Earth is a concept that every digital data must be processed or visualized to be shown on the same framework with other data. Inter-disciplinary data preview, in space and/or in time, makes our global and functional understanding of the Earth system. Immersive visualization may work effectively to understand or discover any interactions between data.



## Current trends of international assessments of greenhouse gas emission mitigation scenarios

AKIMOTO, Keigo<sup>1\*</sup>

<sup>1</sup>Research Institute of Innovative Technology for the Earth

The IPCC 5th Assessment Report (AR5) are scheduled to be completed in 2014. The Working Group III assesses mitigation options and the report "Climate Change 2014: Mitigation of Climate Change", will be released in April 2014 after the approval in the 39th Session of IPCC. Scenario analysis and modeling exercise by the integrated assessment model (IAM) provide a key element in the AR5 report. A number of international inter-model comparison projects are formulated mainly in the United States and EU countries in an effort to make contribution to the IPCC AR5 report.

This paper introduces that the current trends of international assessments of greenhouse gas (GHG) emission mitigation scenarios with the key points which have been described in the AR5 and the key outcomes of the international IAM comparison projects. In addition, international research cooperation activities for harmonizing socioeconomic scenarios for the future IAM assessments, which is named SSPs (Shared Socioeconomic Pathways), will be introduced.

The Fourth Assessment Report (AR4) of IPCC WGIII which was published in 2007 provided six categories for broad ranges of several emission pathways provided by IAM estimations. The lowest level of GHG concentration stabilization is 445-490 ppm CO<sub>2</sub>eq and the emission pathways correspond to 85-50% reductions of global emission by 2050 relative to the 2000 level. The report summarized that the emission pathways will be expected to the equilibrium global mean surface temperature of 2.0-2.4C increase relative to pre-industrial level. The assessment had a strong impact on the international climate change negotiations and domestic measures of climate change response. Long-term target of 2C and halving global emissions by 2050 have been widely discussed in international negotiations such as UNCCC/COP and G8 after the release of AR4, while IPCC never recommends a specific target and policy.

A lot of assessments for emission reduction scenarios by IAMs particularly for deep emission reduction scenarios such as 450 ppm CO<sub>2</sub>eq, have been conducted after the AR4. The assessments also include many overshoot scenarios which are temporally over 450 ppm CO<sub>2</sub>eq and then achieve 450 ppm CO<sub>2</sub>eq in 2100 as well as 450 ppm stabilization scenarios, because current global emission increases are large due to the increases in developing countries, and it is difficult to develop emission reduction pathways with reality in near-term emissions for 450 ppm CO<sub>2</sub>eq stabilization without overshoot.

One of the inter-model comparison projects, AMPERE (Assessment of Climate Change Mitigation Pathways and Evaluation of the Robustness of Mitigation Cost Estimates) project which was funded by the European Commission provided the feasibility of significant emissions reduction for a variety of mitigation technology portfolios. The project assessed that the feasibility for deep emission reductions such as 450 ppm CO<sub>2</sub>eq and the emission reduction costs under several conditions of technology unavailability and the near-term emissions locked into by the Cancun pledges. With significant emission reduction until 2030, the required annual emission reduction to meet 450 CO<sub>2</sub>eq target diverges from the historical rates of change. If the emissions pathways are locked into the low ambitious Cancun pledges to 2030, further improvement is required after 2030. There are many infeasible results to meet the stringent target in model calculation, if there are technological constraints in the availability of CCS, nuclear and renewable energy particularly under the near-term emissions locked in. The emission reduction costs are also very high and almost double or more compared with the idealistic conditions. These assessments which consider realistic conditions in IAMs are one of the progresses after the AR4.

The AR5 of IPCC will include such new assessments will make impacts on international climate policies after the release.

Keywords: climate change, global warming mitigation, emissions scenarios, IPCC, integrated assessment model

## Integrated assessment model structure and linkage with climate model

KUROSAWA, Atsushi<sup>1\*</sup>

<sup>1</sup>The Institute of Applied Energy

### 1. History and basic structure of integrated assessment model

Integrated assessment model (IAM) has been developed as a tool to analyze climate change countermeasures. Edmonds-Reilly model in 1980s was the one of initial trials to indicate the importance of the relationship between climate change and energy issues, through explicit analysis of energy CO<sub>2</sub> and global warming. Since 1990s, model development has been active to evaluate comprehensive measures from interdisciplinary knowledge in climate change, energy system, land use, etc. The new keywords of the models developed are 'interdisciplinary', 'large scale', 'very long-term dynamics', 'scale integration'. These models are called IAMs because their scope is very wide in time, space and disciplines. For example, GRAPE model, developed by the GRAPE development team, consists of modules dealing with energy, climate, land use, macroeconomics and environmental impacts. Intergovernmental Panel on Climate Change (IPCC) working group III reviewed IAM intercomparison results such as economic impacts of Kyoto Protocol, multiple GHGs mitigation including non-CO<sub>2</sub> gases mitigation potential and its effects in the past assessment reports.

### 2. Linkage with climate model

There are various types of linkage of climate model in IAMs. Major categories are 'hard-link' and 'soft-link'. The former includes all equations and variables of climate module in the entire model structure, while the latter exchanges the information (e.g. GHG emissions) between climate module and other parts of the model.

DICE model, one region global model, is the one of initial famous IAMs. It uses hard-link optimization methodology and simple one-dimension climate model with two ocean layers and one atmospheric layer. Radiative forcing of CO<sub>2</sub> is calculated endogenously but other aggregated forcing values are exogenously provided. After obtaining the global mean temperature, macroeconomic damage feedback is assessed as the function of temperature rise.

It is great challenge to include large scale climate model in the hard-link type IAMs. Because of climate system nonlinearity and many constraints including inequalities, it is quite difficult to get solutions especially under dynamic climate constraints such as long-term forcing stabilization. Climate module of GRAPE includes carbon cycle representation of one-dimensional version of the ISAM, one of the reference model in IPCC WG I third assessment report. Global carbon stock is distributed to the atmosphere, ocean, and terrestrial biospheres. The ocean part has 40 deep layers and terrestrial biosphere has six boxes. Energy exchange among atmosphere and ocean layers are also modeled.

Recently, coupled analyses combining earth system model and IAMs are in progress in the area of climate impact assessment with fine mesh-scale, or climate feedback of energy consumption level, etc. Climate information is quite useful and essential in these assessments.

### 3. Future issues and summary

GHG reduction would not be on the track to avoid potential dangerous impacts to global climate change because it is difficult to get consensus in global climate policy. Adjustment to climate condition (i.e. 'adaptation') could be the realistic solution in the short to medium term. Vulnerability to climate change varies by region and economic condition, and climate information in the future is important to design regional adaptation policies.

'Geoengineering', such as solar radiation management (SRM) and carbon dioxide removal (CDR), is included in the IPCC working group I fifth assessment report sentences. Negative emission feasibility through implementation of CDR needs further considerations with low GHG emissions scenarios with assistance of climate models.

IAM has close and essential linkage with climate model from initial development stage, and more interaction are crucial to resolve global and regional agenda in the future.

Keywords: Integrated Assessment Model, Climate Model

## Integration of climate and economic modeling studies

MATSUMOTO, Ken'ichi<sup>1\*</sup> ; TACHIIRI, Kaoru<sup>2</sup>

<sup>1</sup>The University of Shiga Prefecture, <sup>2</sup>Japan Agency for Marine-Earth Science and Technology

So far, there have not been many studies which integrate climate modeling and economic modeling research. The purpose of this presentation is to show one way to integrate climate and economic studies with regard to climate change issues. Here, we present an example of the integration of these two areas, which analyzes socioeconomic impact of achieving a specific radiative forcing level considering the uncertainties of Earth system models using a computable general equilibrium (CGE) model.

Although much uncertainty exists in climate system and simulations of future climate profiles with Earth system models (ESMs), it has not been evaluated in relation to socioeconomic aspects. In this study, we analyze the socioeconomic impact (including that on energy) of three emission pathways, all of which possibly achieve 4.5 W/m<sup>2</sup> of radiative forcing in the year 2100 within uncertainties estimated by an ESM of intermediate complexity (EMIC) tuned for full ESMs using a CGE model, a type of economic models. The model used here is a multi-regional and multi-sectoral recursive dynamic CGE model on a global scale, with energy and environmental components. Thus, the model is also called an integrated assessment model or IAM.

The emission pathways considered in this study are allowable emission pathways obtained by using an EMIC with the Representative Concentration Pathway 4.5 scenario. Here, we analyze the emission pathways of the 5th (lower bound), 50th (mean), and 95th (upper bound) percentiles of the weighted ensemble members in the parameter perturbation experiment. Different pathways are derived from different physical and biogeochemical properties. The global CO<sub>2</sub> emissions in 2100 and the cumulative CO<sub>2</sub> emissions in this century in the upper bound case are 5.1 GtC/yr and 917.6 GtC, while those in the mean case are 3.0 GtC/yr and 764.9 GtC respectively, and those in the lower bound case are 0.91 GtC/yr and 619.7 GtC respectively.

The results indicate that the socioeconomic impacts are larger in the lower bound emission pathway to achieve 4.5 W/m<sup>2</sup> as expected, although the economy and energy demand (both primary and final energy demand) increase continuously in this century. For example, the global gross domestic product (GDP) in each emission pathway is \$212 trillion in the lower bound case, \$217 trillion in the mean case, and \$221 trillion in the upper bound case in 2100 (\$30 trillion in 2001), which are 4.2 – 8.1% smaller than that of the reference scenario (\$230 trillion in 2100). On the other hand, the global primary energy demand in 2100 in the lower bound case is slightly larger than in the mean case; this can be interpreted because biomass energy with carbon capture and storage technology is enhanced to achieve very low carbon dioxide emissions in the lower bound case. In a comparison between the upper bound and lower bound emission pathways, the carbon price of the latter is approximately three times higher in 2100. The GDP in the latter is 4.1% smaller than that in the former in 2100, which is equivalent to only a 0.042% decrease in the annual GDP growth rate. Thus, the socioeconomic impacts caused by ESM uncertainties, here evaluated by GDP and energy demand, are not insignificant but are smaller than the differences in the emission pathways to achieve 4.5 W/m<sup>2</sup>.

Keywords: earth system model, computable general equilibrium model, climate change

## Model Inter-comparison projects of Integrated Assessment Models and the Collaboration with Impact Assessments

FUJIMORI, Shinichiro<sup>1\*</sup> ; HANASAKI, Naota<sup>1</sup> ; TAKAHASHI, Kiyoshi<sup>1</sup> ; MASUI, Toshihiko<sup>1</sup> ; KAINUMA, Mikiko<sup>1</sup> ; HIJIOKA, Yasuaki<sup>1</sup> ; HASEGAWA, Tomoko<sup>1</sup>

<sup>1</sup>National Institute for Environmental Studies

This presentation talks about two topics; namely model inter-comparison projects (MIP) of integrated assessment models (IAM) and the collaboration with impact assessments.

MIP of IAM is carried out by sharing main themes, assuming model conditions and parameter settings, and comparing results. The themes dealt with the last couple of years were, for example the influence of the technological availability (e.g. nuclear) and mitigation starting year on the mitigation cost. The outcomes are eventually summarized as special issues of international journals. The harmonization of the scenario assumptions is generally quite limited to narrative story. The numerical future socioeconomic conditions are dependent on individual models. This intends to encourage as many as IAMs participating MIPs since IAMs have several types and some variables which are exogenous parameters for some IAMs can be endogenous variables for others. The activities relevant to model validation have become much more important than before and some MIPs treat such themes. The activities are ongoing now and model documentations, development of model diagnostics protocol and comparison hind-casting with historical observation are discussed. In regard to the collaboration with Impact, Adaptation and Vulnerability (IAV) assessment, we can classify two types according to the way how the IAM is used. First is the case where IAMs are used as a provider of socioeconomic conditions to IAV. RCP (Representative Concentration Pathways) and SSP (Shared Socioeconomic Pathways) are well known such information. Hanasaki, et al. is an example and AIM/CGE provided information to the water assessment model H08. They assessed the water scarcity. Second is the case where IAMs assess climate change impacts by themselves. Hasegawa, et al. is an example and crop productivity model GAEZ calculated a potential crop productivity change and it is fed into AIM/CGE. They assessed a risk of hunger. The fields of water and agriculture overlap with the IAM coverage through land use and energy supply. We expect one of the possibilities for the further studies would incorporate transactions between them. All studies are made by the combination of emissions scenarios and the outcome of the Earth System Models (ESM). The release of SSP would encourage much more IAV studies.

Meanwhile, several issues might remain even after SSP processes are completed. Here we show two issues. First, SSPs exclude information relevant to climate mitigation and the case with climate mitigation would be different from the case without climate mitigation. The combination of the RCP and CMIP5 (Coupled Model Intercomparison Project Phase 5) is not consistent for such case. Second, we would face the case where the stabilization targets other than existing four RCPs needed to be assessed. The accuracy of the pattern scaling would be the key point. If the pattern scaling had an accuracy which is acceptable for IAV, the existing RCP and CMIP5 are available with the pattern scaling. Otherwise, a set of new climate scenarios is required. However, multi-model ensemble examination similar to CMIP5 takes extra a few years and it would be unrealistic for IAV. Hence, a specific combination of IAM and ESM in Japan (e.g. AIM/CGE and MIROC) associated with the new set of emissions scenarios might be one of the solutions. Although it would take many efforts in order to achieve it, we might be able to identify the usefulness for society and scientific novelty. We hope that this presentation would be one of the indications for such discussions.

Hanasaki, N. et al. A global water scarcity assessment under Shared Socio-economic Pathways ? Part 1: Water use. *Hydrol. Earth Syst. Sci.* 17, 2375-2391, doi:10.5194/hess-17-2375-2013 (2013).

Hasegawa, T. et al. Climate Change Impact and Adaptation Assessment on Food Consumption Utilizing a New Scenario Framework. *Environmental science & technology* 48, 438-445, doi:10.1021/es4034149 (2014).

Keywords: Integrated Assessment Models, Impact, Adaptation and Vulnerability, Model inter-comparison projects, Scenarios

## Climate and socioeconomic scenarios for climate change impact and adaptation assessments in Japan

TAKAHASHI, Kiyoshi<sup>1\*</sup> ; HANASAKI, Naota<sup>1</sup> ; HIJIOKA, Yasuaki<sup>1</sup>

<sup>1</sup>National Institute for Environmental Studies

In order to assess the overall impacts of climate change on a nation and investigate effective adaptation measures, it is important to collect scientific understanding beyond academic disciplines, because impacts of climate change emerge every aspect of the society. Modeling is a widely accepted method to assess future climate change impacts: develop climate and socioeconomic environment assumptions in the future (scenarios), run statistical or process based models using the scenarios, and simulate the future situation for each subject and discipline. If a large number of modelers conduct simulations using a set of common scenarios, one can obtain a multidisciplinary national perspective of climate change impacts and potential adaptation strategy.

We have been conducting a strategic research project funded by the Ministry of Environment, which is named 'Comprehensive research on climate change impact assessment and adaptation policies' (Abbr.: S-8 project; Period: FY2010-2014; Project leader: Prof. Nobuo Mimura, Ibaraki University). In S-8 project, we are working on quantitative analyses of climate change impact on various sectors and adaptation in Japan for the purpose of supporting adaptation policy makings as well as of evaluating possibility of the society that can adapt to the anticipated climate change. The sectors covered in the project include water resource, coastal, disaster prevention, natural vegetation, agriculture, and human health. In S-8 project, climate and socioeconomic scenarios for Japan were discussed for climate change impact assessment and adaptation measures investigation by reviewing earlier literature and latest research activities. Based on the discussion, with keeping in step with the research schedule of the project, sets of scenarios were developed twice covering the whole Japan (the 1st version: March 2011, the 2nd version: November 2013), utilizing information available at the respective timings.

For the 2nd version of the S-8 scenario set, we used the climate projection of four climate models and three radiative forcing scenarios of the Coupled Model Intercomparison Project Phase 5 (CMIP5). We utilized the results of dynamical downscaling using a regional climate model which is consistent with the global scenarios after applying bias-correction techniques. Regarding the population projection scenarios, we developed nine scenarios taking into account not only uncertainty range of the total numbers but also uncertainty in its spatial distribution. We also proposed land use scenarios compatible with the population projections.

In the JPGU session, as a case of multidisciplinary collaboration, we will introduce the background and procedure of the S-8 scenarios development. We will also mention future challenges, which have been found in the scenario development process.

Keywords: climate change, climate change impact, adaptation, scenario

## Introduction to global climate change impact assessment

HANASAKI, Naota<sup>1\*</sup>

<sup>1</sup>National Institute for Environmental Studies

In this presentation, a typical methodology used in modern climate change impact assessments is introduced. Some latest research activities to tackle key problems are discussed as well. This presentation mainly focuses on water resources sector at global scale, but the contents can be broadly applicable to other sectors and scales.

Climate change impact assessment requires scenarios on future climatic and socio-economic conditions and a model which quantitatively describes how the system of interest responses to those changes. In this presentation the latest scenarios namely CMIP5, RCP, and SSP are introduced. Then, a global water resources model H08 is explained which delineates the water cycle and water use of the globe.

Climate change impact assessment typically takes three steps. First, a model of interest is prepared and a simulation is conducted using the present climatic and socio-economic conditions. Second, some simulations are conducted using various future scenarios. Third, the differences in outputs between the future and present are examined since these are considered the impact due to climatic and socio-economic change. In this presentation, the geographical spread of water stressed regions and the number of affected population are discussed under 10 different future scenarios.

A number of challenges remain unsolved on climate change impact assessments. Two international research activities are highlighted to address some of the challenges. The first item is quantification of uncertainties in assessments caused by models. Although the models used in climate change impact assessment basically reproduce the present conditions well, none of them is perfect and outputs include errors. An ongoing international research project termed ISI-MIP is introduced which conducts climate change impact assessment by using a set of common scenarios and multiple models. ISI-MIP analyzes the variations in results and reasons. The second item is implementation of adaptation options. Although humans are expected to take adaptation measures when the impacts of climate become intolerable, adaptation is seldom implemented in earlier simulations. Some pioneering works including adaptation are reviewed and future research directions are discussed.

Keywords: climate change, impact, global, water resources

## Impact assessment of natural disaster due to global warming

MORI, Nobuhito<sup>1\*</sup>

<sup>1</sup>Disaster Prevention Research Institute, Kyoto University

Climate changes in give significant impacts on natural disasters such as typhoon, river flooding, storm surge, landside and etc. The different natural disasters require different forcing from GCMS. The spatial and temporal resolutions of forcing also give significant impact on the impact assessment of natural disasters. This study summarize current activity of impact assessment of natural disasters by SOUSEI program in Japan and discuss importance of cooperative research between GCM modelers and IAM group.



## Downscaling in Climate Information and applications

DAIRAKU, Koji<sup>1\*</sup>

<sup>1</sup>National Research Institute for Earth Science and Disaster Prevention

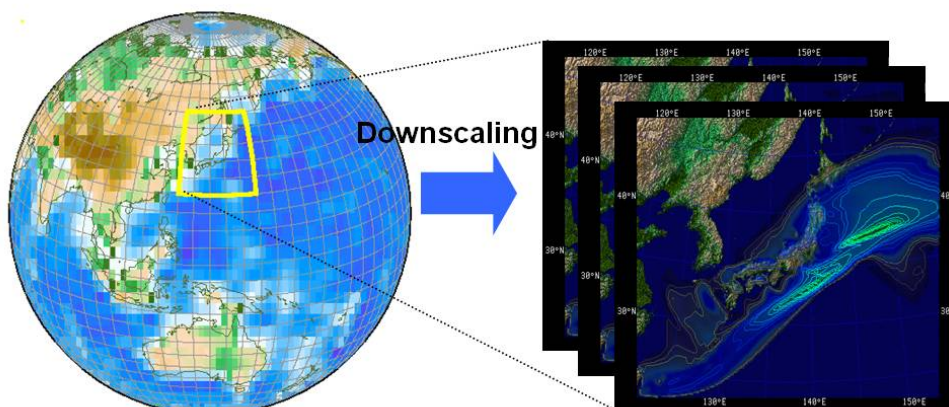
Climate effects caused by human activities will continue for centuries and natural climate influences have always been a risk. Mitigation is a complex, uncertain approach and will need at least several decades. It is necessary, therefore, to put adaptation together immediately. The impacts and potential applications of interest to the stakeholders are mostly at regional and local scales as the essential resources of water, food, energy, human health, and ecosystem function respond to regional and local climate. Climate information and services for Impacts, Adaptation and Vulnerability (IAV) Assessments are of great concern.

Users of climate scenarios produced by global climate models with coarse grid-spacing involve an inadequate mismatch of spatial scale. Downscaling technique is used to obtain the regional climate scenarios, especially in regions of complex topography, coastlines, and in regions with highly heterogeneous land surface covers where those results are highly sensitive to fine spatial scale climate processes. Dynamical and statistical downscaling techniques available for generating regional climate information have the respective strengths and weaknesses. To produce useful climate assessments for decision-making, interaction between the downscaling community and the IAV community are necessary.

To facilitate its interaction, author will present,

- Overview of downscaling techniques in particular for regional climate modelling.
- current International activities (WCRP-CORDEX, etc.)
- Applications of downscaling in Japan from the "REsearch program on Climate Change Adaptation (RECCA)" and the "Program for Risk Information on Climate Change (SOUSEI)" sponsored by the Ministry of Education, Culture, Sports, Science and Technology(MEXT)

Keywords: Downscaling, Regional Climate Model, Climate Change, CORDEX, RECCA, SOUSEI



## Pattern scaling approach for generating regional projections of future extreme events associated with tropical cyclones

TSUTSUI, Junichi<sup>1\*</sup>

<sup>1</sup>Central Research Institute of Electric Power Industry

The assessment of a wide range of greenhouse-gas-emission scenarios in climate change studies employs a simple climate model and pattern scaling based on ensemble projections with complex climate models for a few representative scenarios. The simple climate model deals with the global mean surface temperature as a prediction variable, and the pattern scaling specifies the spatial distributions of different climate variables with prescribed spatial patterns that do not depend on specific scenarios and time points. Although mean temperature and precipitation are typical variables specified by pattern scaling, the present study applies the concept of pattern scaling to extreme events, which are essential for assessing the impact of climate change. An example shown here is a scheme to assess changes in the minimum sea-level pressure and precipitation extreme of the most intense class of tropical cyclones that make landfall in Japan.

This scheme is based on the theory of potential intensity of tropical cyclones and general precipitation extremes. Although real tropical cyclones do not necessarily attain their potential intensities because of various environmental restrictions, the annual cycle of the lower limit of observed minimum sea-level pressures is well represented by climatological potential intensity. An extremely strong tropical cyclone with high societal impact forms only occasionally, within large fluctuations of natural climate variability, regardless of background warming. It is generally difficult to assess relatively small background changes in the intensity of such a rare event by observation statistics or numerical climate projections. The scheme overcomes this difficulty by focusing on large-scale thermodynamic conditions alone, with no consideration of the dynamic conditions that dominantly control the frequency of tropical cyclones. The thermodynamic conditions are scaled with global mean surface temperature anomalies by referring to results (patterns) of ensemble climate model experiments, and reflected in changes in the potential intensity of a target tropical cyclone. Then, the formulation of precipitation extreme incorporates the dynamic effect associated with the intensification of the target tropical cyclone by scaling the vertical structure of the base updraft with that potential intensity change, in addition to thermodynamic change in the amount of water vapor.

Figure 1 shows the assessment results for three different scenarios. The scheme formulates changes in the pressure drop and precipitation extreme of a target tropical cyclone as a function of global mean surface temperature anomaly. The temperature anomaly is calculated using a simple climate model, which has been developed separately, for 3000 cases for each scenario, taking the uncertainty of climate sensitivity into consideration. The computation load of the scheme is negligible, which enables the assessment of many scenarios with different conditions. The scheme also incorporates another uncertainty, not shown here, associated with the amplification of the upper-air temperature anomaly in the troposphere, which greatly affects the minimum sea-level pressure. Thus, the combination of a simple climate model and pattern scaling handles different types of uncertainties in a distinctive way, which is one of the advantages of this approach.

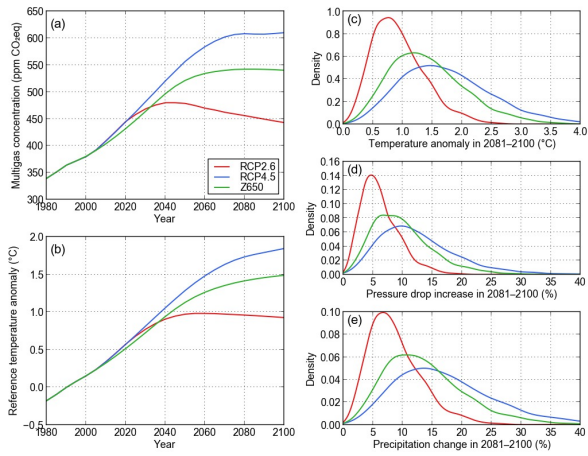
Figure 1: Probabilistic analysis of a target tropical cyclone for three different scenarios labeled RCP2.6, RCP4.5, and Z650. (a), (b): Secular change in the atmospheric multigas concentration and reference global-mean surface temperature anomaly, (c)-(e): Probability density function of the temperature anomaly, increase in pressure drop, and increase in precipitation extreme in 2081-2100 relative to 1981-2000.

Keywords: tropical cyclone, potential intensity, precipitation extreme, pattern scaling, simple climate model, emission scenario

MIS31-16

Room:511

Time:May 2 14:30-14:45



## Emission scenario dependency of pattern scaling and linear additivity of climate forcing-response relationship

SHIOGAMA, Hideo<sup>1\*</sup>

<sup>1</sup>Center for Global Environmental Research, National Institute for Environmental Studies

Human activities are changing the climate, and the consequent impacts on humans and ecosystems are becoming increasingly serious. It has been recognised that adapting to and mitigating anthropogenic climate change is a matter of immediate concern for the world. To inform adaptation and mitigation policies, it is essential to assess the impact of climatic changes under a wide range of scenarios for the stabilization of emissions of greenhouse gases (GHGs) and anthropogenic aerosols (sulfate, black carbon, and organic carbon aerosols). Impact assessments are based on climate change projections from coupled atmosphere-ocean general circulation models (GCMs). Therefore, uncertainties in climate projection propagate to impact assessments and affect subsequent policy decisions for adaptation and mitigation.

Due to the large computational costs of GCMs, only a limited number of emissions scenarios can be made for GCM simulations. To overcome this difficulty and obtain climate scenarios under a wide range of emissions scenarios, the so-called pattern scaling method is often used. By multiplying climate change patterns per 1K of global warming from an AOGCM (called a scaling pattern) by the global mean warming projections from a simple climate model, this method provides projections of precipitation, as well as other variables, at global and regional scales under many emission scenarios. Although the pattern scaling method is widely used, applicability of pattern scaling has been evaluated by only a few studies, and further investigations are clearly warranted.

The basic assumption of pattern scaling method is that scaling patterns are independent on the emission scenarios. Here I show a robust emission-scenario dependency (ESD) in scaling patterns of annual mean precipitation; smaller global precipitation sensitivities occur in higher GHG and aerosol emission scenarios in all the CMIP3 GCM. Different aerosol emissions lead to this ESD. The ESD of precipitation pattern potentially propagates into considerable biases in water resource assessments via pattern scaling.

It is possible to scale climate response patterns to individual forcing agents to obtain climate scenarios. This 'separated pattern' approach is useful to overcome the influences of the ESD. However, this approach requires care in its use. An important assumption of the separated pattern is that individual climate responses to individual forcing agents can be linearly added to obtain the total climate response to the sum of the forcing agents. We explored whether linear additivity holds in 5-year mean temperature/precipitation responses to various combinations of forcing agents in the 20th century and in a future-emissions scenario at global and continental scales. We used MIROC3 GCM, which includes the first and second indirect effects of aerosols. The forcing factors considered were well-mixed greenhouse gases, the direct and indirect effects of sulphate and carbon aerosols, ozone, land-use changes, solar irradiance and volcanic aerosols (the latter three factors were specified only in the 20th-century runs). By performing and analysing an enormous matrix of forcing runs, we concluded that linear additivity holds in temperature responses for all of the combinations of forcing agents at the global and continental scales, but it breaks down for precipitation responses in certain cases of future projections.

Keywords: Climate scenario, pattern scaling, impact assessment

## Evaluation of the nexus of risks under global climate change

YOKOHATA, Tokuta<sup>1\*</sup>; NISHINA, Kazuya<sup>1</sup>; KIGUCHI, Masashi<sup>2</sup>; ISERI, Yoshihiko<sup>3</sup>; SUEYOSHI, Tetsuo<sup>4</sup>; YOSHIMORI, Masakazu<sup>2</sup>; YAMAMOTO, Akitomo<sup>2</sup>; HONDA, Yasushi<sup>5</sup>; HANASAKI, Naota<sup>1</sup>; ITO, Akihiko<sup>1</sup>; MASAKI, Yoshimitsu<sup>1</sup>; SHIGEMITSU, Masahito<sup>6</sup>; IIZUMI, Toshichika<sup>7</sup>; SAKURAI, Gen<sup>7</sup>; IWASE, Kenta<sup>8</sup>; TAKAHASHI, Kiyoshi<sup>1</sup>; EMORI, Seita<sup>1</sup>; OKI, Taikan<sup>2</sup>

<sup>1</sup>National Institute for Environmental Studies, <sup>2</sup>University of Tokyo, <sup>3</sup>Tokyo Institute of Technology, <sup>4</sup>Japan Agency for Marine-Earth Science and Technology, <sup>5</sup>University of Tsukuba, <sup>6</sup>Hokkaido University, <sup>7</sup>National Institute for Agro-Environmental Sciences, <sup>8</sup>Nomura Research Institute

Climate change caused by the increase in atmospheric greenhouse gas has various impacts on human society and ecosystem. Features of the impacts have a large variety, and most part them is adverse impact (damage), although some part is positive impact (benefit) in some locations. It is very important to have reliable predictions of possible damage and benefit (= risks) under the climate change, in order for us to have effective adaptation and mitigation measures.

Future risks caused by the climate change can happen in various sectors. In addition, the various risks are connected across sectors. Especially, a “ nexus ” between the water, food and energy sectors is considered to be very important (Hoff 2011, Understanding the Nexus. Stockholm Environment Institute).

In this study, we are going to present our two activities related to the nexus of risks under the climate change. One is the investigation of qualitative feature of the various links of risks caused by the future climate change. We made a comprehensive list of the possible damage and benefit in the human society and ecosystem possibly caused by the future climate change (“ item of risk ”). This list is generated by the experts of climate, water resources, energy, food, health, security, industry, society, and ecosystem sectors. The experts of these fields in our group members choose all of the possible impacts related to the climate change based on their “ expert judgment ”. The number of items of risks is about 200 currently, such as “ decrease in river runoff ”, “ decrease in crop productivity ”, and “ increase in forest fire ”. Then, we also made a comprehensive list of the possible causal link between the items of risks as described above (“ item of causal link ”). This list is also generated by the experts of the various fields as described above. The number of items of causal link is about 400 currently, such as “ decrease in river runoff ” causes “ decrease in crop productivity ”. Finally, we visualize all of the causal links based on the network diagram using the Fruchtmann & Reingold force-directed layout algorithm. Using the data of item of risks and causal links as well as the network diagram, we are going to discuss the nexus of the risks under the climate change.

The other topic is on the development of a “ terrestrial integrated model ” of our group. We coupled a global climate model called “ MIROC5 ” (Watanabe et al. 2010, J. Climate), global water resources model called “ H08 ” (Hanasaki et al. 2008, HESS), global terrestrial ecosystem model called “ VISIT ” (Ito and Inatomi 2012, Biogeosciences, and global crop model called “ PRYSBI2 ” (Iizumi et al. 2013, J. Agricultural Meteorology). The status of our model development and analysis on the nexus of the risks under the climate change as described above are discussed.

Keywords: climate change, risk, water resources, ecosystem, health, society

---

MIS31-19

Room:511

Time:May 2 15:30-15:45

## Discussion on the challenges for comprehensive global warming studies

TACHIIRI, Kaoru<sup>1\*</sup>

<sup>1</sup>Japan Agency for Marine-Earth Science and Technology

Discussion on the challenges raised.

Keywords: Comprehensive Global Warming Studies

## Atmospheric Chemistry Transport Modeling of Organic Nitrogen Input to the Ocean

ITO, Akinori<sup>1\*</sup> ; LIN, Guangxing<sup>2</sup> ; PENNER, Joyce<sup>2</sup>

<sup>1</sup>JAMSTEC, <sup>2</sup>University of Michigan

Human activities for energy and food production have substantially perturbed the biogeochemical cycle of nitrogen (N) since the industrial revolution. The atmospheric emissions of N-containing compounds from fossil-fuel combustion, intensive agricultural activities, and other anthropogenic processes have substantially increased the supply of reactive N over the oceans downwind of major industrialized regions since 1860. The dominant reactive N species are emitted in the form of nitrogen oxide (NO) and ammonia (NH<sub>3</sub>) from fossil fuel combustion and agricultural practices, are transformed to a number of other nitrogen oxides (NO<sub>y</sub>) and ammonium (NH<sub>x</sub>) during the long-range transport, and then deposited to the oceans. Little is known about the chemical composition of organic N (ON) in the atmosphere or its spatial distribution, due to the limitations of available analytical methods. Over the North Atlantic, a significant fraction of the wet deposition of total soluble N has been measured in the form of soluble ON at coastal and marine locations. The effect of atmospheric ON input on marine ecosystems can either be helpful or harmful depending on the deposition rate and chemical form of ON. Dissolved ON such as urea, amino acids and humic substances can provide an important nutrient source to marine environments. These studies suggest that atmospheric models need to predict the chemical speciation of reactive N species to accurately predict the effects of changes in N inputs on marine ecosystems and climate. Here we use a process-based chemical transport model to investigate global supply of soluble organic nitrogen (ON) from continental sources to the ocean.

Keywords: atmospheric deposition, soluble organic nitrogen, environmental changes

## Ecosystem sustainability of 2 degrees celsius scenario using BECCS

KATO, Etsushi<sup>1\*</sup> ; YAMAGATA, Yoshiki<sup>1</sup>

<sup>1</sup>National Institute for Environmental Studies

Bioenergy with Carbon Capture and Storage (BECCS) is a key component of mitigation strategies in the future socio-economic scenarios to keep mean global temperature rise below 2 °C above pre-industrial, which would require net negative fossil fuel emissions in the end of the 21st century. Large scale BECCS requires additional production of biofuels, which could potentially cause substantial carbon emissions from the land-use change. Developing sustainable low carbon scenarios requires careful consideration of the land-use implications involving large scale BECCS.

We use a global terrestrial biogeochemical cycle model to evaluate effects of land-use change in RCP2.6, which is a scenario with net negative fossil fuel emissions aiming to keep the 2 °C temperature target used in CMIP5. We also use a global crop model to examine BECCS attainability in the land-use scenario of RCP2.6. In the evaluation, we consider deployment of bioenergy with both first-generation second-generation biofuels.

Our analysis reveals that first generation bioenergy crop production would not be sufficient to achieve the required BECCS of RCP2.6 scenario even if we consider the higher fertilizer and irrigation use cases. It would require more than doubling the area for bioenergy crops around 2050 assumed in RCP2.6, however, such scenarios implicitly induce large scale land-use changes that emit significant amount of carbon from deforestation.

Keywords: BECCS, land-use, crop yield, bioenergy



## Climate Restoration via Zero Emissions Stabilization: Examination using Earth System Models

NOHARA, Daisuke<sup>1\*</sup> ; WATANABE, Shingo<sup>2</sup> ; TACHIIRI, Kaoru<sup>2</sup> ; HAJIMA, Tomohiro<sup>2</sup> ; OKAJIMA, Hideki<sup>2</sup> ; TSUTSUI, Junichi<sup>1</sup> ; MATSUNO, Taroh<sup>2</sup>

<sup>1</sup>Central Research Institute of Electric Power Industry, <sup>2</sup>Japan Agency for Marine-Earth Science and Technology

Zero-emissions stabilization is a newly proposed concept that targets reduction of CO<sub>2</sub> emissions to zero in a distant future, after which the atmospheric CO<sub>2</sub> concentration is reduced by a natural atmospheric CO<sub>2</sub> removal process, eventually allowing the atmosphere to reach an equilibrated stable state. The zero-emissions pathway, Z650, has been designed based on this concept as a flexible alternative toward a climate stabilization target. It allows cumulative emissions of 650 GtC during the 21st century and aims to attain zero emissions in the middle of the 22nd century. To confirm the decreases in CO<sub>2</sub> concentrations and temperature that would be achieved with the Z650 pathway, long-term climate and carbon cycle projections have been conducted up to the year 2300 by emission-driven experiment using the Earth system models, CESM1 and MIROC-ESM. Both the models show gradual decreases in the atmospheric CO<sub>2</sub> concentration subsequent to the occurrence of temporal peaks of the concentration due to oceanic and terrestrial CO<sub>2</sub> uptakes. The models also project decreases in the globally averaged surface air temperature after the peak temperature increase. These results imply that the climate is eventually stabilized from a temporal warming state to less warmed under the zero emissions with the Z650 pathway. However, the experiments show considerably different increases in the peak concentration and temperature values, which are attributable to the different carbon and climate sensitivities.

## On the 6th phase of Coupled Model Intercomparison Project

KAWAMIYA, Michio<sup>1\*</sup>

<sup>1</sup>JAMSTEC

From 2013, when the 5th Assessment Report of IPCC WG1 was approved, scientists started discussion on framework of the next (6th) phase of Coupled Model Intercomparison Project (CMIP6). A couple of meetings were held in Aspen, USA in August and in Victoria, Canada in October to arrange a system for implementing CMIP6 protocol for global warming projection experiments. It has been suggested that CMIP6 will be jointly managed by multiple communities in a distributed manner. That is, the "traditional" CMIP community only manages fundamental experiments common to most modeling groups regardless of their specific interest, while other model intercomparison projects (MIPs) cover those specific to their interest: MIPs possibly include, among others, C4MIP for carbon cycle, PMIP for paleoclimate, and GeoMIP for Geoengineering. These activities as a whole will construct CMIP6. The above-mentioned fundamental experiments might include idealized experiments such as CO<sub>2</sub> 1%/y increase, and experiments based on scenarios with and without mitigation policy. According to the schedule currently proposed, the socio-economic scenarios will be developed by the end of 2015, experimental design will be mostly fixed in early 2016, and scenario experiments will be conducted by modeling groups from 2017, whereas those fundamental experiments can be started earlier.

Keywords: CMP6, IPCC, Global Warming Projection, Model Intercomparison Project, Socio-economic Scenario, Climate Model

## 7 years of NanTroSEIZE: Achievements and Lessons Learned

KINOSHITA, Masataka<sup>1\*</sup> ; TOBIN, Harold<sup>2</sup>

<sup>1</sup>JAMSTEC, <sup>2</sup>Univ. Wisconsin-Madison

The objectives of Integrated Ocean Drilling Program (IODP) Nankai Trough Seismogenic Zone Experiment (NanTroSEIZE) include characterizing the nature of fault slip and strain accumulation, fault and wall rock composition, fault architecture, and state variables throughout an active plate boundary system. A deep riser drilling into the locked portion of the Tonankai asperity at IODP Hole C0002F began during IODP Expedition 326 in 2010. After one-year delay due to 3.11 Tohoku event (which gave severe damage to D/V Chikyu), the hole was deepened to 2005 m below seafloor during Expedition 338 in 2012, then deepened to ~3000 m during Expedition 348 in 2013. In addition to the intermittent coring, continuous information was acquired through logging-while-drilling, mud-gas monitoring and cutting analyses. NanTroSEIZE also targets understanding shallow characteristics of subducting Shikoku Basin, forearc slope and Kumano forearc basin.

Through LWD and core analyses, shallow stress state along NanTroSEIZE transect has been revealed. Fault regime changes from normal/strike-slip at <500m to strike-slip in the deeper part (>500 m). Maximum compressional stress is vertical throughout the transect, indicating that the gravitational effect is dominant. Maximum horizontal stress is parallel to the subduction direction, with secondary contribution by the plate convergence. It is consistent with the result from circular air-gun shooting around the vertical seismic array in the central Kumano Basin, which revealed a Vp anisotropy (~5%) in the Kumano Basin that suggests subduction-parallel compression.

Through drilling at two subduction input sites in the Shikoku Basin, we identified a significant Source of fluid in seismogenic zone; ~30 vol% saponite in the basalt sample. This suggests that in the deeper portion of plate boundary, fluid production from basaltic rock (saponite-chlorite) can be greater than from smectite-illite conversion and sediment compaction.

Lab. friction studies in the shallow megasplay fault zone confirmed that shallow faults are velocity-strengthening at slow slip rates. On the other hand, the frictional coefficient during high-velocity (~1 m/s) slips is very low under the undrained condition, suggesting that earthquake rupture propagates easily through clay-rich fault gouge by high-velocity weakening.

Lines of evidence strongly support the activity of shallow portion of megasplay and decollement. Mud breccia in the surface of splay footwall side indicates the earthquake-induced collapse and reworking. Vitrinite reflectance anomaly localized at the fault reveals past thermal anomaly >380degC, indicative of coseismic slip near the seafloor that should have generated a huge tsunami. XRF scanner analysis of microbreccia fault zone in the shallow megasplay indicates an increased illitization relative to surrounding host rock, representing an additional evidence of possible frictional heating and mechano-chemical clay mineral alteration.

Borehole observatories are essential in order to detect and monitor a small and low-frequency deformation that is continuing around the plate boundary. First complex borehole observatory, including geodetic, seismic and hydrological sensors, was successfully installed in the southern Kumano Basin and connected to cable network for realtime monitoring.

So far we drilled at 13 sites, participated by >170 scientists from 15 countries, and published more than 60 scientific papers. Such achievements were made possible by tremendous efforts by CDEX, who tackled with numerous technical challenges such as mechanical setbacks of riser and vessel, concern about the expedition time available (cost and budget), typhoon/low pressure evacuation, and riser drilling in the 5-knot Kuroshio current.

Keywords: IODP, Chikyu, seismogenic zone, Nankai Trough

## Ultra-deep riser drilling into the Nankai accretionary prism: Preliminary results of IODP Expedition 348

HIROSE, Takehiro<sup>1\*</sup> ; TOBIN, Harold<sup>2</sup> ; SAFFER, Demian<sup>3</sup> ; TOCZKO, Sean<sup>1</sup> ; MAEDA, Lena<sup>1</sup> ; KUBO, Yusuke<sup>1</sup> ; KANAGAWA, Kyuichi<sup>4</sup> ; KIMURA, Gaku<sup>4</sup> ; EXPEDITION 348, Scientists<sup>6</sup>

<sup>1</sup>JAMSTEC, <sup>2</sup>University of Wisconsin-Madison, <sup>3</sup>Pennsylvania State University, <sup>4</sup>Chiba University, <sup>5</sup>The University of Tokyo, <sup>6</sup>IODP Expedition 348

The Nankai Trough Seismogenic Zone Experiment (NanTroSEIZE) is a multi-disciplinary scientific project designed to investigate fault mechanics and seismogenesis along subduction megathrusts through seismic imaging, direct sampling, in situ measurements, and long-term monitoring in conjunction with laboratory and numerical modeling studies. As part of the NanTroSEIZE program, International Ocean Discovery Program (IODP) Expedition 348 started on 13 September 2013 and was completed on 29 January 2014. During Expedition 348, the drilling vessel *Chikyu* advanced the ultra-deep riser hole at Site C0002, located 80 km offshore from the Kii Peninsula, from a depth of 860 meters below sea floor (mbsf) to 3058.5 mbsf, the world record for the deepest scientific ocean drilling, and cased it for future access. The drilling operation successfully obtained data on formation physical properties from logging while drilling (LWD) tools, as well as from lithological analyses of cuttings and core from the interior of the active accretionary prism at the Nankai Trough. IODP Site C0002 is the currently only borehole to access the deep interior of an active convergent margin. We will present preliminary scientific results as well as key aspects of riser-drilling operations, including two sidetrack borehole drilling operations conducted in this never-before accessed tectonic environment.

Keywords: IODP, NanTroSEIZE, Nankai Trough, accretionary prism

## Costa-Rica Seismogenesis Program (CRISP) to understand characteristic magnitude of subduction earthquake

SAKAGUCHI, Arito<sup>1\*</sup> ; HARRIS, Robert<sup>2</sup>

<sup>1</sup>Yamaguchi Univ./JAMSTEC, <sup>2</sup>Oregon State University

Variations in earthquake magnitude and recurrence intervals of fault behavior are best understood in the context of regional tectonics. Convergent margins may be divided into two end-member types termed erosive and accretionary plate boundaries (e.g. von Huene and Scholl, 1991; Clift and Vannucchi, 2004). These margins may differ greatly in lithology, physical properties and hydrology. The Nankai accretionary margin has a 1300-year historical earthquake record with a recurrence interval of 100-150 years (Ando, 1975). Great earthquakes at Nankai are typically tsunamigenic and include the 1944 Tonankai (Mw=8.1) and 1946 Nankaido (Mw=8.1) earthquakes (Kanamori, 1977). In contrast, the Middle America trench offshore Costa Rica events of M=7.6 reoccur on average of every 40 years. The CRISP drilling area is offshore Costa Rica just northwest of the Osa Peninsula. Comparisons between these margins may produce insights into mechanisms that influence characteristic magnitudes and recurrence intervals of subduction earthquakes.

The IODP Costa-Rica Seismogenesis Program (CRISP) has carried out the first step toward the deep riser drilling by characterizing the shallow lithologic, hydrologic, stress, and thermal state at offshore Osa Peninsula (Vannucchi et al., 2011; Harris et al., 2013). CRISP drilling reveals that the shallow basement of upper plate crust is forearc basin material consisting of lithic sedimentary units with terrigenous sediment accumulated at a high rate. A large sediment flux to the forearc may have originated from the uplifted back-arc Talamanca Cordillera due to Cocos-Ridge subduction (Lonsdale and Klitgord, 1978; van Andel et al., 1971). Both the Nankai and the CRISP drilling areas are characterized by the subduction of young oceanic crust with high heat flow and active fluid flow (Spinelli and Wang, 2008; Spinelli and Harris, 2011; Harris et al., 2010). The Nankai and Costa Rica margins are ideal areas to better understand the relation between the earthquake magnitudes and other subduction zone factors.

Keywords: Large subduction earthquake, seismogenic fault, accretion and erosive margin

## Estimation of the past bottom-ocean environment of 2Ma based on the benthic foraminifera stratigraphy: IODP Exp. 344

UCHIMURA, Hitomi<sup>1\*</sup>

<sup>1</sup>Graduate School of Science and Technology, Kumamoto University

IODP Exp.344 (Costa Rica Seismogenesis Project: CRISP 2) is designed to understand the processes that control nucleation and seismic rupture of large earthquakes at erosional subduction zones and drilled five sites off the western coast of Costa Rica around the southern end of the Middle America Trench, where the oceanic Cocos Plate is subsiding beneath the Caribbean Plate.

Site U1414 is the reference site and its 2Ma is characterized by lower slope assemblages and also there is not any big change of assemblages. However, a lot of *Chilostomella oolina* are in the upper samples. This means sea bottom environment is a little change from at least 0.12Ma to recent.

The assemblages of Site U1412 are very similar to U1414. The differences are two biozones; one has a lot of *Cibicides mackinnai*, and the other has *Brizalina bicostata*. These species are originally on upper shelf, and that means these zones are allocated layers.

Main objective of this study in the Site U1413 is to understand the tectonic-induced submergence/ uplifting history or paleoslope instabilities in the upper slope area. Benthic foraminifera (BF) are a useful tool to estimate the past bottom-ocean environment. Based on benthic foraminiferal biostratigraphy of U1413, we have recognized the following four biozones for the sequence of past 2 million years and identified plausible slump mass came from the shallower-water environment

The BF divided into Group A (Zone I) is distributed on the lower continental slope in the modern equatorial Pacific. (Smith, 1963, 1964). Group B in Zone II is reported mainly from the lower to middle slope environment of the Pacific. Group C in Zone III is estimated to be distributed in the upper slope. Group D in Zone IV lives in the upper to middle slope as well as the drill site.

On the other hand, some shelf species such as *Brizalina bicostata*, *Cibicides inflatus* and *Uvigerina incilis* (Group E) occur throughout the sequence of the hole. Those species are, however, considered to be reworked specimens from shallower environment, because they co-occurred with deeper water species as Groups A to D, and because a similar occurrence has been reported in the Peru-Chile Trench area by Ingle and Kolpack (1980).

In Zone III, another species group composed of *Brizalina* spp., (Group C), which is distributed mainly in the upper slope areas in the modern oceans. Because Group C is not accompanied by Group D or other deeper-water species, the interval of Cores 17H-11H in Hole A apparently correspond to the upper continental slope, at least shallower than the depth of Group D. Also, the tests of *Brizalina* spp. are well-preserved in contrast to the co-occurred Group E. These results imply that Zone III is allocated Mass transported sediments, like a slump. This interpretation has been also supported by geochemical and logging data. The slump mass has been inferred at the interval between 45-150 mbsf based on the irregular profiles for organic matters and a fold structure plausibly formed by slumping. The slump mass might reflect the active subsidence due to tectonic erosion or passage of subducting seamount at the plate interface.

Keywords: benthic foraminifera, paleobathymetry, Subduction zone

## Limits and Habitability of the Deep Subseafloor Biosphere: New Insights from IODP Expeditions 329 and 337

INAGAKI, Fumio<sup>1\*</sup> ; IODP, Expedition 329 and 337 scientists<sup>2</sup>

<sup>1</sup>Geomicrobiology Group, Kochi Institute for Core Sample Research, JAMSTEC, <sup>2</sup>IODP Expedition 329 and 337 Scientists

In the past decade, the Integrated Ocean Drilling Program (IODP) has offered unique opportunities to explore how life persists and evolves in ecosystems of the Earth interior. There are very few natural environments on surface of the Earth where life is absent; however, the limits to life are expected in the subsurface world. Processes that mediate genetic and functional evolutions of the deep subseafloor life may be very different to those in the Earth surface ecosystems. Previous studies of subseafloor sedimentary habitats demonstrated that activity of microbial communities is generally extremely low, mainly because of the limit of nutrient and energy supply. Nevertheless, microbial activity plays important ecological roles in biogeochemical element cycles over geological timescale.

In 2010, during Expedition 329, we explored limits and habitability of life in deep-sea sediments and basalts in the South Pacific Gyre, the largest oceanic province where surface chlorophyll concentrations and primary productivity in the gyre are lower than any other regions of the world ocean. In 2012, during Expedition 337, we also explored the deep subseafloor coalbed biosphere off the Shimokita Peninsula of Japan. Using riser system of the *Chikyu*, we successfully drilled, cored and logged down to the depth of 2,466 meters below the seafloor.

The IODP Expeditions 329 and 337 represent aerobic and anaerobic subseafloor microbial ecosystems on our planet, respectively, both of which realms have never been explored by previous scientific drilling; therefore, these provide unprecedented opportunities to address the issue of limits and habitability in the deep subseafloor biosphere. A variety of geophysical and geochemical properties, such as temperature, pH, pressure, salinity, porosity, and availability of nutrient and energy are conceivable to constrain biomass and activity of deep life and extent of the subseafloor biosphere. These are systematically investigated by international and multidisciplinary teams of the Expedition 329 and 337 scientists.

## Geophysical logging at the Shimokita IODP Expedition 337

YAMADA, Yasuhiro<sup>1\*</sup> ; SANADA, Yoshinori<sup>2</sup> ; KUBO, Yusuke<sup>2</sup> ; INAGAKI, Fumio<sup>2</sup> ; NAKAMURA, Yasuyuki<sup>2</sup> ; MOE, Kyaw<sup>2</sup>

<sup>1</sup>Kyoto Univ, <sup>2</sup>JAMSTEC

Research achievements using the geophysical logging data obtained at the Shimokita IODP expedition 337 would be presented.



## History of the Mediterranean Sea based on drilled core samples

KURODA, Junichiro<sup>1\*</sup>

<sup>1</sup>Japan Agency for Marine-Earth Science and Technology

Mediterranean Sea has experienced an extreme event called Messinian Salinity Crisis (MSC) that represents a formation of gigantic evaporite deposits in deep basins. Although this event has long been studied, a fundamental question whether the Mediterranean Sea was desiccated or not, still remains unsolved. In this presentation we review the recent achievements of the MSC. To understand hydrological conditions of the Mediterranean Sea during the Miocene-Pliocene, we report a series of Os isotopic record of marine sediment cores from four deep-sea drilling sites in the Balearic Basin, the Tyrrhenian Sea, the Ionian Basin and the Florence Rise, in comparison with the coeval sediments in North Atlantic. Osmium isotopic ratios of the pre-Messinian sediments in the western Mediterranean basin are almost identical to that of the coeval ocean water. In contrast, the pre-Messinian sediments in the eastern Mediterranean basin have significantly low  $^{187}\text{Os}/^{188}\text{Os}$  values. This suggests that Os in the eastern Mediterranean was not fully mixed with western Mediterranean and North Atlantic, and that the basin isolation has already started much earlier than the MSC. The less radiogenic Os would have been supplied to the eastern Mediterranean by selective weathering of ultramafic rocks cropping out in the drainage areas, which contains high amount of non-radiogenic Os. The isotopic compositions of Os in gypsum and halite samples are significantly lower in eastern Mediterranean basins, compared with those of gypsum samples from the western Mediterranean basin, supporting the idea that limited exchange of seawater between eastern and western basins sustained also during the MSC. In all sites Pliocene sediments show more radiogenic Os isotopic ratios, which are close to the coeval oceanic values, indicating that Os started mixing with global seawater again.

Keywords: Mediterranean Sea, Messinian Salinity Crisis, osmium isotope

## Exp. 325 Great Barrier Reef Environmental Changes

YOKOYAMA, Yusuke<sup>1\*</sup>

<sup>1</sup>Yusuke YOKOYAMA

The Great Barrier Reef is the largest coral reef in the world and a world heritage site. Integrated Ocean Drilling Program (IODP) Expedition 325 drilled fossil corals and obtained 225m of core materials from 42 to 167 m below sea-level. The site is suited for reconstructing paleo climate data because: 1) reconstructed sea-level data is relatively immune from isostatic effect since it is located at site far from former ice covered regions (far-field), 2) it locates in or near the Indo Pacific Warm Pool (IPWP) where paleo sea surface temperature (SST) data will constrain climate model strongly, and 3) the growth history of the reef since the LGM is to unlock a key factors for reef system response against environmental changes. Both sea level and climate data have been reconstructed by the science party and they provides new insights of the climate system. In this presentation, I will overview and introduce some key findings of IODP 325 GBR environmental changes (Yokoyama et al., 2011)

Reference: Yokoyama, Y. et al. (2011) "IODP Expedition 325: Great Barrier Reefs Reveals Past Sea-Level, Climate and Environmental Changes Since the Last Ice Age" *Scientific Drilling*, 12, 32-45.

Keywords: Sea level change, Glacier, Last Glacial Maximum, Sea Surface Temperature, Coral, The Great Barrier Reef

## Determination of hydrocarbon gas in drilling mud and cores during Expedition 348 at the Nankai Trough, Japan

FUCHIDA, Shigeshi<sup>1\*</sup> ; HAMMERSCHMIDT, Sebastian<sup>2</sup> ; EXPIDITION 348, Shipboard scientists<sup>3</sup>

<sup>1</sup>Osaka City University, <sup>2</sup>University of Bremen, <sup>3</sup>University of Wisconsin and others

The recent International Ocean Discovery Program (IODP) Nankai Trough Seismogenic Zone Experiment (NanTroSEIZE) Expedition 348 at Site C0002 drilled and cored successfully up to 3058.5 mbsf. During drilling and coring, hydrocarbon and other inorganic gas concentrations were monitored on board. Here, we will report the distribution and origin of the hydrocarbon gas in Holes C0002N (838 to 2330 mbsf) and C0002P (1954 to 3058 mbsf).

Methane, ethane, and propane concentrations in the headspace gas were measured by Geoservices and by using the scientific drilling mud gas monitoring system onboard D/V Chikyu. Total gas concentrations were dominated by methane, with the highest concentrations of up to 8% at around 1305 mbsf. Downhole gas concentrations steadily decreased to values <0.2 %. Ethane and propane were only present in minor concentrations, and higher homologues (i.e. n-butane, i-butane, n-pentane, i-pentane) stayed typically below 0.01 %. Below 2200 mbsf, ethane and propane increase steadily with depth. Bernard diagram (i.e. Bernard parameter vs.  $\delta^{13}C_{CH_4}$ , Bernard et al., 1978) indicates that the gas in Hole C0002NP was gradually changed from biogenic to thermogenic with increasing depth.

Headspace gas samples from cores in Hole C0002P (2160-2220 mbsf) were all dominated by methane, with up to 23455 ppm. Methane concentration in the headspace gas samples was higher than the drilling mud gas samples at the same interval. This underestimation of methane in the drilling mud is due to the influence of drilling parameter (e.g. rate of penetration), mud properties (e.g. mud weight) and degassing efficiency.

Keywords: IODP, Expedition 348, Nantrosize, hydrocarbon

## New approach for subsurface methanogenesis

KANEKO, Masanori<sup>1\*</sup> ; TAKANO, Yoshinori<sup>1</sup> ; OHKOUCHI, Naohiko<sup>1</sup>

<sup>1</sup>JAMSTEC

Quantitative understanding of microbially mediated methanogenesis is important in biogeochemistry for many reasons; Firstly, methanogenesis plays an important role in the carbon cycle on the Earth mediating a terminal process of organic matter degradation and a major metabolic process in anoxic sediments. Secondly, methane produced by methanogens results in methane hydrate formation which is a potential energy resource, while methane released to the atmosphere acts as a greenhouse gas. Thirdly, since methanogens are primitive organisms, clarification of their distribution and environmental factors controlling their activity provides better understanding of subsurface biosphere and environmental constraints for early life.

Although quantitative understanding of distribution and activity of methanogens is requisite for better understanding of methane biogeochemistry, available techniques are restricted to address this issue. Particularly, it is difficult to quantitatively detect a signal of modern methanogenesis from deep marine sediment cores where methanogenic activity is low and complex mixture of organic matter is accumulated during a geologic time scale. However, if function-specific compound directly involved in the methanogenic reaction can be quantified, we would be able to extract information about distribution and activities of methanogens in the marine sediments.

Recently we developed analysis of coenzyme F430. Since F430 catalyzes a terminal step of methanogenesis and possessed by all methanogens, it should be a good biomarker for methanogenesis. High sensitive detection of F430 by LC-MS/MS (sub-femto mol level) allows to detect F430 in marine sediment. We will present the developed methodology and application to sediment core samples.

Keywords: coenzyme F430, methanogenesis, LC-MS/MS, marine sediment

## Lake drilling in Japan: Biwa and Suigetsu

HAYASHIDA, Akira<sup>1\*</sup> ; TAKEMURA, Keiji<sup>2</sup> ; NAKAGAWA, Takeshi<sup>3</sup>

<sup>1</sup>Doshisha University, <sup>2</sup>Kyoto University, <sup>3</sup>University of Newcastle

Lake drilling is an important subject of the International Continental Scientific Drilling Program (ICDP), where several projects were implemented in ancient-type lakes utilizing the GRAD200 and GRA800 systems. However, proposals for attempting lake drilling in Japan have not been submitted to ICDP so far. In 2002, an ICDP workshop, entitled "Lake Biwa and Lake Suigetsu: Recorders of Global Paleoenvironments and Island Arc Tectonics" was held in order to assemble an international team and prepare a full proposal. Subsequently, piston coring and deep drillings were made in Lake Biwa supported by the grant-in-aid from Monbusho. Studies of these core samples are now ongoing in various disciplines including sedimentology, paleomagnetism, organic and inorganic chemistry, and radiocarbon dating. In Lake Suigetsu, an international collaborative research has been carried out aiming to provide a high-resolution paleoenvironmental record of the East Asian monsoon. It also contributed toward establishing a purely terrestrial radiocarbon calibration model, based on analysis of the annually laminated sediment. As the next step of the current researches in Lake Biwa and Lake Suigetsu, we expect a new drilling project targeting a 250-m thick continuous clay member of the Lake Biwa sediments.

Keywords: ICDP, Lake drilling, Lake Biwa, Lake Suigetsu

## How the stress state changes with time in and around faults

OMURA, Kentaro<sup>1\*</sup>

<sup>1</sup>NIED

It is an important factor for forecast a future earthquake how the strength of a fault plane is recovered and how the stress in and around the fault plane accumulate during an earthquake cycle. However, it is difficult to inspect the time variation of stress state in and around a faults in the field because the period of an earthquake cycle is very long. I introduce examples to be concerned with time variations of stress states by downhole in-situ stress measurement (Ikeda et al., 1996a; Ikeda et al., 1996b; Ikeda et al., 2001; Tsukahara et al., 2001; Omura et al., 2004; Yamashita et al., 2004; Hickman and Zoback, 2004; Lin et al., 2007; Yabe et al., 2010; Yamashita et al., 2010; Yabe and Omura, 2011; Kuwahara et al., 2012; Ito et al., 2013; Lin et al., 2013). Those examples indicate that stress increases since after an earthquake toward the next earthquake. However, it is not clear whether the stress increase linearly with time, or change largely just after an earthquake, or increase rapidly just before the next earthquake. We need repeated measurements of in-situ stress to detect directly a time variation of stress state in and around a fault after an earthquake.

Hickman, S., and M. Zoback, 2004, *Geophys. Res. Lett.*, 31, L15S12, doi:10.1029/2004GL020043

Ikeda, R., K.Omura and Y.Iio.,H. Tsukahara, 1996a, Proc. VIIIth Int'l. Symp. on the Observation of the Continental Crust through Drilling, 30-35.

Ikeda,R., Y.Iio and K.Omura, Y.Tanaka, 1996b, Proc. VIIIth Int'l. Symp. on the Observation of the Continental Crust through Drilling, 393-398.

Ikeda, R., Y. Iio and K. Omura, 2001, *The Island arc Special Issue. 10, Issue 3/4*, 252-260.

Kuwahara, Yasuto, Tsutomu Kiguchi, Xinglin Lei, Shengli Ma, Xueze Wen, and Shunyun Chen, 2012, *Earth, Planets and Space*, 64, 13-25.

Lin, W., E.-C. Yeh, H. Ito, J.-H. Hung, T. Hirono, W. Soh, K.-F. Ma, M. Kinoshita, C.-Y. Wang, and S.-R. Song, 2007, *Geophys. Res. Lett.*, 34, L16307, doi:10.1029/2007GL030515.

Lin, Weiren, Marianne Conin, J. Casey Moore, Frederick M. Chester, Yasuyuki Nakamura, James J. Mori, Louise Anderson, Emily E. Brodsky, Nobuhisa Eguchi, and Expedition 343 Scientists, 2013, *Science*, 339, 687-690.

Omura, K., R. Ikeda, T. Matsuda, A. Chiba, and Y. Mizuochi, 2004, *Earth Monthly*, extra edition No.46, 127-134.

Tsukahara, H., Ikeda, R. and Yamamoto, K. , 2001, *Island Arc*, 10, 261-265.

Yabe, Yasuo, Kiyohiko Yamamoto, Namiko Sato, and Kentaro Omura, 2010, *Earth Planets Space*, 62, 257-268.

Yabe, Yasuo and Kentaro Omura, 2011, *Island Arc*, 20, 160-173.

Yamashita, Furoshi, Eiichi Fukuyama and Kentaro Omura, 2004, *Science*, 306, 261-263.

Yamashita, F., Mizoguchi, K., Fukuyama, E. and Omura, K., 2010, *J. Geophys. Res.*, 115, B04409, doi:10.1029/2009JB006287.

Keywords: stress, fault, in-situ measurement, hydraulic fracture, borehole breakout, downhole measurement

## Physicochemical process during earthquake slip: An example from the TCDP

HIRONO, Tetsuro<sup>1\*</sup>

<sup>1</sup>Department of Earth and Space Science, Graduate School of Science, Osaka University

Several fault-drilling projects have been conducted with the common aim of seeking direct access to zones of active faulting and understanding the fundamental processes governing earthquakes and fault behavior, as well as the factors that control their natural variability. Here, we review recent scientific drilling project on the the Chelungpu Fault which slipped during the 1999 Taiwan Chi-Chi earthquake. One of the main findings of fault-drilling research is a better understanding of the physicochemical processes of the primary slip zone during an earthquake, which is closely related to the mechanism of dynamic fault weakening. In the case of the Chelungpu fault, integrated research with borehole experiments, core sample analyses, and numerical simulations were performed, and the results indicate that thermal pressurization occurred during the 1999 earthquake, explain ing the peculiar seismic behavior during the earthquake. Such fault-drilling project related to active fault certainly improve our knowledge and understanding of earthquakes.

Keywords: Onland fault drilling, Active fault

## Deep Fault Drilling Project, Alpine Fault, New Zealand

SHIGEMATSU, Norio<sup>1\*</sup> ; SUTHERLAND, Rupert<sup>2</sup> ; TONWEND, John<sup>3</sup> ; TOY, Virginia<sup>4</sup>

<sup>1</sup>Active Fault and Earthquake Research Center, AIST, <sup>2</sup>GNS Science New Zealand, <sup>3</sup>Victoria University of Wellington, <sup>4</sup>University of Otago

The Alpine Fault is mature (>460 km offset), active (25 mm/yr), and late in its seismic cycle. It ruptured in AD 1717, has a 330 yr return time, and M8 earthquake probability is c. 30% in the next 50 yrs (Berryman et al. 2013). The objective of the Deep Fault Drilling Project (DFDP) is to collect materials, measure ambient conditions, and monitor at depth on the Alpine Fault, to understand earthquake processes and the formation of a continental orogen.

Pilot drilling (DFDP-1) was completed in 2011. Two boreholes were drilled, wireline geophysical loggings collected, and observatory installed. The followings were revealed as Initial results. A low-permeability alteration zone overprints the boundary between fault core and damage zone. The alteration zone significantly affects physical properties and likely evolves during the seismic cycle. There is a fluid pressure step of 0.53 MPa across the fault at 128 m depth, and probable greater difference at greater depth. Geothermal gradient is 63 +/- 2 C/km. Physical properties are highly asymmetric, suggesting a possible (northeastward) preferred rupture direction.

Planning is now underway for the next phase of drilling ("DFDP-2"), which is scheduled to start in 2014. The target total depth (TD) is 1.3 km, with contingency to reach 1.5 km. We drill, sample, and monitor the Alpine Fault to address fault zone evolution via brittle and ductile processes operating in the upper and mid-crust in this novel experiment.

Keywords: Fault zone drilling, the Alpine Fault, Earthquake processes, Brittle and ductile processes



## An Overview of IODP Expedition 346: Asian Monsoon

TADA, Ryuji<sup>1\*</sup> ; MURRAY, Richard W.<sup>2</sup> ; ZARIKIAN, Carlos alvarez<sup>3</sup> ; EXPEDITION 346, Scientists<sup>4</sup>

<sup>1</sup>Graduate School of Science, the University of Tokyo, <sup>2</sup>Earth and Environment, Boston University, <sup>3</sup>Texas A&M University, <sup>4</sup>IODP

In IODP Expedition 346, Joides Resolution (JR) started her cruise from Valdez, Alaska on August 2nd, sailed all the way to the Japan Sea/East Sea (JS/ES), drilled 7 sites in the JS/ES and 2 sites in the northern East China Sea (ECS), and ended her cruise at Pusan, Korea on September 28th. During six weeks of drilling, we recovered 6135.3 m of core, with an average recovery of 101%, which is a record of IODP. The expedition was originally aimed to test the hypothesis that Plio-Pleistocene uplift of Himalaya and Tibetan Plateau (HTP) and/or emergence and growth of the northern hemisphere ice sheets and consequent establishment of the two discrete modes of westerly jet (WJ) circulation is the cause of the millennial-scale variability of the East Asian summer monsoon (EASM) and amplification of the Dansgaard-Oeschger cycles (DOC). The expedition is also aimed to test the hypothesis that surface and deep water conditions of the JS/ES has been controlled by the nature and strength of the water influx through the Tsushima Strait which are strongly influenced by EASM precipitation, eustatic sea level changes, and EAWM cooling.

In order to explore the linkage between WJ circulation and EASM precipitation, it is critical to obtain high-resolution, continuous sedimentary records that preserve proxies of both WJ and EASM. In this respect, the JS/ES is ideal because its hemipelagic sediments contain significant amount of the eolian dust transported from East Asia by the WJ, and alternations of dark and light layers that characterize Quaternary sediments of the sea record variations of EASM precipitation over South China (Tada et al., 1999). Sites are also arranged along the north-south transect to monitor the behavior of the WJ. The sites are arranged to make the depth transect to monitor the behavior of deep water through changes in calcium carbonate compensation depth and bottom water oxygenation level. Northern East China Sea is ideal to monitor changes in EASM precipitation because its surface water salinity and temperature during summer is significantly influenced by the discharge of the Yangtze River whose drainage area covers the majority of the South China where EASM precipitation is most intense (Kubota et al., 2010).

Because of recent advances in drilling technology and newly developed analytical tools, we were able to collect and examine sediment records that were impossible to acquire even a few years ago. The newly engineered half piston core system (called the half APC) enabled us to recover the deepest piston core in DSDP/ODP/IODP history (490.4 m in Hole U1427A). That achievement was also the deepest continuously recovered piston cored sequence, initiated at the mudline and penetrating to the ~500 m depth solely by piston coring. These technological advances delivered a series of new surprises. Examples are pristine dark/light laminae from ~12 Ma sediment recovered by piston core from 410 m core depth below seafloor, Method A [CSF-A] at Site U1425 and from 210 m CSF-A at Site U1430.

Through this expedition, we collected the geological evidence necessary to test the hypotheses described above through drilling in the JS/ES and northern part of the ECS, and are trying to 1) specify the onset timing of orbital and millennial-scale variability of EASM, EAWM and WJ and reconstruct their evolution process and spatial variation patterns, and 2) reconstruct orbital and millennial-scale paleoceanographic changes in the JS/ES to clarify the linkage between the paleoceanography of the JS/ES and EASM, EAWM and/or sea level. Comparison of the obtained results with the uplift history of HTP and/or ice volume changes will enable us to test the hypotheses.

Keywords: IODP, Expedition 346, Japan Sea/East Sea, East China Sea, Dansgaard-Oeschger Cycle, East Asian Monsoon

## Sediment cores recovered from the Sea of Japan/East Sea during IODP Expedition 346 and preliminary result of foraminifer

SAGAWA, Takuya<sup>1\*</sup> ; TADA, Ryuji<sup>2</sup> ; MURRAY, Richard W.<sup>3</sup> ; ALVAREZ-ZARIKIAN, Carlos A.<sup>4</sup> ; EXPEDITION 346, Scientists<sup>5</sup>

<sup>1</sup>Department of Earth and Planetary Sciences, Faculty of Sciences, Kyushu University, <sup>2</sup>Department of Earth and Planetary Science, Graduate School of Science, The University of Tokyo, <sup>3</sup>Earth & Environment, Boston University, USA, <sup>4</sup>Integrated Ocean Discovery Program, Texas A&M University, <sup>5</sup>IODP Expedition 346

Integrated Ocean Drilling Program (IODP) Expedition 346 (29 July-27 September 2013) recovered 6135.3 m of core from seven sites in the Sea of Japan/East Sea and two adjacent sites in the East China Sea. One of the objectives of this expedition is to explore the orbital- and millennial-scale variation and evolution of the East Asian monsoon and its impact on the paleoceanography in the Sea of Japan/East Sea. We recovered centimeter- to meter-scale alternation of dark and light layers in the Pleistocene sediments that could be correlated across the six sites in latitudinal and depth transects of the Sea of Japan/East Sea (U1422-U1426 and U1430), suggesting that the Sea of Japan/East Sea responded as a single system to climatic and/or oceanographic perturbations. Sediments of shallower sites (U1426: 903 mbsl and U1427: 330 mbsl) contain well preserved calcareous fossils and are expected to provide high-quality oxygen isotope stratigraphy that will be a key age controls for the entire region. In particular, high sedimentation rate (~36 cm/kyr) and a complete splice down to ~400 m at Site U1427 make it possible to produce centennial-scale continuous records in shallow water environments for the last ~1.2 Ma. We conducted preliminary oxygen and carbon isotope analyses of benthic and planktonic foraminifera for core catchers from Site U1427A (87 samples). The oxygen isotope variations correspond to lithological change alternating low isotope values in darker clay-rich and high values in light biogenic component-rich sediment and therefore show similar variation to physical properties of the sediment, such as bulk density, magnetic susceptibility, natural gamma ray, and color reflectance. These results confirm high potential of this site for paleoceanographic investigation in orbital, millennial, and centennial timescales.

### Expedition 346 Scientists:

Anderson, W., Bassetti, M-A., Brace, B., Clemens, S., Dickens, G., Dunlea, A., Gallagher, S., Giosan, L., Gurgel, M., Henderson, A., Holbourn A., Ikehara, K., Irino, T., Itaki, T., Karasuda, A., Kinsley, C., Kubota, Y., Lee, G-S., Lee, K-E., Lofi, J., Lopes, C., Peterson, L., Saavedra-Pellitero, M., Singh, R., Sugisaki, S., Toucanne, S., Wan, S., Xuan, C., Zheng, H., and Ziegler, M.

Keywords: IODP, Expedition 346, Asian Monsoon, Sea of Japan/East Sea

## Preliminary results from shipboard research during IODP Expedition 341 (Alaska Tectonics, Climate and Sedimentation)

SUTO, Itsuki<sup>1\*</sup> ; ASAHI, Hirofumi<sup>2</sup> ; FUKUMURA, Akemi<sup>3</sup> ; KIOKA, Arata<sup>4</sup> ; KONNO, Susumu<sup>5</sup> ; MATSUZAKI, Kenji<sup>6</sup> ; NAKAMURA, Atsunori<sup>4</sup> ; OJIMA, Takanori<sup>7</sup> ; EXPEDITION, 341 scientists<sup>8</sup>

<sup>1</sup>Nagoya Univ., <sup>2</sup>Pusan National Univ., <sup>3</sup>Hokkaido Univ., <sup>4</sup>Univ. of Tokyo, <sup>5</sup>Kyushu Univ., <sup>6</sup>Tohoku Univ., <sup>7</sup>Univ. of Tokyo, <sup>8</sup>(none)

The North American Cordillera is an active orogen, which in the Pleistocene is, at times, covered by the Cordilleran Ice Sheet. Ice sheet dynamics are likely impacted by global climate and likely enhanced the erosion in the Cordillera. The melt water discharge to the ocean may play an important role in the rich ecosystem in the Gulf of Alaska by delivering nutrients. In the modern Gulf of Alaska, a rich diversity of marine microorganisms is associated with the seasonal nutrient supply derived from glacial melt water. Continuous paleoceanographic reconstruction by marine microfossils (radiolarians, diatoms, foraminifers etc.) can provide the history of the nutrient supply that may be associated with ice sheet dynamics and glacial runoff into the Gulf of Alaska.

Since the late Miocene, ice sheets formed on the North American continent and intensified around 2.5 Ma during Northern Hemisphere glaciation, which had a strong impact on global and regional environments. On the other hand, the large ice sheet may also have enhanced the erosion process in the higher latitudes and supplied terrigenous inputs such as glacial sediments to the coastal zone. Therefore, it is expected that the sediments in the Gulf of Alaska have recorded directly the history of the Cordillera ice sheet formation and erosion process since the Neogene. In this background, the Integrated Ocean Drilling Program (IODP) Expedition 341 held between May to July 2013, targeted this high-resolution sediment record from late Cenozoic in order to investigate the relevance of climate change in the North Pacific Ocean and the erosion process of Cordilleran glaciers. The drilling was conducted from deep-sea fan to continental shelf occupied by glaciers during glacial expanses.

According to preliminary ship-board results, the sediments recovered during this expedition record paleoceanographic changes in the Gulf of Alaska since the late Miocene and extremely high sedimentation rates which could be one of the greatest achievements in this expedition. In addition, microscopic observation, organic and inorganic chemical analysis and measurement of the physical properties suggest that a large amount of the terrestrial sediments have been transported. A large amount of glacial sediments (ice-rafted debris) have been also recorded. Although it was expected that calcareous microfossils are poorly preserved in this area, the sediment samples obtained in this cruise contained a continuous and rich foraminifera record which will allow the establishment of a long continuous oxygen isotopic curve. Siliceous microfossil and p-mag analyses enable the building of firm chronostratigraphy when combined with the oxygen isotopic curve. Under this well-constrained age determination, other chemical/physical/biological investigations will be done and then we will clarify the paleoenvironmental fluctuation that is unprecedented in the North Pacific.

Keywords: IODP Exp. 341, Gulf of Alaska, land/ocean paleoenvironment, Glacier

## IODP Exp. 345: The first sample of primitive layered gabbros from fast-spreading lower oceanic crust

ABE, Natsue<sup>1\*</sup> ; AKIZAWA, Norikatsu<sup>2</sup> ; HARIGANE, Yumiko<sup>5</sup> ; HOSHIDE, Takashi<sup>4</sup> ; MAEDA, Jinichiro<sup>3</sup> ; MACHI, Sumiaki<sup>2</sup> ; NOZAKA, Toshio<sup>6</sup> ; PYTHON, Marie<sup>5</sup> ; GILLIS, Kathryn<sup>7</sup> ; SNOW, Jonathan<sup>8</sup> ; SHIPBOARD SCIENTIFIC PARTY, Iodp expedition 345<sup>9</sup>

<sup>1</sup>IFREE, JAMSTEC, <sup>2</sup>Department of Earth Sciences, Kanazawa University, <sup>3</sup>AIST, <sup>4</sup>Akita University, <sup>5</sup>Hokkaido University, <sup>6</sup>Okayama University, <sup>7</sup>University of Victoria, B.C., <sup>8</sup>University of Houston, <sup>9</sup>IODP, Texas A&M University

Three-quarters of the ocean crust formed at fast-spreading ridges is composed of plutonic rocks whose mineral assemblages, textures and compositions record the history of melt transport and crystallization between the mantle and the seafloor. However, owing to the nearly continuous overlying extrusive upper crust, sampling in situ the lower crust is challenging. Hence, models for understanding the formation of the lower crust are based essentially on geophysical studies and ophiolites. Integrated Ocean Drilling Program (IODP) Expedition 345 recovered the first significant sections of primitive, modally layered gabbroic rocks from the lowermost plutonic crust formed at a fast-spreading ridge, and exposed at the Hess Deep Rift (Gillis et al., Nature, 2014, doi:10.1038/nature12778).

Keywords: layered gabbro, oceanic lower crust, Hess Deep, fast-spreading ridge, East Pacific Rise, primitive gabbro

## Results of Previous Drilling on Cretaceous Oceanic Plateaus and Future Outlook

SANO, Takashi<sup>1\*</sup> ; NAKANISHI, Masao<sup>2</sup>

<sup>1</sup>National Museum of Nature and Science, <sup>2</sup>Chiba University

Oceanic plateaus, reach volumes of several  $10^6$  to several  $10^7$  km<sup>3</sup>, are characterized by anomalously high rates of mantle melting that represent the largest volcanic events in the Earth's history. There is currently a lively debate about the oceanic plateau volcanism: whether they are built by plume heads from the lower mantle, changes in plate stress, or even meteor impacts. One difficulty with their research is that several of oceanic plateaus (e.g., Kerguelen Plateau) were erupted on remnants of continents where assimilation of continental lithosphere can obscure the primary mantle signature of the lavas. In contrast, Cretaceous oceanic plateaus in the western Pacific (Ontong Java Plateau, Shatsky Rise, and so on) have no effect of the crustal assimilation, permitting its primary origin in mantle to be resolved. The time of productions of the western Pacific plateaus coincides with increases in climate warming, resulting oceanic anoxic event, and eustatic sea level change; and therefore, its origin receives attention from paleo-environment aspects, too. It is proposed that the western Pacific plateaus were formed by the upwelling of very large plume head of mantle material, superplume, that erupted beneath the Pacific basin (Larson, 1991, *Geology*, 19, 547-550). The present-day South Pacific superswell is probably the nearly exhausted remnant of the original upwelling. Moreover, the remnant of the superplume is likely detected by seismic data (e.g., Suetsugu *et al.*, 2009, *Geochem Geophys Geosyst* 10, Q11014).

The plume head phenomenon occurs naturally in numerical and laboratory experiments, but there is currently no unequivocal geological evidence proving that a starting plume head in convecting mantle has operated with Earth. Thus several alternative explanations (described above) or more complex plume head models are proposed to explain origin of the oceanic plateaus.

To test the plume head model, petrological and geochemical data from igneous rocks are important. Although a small number of dredges have recovered basalts from the western Pacific plateaus, almost of all such samples were highly altered. The best way to obtain fresh samples is by drilling of holes. Thus, operations during Ocean Drilling Program (ODP) Leg 192 and Integrated Ocean Drilling Program (IODP) Expedition 324 drilled Ontong Java Plateau and Shatsky Rise, respectively, seeking evidence that would test the plume head hypothesis (Mahoney *et al.*, 2001, *Init Rep ODP*, 192; Sager *et al.*, 2010, *Proc IODP*, 324). Based on drilling of several holes in the oceanic plateaus, both expeditions have extended our knowledge of the compositions and origin of the plateaus magmas considerably. However, both expeditions uncovered complications that do not fit the simple model, so debate over plume head hypothesis continued.

One of the main reasons for the previous failure to test the plume head model is that the previous drilling holes in the oceanic plateaus were too thin; only <300 m basement lavas were recovered among the thick oceanic plateaus (>30 km). The information of such thin drilling holes is difficult to evaluate the plume head model that is proposed by numerical and laboratory experiments. The laboratory experiments of "thermo-chemical" plumes containing both thermal and chemical density anomalies are characterized by a strong time-dependence and could develop for mantle density anomalies lower than 2% (e.g., Kumagai *et al.*, 2008, *Geophys Res Lett*, 35, L16301). Such thermal or chemical density anomalies would be detected by geological researches of long drilling cores (e.g., ~3000 m basement lavas which construct ~10% of total thickness of the oceanic plateaus). To date, such long cores were difficult to recover, but a riser drilling vessel Chikyu has made drilling >3000 m basement lavas technically feasible.

Keywords: oceanic plateau, large igneous province, plume, magma genesis

## Recent progress in paleo- and rock magnetism and its applications produced by IODP

YAMAZAKI, Toshitsugu<sup>1\*</sup>

<sup>1</sup>AORI, University of Tokyo

Paleomagnetists have sailed most of the IODP expeditions, and greatly contributed to the achievement of the aims of individual expeditions. At the beginning of the new phase of IODP, I will review progress in paleomagnetism and rock magnetism and their applications produced by IODP for the last about 10 years.

Results of the two IODP coring programs, one in the North Atlantic (Exp. 303/306) and the other in the east equatorial Pacific (Exp. 320/321), greatly improved our understanding of the past geomagnetic field variations. High-resolution paleointensity records during the Pleistocene with precise age control were obtained from North Atlantic drift sediments. These records led the establishment of the PISO-1500 paleointensity stack, which is now used as the standard curve for paleointensity-assisted chronostratigraphy. Detailed records of polarity reversals and excursions were also obtained. From the equatorial Pacific sediment cores, continuous Miocene to Eocene relative paleointensity records were obtained for the first time, although resolution is not high. Previously, continuous paleointensity records were available only for the last ca. 3 m.y. No discernible relation between paleointensity and polarity length was recognized, despite that a weak positive correlation was suggested previously. On the other hand, volcanic rocks from seamounts (Exp. 330) and oceanic plateau (Exp. 324) were utilized for obtaining absolute paleointensity in the Mesozoic.

Rock- and paleomagnetism was applied to resolve various geological and geophysical problems in IODP. First of all, paleomagnetism contributed progress in the mantle dynamics; paleomagnetic inclinations revealed that the Louisville hotspot did not move in concert with the Hawaiian hotspot (Exp. 330), which is known to have shifted southward about 15 degrees between about 80 and 50 Ma. Magnetic techniques such as the anisotropy of magnetic susceptibility were successfully utilized for studying subduction zone dynamics (NanTroSEIZE, CRIPS). Rock magnetic techniques become widely used in paleoceanographic and paleoenvironmental applications. It was recently revealed using IODP cores that biogenic magnetite prevails in marine sediments (e.g., Exp. 320/321 and 329). Its role to remanent magnetization acquisition processes and potential applications to paleoceanography are attracted attention.

Keywords: paleomagnetism, rock magnetism, IODP, paleointensity

## Chikyu logging review in IODP and future of well logging in scientific drilling

SANADA, Yoshinori<sup>1\*</sup> ; KIDO, Yukari<sup>1</sup> ; KYAW, Moe<sup>1</sup>

<sup>1</sup>JAMSTEC

It has passed seven years since Chikyu joined the IODP expeditions. There were many expeditions where well logging were conducted: NanTroSEIZE exp314 in 2007, expeditions 319 and 322 in 2009, exp332 in 2010, exp338 in 2012-2013, exp348 in 2013-2014; Japan trench fast drilling project (J-FAST) exp343 in 2012; Deep coalbed biosphere off Shimokita exp337 in 2012. The total logged length on Chikyu during IODP Expeditions are 26.2 km in the seven years period. Well logging has increased its importance in science and operations. The reasons are 1) sensor and technological innovation brings more geological and geophysical information, 2) spot or partial interval coring in combination of logging-while-drilling and mudlogging is best option in deepwater expeditions, and 3) need of LWD real time data in decision making for precise location of observatory installation and spot coring. Riser drilling by Chikyu improves hole condition by means of drilling fluid control, which improves logging data quality, and its large hole diameter brings us more selections of tools, measurements, and downhole experiments.

The logging companies have been developing new measurement, higher accuracy and resolution tools. For example, resistivity image tools have wider azimuthal coverage and higher resolution, which help to deeper geological interpretations and breakout analysis. The new sonic tool improves accuracy of velocity in soft sediment and more availability of measurement in shear velocity.

With accessing deeper, more challenging management of time (coring is a time consuming operation), combination of spot coring in the most interesting interval and continuous logging may be one of solutions under limited cruise schedule.

Realtime LWD data acquisition and interpretation were required to install observatory at proper depth. Current LWD technology sends more data to surface, which helps to understand the lithology in real time.

To use large diameter of riser pipes brings us a lot of advantages against lowering logging tools through small drill pipes. Proper tool size and sensor position in the borehole improve data quality. Increasing of tool selection brings more variety of measurement and experiment. FMI resistivity borehole imager covers more image area of borehole wall. Pressure test by dual packer and fluid sampling were available with large diameter tools.

Logging activities and results by Chikyu as part of IODP (2003-2013) will be reviewed and discuss its potential, role, and challenges in the future scientific drilling.

Keywords: logging, Chikyu, IODP

## Mud logging for scientific drilling on D/V Chikyu: results of the past riser operations in the 1st phase IODP

SUGIHARA, Takamitsu<sup>1\*</sup> ; AOIKE, Kan<sup>1</sup> ; MOE, Kyaw thu<sup>1</sup>

<sup>1</sup>CDEX/JAMSTEC

Mud logging has been a key technology for scientific drilling operation by D/V Chikyu. In order to penetrate into deeper formation by riser drilling, full-coring operation to targeted total depth is difficult due to taking much operation time. Therefore mud logging obviously contributes to acquiring continuous geological and geochemical data from formation and circulating fluid in formation to targeted total depth. In the IODP 1st phase, riser drilling operations with mud logging were conducted 4 times by the Chikyu (Expeditions 319, 337, 338, and 348). In this paper, we highlight some results of mud logging operated in the past operation and discuss on technical challenging for future riser operations by the Chikyu.

Mud logging is roughly composed of three components, lithological logging on cuttings, mud gas monitoring, and mud circulation/drilling parameters monitoring. As well known, cuttings lithology logging and mud gas monitoring are important tool to understand geological characteristics beneath drilling site based on results of not only the IODP riser operations by the Chikyu but also ICDP onshore drilling projects (e.g., Unzen and SAFOD). However, potential of mud circulation and drilling parameters monitoring associated with cuttings and mud gas analyses has not been discussed in detail in scientific drilling community. d-exponent is an indicator to detect zone of high pore pressure during drilling and it is well developed in the petroleum industry. d-exponent is defined as normalized rate of penetration (ROP) with rotation speed (RPM) and weight on bit (WOB), and in general case, d-exponent gradually decreases as entering into high pore pressure zone increasing ROP. During Expedition 348, we often faced formation with difficulty of drilling, and supposed there was relatively higher pore pressure zone based on the d-exponent analysis. In this presentation, we will discuss on comprehensive mud logging data analysis including data of d-exponent acquired in the past riser drilling operation and assess its potential for future expeditions.

Keywords: D/V Chikyu, IODP, Mud logging, Cuttings, Mud gas monitoring, Scientific drilling



## Downhole Logging Data Acquisition and Integration: Changing Tactics in the IODP and Its Future Direction

MOE, Kyaw<sup>1</sup> ; KIDO, Yukari<sup>1\*</sup> ; SANADA, Yoshinori<sup>1</sup>

<sup>1</sup>CDEX-JAMSTEC

Since the initiation of IODP in 2003, three drilling platforms, Chikyu, JOIDES Resolution (JR) and Mission Specific Platform (MSP), operated at various environments of global locations using varieties of new techniques. Overcoming many difficulties, longest serving ship JR reached the maximum time in operations with 32 expeditions even ship was modified in dock for 38 months, new riser ship Chikyu with 13 expeditions, and MSP with 5 expeditions. Varying in their capabilities, JR expeditions covered most global areas and research themes where MSP and Chikyu expeditions were targeted to the most challenging and extreme environments. Further addition of riser technology and very shallow locations for MSP brought wider choice of new logging and coring tools, rigfloor parameter, and very high-resolution slim-hole logging tools.

In the downhole logging data acquisition, JR continued her standard set of basic wireline logging with best cost and performance factor but MSP and Chikyu were used expedition/project specific measurements with higher cost and better technology. For the new challenges in the various IODP expeditions, things changed from the previous program were new tools and better measurements, data integration applications and facilities, increased staffing for science support.

Those new techniques covering laboratory and downhole measurements, extended widely in measurement types and improved their capability and efficiency in data integration and onsite decision making. All these large volume of data with wider choice of software further enhanced the integrated studies like cuttings/core-log-seismic integration for the very deep-riser holes.

In this talk, downhole measurements data acquisition and wider data integration in the IODP will be summarized, operational-technical-scientific highlights and lessons will be reviewed, and future direction will be discussed.

Keywords: IODP, Logging, Data Integration, Chikyu, JOIDES Resolution, MSP

## Overview of IODP drilling in Izu-Bonin-Mariana arc

ISHIZUKA, Osamu<sup>1\*</sup> ; TAMURA, Yoshihiko<sup>2</sup>

<sup>1</sup>GSJ/AIST, <sup>2</sup>IFREE, JAMSTEC

What is raw and juvenile continental crust? Furthermore, how does it form and evolve into mature continental crust? The continental crust we observe on the surface of the earth has been deformed, metamorphosed, and otherwise processed perhaps several times from its creation in subduction zones to the present.

Although there are many examples of accreted arc crust on the margins of continents, during- and/or post-collision geochemical changes are widespread, and we do not have the ability to observe active crust-forming processes in modern arcs except by what we can infer from eruptions at the surface, and by remote sensing of arc interiors. ULTRA-DEEP DRILLING INTO ARC CRUST is the best way to sample unprocessed juvenile continental-type crust, to observe these active processes that produce the nuclei of new continental crust, and to examine the nature of juvenile continental crust as first generated at intra-oceanic arcs.

Key questions for comprehending arc crust formation are: (1) What is the nature of the crust and mantle in the region prior to the beginning of subduction? (2) How does subduction initiate and initial arc crust form? (3) What are the spatial changes of arc magma and crust composition of the entire arc? (4) How do the middle arc crust evolve? Possible strategies for answering these questions include drilling by IODP at the Izu-Bonin-Mariana (IBM) arc system. IODP has proposals to drill at the IBM, including three non-riser holes (IBM-1, IBM-2 and IBM-3) and one riser, ultra-deep hole (IBM-4), which answer these questions, respectively, and the four drillings result in comprehensive understanding of the arc evolution and continental crust formation. Drillings by Joides Resolution at three sites (IBM-1, IBM-2 and IBM-3) are scheduled in 2014. This presentation will give an overview of these 3 cruises and their perspectives.

## Tsunami deposits sciences as geohazard research program of ICDP

FUJIWARA, Osamu<sup>1\*</sup>

<sup>1</sup>Active Fault and Earthquake Research Center, AIST

Tsunamis initiated by the 2004 Indian Ocean earthquake (Mw 9.1?9.3) and the 2011 Tohoku-oki earthquake (Mw 9.0) have provided recent demonstrations of the widespread catastrophic damage and loss of life that can be caused by mega tsunamis. Mega tsunamis have dramatic impacts on geological processes as well as on human societies. Large-scale erosion and the mass transport of sediments by tsunamis cause rapid environmental change and biological turnover in coastal areas. Mega tsunamis leave evidence of their passage in the geological record on a time scale far beyond human memory.

Over geological time, mega tsunamis have been caused by events such as subduction-zone earthquakes, volcanic eruptions, landslides (on land and submarine), and meteorite impacts. Large submarine collapses of gas-hydrate-bearing sediments may also have caused mega tsunamis. These facts demonstrate that the risk of catastrophic tsunamis is not limited to active tectonic margins. Although the frequency of these catastrophic events is low compared to a human lifetime, there is no telling when and where the next events will occur.

The 2004 and 2011 events, and the recognition that mega tsunamis have occurred many times on both historical and geological time scales, have prompted international efforts to better understand the hazards associated with tsunamis and to design disaster control strategies at regional and global levels. The foundation on which mega-tsunami risk management is built is hazard assessment, including knowledge of the location, frequency, and magnitude of past events. This basic research leads to a better understanding of the dynamics of geological and biological evolution in coastal regions. Historical documents provide important information for regional analysis of past tsunamis, but their value is limited by the short length of the historical record. Studies of tsunami deposits provide a useful means of extending the length of those records onto a geological time scale.

To solve the above mentioned problems and aim at further development in these study field, following research programs are prospected.

**Understanding past mega tsunamis from geological records.**

- + Mega tsunami events during earth history.
- + Mega tsunami impacts through human history.

**Global coordination of research to develop an inventory of tsunami deposits**

- + Catalogue of mega tsunamis (size, source, age) at plate subduction zones.
- +Catalogue of mega tsunamis (size, source, age) for island countries that have suffered far-field effects of mega tsunamis.

**Outreach to and nurturing of young scientists in the field of tsunami geology**

Keywords: Tsunami deposit, Geohazard, Continental drillig

## Japan Beyond-Brittle Project

ASANUMA, Hiroshi<sup>1\*</sup> ; TSUCHIYA, Noriyoshi<sup>2</sup> ; ITO, Hisao<sup>3</sup> ; MURAOKA, Hirofumi<sup>4</sup>

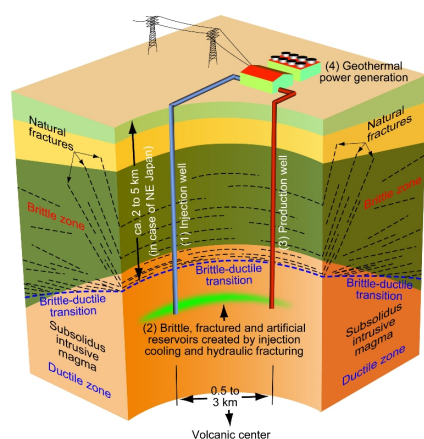
<sup>1</sup>AIST, <sup>2</sup>Tohoku University, <sup>3</sup>Independent Scientist, <sup>4</sup>Hirosaki University

New conventional geothermal energy projects have not been actively promoted in Japan for the last decade because of perceptions of high relative cost, limited electricity generating potential and the high degrees of uncertainties and associated risks of subsurface development. More recently however, EGS (Enhanced Geothermal System) geothermal has been identified as a most promising method of geothermal development because of its potential applicability to a much wider range of sites, many of which have previously been considered to be unsuitable for geothermal development. Meanwhile, some critical problems with EGS technologies have been experimentally identified, such as low recovery of injected water, difficulties in establishing universal design/development methodologies, and the occurrence of induced seismicity, suggesting that there may be limitations in realizing EGS in earthquake-prone compression tectonic zones.

We propose a new concept of engineered geothermal development where reservoirs are created in ductile basement. This potentially has a number of advantages including: (a) simpler design and control of the reservoir, (b) nearly full recovery of injected water, (c) sustainable production, (d) lower cost when developed in relatively shallower ductile zones in compression tectonic settings, (e) large potential quantities of energy extraction from widely distributed ductile zones, (f) the establishment of a universal design/development methodology, and (g) suppression of felt earthquakes from/around the reservoirs.

To further assess the potential of EGS reservoir development in ductile zones we have initiated the "Japan Beyond-Brittle Project (JBBP)". It is intended that the first few years of the JBBP will be spent in basic scientific investigation and necessary technology development, including studies on rock mechanics in the brittle/ductile regime, characterization of ductile rock masses, development of modeling methodologies/technologies, and investigations of induced/triggered earthquakes. We expect to drill a deep experimental borehole that will penetrate the ductile zone in northeast Japan after basic studies are completed. The feasibility of EGS reservoir development in the ductile zone will then be assessed through observations and experimental results in the borehole. An ICDP supported workshop on JBBP has been held March 12-16 in Sendai, Japan, where feasibility, necessary breakthroughs, and roadmap has been discussed from scientific and technological points of view.

Keywords: Geothermal, Brittle-ductile transition, EGS



## Expectations for the new decade of drilling science

YAMADA, Yasuhiro<sup>1\*</sup>

<sup>1</sup>Kyoto Univ

What kind of roles the 'drilling science' should undertake? This presentation proposes directions of 'drilling science' in the coming decades, to bridge the three methods to explore subsurface; exploration geophysics, drilling technology and usage of boreholes, and geology as material science.

## Hydraulic properties and pore structure of the sedimentary rocks at Site C0020, IODP Expedition 337 in Sanriku-oki basin

TANIKAWA, Wataru<sup>1\*</sup> ; TADAI, Osamu<sup>2</sup> ; INAGAKI, Fumio<sup>1</sup> ; KAI-UWE, Hinrichs<sup>3</sup> ; KUBO, Yusuke<sup>4</sup> ; OHTOMO, Yoko<sup>1</sup>

<sup>1</sup>JAMSTEC/Kochi Kore Center, <sup>2</sup>Marine Works Japan Ltd., <sup>3</sup>University of Bremen, <sup>4</sup>JAMSTEC

Microbial biomass in the ocean sediments is controlled by physical, chemical and biological factor and conditions. The biomass in sediments reduces with increasing depth, and the limit of life and the reduction rate of biomass is partly controlled by physical conditions because lithification and diagenesis of oceanic sediments induce reduction of porosity, permeability and pore size. However the relationship between biomass and physical property for deep oceanic sediments is not well known. Therefore, in this study, a series of physical property measurements (Water potential, permeability and porosity) were conducted on the sediment cores at site C0020 from IODP expedition 337 and at site 902 from the Chikyu shakedown cruise (CY06-06) in Sanriku-oki basin. We measured water potential under atmospheric condition and permeability under confining pressure up to 40 MPa. Then we estimated the correlation between water potential and microbial biomass in the sediments.

Keywords: permeability, water potential, water activity, off-Sanriku basin, IODP expedition 337, biomass

## Coring disturbances with the riser drilling system of the D/V Chikyu during IODP Exp. 337 off Shimokita, Japan

MURAYAMA, Masafumi<sup>1\*</sup> ; MORITA, Sumito<sup>2</sup> ; YAMADA, Yasuhiro<sup>3</sup> ; KUBO, Yusuke<sup>4</sup> ; HINRICHS, K-u<sup>5</sup> ; INAGAKI, Fumio<sup>6</sup>

<sup>1</sup>Center for Advanced Marine Core Research, Kochi University, Japan, <sup>2</sup>Institute for Geo-Resources and Environment, National Institute of Advanced Industrial Science and T, <sup>3</sup>Department of Urban Management Engineering, Kyoto University, <sup>4</sup>CDEX, Japan Agency for Marine-Earth Science and Technology, <sup>5</sup>University of Bremen, Germany, <sup>6</sup>Kochi Institute for Core Sample Research, Japan Agency for Marine-Earth Science and Technology

Coring disturbances were observed using the riser drilling system of the D/V Chikyu during IODP Exp. 337 off Shimokita, Japan. Injections of drilling mud and fluid with high density and pressure used in riser drilling during Expedition 337 caused complications to visual core observations. Semiconsolidated materials were commonly observed in this Hole, and drilling mud often easily penetrated the semiconsolidated sandstones and siltstones, causing possible false lamination structure in the cores, which might be misinterpreted as natural sedimentary structure preserved in the cores. Here, we report various kind of coring disturbances which were observed on board with riser drilling system.

Keywords: Coring disturbance, riser drilling, IODP, Exp. 337

## Lithology and XRF analysis data at drilled Site C0020 off the Shimokita Peninsula, IODP Exp. 337

MURAYAMA, Masafumi<sup>1\*</sup> ; HIGASHIMARU, Naotsugu<sup>1</sup> ; IJIRI, Akira<sup>2</sup> ; INAGAKI, Fumio<sup>2</sup>

<sup>1</sup>Center for Advanced Marine Core Research, Kochi University, Japan, <sup>2</sup>KCC/JAMSTEC

Marine subsurface hydrocarbon reservoirs and the associated microbial life in continental margin sediments are among the least characterized Earth systems that can be accessed by scientific ocean drilling. We penetrated a 2,466 m-deep sediment sequence with a series of coal layers around 2 km below the seafloor. Here, we present the 160 XRF data and lithology of sediments and paleoenvironments from drilling Site C0020, IODP Expedition 337. We defined four different lithologic units present in Site C0020. The succession of lithofacies at Hole C0020A also provides insight into the evolution of depositional environments in this region.

Keywords: Lithology, XRF, IODP, Exp.337



## Structural characteristics of Nankai accretionary prism at C0002: Preliminary results from IODP Expedition 348

YAMAMOTO, Yuzuru<sup>1\*</sup>; OHTSUBO, Makoto<sup>2</sup>; BROWN, Kevin<sup>3</sup>; CRESPO-BLANC, Ana<sup>4</sup>; EXPEDITION 348, Scientist<sup>5</sup>

<sup>1</sup>JAMSTEC, <sup>2</sup>AIST, <sup>3</sup>SCRIPS, <sup>4</sup>University of Granada, <sup>5</sup>IODP Expedition 348

Integrated Ocean Discovery Program (IODP) Expedition 348 has deepened hole down to 3058.5 mbsf at Site C0002, and collected cutting and core samples of Upper Miocene Nankai accretionary prism. The structural key observation made on cuttings in Holes C0002N and C0002P, and cores retrieved in Hole C0002P are:

a) The structures observed in intact cuttings include slickenlined surfaces, scaly fabric, deformation bands, minor faults and mineral veins. Slickenlines are observed throughout the whole interval, but scaly fabric is increasingly observed below ~2200 mbsf. The other types of structures are scattered throughout the whole section.

b) The cored interval is characterized by steep bedding planes (more than 75°). A fault zone, 90 cm in thickness, with a few mm-size angular clasts is present in one of the cores (2204.9~2205.8 mbsf). In its present position, the brittle fault zone is associated with a normal faulting sense. It is unclear if this represents an early thrust rotated after its development or late normal fault.

c) SEM images in the upper part of Hole C0002N show little evidence for opal diagenesis, implying  $T < 60-80$  °C at 1225.5 mbsf. In Hole C0002N, the fabric lacks a strongly preferred orientation in clay-rich materials, except along striated micro-faults formed by clays. These zones are extremely localized with a thickness of a few microns or less. In Hole C0002P, below 2200 mbsf, SEM images show the development of a regularly spaced fabric in sandstones, constituted by thin (<0.1 μm), clay-dominated shear planes. Towards the base of the hole, below 2625 mbsf, compaction fabrics in clay-rich materials can be observed. Very thin shear zones with almost no wall damage zone have cut this fabric.

The overall character of the deformation (independent particulate flow with limited evidence for cataclastic deformation) is suggestive of that deformations occurred in a relatively shallow environment (approximately 0-4 km in burial depth).

Keywords: Expedition 348, C0002, Fault zone, Core, Cuttings

## Seismic reflection survey investigating subduction inputs at the Sagami Trough

MIURA, Seiichi<sup>1</sup> ; NO, Tetsuo<sup>1\*</sup> ; SATO, Takeshi<sup>1</sup> ; YAMASHITA, Mikiya<sup>1</sup> ; SAITO, Saneatsu<sup>1</sup> ; TAKAHASHI, Narumi<sup>1</sup> ; KODAIRA, Shuichi<sup>1</sup>

<sup>1</sup>Japan Agency for Marine-Earth Science and Technology

The Sagami Trough is a plate convergent zone of the Philippine Sea Plate underneath the NE Japan including the Kanto area. Varied seismic events occurred associated with the plate convergence. Magnitude (M) 8-class earthquakes, for example 1703 Genroku and 1923 Taisho-Kanto events, damaged the Kanto area seriously. On the other hand, slow-slip events have been observed in the Boso area with 5-7 year interval, whose released energies were comparable to Mw 6. Source depths of the M8-class earthquakes and slow-slip events are almost same. One possible reason of the varied seismogenesis is different subduction inputs at the Sagami Trough. To understand the varied seismogenesis, structural and material information are important. A drilling proposal for subduction input at the Sagami Trough is planned to be submitted. Japan Agency for Marine-Earth Science and Technology was conducted a seismic reflection survey in April, 2013 at the southward of the Sagami Trough on the Philippine Sea Plate. Although a planned seismic line had been 270-km length at the 50-km southward of the trough in WNW-ESE direction, acquired data is limited in half of the planned line for rough weather from volcanic front to landward slope of the trench axis, showing sediment distribution and basement morphology. Sediments can be divided in three units. Basement morphology is rugged as basement highs reaching seafloor at the volcanic front and rising at the Frontal Arc and Outer Arc High of the former arc in the Izu-Ogasawara area, and as depressions as 4-km from seafloor filled by thick sediments. The sediments and basement are comparable to those in the vicinity of the Sagami Trough using conducted seismic profiles at the cross points. In this presentation, we will show the seismic profiles around the Sagami Trough, deduce the ages and materials of sediments and basements comparing previous results, infer the subduction inputs of the Sagami Trough, and discuss the seismogenesis around the Sagami Trough.

Keywords: MCS survey, Sagami Trough, subduction input

## Core quality evaluation with X-CT data

KUBO, Yusuke<sup>1\*</sup> ; AOIKE, Kan<sup>1</sup>

<sup>1</sup>CDEX, JAMSTEC

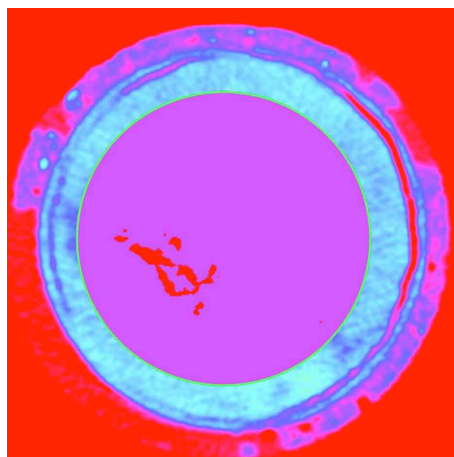
X-ray Computed Tomography (X-CT) is a powerful tool for an observation of internal structures and conditions of core samples. In the laboratory of D/V Chikyu, X-CT data has been used in initial evaluations of sample lithology, structure and physical properties such as density, before splitting the sample. In addition, the non-destructive measurement is particularly useful to evaluate the sample quality, based on which we can optimize the sampling and sample distribution plan. For example, intact pieces are passed to high-priority and contamination-sensitive analyses after observation of X-CT image. However, the evaluation of core quality has been mostly based on visual observation. While visual observation is good for quick evaluation, it sometimes lacked consistency and detailed survey.

In this study we propose a quantitative way to evaluate the core quality from X-CT data. The core quality index (CQI) is calculated as the ratio of area with CT value higher than a threshold value in a sliced image of core sample. The threshold value is determined from the representative CT value in the core section and varies depending on lithology. The data in the region of interest, which is 15 cm<sup>2</sup> of central part of core sample, is binarized with the threshold value to provide normalized index through all sections. The plot of CQI reveals the position and degree of damages inside a core sample.

The method is applied to X-CT data of a total of 176 sections from IODP Exp 337. The results show that CQI profile clearly differentiates intact part and disturbed part of core section. Comparison with other core quality indicators in pore water chemistry and chemical tracer experiments suggests that CQI can be used to identify intervals suitable for contamination-free sampling.

The figure shows an example of binarized X-CT slice of a core sample. Red in the central part (purple) shows porous part in the core sample.

Keywords: Chikyu, IODP, X-CT, core sample



## Comparison of seabeds at <2000 m in water depth off Miyagi before and after the 2011 Tohoku-Oki earthquake

WADA, Ayaka<sup>1</sup> ; KAWAMURA, Kiichiro<sup>1\*</sup> ; ROMER, Miriam<sup>2</sup> ; STRASSER, Michael<sup>3</sup> ; FINK, Hiske<sup>2</sup> ; ARAI, Kazuno<sup>4</sup> ; HINO, Ryota<sup>5</sup> ; ITO, Yoshihiro<sup>6</sup> ; FUJIKURA, Katsunori<sup>7</sup>

<sup>1</sup>Yamaguchi University, <sup>2</sup>University of Bremen, <sup>3</sup>ETH Zurich, <sup>4</sup>Chiba University, <sup>5</sup>Tohoku University, <sup>6</sup>Kyoto University, <sup>7</sup>JAMSTEC

The 2011 Tohoku-Oki earthquake of Mw 9.0 occurred on 11 March 2011. This earthquake excited large tsunamis, which were generated turbidity current as a tsunamigenic turbidity current (Arai et al., 2013). We do not know well how such turbidity currents will record in sediments in the future.

We investigated the impact of the tsunamigenic turbidity currents by seabed observations. Additionally, we discussed how the tsunami event will be preserved in deep-sea sediments.

We observed the video data of six dive surveys. The two dive surveys of 3K#483 and 2K#1220 have done on 5 September 2000 and on 19 September 2000 during the cruise NT00-09 by R/V NATSUSHIMA. A deep-sea camera survey of YKDT#100 has done on 21 June 2011 during the cruise YK11E-04 Leg 2 using R/V YOKOSUKA. The site P08 was dived on 25 September 2011 during the cruise by HAKUYO3000. OFOS-1 and -2 were dived on 18 March 2012 during the cruise SO219A by R/V SONNE. In addition, seabed sectional view were made by PARASOUND in the cruise SO219A.

We observed the change of seabed before and after the Tohoku-Oki earthquake. We could see various alive benthic animals (e.g. sea anemones, sea pens and star fishes) on the muddy mounded seabed. There are no strong flow signals being a strong bottom current from the video observations. We found many dead bodies of benthic animals which were covered with bacterial mats by YKDT#100 and P08 videos. The size of bacterial mats was about 1 m in diameter. After one year from the earthquake, the size of bacterial mats had become small about 10 cm in the OFOS video data. Therefore, the bacterial mats were made after earthquake by seabed disturbance, but bacterial mats would not record in sediment.

On the other hand, we found lines of evidence on the turbidity current which have the potential of preservation in sediments. We observed the bio-fragments scattered on seabed by YKDT#100 and OFOS videos. We measured these direction and we found majority of these faced the SW-NE. Thus, these indicate the direction of the strong flow (e.g. turbidity current) in recent. Our results support the direction of the turbidity current indicated by Arai et al.,(2013). The benthic animals as bio-fragments would record in sediments and would become evidence of tsunami/earthquake events.

Keywords: R/V SONNE, Tsunami deposit, biofragment, paleocurrent

## Evidence of Tohoku-oki earthquake in the deep sea sediment

KANAMATSU, Toshiya<sup>1\*</sup> ; IKEHARA, Ken<sup>2</sup> ; USAMI, Kazuko<sup>2</sup>

<sup>1</sup>Japan Agency for Marine-Earth Science and Technology, <sup>2</sup>Institute of Geology and Geoinformation, National Institute of Advanced Industrial Science and Techn

A study on differences in bathymetric data between before and after 2011 Tohoku-Oki earthquake revealed a large coseismic displacement of the overriding plate, and a seafloor elevation in the Japan Trench axis (e.g. Fujiwara et al. 2012). Detail sub-seafloor structures around the axis obtained after the earthquake image offscraped trench and incoming sediments due to compression during coseismic slip in the plate interface close to the trench (Kodaira et al. 2012, Nakamura et al. 2013). Strasser et al. 2013 suggests that a large scale slump of the wedge toe significantly impacted the geometry and evolution of the plate boundary in the axis of Japan Trench based on data from sediment samples. Kawamura et al., 2012 and Tsuji et al., 2013 also point out that the coseismic displacement of the wedge. These recent researches indicate that remarkable co-seismic deformation and displacement occurred in the toe of slope near to the trench in the case of 2011 Tohoku earthquake. Thus geological evidences for the phenomenon should be recorded in the sediment around the trench axis. We have conducted research cruises to collect surface sediments in order to seek such features as evidences for 2011 and past Tohoku earthquakes. Piston cores were collected from the trench axis and the landward slope in Japan Trench by R/V "Mirai" and R/V "Sonne" in 2012. Intervals in the upper several ten-cm consisting of turbidite units which have been formed just after the earthquake were recovered from the trench axis. This discovery demonstrated that the trench axis is one of the feasible areas to reconstruct Tohoku earthquake history. As ensuring, the older turbidites were also recovered in the area. Contrarily debrite and inclined strata were recovered from the surface of landward slope near to the trench. Those lithologies could be evidences for the wedge displacement or slope failure induced by 2011 or past earthquakes. In the landward slope of Japan Trench, the elongated terrace developed in water depth of 4,000-6,000m is another interesting area to seek evidence related to Tohoku earthquakes. We collected sediment samples from the depth widely using R/V "Natsushima". Frequent thin turbidite occurrences were identified in the several cores. Ductile deformations, probably induced by slope failures, recognized in three cores. Those features could be regarded as evidences of past-other Tohoku earthquakes. Thus it is worth researching farther in these deep-sea areas of Japan trench to document the Tohoku earthquake record. Documentation spatiotemporal distribution of such geological evidences will improve our understanding of Tohoku earthquakes.

Keywords: 2011 Tohoku-oki earthquake, Japan Trench, deep sea sediment

## Turbidites collected from the Japan Trench inner slope, during the NT13-19 cruise

USAMI, Kazuko<sup>1\*</sup> ; IKEHARA, Ken<sup>1</sup> ; MCHUGH, Cecilia<sup>2</sup> ; KANAMATSU, Toshiya<sup>3</sup>

<sup>1</sup>Geological Survey of Japan, AIST, <sup>2</sup>JAMSTEC / Queens College, C.U.N.Y., <sup>3</sup>JAMSTEC

To understand the recurrence of large earthquakes along the Japan Trench, we collected 24 sediment cores from the Japan Trench inner slope, 37.5-40 N, 143.5-144.16 E, water depth 4000-6000 m, during the NT13-19 cruise. Many deep-sea turbidites were intercalated in the sediment cores. We examined the interval and structures of the turbidites using soft-X radiographs. In general, number of the turbidites in a core is high in the southern part off Sendai, but is low in the northern part off Miyako. Meanwhile, intercalated tephra such as Haruna-Ikaho (Hr-FP), Towada-Chuseri (To-Cu) and Towada-a (To-a) were identified in the 13 cores. Based on the eruption ages of the tephra, we estimated the averaged recurrence intervals of 100-500 years in average in almost cores. But there are cores that display different intervals over 1500-2000 years.

Keywords: earthquake, Japan Trench, turbidite, tephra

## Tsunami-generated turbidite as a proxy for large-scale earthquakes

NARUSE, Hajime<sup>1</sup> ; ARAI, Kazuno<sup>2\*</sup>

<sup>1</sup>Graduate School of Science, Kyoto University, <sup>2</sup>Graduate School of Science, Chiba University

We summarize the researches of tsunami-generated turbidites, and examine their possibility to be a proxy for ancient earthquakes. A tsunami-generated turbidity current is a kind of seismically triggered turbidites. Arai et al. (2013) reported the first real-time record of a turbidity current associated with a great tsunami. It was recognized after the Mw 9.0, 2011 Tohoku-Oki event offshore Japan. After the 2011 Tohoku-Oki earthquake and tsunami. An anomalous event on the seafloor consistent with a turbidity current was recorded by ocean-bottom pressure recorders and seismometers deployed off Sendai, Japan. Freshly emplaced turbidites were collected from a wide area of seafloor off the Tohoku coastal region. These measurements and sedimentary records to determine conditions of the modern tsunamigenic turbidity current. It can be anticipated that this discovery is a starting point for more detailed characterization of modern tsunamigenic turbidites, and for the identification of tsunamigenic turbidites in geologic records.

Keywords: Earthquake, turbidite, sediment gravity flow, tsunami

## An abrupt seafloor water-temperature increase in the epicentral region of the 2011 Tohoku earthquake

INAZU, Daisuke<sup>1\*</sup> ; ITO, Yoshihiro<sup>2</sup> ; SAFFER, Demian<sup>3</sup> ; HINO, Ryota<sup>4</sup>

<sup>1</sup>NIED, <sup>2</sup>Kyoto University, <sup>3</sup>The Pennsylvania State University, <sup>4</sup>Tohoku University

We report an abrupt seafloor water-temperature increase observed just after the 2011 Mw9 Tohoku earthquake. Ocean bottom pressure variations during the Tohoku earthquake were observed by a deployment of pressure gauges at eight stations in the epicentral region (Ito et al. 2013 Tectonophys.). The temperature sensors for pressure sensor compensation built into the pressure gauges recorded seawater temperature variations that are presented here.

The temperature data documented the following. Abrupt temperature increases were evident at two stations (TJT1 and GJT3: ocean depth of 3000-6000 m) where maximum slip occurred during the Tohoku earthquake. The temperature increases started less than 10 hours after the earthquake occurrence, reaching up to 0.1 °C above background temperature, and last for a few weeks. Comparable temperature increases were not evident at other stations farther landward, where the ocean depth is less than 2000 m. Prior to the Tohoku earthquake, there were no temperature changes related to other earthquakes at any of the stations. Thus the observed temperature increases are probably associated with the Tohoku earthquake, particularly in the region of maximum coseismic slip.

Geochemical analyses of the seawater sampled near the seafloor suggest that formation pore water was released in the region of maximum coseismic slip following the earthquake. The pore water was thought to originate at about 1 km below seafloor, based on analysis of methane (Kawagucci et al. 2012 Sci. Rep.), with a contribution from the mantle at deeper than 15 km below seafloor as suggested by helium isotope analysis (Sano et al. 2014 Nat. Comm.).

Here we suppose that the observed temperature anomaly is related to pore water release from greater than 1-km depth. In order to explain the timing of the temperature anomalies, required flow velocity of the released water is  $>10^{-1}$  m/s. This is several orders of magnitude more than typical velocities of background fluid flow driven by dewatering of subduction zone sediments ( $10^{-9}$  m/s) (e.g., Sreaton and Saffer 2005 EPSL). The high velocities ( $>10^{-1}$  m/s) most likely reflect fluid flow due to enhanced permeability along fractures and fissures (Tsuji et al. 2013 EPSL) extending to depths of kilometers or more below seafloor, generated by the greatest slip of the Tohoku earthquake.

Keywords: Seafloor water temperature, 2011 Tohoku earthquake



## A sedimentological and paleomagnetic study of deep-sea sediments collected from the Sagami trough

NAKAJIMA, Arata<sup>1\*</sup> ; KAWAMURA, Kiichiro<sup>1</sup> ; KANAMATSU, Toshiya<sup>2</sup> ; SAITO, Saneatsu<sup>2</sup> ; MURAYAMA, Masafumi<sup>3</sup>

<sup>1</sup>Yamaguchi University, <sup>2</sup>JAMSTEC, <sup>3</sup>Kochi University

### Introduction

M7-8 class earthquakes occur repeatedly in the Kanto region, central Japan. We have studied earthquake history around the Kanto region using mainly distribution and geologic age of marine terraces so far (Shishikura, 2012). In contrast to the terrestrial study, we have discussed to identify any seismogenic events from deep-sea sediments (Ikehara, 2001). Recently, Noda et al. (2008) suggested that we could exclude mostly flood deposits by choosing the sampling site carefully. Thus, paleoseismology was developing by these previous studies.

In this study, we collected deep-sea sediments from west Sagami Bay. We described the sediments sedimentologically and paleomagnetically in detail. We discussed a sedimentary process and challenged to extract the earthquake history in the region from these data.

### Studied specimens

We collected two cores from a gentle submarine slope (KT-12-35 PC01; 35:04.00N, 139:12.99E, water depth 991 m and KT-12-35 PC03; 34:58.30N, 139:13.40E, water depth 1,235 m) using a piston corer during the cruise KT-12-35 of Taisei-maru in December 2012. Ikehara et al (2012) reported probable seismogenic turbidites nearby these coring sites.

### Results and discussion

We described and measured the two cores PC01 and PC03 as follows.

1. Sample description using microscope: PC01 and PC03 were mainly olive black hemipelagic sediments including foraminifers and diatoms. Both core were observed several volcanic ash layers and sand layers.

2. X-ray CT analysis: Many sandy clay layers in the hemipelagic sediment layers were confirmed by the difference of CT value. These sandy layers would be event layers (e.g. seismogenic and/or flood events).

3. Physical properties: The porosities in PC01 and PC03 decrease from 72% to 58% and from 76% to 65% with increasing burial depth, respectively. The porosity decreases should result from burial consolidation.

4. Magnetic properties: We analyzed simply a paleocurrent direction using anisotropy of magnetic susceptibility and paleomagnetism. The paleocurrents were roughly judged from E to W in PC01 and PC03 throughout the cores.

5. Volcanic glass: Index properties of volcanic glasses was measured at two horizons at 11 cm and 95 cm below seafloor (hereafter cm-bsf) in PC03. We could identify the 1707 Fuji Houei eruption at 11 cm-bsf and the 838 Tentsujima Tenjyouzan eruption at 95 cm-bsf.

6. C14 dating: We measured C14 for age determination at two horizons at 136 cm-bsf in PC01 and 172 cm-bsf in PC03. We collected  $30820 \pm 210$ BP and  $2850 \pm 30$ BP, respectively. We could calculate the average sedimentation rates as 64 cm/kyr in PC03 and 4 cm/kyr in PC01, even though we could identify the geologic age only at one horizon in PC01.

Based on these results, we discuss the recurrence intervals of the event layers and its depositional processes.

Keywords: Sagami trough, Seismic deposit, XrayCT, Volcanic glass, C14 dating, Magnetic properties

## DEVELOPMENT OF MULTI-PARAMETER BOREHOLE SYSTEM TO EVALUATE THE EXPECTED LARGE EARTHQUAKE IN THE MARMARA SEA, TURKEY

OZEL, Oguz<sup>1\*</sup> ; GURALP, Cansun<sup>2</sup> ; PAROLAI, Stefano<sup>3</sup> ; BOUCHON, Michel<sup>4</sup> ; KARABULUT, Hayrullah<sup>5</sup> ; AKTAR, Mustafa<sup>5</sup> ; MERAL OZEL, Nurcan<sup>5</sup>

<sup>1</sup>Istanbul University-Turkey, <sup>2</sup>Guralp Systems-UK, <sup>3</sup>Geoforschungszentrum-Germany, <sup>4</sup>CNRS-France, <sup>5</sup>Kandilli Observ. & Earthq. Res. Inst.-Turkey

The Istanbul-Marmara region of northwestern Turkey with a population of more than 15 million faces a high probability of being exposed to a hazardous earthquake. The 1999 Izmit earthquake in Turkey is one of the best recorded in the world. For the first time, researchers from CNRS and Kandilli Observatory (Istanbul) observed that the earthquake was preceded by a preparatory phase that lasted 44 minutes before the rupture of the fault. This phase, which was characterized by a distinctive seismic signal, corresponds to slow slip at depth along the fault. Detecting it in other earthquakes might make it possible to predict some types of earthquakes several tens of minutes before fault rupture.

In an attempt to understand where and when large earthquakes will occur, and the physics of the source process prior to large earthquakes, we proposed to install multi-parameter borehole instruments in the western part of Marmara Sea in the frame of an EU project called MARSITE. This system and surrounding small-aperture surface array is planned to be capable of recording small deformations and tiny seismic signals near the active seismic zone of the North Anatolian Fault passing through the Marmara Sea, which should enable us to address these issues.

The objective is to design and build a multi-parameter borehole system for observing slow deformation, low-frequency noise or tremors, and high frequency signals near the epicentral area of the expected Marmara earthquake. Furthermore, it is also aimed to identify the presence of repeating earthquakes and rupture nucleation, to measure continuously the evolution of the state of stress and stress transfer from east to west with high resolution data, and to estimate the near-surface geology effects masking the source related information. The proposed location of the borehole system is right on the Ganos Fault and in a low ambient noise environment in Gazikoy in the western end of the North Anatolian Fault in the Marmara Sea, where the Ganos Fault goes into the Marmara Sea. The proposed instrumentation will be consisted of broadband seismometer with very wide dynamic range, strainmeter, tiltmeter, hydrostatic pressuremeter and thermometer. These instruments will be installed in 150m deep borehole. Additionally, a surface microearthquake observation array, consisting of 8-10 seismometers around the borehole will be established to obtain continuous high resolution locations of micro-seismicity and to better understand the existing seismically active structures and their roles in local tectonic settings.

Keywords: Borehole system, repeating earthquakes, slow motion, microearthquake activity, rupture nucleation, MARSITE

## Seabed topography and geologic structure of 2000~3500 m in water depth, off Miyagi prefecture

HAMADA, Mari<sup>1</sup> ; KAWAMURA, Kiichiro<sup>1\*</sup> ; NAKAMURA, Yasuyuki<sup>2</sup> ; KODAIRA, Shuichi<sup>2</sup>

<sup>1</sup>Yamaguchi University, <sup>2</sup>JAMSTEC

### Introduction

After three days from the 2011 Tohoku-oki earthquake, an emergency seismic survey was carried out in the Japan trench area, off Iwate and Miyagi. By this surveys, we collected seismic reflection images along 16 survey lines from fore-arc basin area at 2500 - 3500 m in water depth to trench floor area at ~7000 m in water depth. We analyzed in detail geologic architecture of the fore-arc basin mainly in the 14 seismic reflection images across the Japan trench.

### Research Overview

The fore-arc basin of the Japan trench consists of two sedimentary units; Paleogene and Neogene. At the base of the Paleogene unit, an Oligocene unconformity overlies Cretaceous rocks. Because of the complexity of the geologic architecture in the Japan trench, it could not easily decipher the spatial distribution of the sedimentary units.

### Results and discussion

Based on the observations of 14 seismic reflection images, we noticed same structural features in the fore-arc basin region (e.g. thickness of seismic units, active faults, deformation structures, topography and so on), so that we divided the region into 5 areas as follows.

#### Area 1:

It is characterized by a thick seismic unit (probably Paleogene unit) above the Oligocene unconformity. The sides of this area are bounded by faults or folds. These features can be seen about 100 km from north to south. This unit thickening might be related to wedge extensional processes as shown in Tsuji et al. (2013).

#### Area 2:

The feature of the Area 2 is similar to that of Area 1. But we found two different points from the Area 1; 1) the continuity of the Area 2 is about 50 km from north to south. This is a half continuity of the Area 1. 2) the Area 2 is located further east (sea) side from the Area 1.

#### Area 3:

It is characterized by erosive features. This area is located in north of Area 2, but there are not features associated with Area 2. This erosive feature might be related to long-term erosion by subduction erosion processes as shown in von Huene et al. (1989).

#### Area 4:

This area is characterized by landward dipping Neogene sedimentary units. The depositional centers were shifted from sea (east) side to land (west) side. This shift might be related to tectonic erosion as shown in Arai et al. (2007).

#### Area 5:

This area is characterized by several active faults that extend and dislocate the seabed. This area is located relatively near the hypocenter of 2011 Tohoku-Oki earthquake, so that here might be active in recent.

### Concluding remarks

In this analysis, we found five unique areas in the fore-arc basin region. These features would be a key to understanding for a further study associated with global and long-term tectonics in this region.

Keywords: Japan Trench, Seismic survey, Forearc Basin, Unconformity, 2011 Tohoku-Oki earthquake

## The development of the self pop-up ocean bottom pressure gauge (OBP) with precision thermometers attached

SUZUKI, Syuichi<sup>1\*</sup> ; ITO, Yoshihiro<sup>2</sup> ; HINO, Ryota<sup>3</sup> ; INAZU, Daisuke<sup>4</sup> ; OSADA, Yukihito<sup>3</sup>

<sup>1</sup>Graduate School of Science, Tohoku University, <sup>2</sup>Disaster Prevention Research Institute, Kyoto University, <sup>3</sup>International Research Institute of Disaster Science, Tohoku University, <sup>4</sup>National Research Institute for Earth Science and Disaster Prevention

We have installed autonomous ocean bottom pressure recorders (OBPRs) off Miyagi and off Nemuro to observe seafloor vertical displacements in response to large earthquakes and aseismic slip. Most notably, an uplift of 5 m due to the 2011 Tohoku-Oki earthquake (Ito et al., 2011) and transient crustal deformations accompanied by slow slip events that occurred before the earthquake (Ito et al., 2013) were measured by the OBPRs which had been installed off Miyagi since 2008. Recent our observations on seafloor show a seawater-temperature anomaly after the 2011 Tohoku-Oki earthquake (Arai et al., 2013.) Here we show our new OBPRs with precise thermometers to observe both of vertical displacement and temperature anomaly on seafloor.

We design the new OBPR with two precise thermometers. The two thermometers are exterior to our ordinal OBPR. A quartz crystal pressure sensor within the ordinal OBPR is firstly equipped with a thermometer, which is used for temperature compensation of output frequency of quartz oscillator. This means the thermometer with the ordinal OBPR measures a temperature within the vessel of the pressure sensor. By the new attached two thermometers, a actual seawater-temperature are measured accurately.

The development of OBPs with precise thermometers attached enables us to record temperatures of seafloor and seawater along with OBP observations. We are planning to deploy these newly developed OBPs around Japan trench and east off North Island of New Zealand. Especially at the landward Japan Trench slope, increase in the amount of water discharge has been reported by the submarine observation after the 2011 Tohoku-Oki earthquake. Therefore, the installation of the new OBPs with thermometers around this area is expected to allow us to observe not only the seafloor vertical displacements accompanying the postseismic deformation but also the time variation of seafloor water temperature associated with the time variation of the amount of water discharge.

Keywords: Two precise thermometers, Sea-bottom water temperature, Ocean bottom pressure gauge

## Sources of freshwater to the Antarctic continental shelf -distributions and multi-decadal changes-

AOKI, Shigeru<sup>1\*</sup>

<sup>1</sup>ILTS, Hokkaido University

The Antarctic continental shelf is the gateway to the global ocean from the Antarctic Ice Sheet, the largest freshwater reservoir on Earth surface. Discharge of the freshwater occurs as the processes such as basal melting of ice shelves and calving of icebergs. On the other hand, sea ice formation and melting on the shelf redistribute the freshwater, affecting the overturning circulations of oceans. These two processes of freshwater transport are closely related to the surrounding oceanic and atmospheric conditions, and therefore estimating their contributions and clarifying their relationships with underlying environments are necessary to quantify the overall impacts to the ocean and its temporal change.

From observed salinity and stable oxygen isotope ratio of sea water with a few assumptions applied, meteoric and sea ice fractions in sea water are estimated on the shelf and their geographical distributions are studied. Meteoric ice fraction is largest in the surface layer of West Antarctica, but the water column inventory is largest in the Ross Sea and surprisingly uniform around Antarctica. The column inventory of meteoric ice retains the broadly consistent signature of ice shelf basal melting, which is proposed by the recent studies, but its oceanic stock is rather homogenized due to the effects such as oceanic advection and basin-scale circulation. Sea ice fraction contributes large production in the areas of strong katabatic wind and shows negligible production/net melting in the West and central East Antarctica. The vigorous vertical mixing due to high production also distributes the meteoric fraction to a wider depth range.

Observed salinity trend suggests a possibility of temporal change in these freshwater transports. The salinity trend at the bottom of the shelf for the recent four decades reveals the salinification in the West Antarctica and freshening in the Ross Sea. Repeated observations on the shelf region off the Adélie Land Coast indicate freshening for the recent two decades. These signatures might be consistent with the accelerating discharge of the west Antarctic ice sheet. The signatures are consistent with the structure of the recent salinity change of Antarctic Bottom Water, suggesting the on-going impact of the Antarctic shelf on the global scale.

## The fourth Antarctic Bottom Water: Cape Darnley Bottom Water

OHSHIMA, Kay I.<sup>1\*</sup>; FUKAMACHI, Yasushi<sup>1</sup>; WILLIAMS, Guy D.<sup>2</sup>; NIHASHI, Sohey<sup>3</sup>; TAMURA, Takeshi<sup>4</sup>; KITADE, Yujiro<sup>5</sup>; HIRANO, Daisuke<sup>5</sup>; AOKI, Shigeru<sup>1</sup>; WAKATSUCHI, Masaaki<sup>1</sup>

<sup>1</sup>Institute of Low Temperature Science, Hokkaido University, <sup>2</sup>Antarctic Climate and Ecosystem Cooperative Research Centre, University of Tasmania, Australia, <sup>3</sup>Tomakomai National College of Technology, <sup>4</sup>National Institute of Polar Research, <sup>5</sup>Tokyo University of Marine Science and Technology

Antarctic Bottom Water (AABW) is the cold, dense water that occupies the abyssal layer of the global ocean, accounting for 30-40 % of its mass (Johnson, 2008). The production of AABW is a key process in the global overturning circulation, representing a significant sink for heat and CO<sub>2</sub>. It is currently recognized that AABW is formed in the Weddell Sea, the Ross Sea and off the Adelie Coast (Orsi et al., 1999). A fourth variety of AABW has been identified in the eastern sector of the Weddell-Enderby Basin (Meredith et al., 2000). However, its production has never been observed, nor its exact dense shelf water (DSW) source located. Recently, satellite-derived estimates of sea ice production suggest that the Cape Darnley Polynya (65-69E), located northwest of the Amery Ice Shelf, has the second highest ice production after the Ross Sea Polynya (Tamura et al., 2008). As such, this polynya is promoted as a strong candidate for DSW source of the AABW identified in the Weddell-Enderby Basin.

As part of the Japanese International Polar Year program, we conducted mooring observations in 2008-2009 offshore from the Cape Darnley Polynya, and revealed that the enhanced sea-ice production in this polynya is the missing source of the AABW (Ohshima et al., 2013). Moored instruments observed overflows of newly formed AABW, about 300 m thick and bottom-intensified, cascading down the canyons north of Cape Darnley. We propose to name this AABW Cape Darnley Bottom Water (CDBW). This result is novel because this AABW is produced purely from sea-ice production without the assistance of an ice shelf and/or large storage volume on the continental shelf, in contrast to the traditional paradigm. We therefore speculate that there could be further AABW-formation discoveries in similar polynyas, particularly those in East Antarctica.

We estimate that 0.3-0.7 Sv of DSW is transformed into CDBW, accounting for 6-13 % of the circumpolar total. The CDBW migrate westward, and increase its volume by gradual mixing with Circumpolar Deep Water, to ultimately constitute part of the AABW in the Weddell Sea (Atlantic sector) referred to as Weddell Sea Deep Water (WSDW). Production of WSDW originating from CDBW is estimated to be 0.65-1.5 Sv, which is about 13-30 % of the Atlantic AABW production. The WSDW is a major component of the AABW driving the lower limb of the meridional overturning circulation (MOC) of the Atlantic Sector. It has been reported that WSDW has been warming since the 1980s, with its volume possibly contracting (Purkey and Johnson, 2012), and that this could result in a weakening of the MOC. Additionally, sediment-core records taken around the CDP indirectly suggest that there has been millennium-scale variability in the local AABW production. It is vital that CDBW be incorporated into the global assessment of the MOC, a key element of the climate system. This will improve numerical simulations predicting its response to long-term climate change.

Keywords: Antarctic Bottom Water, coastal polynya, sea-ice production, dense shelf water, mooring, Cape Darnley

## Southern Ocean: the key factor of climate change

TAMURA, Takeshi<sup>1\*</sup> ; SHIMADA, Keishi<sup>2</sup> ; MATSUMURA, Yoshimasa<sup>3</sup> ; KUSAHARA, Kazuya<sup>3</sup> ; SATO, Tatsuru<sup>3</sup> ; NOMURA, Daiki<sup>3</sup>

<sup>1</sup>National Institute of Polar Research, <sup>2</sup>Tokyo University of Marine Science and Technology, <sup>3</sup>Institute of Low Temperature Science

Ocean keeps a lot of heat, oxygen, CO<sub>2</sub>, and nutrients, and transports these to the world ocean by the global ocean circulation. Polar oceans having sea ice is "Canary of Climate", and are very sensitive to the climate change, e.g., the global warming. Antarctic Bottom Water (AABW) formed in the Southern Ocean is the main actor for these two mechanisms, however, it is still difficult to clarify the whole image of AABW only by the in-situ observation. Our purpose is the estimation of AABW formation, sinking process, and its spread in the bottom layer by the numerical modeling, by using the following three different methods; monitoring of sea ice production by the satellite remote sensing, high-resolution mapping of water temperature and salinity by in-situ observation, and numerical modeling by high-resolution model. This study is challenging to the final and most difficult blank area for the global climate system, and could contribute to the prediction of future climate change.

By our recent results, we got the following two progresses; (1) hemispheric-scale and long-term monitoring of sea ice production which directly links to the AABW formation becomes possible by the accumulation of satellite data and the development and improvement of the algorithms (Tamura et al., 2008) and (2) the result from the numerical modeling could compare to the in-situ results directly by the improvement of the numerical model (Matsumura and Hasumi, 2011). Under these our past works, it is possible to detect the actual dynamics of AABW by the following three independent methods; (a) monitoring of sea ice production by the satellite remote sensing, (b) high-resolution mapping of water temperature and salinity based on the in-situ observation data, and (c) high-resolution ocean modeling.

This study try to clarify the process of AABW formation quantitatively by using our dataset, algorithm, and numerical model. Specifically, our purpose is to estimate the AABW formation, its sinking process, and its expansion in the bottom layer. By using the latest in-situ and satellite data and numerical modeling, we try to clarify the following three questions; Where and how much does the dense water (the origin of the AABW) generate?, How much does the dense water mix with the surrounding water during the process of sinking around the shelf break?, and Where and how much does the AABW exist in the bottom of the world ocean and how does AABW spread?

In our talk, we will introduce updated results for our three ongoing projects; (I) mapping of sea ice production by the satellite remote sensing, (II) improvement of in-situ ocean observation data set, (III) ice shelf-sea ice-ocean coupled modeling, and (IV) micro-scale modeling.

Keywords: Southern Ocean, Antarctic Bottom Water, Sea Ice Production, In-situ Ocean Observation Data Set, Ice shelf - Sea ice - Ocean Interaction, Micro-scale Modeling

## High resolution Modeling on the Antarctic Bottom Water Formation

MATSUMURA, Yoshimasa<sup>1\*</sup> ; OHSHIMA, Kay I.<sup>1</sup> ; HASUMI, Hiroyasu<sup>2</sup>

<sup>1</sup>Institute of Low Temperature Science, Hokkaido University, <sup>2</sup>Atmosphere and Ocean Research Institute, University of Tokyo

At the Antarctic continental margin, a great amount of dense water is created due to intense cooling and active sea ice formation. A part of this dense water descends down to the depth on the continental slope and provides a source of Antarctic Bottom Water (AABW), the densest water mass of the world ocean. This deep water formation drives and controls the global thermohaline circulation. Thus, quantitative understanding of where and how much such dense water descends to which depth with what water mass property is necessary for discussing the structure and intensity of the global thermohaline circulation and hence the earth's climate.

The AABW formation involves various processes with wider range of spatial and temporal scales, such as turbulent mixing induced by vertical velocity shear of descending dense water, influences of small scale submarine ridges and canyons of O(1) km, the surface buoyancy flux highly controlled by openings and closings of coastal polynyas. It is very difficult to perform a numerical simulation which resolves all of these processes because such simulation requires a huge amount of computational resource. Therefore, modeling studies on the AABW formation have been restricted to very idealized experimental settings. In particular, small scale processes such as turbulent mixing and vertical convection cannot be represented by widely used general ocean circulation models with hydrostatic approximation, and a non-hydrostatic model is required. The numerical cost of non-hydrostatic models has been much greater than the hydrostatic models due to the cost of three-dimensional Poisson solver required to diagnose pressure field. To overcome this problem, we developed a non-hydrostatic ocean model with a very numerically-efficient and scalable Poisson solver using the multigrid method. The total cost of our non-hydrostatic model stays less than twice of that of hydrostatic one even with huge amount of grid cells on massively parallel super computers. With using this newly developed model code and present days computational resources, multi-scale and multi-process modeling on the AABW formation, whose results are competent to be quantitatively compared with direct observations, is becoming a reality.

In our talk, we will introduce the outline of the newly developed numerical model and discuss the results of high-resolution AABW formation simulation with focusing on the effects of small scale topographic features and the turbulent entrainment processes induced by Kelvin-Helmholtz instability.

Keywords: Antarctic Bottom Water, non-hydrostatic model



## Modeling basal melting of Antarctic ice shelves

KUSAHARA, Kazuya<sup>1\*</sup> ; HASUMMI, Hiroyasu<sup>2</sup>

<sup>1</sup>Institute of Low Temperature Science, Hokkaido University, <sup>2</sup>Atmosphere and Ocean Research Institute, the University of Tokyo

We have incorporated an ice shelf component into a sea ice-ocean coupled model. Basal melting of all Antarctic ice shelves are investigated with the circumpolar ice shelf-sea ice-ocean coupled model and we have estimated the total basal melting of 770-944 Gt/yr under present-day climate conditions. We present a comparison of the basal melting with previous observational and modeling estimates for each ice shelf in detail. It is found that heat sources for basal melting are largely different among the ice shelves. From a series of numerical experiments, sensitivities of the basal melting to surface air warming and to enhanced westerly winds over the Antarctic Circumpolar Current are investigated. In this model the total basal melting strongly depends on the surface air warming but is hardly affected by the change of westerly winds. The magnitude of the basal melting response to the warming varies widely from one ice shelf to another. The largest response is found at ice shelves in the Bellingshausen Sea, followed by those in the Eastern Weddell Sea and the Indian sector. These increases of basal melting are caused by increases of Circumpolar Deep Water and/or Antarctic Surface Water into ice shelf cavities. By contrast, basal melting of ice shelves in the Ross and Weddell Seas is insensitive to the surface air warming, because even in the warming experiments there is high sea ice production at the front of the ice shelves that keeps the water temperature to the surface freezing point. Weakening of the thermohaline circulation driven by Antarctic dense water formation under warming climate conditions is enhanced by basal melting of ice shelves.

Keywords: Antarctic ice shelves, Ice shelf-sea ice-ocean coupled model, Climate change

## A possible scenario of a drastic change in Antarctic coastal polynyas associated with ice sheet loss

NIHASHI, Sohey<sup>1\*</sup>; OHSHIMA, Kay I.<sup>2</sup>; FRASER, Alexander D.<sup>2</sup>

<sup>1</sup>Department of Mechanical Engineering, Tomakomai National College of Technolog, <sup>2</sup>Institute of Low Temperature Science, Hokkaido University

Coastal polynyas, which are newly-forming sea-ice areas surrounded by pack ice, are formed by divergent ice motion driven by winds and/or ocean currents. Antarctic coastal polynyas are very high sea-ice production areas, because the heat insulation effect of sea ice is reduced significantly in the case of thin ice and accordingly huge heat loss to the atmosphere occurs. The resultant large amount of brine rejection leads to dense water formation. The dense water is a major source of Antarctic Bottom Water (AABW), which is a key player in the global climate system as a significant sink for heat and possibly carbon dioxide. Coastal polynyas are also sites of biological "hot spots", because of much-enhanced primary productivity.

Very recent studies have suggested that landfast sea ice, which is stationary sea ice attached to coastal features such as grounded icebergs and glacier tongues play an important role in the formation of some coastal polynyas by blocking ice advection to cause divergence. Key examples are the Cape Darnley Polynya and Mertz Polynya, both of which are major source areas of AABW.

In this study, we present the first combined circumpolar mapping of Antarctic coastal polynyas and fast ice, based on satellite observation to examine and quantify the linkage between coastal polynyas and fast ice. The map reveals that most coastal polynyas are formed on the western side of fast ice, suggesting that fast ice is an essential element for the formation of most coastal polynyas. Furthermore, we demonstrate that a drastic change in fast ice extent, which is particularly vulnerable to climate change, causes dramatic changes in associated polynyas and possibly AABW formation that can potentially contribute to further climate change.

The map presented in this study reveals that many of the coastal polynyas are formed along the East Antarctic coast where fast ice dominates. In the West Antarctic sector, it was suggested that intrusion of relatively warm Circumpolar Deep Water (CDW) onto the continental shelf causes the basal melting of ice shelves, possibly leading to acceleration of iceberg calving. Future climate change might precipitate a similar situation also in the East Antarctic sector where the location of CDW is relatively close to the continent. This possibly causes drastic changes of fast ice extent directly by melting, or indirectly by acceleration of iceberg calving. The drastic change in fast ice extent is expected to cause a dramatic change in the polynya area and sea-ice production. Further, a huge tabular iceberg can directly affect the polynya area by covering over as shown in the Ross Sea Polynyas area in 2000 and 2002; giant icebergs B-15 and C-19, calved from the Ross Ice Shelf, causing a significant reduction of the polynya area and sea-ice production. The results of this study suggest that fast ice and precise polynya processes should be addressed by next-generation models to reproduce the formation and variability of sea-ice production, dense water, and AABW properly. The mapping presented in this study would give the boundary/validation data of fast ice and sea-ice production for such models.

Keywords: Coastal polynya, Landfast sea ice, Antarctic Bottom Water, Iceberg, Ice sheet

## Wind-buoyancy dichotomy of the Southern Ocean carbon storage

ITO, Takamitsu<sup>1\*</sup> ; TAKANO, Yohei<sup>1</sup> ; DEUTSCH, Curtis<sup>2</sup>

<sup>1</sup>School of Earth and Atmospheric Sciences, Georgia Institute of Technology, <sup>2</sup>School of Oceanography, University of Washington

We use a hierarchy of ocean climate-carbon models to investigate the future scenarios of the Southern Ocean carbon storage. Intensified and poleward-shifted westerly wind is hypothesized to enhance the upwelling of deep water and thermocline ventilation, which may be counteracted by the warming and freshening of the surface waters. We analyze the solubility and biological carbon pumps in the Southern Ocean as simulated by the Climate Model Inter-comparison Project phase 5 (CMIP-5) models. Model-model differences in the regional carbon storage are significant, O(100PgC), reflecting the organized changes in the two carbon pumps. To investigate the underlying mechanisms, we perform a suite of numerical sensitivity experiments using an ocean biogeochemistry model, where we purposefully impose (1) a global warming of sea surface temperature, (2) an intensification of freshwater forcing and (3) an increase in the Southern Ocean wind. Comparing the simulated patterns of carbon and oxygen changes, we find that the future increase in the biological carbon storage is likely due to the warming and freshening of the surface water dominating over the increasing wind.

## Incorporation of trace elements by diatom frustules: Significance of sediment-trap observation in the Southern Ocean

AKAGI, Tasuku<sup>1\*</sup>

<sup>1</sup>Department of Earth and Planetary Sciences, Kyushu University

Diatoms contribute to more than half of the primary production of the oceans and it is well established that the formation and dissolution of diatom opal governs the distribution of dissolved silica in ocean columns (Nelson et al., 1995). Owing to the physical and chemical difficulty in isolating diatom opal from clays (Shemesh et al., 1988; Beck et al., 2002), however, it is difficult to clarify the trace composition of opal and thus to understand how diatoms contribute to the ocean circulation of trace elements. To date, no direct determination of rare earth elements (REEs) in diatoms has been made, and the role of diatoms has not been considered in the circulation of REEs (Sholkovitz et al., 1994; Oka et al., 2009; Siddall et al., 2008; Arsouze et al., 2009; Tachikawa et al., 2003).

The recent study, based on the dissolution kinetics of diatom silica frustules and the incorporation theory of silicic acid complexes, unveiled the composition of diatom frustules and identified the role of diatoms in the oceans (Akagi et al., 2011; Akagi, 2013). Diatoms incorporate metal-silicate complexes, silicate minerals as well as dissolved silica, to form their silica frustules. They recycle rare earth elements in the water column and disintegrate silicate minerals to change rare earth elements in refractory silicates to readily dissolvable forms. Diatom frustules are no longer regarded as pure hydrated silica, but impure matter able to transport some elements to the deep water. In the Bering Sea diatoms are found to incorporate island-arc matter with a high  $\epsilon\text{Nd}$  value (Akagi et al., in press). Diatoms are important in distributing this high  $\epsilon\text{Nd}$  signature to the ocean. This new insight may affect the interpretation of the Nd isotope variation recorded in ferromanganese crusts and foraminifera, which synchronizes with the glacial-interglacial periodical variations.

The new insight on diatom frustules has been established based mainly on sediment trap samples from the Bering Sea, a rather special sea, and ocean chemists tend to treat the insight a rather exceptional case. To generalize the insight, the same line of study should be extended to the sediment trap samples from more normal oceans such as the Southern Ocean.

To date, the possibility of silicic acid complex formation with metal ions has not been explored in the research on marine chemistry. Some elements classified as high field strength elements, HFSEs, are considered to be in the form of OH complex in seawater (Byrne, 2002). Most of elements classified to high field strength elements (HFSEs) have a valency of 3+ or 4+, and considering their thermodynamic properties, it was found that they are likely to have fairly high complex formation constants with silicic acid (Wang et al., 2009; Wang and Xu, 2001). Although silica has been long studied, this study is the first to discover the possibility that it is an important carrier of many elements in marine chemistry. To establish this view, again, studies using trap samples from the Southern Ocean would be highly requested.

Keywords: diatom frustules, trace elements, sediment trap, Southern Ocean

## Millennial-scale sea ice expansion in the glacial Southern Ocean

IKEHARA, Minoru<sup>1\*</sup> ; KATSUKI, Kota<sup>2</sup> ; YAMANE, Masako<sup>3</sup> ; YOKOYAMA, Yusuke<sup>4</sup>

<sup>1</sup>Center for Advanced Marine Core Research, Kochi University, <sup>2</sup>Korea Institute of Geoscience and Mineral Resources (KIGAM),  
<sup>3</sup>JAMSTEC, <sup>4</sup>Atmosphere and Ocean Research Institute, University of Tokyo

The Southern Ocean has played an important role in the evolution of the global climate system. Area of sea ice shows a large seasonal variation in the Southern Ocean. Sea ice coverage on sea surface strongly affects the climate of the Southern Hemisphere through its impacts on the energy and gas budget, on the atmospheric circulation, on the hydrological cycle, and on the biological productivity. In this study, we have conducted fundamental analyses of ice-rafted debris (IRD) and diatom assemblage to reveal a rapid change of sea ice distribution in the glacial Southern Ocean. A piston core COR-1bPC was collected from the Conrad Rise, Indian sector of the Southern Ocean. Core site is located in the Polar Frontal Zone. Sediments are composed of diatom ooze. Age model of COR-1bPC was established by <sup>14</sup>C dating and oxygen isotope stratigraphy of planktic foraminifera. Records of IRD concentration suggest millennial-scale pulses of IRD delivery during the last glacial period. The depositions of rock-fragment IRD excluding volcanic glass and pumice were associated with increasing of sea-ice diatoms, suggesting that the millennial-scale events of cooling and sea-ice expansion were occurred in the glacial South Indian Ocean. Similar episodic IRD depositions were identified in the South Atlantic during the last glacial period (Kanfoush et al., 2000). However, Nielsen et al. (2007) proposed that the tephra-rich grains in the South Atlantic IRD events (SA-IRD events) were mainly derived from South Sandwich Island volcanic arc, and concluded that sea-ice was the dominant ice rafting transport of such IRD grains. Preliminary provenance study of IRD grains suggest that the source of IRD in the South Indian Ocean was also volcanic arc in the South Atlantic, based on chemical compositions of rock-fragment IRD grains. Thus prominent IRD layers in the glacial South Indian Ocean correlate the SA-IRD event, suggesting episodes of sea ice expansion and cooling in the Atlantic and Indian sectors of the Southern Ocean.

Keywords: Southern Ocean, sea ice, millennial-scale, dust

## The ANDRILL Coulman High Project: Japanese contribution to the next phase of the Antarctic Geological Drilling

SUGANUMA, Yusuke<sup>1\*</sup> ; IKEHARA, Minoru<sup>2</sup> ; SUTO, Itsuki<sup>3</sup> ; NOGI, Yoshifumi<sup>1</sup>

<sup>1</sup>National Institute of Polar Research, <sup>2</sup>Kochi Core Center, <sup>3</sup>Nagoya University

The Coulman High Project (CHP) proposes to recover two, high-quality, continuous drill-cores by drilling into Paleogene to lowest Miocene strata beneath the Ross Ice Shelf on the Coulman High in the Ross Embayment, Antarctica. The overarching objective is to establish a history of Cenozoic climate, tectonic and glacial changes in an ice-proximal setting to determine the sensitivity of Antarctica's ice sheets to a range of climatic and tectonic forcings. The sedimentary archives to be recovered in these two ~800-m drill holes will offer a window into the range of environments, ecosystems and tectonic events in the Ross Sea region as it stepped from the warm, high-CO<sub>2</sub> Greenhouse world of the Eocene into the lower-CO<sub>2</sub> and highly variable Icehouse climate of the Oligocene and early Miocene. Antarctica was the keystone in this global climate transition and hosted the growth of ice sheets that started major cryosphere influence on global systems. The sensitivity of the climate system to elevated levels of greenhouse gases, the strength of polar amplification, and the behavior of the AIS in a world warmer than today remain fundamental questions to be addressed by CHP's integrated data-climate modeling studies. These seek to reduce the large uncertainties in predictions of future ice-sheet dynamics and sea level, in part by testing models with ancient scenarios under conditions warmer than today. To improve predictions of long-term future climate and sea level, it is imperative to obtain geological records of past polar climates and ice sheets from time intervals when atmospheric CO<sub>2</sub> was two to four times higher than present levels. Modern observations and instrumental records provide details regarding current and short-term change, but high-fidelity climate records that span previous periods characterized by higher-than-present CO<sub>2</sub> are only available from the Earth's geological records.

The Japanese ANDRILL consortium has decided to join the CHP. In this talk, we will introduce the scientific backgrounds, logistics, and schedule of this drilling project.

## Global circumstance on Geopark

WATANABE, Mahito<sup>1\*</sup>

<sup>1</sup>Geological Survey of Japan,

The concept of Geopark is getting to be known to wide range of people in many countries including Japan, such as researchers, citizens and officials in both municipal and central governments. Every people has every point of view on Geoparks. This situation will contribute to improve the concept of Geopark through the discussion of wide range of people.

Global Geoparks Network (GGN) and UNESCO are discussing about the formal link between them in the working group composed of member country and GGN hosted by Ecology and Earth Science division of UNESCO. When the formalization of Geopark in UNESCO is achieved the present style of evaluating Geopark by GGN may change. As a UNESCO program, support to the least developing countries that try to establish Geopark is important and necessary. The discussion between member countries and GGN is good opportunity to review the activity of Geopark until present with the point of view from outside.

In Japan, on-site evaluation by scientists and manager within Geoparks as well as members of Japan Geopark Committee (JGC) has started in 2012. It was a start of the peer review process between geoparks. Discussion on the policy to evaluate geoparks and candidate areas is getting more active since last May when first meeting on the evaluation policy between evaluators from JGC and geoparks. In those discussion they actively discuss on where Japanese geoparks go and how to promote geopark activity.

The author will present the situation around Geopark as mentioned above and propose issues that should be discussed in the Japanese geopark community.

Keywords: Geopark, UNESCO, Global Geoparks Network, Japanese Geoparks Network, Japan Geopark Committee

## Geoscience in Japanese Geoparks: Significance of Multidisciplinary and Interdisciplinary Geostories

OGATA, Takayuki<sup>1\*</sup>

<sup>1</sup>Faculty of Education, University of the Ryukyus

Geoparks target all geoscientific disciplines consisting of space and planetary sciences, atmospheric and hydrospheric sciences, human geosciences, solid earth sciences, and biogeosciences, presented as the science sections in Japan Geoscience Union (JpGU). In JpGU, academic meetings of geoparks have been held in the public session since 2010 and the multidisciplinary and interdisciplinary session since 2012. However, geostories of Japanese Geoparks Network (JGN) are likely to incline toward specific themes based on URL information uploaded on the JGN official website. Especially, physical geography, such as climatology, hydrology and geomorphology, seems to be slighted in many Japanese geoparks. Physical geography, studying interaction among atmosphere, hydrosphere and geosphere in multidisciplinary and interdisciplinary scopes, should be given more consideration in all Japanese geoparks.

Keywords: geoparks, geostory, geoscience, physical geography, Japanese Geoparks Network, Japan Geoscience Union



## Provision of the Risk Information for Geopark guests in Japan

KOMORI, Jiro<sup>1\*</sup>

<sup>1</sup>Teikyo Heisei University

The exact provision of risk information are important to geopark guests. The possible of the risk on the guests are consulted with the statistical police white paper of the mountain accident in Japan. The consideration shows that the major risk factors on geoparks are fall and slip drop, encounters with dangerous animal and rock fall. However, it is impossible to find an alert, description and discussion regarding their risks in published articles and books which specialized in the geopark activity. Furthermore, more than two thirds of the official geopark websites are devoid of the provision of the risk information. Even the remaining one-third place some simple or little paragraph of hazardous issue. For the safety administration with the advertising of attractiveness of geopark, effective provision through the official websites and printed materials are required in the future.

Keywords: geo-site, geo-tour, alpine accident, alert, accountability, official website

---

MIS35-04

Room:211

Time:May 2 11:45-12:00

## Democratic governance of the Japanese geopark movement

MOKUDAI, Kuniyasu<sup>1\*</sup>

<sup>1</sup>Pro Natura Foundation Japan

Japanese geopark movements needs separation of powers. I would like to propose a model for the governance of a Japanese geopark movement.

Keywords: Japanese Geoparks Network, Japan Geopark Committee, academic society, science communication, bottom-up

## Program of Treasure Stones : Making an original rock specimen using a virtual geotour -

OHNO, Marekazu<sup>1\*</sup>

<sup>1</sup>Unzen Volcanic Area Geopark Promotion Office

We developed a making a rock specimen combined technique of a virtual geotour. To practice this program, a presentation file explaining highlights of geosites, rock samples and an original sheet which put on rock samples. To finish the program within 30 minutes, we limited 5 geosites in explanation and number of rock samples was 10. We carried out this program at Science Agora, which is a big scientific festival holding at Nihon Kagaku Mirai Hall in recent 2 years.

Participants of the program was mainly school students. They selected their favorite stone samples put them on the original sheet with a bond. In the virtual geotour, we explain not only rocks and landscapes but also relationship rock and people, histories of geosites and local foods using local special products. In 2012, we carried the program out with Shimonita Geopark and 151 participated (Sekiya, 2013). In 2013, 129 persons participated the program nevertheless a number of participates was limited. This program was almost popular with participants and received the Science Agora Award in 2012. Furthermore, this program became the fifth place in all programs by a guest popularity vote in 2013.

This program can be carried out regardless of a place, if machine parts and a place are set. And because people participating in this program have many families, various age groups can publicize the highlight of the Geopark. If participates get interests for the geopark, it is expected the increase of tourists of geopark area. In 2014, we hope some of geoparks join the program in Science Agora.

Keywords: Unzen Volcanic Area Global Geopark, virtual geotour, rock specimen, Science Agora

## Development of the textile with a geological map motif-To carry back geo-stories from geopark or natural history museum

SAITO, Makoto<sup>1\*</sup>

<sup>1</sup>Geological Survey of Japan, AIST

The textiles with the Seamless Digital Geological Map of Japan (1:200,000) motif were launched September in 2013. These textiles were developed under the two basic concepts such as making a superior textile by using the geological map as a design of the earth, and the other is making the product which the visitors can carry back a geological story home from natural history museum or geopark. To achieve these concepts, it was important that a designer cooperated with a geologist.

The textiles were developed with Nikko area of the Seamless Digital Geological Map of Japan (1:200,000) motif. The designer changed the color of each legend of the geological map on Geographic Information System (GIS) software and printed it on cloth. The products contained a handkerchief, a porch, and a mini-tote bag with purplish, greenish and pinkish colors each. Because the cloth for product is clipped out from the large cloth which a geological map was printed on, there are 10 areas of porch or 3 areas of mini-tote bag from one printed cloth. As a result, we made the many kinds of textiles such as 3 kinds of handkerchiefs, 30 kinds of porches and 9 kinds of mini-tote bags.

Since the Seamless Digital Geological Map of Japan (1:200,000) is a digital geological map made with a uniform legend throughout Japan, anyone can cut out any local geological map from it. Therefore, it is possible to make the product of the different design every area. If these textiles are made in each geopark, the visitors can carry back the textile with special stories of the geopark.

It is easy to make the T-shirts which a geological map was printed on now. However, it is difficult to make an attractive commercial product, and only an attractive product in cooperation with a designer increases the number of customers. As a result, the product with the geologic map increases the number of people who are interested in geology.

As we push forward a plan to make a product with the geological map of another area motif now, the new products are released soon.

Keywords: textile, geological map, geopark, natural history museum, GIS, geographical Information system

## The accretionary prism experiment for geoparks using powdered sugar, cocoa, and a cooking paper

HAYASHI, Shintaro<sup>1\*</sup>

<sup>1</sup>Fac. of Edu.and Human Studies, Akita Univ.

The analog experiment for understanding an accretionary prism was developed. The experiment is developed for children, students, and the tourists of geoparks. The experiment is simple and is using only familiar materials, such as powdered sugar, cocoa, and a kitchen paper.

Accretionary prism is usual in the Japanese geoparks. But, it is difficult to explain the mechanism of accretion to a child and a student, and the tourist of a geopark.

The accretionary prism experiment proposed until now had a thing adapting a sand box experiment (2004 besides Yamada, 2006, and Kaneda), and flour fault experiment (Okamoto, 1999, 2000).

<The method of an experiment>

Ingredients: powdered sugar, raw cocoa, creep, a cooking paper, a tea strainer, a spoon, a paper cup, the lap for kitchens, papier-mache.

Directions:

1. Papier-mache is wrapped in a lap to make continents.
2. Cut cooking paper into about 40 cm.
3. Build the layer of cocoa (the thickness is around 2mm) on an cooking paper using a tea strainer.
4. Sprinkle powdered sugar with a tea strainer on the layer of cocoa. The thickness is around 2 mm.
5. Wrapped papier-mache "continent" is set at the end of a cooking paper.
6. Sprinkle milk over the continent and continent side of the layer of cocoa and powdered sugar.
7. A cooking paper is pulled.
8. Cocoa and powdered sugar are added to a continent and duplex structure is formed.
9. Put cocoa, powdered sugar, and milk into a paper cup collectively, and pour out and process hot water to make cocoa drink.

Keywords: geopark, accretionary prism, analog experiment, kitchen experiment

## Approach of Educational Activities in Hakusan Tedorigawa Geopark

MOCHIDA, Shuichi<sup>1\*</sup> ; HIROSE, Osamu<sup>1</sup> ; HIBINO, Tsuyoshi<sup>1</sup>

<sup>1</sup>Hakusan Tedorigawa Geopark Promotion Council

The Hakusan Tedorigawa Geopark which was certified as a Japanese geopark in 2011 sets the theme "the journey of water" (water circulation seeing the Tedorigawa River) which is generally easy to understand. The geopark highlights the sites related to earth sciences, nature, people's lives and culture such as fossils, debris flow, an alluvial fan, brewing industry and "haiku" (Japanese poetry).

We have been utilizing these sites for children's education since the beginning, and promoting the activities in school education to popularize the geopark to children. Our aim is also on sustainable local activities.

Although it is said that teachers which don't have the know-how to teach children in the fields have been increasing, the new educational government guidelines given notice in March 2008, show that teachers need to teach children in the nature and daily lives. The activities of the geopark correspond with the guidelines, and it seems that we need to assist the teachers who have less time to study the new course. Study Supporters, who are retired science teachers, have been supporting teachers in the geopark. We aim to teach children in the fields only by in-service teachers.

Keywords: Hakusan Tedorigawa Geopark, educational activity, school education

## Introduction of teaching and materials the theme of Geo, and Disaster awareness of high school students in Shizuoka

KAZUHIDE, Tsuda<sup>1\*</sup> ; MURAKOSHI, Shin<sup>2</sup>

<sup>1</sup>NPO Whole Earth Institute, <sup>2</sup>Faculty of Education, Shizuoka University

### [Introduction]

Science and Environmental Education Project (SEEP) , such as researchers, nature guide school teachers work together , we have developed educational content on the theme of natural science (Tsuda, et al. , 2013 ) . Developing Model class and geoscience materials 12 types aim it at the Izu Peninsula Geopark human resources development projects , and performed on the geo- guide with more than 150 people and described in three years , that capture the characteristics of the earth in Shizuoka Prefecture getting high marks from geo- guides of almost all .

We researched as " Fuji Disaster prevention Fellow training course " , a statistical study of disaster prevention survey of model class.

### [Method]

The subjects were about 320 students in high schools in Shizuoka Prefecture.

As a method we used, hands-on educational materials, interpreter, communication, sub- materials, learning worksheet.

Specifically, you have used the materials of three main lessons. Experimental observation and for each group a stone of four areas of Shizuoka Prefecture, select the age quiz that is specified in the introduction. It captures the age order in the puzzle by geologic province of Shizuoka Prefecture, including the area of each rock is in the deployment. Conclusion, I confirmed the origin of the earth in Shizuoka picture-story show the history of the land in Shizuoka (wood panel) or not there was any such events to the geological era.

### [Results]

In order to know the understanding of the individual, the question, "earthquake", "plate", "Nankai Trough earthquake in the past", "Mount Fuji eruption", "active volcano in the prefecture", "rock in the prefecture", "Geopark". We found that that is not known for most of the Geopark in high school outside of Geopark area.

It resulted in materials (60%) interest in the interpreter (22%) accounted for many, teaching increases the interest geology, geo-on (earth) as the reason

It is expected that by the SPSS statistical analysis, to present a detailed analysis of the data in the announcement.

Keywords: Geoscience materials, Geopark guides training programs, Visiting lectures in high schools, Disaster awareness

## Progress of school education through Geopark Studies in the Itoigawa Global Geopark

TAKENOUCHI, Ko<sup>1\*</sup> ; MIYAJIMA, Hiroshi<sup>1</sup> ; IBARAKI, Yousuke<sup>1</sup> ; TORIGOE, Hiroko<sup>2</sup> ; BROWN, Theodore<sup>2</sup> ; WATANABE, Seigou<sup>2</sup> ; MATSUNAWA, Takayuki<sup>1</sup> ; CHIKAATO, Hisaki<sup>1</sup> ; FUJITA, Eishi<sup>3</sup> ; ICHIKAWA, Satoshi<sup>3</sup>

<sup>1</sup>Itoigawa City Board of Education, <sup>2</sup>Itoigawa Geopark Promotion Office, <sup>3</sup>Itoigawa Science Education Center

Geoparks are parks where visitors can learn about the relationship between mankind and the earth, but they are also part of a movement to develop sustainable regional societies. Education is regarded as one of the most important elements of the Geopark Movement which includes a system to foster the human resources that will manage our sustainable society in future. Itoigawa has begun to construct a sustainable regional society since Global Geopark certification in 2009. The Itoigawa City Board of Education recognized the important role of the Geopark in school education and has included a Geopark Studies program within the compulsory education (elementary and junior high school) curriculum. The first action was to establish a new education plan called the Unified Education Policy for Children Aged 0 through 18 in 2009 in which Geopark Studies was first introduced. Since then, the City Board of Education's continuing support of Geopark Studies has provided the following results: (1) Number of staff member of the Science Education Center has been increased and a Geopark Department has been established in the Itoigawa Teachers Organization's Society of Education Research. (2) Training programs (outdoor and indoor) have been held by these organizations and the Itoigawa Geopark Council, showing educators how geoparks can be used for classroom education. (3) City-wide Geopark Studies Conferences have been held to give students a chance to share what they have learned. (4) Supplementary textbooks for grades 3 through 9 have been published and distributed by various editorial boards, providing invaluable resources for the study of earth science and history as well as regional culture. (5) Geosites have been equipped with information panels and leaflets which cater to school education. (6) The Geopark has become a valuable tool in the teaching of disaster prevention, with a local elementary school receiving national and prefectural awards for its efforts. (7) Every first Wednesday of each month has been set as the geo school lunch date which features regional cuisine made with local ingredients to allow students to learn the relation of Itoigawa's land, cuisine and local produce. (8) And finally, an exchange program has begun for elementary and junior high school students with Itoigawa's Sister Geopark in Hong Kong.

Keywords: geopark, school education, Itoigawa



## CPD program for improvement of guide skill in the San-in Kaigan Geopark

SAKIYAMA, Tohru<sup>1\*</sup> ; MATSUBARA, Noritaka<sup>1</sup>

<sup>1</sup>Graduate School of Management of Regional Resources, University of Hyogo

San-in Kaigan Geopark is the largest global geopark in Japan and there are thirty guide groups in the geopark. Some group members which receive following training programs are registered as official guides of the geopark. (1) Principles of geopark and outline of the San-in Kaigan Geopark, (2) Geology, geography, biology, history and others in the individual area, (3) Manner and technique of guide, (4) Conservation and related ordinances, and (5) Emergency resuscitation methods and system of insurances. License of the official guide is renewed every three years. They must participate at least fifteen seminars and events and improve the skill to guide the geopark during valid period of the license.

It is not easy to prepare enough programs for all official guides because of the wide area of the geopark. On the other hand, there are many educational facilities represented in the San-in Kaigan Geopark. They have many lifelong educational programs independent to the guide training of geopark. But some of them are available to upgrade the guide skill. Accordingly, CPD (continuous professional development) system has been adopted as the improvement program of the official guides in the San-in Kaigan Geopark. Official guides of geopark take the programs provided as CPD program by the educational facilities and they get a CPD-point. Not only such seminars but promotion to out-reach events (symposium, caravan, festival and others) and participation to national and international geopark conferences (GGN, APGN, EGN, JPN and others) is available to CPD-point. In order to renew the license of official guide, they must have fifteen CPD-points in three years.

CPD-program have following effects: (1) Securing of improvement programs for guide, (2) Exchange between people and geopark guides, (3) Deepening of interesting to guide activities, and (4) Development of lifelong education in the geopark.

Keywords: geopark, San'in Kaigan, continuous professional development, lifelong education

## Restoration of the coastal geo-environment along Tottori Sand Dunes

KODAMA, Yoshinori<sup>1\*</sup>

<sup>1</sup>Fac. Regional Sciences, Tottori-Univ.

Along the coast of Tottori Sand Dunes, south-west Japan, dimensions of offshore bars were illustrated from air photos taken in 1968-2008 at 5 year intervals and grain size distributions at berm crests on the beach have been investigated over a half century since 1955. The results show that beach environments have been restoring naturally after damages induced by human activities, such as sand and gravel harvesting in the Sendai River during 1960-1975, which had caused diminishing of offshore bars, coastal erosions and beach sediment coarsening ( $>1.0$  mm) at 1980's and finally vegetation covering of the Tottori Sand Dunes. After stopping sand and gravel harvesting, large floods occurred in 1998 and 2004. These floods transported lots of sediment from upper parts of the drainage area to the main Sendai River. Around 2000, offshore bars along the coast became larger and grain sizes on the beach changes finer ( $<0.4$ mm) after 2011. These grain size values are similar to those in 1955. We are expecting that weeds on the Tottori Sand Dunes will relief naturally by activating blown sand. These phenomena are a good story to get visitors notice well-coordinated natural systems as a geo-park site in the San'in-kaigan Global Geo Park.

Keywords: Tottori sand Dunes, weeding of sand dunes, offshore bar, grain size distribution of beach deposit, sand and gravel harvesting, changes over a last half century

## Various effects that the shape of volcano has brought to the local area: an example of the Takachihonimine volcano

ISHIKAWA, Toru<sup>1\*</sup>

<sup>1</sup>The Council for the Promotion of the Kirishima Geopark

When it comes to a volcanic blessing, it will be reminded of hot springs, spring water, and geothermal energy in many cases. However, these are only partial views of the blessing of a volcano directly useful to a life of people. In order to know deeply what kind of benefit the volcano itself has brought human society, it is necessary to see a volcanic blessing from many sides. As the beginning, this study focuses the shape of volcano.

The Takachihonimine volcano located at the eastern part of the Kirishima Volcano Group, SW Japan is the stratovolcano formed about 7,000 years ago, and has an acute summit and twin volcanoes on its both sides. Such a magnificent shape of the volcano is often dealt with as an icon of Kirishima, and is expected to have brought great influence to people's culture, a sense of values, and a religion view. In this research, I investigate where and how the influence of the topographical features of the Takachihonimine volcano has worked.

Keywords: Kirishima Volcano Group, Takachihonimine, Volcanic blessing

## The Activities of MLIT on the Hakusan Tedorigawa Geopark

KANATANI, Takao<sup>1\*</sup> ; YAMAGUCHI, Takashi<sup>2</sup>

<sup>1</sup>Kanazawa Office of River & National Highway, Ministry of Land, Infrastructure, Transport & Tourism, <sup>2</sup>Hakusan Tedorigawa Geopark Promotion Council

The national flood control project in the Tedorigawa River by MLIT (Ministry of Land, Infrastructure, Transport & Tourism) is deeply related to the Hakusan Tedorigawa Geopark themes 'the journey of water and rocks'.

Some sabo structures in the geopark, constructed in the early Showa era, are designated as a Civil Engineering Heritage and as Registered Tangible Cultural Properties. MLIT, as a member of the Hakusan Tedorigawa Geopark Promotion Council, offers learning opportunities that allow people to look closely at these structures.

A massive flood, the most disastrous in history to that point, occurred in the Tedorigawa River in 1934. A huge rock known as the Shiramine Hyakumangan-no-iwa Rock (literally 4,800 ton rock) that cascaded along with it now sits neatly in the middle of the river. It is a reminder of the sheer scale of the event and is visited on elementary school field trips or on the geo-tours.

Opened in 2001, the Hakusan Sabo Science Museum introduces scientific information on landslide control measures based on the nature, geology, history, and lifestyle of Mt. Hakusan through video and exhibits in cooperation with the Hakusan Tedorigawa Geopark Promotion Council and is visited annually by more than 10,000 people.

The Ishikawa Coast Field Museum, managed in collaboration with the geopark, is an outdoor museum located on a coastal area that offers information on local history and the formation of the coast.

Keywords: Hakusan Tedorigawa Geopark, "Journey of Water", "Journey of Rocks", Sabo at Mt.Hakusan, Ministry of Land, Infrastructure, Transport & Tourism

## The link among Geopark, Biosphere Reserve, and National Park in Hakusan, Japan

NAKAMURA, Shinsuke<sup>1\*</sup> ; SAKAI, Akiko<sup>2</sup> ; MATSUKI, Takashi<sup>3</sup>

<sup>1</sup>Hakusan Tedorigawa Geopark Promotion Council / Mt. Hakusan Biosphere Reserve Council, <sup>2</sup>Graduate School of Environment and Information Sciences, Yokohama National University / JCC for MAB, <sup>3</sup>Hakusan Ranger Office, Ministry of the Environment

Mt. Hakusan (2,702m) is an independent mountain on the Japan Sea side of Central Japan. An area extending over 4 prefectures (Toyama, Ishikawa, Fukui, Gifu) was designated as a national park in 1962, and as a biosphere reserve in 1980 by UNESCO. In 2011, the whole area of Hakusan City (in Ishikawa Prefecture) including the peak of Mt. Hakusan was designated as a Japanese geopark. Therefore, 3 systems on conserving and utilizing nature became to coexist in Mt. Hakusan, and since then, the link among these three is not only a complicated issue but a big chance.

National Parks are locations where human activities are restricted to protect the superb natural landscapes that are representative of Japan and where facilities have been installed to provide essential information and other functions to help visitors come in closer contact with nature (31 national parks in Japan). Biosphere reserves are sites seeking to reconcile conservation of biological and cultural diversity and economic and social development, recognized under UNESCO's Man and the Biosphere (MAB) Programme. To make the 3 functions (conservation, development and logistic support) effective, they have 3 zonations; core area(s), buffer zone(s), and transition area (5 biosphere reserves in Japan). Geoparks are sites enjoying earth and geotourism, supported by UNESCO (6 global geoparks and 27 Japanese geoparks in Japan).

Biosphere reserves and geoparks are both aiming at sustainable development. They attach importance to not only conservation but also utilization of nature, in contrast with the World Heritages. In addition, both form global networks each, which support each site together and diffuse their ideas. However, you can find some differences between these two. For instance, biosphere reserve is an official program of UNESCO, while geopark is a program supported by UNESCO. And the largest difference is that biosphere reserves pay most attention on ecosystems when geoparks pay most attention on earth.

However, they are not only focusing on ecosystems or earth, but they are also focusing on their connections formed with culture or lives. For example, there is a settlement called Shiramine around Mt. Hakusan, located on the river terrace which is a limited flatland in this mountainous area. In Shiramine, fire burned fields were established and forestry was conducted, which could say as a utilization of both topography and biological resources. In the summit of Mt. Hakusan, we could see various alpine vegetations affected by some topographical factors such as the quantity of snow or the formation of the earth. The earth, ecosystems and culture are connected tightly, which connection will be more clarified by both biosphere reserves and geoparks. From this context, you can say that geotours and ecotours might be held as same tours such called geo-ecotours, as it were which Koizumi (2011) said.

National parks are underlying biosphere reserves and geoparks. Both remain under national sovereign jurisdiction, but on the other hand are requested to take effective measures of nature conservation by each state's laws. National parks are representative institution of conservation in Japan, which have some zonations to restrict human activities in phases. Besides, national parks carry out some activities that could be more attractive by cooperating with biosphere reserves and geoparks which have more precise themes.

However, this cooperation depends on the link among the 3 organizations. So in Mt. Hakusan, the secretariats of Hakusan Tedorigawa Geopark Promotion Council and Mt. Hakusan Biosphere Reserve Council are both carried out by Hakusan City, assigning the same staffs, to strengthen the link between these two. Moreover, Ministry of the Environment which manages national parks, takes part in both councils.

The link among the three has just started. We are aiming to create new values and attractions transmitting from Mt. Hakusan, using this beneficial opportunity.

Keywords: Geoparks, Biosphere Reserves, National Parks, Mt. Hakusan, Geodiversity, Biodiversity

## What we learned from the verification of the Dinosaur Valley Katsuyama Geopark reexamination results

YOSHIKAWA, Hirosuke<sup>1\*</sup>

<sup>1</sup>Hirosuke Yoshikawa

We truly feel that reviewing the reexamination results of our geopark verification with local residents and geopark staff members provide us with the opportunity to fundamentally improve its construction. Furthermore, we can use these results to plan future initiatives and development strategies.

We will explain how we can fully utilize these results, such as raising the standards of the overall community and policies and efforts that Katsuyama should undertake as a whole.

Keywords: the reexamination results, our geopark's verification, development strategies, plan future initiatives

## Present state and Future outlook of Mishimamura Geopark Project

OIWANE, Hisashi<sup>1\*</sup>

<sup>1</sup>Mishimamura Village

Mishimamura Village intends to become a member of Japanese Geopark Network deesterilizing its natural, historical, and cultural background. The village consists of three islands. The central island, Satsuma Iwo-Jima is located at the edge of Kikai Caldera, which erupted about 7300 years ago. Its volcanic, fumarolic, and hydrothermal activities are very good resources of tourism. In relation with these activities, historical sulfur mining, sulfur trading, and appearance on palaeographies are also good resources of tourism. In addition, a famous Kabuki actor comes to play because of historical background of the island, and famous djembe player comes to play djembe with children in the island. In spite of these interesting resources, the village has not constructed sightseeing tours that organize these resources. Here, the village started to deesterilize these resources in order to vitalize the village. In this presentation, I will present our original approach and future plan to be a member of Japanese Geopark Network.

Keywords: geopark, caldera

## Introduction of the Nankikumano Geopark activity research project

MORINO, Yoshihiro<sup>1\*</sup> ; TANIWAKI, Tomokazu<sup>2</sup>

<sup>1</sup>Pacific Consultants Co.,Ltd., <sup>2</sup>Natural Environment office of Wakayama Prefectural Government

Various business (spread activity, utilization as education, tourist attractions, the Geopark guide training) is developed mainly on "Nankikumano Geopark promotion meeting" from 2012. "Nankikumano Geopark activity research project" was carried out to plan accumulation and the regional activation of the academic document of the Nankikumano Geopark design in 2013. As for this project, an individual, a local group, a private enterprise work on an academic investigation and the spread together in a Geopark design area.

Keywords: Geo-resources, Local promotion, Geo-tourism



## Plan to aim at the revival and activation of disaster region by disaster heritage of the Great East Japan Earthquake

TANIGUCHI, Hiromitsu<sup>1\*</sup> ; TASHIRO, Kan<sup>2</sup> ; MIYAHARA, Ikuko<sup>3</sup> ; AIHARA, Junichi<sup>4</sup> ; TANAKA, Michi-hisa<sup>5</sup> ; MSC GP, Prep. com.<sup>1</sup>

<sup>1</sup>Tohoku Univ, <sup>2</sup>Tohoku Inst Tech, <sup>3</sup>Miyagi Univ, <sup>4</sup>Tohoku History Museum, <sup>5</sup>Asia Air Survey

The coastal area of Miyagi Prefecture was destroyed almost completely on 11 March 2011 by the Great East Japan Earthquake. Now, many people are working hard and trying to recover from the destruction. As a member of the victims and as a researcher living in the affected areas, we are planning to create a Minami Sanriku Coast Geopark to the affected coastal areas, and to contribute to the reconstruction also.

Simultaneously with general subject such as a stratum, fossil, geographical feature and a cultural heritage, we use the affected heritage which was born in the Great East Japan Earthquake.

At the same time as the scientific understanding of an earthquake or tsunami, the reason to focus on these because we want to help local disaster management in the future. To date, we have finished the investigation of tour point of about 50 places. In the present talk we will focus on an example of Yamamoto town geosite located on the border with Fukushima Prefecture and Miyagi Prefecture.

Keywords: geopark, Minami Sanriku Coast, disaster heritage, revival, Yamamoto Town

## ”100 Earth Heritages” and its Geographical Concept

ARIMA, Takayuki<sup>1\*</sup>

<sup>1</sup>AJG Geopark Committee, Committee for ”100 Earth Heritages” Selection

### 1. The Association of Japanese Geographers and ”100 Earth Heritages”

Geopark Committee in the AJG aims to choose ”100 Earth Heritages”. They organized three symposiums and four questionnaire surveys. Furthermore, Committee of 100 Earth Heritages Selection has launched in 2012 and started the selection. This committee has members of the AJG who are both researchers of physical and human geographies. This article introduces a manner of the selection work for understanding a priority of value in Japanese geography.

### 2. Manner of 100 Earth Heritages Selection

The committee proposed questionnaire survey to members of the AJG several times in order to reflect their opinions in the selection. As a result, 264 places of proposed sites were shown (including some overlap); 155 from speakers and 40 from the audiences in March of 2012, 7 from speakers and 38 from the audiences in March of 2013, 20 from questionnaire respondents and 4 from questionnaire on the web. Based on the list of a total 264 places of proposed sites, the vote by the member of the committee and an argument were performed in July, 2013, and an 65 Earth Heritages were picked up. Enumeration and the vote of the new proposed site by the committee have been held again, and 33 Heritages were added afterwards. It has remaining two places at January 31th, 2014.

### 3. Contents of 100 Earth Heritages

In January 2014, 98 places of Earth Heritages are chosen. As for the Earth Heritages, 47 prefectures have one heritage at least. It depends on consideration in that the heritages should be used for geographical education in schools in Japan. However, on the other hand, the difficulty of the evaluation of the geographical value hides in the back of this consideration. In other words, geographical valuableness can insist on in area wherever of Japan.

### 4. Geographical Values from the perspectives of 100 Earth Heritages

For each heritage, the commentary sentence for choice reason is written. This article clarifies geographical value by considering the contents of the commentary sentence. The contents of sentences mostly consist of the plural sites. This is because a certain reciprocal viewpoint (story) was made between the sites. A nature and human reciprocal relations are seen in the contents. For example, in one of Yoshino River District, this district has mountains of steady sedimentary rocks and rivers cutting sharply between the mountains, this becomes the precondition of the creations of small and unique bridges for movements between the villages for settlements. Such nature and human relations are frequent in the commentary sentences of other heritages. In other words, it is thought that the geographical value from ”100 Earth Heritages” is these reciprocal relationships.

On the other hand, the contents of the commentary sentence can point out the problem, too. This article points out two dimensions. First one is seen in the contents. A writer of the commentary sentence is only physical geographer or humanities geographer. Therefore the contents are slightly deflected to physical or human geographical contents so that they should start to learn about each other’s fields. The second problem can point out that there is a giving an environmental determinism like impression for a reader, because a natural condition is described as a precondition in the sentence. So, it may be said that it is necessary for geography to discuss the environmental determinism. If the general relationship of a natural phenomenon and the humanities phenomenon is proved scientifically, it is one of the geographical directionality for Geoparks.

Keywords: Earth heritages, Physical geography, Human geography, Regional geography, Environmental determinism

## Activity support for the educational continuity from primary through early secondary levels in the Mikasa Geopark

KURIHARA, Ken'ichi<sup>1\*</sup> ; NII, Tadahiro<sup>2</sup>

<sup>1</sup>Mikasa City Museum, <sup>2</sup>Promotion Policy Division, Mikasa City Office

In the Mikasa Geopark, the educational continuity from primary through early secondary levels has been carried out since 2005. In this educational project, there is a subject "Regional Studies", which learns about attributes of Mikasa (eg., history, nature, and industry).

On the other hand, the Mikasa City Museum was established in 1979 to preserve materials of human, natural, and industrial histories of Mikasa. The curators of the museum have supported the subject "Regional Studies" as a museum activity since the first year (2005) of the educational project. Recently, the cooperation program between the educational and geopark activities is exploring.

In the presentation, we introduce the cooperation among the educational, museum, and geopark activities, and discuss the results and subjects.

Keywords: educational continuity, regional study, museum activity, geopark activity, Mikasa Geopark

## The effects of experience-based science and environmental education on Byobugaura geosite in Choshi Geopark

ANDO, Takao<sup>1\*</sup>

<sup>1</sup>Chiba Institute of Science

Choshi geopark is certified by Japan Geopark Committee (JGC) at September 24, 2012. In this study, we will introduce the contents and the effects of geoscience education program for junior high school students using Byobugaura geosite in Choshi Geopark.

Choshi, located at the east end of the Boso peninsula, 100km east of Tokyo, Chiba prefecture, Japan, has many geological heritages that should be preserved and passed on to future generations. Representative geological features in Choshi are as follows. First, the Biobugaura geosite, comprising Pliocene and Pleistocene sedimentary rocks, is approximately 9 km in length and 30~50 m in height and faces the Pacific Ocean. This topography, which is also called "Dover in the East", consists of sharp cliffs formed by land erosion resulting from sea waves. According to a previous report, the speed of erosion is 5~6 m per year. To prevent erosion, seawall was constructed in 1966. The seawall was a necessity for the residents' safety even though it negatively affected the geo-heritage. Second, Inubouzaki geosite, the Cretaceous shallow sea sediments, designated as a government national monument, are exposed in the Inubouzaki coastal area at the east end of the Choshi peninsula. Third, the "Inuiwa" geosite, carried on the tradition of the "Yoshitune legend" which is a legend concerning a samurai warrior in the medieval period of Japan, are composed of Jurassic greywacke, mud stones, and conglomerates that includes calcareous coarse fragments with fusulina fossils.

Our education program using Byobugaura geosite designed it to be usable by a curricular science class of the junior high school, and it conclude for one day. The contents of this program compose two parts, the morning part contain geotour and tephra sampling in the Byobugaura geosite, and the afternoon part consisted of geological lecture and stereomicroscope observation of tephra constituents, e.g. volcanic glass and minerals etc.

The results of questionnaire analysis for participants show (1) this program is understandable for major part of attended students, (2) this program have good effects for induction of affection for local environment, and (3) this program increase desiring to learn for earth science.

Keywords: Geopark, Choshi, Science education, tephra, Byobugaura, Life cycle thinking

## Analuzing the Efficcy of Natulal Disaster Awareness Programs based on the Understanding of Geophysical Mechanisms

SUZUKI, Yusuke<sup>1\*</sup> ; KOYAMA, Masato<sup>2</sup> ; UENISHI, Tomoki<sup>3</sup>

<sup>1</sup>Izu Peninsula Geopark Promotion Council, <sup>2</sup>CIREN, Shizuoka University, <sup>3</sup>Izu-sogo High-school

Izu Peninsula was once a submarine volcano situated in the south sea. This area collided with Honshu with the Northward movement of the Philippine sea plate and formed a peninsula from about 10 Million years back.

After this land volcanism took place that formed multiple large volcanoes. In this geopark we made attempts to popularize earth science and disaster management by conqutting questionnaires with local schools. As a result we understood the efficacy of natural hazards education by using familiar examples. From the participants there were even demands for more information and more comprehensive training programs.

Keywords: Geopark, Disaster Mitigation Education

## Detection, Observation, Preservation, and Utilization of Sand Boiling Traces along an Active Fault : Effort of Hakusan T

KOZAKA, Yutaka<sup>1\*</sup> ; HIRAMATSU, Yoshihiro<sup>2</sup>

<sup>1</sup>Hakusan Tedorigawa Geopark Promotion Council, <sup>2</sup>Kanazawa University

The Morimoto-Togashi Fault Zone which goes through Kanazawa City to Tsurugi District, Hakusan City, is one of geosites where people can learn about the formation of earth in the Hakusan Tedorigawa Geopark. On the eastside of the fault mountains (elevation of 650 meters) were formed by the upheaval. On the other hand, on the westside of the fault the Tedorigawa River transported much sediment, and an alluvial fan was formed by them.

In recent years two excavation surveys of the buried cultural properties were carried out in the western margin of the active Togashi Fault. One at the Bunyudo ruins (Hiramatsu and Kozaka, 2013) and the other at the Netsuno ruin which was excavated in 2013. Sand boiling traces were found in the both ruins, which showed a huge earthquake occurred between the late Yayoi Era and the Heian Era. It is difficult to identify the active fault which the earthquake happened, causing the sand boiling traces. However, from a survey in Umeda District along the Morimoto Fault, it was reported that the latest activity occurred after approximately 2000 years ago, prior to the fourth century (Headquarters for Earthquake Research Promotion, 2013). Therefore, the sand boiling traces are likely to be caused by the activity of the Togashi Fault, considering that the sedimentary layer which the sand boiling traces were found is correlated to the era the fault movement occurred.

We report people's activities related to these ruins where they are located on slight elevations of the alluvial fan, together with an introduction of the sand boiling traces. Additionally, we report about a study tour held in 2013 for the citizens to walk around and observe the both ruins and the Togashi Fault.

The Hakusan Tedorigawa Promotion Council is planning to peel off the sand boiling traces, panel it, and then utilize it as learning materials of the geopark to learn about the formation of earth and disaster prevention.

Keywords: Hakusan Tedorigawa Geopark, Active Fault, Morimoto-Togashi Fault Zone, Sand boiling traces, ruins

## A practical use of geoparks as university educational materials

NIINA, Atsuko<sup>1\*</sup>

<sup>1</sup>Regional Innovation Research Center, Tottori University of Environmental Studies

The purpose of this presentation is to show the practical use of geoparks as university education and to discuss the relationship between local universities and local communities. Tottori University of Environmental Studies opens four classes of *Project Research* for freshmen and sophomore. The classes of Geoparks started in 2012. The aim of the geopark classes is to learn the method of a field survey. There were various topics on geoparks; for freshmen, the development of virtual geotour, the land use survey of Yoshioka hot springs town and the development of geo product, and for sophomore, the development of geo guided tour at Aoshima of Koyamaike Lake and the regional survey of Yoshioka. These output share with local communities and geoparks. It becomes clear that a geopark makes a good use of social learning.

Keywords: university education, regional survey, social learning, San'in Kaigan Geopark, Tottori University of Environmental Studies

## Geopark guide training program in Amakusa area

UGAI, Hiroaki<sup>1</sup> ; HASE, Yoshitaka<sup>1\*</sup>

<sup>1</sup>Amakusa Geopark planning promotion committee

Amakusa Geopark planning promotion committee trained 149 geopark guides in Amakusa area in 2013. We introduce a state of the Geopark guide training at the geosites.

"Amakusa Geopark plan" is an action for "Amakusa Geopark" aiming at authorization of the Japanese Geoparks Network. The five elements, geology, geography, viewing point, culture and industry, comprise the main core of the Amakusa area which is shown at the geosites throughout the islands.

The purpose of Geopark guide training program, through a lecture in room and the local training in field, is aimed for the interpreter of the local geology, creature, culture and industry. The committee confers the qualification of the guide to the person who passed an authorized examination. Geopark guides perform their activity after the enrollment to each local tourism guide association.

Through this program we expect an effect guide authorization, common knowledge of the activity for local inhabitants and the interpreter for geopark which can convey resources in this area to anyone clearly. Geopark guide is important as a diffuser explaining "What is geopark" precisely and is necessary for an action united with local inhabitants or the education spread.

Residents and officials alike collaborate to preserve the geologic inheritance of Amakusa with an educational perspective. Exposing the unique beauty of this inheritance as a tourist attraction in conjunction with the history and culture of the area, an attractive geo-tourism will be found aim at the promotion of the Amakusa area.

Point of the local promotion by the tourism is comment on an earth science-like element for constitution of the earth and a story about the local history and culture.

Keywords: geopark, guide, inhabitants



## Program for broadening the knowledge base and awareness of geopark guides -An example of Amakusa Goshoura Geopark-

HASE, Yoshitaka<sup>1\*</sup> ; UGAI, Hiroaki<sup>1</sup> ; HIROSE, Koji<sup>1</sup> ; TSURUOKA, Seiya<sup>2</sup>

<sup>1</sup>Goshoura Cretaceous Museum, <sup>2</sup>Association of Goshoura Geo-Tourism Guide

It is very important for any geopark that its guides are actively involved in geo-tourism. Guides must strive to continually increase their awareness and broaden their knowledge base of not only their geopark, but also of neighboring areas. We will use the Amakusa Goshoura Geopark as an example to demonstrate a guide awareness-raising program in action with regard to the geology, geography, history and culture of its neighboring areas.

The Amakusa Goshoura Geopark contains strata and fossils in deposits spanning 100 million years. The strata were deposited in the Cretaceous and Paleogene periods of earth's history, and contain abundant fossils including dinosaurs from the Cretaceous period and large mammals common to the Paleogene.

From the peak of Karasu-toge, a geosite in the geopark, we can see a 360-degree panoramic view of the Yatsushiro Sea and landscape of Kyushu Island including Fugen-dake, Yatsushiro Plane, Aso Mountain, Hitoyoshi Basin, Mt. Shiraga, Ontake and Yahazudake on the Hisatsu Volcanic Plateau, Izumi Plane, Mt. Shibi, Nagashima, Shishijima and Koshikijima.

Members of the Association of Goshoura Tourism Guide group are trained to explain not only about the panorama from Karasu-toge including geologic composition and topographical features of Kyushu Island, but the wealth of information stored in its strata. As an example, the association had a tour to study the geology, geography, history and culture on the coastal area from Ashikita to Nagashima along the Yatsushiro Sea in 2014. Similarly, it will take part in the study of the Shimabara peninsula at the Shimabara Global Geopark in the near future. Training programs like these have been instituted as a means of support for the Amakusa Goshoura Geopark guide's continuing education.

Keywords: Geopark guide, neighboring areas, broadening knowledge

## Mt. Apoi Geopark telling a global dynamic movement of the earth

NIIDA, Kiyooki<sup>1\*</sup> ; MT. APOI GEOPARK, Promoting council<sup>2</sup>

<sup>1</sup>Hokkaido Univ. Museum, <sup>2</sup>Samani

Mt. Apoi geopark is located at the southwestern end of the Hidaka mountains, facing to the Pacific southward. Recently, a tectonic map showing a distribution of major plates in the northern hemisphere and suggesting a global sense of plate motion between the North American plate and the Eurasian plate was published. This map gives an easy understanding on a background of the Hidaka mountain building and a simultaneous interpretation on a global dynamic movement of the earth.

We have an excellent example of global mobile belt of the earth, which is the Tethys ophiolite belt from the European Alps ~Greek ~Turkey ~Iran ~Oman ~Pakistan ~Indus Suture ~Andaman ~Great Sunda toward the east, including the continent-continent collisions between Africa and Europe, and India and Asia. Also, we have an above example of active tectonic event such as the Hidaka mountain building, here in Mt. Apoi geopark, Hokkaido, Japan.

Keywords: Mt. Apoi geopark, peridotite, upper mantle, basaltic magma, plate boundary, global dynamic movement

## Communication of Information on the Internet By Geopark: Case Study of Sanriku Geopark

ITO, Taku<sup>1\*</sup> ; HASHIMOTO, Tomoo<sup>1</sup> ; UENO, Ayumi<sup>2</sup>

<sup>1</sup>Chuo Kaihatsu Co., <sup>2</sup>Sanriku Geopark Promotion Conference

The Sanriku geopark certified the Japanese geopark in 2013. It is the largest geopark in Japan that consists of 16 cities in Aomori, Iwate, and Miyagi prefecture. The Sanriku geopark promotion conference is disseminating information at the Internet.

In February 2011, we created the general-oriented website which summarized geological history and the highlight of Sanriku regions. Then, in response to the Great East Japan Earthquake, we have created a new web site for education travel and academic investigation in September 2011, and then, the variety of information was added to the general-oriented website towards the authorization to a Japanese geopark.

Furthermore, through the information by SNS, such as a blog, Facebook and Twitter, we increase the update frequency of information, promotion meeting was to update the content and functionality depending on the purpose or object. We increased the updating frequency of informaton, and updated contents and function according to the purpose.

Now, the degree of name recognition or comprehension of the “ geopark ” are not increasing. However, exposure to mass media and concern of local and a surrounding area are increasing in response to Japanese geopark authorization of Sanriku regions. In order to correspond to this, we decided to newly renew a website in 2014.

In this presentation, we introduce our renewal case and information transmission method and the results of a survey of website on other geoparks.

Keywords: geopark, communication of information, internet, Sanriku

## Utilization of Earth sciences for regional development

ONUMA, Saori<sup>1\*</sup> ; KORIYAMA, Suzuka<sup>1</sup> ; MAEDA, Tomoyuki<sup>1</sup> ; KIKUTA, Ryota<sup>1</sup> ; ISHIKAWA, Natsumi<sup>1</sup> ; IKETO, Hirokuni<sup>1</sup> ; MATSUHISA, Yuko<sup>1</sup> ; FUKUNAGA, Chie<sup>1</sup> ; SAWAHATA, Yurie<sup>2</sup> ; FURUKAWA, Yohei<sup>2</sup> ; HOSOI, Jun<sup>2</sup> ; AMANO, Kazuo<sup>1</sup>

<sup>1</sup>Faculty of Science, Ibaraki University, <sup>2</sup>Graduate School of Science and Engineering, Ibaraki University

The information on earth sciences is useful for disaster prevention of a natural hazard like earthquake and volcanic eruption etc. The new trend utilizing the information of earth sciences to lifelong learning and tourism occurred in recent years. The geopark can be the best place providing this information.

Ibaraki University Geological Information Utilizing Project team is providing geological informations for the management of North Ibaraki Geopark. Main act is creation of 15 sightseeing guidance maps. Now, we are improving the contents of previous maps. Furthermore, we are having strong cooperation with local residents and companies for the regional development.

Keywords: Geopark, North Ibaraki Geopark, regional development

## Activity of Misato-Kai in Sado Island Geopark

ICHIHASHI, Yayoi<sup>1\*</sup>

<sup>1</sup>Sado city board of education Geopark promotion office

We introduce the activity of Misato-Kai, which played an important role for Sado Island Geopark to be a member of Japanese Geoparks Network.

Misato-Kai is the association that was established in 2006 by hostesses of local Japanese inns and hotels to keep close relationship with each other and revitalize tourism in Sado Island. Until now, they've made eco-friendly chopsticks and OMOTENASHI pocket notebooks.

Also, they make place mats as their activities. These mats are made of paper and have some pictures and captions on them to introduce some tourist attractions and promotional programs to guests. This time, they made the place mat under the theme of Sado Island Geopark and many groups and associations such as, Misato-Kai, Sado City and welfare facilities give much support to make it. The cooperation is the significant feature for this activity.

Now, these place mats are attracting favorable comments from hotel guests. Some guests bring it home and others leave some messages on it for people of welfare facilities in Sado Island. It is a useful tool for communication between the hotel guests and the hostesses in local Japanese inns.

In Sado Island, many associations are extremely active. They are very important for Sado Island Geopark activities. We hope that we can work together for our geopark in the future.

Keywords: Sado Island Geopark, Misato-Kai, tourism

## Let us Enjoy Geo-Tetsu - the Sixth Geo-tour through Train Windows, Nakamura and Sukumo Line of the TOSA KUROSHIO RAILWAY

FUJITA, Masayo<sup>1\*</sup> ; YOKOYAMA, Shunji<sup>1</sup> ; KATO, Hironori<sup>1</sup> ; UENO, Shoji<sup>1</sup> ; YASUDA, Tadashi<sup>1</sup> ; IMAO, Keisuke<sup>1</sup> ; SUGA, Yasumasa<sup>1</sup>

<sup>1</sup>Geo-Tetsu Project Committee of the Fukada Geological Institute

### 1. Aims of Geo-Tetsu activities

Geo-Tetsu is the name of the activity that shows everyone ways to enjoy and learn about geology and related sciences, using railways (Kato et al., 2009). Following five year's Geo-Tetsu promote activities are continued by geological engineers who love railways, organized with the corporation of the Fukada geological institute since 2009 (Fujita et al., 2013) and established Geo-Tetsu Project Committee since 2013.

Geo-Tetsu offers the chance to get acquainted with geological features, not only through train windows but also along paths accessible from the stopovers alongside the railway routes. We selected enjoyable Geo-Tetsu courses and Geo-points. As much information is obtainable and can be gathered from various perspectives; the railway itself, geology, geography, cultural heritage and sight-seeing as well. We hope that the general public will enjoy a new style of railway traveling provided by the Geo-Tetsu. The Nakamura and Sukumo Line of TOSA KUROSHIO RAILWAY is presented in this as sixth route of Geo-tetsu.

### 2. The Nakamura and Sukumo Line, the sixth Geo-Tetsu project

#### (1) Abstract of the Nakamura and Sukumo Line

The Nakamura and Sukumo Line run from Kubokawa at Shimanto Town to Sukumo City in the western region of Kochi Prefecture. The railway connects from Kubokawa to Nakamura at 43.0km, and from Nakamura to Sukumo at 23.6km. Both are single track, and the route not electrified. In the line, there are characters designed by Takashi YANASE. Additionally, they have seven wrapped vehicles of municipalities. John Mung (Manjiro Nakahama), Whales, Whale Sharks, Kashiwa-jima Island, Kyoto cultures of the Shimanto City, and the event character of the Sukumo City etc. are painted there. The vehicles not only transport passengers but also inform the charms of the western region of Kochi Prefecture.

The Nakamura Line and the Sukumo Line have a different history of construction. At first, the construction of the Sukumo Line had been promised. However, the Nakamura Line was given to priority by the political motivation. The Nakamura Line was started constructing in 1956, and opened in 1970. On the other hand, the Sukumo Line was started constructing in 1974, but it was interrupted by the Japanese National Railways reconstructing promote measure law in 1981. Afterwards, both routes were succeeded by TOSA KUROSHIO RAILWAY Ltd. as the third sector railway. At last, when the Sukumo Station opened, it became a present route in October, 1997.

#### (2) The rich geological and sight-seeing resources of the Nakamura and Sukumo Line

The Nakamura and Sukumo Line runs on the Shimanto terrane that consists of sandstone and the mudstone from Cretaceous to Paleogene. The train leaves Kubokawa Station (asl 210m) and goes to Kaina Station (asl 47m), descending the inclination of 23 permil or less. Especially, "the First Kawaoku Tunnel (2031m)" is well worth as loop of 350m in radius, descending 20 permil, and the exit appears below by 40m. If you have the compass, you can confirm its needle will be made one rotation in the tunnel. When we goes out there, train runs along Iyoki River. Soon we arrive at the Tosa-Saga Station in famous of bonito's single-hook fishing. The train passes under a lot of short tunnels with the outcrops of turbidite of Shimanto terrane around Tosa-Shirahama. Between Ukibuchi and Tosa-Irino Station, you can visit the river-mouth deviation of the Fukiage River. There are almost stone monuments of the Nankai Earthquake at the Kamo shrine in woods of pine at Irino.

Through the Kotsuka Station, the train changes front to the west. It crosses the Shimanto River in parallel to a red bridge as old national road. In the downstream, there is a long dam for the flood disaster evasion. The train advances straight in the Nakasuji lowland (Kano et al., 2003), which understood the slope-basin deposit (Domeki Formation). Lastly, the train comes out of Hijirigaoka Tunnel (5084m), we arrive at the Sukumo Station.

Keywords: Geo-Tetsu, Geo Point, Nakamura and Sukumo Line of the TOSA KUROSHIO RAILWAY, loop tunnel, Shimanto terrane, Nakasuji lowland

## Collectivity and individuality of particle dispersion under gravity

HARADA, Shusaku<sup>1\*</sup>

<sup>1</sup>Faculty of Engineering, Hokkaido University

Collective motion of fine particles in liquid can be widely seen not only in engineering processes but also in natural phenomena such as water treatment [1], sediment transport [2], bio-convection [3] and lava convection [4]. It is well-known that the spatial variance of particle concentration brings about large-scale convection flow under gravity and sometimes it affects macroscopic motion of particles. In this study, of particular interest is whether collective or individual motion of particles reveals in liquid under the gravity field. The existence of concentration interface, which is an ambiguous interface between suspended particles and pure fluid, plays a significant role in these extreme behaviors.

Figure indicates the settling behaviors of stratified-suspended particles in a vertical Hele-Shaw cell filled with liquid [5]. In cases of small particle size with high concentration, the interfacial instability occurs at the lower concentration interface and the suspended particles behave as an immiscible fluid even though there is no distinct border with pure fluid [6]. Consequently the settling velocity is much faster than that of an isolated particle. On the other hand, in case of large particles with low concentration, the concentration interface is less distinct and the suspended particles settle individually. The transition from these collective to individual motions of suspended particles is controlled by the border resolution of concentration interface. We define the dimensionless parameter which describes the border resolution of concentration interface by the ratio of average particle distance  $d_p/\phi^{1/3}$  ( $d_p$ : particle diameter,  $\phi$ : concentration) to the dominant wavelength of the instability  $\lambda$ . As can be seen in Figure, the dimensionless parameter well describes the transition from fluid-like to particle-like behaviors. The suspended particles (and the interstitial fluid) perfectly behaves as continuum for  $d_p/\phi^{1/3}\lambda < 0.03$  and behaves individually relative to fluid for  $d_p/\phi^{1/3}\lambda > 0.2$  [5].

The similar collective motion of suspended particles has been studied on the settling of particle clouds in viscous fluid. Some researchers have suggested that the collective motion of particles in clouds can be explained by the swarm of Stokeslet [7]. They have found that the particle cloud behaves collectively when the flow generated by each particle (Stokeslet) enough screens the surrounding flow. If the above parameter is rewritten by number density of particles  $N$ , it is expressed as  $(6/\pi)^{1/3}/N^{1/3}\lambda$ . Therefore the border resolution of concentration interface express the discretization of space by Stokeslet  $1/N^{1/3}$  for a given lengthscale  $\lambda$ .

One more interesting similarity to previous study is the wavelength of instability. From the linear stability analysis of Rayleigh-Taylor instability on both miscible and immiscible interfaces of pure fluids [8], it is found that the dominant wavelength of miscible interface with no diffusion and immiscible interfaces with no interfacial tension are asymptotically close to constant value. The wavelength at concentration interface is also close to the asymptotic value [9]. From this point of view, the concentration interface can be interpreted both as the the immiscible interface with no interfacial tension and the miscible interface with no diffusion.

### References

- [1] E. Guyon et al., Physical Hydrodynamics, Oxford University Press (2001).
- [2] J. D. Parsons et al., Sedimentology, 48, 465-478, (2001).
- [3] T. J. Pedley and J.O. Kessler, Annu. Rev. Fluid Mech., 24, 313-358, (1992).
- [4] H. Michioka and I. Sumita. Geophys. Res. Lett., 32, L03309, (2005).
- [5] S. Harada et al., Eur. Phys. J. E, 35, 1-6, (2012).
- [6] C. Voltz et al., Phys. Rev. E, 65, 011404, (2001).
- [7] B. Metzger et al., J. Fluid Mech., 580, 283-301, (2007).
- [8] J. Fernandez et al., Phys. Fluids, 13, 3120-3125, (2001).
- [9] S. Harada et al., Chem. Eng. Sci., 93, 307-312, (2013).

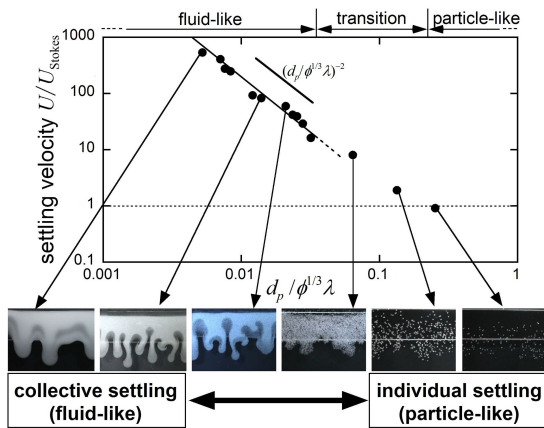


Figure 1: Collective and individual settlings of suspended particles in Hele-Shaw cell.



## Reverse chemical garden reaction of cementitious materials

SATOH, Hisao<sup>1\*</sup> ; FURUKAWA, Erika<sup>2</sup> ; KIMURA, Yuki<sup>2</sup>

<sup>1</sup>Mitsubishi Materials Corporation, <sup>2</sup>Tohoku University

Recent advances in the nano-scale mineralogy extend from the extraterrestrial materials known as in cosmic dusts and asteroids to ordinary industrial materials like the cementitious materials. The distinct property of nano materials can be characterized from the points of view of (1) nucleation, (2) self-assembly behavior and (3) flexibility in the form.

A very common industrial material, cement is a typical one consisted of nano particles of calcium silicate hydrates (C-S-H).

Crystal growth experiment of cementitious materials can be recently performed using interferometric and nanoscopic techniques. Although the cement reaction producing C-S-H from silicates with Ca(OH)<sub>2</sub> (portlandite: CH) or more alkaline solution is extensively occurring at buildings under and after construction, similar reaction is expected at the interface of natural rock and concrete-building such like tunnel, dam and underground repository for radioactive wastes.

Hyper alkaline alteration experiment using vertical scanning interferometer revealed the precipitation behavior of C-S-H by reverse chemical garden reaction on natural rock (Satoh et al., in press). Very slow growth rate of the C-S-H on rock was observed to be  $\sim 2.4E-3$  nm/s. The ionic selection of the solutes through the C-S-H wall having nanopores like membrane was also confirmed.

Most recently, we applied newly developed ultramicroscopic technique with fluid reaction TEM (FR-TEM: Poseidon) for study of reverse chemical garden reaction between silica fume (Elkem Microsilica 940-U,  $\sim 150$  nm) and CH-saturated solution. It revealed that the reaction caused silica hydration (volume expands) and subsequently form string and veil of C-S-H. The growth rate of string C-S-H was calculated to be  $\sim 4.5E-2$  nm/s, which is fast enough to form frame network preparing veil-formation. It was chemically confirmed by FESEM-EDS that this C-S-H veil evolved toward Ca-rich over time. Our observed result could be a fundamental process of reverse chemical garden reaction, i.e., cement-solidification.

Ultramicroscopic investigation of C-S-H growths may improve the simulation of groundwater conditions in the future.

Keywords: reverse chemical garden reaction, cementitious material, C-S-H, fluid reaction TEM

## General nature of liquid-liquid transition in aqueous organic solutions

MURATA, Ken-ichiro<sup>1\*</sup> ; TANAKA, Hajime<sup>1</sup>

<sup>1</sup>Institute of Industrial Science, University of Tokyo

Contrary to the conventional wisdom that there exists only one unique liquid state for any material, there are growing experimental and numerical pieces of evidence for the existence of more than two liquid states in a single component substance. The transition between them is called liquid-liquid transition (LLT). LLT has attracted considerable attention because of its importance in the fundamental understanding of the liquid state. However, the physical nature of the transition has remained elusive. Particularly for water, the possible existence of LLT has special implications not only on its fundamental understanding, but also on a link of various thermodynamic and transport anomalies with critical anomaly associated with LLT. Here we reveal that 14 aqueous solutions of sugar and polyol molecules, which have an ability to form hydrogen bonding with water molecules, exhibit liquid-liquid transitions. We find evidence that both melting of ices and liquid-liquid transitions in all these aqueous solutions are controlled solely by water activity, which is related to the difference in the chemical potential between an aqueous solution and pure water at the same temperature and pressure. Our theory shows that water activity is determined by the degree of local tetrahedral ordering, indicating that both phenomena are driven by structural ordering towards ice-like local structures. This has a significant implication on our understanding of the low-temperature behaviour of water.

Keywords: liquid-liquid transition, water and aqueous solution, supercooled liquids and glasses

## Direct Observation of Crystallization Process in a Solution using Transmission Electron Microscopy

KIMURA, Yuki<sup>1\*</sup>; YAMAZAKI, Tomoya<sup>1</sup>; FURUKAWA, Erika<sup>1</sup>; NIINOMI, Hiromasa<sup>2</sup>; TSUKAMOTO, Katsuo<sup>1</sup>; GARCIA-RUIZ, Juan M.<sup>3</sup>

<sup>1</sup>Tohoku University, <sup>2</sup>Nagoya University, <sup>3</sup>Universidad de Granada

Nucleation is a fundamental event that determines the size, number and morphology of produced crystals. Therefore, the nucleation process must be clarified to form products efficiently and to predict mineralization in various environments. The direct approach to understanding nucleation would be atomic-scale in-situ observation, for which a transmission electron microscope (TEM) would be a most powerful tool. However, the experimental conditions for TEM are limited, and there have been only a few reports on the in-situ observation of nucleation processes to date. In particular, since TEM needs a high vacuum, crystallization experiments in a solution are generally impossible. Recently, the processes of formation of nanoparticles and coalescence in a solution were finally observed using specially designed cells in a TEM [1-3]. However, live observation of the dynamics of the earliest stages of nucleation - those taking place before the formation of a stable crystal - had never been achieved before our recent work [4]. We overcame the difficulty by using an ionic liquid, which has negligible vapor pressure and is not charged up by the electron beam due to its relatively high electron conductivity, and by aiming to visualize the dynamics of nucleation under conditions very close to equilibrium, where the nucleation rate must be small but the conditions for TEM observation are more stable. We used two TEMs at an acceleration voltage of 200 kV (Hitachi H-8100, installed at Tohoku University, Japan) for the nucleation experiment and 300 kV (Hitachi H-9500, installed at Hitachi High-Technologies Corporation, Ibaraki, Japan) for the in-situ heating experiment.

An ionic solution could be observed stably under normal electron irradiation conditions as expected. Nucleation of sodium chlorate crystals was directly observed in the TEM at room temperature. Then, the sample was heated up in the TEM. The main results of the heating experiment were as follows:

1. Nanocrystals were not only dissolved but also newly formed even in the totally dissolving system, i.e., probably an under-saturated condition.
2. Both stable and metastable crystals nucleated independently of their respective solubility. However, metastable crystals were dissolved in a shorter residence time.
3. The total number of smaller particles decreased with the formation of new particles by the Ostwald ripening at or near equilibrium conditions.
4. High-density fluctuations may lead to nucleation even under equilibrium conditions.

We describe the ongoing results to elucidate the dynamics of nucleation at the nanoscale, as well as the growth, coalescence and dissolution of nanocrystals in a solution.

[1] Yuk, J. M., Park, J., Ercius, P., Kim, K., Hellebusch, D. J., Crommie, M. F., Lee, J. Y., Zettl, A. & Alivisatos, A. P. High-resolution EM of colloidal nanocrystal growth using graphene liquid cells. *Science* **336**, 61-64 (2012).

[2] Li, D., Nielsen, M. H., Lee, J. R. I., Frandsen, C. Banfield, J. F. & De Yoreo, J. J. Direction-specific interactions control crystal growth by oriented attachment. *Science* **336**, 1014-1018 (2012).

[3] Liao, H.-G., Cui, L., Whitlam, S. & Zheng, H. Real-time imaging of Pt<sub>3</sub>Fe nanorod growth in solution. *Science* **336**, 1011-1014 (2012).

[4] Kimura, Y., Niinomi, H., Tsukamoto, K. & Garcia-Ruiz, J. M. In-situ live observation of nucleation and dissolution of sodium chlorate nanoparticles by Transmission Electron Microscopy. *J. Am. Chem. Soc.*, DOI: 10.1021/ja412111f. (2014).

Keywords: Nucleation, In-situ observation, TEM, Ionic liquid

## Emergence and Amplification of Chirality via Achiral-Chiral Polymorphic Transition in Sodium Chlorate Solution Growth

NIINOMI, Hiromasa<sup>1\*</sup>; HARADA, Shunta<sup>1</sup>; UJIHARA, Toru<sup>1</sup>; MIURA, Hitoshi<sup>2</sup>; KIMURA, Yuki<sup>3</sup>; UWAHA, Makio<sup>4</sup>; TSUKAMOTO, Katsuo<sup>3</sup>

<sup>1</sup>Graduate School of Engineering, Nagoya University, <sup>2</sup>Graduate School of Natural Sciences, Nagoya City University, <sup>3</sup>Graduate School of Science, Tohoku University, <sup>4</sup>Graduate School of Science, Nagoya University

Chirality is the concept that widely spreads in nature at various levels from elementary particles to morphology of plants. Although both the enantiomers have equal stability, lives on the earth preferentially selects one-type of the two enantiomers. This phenomenon is called homochirality, and its origin (the emergence of chirality) and the amplification of chirality are great puzzles in the evolution of life on the primitive earth. One candidate of the origin includes chiral crystallization of achiral compounds. Sodium chlorate ( $\text{NaClO}_3$ ) undertakes chiral crystallization from achiral solution.  $\text{NaClO}_3$  has chirality in its crystal structure due to the enantiomorphic space group of  $P2_13$  (cubic). A *static* solution of the compound yields statistically equal numbers of the two enantiomorphs. However, Kondepudi *et al.* have strikingly revealed that a *stirred* solution yields only one-type of the enantiomorphs[1]. The mechanism of the significant chiral bias has not been elucidated. Diverse crystallization experiments have implied that the emergence and the amplification proceed during the early stage of crystallization. However, a direct investigation of the early stage is still missing. We therefore have carried out in-situ observations focusing on the early stage. The observations have revealed that achiral metastable crystals having  $P2_1/a$  symmetry (monoclinic) appear prior to the formation of chiral crystals. The authors have reported this result in JpGU 2011[2]. Here, we present more detailed observations, and demonstrate that polymorphic transformation from the achiral phase to the chiral phase can be responsible for the emergence and the amplification.

A droplet (6  $\mu\text{l}$ ) of  $\text{NaClO}_3$  aqueous solution saturated at 22 °C was put on a glass slide whose temperature is controlled at 22 °C by a Peltier device, allowing the droplet to evaporate isothermally. We observed crystallization process induced by the evaporation using a polarized light microscope. The microscope enables us to distinguish cubic crystals from non-cubic crystal by detecting birefringence, allowing us to distinguish chiral crystals from achiral crystals, and it can identify handedness of the chiral crystals by detecting optical rotation.

Polymorphic transformation from an achiral crystal to a chiral crystal was observed. The transformation could be classified into two kinds according to their transition rate. The slower one proceeds at 35  $\mu\text{m}/\text{sec}$  (Fig.A), and the faster did at 2000  $\mu\text{m}/\text{sec}$  (Fig.B). The slower transformation was induced by a contact with a chiral crystal. It is noteworthy that the resulting enantiomorph generated through the contact-induced transformation was certainly the same as the enantiomorph that contacted with the achiral crystal. The double digit difference in a rate of the two transformations is probably ascribed to difference in the mechanism, indicating the slower transformation and the fast one are solvent-mediated phase transformation (SMPT) and structural phase transition (SPT), respectively. The SPT probably generates both the enantiomorphs in equal probability since the activation energy required to transform should be equal. In contrast, the contact-induced SMPT preferentially generates the same enantiomorph as the contacted crystal. This inheritance of chirality through the contact-induced SMPT is possibly responsible for the amplification of chirality.

So far, the emergence and the amplification have been explained by primary nucleation of a chiral crystal and secondary nucleation from the crystal. In contrast, our observation provided a new sight based on the achiral-chiral polymorphic transformation: the emergence of chirality through the SPT and its amplification through the contact-induced SMPT.

### References

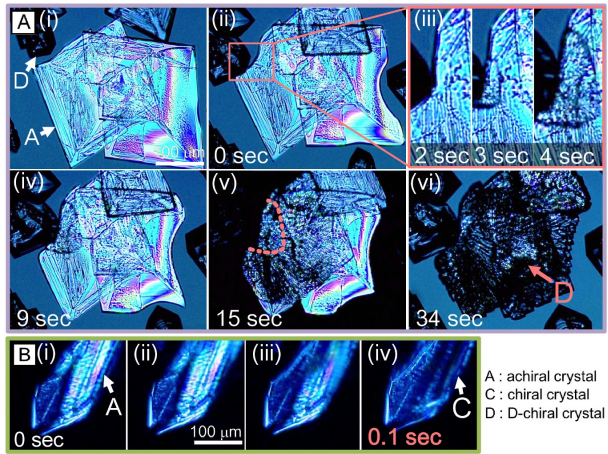
- [1] D.K. Kondepudi, R. J. Kaufman & N. Singh, (1990). *Science*, Vol. 250, pp.975-976.
- [2] H. Niinomi, T. Kuribayashi, H. Miura & K. Tsukamoto, Japan Geoscience Union Meeting 2011, MIS020-06.

Keywords: sodium chlorate, chiral symmetry breaking, chiral crystallization, metastable phase, polymorphic transformation, in-situ observation

MIS36-05

Room:314

Time:May 1 11:45-12:00



## Theoretical analysis on the stability of divalent cations in the surface sites and clusters of calcium carbonate

KAWANO, Jun<sup>1\*</sup> ; SAKUMA, Hiroshi<sup>2</sup> ; NAGAI, Takaya<sup>3</sup>

<sup>1</sup>CRIS, Hokkaido Univ., <sup>2</sup>NIMS, <sup>3</sup>Grad. School of Science, Hokkaido Univ.

Formation process of calcium carbonate polymorphs, calcite, aragonite and vaterite has been extensively investigated, and impurity effect has been proposed as controlling phenomena in order to account for the formation of a particular polymorph. For example, it has been reported that an addition of  $Mg^{2+}$  in a solution inhibits calcite formation and promotes aragonite formation, however incorporation mechanism of this kind of impurities is poorly understood.

In general, smaller divalent cations than  $Ca^{2+}$ , like  $Mg^{2+}$ , cannot form solid solution with aragonite. However, the structure of a crystal surface or small cluster forming at an initial stage of crystal growth can be different from the bulk crystal because of its flexibility, and it can act as the site for incorporation of ions which is unstable in the bulk structure. In the present study, the stability of divalent cations, especially  $Mg^{2+}$ , (1) on hydrated aragonite surface and (2) in the cluster forming in an early stage of nucleation was investigated by quantum-chemical calculations, and the impurity effects on the formation of polymorphs were discussed.

The calculation results show that  $Mg^{2+}$  is easier to be incorporated into a small cluster, while the hydration energy of  $Mg^{2+}$  is higher than that of other divalent cations. This indicates that  $Mg^{2+}$  is difficult to be released from hydration shell, however, once released, it is easy to incorporate into the cluster. Atomic arrangement of these clusters including  $Mg^{2+}$  is different from that of additive-free  $CaCO_3$  clusters. Furthermore,  $Mg^{2+}$  on the aragonite surface considerably affects the surface structure and has an influence on the stability of aragonite. Thus, incorporation of  $Mg^{2+}$  into the clusters and surfaces sites should play an important role on the formation of the crystalline nuclei and the consequent crystal growth.

Keywords: calcium carbonate, impurity, crystal growth

## Atomic scale in situ observation of solid-liquid interface of calcite

ARAKI, Yuki<sup>1\*</sup>; TSUKAMOTO, Katsuo<sup>2</sup>; KIMURA, Yuki<sup>3</sup>; MIYASHITA, Tomoyuki<sup>4</sup>; OYABU, Noriaki<sup>5</sup>; KEI, Kobayashi<sup>6</sup>; YAMADA, Hirofumi<sup>5</sup>

<sup>1</sup>Graduate school of Science, Kobe University, <sup>2</sup>Graduate school of Science, Tohoku University, <sup>3</sup>Institute of Low Temperature Science, Hokkaido University, <sup>4</sup>Faculty of Biology-Oriented Science and Technology, Kinki University, <sup>5</sup>Department of Electronic Science and Engineering, Kyoto University, <sup>6</sup>The Hakubi Center for Advanced Research, Kyoto University

Calcium carbonate is one of common minerals on the earth. Calcium carbonate crystals are utilized industrially in various fields, so that the control of crystal growth is required. It has been known that organisms control the morphology and polymorph of calcium carbonate crystals by utilizing inorganic and organic additives in biomineralization. Understanding the additive effects on growth of calcium carbonate crystal is necessary to control the crystal growth.

The effect of additives on growth of calcite which is a stable polymorph of calcium carbonate has been investigated. The additive effect on calcite surface, such as incorporation of magnesium ions into calcite and pinning of step propagation by organic molecules has been confirmed. On the other hand, the additive effect on hydration of calcite has remained unclear even if that effect has been suggested by the measurement of growth rate of calcite in the presence of additives. Hydration affects adsorption and surface diffusion of ions on calcite surface. Also, the dehydration has been considered as rate-determining process in solution growth by the estimation of energy barriers of solution growth processes. Therefore, hydration is a key to control the kinetics of calcite growth.

Hydration at the vicinity of calcite surface has been measured by surface X-ray diffraction. Although this technique made the description of hydration structure clear, it does not show the local difference of hydration structure between on the terrace and the step front which is capture site of ions. Hence, we employed the newly frequency modulation atomic force microscopy (FM-AFM) for in situ observation of local hydration structure in atomic scale. This technique is expected to provide insight into the atomic scale distribution of hydrated water molecules in growth solution even at step front. This study describes the first in situ examination of the additive effect of organic molecules and magnesium ions on local hydration structure of calcite surface in atomic scale utilizing FM-AFM. The hydration images were compared with the growth rate of calcite measured using phase shift interferometry so as to validate the influence of hydration on the growth rate of calcite.

The findings are summarized as follows:

- (1) The synthetic polypeptide, even that with high hydrophilicity, does not affect hydration at the surface of calcite.
- (2) Combination of magnesium ions and the synthetic polypeptides provides a rigid hydration on calcite surface.
- (3) Magnesium ions and the synthetic polypeptides influence hydration and the surface pattern of calcite, respectively.
- (4) Structured water distribution eases the energy gap between the calcite surface and solution. As a result, the interfacial tension between the calcite surface and the solution is decreased.
- (5) Magnesium ions and the synthetic polypeptide act in unison to accelerate nucleation via changes in hydration structure.
- (6) Hydration contributes to interfacial energy between the calcite and the solution, but not for the adsorption of ions on the calcite steps.

This study demonstrated that additives affect the interfacial tension via altering hydration structure by application of FM-AFM for crystal growth experiment for the first time. Our results also showed that there is hardly any change in the adsorption of ions on calcite surface due to the hydration structure. That suggests that dehydration is not a rate-determining process, an observation that is contrary to the currently prevailing theory. The further observation of hydration of step front will be carried out by FM-AFM to demonstrate the effect of hydration on adsorption of ions. These findings indicate that the control of interfacial tension is possible utilizing the additive effect on hydration. That provides a new knowledge to regulate the polymorphism of calcium carbonate.

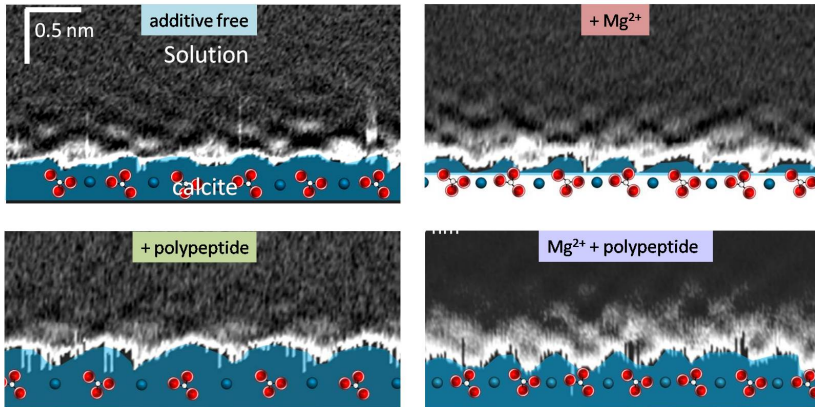
Keywords: Calcite, Hydration, FM-AFM

MIS36-07

Room:314

Time:May 1 12:15-12:30

FM-AFM images of Hydration structure on calcite





## Impurity partitioning in colloidal crystallization

NOZAWA, Jun<sup>1\*</sup> ; HU, Sumeng<sup>1</sup> ; KOIZUMI, Haruhiko<sup>1</sup> ; FUJIWARA, Kozo<sup>1</sup> ; UDA, Satoshi<sup>1</sup>

<sup>1</sup>Institute for Materials Research, Tohoku University

Colloidal crystals are regarded as a promising tool to investigate diverse basic physical phenomena. We have applied this colloidal crystal to impurity partitioning in the melt growth. Since no research has been focused to detail partitioning behavior of colloidal crystals, the objective of the present work is to reveal a partitioning behavior during colloidal crystallization.

A few amount of impurities (2 percent) were doped to the colloidal dispersion, from which colloidal crystals were grown with convective assembly method. Polystyrene particles (PS) were used for fabricating colloidal crystals, and different sizes of PS and fluorescent bearing PS (w/fluor.) were doped as impurity particles.

In each particle size for two kinds of impurity, effective partition coefficient ( $k_{eff}$ ) were measured at various growth rates. Obtained  $k_{eff}$  gives  $k_0$  by using BPS plot. The  $k_0$  is decreased as the difference between the size of the impurity and the 500 nm host particle increased. The  $k_0$  of each w/fluor. was larger than that of the corresponding pure PS. Moreover, the value of  $k_0$  for the 520 nm w/fluor. surpassed unity, whereas the PS is always less than unity.

We have employed a Thurmond and Struthers (T&S) model (J. Phys. Chem. 57, 831 (1953)) to discuss the difference of  $k_0$  for PS and w/fluor. particles. T&S model shows  $k_0$  as;  $k_0 = \exp((\Delta G_{Tr} - \Delta H)/RT)$ . Here,  $\Delta G_{Tr}$  is free energy difference between the solid and liquid phases of an impurity at the transition temperature, T,  $\Delta H$  is the excess enthalpy which is caused by incorporation of the impurity into the host material, and R is a gas constant. We have determined the phase transition volume fraction for PS and w/fluor. to evaluate the  $\Delta G_{Tr}$ . It was shown that  $\Delta G_{Tr}$  of w/fluor. is positive whereas PS is zero. This leads to larger  $\Delta G_{Tr} - \Delta H$  of w/fluor. than that of PS, which corresponds to larger  $k_0$  of w/fluor., and in a small  $-\Delta H$  range,  $k_0$  of w/fluor. surpasses unity. We have found the difference of  $k_0$  for different kinds of impurity particles, and succeeded in applying concept of T&S model to partitioning of colloidal crystals.

Keywords: Colloidal crystal, Impurity partitioning

## Mechanism of ice nucleation on (100) plane of calcium oxalate monohydrate: a molecular dynamics simulation study

NADA, Hiroki<sup>1\*</sup>; ISHIKAWA, Masaya<sup>2</sup>; ECHIGO, Takuya<sup>3</sup>

<sup>1</sup>EMTECH, National Institute of Advanced Industrial Science and Technology (AIST), <sup>2</sup>National Institute of Agrobiological Sciences, <sup>3</sup>Shiga University

Calcium oxalate monohydrate (COM) is the most thermodynamically stable polymorph of calcium oxalate. COM is known as an organic mineral formed on the surface of the Earth, under the bottom of sea, in atmosphere, in meteorites, in plants and in kidney stones. So far, COM has been studied in fields of mineralogy, biology and medical science.

Recently, Ishikawa et al. suggested that COM plays as an ice nucleation promoter, like silver iodide and ice nucleation-active bacteria. They speculated that the structure of COM (100) plane induces ice nucleation. Studies on the mechanism of ice nucleation promotion by COM are important, because the studies may help provide development of new materials to make artificial snow. Molecular dynamics (MD) simulation is a helpful method to investigate the mechanism of ice nucleation at the molecular scale. Thus, we performed a MD simulation to elucidate the mechanism of ice nucleation on the (100) plane of COM.

In the simulation, the intermolecular interaction between a pair of water molecules was estimated using a six-site model. The water-COM interaction was estimated using a COM potential model proposed by Tommaso et al. In the <100>direction of COM, two different molecular layers are piled up by turns; one is positively-charged Ox-1 layer consisting of calcium ions and oxalate ions, and the other is negatively-charged Ox-2 layer consisting of oxalate ions and water molecules. In this study, the simulation was performed for a rectangular parallelepiped system in which supercooled water consisting of 4000 water molecules was sandwiched by Ox-1 and Ox-2 layers. Temperature was set to 268 K. Total run was 4 ns or longer. The simulation indicated the formation of a polar cubic ice structure near the Ox-2 layer. However, the formation of a hexagonal ice structure was not observed. Details of the simulation results will be shown at the presentation.

This work was supported by a Grant-in-Aid for Scientific Research (No. 22107004) on Innovative Areas of "Fusion Materials (Area No. 2206)" from the Ministry of Education, Culture, Sports, Science and Technology (MEXT).

Keywords: crystal growth, nucleation, ice, organic mineral, computer simulation, calcium oxalate

## Observation of admolecule on the crystal surface in liquid by non-contact atomic force microscopy

NAGASHIMA, Ken<sup>1\*</sup>

<sup>1</sup>Institute of Low Temperature Science, Hokkaido University, Japan

The highest resolution AFM images are obtained by non-contact atomic force microscopy (NC-AFM). Fukuma et al. (2005) succeeded in obtaining true atomic resolution images by NC-AFM in spite of the liquid environment [1]. We are interested in the crystal growth process. However, previous NC-AFM studies were only about insoluble crystals in liquid. NC-AFM is not good at investigating the moving surface because NC-AFM is a very sensitive method for detecting weak interaction force. Therefore, we tried to observe several soluble crystals in liquid by NC-AFM at first.

At first, we observed tetragonal lysozyme (110) face in saturated solution by using homebuilt Non-Contact AFM (NC-AFM). We could observe individual molecules on the lysozyme (110) face in liquid for the first time and determine the crystallographic position of each molecule [2]. In addition, we also observed admolecule and point defect on the lysozyme surface in liquid.

### Acknowledgments

We thank Prof. S. Morita of Osaka University, M. Abe of Nagoya University, and Shimadzu Corporation for observation of AFM.

[1] T. Fukuma et al., Appl. Phys. Lett. 87, 034101 (2005).

[2] K. Nagashima et al., J. Vac. Sci. Technol. B 28, C4C11 (2010).

Keywords: AFM, Crystal growth, Atomic resolution image, Admolecule, Protein crystal

## In-Situ Observation of Protein Crystal Growth in The International Space Station

MURAYAMA, Kenta<sup>1\*</sup> ; YOSHIZAKI, Izumi<sup>2</sup>

<sup>1</sup>Katsuo Tsukamoto, <sup>2</sup>JAXA

In-situ observation of protein crystal growth was conducted at the international space station in 2012. Both growth rate and surface topography of lysozyme crystals vs supersaturation and purity of the solution were measured for the first time by interferometry in space. The differences from ground-based experiments became clear to answer the question "Why better crystal could be grown in space?".

Keywords: crystal growth, space experiment, microgravity

## In situ simultaneous SEM/STEM observation of Pt/C catalysts in a gaseous atmosphere

SATO, Takeshi<sup>1\*</sup> ; MATSUMOTO, Hiroaki<sup>1</sup> ; NAGAOKI, Isao<sup>1</sup> ; NAGAKUBO, Yasuhira<sup>1</sup> ; YAGUCHI, Toshie<sup>1</sup>

<sup>1</sup>Hitachi High-Technologies Corporation

In order to gain fundamental understanding of the degradation mechanisms of Pt/C catalyst, there is an increasing demand on the nanostructural characterization using TEM. We have developed the humid-air supply system in TEM, H-9500 300 kV TEM and we have success the deterioration mechanism of fuel cell electrocatalyst<sup>1</sup>. Recently, we developed in situ simultaneous SEM/STEM observation technique for surface analysis of catalyst materials using a HF-3300 Cold-FE TEM with SEM/STEM function. We succeeded in visualizing of three-dimensional movement of the Pt particles on the carbon support in the gas atmosphere by this observation technique.

In situ simultaneous SEM/STEM observation of the platinum catalysts on carbon support (Pt/C; Pt: 29 wt.%) in the air conditions were carried out using HF-3300 equipped with the Cold-FE gun and the SEM/STEM function. A gas injection-heating specimen holder<sup>2</sup> was used for the Pt/C powder heating and gas injection. Pt/C powder mounted on the tungsten wire was heated to 200 deg C in a TEM, and then, while air was spraying (up to  $1.2 \times 10^{-2}$  Pa) from the injection nozzle to the Pt/C, the behavior of the Pt/C was recorded as the movie file. After the air injection at about  $1.0 \times 10^{-3}$  Pa, the coalescence growth between Pt particles on the carbon support was observed, and the Pt particles gradually started inserting into the carbon support. After that, most all of the Pt particles on the carbon support disappeared from the surface of the carbon support. And the carbon support structure was changing into a porous morphology.

We can observe that the behavior of the Pt particles on the carbon support was penetrated into the carbon support by in situ simultaneous SEM/STEM observation. These results demonstrate that the penetration of Pt particles to carbon support affects the degradation mechanism of a Pt/C electrocatalyst.

1. T. Yaguchi et. al., Journal of Electron Microscopy 60(3), 217?225, (2011)
2. T. Kamino et. al., Journal of Electron Microscopy 54(6), 497?503, (2005)

Keywords: electron microscope, in situ observation

## Low temperature crystallization of free-flying silicate nanoparticles investigated by in-situ IR measurement experiment

ISHIZUKA, Shinnosuke<sup>1\*</sup> ; KIMURA, Yuki<sup>1</sup> ; SAKON, Itsuki<sup>2</sup>

<sup>1</sup>Department of Earth and Planetary Science, Tohoku University, <sup>2</sup>Department of Astronomy, University of Tokyo

Dust is typically 100 nm sized nanoparticles which can be observed ubiquitously in the universe. Dust forms from the high temperature gas in the out flow of evolved stars and dispersed into interstellar space. Silicate dust is one of the most abundant minerals in the universe including, shells around evolved stars [1], disks around young stars [2], comets [3] and so on. So its formation mechanism is the key process to understand the lifecycle of dust. Especially, 10  $\mu\text{m}$  IR band structure from 8  $\mu\text{m}$  to 12.5  $\mu\text{m}$  in wavelength arising from Si-O stretching provides us mineralogical character of silicate. The Infrared Space Observatory mission revealed the existence of crystalline silicates around evolved stars based on the 10  $\mu\text{m}$  band feature mainly attributed to amorphous silicate [4]. Numerous laboratory experiments to reproduce the observed spectra such as direct condensation [e.g. 5] and annealing of amorphous silicates [e.g. 6] showed variation in the IR spectra due to structure, chemical composition, temperature, size and shape, and proposed formation mechanisms of crystalline silicates. Nevertheless the scenario is not fully understood. One of the most important discrepancies concerning the dust formation process is a detection of an IR feature attributed to crystalline silicates at low temperature region, typically <300 K [1] in contrast to amorphous silicates at high temperature region [4]. Low temperature crystalline silicates cannot be explained by direct condensation or annealing involving high temperature process.

Recently, we have investigated new IR measurement technique for free-flying nanoparticles which enabled direct comparison with astronomical observation without KBr medium effects which pervert its band structure such as peak wavelength, FWHM and relative intensity [7]. Applying the new IR technique, we investigated condensation of Mg-bearing silicate from thermally evaporated magnesium and silicon oxide under the atmosphere of O<sub>2</sub> and Ar based on 10  $\mu\text{m}$  band.

*In-situ* IR measurement revealed initial condensates were amorphous or droplet of Mg-bearing silicate and its crystallization took place at <500 K. Furthermore, crystallization kept proceeding through lower temperature region. Produced particles showed core-mantle like structure, amorphous silica covered with polycrystalline forsterite observed by Transmission Electron Microscope.

Prevailing annealing experiments reported that 1000 K is required for crystallization of forsterite [8]. This critical discrepancy may be explained by nano size effects. When immoderately small particle nucleates, a particle takes metastable amorphous or droplet phase because of lower melting point of a nanoparticle [9] and larger diffusion coefficient of molecules in a nanoparticle distinct from in bulk [10]. In case the condensates were droplet due to the size effects, activation energy of crystallization is significantly low compared to amorphous [11]. We concluded such characteristic phenomena in nanometer scale enabled low temperature crystallization in the same way as the circumstellar environments.

References: [1] Waters, L. B. F. M., et al. 1996, A&A, 315, L361, [2] Bouwman, J., et al. 2001, A&A, 375, 950, [3] Hanner, M., et al. 1994, ApJ, 425, 274, [4] Molster, F., & Kemper, C. 2005, Space Sci. Rev., 119, 3, [5] Tsuchiyama, A. 1998, Mineralogy journal, 20, 59, [6] Hallenbeck, S. L., et al. 2000, ApJ, 535, 247, [7] Bohren, C. F., & Huffman, D. R. 1983, Absorption and Scattering of Light by Small Particles (New York: Wiley), [8] Koike, C., et al. 2010, ApJ, 709, 983, [9] Qi., 2005, Physica B, 368, 46, [10] Yasuda, H., et al. 1992, JEM, 41, 267, [11] Tanaka, K., K. et al. 2008, JCG, 310, 1281

Keywords: astromineralogy, nanoparticle, experiment, IR

## Free energy of cluster formation and a new scaling relation for the nucleation rate

TANAKA, Kyoko<sup>1\*</sup> ; DIEMAND, Juerg<sup>2</sup> ; ANGELIL, Raymond<sup>2</sup> ; TANAKA, Hidekazu<sup>1</sup>

<sup>1</sup>Institute of Low Temperature Science, Hokkaido University, <sup>2</sup>University of Zurich

Recently we performed molecular dynamics (MD) simulations of homogeneous nucleation from vapor for systems of  $(1-8) \times 10^9$  Lennard-Jones atoms [Diemand et al. J. Chem. Phys. 139, 074309 (2013)]. The very large MD simulations allow us to determine the formation free energy of clusters accurately over a wide range of cluster sizes, for the first time. This is now possible because such large simulations allow for very precise measurements of the cluster size distribution in the steady state nucleation regime. The peaks of the free energy curves give critical cluster sizes, which agree well with independent estimates based on the nucleation theorem. Using these results, we derive an analytical formula and a new scaling relation for nucleation rates:  $\ln J' / \eta$  is scaled by  $\ln S / \eta$ , where the supersaturation ratio is  $S$ ,  $\eta$  is the dimensionless surface energy, and  $J'$  is a dimensionless nucleation rate. This relation can be derived using the free energy of cluster formation at equilibrium which corresponds to the surface energy required to form the vapor-liquid interface. At low temperatures (below the triple point), we find that the surface energy divided by that of the classical nucleation theory does not depend on temperature, which leads to the scaling relation and implies a constant, positive Tolman length equal to half of the mean inter-particle separation in the liquid phase.

Keywords: nucleation, molecular dynamics simulation, nucleation rate, scaling, free energy of cluster formation

## High-speed polarized in-situ observation in a nucleation process of nanoparticles produced by the gas evaporation method

KIMURA, Yuki<sup>1\*</sup>; MIHARA, Arata<sup>2</sup>; ONUMA, Takashi<sup>2</sup>; ISHIZUKA, Shinnosuke<sup>1</sup>; MURAYAMA, Kenta<sup>1</sup>; TSUKAMOTO, Katsuo<sup>1</sup>

<sup>1</sup>Tohoku University, <sup>2</sup>Photron

The gas evaporation method has been investigated for more than half a century since the Kubo effect was reported (1962). There have been many studies on the produced nanoparticles mainly using a transmission electron microscope, which have elucidated the different physical properties of nanoparticles from those in bulk. On the other hand, there have been almost no reports on nucleation in smoke related to crystal growth. Recently, we achieved in-situ observation of the nucleation process in smoke using a double-wavelength Mach-Zehnder-type interferometer, which can determine the temperature and pressure at the nucleation simultaneously. A series of experiments clearly showed that smoke particles condense homogeneously only in a very high supersaturated environment [1-3]. In a preliminary experiment using tungsten trioxide, the smoke particles condensed with a degree of supersaturation as high as  $\sim 10^6$ . In this process, since evaporant is continuously supplied into the surrounding of the evaporation source, the flow of smoke after the nucleation and growth of nanoparticles has been simply considered as a consecutive process. The nucleation and growth of smoke particles should be a rapid process (ms order) due to high supersaturation, so the concentration of the evaporated vapor drastically decreases. However, the details of the formation process remain unknown.

In this study, we attempted to visualize the nucleation of nanoparticles and motion of smoke using a high-speed polarization image sensor (Photron Inc.) to clarify the details of the nucleation process of smoke particles. Since the sensor itself has pixels with micro-polarizers, a phase shift interferogram can be obtained in less than a millisecond because of the lack of mechanical movement free, and can therefore be applied to rapid phenomena such as nucleation in vapor phase. Here, we show the preliminary results of homogeneous nucleation of tungsten oxide from vapor phase.

[1] Y. Kimura, H. Miura, K. Tsukamoto, C. Li, T. Maki, Interferometric in-situ observation during nucleation and growth of  $WO_3$  nanocrystals in vapor phase, *Journal of Crystal Growth*, 316 (2011) 196-200.

[2] Y. Kimura, K. Tsukamoto, Interferometric observation of temperature distributions in the smoke experiment, *J. Jpn. Soc. Microgravity*, 28 (2011) S9-S12.

[3] Y. Kimura, K. K. Tanaka, H. Miura, K. Tsukamoto, Direct observation of the homogeneous nucleation of manganese in the vapor phase and determination of surface free energy and sticking coefficient, *Crystal Growth & Design*, 12 (2012) 3278-3284.

Keywords: Nucleation, High-speed polarized camera, in-situ observation



## In-situ observation of nucleation process of calcium carbonate by the fluid-reaction TEM

YAMAZAKI, Tomoya<sup>1\*</sup>; FURUKAWA, Erika<sup>1</sup>; KIMURA, Yuki<sup>1</sup>

<sup>1</sup>Tohoku University

Recent studies have reported achievements of in-situ observation of the nucleation and crystallization studies using transmission electron microscope (TEM), and several new perspectives for non-classical pathway of crystallization [1-4]. Calcium carbonate generates a lot of attention because of complex nucleation due to appearance of various polymorphs in addition to availability for industrial materials such as paper and paint, and reservoir of carbon dioxide, and biomineralization. We also focus on the calcium carbonate in view of selection of polymorph in nucleation process. In case of nucleation from relatively higher supersaturated solution, nucleation of amorphous phase prior to crystalline phase has been known [5,6]. Kawano et al. have been reported an in-situ observation of solution-mediated phase transition from amorphous phase into crystalline phase under optical microscope [6]. The Ostwald law of stages has been believed to occur in many cases. Contribution of prenucleation cluster, which was confirmed by using the cryo-TEM [8], to the nucleation has also been reported [7]. However the generality or solution condition to take these processes is still not obvious.

Now, we have performed energetically a project to observe crystallization and dissolution processes in an aqueous solution using ionic liquid instead of water or the "Poseidon" (Protochips Inc.), which is a sample holder having a liquid cell for TEM observation. We call our TEM fluid-reaction TEM (FR-TEM), which is able to perform crystallization experiments in a solution including both methods. Here, we have been tried to observe whole the process of crystallization of calcium carbonate via amorphous phase using fluid-reaction TEM and actually observed a solid-state phase transition from amorphous phase into a crystalline phase by in-situ observation.

- [1] Yuk, J. M., Park, J., Ercius, P., Kim, K., Hellebusch, D. J., Crommie, M. F., Lee, J. Y., Zettl, A. & Alivisatos, A. P. *Science* **336**, 61-64 (2012).
- [2] Li, D., Nielsen, M. H., Lee, J. R. I., Frandsen, C., Banfield, J. F. & De Yoreo, J. J. *Science* **336**, 1014-1018 (2012).
- [3] Liao, H.-G., Cui, L., Whitlam, S. & Zheng, H. *Science* **336**, 1011-1014 (2012).
- [4] Kimura, Y., Niinomi, H., Tsukamoto, K. & Garcia-Ruiz, J. M. *J. Am. Chem. Soc.*, DOI: 10.1021/ja412111f. (2014).
- [5] Ogino, T., Suzuki, T. & Sawada, K. *Geochim. et Cosmochim. Acta*, **51** (1987) 2757.
- [6] Kawano, J., Shimobayashi, N., Kitamura, M., Shinoda, K., & Aikawa, N. *J. Cryst. Growth*, **237** (2002) 419.
- [7] Gebauer, D., & Colfen H. *Nano Today*, **6** (2011) 564.
- [8] Pouget, E.M., Bomans, P. H., Goos, J.A.C.M., Frederik, P.M., de With, G. & Sommerdijk, N. A. *Science*, **323** (2009) 1455.

Keywords: Fluid-reaction TEM, In-situ observation, Calcium carbonate, Nucleation

## In-situ TEM observation of dissolution processes in aqueous solutions using "Poseidon"

FURUKAWA, Erika<sup>1\*</sup> ; YAMAZAKI, Tomoya<sup>1</sup> ; KIMURA, Yuki<sup>1</sup>

<sup>1</sup>Tohoku University

Recently, we started a new project to observe crystallization and dissolution processes of crystals in a solution using two different methods under transmission electron microscope (TEM). To overcome the difficulties to introduce a solution into a TEM, Kimura et al. used ionic liquid to avoid evaporation of a solvent in the high-vacuum of a TEM [1]. As the result, several new insights were found: solubility-independent formation of polymorph; crystals do not dissolve smoothly but in a fluctuating manner; and new crystals form even in a totally dissolving system. Another advantage of this method is that the growing crystal does not have a hydrated layer on their surface. It has been believed that dehydration process has a largest potential barrier to incorporate a unit cell into the crystal. However, no one ever visualized the process and it has been totally veiled. The water free experiment using an ionic liquid may give us a new perspective on the dehydration process by comparison with experiments in general aqueous solutions. Now, we are forwarding a project to observe crystallization and dissolution processes in an aqueous solution in atomic-scale using the "Poseidon", which is a sample holder having a liquid cell for TEM observation. We call our TEM fluid-reaction TEM (FR-TEM) including both solution growth experiments using an ionic liquid and the Poseidon.

Poseidon (Protochips Inc.) give us the opportunity to visualize the three-dimensional process with several advantages compared with previous works using an atomic force microscope, which is able to observe only two-dimensional, and an optical microscope, which has much less lateral resolution. Growth and dissolution processes at the first top layer (surface) of a crystal have been energetically studied long time using these tools. However, the detail process in atomic scale has been observed very limited. Therefore, the aims of our project is understanding of three dimensional nucleation including Ostwald law of stages based on phase determination by electron diffraction, determination of very slow dissolution rates, and dissolution process in terms of an influence of defects. Here, we will show the first pictures about the movements of nanoparticles and dissolution of amorphous silica and crystalline silicate samples.

[1] Kimura, Y., Niinomi, H., Tsukamoto, K. & Garcia-Ruiz, J. M. In-situ live observation of nucleation and dissolution of sodium chlorate nanoparticles by Transmission Electron Microscopy. *J. Am. Chem. Soc.*, DOI: 10.1021/ja412111f. (2014).

Keywords: Fluid-reaction TEM, Dissolution, In-situ observation

## Mineral size distribution modeling during dissolution of montmorillonite

YAMAGUCHI, Kohei<sup>1\*</sup>; MIURA, Hitoshi<sup>2</sup>; SATOH, Hisao<sup>1</sup>

<sup>1</sup>Mitsubishi Materials Co., <sup>2</sup>Nagoya City University

In the geological disposal of radioactive waste, the waste is sealed by cement-based materials and bentonite-based material to prevent leakage into environment. The bentonite-based material protect the radioactive waste from the groundwater flow around the geological disposal area, so its low permeability should be maintained for a long term. The low permeability could be achieved by the swelling of montmorillonite in the bentonite-based material. However, montmorillonite will dissolve by a reaction with high-alkaline pore water, spoiling the low permeability of the bentonite-based material. In addition, precipitation of secondary minerals such as zeolite will promote the dissolution of montmorillonite through changes in composition of the pore water. In order to assess the long-term permeability of the bentonite-based material, it is necessary that the dissolution of montmorillonite and crystallization of secondary minerals are comprehended over a long time of several tens of thousands years.

In the pore water, there are numerous montmorillonite particles of various sizes. When montmorillonite of various sizes co-exists in the same solution, the smaller particle dissolves faster than the larger one because of the Thomson-Gibbs effect. The mean size of montmorillonite will increase gradually, leading to a delay of further dissolution. In addition, an evolution of size distribution is also important for the crystallization process of the secondary minerals, e.g., zeolite. Since zeolite is not present in the initial solution, the crystallization process is described in the nucleation and subsequent growth. Evolution of the size distribution of zeolite affects the dissolution of montmorillonite through changes in solution composition. This implies that the evolution of the size distribution of montmorillonite and zeolite should be considered to assess the long-term behavior of the permeability of the bentonite-based materials. However, in the previous chemical equilibrium calculations, the evolution of the size distribution has not been considered.

In this report, we numerically modeled the time evolution of the size distribution of montmorillonite due to dissolution according to a theoretical model described in Yao et al. (1993). The crystallization of zeolite was neglected as a first step. We consider the dissolution of montmorillonite in a closed system. The evolutions of the size distribution, bulk concentration of solution, and mean radius of montmorillonite were successfully calculated.

The model given in this report is a model in a closed system. On the other hand, the geological disposal environment is not a closed system because there is an actual mass transfer due to the flow of groundwater and diffusion. To couple the local mineral dissolution/crystallization and the global mass transfer, some chemical reaction-mass transfer calculation codes have been developed. However, these codes assumed chemical equilibrium, so the evolution of the size distribution of minerals did not considered. The evolution of the size distribution of minerals would significantly affect the long-term behavior of the permeability of the bentonite-based materials. Therefore, it is important to compare the calculation results of the model with the evolution of the size distribution and chemical equilibrium calculation result.

Keywords: montmorillonite, dissolution, Mineral size distribution

## Advanced techniques in the latest quantitative image analysis for crystal growth experiments

YOKOMINE, Makoto<sup>1\*</sup>; SATOH, Hisao<sup>2</sup>; TSUKAMOTO, Katsuo<sup>3</sup>; SAZAKI, Gen<sup>4</sup>

<sup>1</sup>TOYO Corporation, <sup>2</sup>Mitsubishi Materials Corporation, <sup>3</sup>Tohoku University, <sup>4</sup>Hokkaido University

In the research field of crystal growth science, the targeted scales are varied from nano-scaled small space to visible large space. Recently the spatial scale expands toward underground or orbital space. In the metrology field, there is the scaling-law for xyz-t space-time space, beyond which we extend the measurable limits.

The contactless microscopes like interferometers or laser microscopes are very valuable tools for analyzing crystal growth in long time and surface-features in wide area because they have advantages to obtain data in high speed without spoiling the sample surface. Their time-scale is variable in the off-line processing, if the data were sequentially obtained by auto-measurements, so that we can trace the real growth phenomena. By this method, we succeeded to observed lysozyme growths in the International Space Station laboratory, ice-water interface and dissolving clay.

Moreover, the spatial scale can be changed by shifting the field of view with observing and the off-line process of these obtained images as stitching. In general, huge data fragments measured by certain time interval or position shifting contain offsets or distortions and the data amount is much bigger than the speed of manual corrections. Hence, there are many cases that whole data cannot be utilized for final analysis. We attempted to eliminate artifacts generated by microscopes using a system consist of commercially supplied software and dedicated plug-in programs for consistent normalizations and corrections between planes to be stitched.

In this session, we will introduce some examples tried quantitative analysis of huge multiple data including the time-line display expressing time-based changes at certain line on a plane of growing and dissolving crystal surfaces.

Keywords: image analysis, time-space scale, topography, huge stitching

## IP6 as a silver carrier agent and formation of Ag nanostructures

TATSUOKA, Hirokazu<sup>1\*</sup> ; MENG, Erchao<sup>2</sup> ; KOBAYASHI, Tsuyoshi<sup>3</sup> ; SHIMOMURA, Masaru<sup>1</sup> ; TOMODA, Waichi<sup>1</sup> ; MIYABAYASHI, Keiko<sup>1</sup>

<sup>1</sup>Graduate School of Engineering, Shizuoka University, <sup>2</sup>Graduate School of Science and Technology, Shizuoka University, <sup>3</sup>Koba Technology

In recent years, people have become aware of the importance of natural organic materials in geological systems. It would be important to clarify the interaction between natural organic materials and metallic ions.

Phytic acid, known as inositol hexakisphosphate (IP6), or phytate,  $C_6H_{18}O_{24}P_6$ , is found within the hulls of nuts, seeds, and grains, and it is the principal storage form of phosphorus in many plant tissues, especially bran and seeds. IP6 is not digestible to humans and animals, and phytic acid chelates make unabsorbable certain important minerals such as zinc, iron, calcium and magnesium.

On the other hand, for many years, it has been known that silver works for its catalytic activities, anti-microbial activities, and used to avoid infections and prevent spoilage. Many researchers have focused on the anti-bacterial, ability to kill microorganisms and multi-functional properties of silver nano-particles.

In this study, it is demonstrated that IP6 plays a role as a metal carrier agent for the formation of metallic nanostructures. For the preparation of the IP6 with Ag elements (Ag-IP6), The commercial IP6 solution (50 %) was diluted with distilled  $H_2O$  at the  $H_2O:IP6$  solution ratio of 9:1, then 1g of  $AgNO_3$  was added to the diluted IP6 solution of 100 ml, and long-term stabilized small Ag clusters were formed in the solution. A drop of the solution was dripped onto metallic substrates, then kept for the treatment time of 10 s to several min at room temperature. The solution was immediately dried using a gas burner or hot plate. Then, the reaction of the Ag-IP6 with several kinds of metals was examined. The structural and morphological properties of the Ag nanostructures were characterized by scanning electron microscopy (SEM) along with energy dispersive X-ray spectroscopy (EDS), transmission electron microscopy (TEM) and scanning transmission electron microscopy (STEM) with EDS. In addition, the surface condition of the Ag nanostructures reacted with Cu or Al and dried IP6 complexes was characterized by X-ray photoelectron spectroscopy (XPS) using a VG, ESCA-LAB Mk II with a non-monochromatized Al  $K\alpha$  source ( $h\nu = 1486.6$  eV). The energy calibration for a charge correction in the spectra was made using the C1s peak. The FTIR spectra of the dried IP6 complexes were measured using KBr disks. Each disc was composed of powders consisting of IP6:KBr~1:100. The spectra were recorded in the range of 400 to 1400  $cm^{-1}$ . Raman spectra were obtained using an NR-1800 triple Raman system with backscattering geometry using the SHG(532 nm) of a Nd:YAG laser as the excitation source. All measurements were carried out at room temperature. It was found that various kinds of Ag nanostructures were formed with additional metallic sources using the Ag-IP6. Ag nanostructures with the three-dimensional dendritic structures replaced by Cu and Mn, the two-dimensional dendritic structures replaced by  $CaSi_2$  and Mg, the two-dimensional fractal structures replaced by Fe, Ti, Al and Ni, the particles replaced by  $SrSi_2$  and the nanowires replaced by Mo and W were formed. It is noted that the IP6 plays an important role as a silver carrier agent to control the structure and morphology of the Ag nanostructures. In addition, the experimental results suggest that the structural evolution of the Ag-IP6 reacted with Cu takes place to form the Cu-IP6 complex. However, the reaction of Ag-IP6 with Al is not active.

The structural properties of the Ag nanostructures were examined, and the growth evolution of the nanostructures was discussed. The results would help us to understand the nanostructure formation by the reaction between natural organic materials and metals in nature.

Keywords: IP6, nanostructure, dendrite growth, silver

## Development and application of 3-D interferometer for analysis of the concentration field in protein crystal growth

MURAYAMA, Kenta<sup>1\*</sup> ; TSUKAMOTO, Katsuo<sup>1</sup>

<sup>1</sup>Graduate School of Science, Tohoku University

When the crystal is growing in a supersaturating solution, the solute concentration is decreasing towards the crystal/ solution interface because the crystal consumes solute in the solution as it grows. Due to this large vertical concentration gradient, buoyancy driven solutal convection develops. As a result, the distribution of concentration around the crystal become complicated compared to the case when there is no convection.

Thus, not only concentration gradient but also the flow and convection of the solution influences the state of the crystal surface. So that visualizing the whole concentration field of a crystal interface including convection is required.

There have been many reports concerning the measurement of the concentration field, but many of them were two-dimensional (2-D) observations, namely, the objects were observed only from one direction. The information obtained by the 2-D observations is integrated in average along the direction of the observation, so the local information, e.g., concentration distribution around the crystal-liquid interface, was not obtained.

To improve the disadvantage on the 2-D observation, a method of computer tomography (CT) has been adopted in this study. By using the CT method, we can reconstruct the information of the three-dimensional (3-D) concentration field around the growing crystal based on 2-D observations obtained from several directions (3-D observation).

In this study, 3-D measurement of the concentration field with convection and without convection around inorganic and protein crystals was carried out to reveal the concentration distribution over the crystal surfaces. Normal growth rate of the face from points to points are also measured to discuss the effect of concentration distribution on the surface.

Keywords: interferometer, lysozyme, convection

## Dependence of impurity adsorption on the step morphologies and growth rate of tetragonal lysozyme crystal

OSHI, Kentaro<sup>1\*</sup> ; YOSHIZAKI, Izumi<sup>2</sup> ; KIMURA, Yuki<sup>1</sup> ; YAMAZAKI, Tomoya<sup>1</sup> ; TSUKAMOTO, Katsuo<sup>1</sup>

<sup>1</sup>Graduate School of Science, Tohoku University, <sup>2</sup>Japan Aerospace Exploration Agency (JAXA)

High quality protein crystals are required to get the information of the 3-dimensional structure of protein molecules. Impurities, mainly dimer molecules, affect the quality of protein crystal strongly (Yoshizaki et al., 2006). In addition, it is known that the step morphology on {110} faces of the tetragonal lysozyme crystal is changed by impurities. Until now, a lot of space experiments were carried out to get high quality protein crystals under microgravity conditions (McPherson, 1993, etc.). However, the relevance between impurity effects and microgravity condition is not clear. In addition, the step morphology corresponding to the crystal external form is not observed in preceding studies.

We performed "in situ" observations under terrestrial environment and space environment using a tetragonal lysozyme crystal as the model protein. The purpose of this paper is to reveal "the influence of microgravity condition to the impurities adsorption on the {110} faces" and "the reason why the step morphology corresponding to crystal external form does not appear". We made it possible to observe the step morphology and to measure the face growth rate at the same time by using a Michelson type interferometer.

As a result of growth rate measurement, the face growth rate under microgravity condition was higher than that under terrestrial condition. An impurity works to suppress the growth rate of a crystal. Because the buoyancy-driven convection was suppressed under the microgravity condition, we assumed that the larger impurity-depletion-zone was formed around a crystal.

As a result of the observation of the step morphology, we succeeded in observing the lozenge shape step which was corresponding to an external form by a space experiment for the first time. In addition, the step morphologies were classified in four types. It is considered that the impurity adsorption on the crystal surface is different depending on the crystal orientation of the step.

## A Report of Big-Data Processing and Operation of the NICT Science Cloud

MURANAGA, Kazuya<sup>1\*</sup>; UKAWA, Kentaro<sup>1</sup>; YUTAKA, Suzuki<sup>1</sup>; MURATA, Ken T.<sup>2</sup>; WATANABE, Hidenobu<sup>2</sup>; MIZUHARA, Takamichi<sup>3</sup>; TATEBE, Osamu<sup>4</sup>; TANAKA, Masahiro<sup>4</sup>; KIMURA, Eizen<sup>5</sup>

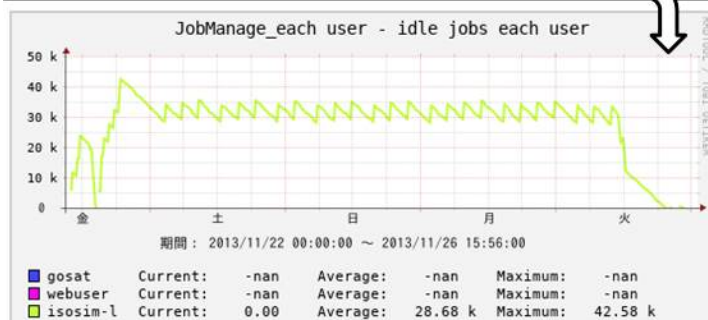
<sup>1</sup>Systems Engineering Consultants Co., LTD., <sup>2</sup>National Institute of Information and Communications Technology, <sup>3</sup>CLEALINKTECHNOLOGY Co.,Ltd., <sup>4</sup>University of Tsukuba, <sup>5</sup>Ehime University

This paper is to propose a cloud system for science, which has been developed at NICT (National Institute of Information and Communications Technology), Japan. The NICT science cloud is an open cloud system for scientists who are going to carry out their informatics studies for their own science.

The NICT science cloud is not for simple uses. Many functions are expected to the science cloud; such as data standardization, data collection and crawling, large and distributed data storage system, security and reliability, database and meta-database, data stewardship, long-term data preservation, data rescue and preservation, data mining, parallel processing, data publication and provision, semantic web, 3D and 4D visualization, out-reach and in-reach, and capacity buildings.

In the present talk we discuss the basic concept of the NICT Science Cloud: (1) data transfer and crawling, (2) data preservation and stewardship and (3) data processing and visualization. After brief introductions of several functions and tools for them, we discuss systems via mash-up of these technologies, which are for practical research works.

ISOSIM-L処理:サイエンスクラウドでTorque/Maui  
ジョブ投入環境整備・19万を超えるタスクを分割投入





## High-speed File Transfer Tool with the Gfarm File System

WATANABE, Hidenobu<sup>1\*</sup> ; KUROSAWA, Takashi<sup>2</sup> ; MURATA, Ken T.<sup>1</sup>

<sup>1</sup>National Institute of Information and Communications Technology, <sup>2</sup>Hitachi Solutions East Japan, Ltd.

A distributed storage system of scale-out type is gradually being used in the High Performance Computing (HPC) to store large scale data. NICT is also running an about 3 petabyte-scale (PB) distributed storage system with the Gfarm file system and a 10Gbps Layer 2 network (JGN-X) in Japan. Gfarm is open source software of a distributed file system for a petabyte-scale grid computing, and has been adopted as a shared storage of the High Performance Computing Infrastructure (HPCI).

When Gfarm copies data between storage servers in long-distance network, it uses a multiple TCP streaming technique to transfer data faster because TCP single streaming is known to produce a low network throughput in a long distance network. However, efficiency of high-speed by the technique becomes low as more distant.

We developed a high-speed file transfer tool worked with Gfarm. The tool adopts the UDT protocol as a data transfer protocol and has a control function for a parallel data transfer. UDT is a reliable UDP based application level data transport protocol over wide area high-speed networks, and uses UDP protocol to transfer bulk data with its own reliability control and congestion control mechanisms. In fact, UDT can provide a high network throughput than TCP in a long distance network.

We explain our tool and report the performance results of the tool in basic evaluation.

## An Examination of Data I/O Speed on a Parallel Data Storage System

MURATA, Ken T.<sup>1\*</sup>; WATANABE, Hidenobu<sup>1</sup>; UKAWA, Kentaro<sup>2</sup>; MURANAGA, Kazuya<sup>2</sup>; YUTAKA, Suzuki<sup>2</sup>; TATEBE, Osamu<sup>3</sup>; TANAKA, Masahiro<sup>3</sup>; KIMURA, Eizen<sup>4</sup>

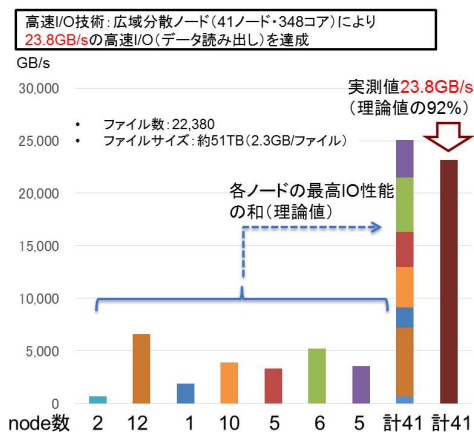
<sup>1</sup>National Institute of Information and Communications Technology, <sup>2</sup>Systems Engineering Consultants Co., LTD., <sup>3</sup>University of Tsukuba, <sup>4</sup>Ehime University

This paper is to propose a cloud system for science, which has been developed at NICT (National Institute of Information and Communications Technology), Japan. The NICT science cloud is an open cloud system for scientists who are going to carry out their informatics studies for their own science.

The NICT science cloud is not for simple uses. Many functions are expected to the science cloud; such as data standardization, data collection and crawling, large and distributed data storage system, security and reliability, database and meta-database, data stewardship, long-term data preservation, data rescue and preservation, data mining, parallel processing, data publication and provision, semantic web, 3D and 4D visualization, out-reach and in-reach, and capacity buildings.

In the present study, we examine performance of parallelization of I/O on the NICT Science Cloud system. We examine two types of data file system; parallel file system (GPFS) and distributed file system (Gfarm). The later file system shows a tremendous fast I/O, as fast as 23 GB/sec using only 30 servers. We should pay attention to this I/O speed (23GB/sec is 184 Gbps) from the viewpoint of network speed. Since general network speed so far is 10 Gbps or 40 Gbps in a cloud system, this 184 Gbps is fast enough that the I/O cannot be a bottle-neck for big data processing.

We also discuss that the distributed file system shows better scalability compared with the GPSF system. Parallelization efficiency in the present examination is higher than 90% in case of parallel file system. This suggests that, in the near future, we can expect higher I/O speed using more file servers. For instance, if the I/O speed is as fast as 100 GB/sec, it takes only 1,000 sec. (17 min.) to read 100 TB data files.



## STARS touch: A web-application for time-dependent observation data

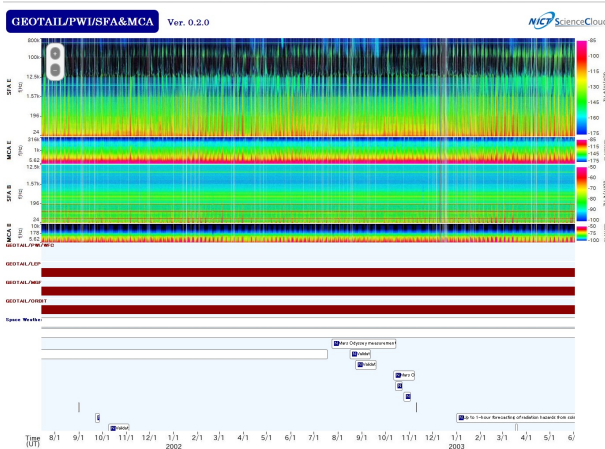
UKAWA, Kentaro<sup>1\*</sup> ; MURANAGA, Kazuya<sup>1</sup> ; YUTAKA, Suzuki<sup>1</sup> ; MURATA, Ken T.<sup>2</sup> ; SHINOHARA, Iku<sup>3</sup> ; KOJIMA, Hirotsugu<sup>4</sup> ; NOSE, Masahito<sup>4</sup> ; WATANABE, Hidenobu<sup>2</sup> ; TATEBE, Osamu<sup>5</sup> ; TANAKA, Masahiro<sup>5</sup> ; KIMURA, Eizen<sup>6</sup>

<sup>1</sup>Systems Engineering Consultants Co., LTD., <sup>2</sup>National Institute of Information and Communications Technology, <sup>3</sup>Japan Aerospace Exploration Agency, <sup>4</sup>Kyoto University, <sup>5</sup>University of Tsukuba, <sup>6</sup>Ehime University

This paper is to propose a cloud system for science, which has been developed at NICT (National Institute of Information and Communications Technology), Japan. The NICT science cloud is an open cloud system for scientists who are going to carry out their informatics studies for their own science.

The NICT science cloud is not for simple uses. Many functions are expected to the science cloud; such as data standardization, data collection and crawling, large and distributed data storage system, security and reliability, database and meta-database, data stewardship, long-term data preservation, data rescue and preservation, data mining, parallel processing, data publication and provision, semantic web, 3D and 4D visualization, out-reach and in-reach, and capacity buildings.

In the present study, we discuss a Web application for time-dependent science data, which is named "STARS touch". This Web application is based on a technique of asynchronous data transfer of graphic files for several types of data plots. The cloud system create a huge number of data plots with various time scale (e.g., from few minutes to few years) for each data-set. Parallel processing techniques to create such huge number of graphic data files are also discussed. We also make a live demonstration of the STARS touch to show several types of applications not only for research works but also for social data previews.



## High performance data processing for detection of bipolar waveforms from KAGUYA/WFC-L using the NICT Science Cloud

DAISUKE, Yagi<sup>1\*</sup> ; MURATA, Ken T.<sup>2</sup> ; KASAHARA, Yoshiya<sup>1</sup> ; GOTO, Yoshitaka<sup>1</sup>

<sup>1</sup>Kanazawa Univ, <sup>2</sup>National Institute of Information and Communications Technology

Lunar orbiter named KAGUYA was launched in September, 2007, and was operated until June, 2009. The WFC (waveform capture) onboard KAGUYA measures plasma waves below 1MHz around the moon. The WFC-L, one of subsystems of WFC, is a waveform receiver measuring waveform from 100 Hz to 100 kHz with its sampling frequency at 250 kHz. Characteristic bipolar waveforms which can be classified into some patterns were observed by the WFC-L. We developed an automatic detection algorithm to pick up these bipolar waveforms, but it takes huge computation time because the total amount of the WFC-L data is about 190 GB.

In the present study, we introduced the Science Cloud system served by National Institute of Information and Communications (NICT) in order to improve the performance of trial and error process for the development of detection algorithm. The NICT Science Cloud is a cloud system built for scientific research and data service especially for big data science. We utilized parallel data processing under the work flow control implemented in the NICT Science Cloud. We report the performance of the NICT Science Cloud in the present paper.

In order to define an appropriate workflow to the data processing servers, Pwrake (Parallel Workflow extension for Rake) was introduced as a task scheduler. Pwrake is extended for file sharing systems from Rake which is a build tool described by Ruby language. It is possible to assign tasks to each node and to perform parallel data processing by describing the contents of processing, the node to be used, and the number of cores.

We confirmed that total processing time reduced down to 1/140 times compared with a case of 1 node and 1 core, when we used 10 nodes and 24 cores. Because of the effect of hyper-thread technology, processing speed is not proportional to the number of the resources. By utilizing the system, it is expected that a higher-precision detection algorithm can be developed efficiently. As further works, development of more intelligent detection algorithm as well as evaluation of the performance using much larger resources of the NICT Science Cloud will be necessary.

Keywords: Lunar Orbiter KAGUYA, Waveform Capture, NICT Science Cloud, parallel processing

## Comparison of grid data formats in meteorology: the reason for indexed sequential access method (ISAM) used in JMA

TOYODA, Eizi<sup>1\*</sup>

<sup>1</sup>NPD, Japan Meteorological Agency

Many format standards are used for grid data of simulation such as numerical weather prediction (NWP). Wright and Gao (2008) argued there are direct-access and sequential formats, and a choice is needed between fastness of partial read and compactness of data files. However, a JMA's local standard NuSDaS (Toyoda, 2001) uses the third category, ISAM (indexed sequential access method) which achieves both fastness and compactness. These three types of file formats are compared (Table 1).

In the operational NWP (1) data structure is often sparse, (2) each file is written by a single process, and (3) many subsequent processes read a part of data file. In this situation the weakness (cost of indexing) is not outstanding and the strength (fastness and compactness) are enjoyed.

It is also noted that the weakness of sequential access (full scan for partial data) will be aggravated in the future computing with larger data size.

### References

Bruce WRIGHT and Feng GAO, 2008: GRIB vs NetCDF: Evaluation of the Technical Aspects. WMO ET-ADRS Doc.2.3(1) <http://goo.gl/AFrsls>

TOYODA Eizi, 2001: NuSDaS: Numerical Prediction Standard Data-set System. JpGU presentation A2-011 <http://goo.gl/JE0a3M>

Keywords: GRIB, netCDF, NuSDaS, grid data, indexed sequential access method

## Types of File Structure

	Sequential Access	Direct Access	Indexed Sequential Access Method (ISAM)
Partial Write	<b>Simple:</b> append to EOF (end of file)	<b>Simple:</b> seek and write	<b>Complex:</b> append to EOF, then index location
File Size	<b>Most Compact</b>	Sparse array <b>Bloated</b>	<b>Compact</b>
Partial Read	<b>Slow:</b> all records must be scanned	<b>Fastest:</b> only seek and read	<b>Fast:</b> look up index, seek and read
Other Strength	No definition needed when creating file	Parallel write to single file	
Meteorological Examples	GRIB GTOOL3	GrADS Binary netCDF	NuSDaS

## Construction of the Large-Scale Statistical Analysis Environment of the STP field data based on the NICT Science Cloud

YAMAMOTO, Kazunori<sup>1\*</sup> ; NAGATSUMA, Tsutomu<sup>1</sup> ; KUBOTA, Yasubumi<sup>1</sup> ; MURATA, Ken T.<sup>1</sup> ; WATARI, Shinichi<sup>1</sup> ; TATEBE, Osamu<sup>2</sup> ; TANAKA, Masahiro<sup>2</sup> ; KIMURA, Eizen<sup>3</sup>

<sup>1</sup>National Institute of Information and Communications Technology, <sup>2</sup>University of Tsukuba, <sup>3</sup>Ehime University

There are two major research methods for geo-space science; one is computer simulation, and the other is satellite and/or ground-based observation. Both methods have their advantages and disadvantages: Computer simulations can provide data in whole time and space in the simulation domain, whereas satellite observation data are expected to provide more accurate information. Therefore it is effective for the improved reliability of data and the increased possibilities of explaining phenomena to utilize multi-satellite observation data in combination with sophisticated simulation data with high time resolution. It has a potential to lead to data assimilations in the future.

However, the amount of both multi-satellite observation data and simulation data with high time resolution is very large. We need computational techniques to analyze both data simultaneously. For statistical analysis and visualization, the typical data processing of both multi-satellite observation data and simulation data with high time resolution is called data intensive processing. In the data intensive processing, the same processing is applied to plenty of data files.

We have built a large-scale environment for the statistical analysis where the data obtained through satellites observations and computer simulation are used to construct a uniform, integrated dataset. In this environment, plenty of data are integrated in the following manner: (1)Archiving large quantities of data files, (2)Resampling time series and convert coordinates, (3)Extracting parameters from simulation data, and (4)Merging both data into one file.

**(1)Archiving large quantities of data files:** Using the STARS (Solar-Terrestrial data Analysis and Reference System) meta-database that provides meta-information of observation data files managed at distributed observation data sites over the internet, users download data files without knowing where the data files are managed. On the other hand, simulation data is saved from supercomputer to petabyte-scale distributed storage that is connected to 10GbE (JGN-X).

**(2)Resampling time series and convert coordinates:** We developed an original data class (SEDOC class) to support our reading of data files and converting them into a common data format. The data class defines schemata for several types of data. Since this class encapsulates data files, users easily read any data files without paying attention to their data formats. The SEDOC class supports a function of resampling time series through linear interpolations and converting them into major coordinates systems.

**(3)Extracting parameter from simulation data:** We have developed a 3-D visualization system that visualizes both of these data simultaneously and extract parameters from simulation data in the arbitrary coordinate value.

**(4)Merging both data into a single file:** Time scale and coordinate are regularized over data files.

We found a practical problem of the system, especially in case of long durational data analyses. It is the problem of the computational load on the processes two to four. It is necessary to solve this problem in order to achieve data-intensive processing for plenty of data files with non-negligible file I/O and CPU utilization.

To overcome this problem, we developed a parallel and distributed data analysis system using the Gfarm and Pwrake based on the NICT Science Cloud. The Gfarm shares both computational resources and perform parallel distributed processing. In addition, the Gfarm provides the Gfarm file system which behaves as a virtual directory tree among nodes. The Pwrake throws a job for each Gfarm node that has a target data file in the local disk. It utilizes local disk I/O to achieve effective load balance.

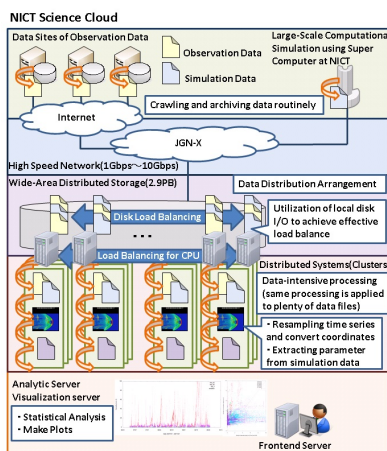
In today's presentation, we show latest results using archived long durational data and discuss the present Gfarm+Pwrake system extended to wide area.

Keywords: computer simulation data, satellite observation data, parallel distributed processing, Gfarm, Pwrake, NICT Science Cloud

MGI37-P01

Room:Poster

Time:April 29 18:15-19:30



## Radio observation network of Tohoku University

YAGI, Manabu<sup>1\*</sup> ; OBARA, Takahiro<sup>1</sup> ; KAGITANI, Masato<sup>1</sup> ; YONEDA, Mizuki<sup>1</sup> ; KUMAMOTO, Atsushi<sup>1</sup> ; MISAWA, Hiroaki<sup>1</sup> ; TSUCHIYA, Fuminori<sup>1</sup> ; IWAI, Kazumasa<sup>2</sup> ; TERADA, Naoki<sup>1</sup> ; OHYA, Hiroyo<sup>3</sup>

<sup>1</sup>Tohoku Univ., <sup>2</sup>NAOJ, <sup>3</sup>Chiba Univ.

Planetary Plasma and Atmospheric Research Center (PPARC) of the Tohoku University is now in progress to build a upper atmosphere, planetary, and space physics database under collaboration with the Inter-university Upper atmosphere Global Observation NETWORK (IUGONET). The core data of the database are planetary and solar radio observation by Iitate Planetary Radio Telescope (IPRT) and Jupiter/galaxy decameter radio receiver working in Iitate observatory, that is one of the observatory of Tohoku University. Development of database of LF/VLF wave observation at Athabasca, Ny-Alesund, and Asia VLF Observation Network (AVON) are undergoing collaborated with Chiba University. In the presentation, we will introduce the observations of solar radio burst with high time resolution using the AMATERAS spectrometer of IPRT, as well as lightning and precipitation of high energy electrons into the atmosphere observed by LF/VLF wave.

Keywords: radio observation, database, upper atmosphere



## Cs-bearing spherical particles emitted from an early stage of the FDNPP accident

ADACHI, Kouji<sup>1\*</sup> ; KAJINO, Mizuo<sup>1</sup> ; ZAIZEN, Yuji<sup>1</sup> ; IGARASHI, Yasuhito<sup>1</sup>

<sup>1</sup>Meteorological Research Institute

We found radioactive Cs-bearing, spherical particles from the filters collected in March 14 and 15, 2011, just after the Fukushima Daiichi Nuclear Power Plant (FDNPP) accident, in Tsukuba. These particles mainly consist of Fe and Zn but contain detectable amounts of Cs using a scanning electron microscope (SEM) and energy-dispersive X-ray spectrometer (EDS). They are several micro meter and are hardly water soluble. They are mostly spherical, suggesting they formed through rapid cooling of radioactive materials. These particles were only found in the filters collected on March 14 and 15, 2011, and these filters had many spots of radioactive materials when measured using an imaging plate (IP). To date, we have identified six such Cs-bearing particles in the filter.

The finding of such Cs-bearing spherical particles suggests the following implications; understandings of the accident and health effects for the radioactive materials emitted at the early stage of the accident and estimations of the current and future environmental radioactivity contaminated by the particles.

Reference: Adachi K., Kajino M., Zaizen Y., and Igarashi Y., Emission of spherical cesium-bearing particles from an early stage of the Fukushima nuclear accident, Scientific Reports, 2013, 3, Article number: 2554.

Keywords: Cesium, electron microscope, aerosol, radioactive material

## Measurement of Cs-137 in atmospheric aerosols in Fukushima prefecture and the surrounding area

NINOMIYA, Kazuhiko<sup>1\*</sup> ; ZHANG, Zijang<sup>1</sup> ; OSUMI, Yuji<sup>1</sup> ; MATSUNAGA, Shizuka<sup>1</sup> ; KAKITANI, Shunsuke<sup>1</sup> ; YAMAGUHI, Yoshiaki<sup>2</sup> ; TSURUTA, Haruo<sup>3</sup> ; WATANABE, Akira<sup>4</sup> ; KITA, Kazuyuki<sup>5</sup> ; SHINOHARA, Atsushi<sup>1</sup>

<sup>1</sup>Graduate School of Science, Osaka University, <sup>2</sup>Osaka University Radioisotope Research Center, <sup>3</sup>Atmosphere and Ocean Research Institute, University of Tokyo, <sup>4</sup>Fukushima University, <sup>5</sup>Ibaraki University

A large amount of radioactive materials were released in the environment by the accident at the Fukushima Daiichi Nuclear Power Station. We have been collecting air-dust using high volume air sampler at Fukushima city (Fukushima Pref.), Marumori town (Miyagi Pref.) and Hitachi city (Ibaraki Pref.) since the accident. We identified the radioactivities of <sup>134</sup>Cs and <sup>137</sup>Cs in filters using HPGe detector. We will discuss time variations of radioactive cesium concentration.

Keywords: Atmospheric observation, Air dust, Radioactivity Measurement, Cs-137 concentration

## Estimate of possible sources of high Cs-137 in atmospheric aerosols measured in south Miyagi during 2 years (2012-2013)

TSURUTA, Haruo<sup>1\*</sup> ; SHIBA, Kaoru<sup>1</sup> ; YAMADA, Hiroko<sup>1</sup> ; KUSAMA, Yuko<sup>1</sup> ; ARAI, Toshiaki<sup>1</sup> ; WATANABE, Akira<sup>2</sup> ; NAGABAYASHI, Hisao<sup>3</sup> ; KITA, Kazuyuki<sup>4</sup> ; SHINOHARA, Atsushi<sup>5</sup> ; NINOMIYA, Kazuhiko<sup>5</sup> ; ZHANG, Zijian<sup>5</sup> ; YOKOYAMA, Akihiko<sup>6</sup> ; KAJINO, Mizuo<sup>7</sup> ; NAKAJIMA, Teruyuki<sup>1</sup>

<sup>1</sup>AORI, The University of Tokyo, <sup>2</sup>Fukushima University, <sup>3</sup>Nihon University, <sup>4</sup>Ibaraki University, <sup>5</sup>Osaka University, <sup>6</sup>Kanazawa University, <sup>7</sup>Meteorological Research Institute

A volunteer team organized by the Japan Geoscience Union has started an intensive field study to monitor radioactive materials in the atmosphere, which were released by the Fukushima Daiichi Nuclear Power Plant (FD1NPP) accident, and by re-suspension of radioactive materials from soils and forests in a regional scale in and surrounding Fukushima area since April 2011. At present, the continuous measurement has been made at Marumori town in Miyagi prefecture, Fukushima city and Koriyama city in Fukushima prefecture, and Hitachi city in Ibaraki prefecture. In this paper, a case study on high concentrations of atmospheric radiocesium frequently measured at Marumori will be reported. At the Marumori town office in south Miyagi, atmospheric aerosols have been collected since December 2011, on a quartz fiber filter every several days by using a high volume air sampler, and radioactive materials in the aerosols were measured with a Ge detector. Forward trajectory analysis by a Lagrangian model was made to trace air masses started from the FD1NPP for 48 hours. The atmospheric concentration of Cs-137 at Marumori was in a level of  $10^{-4}$  Bq m<sup>-3</sup> until April 2012, and then gradually decreased to the level of  $10^{-5}$  Bq m<sup>-3</sup> in the latter half of 2013. High concentrations of Cs-137 more than  $10^{-4}$  Bq m<sup>-3</sup> were measured in the winter and early spring of 2012 and 2013 when the wind speed was high and relative humidity was low. It strongly suggests that the possible source of high Cs-137 could be re-suspension of radioactive materials from soils. In September and November 2012 and from May to August 2013, however, high concentrations more than  $10^{-4}$  Bq m<sup>-3</sup> were also frequently measured, and the highest concentration of  $4.6 \times 10^{-3}$  Bq m<sup>-3</sup> was measured in a sampling period of 16-20 August 2013. On 19 August, unusual high Cs-137 concentration of  $7.1 \times 10^{-1}$ - $8.7 \times 10^{-1}$  Bq m<sup>-3</sup> and  $5.8 \times 10^2$  Bq m<sup>-3</sup> was measured at a monitoring post of Koriyama in Futabamachi 2.8 km north of the FD1NPP, and in front of a building inside the FD1NPP, respectively. According to the forward trajectory analysis, the air masses started from the FD1NPP at 09:00 and 12:00 on August 19 2013 arrived at Marumori on the afternoon of 15:00 and 18:00, respectively. It indicates that radioactive materials released from the FD1NPP were directly transported to Marumori about six hours later. The transport pathways similar to those on August 19 were also shown by the forward trajectory analysis in the other periods when the high Cs-137 concentrations were measured except for winter and early spring. These results clearly demonstrate that radioactive materials were still released into the atmosphere from the FD1NPP. We acknowledge the staff members of the Marumori town office for continuous sampling of atmospheric aerosols for these two years.

Keywords: atmospheric aerosols, radiocesium, source estimate, forward trajectory analysis

## Study on the carrier of airborne radiocesium collected for six month in Tsukuba after the Fukushima nuclear accident

KANEYASU, Naoki<sup>1\*</sup> ; KOGURE, Toshihiro<sup>2</sup> ; MUKAI, Hiroki<sup>2</sup> ; OHASHI, Hideo<sup>3</sup> ; SUZUKI, Fumie<sup>3</sup> ; AKATA, Naofumi<sup>4</sup> ; OKUDA, Tomoaki<sup>5</sup> ; IKEMORI, Fumikazu<sup>6</sup>

<sup>1</sup>National Institute of Advanced Industrial Science and Technology, <sup>2</sup>Graduate School of Science, The University of Tokyo, <sup>3</sup>Tokyo University of Marine Science and Technology, <sup>4</sup>National Institute for Fusion Science, <sup>5</sup>Faculty of Science and Technology, Keio University, <sup>6</sup>Nagoya City Institute for Environmental Sciences

To obtain the knowledge on the physico-chemical properties of airborne radionuclides, we had been collected size-resolved aerosol in Tsukuba, Japan, since April 28, 2011, although the data obtained do not include the first radioactive plumes that reached to Tsukuba on March 15, 2011. From the initial result, we proposed a hypothesis that the sulfate aerosol was the potential carrier of the <sup>134</sup>Cs and <sup>137</sup>Cs that had undergone the middle- to long-range transport from the damaged reactor. We further inferred that re-suspended soil particles that attached radionuclides were not the major airborne radioactive substances from late April to May, 2011 (Kaneyasu et al., 2012).

Nevertheless, there are some issues to be addressed on the nature of airborne radionuclides. Those are, a) until when the sulfate aerosol acted as a carrier of the radiocesium released from the reactor, or the other substances acted as carriers instead, and b) what is the carrier substance when the re-suspension or re-emission of became the dominant source in the airborne radiocesium.

In this study, we address these subjects by analyzing the long-term aerosol samples collected later than those presented in the previous study. The temporal change in the activity size distribution of radiocesium for six month will be discussed. In addition, the carrier substance of radiocesium in the coarse mode size range aerosol is investigated by use of the autoradiograph and scanning electron microscope to the aerosol sample collected in 2011 summer.

Keywords: radiocesium, size distribution, re-suspension, electron microscope, autoradiograph

## Resuspension of radioactive cesium from soil and forest

KITA, Kazuyuki<sup>1\*</sup> ; TANAKA, Misako<sup>1</sup> ; KINASE, Takeshi<sup>1</sup> ; FUJISAWA, Haruka<sup>1</sup> ; YAMAGUCHI, Ryusuke<sup>1</sup> ; KINO, Himiko<sup>1</sup> ; DEMIZU, Hiroyuki<sup>1</sup> ; IGARASHI, Yasuhito<sup>2</sup> ; MIKAMI, Masao<sup>2</sup> ; ADACHI, Kouji<sup>2</sup> ; YOSHIDA, Naohiro<sup>3</sup> ; TOYODA, Sakae<sup>3</sup> ; YAMADA, Keita<sup>3</sup> ; SHINOHARA, Atsushi<sup>4</sup> ; NINOMIYA, Kazuhiko<sup>4</sup> ; OKOUCHI, Hiroshi<sup>5</sup> ; ISHIZUKA, Masahide<sup>6</sup> ; KAWASHIMA, Hiroto<sup>7</sup> ; NAKAI, Izumi<sup>8</sup> ; ABE, Zenya<sup>8</sup> ; ONDA, Yuichi<sup>9</sup>

<sup>1</sup>Ibaraki University, <sup>2</sup>MRI, <sup>3</sup>TiTech, <sup>4</sup>Osaka Univ., <sup>5</sup>Waseda Univ., <sup>6</sup>Kagawa Univ., <sup>7</sup>Akita Pref. Univ., <sup>8</sup>Tokyo univ. of Science, <sup>9</sup>Tsukuba Univ

Radionuclides emitted from the Fukushima dai-ichi nuclear power plant (FNDPP) accident have been deposited on the soil, ocean and vegetation. Re-suspension of radioactive cesium from the soil and vegetation to the atmosphere may be one of significant path in the diffusion of radionuclides after the accident. Therefore, the quantitative understanding of these re-suspensions is important to understand future transition of radionuclides. Identification of aerosol species which bring Cs-134/137 is necessary to understand the mechanism of re-suspension, and its efficiency.

We have measured atmospheric concentration of radiation by Cs-134/137 in Namie high school Tsushima-branch where is away 30km from FNDPP. Relationship between Cesium radioactivity and aerosol size distribution show that multiple re-suspension mechanisms contribute and their contribution varies with the season. The mechanisms of re-suspension will be shown and discussed.

## Evaluation of radioactivity resuspension by dust emission using a size-resolved 1-D vertical model in Namie, Fukushima

ISHIZUKA, Masahide<sup>1</sup> ; MIKAMI, Masao<sup>2\*</sup> ; TANAKA, Yasuhito<sup>2</sup> ; IGARASHI, Yasuhito<sup>2</sup> ; KITA, Kazuyuki<sup>3</sup> ; YAMADA, Yutaka<sup>4</sup> ; YOSHIDA, Naohiro<sup>5</sup> ; TOYOTA, Sakae<sup>5</sup> ; SATO, Yukihiko<sup>6</sup> ; TAKAHASHI, Yoshio<sup>7</sup> ; NINOMIYA, Kazuhiko<sup>8</sup> ; SHINOHARA, Atsushi<sup>8</sup>

<sup>1</sup>Kagawa University, <sup>2</sup>Meteorological Research Institute, <sup>3</sup>Ibaraki University, <sup>4</sup>RIKEN, <sup>5</sup>Tokyo Institute of Technology, <sup>6</sup>Tsukuba University, <sup>7</sup>Hiroshima University, <sup>8</sup>Osaka University

Radioactive materials released into the atmosphere by the Fukushima Daiichi Nuclear Power Plant Accident in March 2011 were deposited over a wider area. Those materials adhered to the soil particles (dust particles) and its resuspension by strong winds is apprehensive about as secondary emissions. We have proposed a size-resolved, one-dimensional resuspension scheme to calculate the concentration of radioactivity in the atmosphere, in the last annual meeting. The results underscore the importance of taking into account soil texture when calculating the concentrations of resuspended, size-resolved atmospheric radioactivity. However, various assumptions were incorporated into both the scheme and evaluation conditions. In this study, we made analyses of soil particle size distribution and soil radioactivity at a school ground in Tsushima District, Namie Town, Fukushima, which was heavily polluted by the accident. The model results were compared with in situ observational data of the size spectrum of atmospheric radioactivity. We validated the applicability of the scheme and the behavior of resuspended radioactive aerosols.

Keywords: Secondary emission, Radioactive aerosol, Dust, Fukushima accident

## Simulation of I-131 in the atmosphere emitted from the Fukushima Daiichi Nuclear Power Plant

TAKIGAWA, Masayuki<sup>1\*</sup> ; TSURUTA, Haruo<sup>2</sup>

<sup>1</sup>JAMSTEC, <sup>2</sup>AORI, Univ. of Tokyo

A large amount of radioactive materials was released into the atmosphere after the accident of the Fukushima Daiichi Nuclear Power Plant (FD1NPP). Inhalation of iodine 131 is important for internal exposure, but the observation of iodine is quite limited especially in the early phase of the accident. We have conducted the simulation of radionuclides using a regional chemical transport model for March 2011. Calculated accumulated deposition of iodine 131 and caesium 137 was compared with the estimation using aircraft monitoring by MEXT and DOE (Torii et al., 2013). The model well captured the meridional gradient in the ratio of iodine 131 to caesium 137 around FD1NPP. The ratio of iodine 131 to caesium 137 is larger than 15 in the south of FD1NPP, and relatively small (around 0.7) in the northwest. This result implies that the regional model and the source term estimated by JAEA can generally reproduce eventual releases which cause large depositon offer the land in March 2011.

Keywords: numerical simulation, atmospheric environment

## The applicability of lichens as indicator of radiocaesium fall-out following the Fukushima Daiichi nuclear accident

DOHI, Terumi<sup>1\*</sup> ; OHMURA, Yoshihito<sup>2</sup> ; KASHIWADANI, Hiroyuki<sup>1</sup> ; FUJIWARA, Kenso<sup>1</sup> ; IJIMA, Kazuki<sup>1</sup>

<sup>1</sup>Japan Atomic Energy Agency, <sup>2</sup>National Museum of Nature and Science

Lichens are symbiotic organisms consisted of fungi and algae. A number of studies was carried out after the nuclear weapons tests and Chernobyl accident, and demonstrated that lichens were useful for indicator of radioactive fallout because (i) they spread in almost all terrestrial habitats e.g. on rocks, tree barks, and soils, (ii) they could take up large amount of radionuclides directly from their thallus due to lack of root system and retain them, and (iii) they were long-lived. It is necessary to understand the behavior of radiocaesium released into the environment from the Fukushima Daiichi nuclear power plant (FNPP) on March 2011, because it is considered to migrate in the ecosystem over a long period. For this purpose, some indicators of initial amount of deposited radiocaesium are required to be compared. Though, the amount of deposited radiocaesium on the topsoil gradually decreases by weathering, while lichens are expected to retain radiocaesium for long time. However, very little work is currently available on the concentration of radiocaesium in lichens and there is no experience of applying lichens to indicator of fall-out in Japan.

In this study, an applicability of lichens as an indicator for amount of deposited radiocaesium was discussed based on the following investigations related to the Fukushima Daiichi nuclear accident. The lichens were widely collected from the area in Fukushima prefecture (mainly west side) and Kanto region affected by the accident since December 2012. Lichen species were focused on parmelioid lichens which were widely distributed around FNPP. (1) After the lichens were removed from barks and dried, the concentrations of <sup>134</sup>Cs and <sup>137</sup>Cs in the lichens were measured with a CsI scintillation detector or a Ge semiconductor detector and compared to amount of <sup>137</sup>Cs deposited on the topsoil on June 2011 and air dose rate. (2) The retention capability of radiocaesium was evaluated by comparing radiocaesium concentrations in lichens to those of barks of lichen habitat.

The radiocaesium concentrations in lichens tended to be higher than those of barks, indicating that parmelioid lichens had retention capability of radiocaesium than tree barks. It was observed that the radiocaesium concentrations in lichens increased with increasing the amount of <sup>137</sup>Cs deposited on the topsoil and air dose rate. These results suggested the applicability of parmelioid lichens as an indicator of radiocaesium fall-out in Fukushima.

Keywords: Fukushima daiichi nuclear accident, Parmelioid lichens, radiocaesium



## Estimation of radioactive cesium translocation by litterfall, stemflow and throughfall in the forest of Fukushima

ENDO, Izuki<sup>1\*</sup> ; OHTE, Nobuhito<sup>1</sup> ; ISEDA, Kohei<sup>1</sup> ; HIROSE, Atsushi<sup>1</sup> ; KOBAYASHI, Natsuko<sup>1</sup> ; TANOI, Keitaro<sup>1</sup>

<sup>1</sup>The University of Tokyo

The accident of Fukushima Daiichi nuclear power plant after the earthquake and Tsunami in March 11th 2011 caused large amount of radioactive cesium (Cs) deposition onto the forest in surrounding areas. Deposited radioactive Cs that were caught by the tree canopy, reaches to the forest floor via various several pathways. To estimate the annual flux of radioactive Cs translocate to forest floor, we investigated the component and amount of those which move from tree canopy based on the measurements of litterfall, stemflow and throughfall.

Field study was conducted in a forest at the upstream part of the Kami-Oguni River catchment, northern part of Fukushima Prefecture. Three plots (2 deciduous-pine (*Pinus densiflora*) mixed stands and 1 Japanese cedar (*Cryptomeria japonica*) plantation) were set in the forest. Five litter traps were set in each plot and collected every month from October 2012 to September 2013. Litter samples were sorted among tree species and also branches, seeds and barks. Throughfall and stemflow were collected every 1 or 2 months. Water samples were filtered and particulate matters were collected for radioactive Cs measurement. Radioactive Cs concentration of all samples were measured by germanium semiconductor detector and NaI(Tl) scintillation counter. Both concentrations of <sup>137</sup>Cs and <sup>134</sup>Cs were measured but only data for <sup>137</sup>Cs were discussed in this report.

The concentration of <sup>137</sup>Cs in leaf litter samples varied from non-detected level to above 30 kBq/kg. The <sup>137</sup>Cs concentration was highest in pine needles and followed by cedar. Leaf litters of deciduous tree species showed significantly lower concentration compared to those of evergreen trees. This was because deciduous trees were before leafing stage at the time of the accident. However, significant levels of <sup>137</sup>Cs in the leaves even of deciduous trees suggest that <sup>137</sup>Cs have been translocated from some part of tree body. On the other hand, deposited <sup>137</sup>Cs at the time of the accident still remains on the leaves of evergreen tree. Amount of <sup>137</sup>Cs translocated from canopy to forest floor in cedar plantation was about 3 times higher than that of deciduous-pine mixed forest. This was due to higher <sup>137</sup>Cs concentration and larger litter biomass of cedar.

<sup>137</sup>Cs concentration of throughfall and stemflow were comparable. Since the amount of throughfall was larger than that of stemflow, significant amount of <sup>137</sup>Cs moved to the forest floor by throughfall. Higher <sup>137</sup>Cs translocation occurred according to the high precipitation. <sup>137</sup>Cs concentration fluctuated depending on the season, but there was no apparent tendency to decrease between 2013 and 2012. Since the concentration of <sup>137</sup>Cs in open rainwater was below the detection limit, it is suggested that <sup>137</sup>Cs is still supplied constantly from the tree canopy and source limitation is not occurring from leaves and trunks, despite the fact that it has past more than one and half year from the fallout.

## Effect of Radiocesium Transfer on Ambient Dose Rate in Forest Environment

KATO, Hiroaki<sup>1\*</sup> ; ONDA, Yuichi<sup>1</sup> ; LOFFREDO, Nicolas<sup>1</sup> ; HISADOME, Keigo<sup>2</sup> ; KAWAMORI, Ayumi<sup>3</sup>

<sup>1</sup>Center for Research in Isotopes and Environmental Dynamics, University of Tsukuba, <sup>2</sup>Asia Air Survey Co., LTD., <sup>3</sup>Masters Program of Environmental Sciences, University of Tsukuba

We investigated the transfer of canopy-intercepted radiocesium to the forest floor following the Fukushima Daiichi nuclear power plant accident. The cesium-137 (Cs-137) contents of throughfall, stemflow, and litterfall were monitored in two coniferous stands (plantation of Japanese cedar) and a deciduous broad-leaved forest stand (beech with red pine). We also measured an ambient dose rate at different height in the forest by using a survey meter (TCS-172B, Hitachi-Aloka Medical, LTD.) and a portable Ge gamma-ray detector (Detective-DX-100T, Ortec, Ametek, Inc.).

In decreasing order of total Cs-137 deposition from the canopy to forest floor were the mature cedar stand, the young cedar stand, and the broad-leaved forest. The ambient dose rate in forest exhibited height dependency and its vertical distribution varied by forest type and stand age. The ambient dose rate showed an exponential decrease with time for all the forest sites, however the decreasing trend differed depending on the height of dose measurement and forest type. The ambient dose rates at the canopy (approx. 10 m-) decreased earlier than physical attenuation of radiocesium, whereas those at the forest floor varied among three forest stands. These data suggested that an ambient dose rate in forest environment can be variable in spatially and temporally reflecting the transfer of radiocesium from canopy to forest floor.

Keywords: Fukushima Daiichi NPP accident, Cesium-137, Forest environment, Canopy interception, Transfer, Ambient dose rate

## Three different structures of radionuclide ratios on the surface soil in the northwestern area from the FDNPP

SATOU, Yukihiko<sup>1\*</sup>; SUEKI, Keisuke<sup>1</sup>; SASA, Kimikazu<sup>1</sup>; MATSUNAKA, Tetsuya<sup>1</sup>; SHIBAYAMA, Nao<sup>1</sup>; TAKAHASHI, Tsutomu<sup>1</sup>; KINOSHITA, Norikazu<sup>2</sup>

<sup>1</sup>AMS Group, University of Tsukuba, <sup>2</sup>Institute of Technology, Shimizu Corporation

The Fukushima Dai-ichi Nuclear power plant (FDNPP) accident caused radioactive contamination on the surface soil at Fukushima and its adjacent prefectures. Substantial contamination has been found in the northwestern area from the FDNPP, according to the airborne monitoring survey and the ground base survey by MEXT, Japan. Radionuclide ratios would have characteristic information on emission source because each nuclear reactor at the FDNPP had different amount of radionuclide and different activity ratio. The activity ratios can be used to make emission source and transport process in the contamination more obvious. We address the issue of radioactive contaminated process, we have measured radionuclides on the surface soil at the town of Namie in the northwestern region from the FDNPP, in the viewpoint of activity ratio.

This study focused on the gamma-ray emitting radionuclides of <sup>134</sup>Cs, <sup>137</sup>Cs, and <sup>110m</sup>Ag. The activities were decay-corrected as of 11 March 2011 when all nuclear reactors scrammed. Data of activity ratios by our results and the Japanese official report classified the investigated northwestern region into 3 groups. Ratios of 0.02 for <sup>110m</sup>Ag/<sup>137</sup>Cs and 0.90 for <sup>134</sup>Cs/<sup>137</sup>Cs were observed northern area of inside 15 km from the FDNPP. On the other hand, two kinds of <sup>110m</sup>Ag/<sup>137</sup>Cs ratios of 0.005 and 0.002 were distributed broadly in the area 60 km away from the plant. The <sup>134</sup>Cs/<sup>137</sup>Cs ratio was 0.98 there.

The activity ratio in the northern area from the FDNPP corresponds to those of nuclear fuel in Unit 1 according to estimation using the ORIGEN code. The <sup>134</sup>Cs/<sup>137</sup>Cs in the northwestern area from the FDNPP agrees with that of Unit 2 and 3. The <sup>110m</sup>Ag/<sup>137</sup>Cs ratios of 0.005 and 0.002 are 1/5 ? 1/10 of the Unit 2 and 3. Official report has announced that discharges of radionuclides from Unit 2 and 3 occurred on 14th March. It is known that contamination in the northwestern area from the FDNPP took place on 15th March. Ag has higher boiling point than Cs. Reactor core would be cooled down to lower temperature below the boiling point of Ag at the timing when contamination occurred. Thus, Ag with higher boiling point was not much released than Cs with lower boiling point. The <sup>110m</sup>Ag/<sup>137</sup>Cs ratio has served to identify the specific sources of contamination in the northwestern area from the FDNPP.

Keywords: Fukushima Nuclear Power plant Accident, 110mAg/137Cs ratio, Surface soil

## Depth profiles of $^{129}\text{I}$ and $^{137}\text{Cs}$ in soil before and after the FDNPP accident

MATSUNAKA, Tetsuya<sup>1\*</sup>; SASA, Kimikazu<sup>1</sup>; SUEKI, Keisuke<sup>1</sup>; TAKAHASHI, Tsutomu<sup>1</sup>; MATSUMURA, Masumi<sup>1</sup>; SATOU, Yukihiko<sup>1</sup>; SHIBAYAMA, Nao<sup>1</sup>; KITAGAWA, Jun-ichi<sup>2</sup>; KINOSHITA, Norikazu<sup>3</sup>; MATSUZAKI, Hiroyuki<sup>4</sup>

<sup>1</sup>University of Tsukuba, <sup>2</sup>High Energy Accelerator Research Organization, <sup>3</sup>Shimizu Corporation, <sup>4</sup>The University of Tokyo

Massive nuclear fission products such as radioiodine and radiocesium were deposited on the land surface of Fukushima via radioactive pollution plumes derived from the Fukushima Dai-ichi Nuclear Power Plant (FDNPP) accident. In order to evaluate inventory and penetration of accident-derived  $^{129}\text{I}$  and  $^{137}\text{Cs}$  in the land surface, depth profiles of  $^{129}\text{I}$ ,  $^{129}\text{I} / ^{127}\text{I}$  atomic ratio and  $^{137}\text{Cs}$  in 30-cm-long soil cores before (May 2008) and after (November 2012) the accident were compared at two sites (Iw-2 and Iw-8) on the western area within 10 km from the FDNPP.

Total  $^{129}\text{I}$  inventories in soil core at two sites after the accident were estimated to be 0.74 - 1.96 Bq m<sup>-2</sup>, 14 - 34 times higher than those before the accident (53.6 - 57.0 mBq m<sup>-2</sup>). Average  $^{129}\text{I} / ^{127}\text{I}$  ratios ((1.4 - 6.2) × 10<sup>-7</sup>) in soil core after the accident were consistent with the  $^{129}\text{I} / ^{127}\text{I}$  ratio of the radioactively-contaminated surface soils in Fukushima (1.5 × 10<sup>-8</sup> - 7.2 × 10<sup>-6</sup>, Miyake et al., 2012). We also estimated that total  $^{137}\text{Cs}$  inventories after the accident were 0.60 - 3.15 MBq m<sup>-2</sup>, 280 - 470 times higher than those before the accident (2.1 - 6.7 kBq m<sup>-2</sup>). Average  $^{134}\text{Cs} / ^{137}\text{Cs}$  activity ratios (1.07 - 1.08) in soil core fell within the activity ratio in Unit 1 - 3 (0.94 - 1.08) of the FDNPP calculated by ORIGEN2 code (Nishihara et al., 2012). These results suggested that accurate total inventories of accident-derived  $^{129}\text{I}$  and  $^{137}\text{Cs}$  in soil could be determined by deduction of those backgrounds at almost same site, thus, the FDNPP accident caused  $^{129}\text{I}$  deposition of 0.69 - 1.90 Bq m<sup>-2</sup> and  $^{137}\text{Cs}$  deposition of 0.59 - 3.14 MBq m<sup>-2</sup> on the western area within 10 km from the FDNPP. Moreover, deposited  $^{129}\text{I}$  and  $^{137}\text{Cs}$  at Iw-2 (4.2 km west from the FDNPP) were respectively, 2.9 and 5.3 times higher than those at Iw-8 (8.4 km west from the FDNPP).

Depth profiles of  $^{129}\text{I}$  concentration,  $^{129}\text{I} / ^{127}\text{I}$  atomic ratio and  $^{137}\text{Cs}$  concentration before the accident were essentially declined from upper layer with depth at two sites. On the basis of the highest values in these profiles, background levels were determined to be 420 ± 11 Bq kg<sup>-1</sup> for  $^{129}\text{I}$ , 1.6 ± 0.1 × 10<sup>-8</sup> for  $^{129}\text{I} / ^{127}\text{I}$  and 48 ± 2.5 Bq kg<sup>-1</sup> for  $^{137}\text{Cs}$ . After the accident, significant elevated values of  $^{129}\text{I}$  (40.2 - 130 mBq kg<sup>-1</sup>),  $^{129}\text{I} / ^{127}\text{I}$  ((0.9 - 9.3) × 10<sup>-6</sup>) and  $^{137}\text{Cs}$  (44.6 - 255 kBq kg<sup>-1</sup>) were found in the uppermost layer at the two sites, then these profiles exponentially declined with depth. Approximately 90% of deposited  $^{129}\text{I}$  and  $^{137}\text{Cs}$  at two sites were absorbed upper 37.4 - 50.5 kg m<sup>-2</sup> (4.1 - 4.3 cm) and upper 13.3 - 21.3 kg m<sup>-2</sup> (1.0 - 3.1 cm) in depth, respectively. In addition, since the relaxation mass depths ( $h_0$ ) of  $^{129}\text{I}$  were 9.2 - 12.8 kg m<sup>-2</sup> greater than those of  $^{137}\text{Cs}$  (6.8 - 11.7 kg m<sup>-2</sup>) at two site, radioiodine was considered to penetrate slightly deeper than radiocesium in upper layer of both sites as Kato et al. (2012) found at 40 km northwestern site from the FDNPP. This is not contradicting to increasing tendency of  $^{129}\text{I} / ^{137}\text{Cs}$  activity ratio with depth at both sites. Based on the fact that both  $^{129}\text{I}$  and  $^{129}\text{I} / ^{127}\text{I}$  in soil after the accident declined to a background level under 84.8 kg m<sup>-2</sup> in depth at Iw-2 and under 133 kg m<sup>-2</sup> in depth at Iw-8, about 8 - 9% of accident-derived  $^{129}\text{I}$  were likely to penetrated 37.4 - 84.8 kg m<sup>-2</sup> (4.3 - 8.6 cm) in depth at Iw-2 and 50.5 - 133 kg m<sup>-2</sup> (4.1 - 10.2 cm) in depth at Iw-8.

Keywords: FDNPP accident, Radioiodine, Radiocesium, AMS, Gamma-ray analysis, Soil profile

## Distribution of $^{129}\text{I}$ in the environment released from the FDNPP accident and estimation of $^{131}\text{I}/^{129}\text{I}$ ratio

SASA, Kimikazu<sup>1\*</sup> ; MATSUMURA, Masumi<sup>1</sup> ; SUEKI, Keisuke<sup>1</sup> ; TAKAHASHI, Tsutomu<sup>1</sup> ; MATSUNAKA, Tetsuya<sup>1</sup> ; SATOU, Yukihiko<sup>1</sup> ; SHIBAYAMA, Nao<sup>1</sup> ; KINOSHITA, Norikazu<sup>2</sup> ; NISHIHARA, Kenji<sup>3</sup> ; MATSUZAKI, Hiroyuki<sup>4</sup>

<sup>1</sup>University of Tsukuba, <sup>2</sup>Shimizu Corp., <sup>3</sup>Japan Atomic Energy Agency, <sup>4</sup>The University of Tokyo

Radioiodine is one of the most important radionuclides released from the Fukushima-Daiichi Nuclear Power Plant (FDNPP) accident.  $^{131}\text{I}$  (half-life: 8 d) has a short half life time. Because of the difficulty of measuring  $^{131}\text{I}$  at this time, it is expected to estimate  $^{131}\text{I}$  precipitation from  $^{129}\text{I}$  (half-life:  $1.57 \times 10^7$  y) with the long half-life in the surface soil. We have measured  $^{129}\text{I}$  concentrations in the surface soil at Fukushima.  $^{129}\text{I}/^{127}\text{I}$  ratios were measured by accelerator mass spectrometry (AMS) at the MALT, the University of Tokyo (Matsuzaki et al., 2007). Stable iodine of  $^{127}\text{I}$  was determined by inductively coupled plasma mass spectrometry (ICP-MS). We already got a result that the average  $^{129}\text{I}$  concentration was  $(2.74 \pm 1.35) \times 10^8$  atoms/g prior to the FDNPP accident as  $^{129}\text{I}$  background at Fukushima. After the accident, average isotopic ratio of  $^{131}\text{I}/^{129}\text{I}$  at Fukushima is estimated to  $(4.02 \pm 0.81) \times 10^{-2}$  as at March 11, 2011. The results of calculation about  $^{131}\text{I}/^{129}\text{I}$  ratio made by the ORIGEN2 code are  $3.18 \times 10^{-2}$  for the Unit 1,  $4.57 \times 10^{-2}$  for the Unit 2 and  $4.81 \times 10^{-2}$  for the Unit 3 (Nishihara et al., 2012). In this presentation, we report the distribution of  $^{129}\text{I}$  in terrestrial environment at Fukushima and  $^{131}\text{I}/^{129}\text{I}$  ratios by region.

Keywords: FDNPP accident, Radioiodine,  $^{131}\text{I}/^{129}\text{I}$ , AMS

## Desorption behavior of intrinsic cesium in smectite: Effect of aggregation on the cesium fixation in clay particles

FUKUSHI, Keisuke<sup>1\*</sup> ; SAKAI, Haruka<sup>2</sup> ; ITONO, Taeko<sup>3</sup> ; TAMURA, Akihiro<sup>3</sup> ; ARAI, Shoji<sup>3</sup>

<sup>1</sup>Institute of Nature and Environmental Technology, Kanazawa University, <sup>2</sup>College of Science and Engineering, Kanazawa University, <sup>3</sup>Graduate School of Natural Science and Technology, Kanazawa University

The radiocesium from the Fukushima Daiichi nuclear power plant accident is retained at the surface soils around the power plant. The expandable fine grained clay minerals such as smectite and vermiculate are the candidates for the host phases of radiocesium. The sorption mechanism of cesium in the clay minerals is expected to be cation exchange reaction in the interlayer of the clay minerals. Therefore, the retained Cs must be desorbed to the solutions in the presence of high concentrations of major cations. On the other hand, some natural observations after the Fukushima accident have shown that the radiocesium in the contaminated soils or sediments is merely desorbed to the water even in saline solutions (e.g. Aoi et al 2013 JPGU meeting). The purpose of the study is to reproduce the unexpected fixation of cesium in clay minerals from the laboratory experiment by using standard well characterized smectite (Kunipia-F). The desorption behavior of intrinsic trace Cs (10 nmol/g from LA-ICP-MS) in smectite by major cations were systematically examined. The results of the present study showed that the aggregation of smectite by the presence of the divalent cations or high concentration of monovalent cations lead to the fixation of cesium in the clay aggregates.

Keywords: cesium, smectite, desorption, fixation, aggregation

## Evaluation of the migration of radiocesium based on chemical speciation

TANAKA, Kazuya<sup>1\*</sup>; FAN, Qiaohui<sup>2</sup>; KONDO, Hiroaki<sup>2</sup>; SAKAGUCHI, Aya<sup>2</sup>; TAKAHASHI, Yoshio<sup>2</sup>

<sup>1</sup>ISSD, Hiroshima University, <sup>2</sup>Graduate School of Science, Hiroshima University

Chemical form of radiocesium is fundamental information for evaluation of its migration in the environment. After the Fukushima Daiichi Nuclear Power Plant (FDNPP) accident, we analyzed <sup>137</sup>Cs in aerosols, rock, soil, leaves, river suspended sediment and river water collected in Fukushima. Here, we review the migration of radiocesium in the environment based on our up-to-date data.

Many particles with high radioactivity were found in aerosols collected in March, 2011, where 50% to 90% of radiocesium was water-soluble. This means that radiocesium was still present mostly in a water-soluble fraction of aerosols before deposition and just after deposition on the ground. However, it was found that little amount of radiocesium was contained in a soluble fraction in soil and weathered rock samples by leaching experiments with water at various pH conditions. Possibly, such a soluble fraction of radiocesium was strongly fixed on rock and soil particles after dissolution in water (e.g. rainfall) on the ground. At the moment, chemical species of radiocesium would have changed from soluble to insoluble form. This strong fixation of radiocesium in soils can be explained by formation of inner-sphere complex in phyllosilicate minerals of clay minerals, which was confirmed by extended X-ray absorption fine structure (EXAFS) analysis. Field-scale observation reflected well the strong adsorption of radiocesium because most of the radiocesium stayed within 5 cm from the surface in soil layers.

In particular, in river and ocean systems, whether radiocesium is particulate or dissolved form is closely related to uptake by organisms and incorporation into food chain in ecosystems. We have monitored radiocesium concentrations in the Abukuma River system since summer in 2011. Total <sup>137</sup>Cs concentration in river water including both dissolved and particulate fractions decreased drastically from summer to winter in 2011, and then gradually decreased with time except at heavy rainfall events. From the strong fixation of radiocesium on soil particles, it was expected that radiocesium was predominant in particulate matter in river systems. More than 70% of radiocesium was particulate form, where the contribution of silt size (3 ~ 63 μm) fraction was the largest. However, radiocesium in dissolved fraction suggested an increase at estuary. This implies desorption of radiocesium from particulate matter because of an increase in salinity.

We made adsorption experiments to determine distribution coefficient,  $K_d$ , between fluvial sediment and river water, and further desorption experiments to examine the reversibility of adsorption-desorption process.  $K_d$  values determined by adsorption and desorption experiments were consistent, indicating that radiocesium adsorption was a reversible process. In addition, when artificial seawater was used for desorption experiment, the resulting  $K_d$  value was lower than that obtained using river water. This clearly demonstrated the influence of ionic strength on adsorption-desorption process through competition of cesium ions with other ions (e.g.,  $K^+$ ,  $Na^+$  and  $Ca^{2+}$ ), which is consistent with the field observation as noted above. Furthermore, we applied generalized adsorption model (GAM) to predict the distribution of radiocesium between particulate matter and water in the Abukuma River system. As a result, it was demonstrated that GAM can predict the apparent  $K_d$  values calculated from <sup>137</sup>Cs concentrations in fluvial sediment and river water as well as lower  $K_d$  values at estuary.

Keywords: Fukushima, Radiocesium

## Radiocesium wash-off associated with soil erosion from various land uses after the Fukushima Dai-ichi NPP accident

WAKIYAMA, Yoshifumi<sup>1\*</sup>; ONDA, Yuichi<sup>1</sup>; YOSHIMURA, Kazuya<sup>2</sup>; KATO, Hiroaki<sup>1</sup>

<sup>1</sup>Center for Research in Isotopes and Environmental Dynamics, University of Tsukuba, <sup>2</sup>Headquarters of Fukushima Partnership Operations, IAEA

Soil erosion is the initial process which drives radiocesium into the aquatic systems and therefore the quantification of radiocesium wash-off associated with soil erosion is indispensable for mitigating the risks. This study presents two year's observation of soil erosion and radiocesium wash-off to quantify differences in radiocesium behavior in various land uses. Seven runoff plots were established in four landscapes; uncultivated farmland (Farmland A1, Farmland B1), cultivated farmland (Farmland A2, Farmland B2), grassland (Grassland A, Grassland B) and Japanese cedar forest (Forest) in Kawamata town, an area affected by the Fukushima Dai-ichi Nuclear Power Plant accident. The discharged sediments were collected approximately every two weeks. In laboratories, collected sediments were dried and weighed for calculating soil erosion rates ( $\text{kg m}^{-2}$ ) and served for measurements of radiocesium concentration ( $\text{Bq kg}^{-1}$ ) with HPGe detectors. The erosivity factor of the Universal Soil Loss Equation (R-factor:  $\text{MJ mm ha}^{-1} \text{hr}^{-1} \text{yr}^{-1}$ ) was calculated based on the data of precipitation. Standardized soil erosion rates ( $\text{kg m}^{-2} \text{MJ}^{-1} \text{mm}^{-1} \text{ha hr yr}$ ), observed soil erosion rates divided by R-factor, was  $1.8 \times 10^{-4}$  in Farmland A1,  $6.0 \times 10^{-4}$  in Farmland A2,  $1.5 \times 10^{-3}$  in Farmland B1,  $8.3 \times 10^{-4}$  in Farmland B2,  $9.6 \times 10^{-6}$  in Grassland A,  $5.9 \times 10^{-6}$  in Grassland B and  $2.3 \times 10^{-6}$  in Forest. These erosion rates were basically proportional to their vegetation cover of soil surfaces except for cultivated farmlands. Concentrations of Cs-137 in eroded sediments basically depended on the local deposition of Cs-137 and varied enormously with ranging several orders of magnitude in all the landscapes. For the observation period of time decreasing trends in concentrations of Cs-137 in eroded sediments were not obvious. To compare these results with those of Chernobyl, we calculated normalized solid wash-off coefficient ( $\text{m}^2 \text{g}^{-1}$ ) with dividing the mean total concentration of Cs-137 in sediments by local deposition of Cs-137 (Konoplev et al., 1992). The coefficient was  $4.4 \times 10^{-5}$  in Farmland A1,  $1.3 \times 10^{-5}$  in Farmland A2,  $6.4 \times 10^{-5}$  in Farmland B1,  $1.0 \times 10^{-5}$  in Farmland B2,  $2.2 \times 10^{-5}$  in Grassland A,  $1.0 \times 10^{-5}$  in Grassland B and  $8.2 \times 10^{-5}$  in Forest. High erodibilities and relatively low values of normalized wash-off coefficients in cultivated farmlands can be attributed to the mixing of surface soil by ploughing. These values almost corresponded to those of Chernobyl. It was found that the total solid wash-off coefficient of radiocesium from farmlands is high and for 2 years period of time after the accident reaches 10%. Generally high precipitation in the region and steep slopes promote higher wash-off of radiocesium as compared to the Chernobyl case. Also, normalized wash-off coefficients exhibited relatively less volatility than erodibilities in the landscapes. These results suggest that soil erosion management is crucial for mitigating risks of radiocesium.

Keywords: soil erosion, erosion plot, Cs-137



## The distributed models to predict interannual changes in inventory and discharge of rCs from river basin

KONDOH, Akihiko<sup>1\*</sup> ; ONDA, Yuichi<sup>2</sup>

<sup>1</sup>CEReS, Chiba University, <sup>2</sup>CRiED, University of Tsukuba

Radioactive materials emitted from Fukushima Dai-ichi Nuclear Power Plant (FDNPP) in March 11, 2011, are spreading to wide area and deposited on the ground. Abukuma mountains where vast amount of radioactive nuclides are deposited, is mostly covered by forest. Transition of radioactive nuclides arises with hydrologic and material cycles in forested mountain watershed, and the redistribution will proceed for a long time. Monitoring of the distribution and time changes in radioactive materials are necessary. At the same time, the prediction of long term behavior of radioactive materials is necessary to make use of restoration of contaminated area. The purpose of the study is to calculate erosion rate in wide area, and predict long term change in the inventory of radioactive cesium, especially cesium 137, by distributed parameter model.

Spatial resolution of the distributed model is 25m, same as aerial monitoring of dose rate and inventory maps published by MEXT. The area of calculation is the extent of 36 river catchment within the 80 km zone from FDNPP including Abukuma River Basin.

Members of USLE (Universal Soil Loss Equation) to calculate erosion rate are derived from observation in USLE plots established in different land cover in Yamakiya District, Kawamata Town, Fukushima Prefecture, by team Tsukuba University.

Land use type for each grid cells is derived from present vegetation map prepared by Ministry of Environment. Gridded land use map with 25m resolution is created from shape file of the vegetation map. Topographic parameters are extracted from 25m resolution DEM re-constructed from 10m DEM by GSJ (Geospatial Information Authority of Japan). Vegetation cover ratio map is created from MODIS NDVI datasets with 250m resolution processed by Tokyo University of Information Sciences.

Erosion rates on each grid cell are calculated and make distribution map. Erosion rate is high in crop land, and low in forested area. Average erosion rate in crop land is about 1.4 ton/ha/year, and the one in forested area is about 0.1 ton/ha/year.

The model that calculate the transition of cesium-137 is developed and the changes in the inventory from 2011 to 2041 are calculated. The erosion rate is annual value, so time step is set to one year. The eroded sediment is transported to down slope. Sediment Delivery Ratio (SDR), the ratio of transported sediment over total sediment, should be determined, however, the proper SDR is not known, so SDR=1 is adopted in the calculation and maximum transportation rate is assumed.

The amount of cesium-137 is calculated by introducing  $Sc$ .  $Sc$  is the ratio of effluent cesium-137 (Bq/kg) over inventory (Bq/m<sup>2</sup>).  $Sc$  is determined by observations at the USLE plots of different land use. Out flowing cesium-137 is calculated by erosion rate multiplying by  $Sc$ .

The movement of debris along the slope is generally very slow, however, after the debris reach to the valley bottom, where saturation usually occur at the precipitation events, sediment is removed by flowing water. DEM is used to calculate Topographic Index (TPI) to designate the area of stream flow generation. When sediments reach to the area, cesium-137 flushes to the outlet of the watershed. In this calculation, all the cesium-137 is considered to be removed to the cell, and flushes to the outlet.

The calculation shows the average inventory of cesium-137 is about 10% lower than the one that only radioactive decay is considered. Total amount of discharge of cesium-137 at Iwanuma point, Abukuma River, is the order of  $10^{13}$  Bq in both case in the first year after the deposition of radioactive materials. Discharge of cesium-137 sharply decrease in the first years, after the sharp drop, discharge decreased in exponential form.

The result of the study is based on the empirical model, however, it considers the established knowledge in the field of stream flow generation. The results reflect the actual condition of cesium-137 transition.

Keywords: Universal Soil Loss Equation, erosion rate, radioactive cesium, inventory change, distributed model, FUKUSHIMA

## Cs-134 and Cs-137 radioactivity of riverine suspended solids in the Abukuma River after the heavy rain in June 2012

NAGAO, Seiya<sup>1\*</sup> ; KANAMORI, Masaki<sup>2</sup> ; OCHIAI, Shinya<sup>1</sup> ; TOMIHARA, Seiichi<sup>3</sup> ; YAMAMOTO, Masayoshi<sup>1</sup>

<sup>1</sup>LLRL, INET, Kanazawa University, <sup>2</sup>Grad. School of NST, Kanazawa University, <sup>3</sup>Environmental Aquarium Aquamarine Fukushima

About 15 PBq of both Cs-134 and Cs-137 was released from the Fukushima Daiichi Nuclear Power Plant (NPP) after the 2011 Tohoku earthquake and tsunami. Surface deposition pattern of Cs-134 and Cs-137 occurred at Fukushima, Tochigi and Gunma Prefecture by a combination with wind direction and precipitation. It is important to elucidate the short-term to long-term impacts of the Fukushima Daiichi NPP accident on ecosystems of river watershed environments. This study was conducted to investigate transport of Cs-134 and Cs-137 in the Abukuma River running through Fukushima and Miyagi Prefecture in Japan, 15 months after the Fukushima Dai-ichi NPP accident. Field experiments were carried out at Shirakawa (upper), Motomiya, Data (middle) and Iwanuma (lower) during June 19-21, 2012. We also carried out the research at the Uta, Niida, Natsui and Same Rivers. Typhoon Guchol struck Japan on June 20. Fukushima Prefecture had rainfall of 77-136 mm during June 19-21. The suspended particles were separated using continuous centrifugation. The radioactivity of Cs-134 and Cs-137 was measured with gamma-ray spectrometry after drying them by freeze-dry method.

Total radioactivity of Cs-134 and Cs-137 in river waters was 0.091-3.83 Bq/l in high flow conditions by heavy rain. The particulate fractions of Cs-134 and Cs-137 were 77-89% at the normal flow condition, but were close to 100% after the typhoon. The radioactivity of Cs-134 and Cs-137 increased from 500 Bq/kg-ss in the upper site (Shirakawa) to 3470 Bq/kg-ss in the lower site (Iwanuma). The Cs-137 radioactivity was 3200 Bq/ kg-ss in the Uta River, 42440 Bq/ kg-ss in the Niida, 850 Bq/ kg-ss in the Natsui River and 550 Bq/ kg-ss in the Same River. These results indicate that the input of radiocesium associated with suspended particles from the watershed to the river water is controlled by the accumulation of radiocesium on the ground surface in the river watershed and transport processes of suspended solids in the river systems.

Keywords: river water, radioesium, particulate forms, migration, heavy rain event

## Transportation of radiocesium through rivers in Fukushima

TANIGUCHI, Keisuke<sup>1\*</sup>; YOSHIMURA, Kazuya<sup>2</sup>; SMITH, Hugh<sup>3</sup>; BLAKE, Will<sup>4</sup>; TAKAHASHI, Yoshio<sup>5</sup>; SAKAGUCHI, Aya<sup>5</sup>; YAMAMOTO, Masayoshi<sup>6</sup>; ONDA, Yuichi<sup>1</sup>

<sup>1</sup>Center for Research in Isotopes and Environmental Dynamics, University of Tsukuba, <sup>2</sup>JAEA, <sup>3</sup>University of Liverpool, <sup>4</sup>School of Geography, Earth and Environmental Sciences, Plymouth University, <sup>5</sup>Department of Earth and Planetary Systems Science, Graduate School of Science, Hiroshima University, <sup>6</sup>Low Level Radioactivity Laboratory, Kanazawa University

Due to Fukushima Daiichi Nuclear Power Plant accident, radioactive materials including Cs-134 and Cs-137 were widely distributed in surrounded area. The radiocesiums have been transported in river networks. This study showed the monitoring results of radiocesium concentration in river waters and suspended sediments in Abukuma river basin and smaller coastal river catchments.

The monitoring started at 6 sites from June 2011. Subsequently, additional 24 monitoring sites were installed between October 2012 and January 2013. Flow and turbidity (for calculation of suspended sediment concentration) were measured at each site, while suspended sediments and river water were collected every one or half month to measure Cs-134 and Cs-137 activity concentrations by gamma spectrometry.

Activity concentrations of Cs-134 and Cs-137 on suspended sediments were generally decreasing at all sites. The decreasing rate changed lower at about one year later from the accident. Activity concentration in river waters also showed the same tendency although there are only few data within 1 year from the accident.

Activity concentrations measured at the same day are proportional to the mean catchment inventory. Therefore, the activity concentration can be normalized by the mean catchment inventory. The normalized activity can be fitted to following double exponential function:

$$[At] = 1.551 \exp(-5.265 t) + 0.069 \exp(-0.266 t), \text{ where } t \text{ is the time from the accident [year].}$$

Radiocesium flux at a monitoring site was measured from the flow and turbidity data and the radiocesium concentration. Suspended sediment concentration (SSC) could be estimated from the turbidity data. Suspended sediment flux was calculated by multiplying the SSC by flow rate. Then, multiplying the suspended sediment flux by radiocesium concentration gave the radiocesium flux. The highest radiocesium flux occurred in Sep. 2011 due to the typhoon roke. Then, the radiocesium flux declined, however the flux increased in the summer and autumn of 2013 due to typhoon events.

There is no time evolution of Kd between suspended sediments and river water. Instead, Kd was varied spatially. Although the reason of the spatial variation is not clear for now, geology of the catchment (i.e. mineral composition of suspended particles) seems to relate the variation.

Keywords: Radiocesium concentration, suspended sediment

## A sediment transport model for analyzing the environmental dynamics of radionuclides in estuarine and coastal oceans

UCHIYAMA, Yusuke<sup>1\*</sup> ; YAMANISHI, Takafumi<sup>1</sup> ; TSUMUNE, Daisuke<sup>2</sup> ; MIYAZAWA, Yasumasa<sup>3</sup>

<sup>1</sup>Kobe University, <sup>2</sup>Central Research Institute of Electric Power Industry (CRIEPI), <sup>3</sup>Japan Agency for Marine-Earth Science and Technology (JAMSTEC)

Several oceanic dispersal modeling have been conducted by multiple institutions on dissolved radionuclides leaked at the Fukushima Dai-ichi Nuclear Power Plant (FNPP). Among others, we developed a multi-nesting oceanic model at the lateral grid resolution down to 1 km and performed the comprehensive dispersal reanalysis of the direct release of <sup>137</sup>Cs from FNPP occurred in March and April 2011 (Uchiyama *et al.*, 2013, *J. JSCE*). The model reveals that the current field on the continental shelf off Fukushima varied with surface wind stress and largely confined in the narrow coastal strip by about 30 km offshore. The spectral coherence analysis suggests that predominant alongshore transport of nuclides is caused by coastal jets on the shelf, presumably as forced shelf waves associated with the alongshore component of the wind stress. The coastal dispersal of the radionuclides is affected not only by direct release but also by atmospheric fallout (deposition) and discharge from the rivers. The last process introduces a time lag behind the direct release with hydrological process because the nuclides mostly attach to suspended particles (sediments) that are transported quite differently to the dissolved matter in the ocean.

In the present study, an Eulerian sediment transport model as an active tracer conservation equation with a prescribed settling velocity added to the vertical advection term, a wave-enhanced bed boundary layer model and a simple stratigraphy model proposed by Blaas *et al.* (2007) are implemented into ROMS (Shchepetkin and McWilliams, 2005, 2008). Three classes of sediments, viz., fine sand, silt and clay fractions, are considered here. The modeling procedure is approximately the same as Uchiyama *et al.* (2013), whereas the third embedding is done at the horizontal resolution dx of 250 m within the existing 1-km domain to develop the triple nested configuration forced by the assimilative JCOPE2 reanalysis (Miyazawa *et al.*, 2009) as the outer-most boundary conditions. Thus the grid refinement occurs from JCOPE2 (dx ~ 10 km) to ROMS-L1 (dx = 3 km), to ROMS-L2 (dx = 1 km), and finally to ROMS-L3 (dx = 250 m). Sediments are taken into account in ROMS-L3 model carried out for March through August 2011. The bed skin stress is evaluated by a combined wave-current stress model of Soulsby (1995) with the wave field computed by a SWAN spectral wave modeling at dx = 1 km embedded in the JMA GVP-CWM spectral wave reanalysis. The bathymetry is provided by the 50-m resolution dataset compiled by Japan's Cabinet Office. The initial distributions of fractions of the marine bed sediment classes are estimated with an optimally interpolated field of the observations reported by Miyagi and Fukushima Prefectures (1991, 2013). Daily discharges of 6 major rivers and 14 minor rivers in the L3 domain are provided from the hydrological surface water model HYDREEMS conducted in CRIEPI. An empirical, mean relation between river discharge and sediment flux based on Takekawa *et al.* (2013) is employed for estimating the section-averaged sediment flux at each river mouth. Fraction of sediment classes in the river water is estimated from a USLE based river model conducted by JAEA (2013). The passive tracer is additionally considered to track dissolved <sup>137</sup>Cs released from FNPP as the direct release, whereas its absorption and desorption to the sediments (i.e., suspended <sup>137</sup>Cs) are not considered yet.

We intend to talk at the conference on initial dispersal of dissolved <sup>137</sup>Cs at dx = 250 m, extent of the land-derived sediments from each river mouth, resuspension and recirculation of the deposited bed sediments during storm conditions, in conjunction with corresponding oceanic states. We will further touch on potential distribution of suspended and dissolved <sup>137</sup>Cs if absorption and desorption occur.

Keywords: multi-class sediment transport model, radioactive cesium 137, multiple nesting approach, ROMS (Regional Oceanic Modeling System)

## Distribution of radionuclides in the surface seawater developed by aerial radiological survey

INOMATA, Yayoi<sup>1\*</sup> ; AOYAMA, Michio<sup>2</sup> ; HIROSE, Katsumi<sup>3</sup> ; SANADA, Yukihisa<sup>4</sup> ; TORII, Tatsuo<sup>4</sup> ; TSUBONO, Takaki<sup>5</sup> ; TSUMUNE, Daisuke<sup>5</sup> ; YAMADA, Masatoshi<sup>6</sup>

<sup>1</sup>Asia Center for Air Pollution Research, <sup>2</sup>Fukushima University, <sup>3</sup>Sophia University, <sup>4</sup>Japan Atomic Energy Agency, <sup>5</sup>Central Research Institute of Electric Power Industry, <sup>6</sup>Hirosaki University

This study investigated the distribution of anthropogenic radionuclide in the surface seawater derived from the Fukushima Dai-ichi Nuclear Power Plant (FNPP1) observed by aerial radiological survey as an initial attempt. The aerial radiological survey over the coastal region was performed by the U.S. Department of Energy National Nuclear Security Administration (DOE/NNSA) within a 30 km radius of the FNPP1 on 18 April 2011. We found good correlations between the in-situ activities of radionuclide (<sup>131</sup>I, <sup>134</sup>Cs, <sup>137</sup>Cs) in the surface seawater and gamma-ray peak count rates by aerial radiological surveys (correlation coefficients for <sup>131</sup>I, 0.89; <sup>134</sup>Cs, 0.96; <sup>137</sup>Cs, 0.92). Based on these relations, we find that the area with high concentrations extend south-southeast from the FNPP1. The maximum concentrations of <sup>131</sup>I, <sup>134</sup>Cs, and <sup>137</sup>Cs reached 329, 650, and 599 Bq L<sup>-1</sup>, respectively. The <sup>131</sup>I/<sup>134</sup>Cs ratios in surface waters of the high activities area on 18 April were about 0.6-0.7. Considering the radioactive decay of <sup>131</sup>I (half-life: 8.02 d), we determine that the radionuclides in this area are due to direct release from FNPP1 to the ocean. These also confirm that the aerial radiological survey might be very effective to investigate the surface distribution of anthropogenic radionuclides in the surface seawater. Furthermore, the model reproduced the distribution pattern of the FNPP1 derived radionuclides, although simulated results by regional ocean model are underestimated.

**Keywords:** Airborne surveys, Ocean, Anthropogenic radionuclide, Gamma-ray peak count, Regional Ocean Modeling System, Fukushima Daiichi Nuclear Power Plant

## Approach taken by oceanography specialists toward building emergency system and analyzing radiocesium in bottom sediment

IKEDA, Motoyoshi<sup>1\*</sup>

<sup>1</sup>Hokkaido University

Eastern Japan along the Pacific coast has been damaged seriously and is still trying to recover after the nuclear power plant accident in Fukushima due to the magnitude-9 earthquake on March 11, 2011. In addition, we should prepare ourselves for another accident in future. The necessary system is to predict and monitor radionuclide distributions immediately following a possible accident, even if it is a rare case. We have started a plan of testing an emergency system based on ocean simulation models. The other actions include monitoring and modeling of radiocesium concentration, which still keeps a high level in the bottom sediments. The dedicated members of the Oceanographic Society of Japan have been making estimations and discussion to find which processes are responsible for the high concentration, while symposia have been held from time to time. We have so far reached the tentative conclusion that any process could be a possible one for the present condition among absorption/adsorption by plankton, detritus and disturbed sediments, direct adsorption of seawater cesium and inflow of suspended solids from rivers, with a particular attention to re-suspending sediments.

Keywords: radionuclide, emergency system, sediments

## Long-term behavior of Cs-137 activity in the ocean following the Fukushima Daiichi Nuclear Power Plant Accident

TSUMUNE, Daisuke<sup>1\*</sup> ; AOYAMA, Michio<sup>2</sup> ; TSUBONO, Takaki<sup>1</sup> ; TATEDA, Yutaka<sup>1</sup> ; MISUMI, Kazuhiro<sup>1</sup> ; HAYAMI, Hiroshi<sup>1</sup> ; TOYODA, Yasushi<sup>1</sup> ; YOSHIDA, Yoshikatsu<sup>1</sup> ; UEMATSU, Mitsuo<sup>3</sup>

<sup>1</sup>Central Research Institute of Electric Power Industry, <sup>2</sup>Fukushima University, <sup>3</sup>Tokyo University

A series of accidents at the Fukushima Dai-ichi Nuclear Power Plant following the earthquake and tsunami of 11 March 2011 resulted in the release of radioactive materials to the ocean by two major pathways, direct release from the accident site and atmospheric deposition.

We reconstructed spatiotemporal variability of Cs-137 activity in the ocean by the comparison model simulations and observed data. We employed a regional scale and the North Pacific scale oceanic dispersion models, an atmospheric transport model, a sediment transport model, a dynamic biological compartment model for marine biota and river runoff model to investigate the oceanic contamination.

Direct releases of Cs-137 were estimated for two years and six months after the accident by comparing simulated results and observed activities very close to the site. The estimated total amounts of directly released was  $3.6 \pm 0.7$  PBq. Directly release rate of Cs-137 decreased exponentially with time by the end of December 2012 and then, was almost constant. The daily release rate of Cs-137 was estimated to be  $3.0 \times 10^{10}$  Bq/day by the end of September 2013. The activity of directly released Cs-137 was detectable only in the coastal zone after December 2012. Simulated Cs-137 activities attributable to direct release were in good agreement with observed activities, a result that implies the estimated direct release rate was reasonable, while there is no observed data of Cs-137 activity in the ocean from 11 to 21 March 2011. Observed data of marine biota should reflect the history of Cs-137 activity in this early period. We reconstructed the history of Cs-137 activity in this early period by considering atmospheric deposition, river input, rain water runoff from the 1F NPP site and absorption in sediment. The comparisons between simulated Cs-137 activity of marine biota by a dynamic biological compartment and observed data also suggest that simulated Cs-137 activity attributable to atmospheric deposition was underestimated in this early period. In addition, river runoff model simulations suggest that the river flux of Cs-137 to the ocean was effective to the Cs-137 activity in the ocean in this early period. The sediment transport model simulations suggests that the inventory of Cs-137 in sediment was less than 10% of total released Cs-137. Sediment is not dominant sink of Cs-137 in the ocean.

Keywords: Fukushima Daiichi NPP accident, Regional Ocean Model System, Cesium 137

## Characteristics of radioactive Cs in reservoir sediment in Iwaki, Fukushima prefecture

AOI, Yusuke<sup>1\*</sup> ; FUKUSHI, Keisuke<sup>2</sup> ; TOMIHARA, Seiichi<sup>3</sup> ; NAGAO, Seiya<sup>2</sup> ; ITONO, Taeko<sup>1</sup>

<sup>1</sup>Graduate School of Natural Science and Technology, Kanazawa University, <sup>2</sup>Institute of Nature and Environmental Technology, Kanazawa University, <sup>3</sup>Aquamarine Fukushima

Large amount of radioactive elements, mainly Cs, were emitted from Fukushima Daiichi Nuclear Power Plant (FDNPP) because of Tohoku Earthquake occurred in March, 2011 and Fukushima prefecture and prefectures of the neighborhood were contaminated. Nuclear Regulation Authority, Japan (2013) reported that air dose rates evaluated based on the airborne monitoring results clearly show larger declines than those calculated based on the physical half-life of radioactive Cs. The reasons for such larger declines may include the effects of natural environmental erosion, such as rainfall. We have applied the sediment trap to sample the reservoir sediment. Sediment trap can observed the erosion continuously. Our purpose is to examine the characteristics of Cs contaminated soil continuously from summer to winter in 2013 in detail in Iwaki city, Fukushima prefecture.

Keywords: Radioactive Cs, Sediment, Erosion, Soil, Clay mineral



## Deposition and Migration of Radioactive Cs in the Matsukawa Ura and Feeder Rivers, Fukushima, Japan (Preliminary report)

KAMBAYASHI, Shota<sup>1\*</sup> ; ZHANG, Jing<sup>2</sup> ; NARITA, Hisashi<sup>3</sup> ; SHIBANUMA, Seiichiro<sup>4</sup> ; SOMA-FUTABA FISHERIES COOPERATION, Members<sup>5</sup>

<sup>1</sup>Graduate School of Science and Engineering for Education, University of Toyama, <sup>2</sup>Graduate School of Science and Engineering for Research, University of Toyama, <sup>3</sup>School of Marine Science and Technology, Tokai University, <sup>4</sup>Cbec, <sup>5</sup>Soma-Futaba Fisheries Cooperation Matsukawa Ura Branch

Radionuclides were released into the environment by the associated accident at the Fukushima Daiichi Nuclear Power Plant (FDNPP). Radioactive Cs that are released from FDNPP and is deposited on the land will migrate to the ocean finally through the surface flow. In this study, we were intended to determine the actual transport of radioactive material in the system of river - estuary - ocean as a model area the feeder rivers and Matsukawa Ura located in Soma City, Fukushima Prefecture. Sediment sampling were continuously obtained from Matsukawa Ura and feeder rivers (Uda River, Koizumi River, Ume River and Nikkeshi River) from September 2013. The radioactivity of the Gamma ray nuclide was measured using a Ge semiconductor detector. Radioactive Cs activity in the Ume River and Nikkeshi River, which are located on the south side were higher than that in the Koizumi River and Uda River, located on the north side, because that reduced rainfall led to the increases in radioactive Cs concentration, except for the Nikkeshi River effected by heavy rain. Thus, it is thought there is a strong correlation between precipitation and radioactive Cs inventory of Matsukawa Ura, and the river flow in brackish area is dominant by the increasing precipitation which led to the increasing of flow rate, result in the river bed sediment inflowing to Matsukawa Ura. So it suggests that radioactive Cs activity has decreased because of increasing precipitation. In the Nikkeshi River, radioactive Cs activity was increased and sediment was changed to fine grain size at the same time after heavy rain as compared with before. This is considered that fine particles have been transported due to salt water intrusion during returning from overflow to the calm water after the heavy rain event. Transport situation of radioactive material in the river - estuary - ocean system revealed that physical and chemical process contributes significantly influence on it such as water flow and dynamics of fine sediment.

Keywords: Radioactive Cs, Matsukawa Ura, Brackish water area

## Rapid determination of Radiostrontium in seawater sample using DGA Resin

TAZOE, Hirofumi<sup>1\*</sup> ; YAMAGATA, Takeyasu<sup>2</sup> ; OBATA, Hajime<sup>3</sup> ; YAMADA, Masatoshi<sup>1</sup>

<sup>1</sup>Institute of Radiation Emergency Medicine, Hirosaki University, <sup>2</sup>College of Humanities and Sciences, Nihon University,

<sup>3</sup>Atmosphere and Ocean Research Institute, the Tokyo University

A large amount of radionuclides were dispersed to the environment as a result of the accident at the Fukushima Daiichi Nuclear Power Plant in March 2011. Assessment of Sr-90, one of the major fission products, is crucial from the perspective of its bioavailability depending on behaviour similar to that of Ca, although few reports exist, so far. Traditional analytical procedures applies harmful huming nitric acid or large scale ion chromatography in order to separate between Sr and Ca prior to beta counting. In this study, rapid and robust purification technique for the daughter radionuclides yttrium-90 of Sr-90 using DGA chelating resin (Eichrom) without separation of Sr from Ca. DGA resin shows high distribution coefficient in high hydrochloric and nitric acid concentrations. Furthermore, we optimize the preconcentration method of Sr in seawater.

Keywords: Sr-90, Yttrium, Fuskuhima, Nuclear power plant, seawater

## Synchrotron radiation X-ray analyses of the radioactive single airborne particle emitted by the Fukushima nuclear accident

IIZAWA, Yushin<sup>1\*</sup> ; ABE, Yoshinari<sup>1</sup> ; NAKAI, Izumi<sup>1</sup> ; TERADA, Yasuko<sup>2</sup> ; ADACHI, Kouji<sup>3</sup> ; IGARASHI, Yasuhito<sup>3</sup>

<sup>1</sup>Tokyo University of Science, <sup>2</sup>JASRI/SPring-8, <sup>3</sup>Meteorological Research Institute

The Fukushima Daiichi nuclear power plant (FDNPP) accident released radioactive materials into the air environment over the entire Northern Hemisphere in March 2011. In order to elucidate environmental transfer of the radioactive materials from the FDNPP accident, a large number of studies have been carried out until today. However, we still do not know the exact physical and chemical properties of the radioactive materials. Such knowledge is necessary to construct the numerical models to estimate the geographical distributions and to evaluate the human exposures during and after the FDNPP accident. Therefore, we studied the radioactive materials which were released in the air environment by a FDNPP accident based on the multiple SR (synchrotron radiation) X-ray analyses of the single airborne particles with strong radioactivity trapped in Tsukuba, Ibaraki Prefecture at the time of the FDNPP accident. The samples were the radioactive single particles collected on quartz fiber filter at the Meteorological Research Institute, Tsukuba using a high-volume aerosol sampler on March 14-15. We selected the radioactive single particles out of this filter using micromanipulator and transferred to the KaptonR tape on an acrylic plate for SR X-ray analyses.

SR experiments were performed at the beam line BL37XU of SPring-8. The monochromatic SR X-ray beams were focused to about 1  $\mu\text{m}$  (horizontal) x 1  $\mu\text{m}$  (vertical) by K-B mirror. Two excitation X-ray energies were selected depending on the target elements for analysis: i.e., 15.0 keV (low-energy mode) and 37.5 keV (high-energy mode). SR X-ray fluorescence (XRF) imaging was applied to obtain elemental distribution, and X-ray absorption near edge structure (XANES) analysis was used for chemical state analysis, and X-ray powder diffraction (XRD) analysis was carried out to obtain crystal structural information of the particles.

We have successfully analyzed three radioactive single airborne particles. XRF analysis has revealed the existence of Cs in all of them. We were able to detect various elements shown below depending on the excitation energy. In addition, XRF imaging shows that each element exhibited uniform distribution in the particles.

High-energy mode: Cs, Ba, Te, Sn, Mo, Zr, Rb, Zn, Fe

Low-energy mode: Fe, Mn, Cr, Zn, Ti

Each particle showed different chemical compositions. XANES analysis of Sn, Mo, Zn, Fe in the particles showed that these metallic elements existed in high oxidation states in glass matrix. Furthermore, XRD analysis shows that the particle was amorphous because no diffraction line was observed. These results suggest that the detected elements are components of materials constituting the reactor and fission products. It is presumed that the reactor materials including the nuclear fuel melted at a high temperature and quenched by releasing to the air environment as a glassy materials.

Keywords: Fukushima Daiichi nuclear power plant, Synchrotron radiation X-ray analysis, airborne particle, strong radioactive particle

## An approach to chemical reactions in the atmosphere

AOYAMA, Tomoo<sup>1\*</sup>; WAKAZUKI, Yasutaka<sup>1</sup>

<sup>1</sup>Center for Research in Isotopes and Environment Dynamics, University of Tsukuba

### 1. Introduction

We discuss an approximate approach to simulate time series reactions in the atmosphere. At first, we write a reaction at definition time- $t$ , as  $A+B=C$ . Next, we suppose that densities of the compounds are written by Gaussians. The Gaussian is a solution for general small particles diffusion processes. The time- $t$  is discrete about the interval is  $dt$ . If 2 particles of compound A and B are interacted within the interval, the reaction reaches equilibrium, and a compound C is generated.

### 2. Descriptions

Considering properties of the atmosphere, we adopt Gaussian having different parameters for the horizontal and vertical directions.

$$GA\{A\}(r,z)=QA\{A\}\exp\{-\alpha A(r-rA)^2-\beta A(z-zA)^2\}, (1)$$

The suffix A corresponds to compound A. The Q is density and the unit is [M/volume] of compounds. In case of uncertain compounds chemically, it is replaced by [kg/volume]. A vector  $r$  is for  $x$ - and  $y$ -coordinates, and  $z$  is for  $z$ -coordinate. The function  $\exp$ (whose arguments is 3-dimensional distance) is a kind of the volume. Eq. (1) is a relation of [M]; that is, a reaction equation, which is defined at any time.

The  $\alpha$  and  $\beta$  (which are positive) are diffusion parameters and they depend with elapsed time from the generation. The dependency is very complex and the evaluation is difficult. In the puff-model approach, it is calculated by many turbulence parameters. However; we wonder that model is significant in case of very diffused case. We wish to adopt Lagrangian particles (L-particles), where alpha-beta-parameters are not, and effects of the turbulence are expressed by random numbers.

L-particles are a finite volume of the air, and have no shape. Therefore; we redefine it to be Gaussian. The multiply of Gaussians is a Gaussian; it is an appropriate function to express reactions.

Under the representation, alpha-beta-parameters are fixed coefficients to define a unit volume. They are a kind of mesh intervals. The re-defined Gaussians are moved by meteorological fields, as if they were L-particles. The Gaussian is like as a mesh-unit in Euler approach, which has a finite volume. They are in a space, and are moved by wind fields; however, they are not arranged orderly in Euler approach. Here, if the arrangement is introduced as following;

A transformation between L-particle and Euler-mesh:

$$Q(\text{mesh coordinates})=\text{Integral}\{GA(r,z)G(\text{on mesh})dv\},$$

$$\{GA(r,z)\}\rightarrow\{Q(\text{on mesh})\}.$$

The transformation seems to be usable to evaluate diffused mist.

### 3. Reactions

In an interval time, chemical equilibrium is,

$$Keq=[C]/([A][B]). (2)$$

For every times,

$$QA(t+dt)=QA(t)-QC(t), QB(t+dt)=QB(t)-QC(t), (3)$$

$$rA(t+dt)=rA(t)+\{u,v\}Adt+\text{Rand}(), (4)$$

$$ZA(t+dt)=ZA(t)+\{w\}Adt+\text{Rand}(), (5)$$

Where, a vector  $\{u,v,w\}$  is wind speeds.  $\text{Rand}()$  is normal distributed random numbers.

In another reaction,  $A+B=C+D$ , we get,

$$Keq=(C[D])/([A][B]), (6)$$

Since the distributions of C and D are same at the first step,

$$GC=GD=(KeqGAGB)^{0.5}. (7)$$

### 4. Progress of the research

We try to simulate some reactions in the atmosphere now.

Keywords: atmospheric reaction, SPM, L-particle

## Secular distribution of radioactive strontium concentration in the atmosphere after after the accident of FD-NPP

ZHANG, Zi jian<sup>1\*</sup> ; NINOMIYA, Kazuhiko<sup>1</sup> ; TAKAHASHI, Naruhito<sup>1</sup> ; YAMAGUCHI, Yoshiaki<sup>2</sup> ; YOSHIMURA, Takashi<sup>2</sup> ; SAITO, Takashi<sup>3</sup> ; KITA, Kazuyuki<sup>4</sup> ; TSURUTA, Haruo<sup>5</sup> ; WATANABE, Akira<sup>6</sup> ; SHINOHARA, Atsushi<sup>1</sup>

<sup>1</sup>Graduate School of Science, Osaka University, <sup>2</sup>Radioisotope Research Center, Osaka University, <sup>3</sup>Faculty of Comprehensive Human Sciences, Shokei Gakuin University, <sup>4</sup>College of Science, Ibaraki University, <sup>5</sup>Atmosphere and Ocean Research Institute, the University of Tokyo, <sup>6</sup>Fukushima University

### 1.Introduction

On March 12, 2011, a large amount of radioactive nuclides have been released into the environment by the nuclear accident at the Fukushima Daiichi Nuclear Power Station. Measurement about radioactive nuclides will give us much information about the accident circumstance. Furthermore, radioactivities in the air dust are critical for estimation of internal exposure. There are many measurements results of I-131, Cs-134, Cs-137 in environment samples. However, in other nuclides, such as the pure beta emitter nuclide Sr-90 has not been measured sufficiently. Sr-90 is considered one of the harmful radioactive nuclides. Therefore, measurement of Sr-90 in the air dust is important for calculating exposure. We developed a new simple and quick strontium isolation technique using solid-phase extraction for determination Sr-90 in the air dust by liquid scintillation counter (LSC).

### 2. Method

In this study, we used 3M Empore<sup>TM</sup> Strontium Rad Disk to extract strontium ion from air dust samples. This filter can collect Sr<sup>2+</sup> ion efficiently. However, it is known that this filter also catches Pb<sup>2+</sup>. Natural radioactive nuclide Pb-210 seriously will be interferences in Sr identification in beta ray counting. In this study, cation exchange with EDTA adopted for Sr isolation. We made test experiments with radioactive Sr tracer and obtained that the chemical yield was about 90 %. The time for chemical operation was about 3-4 hours. To determine Sr-90, Cherenkov radiation of Y-90 has been measured by LSC, 1220 QUANTULUSTM Ultra Low Level Liquid Scintillation Spectrometer. With Sr-90 standard solution, we obtained that the Y-90 Cherenkov light detection efficiency was 68.7% and the Sr-90 detection limit was 0.004 Bq. With sequential measurement, the growth curve of Y-90 was described to determinate activity of Sr-90.

### 3.Results

We measured Sr-90 in the air dust samples of Fukushima, Hitachi, Kawasaki and Osaka. We chose some air dust samples that have high Cs-137 activity for Sr-90 measurement. Strontium isolation with solid phase extraction was performed. In Hitachi, the Sr-90 activity concentration in air is decreased with time and the ratio of Sr-90/Cs-137 is about 10-3. It is possible that after April, Sr-90 has been the same behavior of Cs-137. We observed a long time variation of Sr-90 air concentration in Hitachi and Fukushima and found that the Sr-90/Cs-137 activity ratio increased over time. We are going to discuss about behaviors of the Sr-90 and Cs-137 in the atmosphere.

## Correlation between Atmospheric Re-entrainment of Radioactive Cs and Meteorological Phenomena Conditions.

KINO, Himiko<sup>1\*</sup>; KITA, Kazuyuki<sup>1</sup>; TANAKA, Misako<sup>1</sup>; KINASE, Takeshi<sup>1</sup>; DEMIZU, Hiroyuki<sup>1</sup>; IGARASHI, Yasuhito<sup>2</sup>; MIKAMI, Masao<sup>2</sup>; KAJINO, Mizuo<sup>2</sup>; ADACHI, Kouji<sup>2</sup>; KIMURA, Toru<sup>2</sup>; ISHIZUKA, Masahide<sup>3</sup>; KAWASHIMA, Hiroto<sup>4</sup>; YOSHIDA, Naohiro<sup>5</sup>; TOYODA, Sakae<sup>5</sup>; YAMADA, Keita<sup>5</sup>; OKOCHI, Hiroshi<sup>6</sup>; SHINOHARA, Atsushi<sup>7</sup>; NINOMIYA, Kazuhiko<sup>7</sup>; ONDA, Yuichi<sup>8</sup>

<sup>1</sup>Ibaraki University, <sup>2</sup>Meteorological Research Institute, <sup>3</sup>Kagawa University, <sup>4</sup>Akita Prefectural University, <sup>5</sup>Tokyo Institute of Technology, <sup>6</sup>Waseda University, <sup>7</sup>Osaka University, <sup>8</sup>Tsukuba University

### 1.Introduction

Massive earthquake attacked the eastern Japan on March 11 2011. It triggered the Fukushima Daiichi Nuclear Power Point accident, where large amount of radioactive substances were released. Released radioactive substances are diffused with atmospheric diffusion process, and eventually deposit on the ground surface and vegetation. Deposited radioactive Cs are released again from the ground surface and vegetation.

Today's main factor of atmospheric radiation concentration fluctuation is atmospheric Re-entrainment of radioactive Cs. Re-entrainment mechanism of radioactive Cs is a complex and unprecedented problem. We must consider an interdisciplinary study on deposited radioactive Cs for long-term estimation.

We infer that so Cs has a property that is taken in by clay minerals in soil that one of carriers of radioactive Cs is soil particles. The purpose of this study is to make clear how long does atmospheric radiation concentration increase by its re-entrainment, under what meteorological phenomena conditions.

### 2.About sampling

Since December 2012, we have been observing atmospheric radiation concentration of radioactive Cs by High-Volume Air Sampler on ground at Namie high school. It collects aerosols by passing through quartz filter. Wind velocity is measured at three altitudes by Three Cup Anemometer..Soil moisture is measured by Moisture Meter of Time Domain reflectometry system.

### 3.Correlation between seasonal re-entrainment of radioactive Cs and meteorological phenomena conditions

### 4.Investigation of direct transport by back-trajectory analysis

Keywords: Radioactive Cs, Atmospheric Re-entrainment, Fukushima Daiichi Nuclear Plant accident, Environmental Radioactivity

## Estimate of relationship between composition of aerosol and radioactive cesium observed in Namie Town, Fukushima Pref.

TANAKA, Misako<sup>1\*</sup>; KITA, Kazuyuki<sup>1</sup>; KINASE, Takeshi<sup>1</sup>; KINO, Himiko<sup>1</sup>; DEMIZU, Hiroyuki<sup>2</sup>; IGARASHI, Yasuhito<sup>3</sup>; MIKAMI, Masao<sup>3</sup>; ADACHI, Kouji<sup>3</sup>; KIMURA, Toru<sup>11</sup>; KAWASHIMA, Hiroto<sup>4</sup>; YOSHIDA, Naohiro<sup>5</sup>; TOYODA, Sakae<sup>5</sup>; YAMADA, Keita<sup>5</sup>; OKOCHI, Hiroshi<sup>6</sup>; YAMANOKOSHI, Eri<sup>6</sup>; SHINOHARA, Atsushi<sup>7</sup>; NINOMIYA, Kazuhiko<sup>7</sup>; NAKAI, Izumi<sup>8</sup>; ABE, Yoshinari<sup>8</sup>; ISHIZUKA, Masahide<sup>9</sup>; ONDA, Yuichi<sup>10</sup>

<sup>1</sup>Faculty of Science, Ibaraki University, <sup>2</sup>Faculty of Engineering, Ibaraki University, <sup>3</sup>Meteorology Research Institute, <sup>4</sup>Akita Prefectural University, <sup>5</sup>Interdisciplinary Graduate School of Science and Engineering, Tokyo Institute of Technology, <sup>6</sup>Faculty of Science and Engineering, Waseda University, <sup>7</sup>Graduate school of Science, Osaka University, <sup>8</sup>Faculty of Science, Tokyo University of Science, <sup>9</sup>Faculty of Engineering, Kagawa University, <sup>10</sup>Center for Research in Isotopes and Environmental Dynamics, Tsukuba University, <sup>11</sup>ATOX Co., Ltd.

Radionuclides emitted from the Fukushima dai-ichi nuclear power plant (FNDPP) have been deposited on the soil, ocean and vegetation. Re-suspension of radioactive cesium from the soil and vegetation to the atmosphere may be one of significant path in the diffusion of radionuclides after the accident. Therefore, the quantitative understanding of these re-suspensions is important to understand future transition of radionuclides. Identification of aerosol species which bring Cs-134/137 is necessary to understand the mechanism of re-suspension, and its efficiency.

We have measured atmospheric concentration of radiation by Cs-134/137 in Namie high school where is away 30km from FNDPP. We have set seven high-volume air samplers (HV) at the site and one operated for 24 hours day by day.

Then gamma-ray emission from HVsamples was measured with Ge detector.

In this way we have gotten atmospheric concentration of radiation which interval is one day.

While sampling, we measure atmospheric concentration of aerosol: black carbon, sulfate, and the number of particle which have size dependence using Electrical Low Pressure Impactor (ELPI).

We have analyzed the aerosols which had collected on HV filter with chemical analysis such as chromatograph.

We examined for correlation between the results of analysis and atmospheric concentration of radiation. And we examined what factor affects atmospheric concentration of radiation, and where the factor comes from using Positive Matrix Factorization (PMF). The PMF is multivariate analysis which estimates factor profile and factor contribution from observed value. The analysis needs only the observed value and number of factor (i.e. need not source profile), so there is possibility of finding the unexpected source.

This study used the date of March and August, 2013.

Keywords: Fukushima daiichi nuclear plant accident, environmental radioactivity

## The trial which presupposes the surface ground motion using an underground seismograph; MeSO-net

SAKAI, Shin'ichi<sup>1\*</sup> ; NAKAGAWA, Shigeki<sup>1</sup> ; HIRATA, Naoshi<sup>1</sup>

<sup>1</sup>Earthquake Research Institute, University of Tokyo

We have been constructing an ultra dense seismic observation network; Metropolitan Seismometer Observation Network; MeSO-net. MeSO-net consists of 296 seismic stations. The signals from seismometers are sampled 200 Hz by a 24-bit analog to digital converter at the bottom of 20m-borehole. The surface ground motion differs from the waveform observed at the underground. Then, we tried presumption of the surface ground motion using an underground seismograph.

The present study is supported by two Special Projects for Earthquake Disaster Mitigation in Tokyo Metropolitan Area and reducing vulnerability for urban mega earthquake disasters from the Ministry of Education, Culture, Sports, Science, and Technology of Japan.

Keywords: ground motion, MeSO-net



## Attenuation Structure beneath Kanto Region using Maximum Amplitude

SEKINE, Shutaro<sup>1\*</sup>; TAKEDA, Tetsuya<sup>2</sup>; KASAHARA, Keiji<sup>1</sup>

<sup>1</sup>Association for the Development of Earthquake Prediction, <sup>2</sup>National Research Institute for Earth Science and Disaster Prevention

### Introduction

The seismic attenuation structure beneath the Japanese islands should be three-dimensionally complex to a similar degree as the velocity structure. Especially, in the Kanto region, the similarity with the velocity structure is unlikely to be seen in other parts of the Japanese islands because seismic attenuation implies inelasticity or scattering, whereas seismic velocity represents elastic properties. A precise estimate of the seismic attenuation leads to a better estimate of the strength of an earthquake source, in turn allowing for proper scaling. Information on seismic attenuation is also important in the simulation of strong ground motions. In this study, tomographic inversions are performed for the three-dimensional (3D) attenuation structure beneath the Kanto Region.

### Data and Grid setting

In this study, tomographic inversions are performed for the three-dimensional (3D) attenuation structure beneath the Japanese islands from NIED Hi-net catalog. Vertical amplitudes of ground velocities reported between January 2004 and February 2009 are used in this study. Amplitudes from 11766 earthquakes are selected for P- and S-wave tomography. The number of the ray is 552,935 for P and 393052 for S, respectively. A grid with interval of 0.1 in Kanto region and 0.5 in other region is applied to this region at depths of every 5 km.

### Results

We estimate regional detail attenuation structure in Kanto region using tomography method with NIED Hi-net maximum amplitude data. In Kanto region, a High-Q zone is clearly found along the upper boundary of the Philippine Sea slab, and below the slab, we found a distinct wedge mantle low-Q zone.

Keywords: Q, Attenuation Structure, Kanto Region

## A highly attenuative zone beneath the Tokyo Metropolitan area.

PANAYOTOPOULOS, Yannis<sup>1\*</sup> ; HIRATA, Naoshi<sup>1</sup> ; SAKAI, Shin'ichi<sup>1</sup> ; NAKAGAWA, Shigeki<sup>1</sup> ; KASAHARA, Keiji<sup>2</sup>

<sup>1</sup>Univ. Tokyo, ERI, <sup>2</sup>Assoc. Develop. Earthquake Prediction

The material properties of the complex subduction zone beneath the Tokyo Metropolitan area can be estimated by the seismic attenuation  $Q$  of seismic waves observed at local seismic stations. Previous studies have provided us only with the large scale attenuation structure for all Japan (Jin & Aki, 2005; Nakamura et al., 2006; Edwards & Rietbrock, 2009) or only for the shallow part inside the Kanto basin (Kinoshita, 1994; Yoshimoto & Okada, 2009). In this study we aim to derive a detailed picture of the attenuation structure in the crust and upper mantle beneath the Kanto basin. The waveform data used in this study are recorded at the dense seismic array of the Metropolitan Seismic Observation network (MeSO-net). The station network is distributed on five lines with an average spacing of 3 km and in an area with a spacing of 5 km in the central part of Kanto plane. The 296 MeSO-net stations are equipped with a three-component accelerometer at a bottom of a 20-m-deep borehole, signals from which are digitized at a sampling rate of 200 Hz with a dynamic range of 135 dB. The attenuation of seismic waves along their path is represented by the  $t^*$  attenuation operator that can be obtained by fitting the observed seismic wave amplitude spectrum to a theoretical spectrum using an omega square source model. In order to accurately fit the spectral decay of the signal, only earthquakes that are recorded with intensity greater than 1 in the Japan Meteorological Agency (JMA) intensity scale are selected. The waveforms of 154 earthquakes were selected from the JMA unified earthquake list from January 1st 2010 to May 31st 2011. A grid search method is applied to determine the  $t^*$  values by matching the observed and theoretical spectra. The  $t^*$  data were then inverted to estimate a 3D  $Q_p$  structure under the Tokyo Metropolitan area, using a layered initial  $Q$  model. Grid points were set at 15 km spacing in the horizontal direction and with 10 km spacing at depth. We implemented the 3D velocity model estimated by Nakagawa et al., 2012 and in addition we set the initial  $Q$  values at 116 for the 0 km grids and to 400 for all the grids below them. The obtained model suggests average  $Q$  values of 50~100 inside the Kanto basin. Furthermore, a low  $Q$  zone is observed in the area where the Philippine Sea plate meets the upper part of the Pacific sea plate. This area is located at approximately 40 km depth, beneath the north-east Tokyo and west Chiba prefecture areas and is represented by  $Q$  values of 100~200. Earthquakes occurring on the Pacific plate pass through this low  $Q$  area inside the Philippine sea plate and are attenuated significantly. Combined with the detailed velocity structure beneath the Kanto basin, our results help us to understand the material properties of the subducting plates. The implementation of our findings in strong motion simulation studies could help towards a better understanding of the damage area of future earthquakes and mitigate the disaster of the affected areas.

Keywords: attenuation, tomography, MeSO-net

## Viscoelastic effects on stress on the active faults around the Tokyo metropolitan area after the 2011 Tohoku earthquake

HASHIMA, Akinori<sup>1\*</sup> ; FREED, Andrew<sup>2</sup> ; BECKER, Thorsten<sup>3</sup> ; SATO, Hiroshi<sup>1</sup> ; OKAYA, David<sup>3</sup> ; SUITO, Hisashi<sup>4</sup> ; HATANAKA, Yuki<sup>4</sup> ; MATSUBARA, Makoto<sup>5</sup> ; TAKEDA, Tetsuya<sup>5</sup> ; ISHIYAMA, Tatsuya<sup>1</sup> ; IWASAKI, Takaya<sup>1</sup>

<sup>1</sup>Earthquake Research Institute, the University of Tokyo, <sup>2</sup>Purdue University, <sup>3</sup>University of Southern California, <sup>4</sup>Geospatial Information Authority of Japan, <sup>5</sup>National Research Institute for Earth Science and Disaster Prevention

Beneath the Japan islands, the Pacific plate descends from the east and the Philippine sea plate descends from the south, causing interaction of two slabs at depth. The 2011 M9 Tohoku earthquake in northern Japan had a source region with a length of ~500 km and a width of ~200 km and forced broad lithospheric and mantle regions to deform. In addition, seismicity rates in the surrounding regions drastically increased. As the effect of the Tohoku earthquake on crustal deformation and seismicity in the Japan region is so large, it is required to quantitatively evaluate the temporal change of stress due to this earthquake. On the other hand, the mechanism of postseismic deformation is considered to be afterslip around the source region, viscoelastic stress relaxation in the asthenosphere and so on. Here, we investigate the effects of slab geometry and 3D heterogeneity on the inversion of inferred coseismic slip, the resulting broad coseismic deformation and the propagation of stress throughout the region.

We construct a 3-D finite element model (FEM) to generate Green functions for use in a coseismic inversion study that allows the influence of complex slab geometry as well as heterogeneities in elastic structure on inferred slip. We utilize the large, land-based Japan GPS array as well as seafloor geodetic constraints in the inversion. We are particularly interested in how coseismic seafloor constraints influence inversion results. Our FEM considers a region of 4500 km x 4900 km x 670 km, incorporating the Pacific and the Philippine sea slabs by interpolating models for the Tohoku region and the Nankai trough, as well as the Kuril, Ryukyu and Izu-Bonin arcs. As the geometry of the plate boundaries, we used the model interpolating the existing local plate boundary models. As the crustal thickness, we simply take the uniform value of 30 km for the continental plate and 6 km for oceanic plates. For the underlying mantle, we give the elastic constants according to the PREM model. The slabs are assumed to have 5 % higher P- and S-wave velocity than the surrounding mantle. The model region is divided into about 500,000 tetrahedral elements with average dimension ranging from 5-100 km. We also test the role of gravity on coseismic results, with initial results suggesting that gravitational loading is not an important factor because of the shallow dip of the upper Pacific slab. Based on the coseismic slip obtained by the inversion, we computed the temporal change of the Coulomb failure stress change on the active faults in the Tokyo metropolitan area considering viscoelastic relaxation in the asthenosphere. Our long-term objective is to study the influence of the Tohoku earthquake on evolution of stresses throughout Japan due to both coseismic and postseismic processes, the latter including afterslip and viscoelastic relaxation. An accurate accounting of coseismic slip is very important to such an endeavor.

Keywords: 2011 Tohoku earthquake, Coulomb failure stress change, Crustal structure, Active fault, Finite element modeling, Viscoelasticity

## Distribution and structures of blind thrust faults beneath the Tokyo metropolitan area

ISHIYAMA, Tatsuya<sup>1\*</sup> ; SATO, Hiroshi<sup>1</sup> ; KATO, Naoko<sup>1</sup> ; ABE, Susumu<sup>2</sup> ; WATANABE, Hidehisa<sup>3</sup> ; SHIGA, Nobuhiko<sup>3</sup>

<sup>1</sup>Earthquake Research Institute, University of Tokyo, <sup>2</sup>R&D Department, JGI, Inc, <sup>3</sup>Mitsui Mineral Development Engineering Co., Ltd.

We show subsurface geometries of several active blind thrusts beneath this highly urbanized area, based on tectonic landforms, high-resolution seismic reflection data, gravity anomaly data, and Quaternary stratigraphy. Deep seismic reflection profiles corroborate the notion that steeply dipping blind thrusts are reactivated normal faults originally formed by middle Miocene extensional tectonics. Despite very slow (less than 0.1 mm/yr) late Quaternary slip rates, our work suggests the presence of previously unrecognized faults that pose more seismic hazards to Tokyo and outlying communities, and urges more intense efforts to shed more light on the recent slip rates, magnitude and recurrence of the past earthquakes on them.

## Tsunami damage in Tokyo Bay from the 1703 Genroku Kanto Earthquake

MURAGISHI, Jun<sup>1\*</sup> ; SATAKE, Kenji<sup>1</sup>

<sup>1</sup>Earthquake Research Institute, the University of Tokyo

The 1703 Genroku Kanto earthquake was a great inter-plate earthquake along the Sagami Trough on December 31st, 1703 and caused severe damage in southern Kanto region (Usami et al., 2013). For the tsunamis in Boso Peninsula, Hatori (1975, 1976) and Koyama (1982, 1983, 1987) investigated historical documents and stone monuments recording casualties, and Tsuji (2003) revealed the number of washed-away houses at each village.

For the tsunami in Tokyo Bay, Hatori (1976, 2006) estimated the tsunami heights as 2 m in his compilation of tsunami heights in the Kanto region. While this height has been often used for tsunami countermeasure in Tokyo Bay, the ground for this estimation is not clear.

On the other hand, the Cabinet Office (2013) concluded that no tsunami damage occurred in the eastern coast of Tokyo Bay, although some tsunami description is recorded in Edo, the capital in those days. It is necessary to conduct an investigation of tsunami damage along the coast of Tokyo Bay through historical documents.

The notice from Edo-Machi-Bugyo (Edo City Commissioners) to residences in Edo recorded that there were four major arrivals of tsunami along the Uchikawa River (Sumida River), and tsunami came up to the upper limit of the river. According to the “ Omurochuki ” , tsunami inundated up to the Eitai-bashi Bridge. There were seven ebbs and flows of tide. Tides were filled twelve times on the next day after the earthquake. “ Saihen-onkoroku ” recorded that the person(s) were thrown off their ship during their evacuation.

There is a document which recorded tsunami damage in Funabashi City, Chiba Prefecture. Petition from fishermen to public office, which was written 41 years after the 1703 Genroku earthquake, recorded that fishing boats and tools for fishermen such as fishing nets were washed away, and that fishermen requested the public assist for the poor catch of fish due to the lack of sea weeds.

“ Shiohama-Yuraigaki ” reported the origin of salt farm and its damage at Ichikawa City due to the subsidence accompanied by the 1703 earthquake. These historical records are materialized in 1756 and afterwards. The embankments were collapsed and the salt farm has been ruined. However, no tsunami damage is described. This document described storm surge damage on September 28, 1680. It says that 55 persons were killed in Kakemama-mura by the storm surge, 100 persons died and millets and household goods were completely washed away in Hanzaemon Ina ’ s territory. It seems that there was wide range and large-scale storm surge damage according to the historical record. Although the 1680 storm surge damage is recorded in detail, there is no record of the 1703 tsunami, indicating that the 1703 tsunami damage, if any, must be smaller than the storm surge of 1680.

We found the historical records which had not been used in previous tsunami studies, and revealed that the 1703 Genroku tsunami caused some damage in inner Tokyo Bay area. We would like to continuously collect historical-records and examine the tsunami damage and heights.

### Acknowledgements

This study was supported by the Special project for reducing vulnerability for urban mega earthquake disasters from the Ministry of Education, Culture, Sports, Science and Technology of Japan.

Keywords: the 1703 Genroku Earthquake, Historical earthquakes, Tsunami

## A new direction of the MeSO-net

HIRATA, Naoshi<sup>1\*</sup> ; SAKAI, Shin'ichi<sup>1</sup> ; NAKAGAWA, Shigeki<sup>1</sup> ; KASAHARA, Keiji<sup>2</sup> ; KIMURA, Hisanori<sup>3</sup> ; HONDA, Ryou<sup>4</sup>

<sup>1</sup>Earthquake Research Institute, the University of Tokyo, <sup>2</sup>ADEP, <sup>3</sup>NIED, <sup>4</sup>Hot Springs Research Institute of Kanagawa Prefecture

We have developed the Metropolitan Seismic Observation network (MeSO-net) under the Special Project for Earthquake Disaster Mitigation in Tokyo Metropolitan Area (FY2007-FY2011) and maintain it by the Special Project for Reducing Vulnerability for Urban Mega Earthquake Disasters (FY2012-FY2016), which are supported by MEXT. The network consists of 296 seismic observation stations, from which data are continuously transmitted and recorded at a data management center in ERI. We developed an intelligent data transmission protocol for MeSO-net System, which is referred to as Autonomous Cooperative data Transfer (ACT)(Morita et al., 2010) . As culture noise in urban areas is very high, we use a 20-m-deep shallow borehole to install wide-band accelerometers but a signal-to-noise ratio is still low. A large number with short interval of station configuration helps us to obtain better resolution and high quality seismic data. We are now developing a new automatic data processing function in the MeSO-net: automatic event detection and P- and S-phase picking. We also develop a method to predict ground and building motions from the MeSO-net data.

Keywords: MeSO-net, accelerometer, continuous recording, Autonomous Cooperative data Transfer, automatic event detection, seismic tomography

## Overview of 'Maintenance and Recovery of Functionality in Urban Infrastructures'

NAKASHIMA, Masayoshi<sup>1\*</sup> ; KOSHIKA, Norihide<sup>2</sup> ; KAJIWARA, Koichi<sup>3</sup> ; NOZAWA, Takashi<sup>1</sup>

<sup>1</sup>Disaster Prevention Research Institute Kyoto University, <sup>2</sup>Kobori Research Complex, <sup>3</sup>Hyogo EERC, NIED

The 2011 Tohoku earthquake caused unprecedented damage to the island of Japan. The damage was spread to the Tokyo Metropolitan Area, hundreds kilometers away from the epicentral region, which sustained serious disruption, most notably to businesses. Measures have to be taken to reduce such disruption before the island of Japan receives another mega earthquake, which is expected by the middle of this century. Issues to be addressed:

1. Quantification of collapse margin of high-rise buildings.
2. Monitoring and prompt condition assessment of buildings.

The project deals with high-rise buildings which are prevalent in urban areas and focuses on the following three themes.

- (1) Quantification of collapse margin of high-rise building structures.
- (2) Monitoring and condition assessment for the health of buildings.
- (3) Evaluation and monitoring of soil-foundation-structure interaction systems.

To achieve these goals, state-of-the-art theory and high-fidelity simulation are utilized, together with a series of large-scale tests as well as continuous observation of vibrations to actual structures. The project will offer technical guidelines and associated materials useful for the design, construction, and maintenance of buildings and urban infrastructure systems. A research team consisting of members from industry, academia, and government authorities has been formed to run the project most effectively.



鉄骨造試験体  
の最終崩壊形

## Urban Resilience

HAYASHI, Haruo<sup>1\*</sup>

<sup>1</sup>Disaster Prevention Research Institute, Kyoto University

With a high probability in the first half of 21st century, Nankai Trough earthquakes will cause a tremendous amount of damage and losses which might exceeds Japanese national annual budget. In addition, we might take into account the possible occurrence of Tokyo Metropolitan earthquake which may cause a serious threat to our national security. It is virtually impossible to complete all the works needed to prevent those possible damage and losses due to these mega earthquakes before they will happen. It means that we need to develop a science and technology to minimize the resulting damage and losses due to these mega scale earthquake disasters and to realize high disaster resilience for quick and steady recovery based on the lessons taken from past earthquake disasters including 3.11 Tohoku Earthquake and Tsunami Disaster in 2011.

Recent progress in information and communication technology such as internet and mobile device with GPS should be adapted for effective disaster response and recovery. In this project, we will develop two ICT based system for creating common operational pictures among stakeholders. First system will be web-GIS system to provide an informational platform in which various kinds of information provided from seismology to social psychology will be mashed up for creating a new value. Second system will be Micro Media Service which will provide the information selected for each uses to meet their needs.

It is our ultimate goal to improve disaster preparedness of each individual who might be function as disaster response personnel or disaster victims. We will develop a Web portal site named as Disaster Literacy Hub to provide educational materials prepared for all disciplines related for earthquake disaster reduction based on the theory of instructional design.

All the academic achievements will be presented through the website shown below:





## Past large earthquakes beneath metropolitan Tokyo: Issues for estimation of occurrence probability and disaster

SATAKE, Kenji<sup>1\*</sup> ; ISHIBE, Takeo<sup>1</sup> ; MURAGISHI, Jun<sup>1</sup>

<sup>1</sup>Earthquake Research Institute, the University of Tokyo

Two types of large earthquakes, great interplate ( $M \sim 8$ ) earthquakes along Sagami Trough and  $M \sim 7$  earthquakes beneath southern Kanto region, have caused damage in metropolitan Tokyo and are expected to occur in the future. The 1923 Taisho Kanto earthquake (September 1,  $M 7.9$ ) and the 1703 Genroku Kanto earthquake (December 31,  $M 8.2$ ) are the first type, and the typical example of the second type is the 1855 Ansei Edo earthquake (November 11,  $M 7.0$ ).

The Cabinet office and the Earthquake Research Committee of the Japanese government recently re-examined the source area of the interplate earthquake along Sagami Trough, estimated that the maximum possible size would be  $M 8.6$ , and that the 1703 earthquake may be closer to the maximum size. Previous Kanto earthquakes have not been well studied; recent studies of tsunami deposits (Shimazaki *et al.*, 2011, JGR) concluded that the 1293 earthquake (May 20) was the Kanto earthquake along Sagami Trough. The 1495 earthquake (September 3) has been considered as a fake earthquake, possibly confused with the 1498 Meio earthquake along Nankai Trough, but Kaneko (2012, Ito-shi Kenkyu) proposed that the 1495 earthquake was another interplate earthquake along Sagami trough. Studies of historical documents and tsunami deposits have revealed the recurrence of Kanto earthquakes. Details of each event, such as the source area or possibility of simultaneous rupture on Kozu-Matsuda fault, need to be studied to clarify the diversity of recurrent interplate earthquakes.

A hypothetical earthquake beneath Tokyo at the deeper plate interface, the northern Tokyo Bay earthquake, had been considered for disaster estimation of metropolitan Tokyo. Recent damage estimation by the Cabinet Office (2013), however, assumed an earthquake in the Philippine Sea Plate, which would cause similar seismic intensity with the 1855 Ansei Edo earthquake. The hypocenter of the 1855 earthquake has been studied on the basis of seismic intensity and damage distribution from historical literature, and various estimates ranging from a shallow crustal source to 100 km deep source within the Pacific Plate have been proposed. The seismic intensity distribution in Kanto region is strongly influenced on both deep and shallow subsurface seismic velocity structures, hence quantitative comparison with recent earthquakes or simulation on three-dimensional velocity structure would be necessary to accurately estimate the 1855 hypocenter.

The Earthquake Research Committee (2004) estimated the 30-year probability of  $M \sim 7$  earthquake in southern Kanto region as 70 %, on the basis of five earthquakes since 1885 and the Poisson process. The five events are: 1894 Meiji Tokyo earthquake, 1895 and 1921 Ibraki earthquakes, 1922 Uraga channel earthquake, and 1987 eastern Chiba earthquake. Among them, at least three (1921, 1922 and 1987) occurred in the Philippine Sea Plate, and one (1895) occurred in the Pacific Plate (Ishibe *et al.*, 2012, Coord. Comm. Earthquake Prediction). For more accurate estimation of future probability, studies of older earthquakes from historical records and estimation of their epicenter, depth and earthquake types are required.

Keywords: Tokyo Metropolis, historical earthquake, Kanto earthquake, long-term forecast

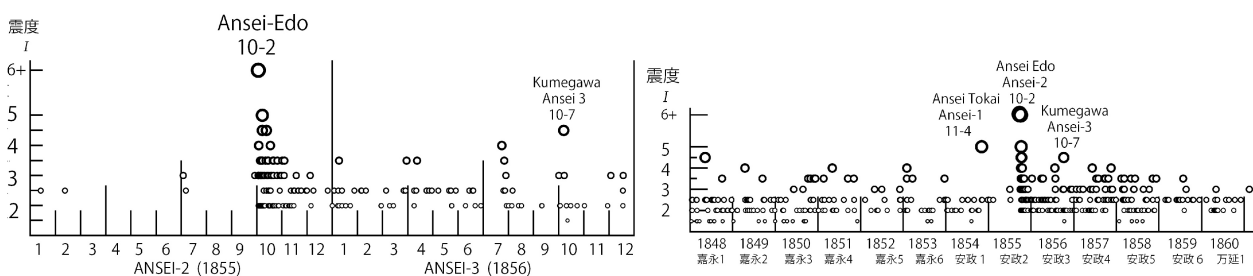
## Activity change of aftershocks of the Ansei Edo earthquake of November 11th, 1855

TSUJI, Yoshinobu<sup>1\*</sup> ; MATSUOKA, Yuya<sup>2</sup>

<sup>1</sup>Fukada Geolog. Inst., <sup>2</sup>Editorial Room of Chronicle, Sendai City Museum

Ansei Edo earthquake occurred at 11 PM, November 11th, 1855 at a point just below the city zone of Edo (Tokyo at present). Due to this earthquake, it is suggested that more than 10,000 people were killed in Edo. The location of the epicenter, its magnitude, and its fault mechanism is still not clarified. In the present study, we studied on the activity change of aftershocks by using descriptions of felt earthquakes written in diaries. We made a data base of felt earthquakes occurred in the period between the beginning of the first year of Kaei (1848) and the end of the first year of Man-en (1860) in Kanto district including the Edo city zone. In general, more than ten kinds of diaries were kept in the Tokyo city zone. Most reliable one is "Reiken Kobo" which is the diary kept at the Edo Astronomical Observatory in Kudan-Ue street. Diaries with descriptions of felt earthquakes were kept at more than ten cities on the Kanto Plain. We compiled a database of those records of felt earthquakes. We gathered electronic 3,192 cards of records of felt earthquakes in total. It is clarified that earthquakes were felt at Tokyo 543 times in total. The left figure shows the diagrams of felt earthquakes at Edo in two two years from the beginning of 1855 to the end of 1856. We can recognize that the aftershock period is finished generally at May 1856. An eminent earthquake occurred at Tokorozawa, about 40 kilometers WNW of Tokyo, which is considered as an earthquake induced by the Ansei Edo Earthquakes (an aftershock in wider sense). The right figure shown diagram of felt earthquakes in the period of 13 years between 1848 to 1860. The activity of earthquakes induced by the Ansei Edo earthquakes continued up to the end of the year of Ansei 5 (1858).

Keywords: historical earthquake, earthquake in metropolitan zone, aftershocks, the 1855 Ansei Edo Earthquake



## Compiling S-P times and first motion polarities for recent eqks and classification of the 1921 and 1922 eqks

ISHIBE, Takeo<sup>1\*</sup> ; SATAKE, Kenji<sup>1</sup> ; MURAGISHI, Jun<sup>1</sup> ; TSURUOKA, Hiroshi<sup>1</sup> ; NAKAGAWA, Shigeki<sup>1</sup> ; SAKAI, Shin'ichi<sup>1</sup> ; HIRATA, Naoshi<sup>1</sup>

<sup>1</sup>Earthquake Research Institute, the University of Tokyo

We compiled S-P times and first-motion polarities for earthquakes in Kanto region, central Japan on the basis of seismic phase data from 1923 to 2011 provided by the Japan Meteorological Agency (JMA), and that for 3,086 earthquakes which occurred from April 1st, 2008 to June 5th, 2012, from the Metropolitan Seismic Observation Network (MeSO-net). The number of target stations, where these data can be comparable with 26 stations which had operated in early stage of instrumental observations is 69 by JMA, and 19 by MeSO-net and other networks.

These data would be helpful for determining hypocenters and focal mechanism solutions of old earthquakes with limited instrumental data by comparing with S-P times and first-motion polarities for old earthquakes. As an example of application, we then compiled the characteristics of S-P times and first-motion polarities in southwestern Ibaraki and northwestern Chiba regions where the inter-mediate depth earthquakes frequently occur, and inferred the hypocenters and focal mechanism solutions of the 1921 Ibaraki-Ken-Nambu (M7.0) and 1922 Uraga-Channel (M6.8) earthquakes. Eleven first-motion polarities for the 1921 event are inconsistent for inter-plate earthquakes between the Okhotsk and Philippine Sea plates, and between the Philippine Sea and Pacific plates. Fourteen first-motion polarities and six S-P times for the 1922 event are similar for intra-slab earthquakes within PHS in and around southwestern Chiba with strike-slip fault mechanisms. These results strongly suggest that both the 1921 and 1922 events were not inter-plate earthquakes but intra-slab earthquakes.

In Japan, instrumental observation started in 1870's and seismographs and phase data (e.g., arrival times of typical phases, maximum amplitudes, first-motion polarities) have been persisted while some data were lost due to the fire. On the basis of these data, source parameters (hypocenters, focal mechanism solutions, and magnitude) for old earthquakes with limited instrumental data were estimated and cataloged. Determining hypocenters and focal mechanisms as back as possible prior to the start of JMA catalog is important to discuss long-term changes in seismicity. In Kanto, this period is especially important because it corresponds several tens of years before the 1923 Kanto earthquake and damaging earthquakes frequently occurred. However, the determinations of source parameters for old earthquakes have some difficulties. By using S-P times and first-motion polarities for recent earthquakes as "template", the accuracies in hypocenter locations and focal mechanism solutions for old earthquake would improve.

### Acknowledgements

We used phase data for earthquakes provided by JMA and that by the MeSO-net. We also used focal mechanism solutions for earthquakes provided by National Research Institute for Earth Science and Disaster Prevention and JMA, and a program modified from HASHv2 (Hardebeck and Shearer, 2002) to calculate the azimuths and take-off angles for first-motion polarities at each observation station. This study was supported by the Special project for reducing vulnerability for urban mega earthquake disasters from the Ministry of Education, Culture, Sports, Science and Technology of Japan.

Keywords: S-P time, first motion polarity, 1921 Ibaraki-Ken-Nambu earthquake, 1922 Uraga-Channel earthquake

## Field Survey for the Memorial Matters from the 1923 Great Kanto Earthquake in Central Kanagawa Prefecture

TAKEMURA, Masayuki<sup>1\*</sup>

<sup>1</sup>Disaster Mitigation Research Center, Nogoya-Univ.

Many memorial towers and monuments have been constructed for the heavy toll of life and for the restoration of villages or cities in Southern Kanto district. Death claimed a toll of about 105000 totally from the 1923 Great Kanto earthquake. These towers and monuments must be forever witnesses to the tragedy of the earthquake damage and spokesmen for the victim's dying wish "don't repeat such damages". However, most of them have been already forgotten by the citizens. We thought its sacrilege and must use them for the public education of earthquake disaster prevention. This manuscript is a report on the field survey for the memorial matters from the Great Kanto earthquake in Central Kanagawa Prefecture. The number of the matters is 126. This survey will be continued next two years in Western and Eastern Kanagawa Prefecture.

Keywords: memorial tower, Great Kanto Earthquake, Kanagawa Prefecture

## Composition of the subducted slab beneath Izu collision zone, Japan

ISHIKAWA, Masahiro<sup>1\*</sup>

<sup>1</sup>Graduate School of Environment Information Sciences, Yokohama National University

The Philippine Sea plate subducts northwestward under the Honshu arc, Japan. The presence of the Izu-Bonin arc within the Philippine Sea plate causes a complex tectonic environment. In eastern Kanto area, an accretionary wedge composed of late Cenozoic sediments overlies the downgoing Philippine Sea plate. In western Kanto area, the Izu-Bonin arc has collided with the Honshu crust; remnant pieces of the Izu-Bonin arc such as the Tanzawa block were accreted to the Honshu crust. A megathrust separates the Philippine Sea slab from the Honshu crust. According to seismic survey (Sato et al., 2005), the megathrust fault separates the upper/middle crust from the Izu-Bonin arc beneath the Izu collision zone. Devastating M8-class earthquakes occur on the megathrust fault, and the epicenter of the Kanto earthquake of 1923 (M7.9) is located in the Izu collision zone. To evaluate seismic hazard in the Greater Tokyo Area of Japan we need to clarify the lithological properties of Izu collision zone.

This study presents an interpretation of the crustal structure of the Izu collision zone. This study infers that amphibole is a main constituent mineral of the subducted lower crust of the Izu-Bonin arc. Dehydration embrittlement process resulting from the dehydration of hydrous minerals (e.g. amphibole) in the subducting lower crust is expected, and it may have induced the microearthquakes by enhancing pore pressures along the pre-existing faults/fractures in the subducting lower crust beneath the Izu collision zone. Stability field of amphibole within the gabbroic composition from the Tanzawa plutonic complex was calculated by Theriak-Domino software, and the phase diagram shows hot subduction can account for seismicity of the microearthquakes beneath the Tanzawa Mountains and the resulting dehydrated dry slab may therefore account for the observed absence of seismicity below the northern part of Tanzawa Mountains and Kanto Mountains.

Keywords: collision zone, slab

## Tsunami Heights of the 1854 Ansei-Tokai Earthquake Tsunami in Gokasho Bay Region, Mie Prefecture

NARUHASHI, Ryutaro<sup>1\*</sup> ; SATAKE, Kenji<sup>1</sup>

<sup>1</sup>Earthquake Research Institute, Univ. Tokyo

The Kumano-nada Sea coastal area has been repeatedly attacked by tsunamis from the Nankai Trough subduction-zone earthquake. For historical tsunamis, since this area is close to Kinki region, many historical records exist. For the recent 1944 Showa-Tonankai earthquake tsunami and the 1854 Ansei-Tokai earthquake tsunami, not only historical records and monuments but also many folklores still remain. However, the 1944 Showa Tonankai earthquake tsunami has a comparatively small scale, and is unsuitable for examining the average scale about the tsunami from the Nankai Trough. Based on above-mentioned reason, we studied for the 1854 Ansei-Tokai earthquake tsunami.

Gokasho Bay is a blockade inner bay which has typical ria coasts and drowned valleys. It is located in central Kii Peninsula and faced with the Nankai Trough. In this bay area, measurement points of the tsunami height for the 1854 Ansei-Tokai earthquake tsunami and the data on height were mainly based on historical records and oral traditions. In particular, in Konsa district, it is based on the words of the Bon festival dance currently kept in there called "Shongai kudoki" or "Tsunami kudoki". Tsunami heights were measured by level measurement using laser range finder TruPulse360 and a hand level on the basis of the spot elevation given by 1/2500 topographical maps.

As a result, a total of 40 points of tsunami height were obtained in Gokasho Bay region. The average inundation height of whole bay area was approximately 4 - 5 m.

In Konsa, located in the most closed-off section of the bay, dendritic valley plains which have small-sized rivers spread. According to distribution of both inundation and run-up points by this research, it is supposed that tsunami ran-up to every valleys of those. Tsunami heights in Konsa ranged 4 - 11 m, and were higher than those in other districts. The maximum run-up height was 11.5 m in the valley of Ushiroguchi.

Keywords: Gokasho Bay, 1854 Ansei-Tokai Earthquake Tsunami, tsunami height, run-up height, inundation height

## Publication of the Japan University Network Earthquake Catalog of First-Motion Focal Mechanisms (JUNEC FM<sup>2</sup>)

ISHIBE, Takeo<sup>1\*</sup> ; TSURUOKA, Hiroshi<sup>1</sup> ; SATAKE, Kenji<sup>1</sup> ; NAKATANI, Masao<sup>1</sup>

<sup>1</sup>Earthquake Research Institute, the University of Tokyo

We determined focal mechanism solutions for 14,544 earthquakes that occurred in and around the Japanese Islands from July 1985 to December 1998 by using first-motion polarities reported by the Japan University Seismic Network, and compiled the Japan University Seismic Network Earthquake Catalog of First-Motion Focal Mechanisms (JUNEC FM<sup>2</sup>). JUNEC can be obtained from ftp site provided by ERI: <ftp://ftp.eri.u-tokyo.ac.jp/pub/data/junec/hypo/>. JUNEC FM<sup>2</sup> also can be obtained via ftp site: <ftp://ftp.eri.u-tokyo.ac.jp/pub/data/junec/mech/>. The Earthquake Research Institute, the University of Tokyo has compiled observed data with the cooperation of universities and determined hypocenters amounting to about 190,000.

This catalog covers small-magnitude earthquakes ( $M \geq 2.0$ ) prior to the recent development of seismic observation networks and automated waveform data processing systems, and it will prove helpful in understanding the spatial and temporal heterogeneities of stress fields by combing recent focal mechanism solutions. Abundant focal mechanism solutions will be useful for statistical analyses. Their distribution is spatially and temporally heterogeneous, and it clearly reflects both the development of observation station network and spatial variations of first motion polarity report rate (i.e., first motion polarity report number / the number of picked onsets). Determined focal mechanisms are basically consistent with previously reported ones such as Full-range Seismograph Network of Japan (F-net; Okada et al., 2004) moment tensor solutions provided by National Research Institute for Earth Science and Disaster Prevention (NIED), or P-wave first motion focal mechanisms provided by the Japan Meteorological Agency (JMA) though some focal mechanisms are significantly different from them.

In Japan, an abundance of first-motion focal mechanism solutions for earthquakes have been determined after the 1995 Kobe earthquake (magnitude according to JMA-,  $M_{JMA}$  7.3) through the development of the High Sensitivity Seismograph Network Japan (Hi-net). In addition, moment tensor solutions for moderate- to large-magnitude earthquakes have been routinely determined since 1997 using the F-net and improved data processing systems. These focal mechanism solutions have provided a good understanding of the fault structures and the local/regional stress fields in which earthquakes occur. However, focal mechanism solutions for earthquakes covering the Japanese Islands prior to the development of recent seismic observation networks have been very limited, barring a few studies (e.g., Ichikawa, 1961, 1971). Following the 2011 off the Pacific coast of Tohoku earthquake (moment magnitude according to the JMA,  $M_w$  9.0), the distribution of focal mechanism solutions has drastically changed especially in and around the source region. This indicates that stress fields or focal mechanism solutions are temporally variable. In light of this, data on the focal mechanisms of earthquakes extending as far back as possible are desirable in order to investigate intermediate- to long-term spatial and temporal heterogeneities of focal mechanism solutions and local/regional stress fields.

### Acknowledgements

We used a program modified from HASH (Hardebeck and Shearer, 2002) to estimate the focal mechanism solutions and the pick files observed by Hokkaido University, Hiroshima University, Tohoku University, the Earthquake Research Institute of the University of Tokyo, Nagoya University, the Disaster Prevention Research Institute of the Kyoto University, Kochi University, Kyushu University, and Kagoshima University. We also used focal mechanism solutions for earthquakes provided by NIED and JMA. This study was supported by the Special project for reducing vulnerability for urban mega earthquake disasters from the Ministry of Education, Culture, Sports, Science and Technology of Japan.

Keywords: first-motion focal mechanism solution, Japan University Network Earthquake Catalog (JUNEC)

## Three-dimensional earthquake forecasting model for the Kanto district: Completeness magnitude of earthquake catalogs

YOKOI, Sayoko<sup>1</sup> ; TSURUOKA, Hiroshi<sup>1\*</sup> ; HIRATA, Naoshi<sup>1</sup>

<sup>1</sup>Earthquake Research Institute, The University of Tokyo

We started to construct a 3-dimensional (3D) earthquake forecasting model for the Kanto district in Japan under the Special Project for Reducing Vulnerability for Urban Mega Earthquake Disasters based on the Collaboratory for the Study of Earthquake Predictability (CSEP) experiments. Because seismicity in this area ranges from shallower part to a depth of 80 km due to subducting Philippine-Sea and Pacific plates, we need to study the effect of earthquake depth distribution.

We tried to construct a prototype of 3D earthquake forecasting model for the area based on the Relative Intensity model (Nanjo, 2011) which forecasts earthquake probabilities using historical data. For a large earthquake forecasting, we need a longer period of earthquake data than current studies. Therefore, we analyzed completeness magnitude ( $M_c$ ) every 10 km in a depth from 0 to 100 km of earthquake catalogs of Utsu (1979, 1982), Japan Meteorological Agency (JMA) and National Research Institute for Earth Science and Disaster Prevention (NIED) which are partially covered from 1885 to 2013 by the Maximum curvature method (Wiemer and Wyss, 2000) to assess a quality of their catalogs considering a depth of hypocenters. In the case of JMA catalog, an average and its standard deviation of  $M_c$  for a year from 1923 to 1970's showed 3.7 and 0.4, respectively. Then, they decreased from 1970's to 2000, which means that quality of the catalog improved with time. After the 1980's,  $M_c$  showed heterogeneous distribution with depth.  $M_c$  in shallower depth are smaller than that in deeper one. For example, averaged  $M_c$  and its standard deviation from 2000 to 2010 is 0.25 and 0.14 with 0 to 30 km in depth against 0.67 and 0.10 with 60 to 100 km in depth. In this presentation, we discuss how use the heterogeneous catalog to develop a 3-dimensional forecasting model in Japan.

The authors thank JMA and NIED for their earthquake catalogs. This work is sponsored by the Special Project for Reducing Vulnerability for Urban Mega Earthquake Disasters from Ministry of Education, Culture, Sports and Technology of Japan.

**Keywords:** Three-dimensional forecasting model, Kanto district, Collaboratory for the Study of Earthquake Predictability, earthquake catalogs



## Sparse Modeling to Estimate Spatial Distribution of Ground Motion Required for Rapid Prediction of Structural Damages

MIZUSAKO, Sadanobu<sup>1\*</sup> ; NAGAO, Hiromichi<sup>1</sup> ; HIROSE, Kei<sup>2</sup> ; KANO, Masayuki<sup>3</sup> ; HORI, Muneo<sup>1</sup>

<sup>1</sup>Earthquake Research Institute, The University of Tokyo, <sup>2</sup>Graduate School of Engineering Science, Osaka University, <sup>3</sup>Graduate School of Science, Kyoto University

A rapid prediction of structural damages due to a large earthquake is important to prevent secondary disasters. The first step of the prediction is to estimate ground motion at a targeted construction from observed seismic data, and the second step is to predict structural damage using the estimated ground motion. An accurate damage prediction requires ground motions with spatially-high resolution although the spatial density of constructions is much higher than that of seismometers in urban area. We have been developing a statistical method to model such ground motions using seismograms obtained by a seismometer array. Our target is Tokyo metropolitan area in which seismogram of MeSO-net (Metropolitan Seismic Observation network) is available.

Mizusako[2013, graduation thesis] proposed a method based on the Taylor expansion, and applied it to MeSO-net data when the Great East Japan Earthquake occurred. This method was found never to account for ground motions higher than 0.15 Hz, which was insufficient when considering that the eigenfrequency of constructions is usually between 1-10 Hz. Mizusako[2013] determined the partial differential coefficients, which appear in the Taylor expansion, from five nearest observatories with a truncation of the first order, but a better selection of a truncation of order and a group of observatories, which is hereinafter called " cluster " , could more accurately explain ground motions higher than 0.15 Hz.

We propose an algorithm based on sparse modeling that automatically and objectively determine the truncation of order and the size of the cluster. Our algorithm adopts the lasso, which is able to select dominant partial differential coefficients owing to the L1-norm regularization term. Moreover, the group lasso is implemented on our algorithm in order to select the coefficients of the same order associated with different components. We will report initial results obtained by the proposed method, comparing with the results of Mizusako[2013].

Keywords: Sparse modeling, lasso, urban disaster, MeSO-net

## Let's make a space food by using Peucedanum Japonicum which is medicinal herbs

WAKITA, Mari<sup>1\*</sup> ; TAKASE, Yoshimi<sup>1</sup> ; KAWAI, Mika<sup>1</sup> ; HAYASHI, Yoshino<sup>1</sup> ; KOBAYASHI, Mizuki<sup>1</sup> ; KAJIWARA, Satomi<sup>1</sup> ; KATAYAMA, Naomi<sup>1</sup>

<sup>1</sup>Nagoya Women's University

### Purpose

In a long-term stay in the space, the meal is very important. It is necessary to have the balanced meal every time not to get sick. Therefore it is necessary for space foods to prepared dishes with medicinal herbs. The reinforcement or cancer prevention of immunity were intended that superior efficacy made space foods using prospective Peucedanum japonicum. The Peucedanum japonicum has bitter taste, but considered the method that we could use Peucedanum japonicum as snacks, deliciously.

### Method

At first we made a liquid of Peucedanum japonicum by using a mixer. I made three kinds of snacks which are pound cake, dumpling and shortbread with the liquid of the Peucedanum japonicum. We did a sensuality test for subjects and we get the result of taste and the result of smell. The perfect scores of sensuality test is 10 points. To make a pound cake, we mixed 200 g of pancake mixture with 180g of Peucedanum japonicum. And we baked it by using 180 degree oven during 30 minutes. Furthermore, I made the poundcake which I added 10 g of powdered green tea in this basic recipe. In addition, the dumpling mixed 150 g of powder with 130g of nonglutinous rice powder. And we mixed Peucedanum japonicum in that dumpling. We steamed it with 100 degrees for 30 minutes. The shortbread mixed 250 g of weak flour, powder from nonglutinous rice 50 g, sugar 80 g, butter 175 g, Peucedanum japonicum 25 g and leaf 6 g of the mint. And we baked it at 170 degrees for 45 minutes.

### Result

We were able to eat deliciously without feeling bitterness of the Peucedanum japonicum by eating snacks. I judged even a sensuality examination to be delicious from a primary schoolchild to an elderly person. By butter, by wheat flour and by the cooking process, Peucedanum japonicum taste is better than before. It is easy to eat after cooking.

### Consideration

The Peucedanum japonicum taste was not bitter after cooking. And it was able to eat. Peucedanum japonicum have cancer protective efficacy. It is necessary to take as medicinal herb to keep our body health in the space. The space radiation including danger of the carcinogenesis may be accompanied in the space. Next, we would like to make the side dish by using peucedanum japonicum. And we would like to say utilization of medicinal herbs widely generally in future.

Keywords: Space foods, medicinal herbs, medicinal meal, Peucedanum Japonicum, snacks

## Low GL menu by using Low GI food is good as Space food

KOBAYASHI, Mizuki<sup>1\*</sup> ; KAJIWARA, Satomi<sup>1</sup> ; WAKITA, Mari<sup>1</sup> ; TAKASE, Yoshimi<sup>1</sup> ; KAWAI, Mika<sup>1</sup> ; HAYASHI, Yoshino<sup>1</sup> ; KATAYAMA, Naomi<sup>1</sup>

<sup>1</sup>Nagoya Wone's University

### Purpose

We became able to stay in the space for a long term. The offer of the meal appropriate to the active mass in the space is necessary. Therefore a menu offer to become the meal contents which are hard to go up of the blood sugar level is necessary. Metabolic syndrome becomes the problem on the earth. It is necessary to inform how it is important that we prevent hyperglycosemia after a meal widely. Similarly, in the space, you should consume the meal which is hard to go up of the blood sugar level. It is important that we do disease prevention. Therefore in this study, we made a menu (low GL food menu) which was hard to go up of the blood sugar level using food (low GI food) which was hard to go up of the blood sugar level.

### Method

We collected low GI foods. We put low GI food together and made the low GL food menu which was hard to go up of the blood sugar level. This menu is Unpolished rice, Wheat, Miso soup, Meuniere of the salmon, Boiled vegetables, Black sugar syrup agar. We use this menu and we measured blood sugar level by using peripheral blood. We checked our menu which is really became the low GL by using peripheral blood. We check our blood sugar level by using Kit (product made in Terumo Corporation), before eating this food and after 15 minutes, 30 minutes, 45 minutes, 60 minutes, 90 minutes and 120 minutes.

### Result

Cooking method was very important to make low GL menu. When we make soft food and eat it, our blood sugar level become high easily. Because when we make rice and boiled vegetables softly, the GL level of the actual survey became higher.

### Discussion

We think that it is desirable to perform by using low GI food to make low GL menu. And we think that the cooking method is very important to low GL menu. The space food must be good balance diet. By feeling of satisfaction and slow digestion and slow absorption, it is possible to prevent a sudden rise of the blood sugar level.

Keywords: Low GI, Low GL, Blood sugar level, Diabetes, Spece food

## Two weeks stay in Mars Desert Research Station(MDRS)

KATAYAMA, Naomi<sup>1\*</sup>

<sup>1</sup>Nagoya Women's University

I obtained an opportunity to participate in MDRS137. I cooked food for crew in MDRS137.

I made a menu using the commercial article that long-term preservation was possible as space foods. The basic meal was that, rice of the freeze dry, vegetables of the freeze dry, soup of the freeze dry, a retort pouch, canned food, dried fruit, a cookie and a candy. I can keep that food during long time.

Three women and five men participated in this study. The nutrient and the energy of the meal calculated it in consideration of the age, sex and active mass of the subject. I provided a meal of 1600kcal to woman 53 years old. I provided a meal of 1750kcal to woman 21 years old. I provided a meal of 1800kcal to male 50 years old. I provided a meal of 2000kcal to male 41 years old.

The significance of this study is the point that not only the use of the commercial preservation food as space foods but also the food problem at the time of the disaster can solve. It is necessary to make 42 kinds of menus to spend 14 days in MDRS. I thought about a combination of the commercial freeze dry rice and canned food of the fish. In addition, I thought about the combination of freeze dry soup and freeze dry vegetables.

Because 42 menus were gathered up as a booklet, I want to distribute this result widely in future. I hope that people will have interest in the space after to read that booklet. And I can enlighten people about combination of commercial food for the disaster.

Keywords: Closedown space, Life-support system, Space foods

## The recommendation of using the commercial disaster food as Breakfast -To consider it as space foods-

KAJIWARA, Satomi<sup>1\*</sup> ; WAKITA, Mari<sup>1</sup> ; TAKASE, Yoshimi<sup>1</sup> ; KAWAI, Mika<sup>1</sup> ; HAYASHI, Yoshino<sup>1</sup> ; KOBAYASHI, Mizuki<sup>1</sup> ; KATAYAMA, Naomi<sup>1</sup>

<sup>1</sup>Nagoya Women's University

### Purpose

At the present, the people who do not eat breakfast increase in Japan.

The Japanese Government recommends that we have breakfast well. As same as, the importance of the meal in the space rise more. Development of the space food which can store for a long term is urgent business. Because, we think about an exploration and emigration to Mars. Delicious space food is very important for the astronaut to keep their appetite. We perform questionnaire survey about the breakfast. I clarify the frequency of the breakfast intake. In addition, I clarify what kind of breakfast was eaten. Therefore in this study, we examined sensuality of the commercially food which can keep for a long term. And based on the result, we thought about the taste and smell in future space foods.

### Methods

Fifty female college students(20-21 years old) answered the questionnaire about breakfast intake frequency and about contents of breakfast. Fifty female college students (20-21 years old), they eat some commercially available rice things (eight kinds) which can store for 7ve years. And we performed to do sensuality examination for them. Students carried out the sensory examination and scoring (Perfect score is 10) of food. The marketing products are cooked with hot water in 15 minutes and cold water in 60 minutes. Vegetable rice, shrimp pilaff, perilla and seaweed rice, chirashi-sushi, white rice, fried rice, beef rice, dry curry of the magic rice (product made in Satake Corporation) .

### Results

The contents of breakfast were one or two kind of food. People have no time to make breakfast because of busy. An evaluation was high in the taste in order of vegetable rice, dry curry, beef rice, chirashi- sushi, fried rice, perill and seaweed rice, and white rice.

### Conclusion

Because people were busy in the morning, a balanced meal to be able to make in a short time was required. This disaster food is just fit as breakfast very much. As for both the taste and the incense, five vegetable rice, fried rice with meat, vegetables and curry rice, stewed beef rice occupied the high rank. Space foods passing globally are necessary. This commercially available disaster food is suitable for both space foods and breakfast very much. We want to examine not only the rice but also the side dish in future.

Keywords: Breakfast, th ecommercial disaster food, Space food

## The need of the lactic acid beverage in space foods

HAYASHI, Yoshino<sup>1</sup> ; KOBAYASHI, Mizuki<sup>1\*</sup> ; KAJIWARA, Satomi<sup>1</sup> ; WAKITA, Mari<sup>1</sup> ; TAKASE, Yoshimi<sup>1</sup> ; KAWAI, Mika<sup>1</sup> ; KATAYAMA, Naomi<sup>1</sup>

<sup>1</sup>Nagoya Women's University

### Purpose

The long-term space stay makes it possible to perform many studies. We think that the development of space foods will develop more in future. The meal management to maintain the health of an astronaut working busily is important. With lactic acid bacterium beverage, we thought that we want to perform the health care of the astronaut. Therefore we decided to check the effect on bowel movement of the lactic acid bacterium beverage.

### Method

We assumed twenty adult women (average age 20.5 years old) as subjects. Before experiment start, during two weeks, we took the bowel movement record. Twenty students participated in an experiment. We divided it into two groups of ten students of the constipation and ten students of the non-constipation. We boiled Y Company lactic acid bacterium beverage (40% of calorie off) at 100 degrees during three minutes. During two weeks, we let the ten constipation consume the lactic acid bacterium beverage which we boiled and recorded the state of the bowel movement. Another two weeks, we let them consume the lactic acid bacterium beverage which we did not boil and recorded the situation of the bowel movement afterwards. Ten students of the non-constipation tested it in order to reverse-turn with ten students of the constipation. After the experiment end, we recorded the situation of the bowel movement during two weeks. The record contents were the stool frequency, smell, shape and number of times of the gas.

### Result

Stool frequency was improved in the constipation group by the lactic acid bacterium intake. In the case of the non-constipation group, the big change was not seen in stool frequency. However, in both groups, the degree of smell was improved clearly.

### Discussion

In constipation group, stool frequency was increased after drinking of the lactic acid beverage. A bowel movement state might be improved by an oligosaccharide and the lactic acid included in the lactic acid bacterium drink. However, when constipation group stopped the intake of the lactic acid beverage, their stool frequency was not good as before. It is necessary to consume the lactic acid bacterium drink continuously

Keywords: Lactic acid, Beverage, Space foods

## Publication of redesigned multicolor 1:25,000 topographic maps

UNE, Hiroshi<sup>1\*</sup> ; NEMOTO, Masami<sup>1</sup>

<sup>1</sup>Geospatial Information Authority of Japan

With rapid development of the information and communication technology, the national basic map accomplishes a big change. As for the 1:25,000 topographic map produced by the Geospatial Information Authority of Japan ("GSI"), which underpins the geo-science studies, publication of newly designed multicolored 1:25,000 topographic map was started from November 2013, with different production process and more detailed contents which the topography was easy to understand.

New 1:25,000 topographic map is based on "digital Japan basic map (DJBM)", and the production process was greatly changed. A Plotting work using aerial photo, which was the biggest characteristic of the past topographical map making, is not included in the process, and a part of the vector data in the digital Japan basic map is directly clipped and printed.

It is enactment of "the Basic Act on the Advancement of Utilizing Geospatial Information (NSDI act of Japan)" of 2007 that became the starting point of such a change. By this law, it was prescribed in particular that the government shall prepare and use "the fundamental geospatial data (FGD)" as a standard of the positions on the digital map. The GSI executed the production of FGD utilizing 1:2,500 city planning base map and 1:25,000 topographic map to mostly complete for the whole country by the end of 2011, and produced DJBM using FGD as a frame.

New 1:25,000 topographic map is based on DJBM, which means that the contents became more detailed than the conventional one. Furthermore, introduction of process printing enabled multicolor production, and some expression methods were realized for the first time.

Contents becoming more detailed means that the information becomes the precision of 1:2,500 level in city planning area. This comes from that DJBM is maintained at 1:2,500 level in the city planning area, where in the area except it at 1:25,000 level. All the buildings are displayed without being generalized even in the crowded city areas. In addition, the indication density of the road rises because all the roads are displayed without thinning.

Introduction of process printing allowed to add green shadows to grasp the topography intuitively. Orange colored buildings can avoid the congestion with roads or the place names. In addition, expressions using various colors improved the readability of the topographic map, e.g., expressways, national highways and public roads are colored in green, red and yellow respectively, and national highway numbers are displayed in inverse triangle type of the blue.

Besides, GSI started to present "digital topographic map 25,000" to provide image data clipped from DJBM online using internet from 2012. Users can choose the central position, size and the direction of the map image depending on the purpose of use, and can choose colored/monochromatic map and with/without the shadows. It makes it easier to use it as the background map of geo-science study.

As for 1:25,000 multicolored topographical map, around ten sheets a month are published newly for the time being, and conventional topographic maps are going to be replaced several years later.

Keywords: 1:25,000 topographic map, NSDI Act of Japan, Digital Japan Basic Map, process printing

## Design of the PNG Elevation Tile and Rapid Response of Disaster Prevention-related Web Site

NISHIOKA, Yoshiharu<sup>1\*</sup> ; NAGATSU, Juri<sup>1</sup>

<sup>1</sup>Institute of Geology and Geoinformation, AIST

In order to achieve the advancement of elevation data use, we designed the PNG Elevation Tile. We create PNG elevation tiles based on the elevation tile of CSV currently published from the Geospatial Information Authority of Japan, and tested using test applications. In such applications, the redraw which took several minutes until now can be performed in several seconds, and a high-speed response can be realized using the PNG Elevation tile.

Keywords: PNG Elevation Tile, tile, disaster prevention, energy cone, Seamless Geological Map, 3D



## The monitoring of the NIED Hi-net by using the mobile application

EMOTO, Kentaro<sup>1\*</sup>; SAITO, Tatsuhiko<sup>1</sup>; UENO, Tomotake<sup>1</sup>; HARYU, Yoshikatsu<sup>2</sup>; NASU, Kenichi<sup>2</sup>; SHIOMI, Katsuhiko<sup>1</sup>; AOI, Shin<sup>1</sup>

<sup>1</sup>NIED, <sup>2</sup>NIED/ADEP

For the geophysical research and the disaster prevention, monitoring the seismic activity is important. By monitoring of the seismicity, for example, we can detect the unusual event and know the fault plane. Monitoring of the real time wave filed is also important for the early warning. In order to correctly monitor the seismic activity, we have to monitor the seismic stations. The trouble of the station causes the decrease of the accuracy and the wrong interpretation. NIED runs the Hi-net seismic network which has more than 80 seismic stations with the average separation of 20 km all over Japan. NIED provides the waveform data and automatically detected earthquake information through the internet. All stations are always watched and the trouble information is reported. Usually, this watching is done by checking the individual waveform. The map information, however, is easier to understand the station condition than the waveform. In this study, we propose a method to monitor the seismic network by using the mobile device and develop the mobile application. Also we develop the applications to check the automatic hypocenter determination system.

First, we develop the application which shows the seismicity on the map. We plot earthquakes listed on the catalog determined by the Hi-net automatic system on the embedded map application. We also plot the cross section of the seismicity. We can enlarge, reduce and rotate the map. Corresponding to these gestures, the cross section is also changed. Therefore, we can see the subducting slab and the fault plane from arbitrary directions. By plotting the past seismicity on the background, we can check that the recent earthquake is usual or unusual.

Second, we develop the application which shows the wave traces of selected stations and the earthquake information on the same image in order to know whether the automatic hypocenter determination system works properly. On the Hi-net web site, we can see the 100-trace image of selected Hi-net stations. By looking this image, we can roughly know the location, the origin time and the magnitude of the earthquake. We can see some earthquakes are correctly determined but some earthquake is not determined by the automatic system by plotting the earthquake information on the trace image.

Finally, we develop the application for the manager of the Hi-net network, which shows the real time Hi-net records on the map. We get the real time data from the data server of the Hi-net and make the map image of the RMS (1s) velocity amplitude. We stock this image every second and download it from the mobile device. On the device, we can see the real time record of all stations of Hi-net every second. Hence, we can visually find abnormal behaviors of stations. By changing to the map application and showing the detail station information, we can check which station has some troubles. We also plot the information of the rapid source parameter determination system, named AQUA, on the real time map. We can see the wavefield and the source location at the same time. By comparing this information, we can check both AQUA system and station condition.

By using first two and third applications, we check the Hi-net automatically hypocenter determination system and stations, respectively. We can watch the Hi-net in terms of the wavefield, the waveform and the hypocenter by integrating three applications.

Keywords: Hi-net, mobile, real time

## Red Relief Image Map of the terrain representation method of the moon

CHIBA, Tatsuro<sup>1\*</sup> ; KAMIYA, Izumi<sup>2</sup> ; TAKAKUWA, Noriyuki<sup>2</sup> ; SATO, Takenori<sup>2</sup>

<sup>1</sup>Asia Air Survey Co., Ltd., <sup>2</sup>Geospatial Information Authority of Japan

### Summary

Although detailed terrain data of the lunar surface is obtained, terrain representation technique has become an issue. So called Red Relief Image Map (RRIM), which has been developed specifically for volcanic terrain analysis by LiDAR was applied to the topographic representation of the moon that seems to be similar to the volcanic terrain on the earth. The resulted RRIM of the moon showed effectiveness for visual interpretation of the lunar terrain.

### Terrain of the Moon

The moon terrain may be characterized by high land and mariner of basaltic plane. There are several commonly used terrain representation methods. Contouring is very effective method for representing high relief topography, but not quite suitable for enhancing low relief terrain such as lunar surface. Many small scale maps and map atlas employ shaded-relief and/or gradation representation method. Even for the small scale topographic representation of the lunar surface, the shaded-relief and gradient method was used to be employed most of the cases. However, these traditional methods have issues to be solved since there are many craters lie one upon another on the lunar surface. These dipped terrains sometimes erroneously expressed by shaded-relief method depending on the direction of illumination light. Development of more effective terrain representation method is expected to solve these issues.

### The RRIM

The RRIM is a method for enhancing terrain relief and is based on concept of slope map. In the RRIM, the slope is expressed by red gradation, and ridge-valley is expressed by intensity of light. Namely, the steeper the slope, the more ridge area, the lighter, and the valley and more dipped terrain, the darker on the RRIM. This image, although it is single ortho-image, provides 3D perspective.

### The RRIM of the Moon

The RRIM was applied for making map of the moon. Digital terrain data (DEM) used for making the RRIM was acquired by "Kaguya" lunar mission by JAXA. The DEM has 1/20 degree mesh interval. Presently, The RRIM of the moon can publicly be viewed at home page of Geospatial Information Authority of Japan , MILIT. It is also possible to 3D high speed viewing using Secium and Three.js.

### Acknowledgement

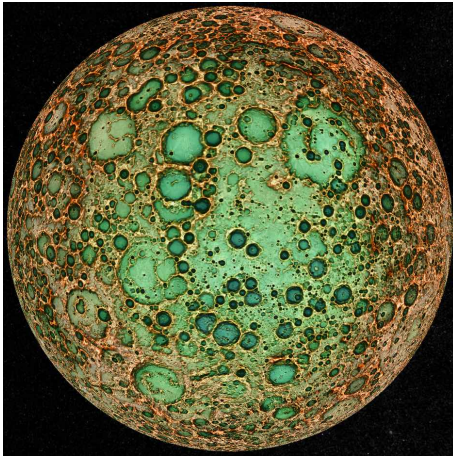
Authors acknowledge JAXA and NAOJ for providing the lunar terrain data from "KAGUYA" mission. .

Keywords: moon, DEM, terrain representation, red relief image map, crater, selene

MTT41-P04

Room:Poster

Time:April 28 18:15-19:30



## Development of the CS (Curvature and Slope) topographical map

TODA, Kenichiro<sup>1\*</sup> ; DAIMARU, Hiromu<sup>2</sup> ; KOARAI, Mamoru<sup>3</sup> ; NAKANO, Takayuki<sup>3</sup> ; IWAHASHI, Junko<sup>3</sup>

<sup>1</sup>Nagano Prefecture Forestry Reserch Center, <sup>2</sup>Forestry and Forest Products Reserch Institute, <sup>3</sup>Geospatial Information Authority of Japan

For the topographical interpretation, we developed CS (Curvature and Slope) topographical map to visualize micro-relief that affect landslide susceptibility in mountain area. The CS topographical map represents valleys by blue color and ridges by red color, simultaneously steep slopes are assigned to dark color. We produced CS topographical map for the entire area of Nagano Prefecture from airborne LiDAR DEM and conducted many micro landslide such as linear depressions in landslide blocks, valley head hollows were recognized, and they were confirmed by subsequent field survey. The CS topographical map provides us with many information about distribution of micro-relief in mountain area, and it may be a prominent tool for evaluating landslide susceptibility.

Keywords: CS topographical map, topographical interpretation, curvature, slope

MTT41-P06

Room:Poster

Time:April 28 18:15-19:30

## The map of a geopark

KOARAI, Mamoru<sup>1\*</sup> ; MOKUDAI, Kuniyasu<sup>2</sup>

<sup>1</sup>GSI of Japan, <sup>2</sup>Pro Natura Foundation Japan

The authors reviewed about the deployment of geopark activity and the practical use of maps of geopark in Japan, and reported the actual condition of the map in the geoparks of all Japan. In this work, the authors collected many pamphlets of geopark with map information, reviewed all pamphlets in the points of view for expression of geographical feature.

There are many maps like tourist resort maps. But, some maps for Geopark had tried geographical feature expression in base map. For example, some maps express the landform using color for each elevation simply, and some maps were carried out 3D expression of the shade figure using DEM. These type maps were considered to be easy to understand the outline of geographical feature, compared with a contour drawing map.

Keywords: geopark, map, expression of geographical feature

## Landslide Geomorphological Map of the Northern Hida Mountains, Japan

SATO, Go<sup>1\*</sup> ; KARIYA, Yoshihiko<sup>2</sup>

<sup>1</sup>Teikyo Heisei University, <sup>2</sup>Senshu University

The northern Hida Mountains located in central Japan consist of high-relief mountain ranges. A previous study has reported the distribution of the glacial topography and explained the landform development caused by glaciers in this region. In 2008, we published the *Landslide Geomorphological Map of the Northern Hida Mountains*. This map revealed the landslide distributions and glaciated topographies. Our poster shows this map and explains the methods and criteria for geomorphological mapping, as well as the development and characteristics of landslide distribution.

Keywords: Geomorphological map, Landslide topography, Glacial topography, Geomorphological development, The Northern Hida Mountains

## Geographic Environment Reconstruction and Geo-visualization using High Resolution DEM and Old Printed Map

SUZUKI, Atsushi<sup>1\*</sup>

<sup>1</sup>Rissho University

This study combines high resolution DEM (5m or 10m) with topographical maps published in the early 20th century and make 2D and 3D maps. By such a work, I try the then geographical environmental reconstruction and geo-visualization.

The main study area is Sakishima Islands of the early 20th century. In Sakishima islands in the first half of the 20th century, 1000 to 2000 malarial patients were reported in every year. According to the old research findings, there was much endemic malaria in Sakishima islands in the island of continentality or volcanic island, and it was distributed over the area where there is a vertical interval of land and the basin system network progressed.

Keywords: High Resolution DEM, Printed Map, Geographical Environment, Geo-visualization

## Visualization of tsunami and circumstances during initial evacuation and its effectiveness for disaster education

KIMURA, Hiroyuki<sup>1\*</sup> ; SUGAWARA, Daisuke<sup>2</sup> ; IMAMURA, Fumihiko<sup>2</sup>

<sup>1</sup>FUKKEN CO.,LTD., <sup>2</sup>International Research Institute of Disaster Science, Tohoku University

Public interests in forthcoming large-scale tsunami have been increasing since the notification of the large-scale projected tsunami scenario along Nankai Trough. It is important for people to keep their high consciousness of tsunami hazards by means of continuous and effective tsunami-disaster prevention education. With regard to safe evacuation from tsunamis, people must evacuate as early as possible, and they should prepare an appropriate plan and method for evacuation, which is corroborated by understandings on tsunami behavior and situations of the initial stage of tsunami evacuation. In this study, we will present visualizations of tsunami behavior and circumstances during initial evacuation activity. We will further investigate effectiveness of the visualization for disaster prevention education.

Coastal areas of the Pacific coast of Tohoku have been photographed before and after the Great East Japan Earthquake. These photographs have been taken as both orthographical and diagonal (oblique) aerial imageries. The diagonal photographs are useful for people to figure out the elevations of features, such as buildings and topography three-dimensional and clearly. The oblique photographs and inundation map computed from the numerical simulation of 2011 Tohoku-oki tsunami are synthesized, to derive a realistic visualization of the tsunami flooding. This visualization will be useful for people to understand tsunami behavior, which is influenced by land use and local topography.

Visualization of circumstances during initial evacuation activity will be useful information for people to understand imminency and available time for tsunami evacuation. Airborne orthographical photographs and satellite imageries are superimposed by concentric circles centered by selected representative points that is familiar with local people, as well as main roads and evacuation facilities, because they are crucial for evacuation plan. It is unlikely that people may stay in their own houses and offices at the time of the earthquake and tsunami. The visualization proposed by this study will lead people to understand plausible circumstances and will provide useful information for various alternative measures for initial evacuation activity, as well as existences of insusceptible areas for evacuation.

Keywords: tsunami behavior, tsunami evacuation, visualization, disaster prevention education



## A Web-based Volcano Hazard Map with Information on Evacuation Shelters, Hospitals and Facilities for Vulnerable People

ISHIMINE, Yasuhiro<sup>1\*</sup>

<sup>1</sup>National Institute of Public Health

National Institute of Public Health is a governmental agency that belongs to Ministry of Health, Labour and Welfare. It provides with training courses related to public health, environmental hygiene and social welfare as well as conducts research on the fields. It revises the countermeasures to protect lives and health of citizens during large-scale disasters on the lessons learned from the experience during the Tohoku Earthquake and Tsunami Disaster. As a part of the revision, I am now developing an information-sharing system to facilitate support teams to effectively and efficiently distribute a limited number of staff and resources during large-scale disasters. The mapping of relevant facilities, such as evacuation shelters and hospitals, is the key function of the information-sharing system because the understanding of geographical relationships is the first step to visit and work in an unfamiliar area during disasters. I adapted the information-sharing system to volcanic eruptions to display potentially hazardous areas. I will show an example of the application by using the hazard map of Mt. Fuji, which has been published by Mt. Fuji Volcanic Disaster Prevention Conference in 2002.

Keywords: Hazard Map, GIS, Volcanic Eruption, Mt. Fuji, Disaster Medicine, Public Health

## Mapping the supply-demand gap in childcare services with GIS: A case study in Tokyo

WAKABAYASHI, Yoshiki<sup>1\*</sup> ; KOIZUMI, Ryo<sup>1</sup> ; KUKIMOTO, Mikoto<sup>2</sup> ; YUI, Yoshimichi<sup>3</sup>

<sup>1</sup>Tokyo Metropolitan University, <sup>2</sup>Oita University, <sup>3</sup>Hiroshima University

The aim of this study is to visualize the spatial pattern of the gap between childcare supply and demand on a map. Study area is Tokyo where the number of children awaiting enrollment in licensed childcare centers is extremely large. To map the supply-demand gap with geographic information systems, we calculated difference between supply and demand densities after converting the vector data concerning childcare supply from the public sector and pre-school children into raster data using kernel density estimation. The result of the analysis showed a spatial imbalance between childcare supply and demand. The map that added the distribution of unlicensed childcare centers proved that the shortage of the childcare supply by the public sector is spatially complemented by the services by the private sector.

Keywords: childcare services, supply-demand gap, kernel density estimation, raster calculation, Tokyo

## Geo-interactive Guidebook Services: Design and Development of LBS Applications Featuring Geo-enabled Illustrations

LU, Min<sup>1\*</sup> ; ARIKAWA, Masatoshi<sup>1</sup>

<sup>1</sup>Center for Spatial Information Science, The University of Tokyo

The current location-based mobile applications for tourists usually use Web maps as base maps with attached objects like POIs (points of interest) to provide relevant guide information. Their services rely on accuracy of positioning functions on the handsets and accessibility of the Web maps. However, their diversity of maps and geo-information representation methods are insufficient, and are regardless of the differences in cultures as well as target users. Meanwhile, such services provide information mainly based on points, but storytelling and plots are less concerned. On the other hand, conventional paper-based guidebooks and magazines are still popular because they are good at dealing with subdivided topics, content arrangement, illustrations and stories to provide tentative travel plans with attractiveness and readability. However, they lack the capability of interactions with readers' actions and locations.

In considering of combining the advantages of positioning-enabled devices and well-designed guidebooks, we researched on a framework to create geo-enabled pages for designing applications and services providing better user experience when traveling in the real world. By analyzing the graphic components of the pages of a guidebook from the viewpoint of geo-information representation, a structured description of both graphic and geographic information of the components is established. Different geo-reference methods for geocoding the components are discussed. Especially, the methods of positioning using illustrated-maps and lines on pages are focused. Possible location-based events in the procedures of interactions with users and their locations are summarized. The design principles of user interfaces for both content creators and final users are discussed.

Finally, prototypes named "Manpo" including a content editor and a content browser are developed based on Apple Inc.'s iOS platform. Contents created by the prototype editor from existing guidebooks were used with Manpo by experimenters, to show the usability of the framework and the potential to be a commercial product.

Keywords: guidebooks, illustrated maps, geo-reference, mobile applications

## Development of a Learning Environment based on Spatio-temporal Historical Story Mapping Animation

INOUE, Yasushi<sup>1\*</sup> ; TSURUOKA, Ken'ichi<sup>1</sup> ; ARIKAWA, Masatoshi<sup>1</sup>

<sup>1</sup>Center for Spatial Information Science, The University of Tokyo

The purpose of leaning history is to have the capability of imaging the future by using the knowledge in historical facts. In history learning, it is important for users to understand effectively causal relationships of events. However, paper textbooks have a limitation of dynamically representing historical stories, because articles of paper textbooks consist of pieces of texts and pictures such as photos, maps, diagrams, and chorological tables. These kinds of articles are fragmental and static descriptions from the viewpoint of visual presentations. A learning environment that the user can easily understand causal relationships of events for a historical story is desired.

For resolving the limitation of paper textbooks, we propose a new framework for visualization of historical stories with relationships of events. A historical story can be defined what to combine causal relationships of events along the axis of time. We classified and defined simple data models for visualization according as time series and locations of events. We have implemented an application software system that has an interactive user interface by displaying sequences of graphics with our data models. Visual representation of our user interface is realized by three basic methods for depicting historical stories as follows:

- (1)Visualization of causal relationships with arrow icons on chorological tables and maps
- (2)Visualization of hierarchies of events with chorological tables and maps
- (3)Visualization of the focal position in storytelling

We are creating animation content telling the story about the government's actions for the aftermath of the 2011 Tohoku earthquake and tsunami by using our prototype system as a model case. The purpose of our study is to realize a learning environment for users to easily understand causal relationships of events, in brief, and to prove effectiveness of historical learning through the model case.

Keywords: History Learning, Visualization, Ubiquitous Mapping

## Integrating Maps in Photos with Relative Spatial References

SI, Ruochen<sup>1\*</sup> ; ARIKAWA, Masatoshi<sup>1</sup> ; LU, Min<sup>1</sup>

<sup>1</sup>Center for Spatial Information Science, The University of Tokyo

### 1. Introduction

Signboard maps are widely distributed in public places, such as parks, subway stations, universities, and so on. Signboard maps are usually designed specially for the local area. POIs are usually highlighted in the maps. Many signboard maps are also drawn in an artistic way, and the mapping styles are various in different signboard maps. Except for the content, the locations of the signboard maps also provide rich information. The locations of the signboard maps are usually important places, such as the entrance of the facility and the place people easily miss the way. However, one of the disadvantage of the signboard maps is that they are not accessible anytime anywhere if users are far from them. To solve the problem, we propose a method to integrate the signboard maps in photos with digital maps to provide location based services with the signboard maps on smart phones.

### 2. Mapping Signboard Maps onto Digital Topographical Maps

An example of a signboard map we are going to integrate is a map of Kashiwa Campus at the University of Tokyo. We took the high resolution photos of the signboard maps in the campus. And we use a digital topographical map provided by The Geospatial Information Authority of Japan as the base maps.

We use the road intersection points as the control points of the photos. All the road intersection points are picked and are given the same coordinates as the corresponding points on the base maps. With the control points, we can map a user's location coordinates onto the photos including the signboard maps. However, factors such as the generalization, exaggeration, and the different of map projection used in the signboard maps make errors of the mapped user's location on the photo. And the errors of relative spatial relations, like locating the user on the wrong side of roads intersection, will easily mislead the users.

To ensure the relative spatial relationship of user's location with roads, we depict the roads on the photos, record their coordinates, and find the corresponding roads on the base maps. Instead of mapping the user's location directly onto the photos, we first map it onto the base map. Then we find the nearest road in the base map from the user's location. Then we map the location from the base map to the photo, so that the relative distance from user's location to the road keeps same and the foot point cuts the road with same proportion. As shown in the figure, AB and A'B' are corresponding roads in base map and in the photo, U and U' are the user's locations, V and V' are the nearest point on the road from user's location. Then,  $AV/VB=A'V'/V'B'$ ,  $UV/AB=U'V'/A'B'$ .

### 3. Integrating Multiple Various Signboard Maps

As we have mentioned, the locations of signboard maps themselves are usually important places. We annotate in each signboard map the locations of other signboard maps. By doing so, we do not only tell the users the locations of other signboards, but also composed different signboard maps, each may refer to a relatively small local area, to form a larger map. While the user is moving out of the current map, we zoom out of the current map and zoom into another map in which the user's location falls.

### 4. Conclusion

The signboard maps are generally more artistic, more stylish and more thematic than commonly used digital navigation maps. And the locations of the signboard maps are also important. We proposed the method to integrate the signboard maps in photos with digital base map to provide location based service with signboard maps on smart phones.

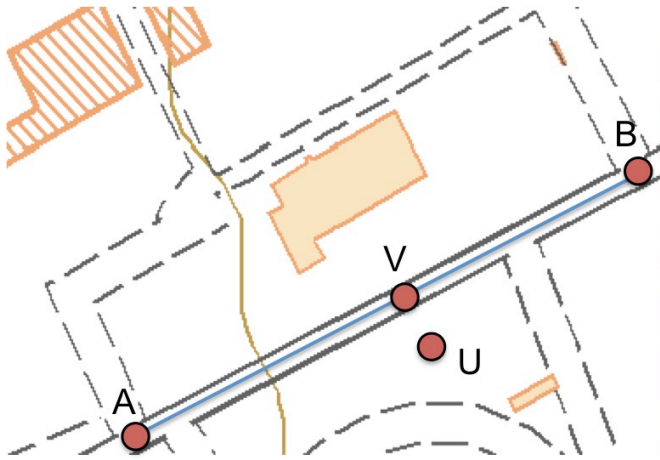
In this paper, we just made the experiment with the signboard maps of Kashiwa Campus at the University of Tokyo. In the future, we are going to cooperate with local governments and communities to collect and integrate more signboard maps on our proposed framework.

Keywords: Signboard Maps, Photos, Location-based Services, Relative Spatial References

MTT41-P14

Room:Poster

Time:April 28 18:15-19:30



## Portrayal and Symbology of Global Map

ANDO, Akifumi<sup>1</sup> ; UBUKAWA, Taro<sup>1</sup> ; SAITO, Toshinobu<sup>1\*</sup> ; YAMADA, Akiko<sup>1</sup> ; UEDA, Maya<sup>1</sup> ; SUGA, Masaki<sup>1</sup> ; YAMAZAKI, Satoko<sup>1</sup>

<sup>1</sup>Environmental Geography Division, Geocartographic Department

Global Map is fundamental geospatial information datasets composed of eight kinds (Population Centre, Drainage, Transportation, Boundaries, Land Use, Land Cover, Vegetation, Elevation) of thematic information based on consistent specifications. It is developed under international cooperation of respective National Geospatial Information Authority (NGIA) around the world. Global Map version 2 (Global Version, Land Cover and Vegetation) was published in July, 2013. Analyzing Global Map with other geospatial information gives good understanding of the relationship between human activities and environmental conditions including forest distribution and land cover conditions. This poster shows our recent achievements in developing new portrayal for Global Map and tiles for WTMS.

Keywords: Global Map, Map Symbology

## Estimation of the Horizontal Positional Accuracy of Geospatial Data

KOSHIMIZU, Hiroshi<sup>1\*</sup> ; MURAKAMI, Masaki<sup>2</sup>

<sup>1</sup>GSI of Japan, <sup>2</sup>GSI of Japan

Expectations for positioning accuracy enhancement vitalize efforts for the advancement of positioning services. For example, various driving assist service with the use of 'Authority map' (which is a large scale map that anyone can use) is being studied in the field of ITS service. It is expected that further disclosure of information about the horizontal positional accuracy of map (which should be combined with positioning information) will be required.

As for the horizontal positional accuracy of map, the threshold (upper limit value) called 'standard deviation' is prescribed in the General Standard of Operation Specifications for Public Surveys for digital topography: 1.75m in the case of the scale 1:2500 (2.50m in the case of editing pre-existing data). However, this 'standard deviation' gives no specific information about probability density functions which are inevitable for the definition of the positional accuracy. Moreover, it is pointed out that above threshold is too large in relation to actual values of public survey works and thresholds of several rules in other countries.

We therefore give the definition of the index 'standard deviation' expressing the horizontal positional accuracy of map with the use of the past research of GreenWalt-Shultz (1968), which had a crucial impact in the FGDC accuracy standards (1998). Let  $X, Y$  be random variables which have horizontal residual component values  $x, y$  as realized values which are obtained from sample points in the map. Here, 'residual value' means the difference of the observed value and the value considered to be true concerning the same point. If a set  $\{(x,y)\}$  contains no bias and outlier, residual value  $(x,y)$  is considered to represent positional accuracy of the point. We assume that realized values of  $X (Y)$  are normally distributed with density function  $f_x (f_y)$  of mean 0 and variance  $s_x^2 (s_y^2)$ . Let  $P(R)$  the probability which a sample point falls in the closed disc with radius  $R$ .  $P(R)$  is represented by the density function  $f$  which has  $f_x$  and  $f_y$  as a marginal density function on  $X \times Y$  with the use of conversion from  $(x,y)$  to polar coordinates. If  $s_x = s_y$  then we can easily show that  $P(s_x) = P(s_y) = 0.3935$ , otherwise  $P(s) = 0.3935$  leads an approximate expression  $s = 0.5(s_x + s_y)$ , which is shown by converting the polar coordinates expression of  $P(R)$  into the form of integral transformation of certain modified Bessel function (of the first kind) and using numerical calculation methods. If  $s_x = s_y$  then  $s_x = s_y = s$ . Therefore, we define the index 'standard deviation' by  $s$ , and call  $s$  'Circular Standard Error' or 'CSE' for short. Estimated value of  $s$  should be calculated by  $\{(x,y)\}$ .

Based on this redefinition, we investigated the horizontal positional accuracy of public survey works for digital topography with the scale 1:2500. We regarded (independently) observed coordinate value of GNSS positioning as true value at the sample point, and removed the effect of bias and outlier as much as possible in advance. As a result, we obtained a rough estimate on the CSE: Estimated average value of CSE is 0.3~0.4m, and estimated threshold (upper limit value) is 0.8m. This estimation indicates the necessity of tightening the threshold for the positional accuracy in the General Standard of Operation Specifications for Public Surveys.

Keywords: positional accuracy



## Effectiveness of the consecutive cross sections expression for the relief representation

ARAI, Riku<sup>1\*</sup> ; MORITA, Takashi<sup>2</sup> ; KUDO, Keisuke<sup>1</sup>

<sup>1</sup>Graduate School of Engineering and Design, Hosei University, <sup>2</sup>Faculty of Engineering and Design, Hosei University

A map that shows the relief topography is having a lot of kinds. For example altitude tints map, and a color shaded relief map, etc. In late years, by a detailed digital altitude model, we can come to express an irregularity of the slight topography. In this way, we can recognize the topography intuitively.

However, like a contour line, it is important that we grasp ups and downs of the topography quantitatively. Therefore we stack a contour line on topography irregularity map and are effective in visualizing the ups and downs between specific two spots by beginning to talk about any section. Furthermore, we may express the topography as a map of the subject by handling shadow in the continuation section that cut and brought down a parallel section to equal distance continually. In addition, it may show former city space structure by grasping ups and downs of such slight topography.

This study made the topography irregularity map around the rich moat of topography ups and downs. Furthermore, I visualize the city space structure that watched "Ichigaya Hachiman" from a geographic characteristic as an example by consecutive cross section expression. And I reevaluate an effect of the consecutive section expression in the topography irregularity map.

As a result, I showed city space structure and ups and downs of the slight topography by an irregularity map clearly as well as superficial contour line and color shaded relief. And the consecutive cross section expression expressed detailed topography incline to supplement an irregularity map.

**Keywords:** topographic map, consecutive cross sections, urban space structure, moat of a Edo castle, hilly sections of Tokyo, shrine

## Mass-independent fractionation of mercury stable isotopes in deep-sea hydrothermal systems

TAKEUCHI, Akinori<sup>1\*</sup> ; TOMIYASU, Takashi<sup>2</sup> ; KODAMATANI, Hitoshi<sup>2</sup> ; YAMAMOTO, Masahiro<sup>3</sup> ; MARUMO, Katsumi<sup>4</sup>

<sup>1</sup>National Institute for Environmental Studies, <sup>2</sup>Kagoshima University, <sup>3</sup>JAMSTEC, <sup>4</sup>University of Toyama

It has been recognized that mercury (Hg) isotope analysis is an important new tool for identifying Hg source and tracking Hg transformations in the environment. Mass-dependent (MDF) and -independent (MIF) fractionations of Hg isotopes are caused by a wide variety of biogeochemical processes including redox reactions and volatilization. Volcanic activities and its associated hydrothermal activities are the main sources of naturally-emitted Hg in the environment. Several previous studies suggested that the naturally-emitted Hg indicated both MDF and MIF. It was thought that the MDF was caused by a process of liquid-vapor partitioning during ascending and the MIF was caused by photoreduction. It was, however, suggested that both photoreduction and volatilization could cause the MIF, and it has never been distinguish from each other in the hydrothermal systems. In this study, geological samples in active deep-sea hydrothermal systems at Izu-Bonin arc were collected and measured their Hg isotopic compositions. They indicate both MDF and MIF. The  $\delta^{202}\text{Hg}$  values range from -1.0 to 0.5 ‰, indicating the liquid-vapor partitioning, whereas the calculated  $\Delta^{199}\text{Hg}$  values are mostly between 0.1 and 0.2 ‰, indicating the MIF in the deep-sea hydrothermal systems without photoreduction. The linear relationship between  $\Delta^{199}\text{Hg}$  and  $\Delta^{201}\text{Hg}$ , ranging from 1.6 and 2.0, also indicates the nuclear volume effect. This result suggest that MDF and MIF of Hg isotopic compositions can be utilized to distinguish naturally-emitted Hg from anthropogenic Hg.

Keywords: Mercury Isotope, MIF, Deep-sea Hydrothermal Systems, CV-MC-ICP/MS

## Speciation of metal ions in water: comparison of their reactivities with oxygen-donor hard ligands

TAKAHASHI, Yoshio<sup>1\*</sup> ; MIYAJI, Asami<sup>1</sup> ; TANAKA, Masato<sup>1</sup>

<sup>1</sup>Graduate School of Science, Hiroshima University

Complexation of metal cations with ligands such as hydroxide ion, carbonate ion, carboxylate ion, and phosphate ion is one of the most important factors controlling behaviors of metal ions in natural environment. Previous studies showed that these ligands were classified as "intermediate hard ligands" having oxygen donor, which favors to form ionic bonding. However, it was found that the reactivity of these ligands depends on ionic radius and that there is a difference of the reactivity between hydroxide ion and other intermediate hard ligands such as carbonate and carboxylate. For example, among divalent alkaline earth metal ions, Mg<sup>2+</sup> mainly precipitates as hydroxide (brucite), while Ca<sup>2+</sup> prefers to form carbonate (calcite) or phosphate (apatite) minerals rather than hydroxide. However, quantitative discussion on the selectivity of metal cations has not been performed.

In this study, we evaluated the standard Gibbs free energy, entropy, and enthalpy for the complex formation of hydrated metal cations with these ligands based on a critical thermodynamic database. As a result, we found that the entropic contribution to the free energy was large in the case of hydroxide complex of smaller cation. In contrast, the entropic contribution to the free energy was small in the case of hydroxide complex of larger cation and other complexes. In addition, the enthalpy contribution was not significant in this reaction. In the aqueous complexation reaction, entropy was controlled by the number of water molecules replaced by the ligand, suggesting that hydroxide complex for large cation was not stable due to the small effect of dehydration.

This suggestion was confirmed by quantum mechanical calculations, which was performed with B3LYP/6-311+G\* level using Gaussian 09. We calculated distance between metal (M) in the center and oxygen (O) in the ligand with the increase of number of water molecules placed in the vicinity of the metal ion. As a result, it was found that the M-O distance for hydroxide complex is larger than that of carbonate in the case of larger cation and vice versa. This means that hydroxide prefers to form outer-sphere complex for larger metal ion, which is not the case of other intermediate hard ligands. This result is consistent with what we suggested based on the thermodynamic data.

Keywords: Speciation, Entropy, Complexation, Hydrolysis, Quantum chemical calculation

## Consistency between fission-track and U-Pb ages of zircon and its implications

IWANO, Hideki<sup>1\*</sup>; DANHARA, Tohru<sup>1</sup>

<sup>1</sup>Kyoto Fission-Track Co.

Following the recommendation by the Fission Track Working Group of the IUGS Subcommittee on Geochronology (Hurford, 1990), the fission-track method was transformed into a simplified and user-friendly dating tool. Standardization based on the common use of international age standards is what is called the zeta calibration. However, the adoption of the standardization scheme in which fission-track ages are determined against reference ages (K-Ar, Ar/Ar, Rb-Sr), and not based on physical parameters directly associated with the fission process, meant that the fission-track method lost its status as an independent geochronometer. Over the last two decades, we have investigated the problems of the absolute calibration approach, and we have finally demonstrated that it works well for zircon when using the external detector method (Danhara and Iwano, 2013). One of our conclusions is that the fission-track age for the Fish Canyon Tuff is 28.4+/-0.2 Ma. This is concordant with the recent zircon U-Pb ages (Schmitz and Bowring, 2001; Bachmann et al., 2007) and slightly older than the sanidine Ar/Ar age of 27.8+/-0.2 Ma, which is the reference age for the zeta calibration. We will discuss the consistency between fission-track and U-Pb ages of zircon from volcanic samples and give some comments on fission-track age standardization.

Bachmann et al. (2007) *Chemical Geology* 236, 134-166.

Danhara and Iwano (2013) *Island Arc*, 22, 264-279.

Hurford (1990) *Chemical Geology*, 80, 171-178.

Schmitz and Bowring (2001) *Geochimica et Cosmochimica Acta* 65, 2571-2587.

Keywords: zircon, fission-track age, U-Pb age, calibration

## Fe isotope measurement of taenite using LA-MC-ICPMS technique with Galvano scanner system

OKABAYASHI, Satoki<sup>1\*</sup> ; HIRATA, Takafumi<sup>1</sup>

<sup>1</sup>Division of Earth and Planetary Sciences, Kyoto University

The laser ablation-multicollector-inductively coupled plasma mass spectrometry (LA-MC-ICPMS) is widely accepted as the powerful technique to reveal the isotope ratios of solid sample. This technique can achieve the in-situ analysis of micro region with swiftness. On the other hand, it is difficult to avoid the mass spectrometric and non-mass spectrometric interferences from coexistent elements in this technique because the produced sample particles by laser ablation are directly introduced into the ICP with carrier gas. Such interferences have a potential to intercept to reveal the precise and accurate isotope data. The effect on the isotope ratios of analyte from coexistent elements can be corrected by using the standard material which include same amount of coexistent elements as the sample. However, synthesis of isotopic homogeneous solid material is extremely difficult.

In this study, we have developed a technique to measure the Fe isotope ratios of taenite in iron meteorites. The Fe isotope signature of iron meteorites is one of the key information to understand the core formation of planetesimals and terrestrial planets. However, the in-situ Fe isotope measurement of taenite is difficult because of the abundant Ni (>25 wt%) in it. In order to overcome this problem, we have applied Galvano mirrors and a telecentric optical system (Yokoyama et al., 2011) for LA-MC-ICPMS technique. In this technique, pure iron (IRMM-014) and pure Ni were ablated at a time using femtosecond laser with Galvano system as the Fe isotope standard. The ablated Ni amount was adjusted to the Ni amount in the taenite sample. The Fe isotope ratios ( $^{56}\text{Fe}/^{54}\text{Fe}$  and  $^{57}\text{Fe}/^{54}\text{Fe}$ ) of taenite phases were measured using MC-ICPMS and the mass fractionation in the mass spectrometry was corrected by sample-standard bracketing technique. The precision and accuracy of Fe isotope data obtained by the presented technique will be discussed in this presentation. The isotope analytical technique developed in this study can be applied not only for taenite phase in iron meteorite but also for other sample which include coexistent elements.

Keywords: ICP-MS, laser ablation, taenite, Fe isotope, Galvano

## High-Pressure Neutron Beamline PLANET for investigating "Water" in the Earth

HATTORI, Takanori<sup>1\*</sup> ; SANO, Asami<sup>1</sup> ; ARIMA, Hiroshi<sup>2</sup> ; INOUE, Toru<sup>3</sup> ; KAGI, Hiroyuki<sup>4</sup> ; YAGI, Takehiko<sup>3</sup>

<sup>1</sup>Japan Atomic Energy Agency, <sup>2</sup>Institute for materials research, Tohoku university, <sup>3</sup>Geodynamics Research Center, Ehime University, <sup>4</sup>Geochemical Laboratory, Graduate School of Science, University of Tokyo

The PLANET is the world's first neutron beamline specialized for high-pressure and high-temperature experiments. The most characteristic feature is the capability to investigate the state of water and hydrogen in minerals at high-pressure and high-temperatures up to 20GPa and 2000K with the multi-anvil high-pressure apparatus. The construction was started in 2008 and the experiments have been conducted since Nov. 2012. In this talk, the design and performance of the PLANET are introduced.

PLANET is designed so as to investigate structures not only of crystalline but also of amorphous (liquid) materials. The resolution of the diffraction pattern ( $\Delta d/d=0.6\%$ ) was found to be almost equal to the designed value(0.5%). The elimination of the background from the sample surrounding materials, which is the most important issue in the high-pressure experiments, was found to be accomplished by using the severe incident and receiving collimators. With this development, PLANET offers very clear patterns even at high pressures. This character made the PLANET one of the most innovative beamlines among several high-pressure neutron beamlines in the world.

Keywords: neutron, high pressure, beamline, hydrous



## High-pressure neutron beamline at J-PARC and applications to earth and planetary sciences

KAGI, Hiroyuki<sup>1\*</sup>; IIZUKA, Riko<sup>2</sup>; KOMATSU, Kazuki<sup>1</sup>; YAGI, Takehiko<sup>2</sup>; NAGAI, Takaya<sup>3</sup>; INOUE, Toru<sup>2</sup>; SANNO, Asami<sup>4</sup>; HATTORI, Takanori<sup>4</sup>

<sup>1</sup>Graduate School of Science, University of Tokyo, <sup>2</sup>Geodynamic Research Center, Ehime University, <sup>3</sup>Graduate School of Science, Hokkaido University, <sup>4</sup>Japan Atomic Energy Agency

Construction of the high-pressure dedicated beamline, PLANET, in Japan Proton Accelerator Research Complex (J-PARC) has been completed in 2012 and scientific programs for general users have just started in 2014. The PLANET beamline has a focusing mirror for incident neutron and two 90-degree detector banks. Each bank has 160 pieces of Position Sensitive Detectors (PSDs) filled with <sup>3</sup>He gas. Each bank has a detector coverage of  $90 \pm 11$  degree against the incident beam in the horizontal direction and  $0 \pm 35$  degree in the vertical direction. Radial collimators are attached in front of the detector banks to reduce the background. The instrumental resolution is 0.6% in  $\Delta d/d$ . The accessible d-spacing is normally 0.2-4.2 Å and is doubled in a double-frame setup. The power of the proton beam is around 300 kW and will be increased to 600 kW in 2014. The most characteristic feature of the PLANET beamline is the multi-anvil apparatus with six independently acting 500-tonne rams (6-axis press called ATSUHIME). Using ATSUHIME, we successfully observed neutron diffraction patterns of hydrous minerals at high pressure and high temperature without any contamination from sample-surrounding materials such as pressure transmitting media, anvils, and so on. This clearly shows that the incident slit and radial collimator installed in the beamline are very effective to obtain the diffractions under high pressure.

We focus on pressure-responses on the structure of materials with hydrogen-bonding networks through neutron diffraction measurements at high pressure. These results will contribute to fundamental understanding of hydrous materials in the deep earth and icy material in the planets.

Keywords: neutron, neutron diffraction, hydrogen, water, high pressure, ices

## Geo-neutrinos for advanced earth studies

TANAKA, Hiroyuki<sup>1\*</sup>

<sup>1</sup>Earthquake Research Institute, The University of Tokyo

Neutrinos generated in Earth (geo-neutrinos) gives us information about the distribution of Uranium (U), thorium (Th), and potassium (K) inside Earth. Beta-decays of radionuclides U/Th/K inside Earth produce low energy anti-electron neutrinos (U and Th produces  $7.41 \times 10^7$  neutrinos  $\text{kg}^{-1}\text{s}^{-1}$  and  $1.62 \times 10^7$  neutrinos  $\text{kg}^{-1}\text{s}^{-1}$  respectively (without considering neutrino oscillation)) that traverse through Earth without being disturbed due to their extremely small interaction cross section with matter. Recent geo-neutrino observations have produced results that have a potential to support and clarify the current concerns of earth science: estimating the amount of contribution to the surface heat flux; constraining existing Earth's compositional estimates; and clarifying the origin of low shear velocity regions found at the core mantle boundary (CMB). Today, there are two detectors capable of measuring geoneutrinos: KamLAND, in Japan, and Borexino, in Italy. The KamLAND research team has found  $116 \pm 28$ , 27 geoneutrino candidate events (generated through the decay processes of  $^{238}\text{U}$  and  $^{232}\text{Th}$ ) during 2,991 days of geoneutrino observation (Gando et al. 2013). The contribution from geonuclear reactions to the heat flow, estimated from examination of the geoneutrino flux, reached  $11.2 \pm 7.9$ , 5.1 TW. Although the volume of the Borexino detector (280 t) is much smaller than that of KamLAND (1,000 t), the background from reactor neutrinos is much lower than that for KamLAND because there are no nuclear power plants in Italy. Borexino detected  $14.3 \pm 4.4$  geoneutrino candidates over 1353 days of observation. Both measurement results are consistent each other, and also reject the fully radiogenic model, which assumes that the total Earth's surface heat flux is completely originated from radiogenic heat from U, Th and K. The upper limit on the fully radiogenic heat flux hypothesis (Herndon 1996) was set to be 4.5 TW at 95% confidence level (Bellini et al. 2013).

Gando A, Gando Y, Hanakago H, Ikeda H, Inoue K, et al. 2013. Reactor on-off antineutrino measurement with KamLAND. *Phys. Rev. D* 88:033001.

Herndon JM. 1996. Substructure of the inner core of the Earth. *Proc. Natl. Acad. Sci. USA* 93:646-48.

Bellini, G., Ianni, A., Ludhova, L., Mantovani, F., McDonough, W.F. 2013. Geo-neutrinos, *Prog.Part.Nucl.Phys.* 73:1-34

Keywords: Neutrino, Uranium, Thorium, Mantle



## Multi-range imaging mass spectrometry using laser ablation-ICP-mass spectrometry

HIRATA, Takafumi<sup>1\*</sup> ; HATTORI, Kentaro<sup>1</sup> ; OHARA, Seiya<sup>1</sup>

<sup>1</sup>School of Science, Kyoto University

Time-resolved elemental and isotopic data can provide key information about the time changes of the geochemical conditions of the surface environment of the Earth, and therefore, critical restriction for the origin or evolutionary sequence of the surface environment of the Earth and the life could be derived. To obtain reliable and exclusive information from the samples, tremendous efforts have been given to develop various analytical techniques, which could provide both the higher elemental sensitivity and higher analytical throughput. Among the analytical techniques, plasma ion source mass spectrometer coupled with the laser ablation sample introduction technique (LA-ICPMS) has now become the most sensitive and user-friendly analytical tool to derive elemental and isotopic distribution among the different phases or minerals. Moreover, in the LA-ICPMS technique, atomization and ionization of the analytes were independently carried out from the sampling (i.e., post ionization technique), and therefore, the sampling and ionization conditions could be separately optimized. The post ionization technique results in the smaller contribution of the matrix effect, which could be the major source of analytical error. Furthermore, for the LA-ICPMS technique, sample was located under the atmospheric pressure sample cell, and laser induced sample aerosols were carried into the ICP ion source using a He carrier gas. This suggests that no evacuation of the sample housing is required, and therefore, biological cell or tissue samples (i.e., wet samples) can be directly subsidized to elemental imaging analysis, obviating the drying or freezing procedure for the analysis. The LA-ICPMS technique has further advantages of imaging analysis for samples with various sizes, ranging from 10 microns to >10 mm. Because of high capability for quantitative imaging of ultratrace-elements, together with high analytical capability to measure large-sized samples, the LA-ICPMS technique has blossomed to become the key analytical technique for the imaging analysis of trace-elementals and isotopes. This is very important to obtain elemental and isotopic images for not only biological samples, but also various rock or minerals. In fact, imaging data for whole rock pierces or minerals can tell us the substantial process for the elemental distribution or diffusion among the samples. We should recall that we could not see the forest for the trees. Despite the obvious success in obtaining the elemental and isotopic imaging data, neither quantitative evaluation of the detection limits for the elements nor the dependence of the analytical conditions (e.g., laser pit size, raster rate, system setup or condition for data acquisition) onto the resulting spatial resolution were made. To investigate these, we have measured imaging analyses of several trace- and ultratrace-elements from meteorite samples and biochemical samples under the various analytical conditions. In this presentation, we will described the effect of the system setup and operational settings onto the resulting spatial resolution and onto the limit of detection for the elements.

Keywords: laser ablation, ICP-mass spectrometry, imaging mass spectrometry, multi-scale imaging, trace-elements, quantitative imaging

## Cavity ring-down spectroscopy for the isotope ratio measurements of water from fluid inclusions in stalagmites

UEMURA, Ryu<sup>1\*</sup> ; NAKAMOTO, Masashi<sup>1</sup> ; GIBO, Masakazu<sup>1</sup> ; MISHIMA, Satoru<sup>1</sup> ; ASAMI, Ryuji<sup>2</sup>

<sup>1</sup>University of the Ryukyus, <sup>2</sup>University of the Ryukyus

Oxygen isotope record in stalagmites is useful to reconstruct past environmental changes. However, the interpretation of calcite isotope record is not straightforward because it is affected by various factors affect such as amount of precipitation and temperature. Water isotope composition of fluid inclusions, and oxygen isotope difference between water and host calcite, from stalagmite are potentially important proxies to estimate the paleo-temperature. Recently, infrared spectroscopy (IRIS) has been widely used for stable isotope ratio measurement of water. Unlike traditional isotope mass spectrometer (IRMS), the IRIS does not require pre-treatment processes (e.g., high-temperature furnace or equilibration device). A limitation of IRIS is that commercially available IRIS systems need large sample volume (1 - 2 micro litres) for liquid water measurement. In this study, we developed a custom-designed device suitable for precise measurement of smaller volume (0.05 to 0.20 microlitres) of water, and tested two extraction methods (thermal extraction and mechanical crushing). Oxygen and hydrogen isotope ratios of water were measured using cavity ring down spectroscopy (WS-CRDS Picarro L2130-i). Stalagmites samples were collected in several caves in Okinawa, Japan. Pieces of stalagmites (80-300mg) subsampled from homogeneous layers, and reproducibilities of the inclusion measurement were 0.2 permil for  $\delta^{18}\text{O}$  and 1 permil for  $\delta\text{D}$ . The measured  $\delta^{18}\text{O}$  and  $\delta\text{D}$  of inclusion water from recently grown stalagmites agrees with modern dripwaters, indicating that our extraction technique is useful to measure isotope ratios of past inclusion water.

Keywords: Stable isotope, Fluid inclusion, Speleothem, Stalagmite, Paleoclimate, CRDS

## Coral growth-rate insensitive Sr/Ca as a robust temperature recorder at the extreme latitudinal limits of Porites

HIRABAYASHI, Shoko<sup>1\*</sup> ; YOKOYAMA, Yusuke<sup>1</sup> ; SUZUKI, Atsushi<sup>2</sup> ; KAWAKUBO, Yuta<sup>1</sup> ; MIYAIRI, Yosuke<sup>1</sup> ; OKAI, Takashi<sup>2</sup> ; NOJIMA, Satoshi<sup>3</sup>

<sup>1</sup>Atmosphere and Ocean Research Institute, The University of Tokyo, <sup>2</sup>National Institute of Advanced Industrial Science and Technology, <sup>3</sup>Amakusa Marine Biological Laboratory, Kyushu University

Corals are rich archives of climatic changes with high-resolution record of seasonal change such as sea-surface temperature (SST), in tropical and sub-tropical seas during recent and distant past. Past SST are commonly reconstructed from the trace elementals present in annually-banded coral skeletons. Recently, reef building corals were found in temperate regions due to coral habitat range shifts and/or expansions. Therefore, it could be a powerful tool for reconstructing climatic changes such as global warming and ocean acidification over long period. However, because of the more stressful environment for corals in temperate region than tropic or subtropics, we have to know how to reconstruct palaeo-SST using temperate corals.

This paper was reported Sr/Ca-based SST reconstructions for temperate Porites corals collected from Kyushu, Japan, near the northern latitudinal extent of hermatypic corals. New, high-resolution Sr/Ca data, measured along the growth axes of Porites from Ushibuka, were compared to previously published  $\delta^{18}\text{O}$  data from the same specimens (Omata et al., 2006). Results indicate that Sr/Ca variations in a low-growth coral remain independent from growth rate, in contrast to the oxygen isotope ratios of the same coral. Results clearly indicate that Sr/Ca robustly reproduces SST variations from regions along the extreme latitudinal limits of hermatypic coral habitat, independent of growth rate variations.

Additionally, Sr/Ca of the other two Porites corals collected in Ushibuka were measured and the inter-colony variation of reconstructed SST was shown. At this stage, it is difficult to reconstruct accurate SST using only one specimen of Porites in temperate region. However, we can reconstruct SST within only 1 °C difference from observed SST if we calibrate Sr/Ca-SST using more than two corals. It is expected that in the future the fossil temperate corals will be commonly used for palaeo-SST reconstruction.

## Maximizing organic records: Recent achievements and future directions

OHKOUCHI, Naohiko<sup>1\*</sup> ; CHIKARAISHI, Yoshito<sup>1</sup> ; TAKANO, Yoshinori<sup>1</sup> ; OGAWA, Nanako<sup>1</sup>

<sup>1</sup>JAMSTEC

Molecular isotopic record in either organisms or sediments has been proven useful for better understanding the bio(geo)chemical processes, reconstructing paleo-environment, etc. During the last decades, target molecules have been expanding from simple lipids to complex physiologically active compounds. There are two key issues to push this molecular tool more useful and more efficient: 1) Purity of the target compounds that are extracted from environmental samples (generally a complex mixture of organic compounds), and 2) sensitivity of isotope-ratio mass spectrometry (IRMS) system for precisely measuring isotopic compositions. In this presentation we will overview the recent advances in these two issues, and how these achievements contributed to the progresses in our knowledge. We also try to mention in the future challenges of molecular isotopic signatures.

Keywords: Organic molecule, isotopic composition, nitrogen, carbon

## Precise and sensitive determination of stable isotopic compositions of amino acids

CHIKARAISHI, Yoshito<sup>1\*</sup> ; TAKANO, Yoshinori<sup>1</sup> ; OHKOUCHI, Naohiko<sup>1</sup>

<sup>1</sup>Japan Agency for Marine-Earth Science and Technology

Amino acids are biologically central and functional organic compounds. Their molecular and stable isotope profiles have been employed as a tool in various fields of studies, particularly for understanding of the trophic energy flow of food web ecology as well as for estimating the origin of amino acid procurers in extraterrestrial samples (e.g., meteorites). One of the most powerful techniques in the stable isotope studies of amino acids is compound-specific isotope analysis (CSIA) by gas chromatography/isotope ratio mass spectrometry (GC/IRMS), which potentially allows a rapid and precise determination of H, C, N, O, and S isotopic compositions of individual amino acids in complex mixture of samples. However, (1) isotopic fractionation and exchange during pretreatment (e.g., hydrolysis, extraction, purification, and derivatization) of samples, (2) chromatographic separation among individual amino acids, and (3) less sensitivity on GC/C/IRMS (i.e., 10-50 nmol of elements is required) are always problematic in CSIA of amino acids.

In the presentation, we will briefly review these issues on CSIA of amino acids, and show current advances in the precise and sensitive determination of C and N isotopic compositions of amino acids (i.e., within 0.4-0.8 permil for a minimum sample amount of 0.5 nmol element), based on the minimizing isotopic fractionation during HPLC purification and derivatization as well as reducing leak and background variation in GC/IRMS instrument. With this method, we can access C and N isotopic signature of wide range of samples including amino acids in bacteria and archea isolated from natural environments as well as amino acid procurers in meteorites.

Keywords: stable isotope, amino acids, food web, meteorite

## On the role of amino acid metabolism and a biogeochemical linkage

TAKANO, Yoshinori<sup>1\*</sup> ; CHIKARAISHI, Yoshito<sup>1</sup> ; OHKOUCHI, Naohiko<sup>1</sup>

<sup>1</sup>JAMSTEC

Deep-sea sediments harbor a novel and vast biosphere with yet unconstrained importance in the global biogeochemical cycle. To explore these habitats is interdisciplinary challenges for the biogeochemical and geomicrobiological scientific community. The limits of deep biosphere are on-going subject, which were not yet known in terms of environmental properties, including depth, temperature, energy availability, and geologic age; however, it is known that seafloor microbes play a significant role in chemical reactions that were previously thought to have been abiotic.

Since the novel classification by Woese and Fox (1977), Archaea, one of three domains of life, had been originally believed to exist in extreme environments including high temperature, high salinity, low oxygen concentration. However, recent advances in molecular and phylogenetic approaches revealed their widespread distribution in marine and terrestrial environment including deep subsurface biosphere. The planktonic and benthic archaeal assemblages include two major phyla Euryarchaeota and Crenarchaeota. The novel phylum have been also proposed recently as Thaumarchaeota, Korarchaeota, and Nanoarchaeota.

In the present study, we reviewed the recent knowledge of prokaryotic ecology and biogeochemistry from molecular-specific isotopic signatures. Among these, we focused on the role of amino acid metabolism and a biogeochemical linkage mediated by deep-sea benthic archaea.

### [ References ]

Ohkouchi, N. and Takano, Y. Organic nitrogen: sources, fates, and chemistry. *Treatise on Geochemistry*, 10: Organic Geochemistry (Edited by Birrer, B., Falkowski, P., Freeman, K.), Vol. 12, Elsevier, pp. 251-289 (2014).

Takano et al., Detection of coenzyme F430 in deep-sea sediments: A key molecule for biological methanogenesis. *Organic Geochemistry*, 58, 137-140 (2013).

Chikaraishi et al., Determination of aquatic food-web structure based on compound-specific nitrogen isotopic composition of amino acids. *Limnology and Oceanography: Method*, 7, 740-750 (2010).

Keywords: amino acid metabolism, deep-sea benthic archaea, a biogeochemical linkage

## Simple method for separation of boron from volcanic rocks for isotopic analysis by MC-ICP-MS

SHINJO, Ryuichi<sup>1\*</sup> ; HAMADA, Yukinori<sup>1</sup>

<sup>1</sup>Univ. Ryukyus

We developed a simple and thus effective method of separation of boron from volcanic rocks.

It has been suggested that easy volatilization of boron and isotopic fractionation during evaporation step after HF decomposition of silicate rock samples; therefore procedure of evaporation at low-temperature (<80C) with mannitol (which suppress volatilization) under boron-free specific experiment environment has been utilized.

Our new method dose not require evaporation step, thus effectively preventing boron volatilization and related fractionation. Contamination opportunity can also be reduced. In our method, supernatant HF solution at sample digestion step is loaded onto mini-column cartridge of Amberlite IRA 743 (0.25mL) with no evaporation step. Recovery yield for silicate rocks was generally >80%. To evaluate our method, the GSJ rock standards (JB-2, JB-3 and JR-2) were analyzed by following the proposed method. Measured boron isotopic compositions for these rocks were in good agreement with preferred values.

## Development on submicron-scale U-Pb dating by Laser post-ionized SNMS

TERADA, Kentaro<sup>1\*</sup> ; NAKABAYASHI, Makoto<sup>1</sup> ; KAMIOKA, Moe<sup>1</sup> ; TOYODA, Michisato<sup>1</sup> ; ISHIHARA, Morio<sup>1</sup> ; NAKAMURA, Ryosuke<sup>2</sup> ; AOKI, Jun<sup>1</sup> ; HINO, Yuta<sup>1</sup>

<sup>1</sup>Graduate School of Science, Osaka University, <sup>2</sup>Office for University-Industry Collaboration, Osaka University

In order to decipher the history of the Solar System, in-situ U-Pb dating method using SIMS (Secondary Ion Mass Spectrometry) has been used over 40 years, of which spatial resolution is 2-10 micron. In general, the secondary ion yield of SIMS is so low (less than 1 %) that it has been the weak point of this in-situ analysis. Here, we report the performance of Pb isotope measurement using the Laser SNMS that consist of of Ga-ion source for primary beam, femto-second laser for post-ionization, and the multi-turn TOF-SIMS for mass spectroscopy (Ishihara et al. 2010).

Keywords: U-Pb dating, mass spectrometry, in-situ analysis, isotope analysis



## Inhibition effect of natural organic matter on adsorption of radiocesium onto particulate matters in Pripyat River

SUGA, Hiroki<sup>1\*</sup>; FAN, Qiaohui<sup>1</sup>; TAKEICHI, Yasuo<sup>2</sup>; TANAKA, Kazuya<sup>3</sup>; KONDO, Hiroaki<sup>1</sup>; KANIVETS, Vladimir<sup>v4</sup>; SAKAGUCHI, Aya<sup>1</sup>; INAMI, Nobuhito<sup>2</sup>; ONO, Kanta<sup>2</sup>; TAKAHASHI, Yoshio<sup>1</sup>

<sup>1</sup>Department of Earth and planetary system science, Hiroshima University, <sup>2</sup>Institute of Materials Structure Science, High-Energy Accelerator Research Organization (KEK), <sup>3</sup>Institute for Sustainable Science and Development, Hiroshima University, <sup>4</sup>Ukrainian Hydrometeorological Institute

Radiocesium have been emitted to environment originated from nuclear weapon tests and nuclear accidents such as in Chernobyl and Fukushima. Among various sources, the nuclear accidents in Chernobyl and Fukushima have caused serious contaminations in land-surface around these areas due to the deposition of the radionuclides dispersed via atmosphere as aerosols. Subsequently, radiocesium can be transported via rivers into oceans. In the soil- river-sediment system, radiocesium has high affinity for particulate matters, in particular for clay minerals. The high affinity has been shown to be the results of specific adsorption to frayed edge site (FES) and interlayer site in 2:1 phyllosilicate as inner-sphere (IS) complexes. However, it has been indicated that cesium adsorption to clay minerals can be blocked by natural organic matters (NOM) that adsorb on the mineral surface. NOM are ubiquitous and play various important roles on the adsorption of metal ions on particulate matters such as (i) promotion of adsorption of metal ions by the complexation with NOM and (ii) inhibition of adsorption by covering the particulate matters. High availability of Cs in soils with relatively high organic matter content was explained in terms of the blocking of access of cesium to specific adsorption sites (such as FES and interlayer site) of the clay mineral.

In river waters in Fukushima, it has been indicated that more than 70% of radiocesium is adsorbed on particulate matters. In contrast, Sansone et al. (1996) showed that more than 70% of radiocesium was in the dissolved fraction in Chernobyl. One critically important difference between the two sites is that peat, which contains large amount of NOM, is the main surface layer in the Chernobyl area. These NOM can be introduced into the Pripyat River that can coat on the particulate matters in river waters. Thus, it is possible that high content of NOM in rivers (e.g., Pripyat River) in Chernobyl can be responsible for the larger fraction of dissolved radiocesium compared with that in Fukushima due to the blocking effect by the NOM. In this study, therefore, adsorption of cesium on particulate matters collected in the Pripyat River with the characterization of the particulate matters have been conducted to study whether the blocking effect is affecting the adsorption behavior of cesium.

Here, we examined Cs LIII-edge extended x-ray absorption fine structure (EXAFS) to study the cesium species adsorbed on the particulate matters collected from Pripyat River and also on the particulate matters after the removal of NOM by the treatment with hydrogen peroxide. To characterize the particulate matter, distribution image of organic substances on the particulate matter was analyzed by compact Scanning Transmission X-ray Microscope (cSTXM) newly developed in Photon Factory, KEK in Tsukuba, Japan. After the cSTXM imaging, characterization of NOM was conducted by near edge X-ray absorption fine structure (NEXAFS) at the C K-edge measured for the NOM by cSTXM.

From this study, blocking effect of cesium adsorption to clay minerals by humic acid was confirmed in natural particulate matter in Pripyat River, which might be related to the larger dissolved fraction of radiocesium around Chernobyl area, compared with that in rivers in Fukushima area.

Keywords: chernobyl, natural organic carbon, STXM

## Development of the technique for determination of I-129 in fish samples as new tracer of marine ecosystem

KUSUNO, Haruka<sup>1\*</sup> ; MATSUZAKI, Hiroyuki<sup>1</sup> ; NAGATA, Toshi<sup>2</sup> ; MIYAIRI, Yosuke<sup>2</sup> ; YOKOYAMA, Yusuke<sup>2</sup> ; OHKOUCHI, Naohiko<sup>3</sup> ; TOKUYAMA, Hironori<sup>1</sup>

<sup>1</sup>School of Engineering, The University of Tokyo, <sup>2</sup>Atmosphere and Ocean Research Institute, The University of Tokyo, <sup>3</sup>Japan Agency for Marine-Earth Science and Technology

The availability of <sup>129</sup>I as a new tracer for marine ecosystem was examined.

The iodine isotopic ratio (<sup>129</sup>I/<sup>127</sup>I) in seawater is determined by the anthropogenic <sup>129</sup>I transferred from the atmosphere, i.e., it shows very high ratio as the order of 10<sup>-10</sup> for <sup>129</sup>I/<sup>127</sup>I at the surface or surface mixing layer and suddenly decreases going deeper to some of 10<sup>-12</sup> or lower. Iodine isotopic ratio (<sup>129</sup>I/<sup>127</sup>I) of marine lives like fish should be determined by their habitats and the ways exchanging iodine with seawater. This means that the iodine isotopic ratio is potential indicator of marine ecosystem. However there have been only few studies using <sup>129</sup>I for marine ecosystem. This is because <sup>129</sup>I is so trace in the marine lives that ordinary analytical techniques cannot detect.

Recent development of analytical technique for <sup>129</sup>I using AMS (Accelerator Mass Spectrometry) enables determine trace amount of <sup>129</sup>I concentration in environmental samples.

In this study the pyrohydrolysis method was applied to extract iodine from fish samples. A freeze-dried and homogenized fish sample, 0.1g to 0.5g, was combusted in the quartz tube under oxygen and water vapor flow. Iodine was extracted into an alkaline solution. An aliquot of this solution was taken for ICP-MS analysis to determine the stable iodine (<sup>127</sup>I) concentration. The remaining was, added with carrier iodine (about 1 mg), purified by solvent extraction and collected as AgI precipitation. <sup>129</sup>I/<sup>127</sup>I ratio was determined by AMS. From the AMS result and the <sup>127</sup>I concentration, the <sup>129</sup>I/<sup>127</sup>I ratio of the fish samples themselves can be calculated.

The extraction yield was evaluated using IAEA-414 fish standard sample. Background in the pyrohydrolysis was also examined.

The preliminary results of fish samples, collected from Suruga-bay (located on Pacific coast in the middle of Honshu, Japan) showed 1×10<sup>-10</sup> to 7×10<sup>-10</sup>, which was consistent with that of surface seawater.

Keywords: Iodine-129, tracer, marine ecosystem, fish, AMS

## Exploring the ecology of catfish through trace elements analyses of otolith by LA-HR-ICPMS to reconstruct palaeo-SST

AMEKAWA, Shota<sup>1\*</sup> ; YOKOYAMA, Yusuke<sup>1</sup> ; KUBOTA, Kaoru<sup>1</sup> ; SAKAI, Saburo<sup>2</sup>

<sup>1</sup>Atmosphere and Ocean Research Institute, The University of Tokyo, <sup>2</sup>Japan Agency for Marine-Earth Science and Technology

Otoliths are incrementally precipitated aragonite biominerals found within the inner ear of all teleost fish. Previous studies show that oxygen isotopes ( $\delta^{18}\text{O}$ ) of otolith aragonite precipitate in equilibrium with those of seawater regarding ambient water temperature (Campana, 1999). Therefore, ( $\delta^{18}\text{O}$ ) of otolith can be used as a strong thermometer for reconstructing the past environment. In the meantime, fish habitats are necessary to be revealed before understanding the palaeoenvironments using otolith due to its nature as biomineral associated with fish. Thus we applied trace element measurements in the specimens to identify the habitable zones namely marine, brackish and freshwater. Strontium abundance in carbonate samples (Sr/Ca) is the best indicator to be employed because of distinct differences in concentration in marine and riverine waters (Walther and Thorrold, 2006). The present study is therefore aiming for identifying the past fish ecology using Sr/Ca in otoliths measured by newly developed laser ablation (ArF excimer) high resolution inductively coupled plasma mass spectrometry (LA-HR-ICPMS). The study area is the Gulf of Kutch in Gujarat district, northwestern part of India. This area is strongly influenced by Indian monsoon, which is characterized as distinct seasonal rainfall (humid summer and dry winter). Salinity distribution within the Gulf of Kutch is unusual compared with general river-estuary system. Lower salinity ( $\sim 37$ ) is observed in the inner part, whereas higher values ( $>40$ ) are observed near the mouth (Vethamony et al., 2007). In this study, we analyze both modern and fossil otoliths. Fossil otoliths were excavated from archaeological sites of Harappan Civilization located in Bagasra and Datrana. According to otolith morphology, they probably the otoliths of Siluriformes Ariidae catfish, known as marine catfish. Trace element concentrations relative to Ca ( $^{23}\text{Na}$ ,  $^{25}\text{Mg}$ ,  $^{55}\text{Mn}$ ,  $^{88}\text{Sr}$  and  $^{137}\text{Ba}$  /  $^{43}\text{Ca}$ ) were measured along with growth bands of otoliths. They are measured using LA-HR-ICPMS. The system is consisted with Thermo Finnigan Element XR high resolution inductively coupled plasma mass spectrometer coupled to Resonetics 193 nm excimer laser ablation system installed at Atmosphere and Ocean Research Institute. Nine modern and 16 fossil otoliths thin sections were prepared and 6 modern and 4 fossil sections were analyzed using LA-HR-ICPMS. Abrupt changes in Sr/Ca with an amplitude of as much as 3 mmol/mol within  $\sim 2$  weeks suggest fish migration between freshwater and the seawater. From a conservative mixing model for Sr/Ca of estuarine water, the fish has migrated to riverine environment sometimes in their life since the model predicts small changes in Sr/Ca of water if salinity is higher than  $\sim 5$  unit. It is rather changes in Sr concentrations in ambient water than that for water temperature or salinity in the gulf.

Keywords: otolith, trace element, oxygen isotope, LA-HR-ICPMS, Gulf of Kutch

## Improved $^{10}\text{Be}$ preparation to reduce analytical background for earth surface process studies

YAMANE, Masako<sup>1\*</sup> ; YOKOYAMA, Yusuke<sup>2</sup> ; MIYAIRI, Yosuke<sup>2</sup> ; HORIUCHI, Kazuho<sup>3</sup> ; MATSUZAKI, Hiroyuki<sup>4</sup>

<sup>1</sup>JAMSTEC, <sup>2</sup>AORI, Univ. Tokyo, <sup>3</sup>Hirosaki Univ., <sup>4</sup>Grad. Sch. Eng., Univ. Tokyo

Due to advancement of Accelerator Mass Spectrometry (AMS), *in situ* produced beryllium-10 ( $^{10}\text{Be}$ ) in quartz has been used for earth surface process studies, such as surface exposure dating (*e.g.* Yamane *et al.*, 2011), erosion rate estimations (*e.g.* Shiroya *et al.*, 2012), tectonic processes (Yokoyama *et al.*, 2005) and so forth (*e.g.* Gosse and Phillips, 2001). In order to expand the applicability of this technique, the sample with low  $^{10}\text{Be}$  concentration need to be measured with high precision. This requires reduction of background that is often affected isobars (boron-10). We have conducted several attempts and found that the length of time exposed to the ambient atmosphere during the oxidization process is the most important step to increase  $^{10}\text{Be}$  background (Yokoyama *et al.*, submitted). In this presentation, we discussed our experimental results and potential improvement of topics for understanding of earth surface process.

Keywords: beryllium-10, background, earth surface process, Accelerator Mass Spectrometry

## Radiocarbon pretreatment system of AORI AMS

MIYAIRI, Yosuke<sup>1\*</sup> ; YOKOYAMA, Yusuke<sup>1</sup> ; YAMANE, Masako<sup>2</sup> ; HIRABAYASHI, Shoko<sup>1</sup>

<sup>1</sup>Atmosphere and Ocean Research Institute, University of Tokyo, <sup>2</sup>Japan Agency for Marine-Earth Science and Technology

The Accelerator Mass Spectrometry(AMS)is effective in radiocarbon dating. By the conventional method, a large tandem accelerator(e.g.Accelerating voltage = 5MV) was used. However, the small accelerator(e.g.Accelerating voltage = 500kV) is used in the new AMS analysis.

The small AMS machine is handy.We installed small AMS machine in our laboratory. We will present the outline of new AMS pretreatment system and the geochemical application research using that.

Keywords: Radiocarbon, AMS, Accelerator Mass Spectrometry, 14C

## Multi-site infrasound observation around Syowa station, Antarctica

KAKINAMI, Yoshihiro<sup>1\*</sup>; OKADA, Kazumi<sup>6</sup>; YAMAMOTO, Masa-yuki<sup>1</sup>; KANAO, Masaki<sup>2</sup>; MURAYAMA, Takahiko<sup>3</sup>; MATSUSHIMA, Takeshi<sup>4</sup>; ISHIHARA, Yoshiaki<sup>5</sup>

<sup>1</sup>Kochi University of Technology, <sup>2</sup>National Institute of Polar Research, <sup>3</sup>Japan Weather Association, <sup>4</sup>Institute of Seismology and Volcanology, Faculty of Sciences, Kyushu University, <sup>5</sup>JAXA Space Exploration Center, Japan Aerospace Exploration Agency, <sup>6</sup>Institute of Seismology and Volcanology, Faculty of Science, Hokkaido University

Infrasound is one of the frontier fields in geophysics to observe atmospheric events. World wide infrasound observing network has been constructed as the CTBTO (Comprehensive Nuclear-Test-Ban Treaty Organization) to detect infrasound signal from huge artificial explosions, however, the CTBTO infrasound observing stations usually catch the natural infrasonic waves generated by many geophysical events, like volcanic eruptions, earthquakes, tsunamis, etc. For example, when a huge meteorite fall was observed near Chelyabinsk, Russia in 2012, the induced infrasonic waves reached to many distant CTBTO stations more than 10,000 km apart from. In the polar region, there exists local infrasound sources generated mainly by the ice sheets on ground, ice field, and glacier motions. Icequakes have been frequently monitored by seismic stations in polar region, however, monitoring of induced atmospheric infrasonic waves through lithosphere-atmosphere coupling is still in progress. We installed an infrasound sensor at Syowa station, Antarctica in 2008 during IPY (International Polar Year) period by JARE (Japanese Antarctic Research Expedition) 49 mission. However, the direction-finding of the infrasonic waves is significant to study the comparison between the seismic data, thus, 2 sensors were added on Syowa to make a triangle sensor array in 2013 by JARE 54. In addition, 5 more sensors were installed at 5 locations around Syowa in 2013 (Murayama et al., 2013).

The infrasound data observed at Syowa can be transferred to Japan via satellite connection, however, the data recorded by data logger at the stations near Syowa cannot be obtained without visiting there. In JARE 55 mission, we obtained one-year infrasound observation data recorded at several stations around Syowa and will return them back to Japan in March 2014. In this paper, we will introduce some preliminary results obtained in Antarctica as the first multi-site infrasound observation at the frozen continent.

Keywords: ifrasound, Antarctica, multi-site observation, JARE, ice quake

## Characteristic features of infrasound waves observed at Antarctica

KANAO, Masaki<sup>1\*</sup> ; MURAYAMA, Takahiko<sup>2</sup> ; YAMAMOTO, Masa-yuki<sup>3</sup> ; ISHIHARA, Yoshiaki<sup>4</sup> ; KAKINAMI, Yoshihiro<sup>3</sup> ; OKADA, Kazumi<sup>5</sup> ; MATSUSHIMA, Takeshi<sup>6</sup>

<sup>1</sup>National Institute of Polar Research, <sup>2</sup>Japan Weather Association, <sup>3</sup>Kochi University of Technology, <sup>4</sup>Japan Aerospace Exploration Agency, <sup>5</sup>Hokkaido University, <sup>6</sup>Kyushu University

Characteristic features of infrasound waves observed at Antarctica reveal the physical interaction involving surface environmental variations in the continent and surrounding Southern Oceans. A single infrasound sensor has been continuously recorded since 2008 at Syowa Station (SYO; 39E, 69S), the Lutzow-Holm Bay (LHB), East Antarctica. The continuously recording data clearly represent a contamination of the background oceanic signals (microbaroms) during whole seasons. In austral summer in 2013, several field stations by infrasound sensors are established along the coast of the LHB. Two infrasound arrays with different diameter size are installed at both SYO (by 100 m spacing triangle) and S16 area on continental ice sheet (by 1000 m spacing triangle). Besides these arrays, two isolated single stations are deployed at two outcrops in LHB. These newly established arrays clearly detected the propagating directions and frequency contents of the microbaroms from Southern Ocean. Microbaroms measurements are a useful tool for characterizing ocean wave climate, complementing other oceanographic and geophysical data in the Antarctic. Moreover, several kind of remarkable infrasound signals are demonstrated, such as regional earthquakes, together with a detection of the airburst shock waves generated from meteorite injection at the Russian Republic on 15 February 2013. Detail and continuous measurements of the infrasound waves in Antarctica could be a new proxy for monitoring a regional environmental change as well as temporal climate variations in high southern latitude.

Keywords: infrasound, array observations, Lutzow-Holm Bay, East Antarctica, microbaroms, surface environment

## Monitoring snow avalanches by using infrasound with an object of establishing remote detection system of snow avalanches

ARAI, Nobuo<sup>1</sup> ; MURAYAMA, Takahiko<sup>1\*</sup> ; IWAKUNI, Makiko<sup>1</sup> ; TANIMOTO, Saki<sup>2</sup> ; TAKAHASHI, Daisuke<sup>2</sup> ; KURIHARA, Yasushi<sup>2</sup> ; ARAKI, Keiji<sup>2</sup> ; YAMAMOTO, Masa-yuki<sup>3</sup>

<sup>1</sup>Japan Weather Association, <sup>2</sup>Railway Technical Research, <sup>3</sup>Kochi University of Technology

It has been demonstrated that avalanches produce strong infrasonic vibrations in air during their movement (Bedard, 1988<sup>[1]</sup>, Hejda, 1995<sup>[2]</sup>). These infrasonic vibrations propagate great distances and can follow the natural relief. This fact shows that it is possible to monitor remotely the snow avalanche by using infrasound detection system.

We aim to establishing remote detection system of snow avalanches. In order to study the feature of the signal associated with snow avalanches, as a first step, we carried out trial infrasound observation simultaneously with the video monitoring and the meteorological observation at mountainous region in Niigata Prefecture from January to April 2013. During the trial observation, some infrasound signals generated by snow avalanches were recorded. We analyzed these data and attempted to extract features from infrasound signals.

### [References]

[1] Bedard, A. J. et al. 1988. On the feasibility and value of detecting and characterizing avalanches remotely by monitoring radiated sub-audible atmospheric sound at long distances. Proc. A Multidisciplinary Approach to Snow Engineering, Santa Barbara, CA.

[2] Hejda, D. 1995. Caracterisation de l'emission acoustique des avalanches, (These de diplome, E. P. F. Lausanne, Suisse.)

Keywords: Infrasound, Snow avalanches, Avalanche monitoring



## Micro-barometric variation associated with rainfall

IYEMORI, Toshihiko<sup>1</sup> ; SANO, Yasuharu<sup>2\*</sup> ; HAYASHI, Taiichi<sup>3</sup> ; ODAGI, Yoko<sup>1</sup> ; AOYAMA, Tadashi<sup>1</sup> ; NAKANISHI, Kunihito<sup>1</sup>

<sup>1</sup>Graduate School of Science, Kyoto University, <sup>2</sup>Asahi University, <sup>3</sup>DPRI, Kyoto University

A sudden rainfall (shower) is often preceded by a micro-barometric variation. To examine quantitative relationships between them, we conducted observations of micro-barometric, rainfall and absorption of BS broadcasting radio waves and recorded the data with one second resolution.

As a result, we often observed the events where a pressure increase starts about one minute before a strong rainfall. Just after the start of the rainfall, micro-barometric variation with period about a few minutes were also observed. These results suggest that the dynamic pressure associated with the falling rain drops pushes the air and observed as a gradual increase of the pressure on the ground. If this is the case, a rarefaction waves may propagate upward over the rain cloud. In this paper, we will show the results obtained from many events.

Keywords: micro-barometric variation, gravity wave, rainfall, acoustic gravity wave

## Ionospheric disturbances by volcanic explosions: Observations with GNSS

NAKASHIMA, Yuki<sup>1\*</sup> ; HEKI, Kosuke<sup>1</sup>

<sup>1</sup>Dept. Natural history sciences, Graduate school of science, Hokkaido Univ.

There have been numbers of reports that atmospheric waves, e.g. internal gravity waves and acoustic waves, excited by various natural or artificial phenomena on the ground, shake up the ionospheric F layer as high as 300 km [Calais et al., 1998 GJI; Heki and Ping, 2005 EPSL]. Acoustic waves from volcanic eruptions are observed as infrasound in near fields, but they also propagate upward and cause ionospheric disturbances [Heki, 2007 GRL]. We try to reveal the characteristics of ionospheric disturbances caused by volcanic explosions using Total Electron Content (TEC) data derived at the dense array of ~1240 Global Navigation Satellite System (GNSS) stations in the Japanese GEONET.

Heki [2006] detected TEC changes of ~0.1 TECU in the region to the south - southeast of the volcano ~10 minutes after the explosion of the Asama Volcano, central Japan, on Sep. 1, 2004, at 11:02 UT. He estimated the atmospheric wave energy from the amplitude of TEC disturbances, and inferred the explosion energy by comparing the TEC change amplitudes with those caused by an artificial explosion with known energy [Calais et al., 1998]. Later, Dautermann et al. [2009 JGR] performed a similar study for the 2003 explosion of the volcano in the Montserrat Island, West Indies.

Here we report on the TEC disturbances caused by the explosion of the Kirishima-Shinmoe volcano, southern Kyushu, Jan. 31 2011, 22:54 UT. According to the JMA documents issued in 2011 January, this explosion induced the infrasound of ~458 Pa, which blasted some window glasses in Kirishima-city, Kagoshima. We also detected 0.2-0.3 TECU peak-to-peak amplitude disturbances after the 2009 October explosion of the Sakurajima volcano, southern Kyushu. They appeared 10 minutes after the explosion and propagated southward with a sound speed at the F layer height. In contrast to the period of ~4 minutes of typical coseismic ionospheric disturbances, TEC changes by volcanic explosions were found to have periods of ~2 minutes or shorter.

In the presentation, we will compare new examples of ionospheric disturbances by volcanic explosions, such as the 2011 Shinmoe and 2009 Sakurajima cases, with older cases such as the 2004 Asama case.

Keywords: GPS, GNSS, infrasound, acoustic wave, volcanic explosion, ionosphere

## Simulation of ionospheric variations caused by acoustic waves generated in the lower atmosphere

SHINAGAWA, Hiroyuki<sup>1\*</sup>

<sup>1</sup>NICT

In the lower atmosphere of the earth, acoustic-gravity waves are generated by various kinds of natural and artificial sources, such as cumulus clouds, tornados, typhoons, earthquakes, tsunamis, volcanic eruptions, meteor impacts, nuclear explosions, rocket launches, etc. Previous theoretical and observational studies have suggested that acoustic-gravity waves induced by such sources can propagate up to the upper atmosphere, producing temporal and spatial variations in the thermosphere and in the ionosphere. However, specific mechanisms of upper atmospheric variations caused by the acoustic-gravity waves have not yet been fully understood because the atmosphere-ionosphere system is an extremely complicated and nonlinear, and it is easily disturbed by many other sources in the atmosphere and in space. In order to quantitatively study the ionospheric variations caused by tsunami-driven acoustic-gravity waves of the 2004 Sumatra earthquake and 2011 Tohoku-oki earthquake, we developed a nonhydrostatic compressible atmosphere-ionosphere model. The model successfully reproduced atmospheric waves and large-scale electron density variations that are caused by tsunami-driven acoustic-gravity waves. We are now developing an atmosphere-ionosphere model with higher spatial resolution and more realistic parameters. We expect that the model is able to reproduce atmospheric-ionospheric phenomena associated with infrasonic and gravity waves produced by various kinds of phenomena. We will report previous results and future prospects.

Keywords: acoustic wave, lower atmosphere, upper atmosphere, ionosphere, simulation, model

## Low-frequency atmospheric pressure waves associated with the outer-rise earthquake on Oct. 25, 2013, 17:10 UTC.

ARAI, Nobuo<sup>1\*</sup> ; IWAKUNI, Makiko<sup>1</sup> ; MURAYAMA, Takahiko<sup>1</sup> ; NOGAMI, Mami<sup>1</sup>

<sup>1</sup>Japan Weather Association

Sensitive microbarographs in and around Japan recorded unequivocal signals associated with the 2011 Off the Pacific Coast of Tohoku, Japan earthquake (Mw = 9.0) (Arai *et al.*, 2011).

These signals retained the original shape of the tsunami and traveled in the atmosphere significantly faster than the tsunami waves in the ocean, therefore, we think that an establishment of a network of infrasound observation along the coast line facing the subduction zone would improve the tsunami warning system.

According to this idea, we deployed three (3) microbarograph stations in Ofunato City, Iwate last July as the first step of the establishment of a network of infrasound observation and are trying to observe atmospheric pressure changes continuously.

The outer-rise earthquake occurred off the Fukushima region on Oct. 25, 2013, 17:10 UTC and the tsunami waves with few tens centimeter heights observed at coastal area of Tohoku region. And some curious atmospheric pressure waves detected at our Ofunato sites. The characteristics of the observed signals are consistent with the features of the tsunami source produced by the outer-rise earthquake.

### Reference:

Arai *et al.* , Atmospheric boundary waves excited by the tsunami generation related to the 2011 great Tohoku-Oki earthquake, *Geophysical Research Letters*, Vol. 38, L00G18, doi:10.1029/2011GL049146.

Keywords: Infrasound, atmospheric pressure change, outer-rise earthquake, detection of tsunami

## Examination on Numerical Simulation of Tsunami-Induced Extremely Low Frequency Sound Waves with Geospatial Information

OKUBO, Kan<sup>1\*</sup> ; KAWASHIMA, Ken<sup>1</sup> ; OSHIMA, Takuya<sup>2</sup> ; TAKEUCHI, Nobunao<sup>3</sup>

<sup>1</sup>Graduate School of System Design, Tokyo Metropolitan University, <sup>2</sup>Faculty of Engineering, Niigata University, <sup>3</sup>Graduate School of Science, Tohoku University

Air pressure changes associated with earthquakes and/or tsunami have been investigated previously. As for air pressure changes associated with tsunami, some observation results have been reported (T. Mikumo (1964), T. Mikumo, et al. (2008) and William L. Donn and Eric S. Posmentier (1964), Y. Tamura (2011), N. Arai, et al. (2011)).

We have measured the air pressure in the terrestrial atmosphere with other meteorological parameters (temperature, humidity, etc.) continuously at Hosokura outdoor observation station (HSK) in Miyagi Prefecture, Japan. The extremely low frequency sound waves (so-called micro barometric waves) are also detected as large changes of air pressure in the 2011 off the Pacific coast of Tohoku Earthquake (M 9.0, origin time;14:46.18JST) (K. Okubo, et al. (2011)).

Although the power failure was caused by the earthquake occurrence, our observation system had been maintained by the UPS system and the private power generation. Therefore, in this earthquake, our observation system successfully observed extremely low frequency sound waves induced by tsunami. The waves were detectable at the observation point on the ground surface sufficiently early before the arrival of tsunami waves at coastal areas, because sound waves propagate faster than ocean waves (tsunami).

These results can encourage early tsunami detection (S. Iwasaki (1992), T. Izumiya (1994)) using multi-site observation and arrival time difference method. That is, detection of tsunamis might be possible by monitoring extremely low frequency sound waves at ground surface observation sites and/or sea-level observation at relatively low cost. It is important to obtain information of tsunami as soon as possible; arrival time, area and scale.

In this study we present a fundamental examination on analysis and visualization of extremely low frequency sound waves caused by tsunami using numeral approach. We employ the numerical simulation using the Finite-Difference method in Time-Domain (FDTD method) (Yee, 1966) with geospatial information for the large-scale sound wave propagation. As an elementary study, it is applied to the estimation of extremely low frequency sound waves' propagation and time-series analysis of sound pressure.

Through our study, we show the numerical results of sound pressure distribution and estimate the propagation phenomena of sound waves, compared with the observed data at HSK. This examination may help the development of the design of early tsunami detection system. In the future, further efforts can suggest new systems for early warning of destructive tsunami using a combination of other measurements.

We are grateful to Hosokura Metal Mining Co. for the maintenance of our site. This research was partially supported by a Grant-in-Aid for Scientific Research from the Japan Society for the Promotion of Science.

Keywords: Numerical Simulation, tsunami, sound field change, microbarometric wave, infrasound, numerical visualization

## Atmospheric Gravity Waves from the 2010 Maule, Chile earthquake (Mw8.8)

MIKUMO, Takeshi<sup>1\*</sup> ; IWAKUNI, Makiko<sup>2</sup> ; ARAI, Nobuo<sup>2</sup>

<sup>1</sup>Kyoto University, <sup>2</sup>Japan Weather Service, <sup>3</sup>Japan Weather Service

Atmospheric pressure waves were recorded after the 2010 Maule, Chile earthquake (Mw=8.8) by microbarographs at seven International Monitoring System (IMS) stations in the distance range up to 7,680 km. By applying bandpass-filtering, we extracted low frequency gravity waves, removing atmospheric noise and higher-frequency acoustic modes, and then estimated their phase velocities around 332-341 m/s. To compare with these observations, we constructed synthetic waveforms, referring to the source dimension and coseismic vertical ground displacements based on geodetic measurements (Moreno et al., 2012), and incorporating a standard atmospheric sound velocity structure up to a height of 220 km. The comparison between the observed and synthetic waveforms provides generally satisfactory agreement, and suggests the time constant of ground displacements between 2 and 3 min in the northern and southern segments of the entire source region extending for about 500 km..

Keywords: 2010Maule, Chile earthquake, Mw=8.8, low-frequency, Atmospheric gravity waves

## High resolution barometer array in Palau, Western Pacific

ISHIHARA, Yasushi<sup>1\*</sup> ; FUKAO, Yoshio<sup>1</sup> ; SHITO, Azusa<sup>2</sup> ; OBAYASHI, Masayuki<sup>1</sup> ; SHIROOKA, Ryuichi<sup>1</sup>

<sup>1</sup>JAMSTEC, <sup>2</sup>Institute for Geothermal Sciences, Kyoto University

The Variety of waves is propagating in the atmosphere, ocean and solid earth. And there are interacting between each layer. For total and integrated understanding, multi parametric measurement over different field is required. We target Palau islands, western Pacific for multi parametric measurement. We are operating broadband seismic station in a station of Pacific Geophysical Network (OHP network). And another seismic station is also under operation due to removing of seismic station. Meteorology group of JAMSTEC has their station including meteorological radar. We think that Palau is fine condition to construct integrated geophysical measurement field. So that we deployed high resolution barometric small array in Palau.

Palau locates tropical zone and its daily weather condition is similar and relative more stable than middle latitude zone and polar area that have some day's variation and passing of front. In our research, one of main focuses is very low frequency band of barometric variation; the ambient condition has merit to get accurate detection of signal.

As for observation system, sensor is quartz oscillation type high resolution barometer and recorder is Linux Box via serial communication. We set to be sampling of 2 sps to get high resolution data. We installed Five(5) stations in Palau whose station interval is about 20km. Two stations of them locate at seismic stations and another station is same area with weather station. The array is operating from August, 2013 and is under operation.

The tentative data review shows atmospheric gravity wave is frequently recorded in longer period of 200sec. Sometimes event pulse-like signals are detected. Apparent velocity of these waves is 20 ? 30 m/s and direction of propagation varies daily. Most signal arrives from outside of this array. We report character of these wave and relation with meteorological condition.

Keywords: atmospheric gravity wave, micro seism

## Improvement and evaluation of optical-type infrasound sensor for multi-site observation

IKEHARA, Kousuke<sup>1\*</sup> ; YAMAMOTO, Masa-yuki<sup>1</sup> ; KAKINAMI, Yoshihiro<sup>1</sup> ; ISHIHARA, Yoshiaki<sup>2</sup>

<sup>1</sup>Kochi University of Technology, <sup>2</sup>JAXA Space Exploration Center, Japan Aerospace Exploration Agency

Infrasound is applicable for remote-sensing methods for detecting geophysical phenomena in the atmosphere. There have been developed and used many types of infrasound sensors, however, typically used infrasound sensors are almost developed by foreign countries, resulting high cost situation in Japan. If we can develop low cost infrasound sensors, multi-site arrayed observation will be realized in near future.

Recently, infrasound signal generated by tsunami was clearly detected by many CTBTO infrasound stations (Arai et al., 2011), suggesting a new era for establishing a dense infrasound sensor network in every prefecture of Japan for preventing or reducing catastrophic disasters. Because the nature of pressure waves with large wavelength, amplitude of infrasound generated by tsunami might be proportional to the size of the disasters. Combination with sensor networks of seismometers on ground and ocean floor, GPS-buoy type wave recorders, and water manometers on ocean floor, establishing a dense network of infrasound sensors with arrayed configuration is desired.

Since 2006, we have been developing new sensing method of infrasound by using piezo film and PSD (Position Sensitive Detectors), achieving frequency range between 0.001 Hz and 10 Hz as well as minimum pressure level of 0.01 Pa (Yamamoto and Ishihara, 2009). In 2013, we tried downsizing the PSD type infrasound sensor developed in 2008 into a size of 0.15 m x 0.15 m x 0.25 m height with calibrating it by using space chamber (0.8 m length x 0.58 m diameter) as an accurate volume pressure reservoir (Manabe et al., 2013). Here, we improved the PSD optical-type infrasound sensor by using 3D printer technology to make many tiny parts designed with 3D CAD software.

By pushing and pulling a small amount of air by a small syringe, calibrating pressure waves with extremely weak amplitude (10 Pa to 0.01 Pa) can be generated in the space chamber, precise measurement of artificially generated infrasonic signals could be realized. The waves were measured by both of the developed PSD sensor and Chaparral Model-2.5 infrasound sensor at the same time. Comparison with output signals by two types of sensors, the downsized PSD type infrasound sensor was carefully studied. In this paper, we will introduce the new design and obtained calibrating datasets.

Keywords: infrasound, multi-site observation, sensor development, optics, measurement, low-cost



## Pressure sensors detected wind noise produced in wind tunnel

IWAKUNI, Makiko<sup>1\*</sup> ; YAMAMOTO, Masa-yuki<sup>2</sup> ; TANIMOTO, Saki<sup>3</sup> ; KAKINAMI, Yoshihiro<sup>2</sup> ; IKEHARA, Kosuke<sup>2</sup> ; OKADA, Kazumi<sup>4</sup> ; ARAKI, Keiji<sup>3</sup> ; KURIHARA, Yasushi<sup>3</sup> ; ARAI, Nobuo<sup>1</sup> ; MURAYAMA, Takahiko<sup>1</sup> ; NOGAMI, Mami<sup>1</sup>

<sup>1</sup>Japan Weather Association, <sup>2</sup>Department of systems engineering, Kochi University of Technology, <sup>3</sup>Railway Technical Research Institute, <sup>4</sup>Institute of Seismology and Volcanology, Hokkaido University

As infrasound and pressure disturbance induced by local wind around infrasound sensors are partially in the same frequency range, amplitude of the infrasound signal is sometimes lower than that of pressure disturbance by strong wind. Thus, obtaining the infrasound signal by analyzing software from the observation data with such wind noises is one of the technical objectives to solve. Usually, some porous pipes connected with the infrasound sensors have been used in order to reduce such local wind disturbances.

To evaluate such system for wind noise reduction, we conducted experimental study by using a wind tunnel with wind speed up to 60 m/s. We used nano-resolution pressure transducer (6000-16B manufactured by Paroscientific Inc., USA) and microphone type infrasound sensors

(Chaparral physics, Model25 manufactured by Univ. of Alaska Fairbanks) in the wind tunnel of the Railway Technical Research Institute (RTRI), Japan. In this presentation, we will show the relationship between the wind speed and porous pipe configuration installed in the wind tunnel.

In this presentation, we show the relation between wind speed and pipe direction.

Keywords: Infrasound, wind noise reduction, pipe reduction system, wind tunnel

## Legacy Technology Still in Use: Lessons from FLOSS Development

BABA, Yoshihiko<sup>1\*</sup>

<sup>1</sup>Ritsumeikan University

### 1. Introduction

In science, including geospatial and earth science, use of the Internet is becoming more and more important. Institutions provide more and more, spatial data and scientists share the information or work on a project regardless of geographical boundary. In such situation, social media will be becoming more and more important, but the popularity changes so easily. On the other hand, there are several social tools which have been around for more than 30 years, such as IRC and CVS/Subversion/git. In this paper, the advantages and disadvantages of the current and legacy social tools.

### 2. Underlying Philosophy

IRC and CVS/Subversion/git are very popular among free and libre open source software (FLOSS) developers. One of the most important factor of free software was revealed by Eric Raymond, who contrasted two different free software development models:

The cathedral model: source code is available with each software release, but code developed between releases is restricted to an exclusive group of software developers.

The bazaar model: the code is developed over the Internet in view of the public.

In fact, all the commercial projects and many FLOSS projects are organized in the cathedral model. The point is, only FLOSS software can be developed in the bazaar model. The most well-known project which adopted the bazaar model is perhaps Wikipedia. What can we learn from the project?

### 3. IRC vs twitter

There are many real time chat tools, such as IRC, Skype, Messenger, Twitter and LINE.

IRC is a communication protocol developed in 1988. In IRC, users join a server (e.g. freenode.net) using IRC clients (e.g. xchat), then joins a room (e.g. #qgis, #grass) to talk and discuss issues. It is said that there are more than 50,000 users on Freenode. The figure may be small, when compared to twitter or LINE. It is noted that the author(s) asked several Fink developers to review this article. IRC can be compared to twitter in that they are both for "short text" and real-time communication.

When using twitter, you can browse information about a certain topic using hash tag (#). However, twitter is in its essence a "twit", expressing one's opinion and rarely becomes a place for conversation/discussion.

ITO (MTT38-01) discusses that the information is well organized at together by a coordinator. By the summary on together is often very difficult to read. On the other hand, chat logs of many IRC channels are very useful without any editing. Perhaps, something can be learned from IRC. But so far, my suggestion is to use IRC for scientific discussion.

### 4. Discussion

As seen in the previous section, there are several legacy tools that are still widely used, especially among FLOSS developers. One of the advantages of these legacy tools is that they have been evolved to support the "cathedral" model explained above.

For geospatial and earth science, such tool may be useful to share the information of, say, open data. There are many institutions, public or private, which offer GIS data on the Internet. The official data, such as shape files provided at [data.gov.uk](http://data.gov.uk) or [nlftp.mlit.go.jp/ksj/](http://nlftp.mlit.go.jp/ksj/), would be more useful when one finds an error, fix it and report and/or redistribute it. The download pages may be more enhanced with wiki, where users can post their ways of using the data. Google maps, or its more "open" alternative, OpenStreetMap, may be more sustainable if they learn more from legacy tools.

MTT44-01

Room:311

Time:May 2 14:15-14:30

#### 5. Conclusion

Several social tools for FLOSS development, which have been developed since 1980s, are reviewed. Some tools, such as IRC, are still used despite the recent advancement of newer social tools. In fact, these tools may be more advanced, in that they give more powers to users, than the recent and more popular social media, such as Facebook and twitter.

Keywords: FLOSS, IRC, CVS, Bug Tracking

**Abstract (English):** In science, including Earth and Planetary Science, software development has played an important role, in many cases with package management systems. Fink Project, one of the package management systems, has been involved in a number of free software to Mac OS X. Such package management systems are supported by a large number of maintainers, with the aid of SourceForge, CVS and/or git, IRC and many other tools.

## Establishing Technology of Environmental Monitoring Using Social Media

ITO, Masaki<sup>1\*</sup>

<sup>1</sup>The University of Tokyo

This paper discuss the way to enable environmental monitoring using social media. Several existing approaches such as development of original software and utilizing crowdsourcing service are introduced with there advantages and disadvantages. Finally the author emphasizes the need of further research on theory and technology.

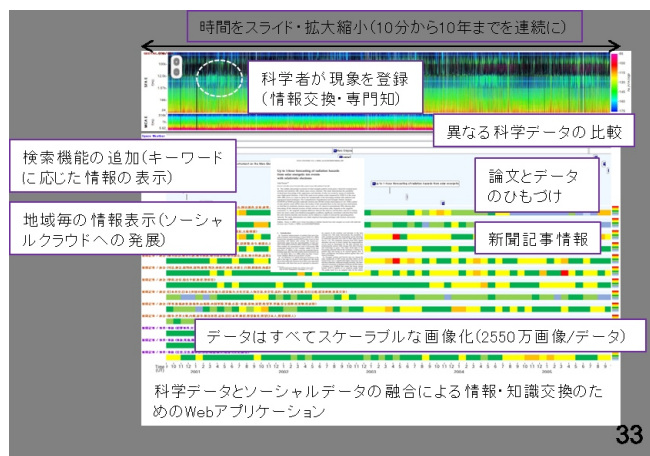
Keywords: Social Media, Environmental Monitoring, Crowdsourcing

## A Web-application for Time-dependent Observation Data for both Scientific and Social Data

MURATA, Ken T.<sup>1\*</sup>

<sup>1</sup>National Institute of Information and Communications Technology

The NICT Science Cloud is one of the science clouds proposed for development of sciences. A variety of science data are collected and stored in the science cloud to be analyzed interdisciplinary. After the Internet is widely used, new concept and information technology have shown up; semantic web and linked open data (LOD). These technologies enable information on the Internet machine readable. In many science fields, it is pointed out that the semantic web will play an important role for the interdisciplinary research works. However, there have been few ideas to be ever proposed as a methodology or roadmap to the interdisciplinary science using semantic web. Herein we present a concept of professional knowledge and academic knowledge following collective knowledge proposed as a Web 2.0. Based on the concept, we design a Web-application for interdisciplinary science. The application (named STARS touch) provides users with an environment of dynamic and light preview of any types of time-dependent data. In the demonstration, we show an example of simultaneous preview of both scientific data (satellite observation data) and social data (newspaper information).



## The trial which carries out information dissemination by SNS at a high school students

AOKI, Kunihiro<sup>1\*</sup>

<sup>1</sup>Nihon univ. BUZAN high school & junior high school

Even if it thinks that a teacher will take communication with a student, it is very difficult to try to be connected with a high school student.

Then, "whether, during session, communication can be taken with a student" is important.

The method for being connected with a student in the first half is reported.

It is what "the atmosphere which a student says easily is built for", and "a lesson which a student tries to hear positively that the talk is" that I take care by the lesson.

Therefore, I am made to prepare time to concentrate only for a short time several times while I accept a student's positive remark.

As a mistake is made in being right, it catches not related to a student's remark and its head is bowed in assent, the boundary of the mistake is clarified if behind right.

Thus, by corresponding from a student's viewpoint, I think that a student opens the heart to a teacher.

If it comes so far, a student will be connected in SNS.

The most is a student and a graduate although the number of the followers of my Twitter is 95 now.

In order to usually disseminate the information on extension and geography of a lesson, or earth science the second half using SNS, practice using SNS is reported.

Even if it can take communication by SNS with the present condition and a student, there is no reaction in the photograph and comment related to geography.

Most of the reasons are a thing with a "petty" photograph, and a thing with "many" character numbers.

For example, even if it shows the photograph of a terrace, only the comment "it is peaceful" comes.

If the number of characters exceeds 70 characters, it is tired of reading a character.

It is adiaborous, even if the contents of the photograph also have a reaction in the direction where the scene is mixed and it shows geographical feature, vegetation, etc.

The photograph about geography is published, and since a result which is considered even if it is going to ask for a comment or is going to offer teaching materials has not come out, I would like to obtain a comment from you, although SNS is convenient.

Keywords: Twitter, Line, Lesson

## Social media as a source of innovative ideas for education and outreach in geoscience

OGUCHI, Takashi<sup>1\*</sup> ; ISHIKAWA, Hajime<sup>1</sup> ; HASHIMOTO, Mari<sup>2</sup>

<sup>1</sup>CSIS, Univ. Tokyo, <sup>2</sup>Meiji Gakuin Univ.

Scientists are often expected to contribute to education and outreach in their specialized fields. They can provide scientifically accurate information about their fields based on deep knowledge. However, they may be much affected by the customs and common sense of their fields, and may not be good at attracting attention of people who do not have specialized knowledge in the fields. Social media contribute to the reduction of this problem, through interactions of people with various backgrounds. Scientists of a particular field often interact with those who are interested in the field but have different backgrounds including non-scientists. Such people sometimes provide scientists with novel ideas for effective education and outreach. Subsequent comments from scientists on the ideas may be useful for those who provided the ideas. In this presentation, we discuss such constructive interactions among persons in social media, with reference to geomorphological examples.

Keywords: social media, education, outreach, interaction among persons

## The possibility and current issues of sharing information with social media in geoparks

NIINA, Atsuko<sup>1\*</sup>

<sup>1</sup>Regional Innovation Research Center, Tottori University of Environmental Studies

This presentation reports on the possibility and current issues of sharing information with social media in the case of San-in Kaigan Global Geopark. Sharing knowledge and experiences is necessary for the development of the geopark network. Communication is one of the best ways to share them among people. There are various ways of communication; for instance, face-to-face communication, non-face-to-face communication, mass media and social media. In the case of San-in Kaigan Geopark which spans across 110 km from east to west and 30 km from north to south, social media is a complementary tool to communicate among local actors, stakeholders and shareholders in the wide territory of the geopark.

Keywords: social media, communication, sharing information, San'in Kaigan Geopark



## ”San’in Kaigan Geopark \*Fortune Cookie in Love” Project

KOYAMA, Makoto<sup>1</sup> ; FURUKAWA, Tomoko<sup>1</sup> ; MATSUBARA, Noritaka<sup>2\*</sup>

<sup>1</sup>San’in Kaigan Geopark Promotion Council, <sup>2</sup>Inst. Nat. Env. Sci., Univ. Hyogo

San’in Kaigan Geopark Promotion Council conducts ”Questionnaire on Recognition of San’in Kaigan Geopark” every year. In a questionnaire survey conducted at PR campaign in Keihanshin area in 2013, San’in Kaigan Geopark recognition was low among 10s (27%) and 20s (24%) compared to 70s over (68%). An issue for the future is considering ways to raise awareness of geopark activities among young people. One of the reasons why many young people are not familiar with geopark is insufficient PR activity through the use of the internet. Now the council provides information available on the official website and Facebook. The problem is that those websites are not well-known to the general public.

For this reason, San’in Kaigan Geopark undertook ”San’in Kaigan Geopark \*Fortune Cookie in Love” Project, which local guides, tourism facilities, local residents, geopark-related officials and researchers dance along ”Fortune Cookie in Love”- by J-pop’s most popular girl group AKB48. We uploaded a video to Youtube on January 31, 2014 and promote the San’in Kaigan Geopark to the general public. There are 43 different scenes and 265 wonderful performers including mascots in about 4-minute video. Organized yet creative dancing entertains those who watch the video. We also advertise it to the media, and people who access to this video on Youtube easily exceed 10,000.

From now on, we will analyze the awareness and the effect of this project through a questionnaire and any changes in the number of visitors across the San’in Kaigan Geopark.

Keywords: sns, youtube, Fortune Cookie in Love, San’in Kaigan, geopark

## San'in Kaigan Geopark Tourism Promotion By Female Bloggers

ANDO, Kazuya<sup>1\*</sup> ; NAKATANI, Hideaki<sup>1</sup> ; OOE, Seiji<sup>1</sup> ; ISHIGAMI, Nobuyuki<sup>1</sup>

<sup>1</sup>San'in Kaigan Global Geopark Promotion Office

While there is a strong trend among independent travelers to gather information and plan trips within Japan through the use of the internet and word-of-mouth information, there is a lack of information regarding geotourism available online. In response to this situation, a number of San'in Kaigan Geopark model tours were operated in Tottori Prefecture. These were promoted by female bloggers who are popular and influential in the independent tourism market. In 2012 and 2013, a total of 70 female bloggers established their own themes and planned trips to the San'in Kaigan Geopark. Each blogger posted their travel reports on their blog sites and on twitter. At the same time, a "San'in Kaigan Geopark Model Tours for Women" facebook page was established so that each of the travel reports could be posted and shared. As a result of this continual availability of travel information, San'in Kaigan Geopark related pages received a high number of online hits, and increased awareness and popularity regarding the Geopark was achieved.

Keywords: San'in Kaigan Geopark, Tours for Women, Geotourism, Female Bloggers

## Effects and issues of information transmission using the social media in a large active geopark

MATSUBARA, Noritaka<sup>1\*</sup>

<sup>1</sup>Inst. Nat. Env. Sci., Univ. Hyogo

The San'in Kaigan Geopark is located in the west of Japan, spanning approximately 120km from its easternmost point, at Kyogamisaki Cape in the city of Kyotango, to its westernmost point, on the Aoyakaigan Coast in the city of Tottori, and measuring a maximum of 30km from north to south.

In terms of administrative jurisdictions, the Geopark spans a total of three cities and three towns in 3 prefectures (Kyoto Prefecture, Hyogo Prefecture, Tottori Prefecture).

Sharing and generating information is difficult in such a large active geopark. Then, we decided to use a social media to share and generate information smoothly. We created fan page of the geopark to Facebook. We have established an administrator in each area to generate regional information.

Keywords: geopark, facebook, San'in Kaigan Geopark, social media

## Utilization of facebook for the management of working groups in North Ibaraki Geopark

AMANO, Kazuo<sup>1\*</sup> ; HOSOI, Jun<sup>2</sup> ; IBARAKI UNIVERSITY, Geological information utilizing project<sup>1</sup>

<sup>1</sup>Faculty of Science, Ibaraki University, <sup>2</sup>Graduate School of Science and Engineering, Ibaraki University

Exchange of information with SNS like Twitter, foursquare, facebook has been done in the North Ibaraki Geopark (Saito et al., 2010; Ito et al., 2011, 2012; Amano et al., 2012, 2013). Facebook is very useful for the management of the North Ibaraki Geopark because it has many capabilities such as file upload and event planning etc. Recently, Utilization of facebook for management of four working groups in the North Ibaraki Geopark is carried out. Members of each working group successfully discuss or communicate many things for the management of the North Ibaraki Geopark.

Keywords: SNS, geopark, North Ibaraki Geopark, facebook

## Study on the socialized development environment in the geospatial informations field

SETO, Toshikazu<sup>1\*</sup>

<sup>1</sup>Center for Spatial Information Science, the University of Tokyo

### 1. Introduction

The deployment of the technology and systems for geospatial information is the spread of the open-source movement and culture since 2000, opening up of technology and information has come to be regarded as important in the GIS field (Sui, 2014). This open culture is expected to spread to social, political, and economic areas, such as Open Government. This is an important point for government that have not gone far enough to implement GIS, but the platform is beginning to be wide open.

The major features of GIS technology since the 2010s have been open source code, various code development platforms and interfaces, translation of software documentation, concept creation for application development, and cloud computing which has led to social interaction and cooperation. In this study, mainly in the Free and Open Source Software for Geospatial (FOSS4G), we examine the actual situation of the socialized open developing environment for GIS technology and consider whether that is a problem and what are its effects.

### 2. Platform to support the socialized developing environment

The Quantum GIS (QGIS) is a desktop open-source GIS software from the Open Source Geospatial (OSGeo) Foundation to support the development and publication of source code that has been made available through repositories such as SourceForge. GitHub is a Web-based hosting service for software development projects, which started gaining popularity around 2010. Transifex, which was founded in 2008, has emerged as a Web-based translation platform. It provides variety and takes better advantage of the version control system than Git, and it tracks changes in programs such as forks that incorporate a user's own code as part of the development project, and it provides for fluid use of source code. In fact, we have started to migrate to system of Git from SVN, the platform for Web maps for applications such as Ushahidi. As a localization system on the Web, Transifex provides convenient visualization of progress and a translation interface. Transifex has been used to translate 20 or more OSGeo projects including QGIS software with Japanese versions of all projects. In addition, translations of QGIS user manuals can be incorporated directly into the software, and the translation of case studies of open data, such as in the use case, do not matter, because they are shared as a target.

### 3. Challenges that the effects of social networking bring to openness

Social networking in open-source software development, such as with Transifex and GitHub, is creating many opportunities for GIS technology. For example, Harvard University has developed an open-source package in which geospatial information from various libraries are combined based on Geonode. Also in Japan, use of platforms such as IdeaLinkData and CityData that allow social sharing of regional data is increasing, and more involvement of various actors using GIS is expected. Additionally, with increased participation opportunities for data users and developers through the Web, and to develop open data events such as Hackathon, which began recently in Japan, this trend in data and source code is also becoming a medium to provide resources directly.

However, while open-source social networking accelerates development, product development itself is being subdivided into code for individual functions and, due to different versions in the library, errors can increase. In addition, mutual information exchange between developers is spread by social networking, with smaller contributors able to lead the development as compared to developers from the English-speaking countries. Therefore, it is expected that social networking will contribute to the generation of open data as well as to software development and translation to support visualization and data manipulation of geospatial information, such as the introduction in GIS education and the creation of opportunities for participation.

Keywords: open culture, FOSS4G, crowdsourcing, GitHub

## Edmund Naumann (1854-1927) and Mt Fuji

YAJIMA, Michiko<sup>1\*</sup>

<sup>1</sup>Tokyo Medican and Dental University

Edmund Naumann (1854-1927) and Mt Fuji  
Michiko YAJIMA

Mt Fuji is the highest mountain in Japan at 3776 m. In 2013 Mt Fuji was added to the World Heritage List as a Cultural Site. Japanese people, young and old, man and woman, climb Mt Fuji for religious reason since the old age. Scientific research on Mt Fuji started at the Meiji Era by the foreigners. Before 1854 Japan closed the doors to the Westerners. Once opened the door to the Westerners, Meiji Government hired many foreign teachers.

Edmund Naumann (1854-1927) came to Japan in 1875, became the first professor of Geology in the University of Tokyo, founded the Geological Survey of Japan and made the good geological reconnaissance map of Japan. He was fascinated by the Mt Fuji just when he reached Japan. At that time many westerners came on boat, the first sight of Japan is Mt Fuji. Western scientists all made the race to climb Mt Fuji. Naumann climbed the Mt Fuji in 1883. His research work is just surrounding Mt Fuji. He made clear the history of measurement of the height of Mt Fuji. He made clear the history of eruption of Mt Fuji. His most important geologic work is proposing the Fossa Magna in the central Japan. He thought the reason of Fossa Magna may be the intrusion of Mt Fuji.

After he came back to Germany he wrote even the script of Opera “ Taketorimonogatari ” that is the old Japanese tale of beautiful lady who came from the heaven and came back to the heaven at Mt Fuji with the smoke of eruption.

Keywords: Naumann, Mt Fuji, Fossa Magna

## The Research on Seitaro Tsuboi Materials: Interpreting his Correspondence

TOCHINAI, Fumihiko<sup>1\*</sup>

<sup>1</sup>Kanazawa Institute of Technology

The author has studied a large quantity of historical materials about a geologist Seitaro Tsuboi (1893-1986) (hereinafter "Tsuboi Materials") since 2010, which have been collected and archived by Multi-media and Socio-information Studies Archive, University of Tokyo. Tsuboi conducted researches on igneous petrogenesis with physical and chemical methods from 1920s to 1950s, which attracted positively or negatively many geologists. Combined with his position, a professor of petrology at (Imperial) University of Tokyo, he had considerable influence on the course of Japanese geological sciences.

Prior to the study of Tsuboi Materials, the author's understanding was that Tsuboi's influence over Japanese geological community rapidly decreased after his retirement from the professorship in 1954. However, the analysis of contents of Tsuboi Materials, such as correspondence with publishers about his books and documents about royalties on his books, suggests that his researches did attract people's interests even in the late 1970s. The details will be introduced in the presentation.

Keywords: History of Science, History of Geology in Japan, Seitaro Tsuboi, Archive

## The Examples of the "puzzle-solving" in the Plate Tectonics Theory

CHIBA, Jun'ichi<sup>1\*</sup>

<sup>1</sup>Yokohama School, O-hara Business College

It is generally considered that the plate tectonics theory has become a paradigm in the field of solid earth science (for instance, Miyashiro, 1998). Indeed, when I was engaged in descriptive research on the structural geology of Boso peninsula when I was studying for the doctoral degree, I would use technical terms of the accretionary prism theory, a sub-theory of the plate tectonics theory, to interpret observed facts. Also, looking at an outcrop in front of me, I was often asking myself, "Which part of an accretionary does this piece correspond to?" in the middle of a field survey. By doing so, I was trying to integrate new observed facts into the framework of the accretionary prism theory, which can be considered in a sense as "puzzle-solving" in normal science as referred to by Thomas Kuhn.

Tomari (2008) describes how the Japanese earth science society accepted the plate tectonics theory, apart from the memoirs of people directly involved in this process. Tomari argued that while geophysicists and seismologist accepted the plate tectonics theory in a relatively smooth manner, it took ten more years for geologists to accept it, which he described as "a lost decade". He ascribes it to the following causes: the geologists were interested less in application of physics and chemistry (principle of the present) than description of the respective geographical features of each region in accordance with the orogenesis theory; also, the geologists who were the leading figures in the Association for the Geological Collaboration in Japan, which accounted for the majority of the geological society in Japan at that time, harshly criticized the plate tectonics theory. Shibasaki(2011) argued against the claim of Tomari, by noting that the Japanese geological society by no means accepted the plate tectonics theory late for the following reasons: geologists who were conducting research on biostratigraphy with the use of Radiolaria fossils from the late 1970s to the early 1980s led the geological society to accept the plate tectonics theory by, for example, successfully explaining some of the problems of areal geology with the accretionary prism theory ? in particular, the problem associated with age determination of block-in-matrices (Radiolaria revolution); as such, they were able make a contribution to a theory on global movements precisely because they were engaged in research on areal geology. She also maintained that since most of the young researchers who contributed to the Radiolaria revolution belonged to the Association for the Geological Collaboration in Japan, while it is certainly true that the researchers who were the leading figures of the association were against the plate tectonics theory, their influence was limited. She then argued that it is necessary to conduct more integrated research on science history.

With regard to the question described above, I argue that it is meaningful to review when the kind of research that corresponds to the "puzzle solving" of the plate tectonics theory began in each of the sub-fields of geology (structural geology, stratigraphy, volcanic petrology, metamorphic petrology and mineralogy, in addition to areal geology). It is because it is possible to determine whether the result of any given research corresponds to the "puzzle-solving" of the plate tectonics theory from its theoretical structure; and by doing so, it is possible to show that the plate tectonics theory functions as a paradigm. In this presentation, I introduce some examples of the geological studies which are regarded as the "puzzle-solving" in the plate tectonics theory.

Keywords: plate tectonics, puzzle-solving, history of science, geology



## A history of mining, mineralogy and geology in the German literature

UENO, Fuki<sup>1\*</sup>

<sup>1</sup>Graduate School of Information Science, Nagoya University

The question of organic or inorganic nature of minerals had been a subject of a debate since the ancient Greece to the Middle Ages. Thales and Pythagoreans believed that stones had souls, whereas Plato and Aristotle believed they possessed an anima. In the view of nature in the Ancient Rome, people believed that leaving mines without mining for a certain period of time would allow them to refill. In the Middle Ages, the relationship between minerals and magic was debated, and people believed stones had anima whereas jewels had magical powers. This thinking was further developed by alchemists, for whom the knowledge and understanding of minerals and jewels was essential.

The idea that minerals have supernatural power is also found in the German literature, especially that of the 18 and 19th century. A lot of novelists at the time studied mining, mineralogy and geology as they had been involved in mining business. In their writings stones have mystic powers.

However, already in the 13th century, Albertus Magnus ridiculed the idea of stones having a soul. Georg Agricola published *De Re Metallica* (1556) a complete and technical treatise on mining and extractive metallurgy in the 16th century, whereas Leibniz created *Protogaea*, an ambitious account of terrestrial history, central to the development of the earth sciences in the 17th century.

I will introduce works of romanticist (Goethe, Novalis, etc.) and philosophers (Leibniz, etc.) involved in mining business, and discuss the gap between their philosophy and reality.

## Wang Mo's role in the history of Japanese and Chinese geography

SHIBATA, Yoichi<sup>1\*</sup>

<sup>1</sup>Institute for Research in Humanities, Kyoto University

Wang Mo is first Chinese graduate of the department of geography at Imperial University of Tokyo, and also founder of second department of geography in China. This paper examines his role in the history of Japanese and Chinese geography.

Keywords: institutionalization of geography, diffusion of geographical thought, Chinese international students in Japan, history of geography

## Theory Change in Science - Case Study on the Solar System Formation

AOKI, Shigeyuki<sup>1\*</sup>

<sup>1</sup>University of Aizu

Philosophy of science today has been particularized, just like particular sciences themselves. Philosophy of earth (and planetary) sciences was active in the 1980s-1990s following the Plate Tectonics Revolution in the 1960s, but seems to be inactive these days. Recent anthology on philosophy of science (Curd & Psillos 2013) discusses biology, chemistry, cognitive science, economy, psychology, social sciences, etc. while making no references to earth sciences. The above-mentioned literature on Plate Tectonics Revolution was based on preliminary historical studies on the earth sciences in the 1960s. In contrast to this, the synthetic process of earth and planetary sciences is not yet documented in detail, so philosophy of earth and planetary sciences has to start with digging up interesting historical data.

This presentation, drawing on Brush(1996), overviews the theoretical developments on the origin and evolution of the solar system in the 20th century, and then discusses which model best explains this process.

Keywords: Philosophy of Science, History of Science, Science Studies

## A rudimentary consideration on anthropogenic climate change and countermeasures to it, "geoengineering" in particular

MASUDA, Kooiti<sup>1\*</sup>

<sup>1</sup>JAMSTEC

The issue called "anthropogenic climate change" (ACC) or "global warming" is such a chain of causes and effects that human industrial activities result in increase of concentration of greenhouse gases such as carbon dioxide in the atmosphere, enhancement of the greenhouse effects, and cause changes of climate which can be characterized by increase of global mean surface temperature. It also have such aspects as sea level rise and changes of dryness, which have impacts on human society. The impacts are given unevenly between regions and between generations.

Since 1998 when the IPCC was established, the countermeasures to ACC has been discussed in terms of "mitigation" and "adaptation". In its 5th Assessment Reports (AR5) to be published in 2013-14, another category called "geoengineering" is added. Here I tentatively follow the categorization of AR5.

The human society has developed within the constraint of the environment, by adapting to it. Climate, including its changes, is part of the environment, and adaptation to it is one of basic functions of the human society. There are a few notable issues, however. Since the start of agriculture, the human society has experienced the climate of Holocene which has extraordinarily small variability in the context of the whole Quaternary era. Also, in the modern world, adaptation by migration has become difficult, since clear national boundaries and land ownership have been developed, and population has increased so much thanks to technologies which also involve utilization of fossil fuel. In addition, with recent development of global ideas of equality between nations and humanitarianism,

people tend to value avoiding such fates where many people die untimely.

In the middle 20th century, it was hoped to technologically control climate within a state favorable to human society. Development of science resulted in two pieces of understanding. One is that the climate is a complex system with large uncertainty due to nonlinearity and difficulty of observation. Another is that emission of carbon dioxide by burning of fossil fuels is an important forcing that shifts the energy balance of the climate system. Then, people tended to think a kind of "passive intervention" by reducing the forcing that human activities already have made as the major countermeasure to the climate change. It has become customarily called "mitigation".

The essence of mitigation is reducing use of fossil fuels. International decision making on it has not been very successful even though 20 years have passed after the establishment of UNFCCC in 1992. It is because energy resources is fundamental to economical development.

In this context, hopes to technologically control climate, e.g. "geoengineering" have risen again. It is still difficult, however. The technology is not finished, and the knowledge about effects, side-effects and costs is uncertain.

Two major sub-categories of "geoengineering" are called "carbon dioxide removal" (CDR) and "solar radiation management" (SRM).

CDR is equivalent to mitigation as far as it reduces the forcing to the atmosphere, but it modifies the environment of geological formations, soil, or ocean, where the carbon dioxide is put. In addition, failure of sequestration is possible. "How much environmental modification and possibility of accidents people can tolerate" will be a subject of social decision making. The decision making can be done within a country if the sequestration is made within its territory.

SRM can cancel the greenhouse forcing in global mean sense, but it will enhance it in some of latitude bands and seasons. Assessments of its impacts is as difficult as regional projection of ACC. The fact that this is intentional makes the issue of liability more serious. Thus, such an international governance regime that is much stronger than the current UNFCCC regime is necessary, in addition to technological feasibility, to include SRM in policy options.

---

MZZ45-07

Room:422

Time:April 29 15:45-16:00

Keywords: anthropogenic climate change, global warming, geoengineering, adaptation to climate change, mitigation of climate change, solar radiation management

## Partial Commensurability: Translations between Multiple Observational Systems in Solid-Earth Physics

MORISHITA, Sho<sup>1\*</sup>

<sup>1</sup>Kyoto University / JSPS

The theme of incommensurability was introduced to philosophy of science by Kuhn and Feyerabend in 1960s. This theme has been discussed as problem of translations between multiple paradigms or conceptual frameworks. However, in 90s, a philosopher of science Ian Hacking extended the problematique ontologically. He argued that incommensurability is the problem of translations between multiple "closed systems" in experimental science [Hacking 1992].

If we apply his argument to observational science, it is outlined as below. Each observational equipments forms closed systems. That is, each equipment has the particular procedure and principle of observation which correspond to the mechanical structure of it. The data are visualized in the peculiar way and analyzed with the unique methods of correction. When observational equipment is different, the methods for articulations and the results are totally different. Therefore, a result from a particular observational equipment is difficult to translate into a result of another observational equipment.

This theme suggest the problem how we can achieve the comparison between different observational systems. In this paper, the author will call such comparison "partial commensuration" and discuss some specific examples of solid-earth physics, such as joint-inversion.

Keywords: Incommensurability, Observational Systems, Translation

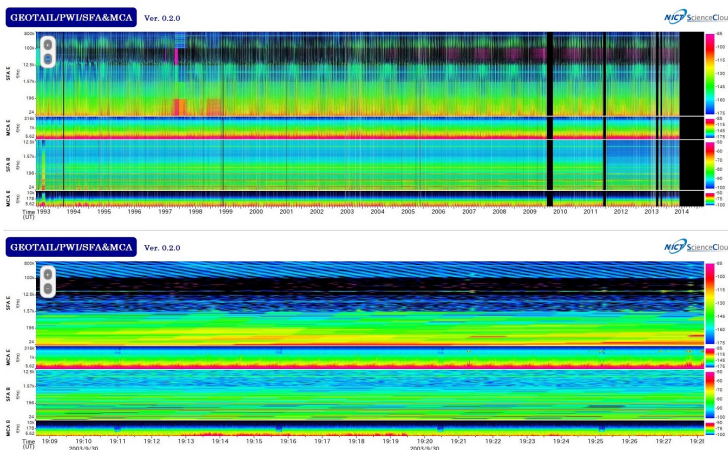
## A Web-application of Dynamic Time-Scale Previewer and its Application for Historical Geoscience Studies

MURATA, Ken T.<sup>1\*</sup>

<sup>1</sup>NICT

The NICT Science Cloud is one of the science clouds proposed for development of sciences. A variety of science data are collected and stored in the science cloud to be analyzed interdisciplinary. After the Internet is widely used, new concept and information technology has shown up; semantic web and linked open data (LOD). These technologies enable information on the Internet machine readable. In many science fields, it is pointed out that the semantic web will play an important role for the interdisciplinary research works. However, there have been few ideas to be ever proposed as a methodology or roadmap to the interdisciplinary science using semantic web. Herein we present a concept of professional knowledge and academic knowledge following collective knowledge proposed as a Web 2.0. Based on the concept, we design a Web-application for interdisciplinary science. The application (named STARS touch) provides users with an environment of dynamic and light preview of any types of time-dependent data. In the demonstration, we show an example of simultaneous preview of both scientific data (satellite observation data) and social data (newspaper information).

Keywords: STARS touch, NICT Science Cloud, Web Application



## Science against Natural Hazard 1960-1993: Has the Natural Disaster Science Overcome the Disasters?

YAMADA, Toshihiro<sup>1\*</sup>

<sup>1</sup>Post-doctoral Fellow of Pedagogy, University of Tokyo

The disastrous Ise-wan Typhoon of 1959 triggered the emergence of the field of Natural Disaster Science in Japan, which was proposed by the geophysicist Hasegawa Mankichi (1894-1970), President of Fukui University. The project, funded by the Ministry of Education and well organized especially by the geologist Matsuzawa Isao (1906-1990), Professor of Nagoya University, was continued until 1990s and provided many opportunities for the researches and activities of geoscientists. This article focuses this project considering the following contexts: 1) the post-war defense conversion in the field of earth sciences; 2) the interrelationship between the two major disciplines, geology and geophysics, in the sciences; and 3) the inclusion of the human and social sciences to cope effectively with such hazards and disasters.

Keywords: Natural Disaster Science, contemporary history of earth sciences, defense conversion, interdisciplinary domain, Hasegawa Mankichi, Matsuzawa Isao



## The reasons why we couldn't avoid the Okawa Elementary School disaster

HAYASHI, Mamoru<sup>1\*</sup>

<sup>1</sup>University of TOYAMA

March 11, 2011. Fifty minutes after the earthquake off the Pacific coast of Tohoku region, the big tsunami hit the Okawa Elementary School at Ishinomaki city. The victims include 74 students and 10 teachers from that school, as well as 3 students from Okawa Junior High School that had come to take children home and unknown number of Okawa district residents. Only 4 children and 1 teacher survived the catastrophe. It is considered the worst tragedy under the school administration since the establishment of the school system in Meiji Restoration.

The role of Earth Planetary Science will be examined considering the fact that the comprehension about magnitude of those involved in science education is still in the 1960's, and the problem concerning the Okawa Elementary School accident verification committee's investigation, which is predictable and not enough to get to the truth about the tsunami catastrophe.

## Characteristics of the modern stone industry and the regional context in each granite production areas in Japan

INUI, Mutsuko<sup>1\*</sup>

<sup>1</sup>School of Science and Engineering, Kokushikan University

Japanese stone industry has been thought to have developed to supply materials for the western architectures that were introduced in Japan in the late 19th century. It is also thought that it simply reduced because the imported stone materials became inexpensive. They are true, in a way, but the fact is more intricate, according to the interview survey carried out in several granite production areas. It is important to learn and record the complexity in the industrial history of one of the Japanese underground resources. Characteristic Japanese manner in the stone industry is described in this article. Difference in the industrial structure and history between several production areas are then documented.

Modern quarrying and stone manufacturing industry in Japan was established shortly after the introduction of western architecture, which used stones. Before that, stone was not popular in architectures. Therefore, stone was accepted in Japanese construction as decorating or finishing material. As the result, the standard manner of stone panelling in Japan became very elaborate, which only allowed beautifully designed stone panels with perfect colors and patterns, without any irregularities. The tradition has lead to low yield ratio (high rate of waste). Japan is also unique in its market of large granite tombstone which became popular after the world war II. Religious monuments are also popularly produced in stones. Stone materials in Japan therefore had two different markets, one for building stones, another for tombstones and religious craftworks.

Grain size, number density and orientation of cracks seems to determine the use of the stone, for building stone or for tombstone. Coarse grained granite with less cracks and veins yields large sized blocks, which is more favorable for architectural use. Some of those granites are used in famous historical buildings in Tokyo (e.g. Shodoshima stone, Kitagi stone). Fine grained granites with greyish colors are favored for tombstones in Japan (e.g. Aji stone, Oshima stone). Those quarries tend to have cracks with high number density and very low yield ratio, resulting in very expensive tombstone products.

Another factors that made difference between the granite production areas are the location of the quarry. Quarries on islands had advantage when principal transportation was seaborne. The transportation however shifted onto land and the islands lost their advantage. The relation between the quarry and the town sometimes restricted the activity of the quarry, concerning the noise or the disturbance on the landscape. Ownership of the mining area seemed to affect the sense of community in the production area.

The scheme and the unique manner of the stone industry in Japan are described. The interview survey revealed the context of each several granite production areas in Japan, and demonstrated how they corresponded to the decrease of stone production in Japan.

Keywords: building stone, tombstone, headstone, granite, quarry, modern industrial history

## History of marble mining in Mine, Yamaguchi Prefecture, Japan, and its use in historic buildings

INUI, Mutsuko<sup>1\*</sup>

<sup>1</sup>School of Science and Engineering, Kokushikan University

Mine District, Yamaguchi Prefecture, Japan, had been the largest marble mine in Japan for several decades until around 1970. Marble of Mine have been used in many buildings built during those period, also in Tokyo. However, import of inexpensive marble started to increase and soon overwhelmed the domestic marble. Most of the domestic marble mines have closed. It is important to remember the role of Japan's marble, one of our precious natural resources, in the developing industry of Japan during those times. The knowledge is also important to assess the building properly. The assessment may determine if the historic buildings should be conserved, renovated, or conversed. The aim of this study is to describe as many Mine marbles as possible for record, concerning e.g. its color, texture, how it was called, the locality of the quarry, during what period it was mined, or in what historic building it was used.

Keywords: marble, Mine district, Japan, stone industry, quarry, historic building

## Review of self-experiments on the cooperative study between EPS and philosophy of science since 2008

KUMAZAWA, Mineo<sup>1\*</sup> ; UENO, Fuki<sup>1</sup>

<sup>1</sup>Nagoya University, <sup>2</sup>Nagoya University

[ **Decoding the Earth's evolution related to philosophy of science** ] Motivation of the interdisciplinary works came up during the planning of the decoding research program (1995-1997) on the whole evolution history of the Earth from its birth at 4.6 billion years ago to the present time. In that program, the Earth history is described by a sequence of several time periods separated by the characteristic big events. We have assigned the present as the 7th big event in the Earth's history, with such a notion that Homo sapiens started science to try to understand everything; life, the Earth and the World. The present time is the boundary of the two different types of research; the past as a target of historical science and the future to predict and control even ourselves so as to fit with what we shall hope. We recognize that the World started self-reference and self-intervention in a way of coevolution between the life and the Earth environments by means of science and technology. The role of science has been evolving to have more influence to social and human subject, thereby more importance is placed on meta-science or philosophy of science.

Traditional philosophy of science with their classic discipline appears helpless, since it does not refer to newer experience and knowledge and deeper thinking having been accumulated lately by science method. This situation is making the philosophers difficult to digest science, a new comer. In addition, there are serious problems on science side; usually scientists do not pay much attention to meta-science; what the science is, why science works, how science contributes to people, etc., simply because most of them are slotted into the specific roles in a big science system. This situation appears serious for the modern society in respect to its survival on such a small friable Earth, as we geoscientists know well.

To face with this difficulty, we tried self-experiments of joint research by geoscientists with Todayama and his collaborators on the subject of common interests since 2009, and some of the results have been reported at JpGU meeting. Fortunately, Todayama School has been trying to open up a new trend, 'naturalized philosophy of science', so the collaboration was really welcome. This work was supported in 2011-2013 by JSPS Grant-in-Aid for Scientific Research (23320005) headed by Dr. Shigeyuki Aoki. The outcomes of research on the history of geoscience were published in Nagoya Journal of Philosophy, Vol.10 (2013), and the works on other topics will appear in the forthcoming volumes.

[ **The problems recognized** ] The collaboration between the scientists and philosophers of science was found still difficult due to the difference in languages, cultures and even in the way of discussions. Whereas it is difficult to review objectively in detail at this moment, we shall keep trying to find out the good ways of collaboration with meta-science for our survival succession. We have obtained a bright hope along this line in the present work.

In conclusion, we found an 'indispensable minimum recipe' of approaching the problem. It is the promotion of education policy for the graduate students to take double tracks striding the boundary between science and human studies to be seamless. We have to remind that the Japanese education system appears far behind the contemporary necessity.

[ **The purpose of this poster presentation** ] We believe that the straightforward discussions are really useful among the research workers of different disciplines for activating the intellectual potential, in particular. The purpose of this presentation is to invite those who are interested in the interdisciplinary communication between science and meta-science to have discussions in front of our poster. Note: Two authors of this presentation were the acting managers of the collaboration works between Geoscience and Todayama School of philosophy of science.

Keywords: Science of Science Phenomena, Meta-Science, Philosophy of Science, Normative Science